Design and Synthesis of New Biologically Active Heterocycles Derived from [2.2]Paracyclophanes and 2-Quinolones

Zur Erlangung des akademischen Grades einer

DOKTORIN DER NATURWISSENSCHAFTEN

(Dr. rer. nat.)

von der KIT-Fakultät für Chemie und Biowissenschaften

des Karlsruher Instituts für Technologie (KIT)

genehmigte

DISSERTATION

von

M. Sc. Lamiaa Elsayed Abd El-Haleem

Minia, Ägypten

Referent: Prof. Dr. Stefan Bräse

Korreferent: Prof. Dr. Joachim Podlech

Tag der mündlichen Prüfung: 19. Oktober 2020

“I have frequently been questioned, especially by women, of how I could reconcile family life with a scientific career. Well, it has not been easy.”

~ Marie Curie

Honesty Declaration

The present work was carried out at the Institute of Organic Chemistry at the Karlsruhe Institute of Technology (KIT), Faculty of Chemistry and Biosciences, Institute of Organic Chemistry (IOC) and at the Faculty of Science at Minia University (Egypt) in the period from 19th September 2017 to 9th September 2020 under supervision of Prof. Dr. Stefan Bräse. During the period from 19th September 2017 to 15th October 2018, the work was scientifically supervised by Prof. A. A. Aly (Minia University).

Die vorliegende Arbeit wurde in der Zeit von 19.09.2017 bis 09.09.2020 am Institut für Organische Chemie der Fakultät für Chemie und Biowissenschaften am Karlsruher Institut für Technologie (KIT), sowie an der Fakultät der Wissenschaften and der Universität Minia (Ägypten) unter der Leitung von Prof. Dr. Stefan Bräse durchgeführt. Im Zeitraum von 19.09.2017 bis 15.10.2018 wurde die Arbeit durch Prof. A. A. Aly (Minia University) wissenschaftlich betreut.

I hereby declare truthfully that I have prepared this thesis autonomously except for the help explicitly stated in the treatise itself; that I have exhaustively and accurately indicated all auxiliary means; and that I have marked all portions taken, verbatim or in altered form, from the work of others or my publications.

Hiermit versichere ich wahrheitsgemäß, die vorliegende Dissertation selbstständig verfasst und ohne unerlaubte Hilfsmittel angefertigt, andere als die angegebenen Quellen und Hilfsmittel nicht benutzt und die den verwendeten Quellen wörtlich oder inhaltlich entnommenen Stellen als solche kenntlich gemacht habe. Die Arbeit wurde bisher in gleicher oder ähnlicher Form noch keiner anderen Prüfungsbehörde vorgelegt und auch nicht veröffentlicht. Ich habe die Regeln zur Sicherung guter wissenschaftlicher Praxis am Karlsruher Institut für Technologie (KIT) in der gültigen Fassung beachtet.

Karlsruhe, 08.09.2020 Lamiaa Elsayed Abd El-haleem

The German title of this thesis

Design und Synthese von neuartigen bioaktiven Heterozyklen basierend auf [2.2]Paracyclophanen und 2-Chinolonen

Table of Contents

Abstract

Five-membered heterocycles form by far the largest of the classical molecular divisions in organic chemistry. Moreover, the synthesis of novel *N*-containing five-membered heterocycles and the investigation of their chemical behavior and pharmacological activities have gained more importance in recent decades. Cancer is one of the main causes of death, ranked only after heart disease, developing novel anticancer drugs has become one of the most important areas of research today. The aim here is to found a method to develop new drugs by combining different compound classes that have importance in synthetic and drug chemistry.

Thiosemicarbazides are carbothioamide derivatives, they are ideal candidates and valuable building blocks for the synthesis of various five-membered heterocyclic rings. Additionally, [2.2]paracyclophanes have recently been established in the field of stereoselective synthesis and have also been incorporated into heterocyclic structures. On the other hand, the chemistry of 4-hydroxy-2-quinolones is unique due to their roles in the biological and pharmacological activities of many of their derivatives. Therefore, the presented thesis is based on the synthesis and applications of novel *N*-containing five-membered heterocycles from new synthesized substituted thiosemicarbazides attached to [2.2]paracyclophane, as well as the synthesis of new five-membered heterocycles fused with 4-hydroxy-2-quinolones.

Firstly, the synthesis and linked between [2.2]paracyclophane and thiosemicarbazides is obtained, afterward, different classes of five-membered heterocycles are designed and synthesized *via* cyclization reaction and donor-acceptor interaction of [2.2]paracyclophanyl-*N*-substituted hydrazinecarbothioamide (as donors) and several types of acceptors like dimethyl acetylenedicarboxylate, dicyanomethylene-1,3-indanedione, 2,3-dichloro-1,4-naphthoquinone and 2-bromo-2′-aceto-naphthone.

Secondly, all of the obtained target compounds were screened against 60 cancer cell lines. Some of them displayed a moderate to weak activity on most of the tested cancer cell lines. Some others displayed anticancer activity against the leukemia subpanel namely RPMI-8226 and SR cell lines, and others displayed anticancer activity against the SK-MEL-5 melanoma cancer cell line.

Lastly, a novel series of fused five-membered heterocyclic rings attached to 4-hydroxy-2-quinolones were synthesized *via* reactions between 4-hydroxy-2-quinolones as donors and different classes of acceptors like 3,4,5,6-tetrachloro-1,2-benzoquinone, 2,3-dichloropyrazine, and *E*-dibenzoylethene.

Kurzzusammenfassung

Fünfgliedrige, stickstoffhaltige Heterozyklen bilden eine der größten Molekülsparten in der organischen Chemie und die Untersuchung ihres chemischen Verhaltens und ihrer pharmakologischen Aktivitäten hat in den letzten Jahren stetig zugenommen. Krebs ist eine der häufigsten Todesursachen und wird statistisch gesehen nur durch Herzkrankheiten übertroffen. Daher ist die Entwicklung von neuartigen Krebsmedikamenten einer der wichtigsten Bereiche der Wissenschaft der heutigen Zeit. Das Ziel ist eine Methode zu finden und zu etablieren, mit welcher neue Wirkstoffe entwickelt werden, indem man verschiedene Substanzklassen kombiniert, welche in der synthetischen und pharmazeutischen Chemie bedeutsam sind.

Thiosemicarbazide sind Derivate der Carbothioamide und ideale Kandidaten und wertvolle Bausteine der Synthese von verschiedenen fünfgliedrigen Heterozyklen. Darüber hinaus haben sich [2.2]Paracyclophane auf dem Gebiet der stereoselektiven Synthese etabliert und wurden in heterozyklische Strukturen eingebaut. Des Weiteren ist die Chemie der 4-Hydroxy-2-chinolone aufgrund der biologischen und pharmakologischen Bedeutung der Derivate dieser Substanzklasse einzigartig. In der vorliegenden Arbeit werden die Synthesen und Anwendungen von neuartigen stickstoffhaltigen Heterozyklen sowohl basierend auf substituierten und mit [2.2]Paracyclophanen verbundenen Thiosemicarbaziden, als auch die Synthese und Anwendung von mit 4-Hydroxy-2-chinolonen verbundenen fünfgliedrigen Heterozyklen untersucht.

Zunächst wurde hierfür die Synthese und Verlinkung von [2.2]Paracyclophanen und Thiosemicarbaziden vorgenommen. Anschließend wurden verschiedene Klassen von fünfgliedrigen Heterozyklen entworfen und mittels Zyklisierungsreaktionen und Donor-Akzeptor-Interaktion zwischen [2.2]Paracyclophanyl-*N*-substituierten Hydrazincarbothiamiden und verschiedenen Akzeptoren synthetisiert. Im Anschluss wurden die erhaltenen Substanzen gegen 60 Krebszell-Linien getestet. Einige der Substrate zeigten antikanzerogene Aktivität gegen die Leukämie-Zelllinie RPMI-8226 und SR-Zelllinien oder auch gegen SK-MEL-5 Melanom-Krebszellen. Schließlich wurde eine neuartige Serie von fusionierten fünfgliedrigen Ringen, welche mit 4-Hydroxy-2-chinolonen verbunden sind, synthetisiert. Die Synthese erfolgte mittels der Reaktion zwischen 4-Hydroxy-2-chinolonen als Donoren und verschiedenen Akzeptor-Klassen wie 3,4,5,6-Tetrachloro-1,2-benzochinonen, 2,3-Dichloropyrazinen und *E*-Dibenzoylethenen.

1. Introduction

In recent years, the chemistry of five-membered heterocyclic rings has received considerable attention because of their synthetic challenges and biological and pharmaceutical importance.[1] There are two classes of five-membered heterocyclic rings (Figure 1): saturated five-membered rings containing one heteroatom like tetrahydrofuran, pyrrolidine, tetrahydrothiophene, and unsaturated five-membered rings with *one* heteroatom like furan, pyrrole, thiophene. These unsaturated five-membered ring compounds are aromatic and called "heteroaryls".[2-3]

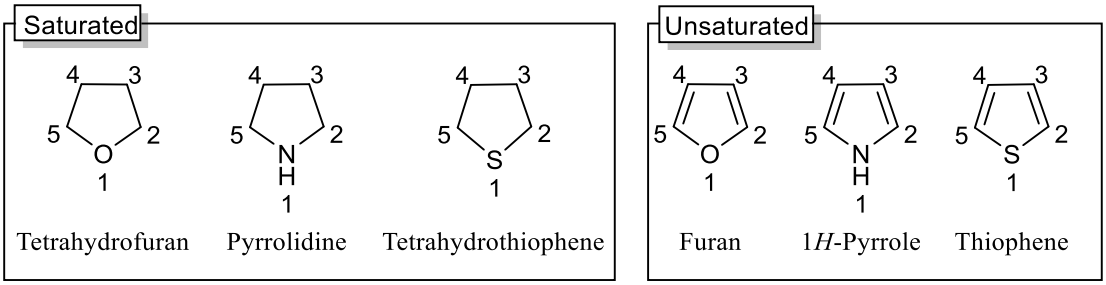

Figure 1: Examples of saturated and unsaturated five-membered heterocyclic compounds.

Azoles are a class of five-membered heterocyclic compounds containing a nitrogen atom and an additional heteroatom (nitrogen, sulfur, or oxygen) in the ring.[4] Azoles which have a vast biologically active nature have motivated many researchers throughout the world to exploit their biological potential to design and develop newer therapeutic agents (Figure 2).[5]

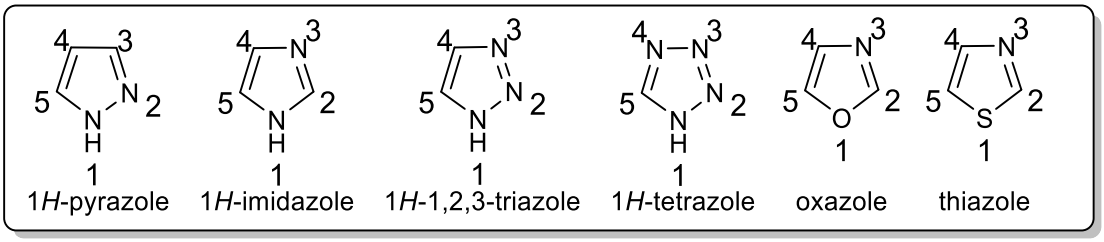

Figure 2: Examples for azole compounds.

Azoles are present in some of the most common biologically important molecules. Drimentine G (**1**) is a prime example of the importance of azoles in biologically active compounds. This specific compound has anticancer and antibacterial activities, while Captopril (**2**) is an ACE inhibitor used for the treatment of hypertension (Figure 3).[6-9] Thiazole analogs have continued to attract interest in the field of medicinal chemistry due to their wide-ranging biological activities. A literature survey revealed some reported antibacterial FabH inhibitors that possess a thiazole scaffold similar to the 2-arylidenehydrazinyl-4-arylthiazole analogs **3**, **4,** and **5**.[10-13]

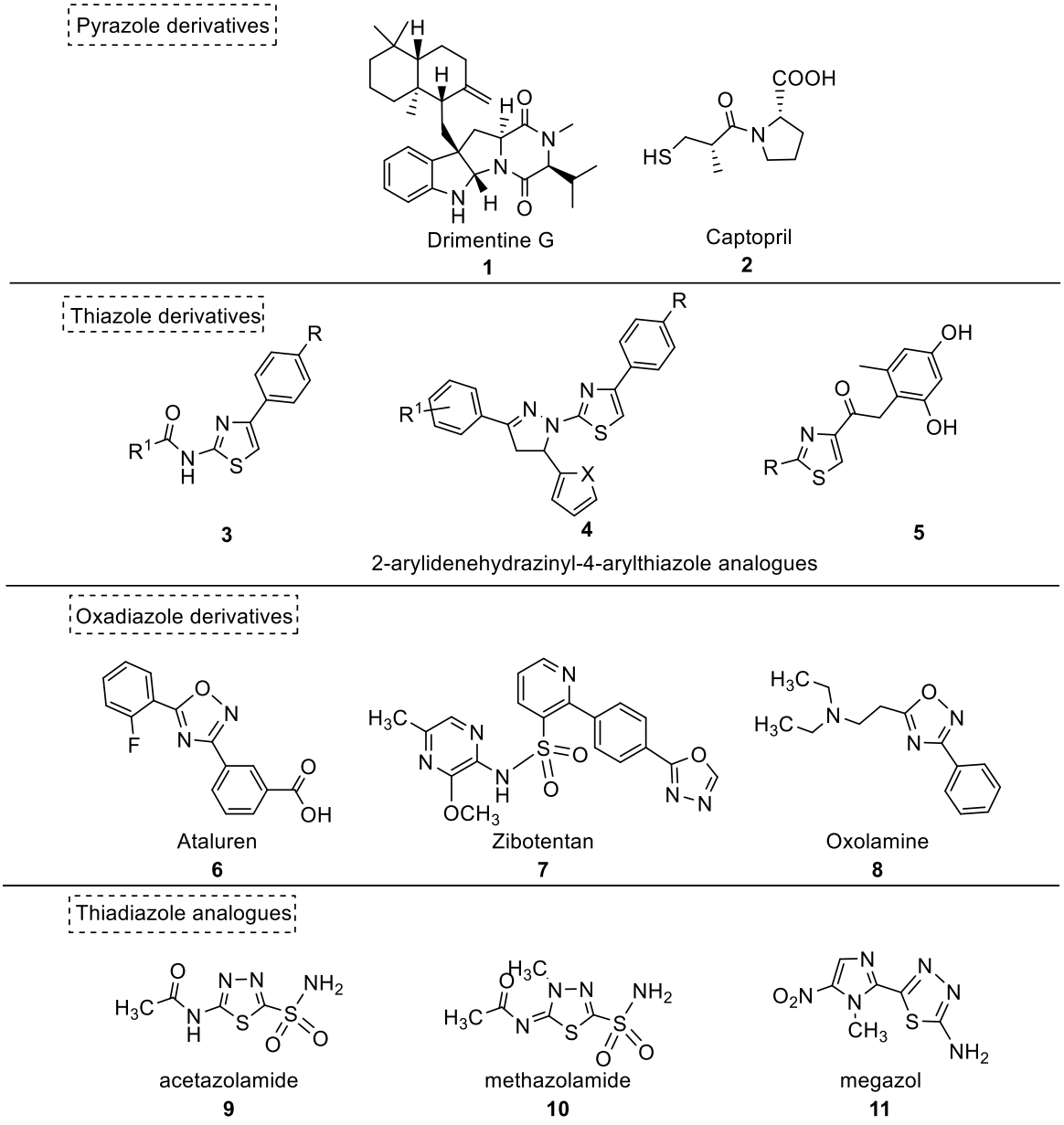

Figure 3: Selected example of current drugs containing heterocyclic scaffold.

Furthermore, these structural motifs are also present in many pharmaceutically active compounds (Figure 3).[10] Moreover, they are many 1,2,4-oxadiazoles derived drugs like ataluren (**6**), oxolamine (**7**), and 1,3,4-oxadiazoles like zibotentan (**8**) are widely used in several drugs, researchers report it as important bioisosteres to replace amide and ester functionalities in the compounds making them resistant to enzyme-catalyzed hydrolysis which improves their biological and pharmacokinetic properties (Figure 3).[14-15] In recent studies, it was found that also 1,3,4-thiadiazole derivatives, like for example acetazolamide (**9**), methazolamide (**10**), and megazol (**11**) (Figure 3).[16-17] have a broad spectrum of pharmacological activities which can

be classified into the following categories: antibacterial and antifungal activity,[18-19] anticancer activity,[20] anti-inflammatory activity,[21] and antiviral activity.[22-23]

1.1 *N*-Containing Five-membered Rings

1.1.1 Nomenclature and Isomerism

The standard method for naming five-membered heterocyclic rings is the Hantzsch-Widman nomenclature system.[24] The identity of the heteroatom in the ring is established by using different prefixes and numbers are assigned to the atom denoting the heteroatoms´ position. The degree of unsaturation is described by the suffix at the end (Table 1).[24-25]

Table 1: Hantzsch-Widman nomenclature for five-membered heterocyclic compounds.

Order of Seniority	Prefix	Suffix
1	-oxa for oxygen	-*ole* for an unsaturated ring
2	-thia for sulfur	-*olane* for a saturated ring with only O or S
3	-aza for nitrogen	-*olidine* for a saturated ring with N
4	-phospha for phosphorus	
5	-bora for boron	

Isomerism in five-membered heterocyclic compounds with one-heteroatom depends on the number and type of substitutions present in the molecule. Figure 4 shows the possible isomers of mono- and di-substituted heterocyclic pyrroles.[25]

1.1.2 Synthesis of *N*-Containing Five-membered Rings

N-Containing five-membered rings are found in nature and occur in coal tar, bone oil, and many other naturally occurring substances such as chlorophyll and vitamin B12.[25]

1.1.2.1 General Synthesis Methods

Pyrrole

Synthesis of pyrrole derivatives *via* a gold-catalyzed intramolecular variant of the acetylenic Schmidt reaction was reported by Toste. Homopropargylic amines **12** undergo cyclization, when treated with a combination of gold dichloride and silver hexafluoroantimonate, to yield 2,3,5-trisubstituted pyrroles **13** (Scheme 1).[26]

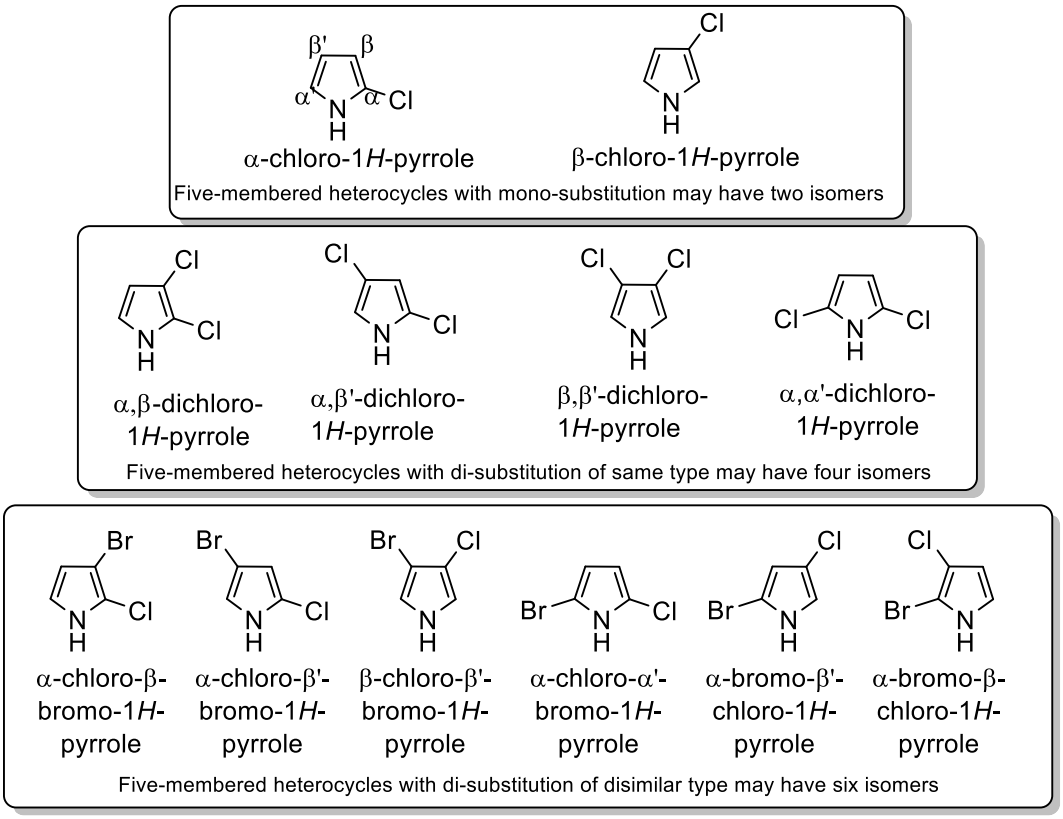

Figure 4: Isomerism in five-membered heterocycles.

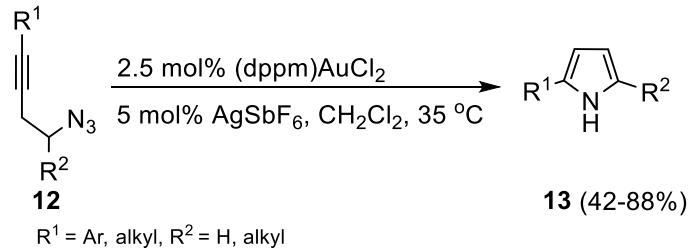

Scheme 1. Synthesis of 2,3,5-trisubstituted pyrroles **13**.

Thiazole and Oxazole

Diazocarbonyl compounds **15** can react with primary amides **14** in the presence of dirhodium tetraacetate as catalyst and 1,2-dichloroethane as a solvent, to form α-acylaminoketones **16**, which are subsequently cyclized into thiazole and oxazole derivatives (Scheme 2). The treatment of 1,4-dicarbonyl intermediates with Lawesson's reagent yields the corresponding thiazoles **17**, while oxazoles **18** can be obtained *via* a cyclodehydration reaction with triphenylphosphine-iodine-triethylamine.[27]

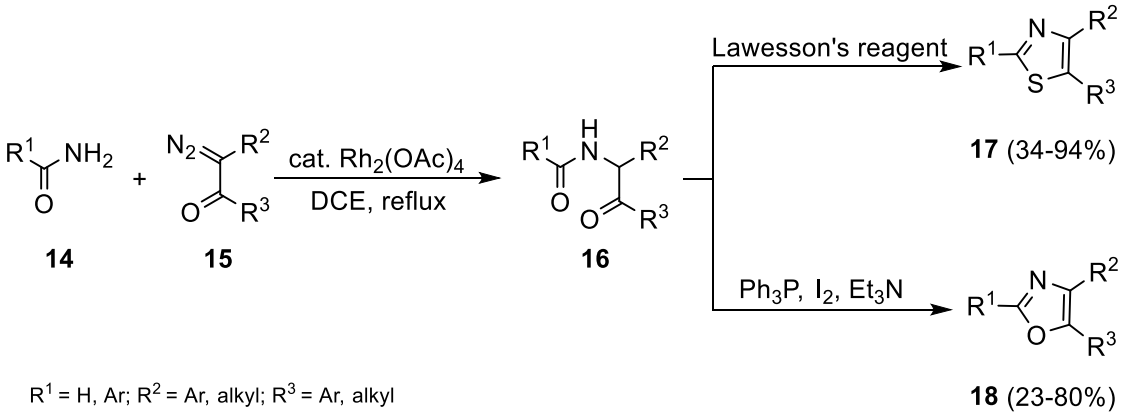

Scheme 2. Formation of thiazoles **17** and oxazoles **18**.

Pyrazoles

Pyrazole derivatives **20** can be synthesized by a reaction between *β*-alkoxyvinyl trichloromethyl ketones **19** with hydrazine hydrochloride. The double nucleophilic character of hydrazines allows them to react with each carbonyl group of a 1,3-keto-aldehyde masked as enol ether or acetal to form the corresponding pyrazole derivatives **20** (Scheme 3).[28]

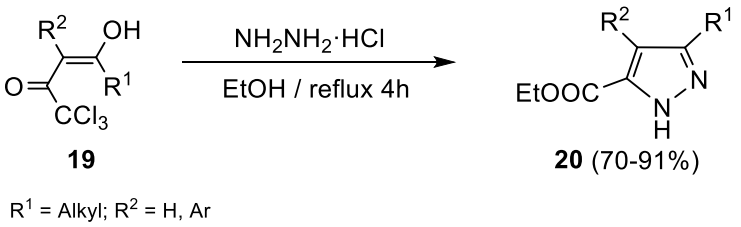

Scheme 3. Synthesis of pyrazole derivatives **20**.

Triazole

In 1986 Sakai *et al.* described the formation of substituted triazoles **23**. The Sakai approach relies on the condensation of primary amines and α,α-dichlorotosylhydrazones **21** in methanol to regioselectively form 1,4-substituted triazoles **23** under ambient reaction conditions (Scheme 4).[29]

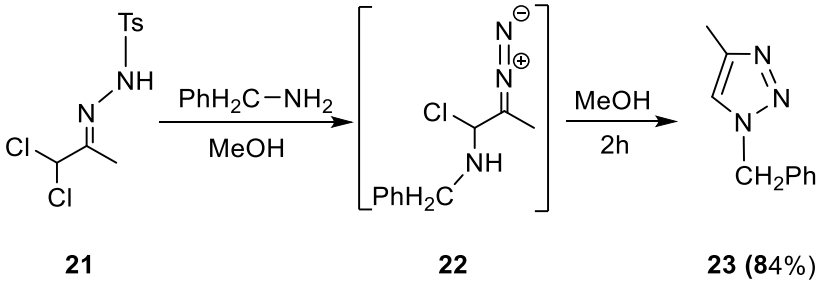

Scheme 4. Synthesis of 1,4-substituted triazoles **23**.

1.1.2.2 Synthesis of *N*-Containing Five-membered Rings from Thiosemicarbazides

The reactivity of thiosemicarbazides makes them valuable as building blocks for the synthesis of heterocyclic motifs, especially five-membered rings (Figure 5). The structures of hydrazinecarbothioamide and its derivatives are related to compounds described by the formula of $R^1NHNHCSNHR^2$ (Figure 5). This class is called thiosemicarbazides,[30] and it has a wide range of applications, for example as antibacterial, antifungal, chemotherapeutic, and bio-analytical reagents.[31-33]

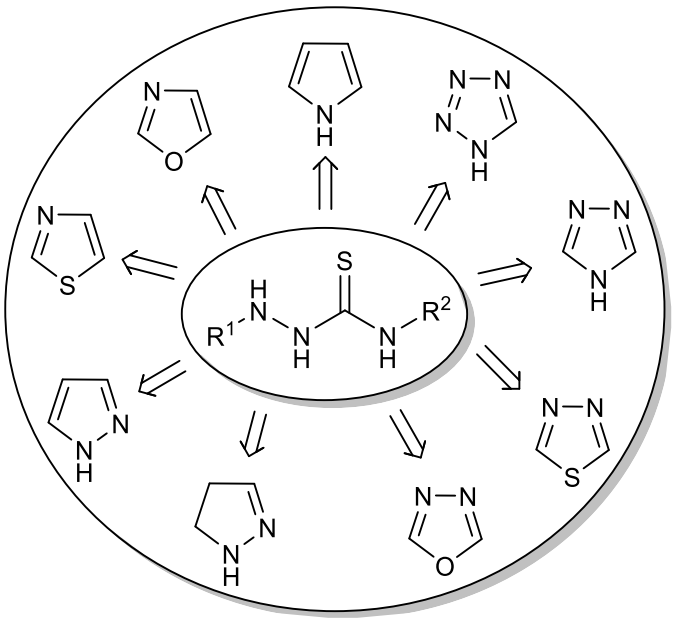

Figure 5: Thiosemicarbazides as building-blocks in the synthesis of heterocyclic compounds.

Synthesis of Thiosemicarbazides.

Thiosemicarbazides can be prepared by several methods, the most common ones are from aldehydes, amines, or carbohydrazides, general examples for preparation will be discussed as follows:

From 1-Chloro-3,4-dihydronaphthalene-2-carbaldehyde

In two successive steps, substituted thiosemicarbazide can be prepared by the condensation of 1-chloro-3,4-dihydronaphthalene-2-carbaldehyde (**24**) with hydrazine hydrate in ethanol to afford Schiff's base. By adding compound **25** to phenyl isothiocyanate in boiling dioxane (*E*)-2-((1-chloro-3,4-dihydronaphthalen-2-yl)methylene)-*N*-phenylhydrazinecarbothioamide (**26**) can be obtained. Alternatively, heating compound **24** with thiosemicarbazide **27** in ethanol gives (*E*)-2-((1-chloro-3,4-dihydronaphthalen-2-yl)methylene)hydrazine-1-carbothioamide (**28**) (Scheme 5).[34]

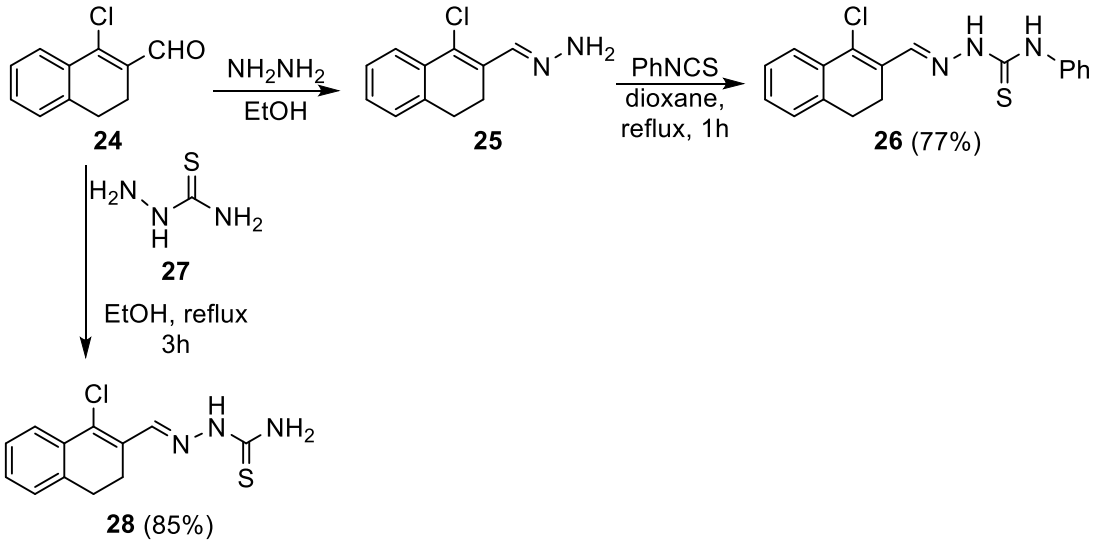

Scheme 5. Synthesis of thiosemicarbazides **26** and **28**.

From Substituted Amines

The addition of carbon disulfide and trimethylamine to a solution of substituted aniline derivatives **29** in THF affords dithiocarbamic acid salts, which can then be added to Boc_2O and DMAP to give the corresponding isothiocyanates **30**. Then, the isothiocyanates **30** reacted with the substituted hydrazines **33** and triethylamine (Et_3N) to form thiosemicarbazides **34** (Scheme 6).[35]

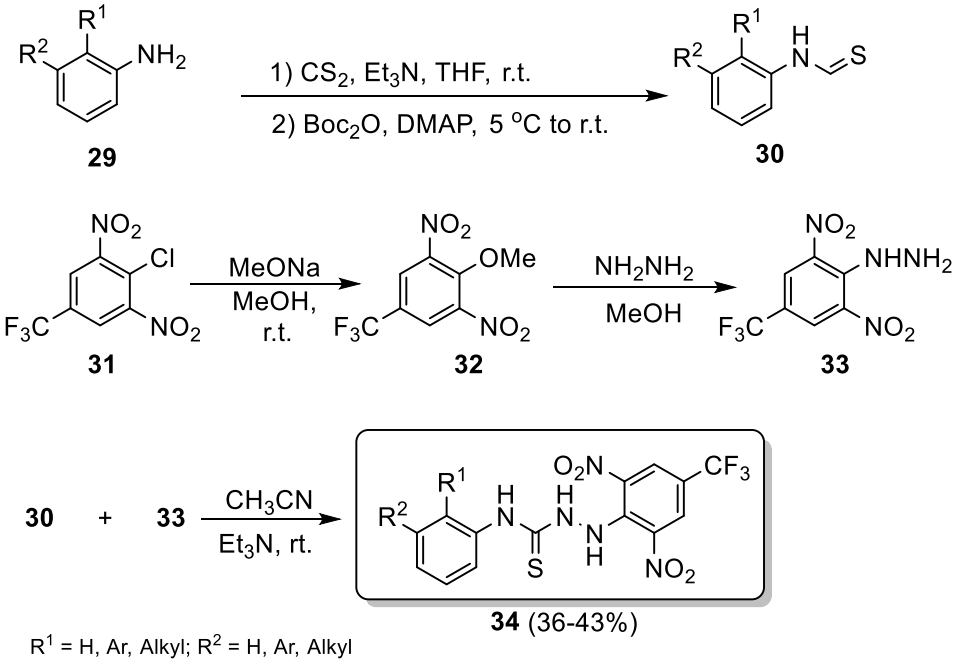

Scheme 6. Formation of thiosemicarbazide **34** from substituted aniline derivatives **29**.

From Carbohydrazide

Carbohydrazides **36** are commonly prepared by reactions of hydrazine with acyl derivatives **35** including esters, cyclic anhydrides, and acyl halides. The corresponding aroyl-thiosemi-carbazides **37** can be synthesized by reacting carbohydrazide **36** with different isothiocyanates in ethanol (Scheme 7).

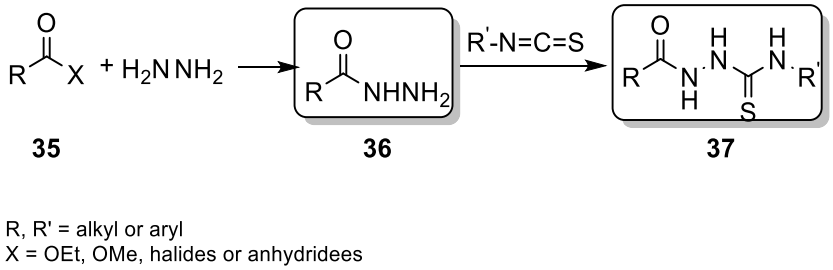

35 **36** **37**

Scheme 7. A general method for the synthesis of substituted aroylthiosemicarbazides **37** from carbohydrazides **36**.

An example of the syntheses of substituted aroylthiosemicarbazides **41** is the conversion of diflunisal (2',4'-difluoro-4-hydroxybiphenyl-3-carboxylic acid) (**38**) to its corresponding diflunisal ester **39**. The desired diflunisal hydrazide **40** can be obtained by using hydrazine hydrate. The reactions of hydrazide **40** with various aryl isothiocyanates afford substituted hydrazinecarbothioamides **41** (Scheme 8).[36]

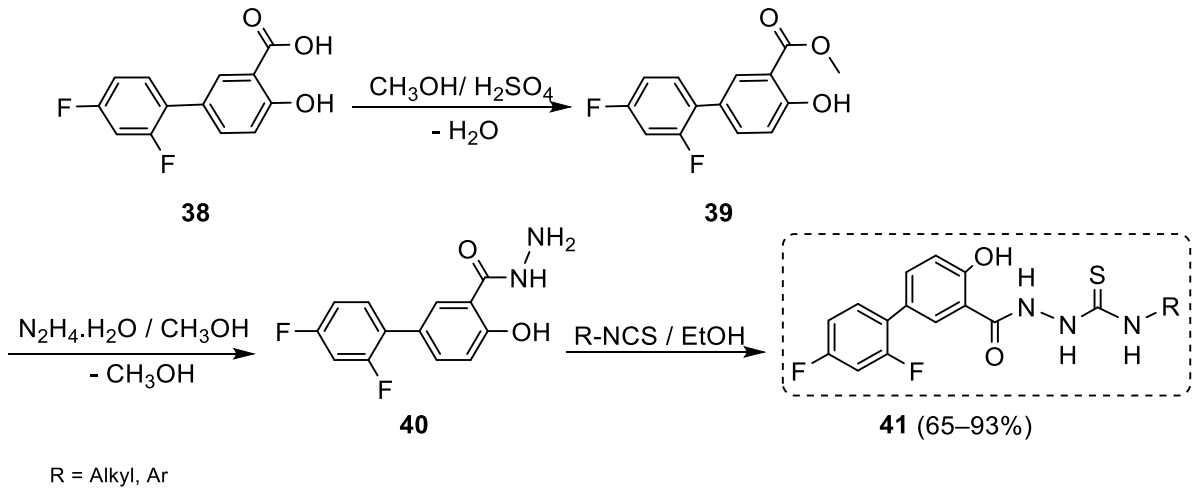

38 **39** **40** **41** (65–93%)

Scheme 8. Synthesis of hydrazinecarbothioamides **41**.

Aroylthiosemicarbazides in the Synthesis of Bio-active Five-membered Heterocycles

This study focuses on the synthesis of different bioactive substituted *N*-containing five-membered rings from substituted aroylthiosemicarbazides.

Synthesis and Biological Activity of Pyrrolidine Derivatives

Substituted pyrrolidine-2,5-dione **44** can be synthesized by condensation of carbohydrazide derivatives **42** with succinic anhydride **43** in refluxing glacial acetic acid (Scheme 9).[37] Compound **44** shows epidermal growth factor receptor (EGFR) inhibitory activity which evaluates for its antiproliferative activity on human breast cancer cell line (MCF-7).

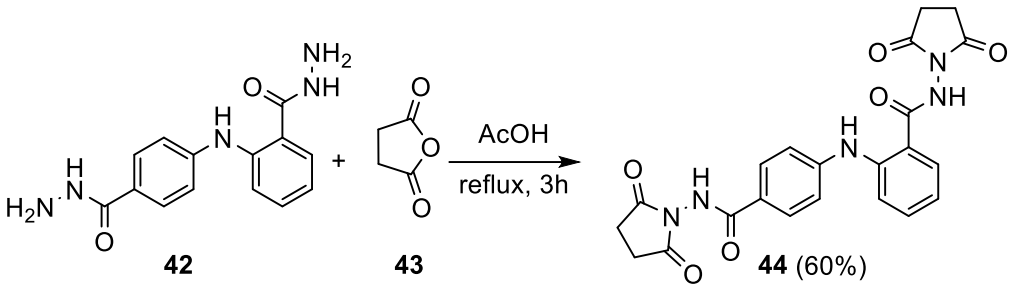

Scheme 9. Synthesis of substituted pyrrolidine-2,5-dione **44**.

Synthesis and Biological Activity of Thiazole Derivatives

Substituted thiazoles can be synthesized by refluxing *N*-phenyl thiosemicarbazide **45** with chloroacetic acid **46** and sodium acetate in ethanol to afford *N*'-(4-oxo-3-phenylthiazolidin-2-ylidene)benzohydrazide **47**, which can undergo condensation reactions with a variety of aromatic aldehydes **48a-c** in acetic acid and sodium acetate to furnish the corresponding 5-arylidenethiazolidin-4-one compounds **49** (Scheme 10). By screening compounds **49a-c** as an antioxidant, the best antioxidant potentiality was found to be **49b**, followed by **49c** and **49a**. The results indicate that a combination of the nicotinonitrile moiety and thiazole ring promotes the antioxidant activity to the highest percentual inhibition ranging from 82% to 86%.[38]

Furthermore, 3-thiazolylcoumarin derivatives **52** were synthesized by reactions of thiosemicarbazide derivatives **50** and 3-(bromoacetyl) coumarin **51** (Scheme 11). Compounds **52** were screened for *in vitro* α-glucosidase inhibitory activity and cytotoxicity. The results show that all compounds are non-cytotoxic but have excellent inhibitory activity in the range of IC_{50} = 0.12 ± 0.01-16.20 ± 0.23 μM when compared to the standard acarbose (IC_{50} = 38.25 ± 0.12 μM).[39]

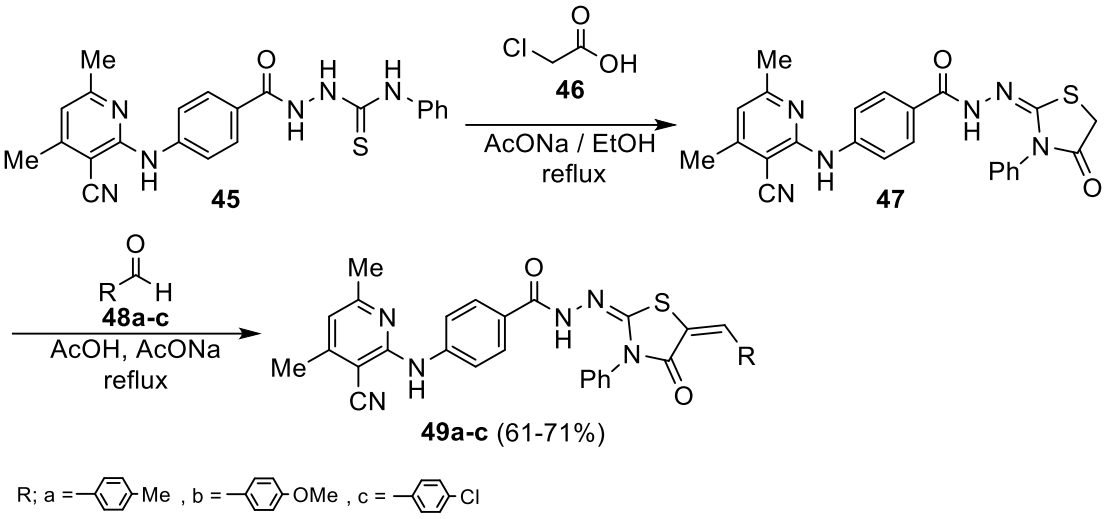

Scheme 10. Synthesis of antioxidant 5-arylidenethiazolidin-4-one compounds **49a-c**.

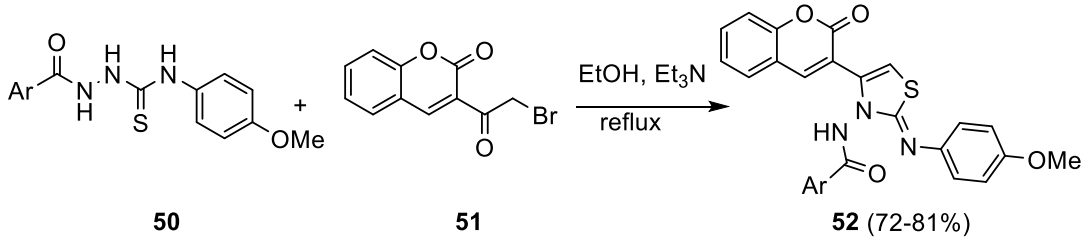

Scheme 11. Synthesis of α-glucosidase inhibitor and non-cytotoxic 3-thiazolylcoumarin derivatives **52**.

Synthesis and Biological Activity of Pyrazole and Imidazolidine Derivatives

By the reaction of substituted carbohydrazides **53** with acetylacetone **54**, the pyrazole-containing 2-((4-(3,5-dimethyl-1*H*-pyrazole-1-carbonyl)phenyl)amino)-4,6-dimethylnicotinonitrile **55** can be synthesized. Similarly, the reaction of carbohydrazide **53** with ethyl acetoacetate **56** leads to the formation of the corresponding 2-((4-(3-methyl-5-oxo-1*H*-pyrazole-1-carbonyl)phenyl)amino) nicotinonitrile derivative **57** (Scheme 12).[38]

The formation of N^1-[4-(phenylsulfonyl)benzamide]-N^3-(2-methoxyphenyl)-2-thioxo-4,5-imidazolidinedione **60** can be achieved by stirring N^1-[4-(phenylsulfonyl)benzoyl]-N^4-(2-methoxyphenyl)thiosemicarbazide **58** with oxalyl chloride **59** and refluxing the formed precipitate in ethanol (Scheme 13). The preliminary results of antimicrobial activity tests indicate that the tested compounds inhibit the growth of some gram-negative bacteria such as *Escherichia coli, Pseudomonas aeruginosa,* gram-positive bacteria like *Bacillus subtilis,* and fungi like *Candida scotti.*[40]

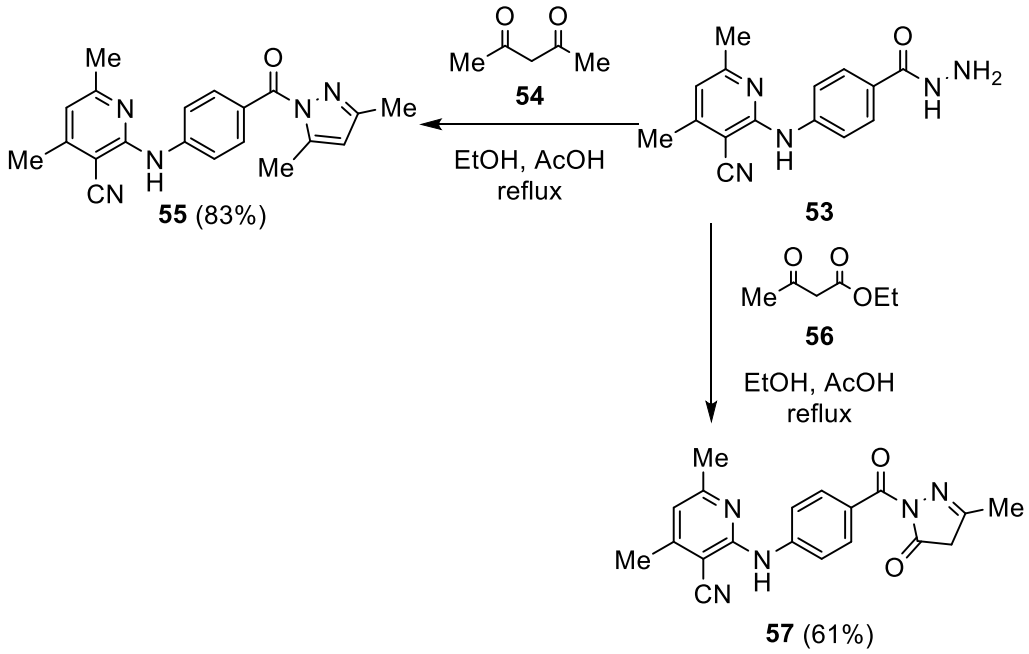

Scheme 12. Synthesis of different substituted pyrazole rings **55** and **56** from carbohydrazide **53**.

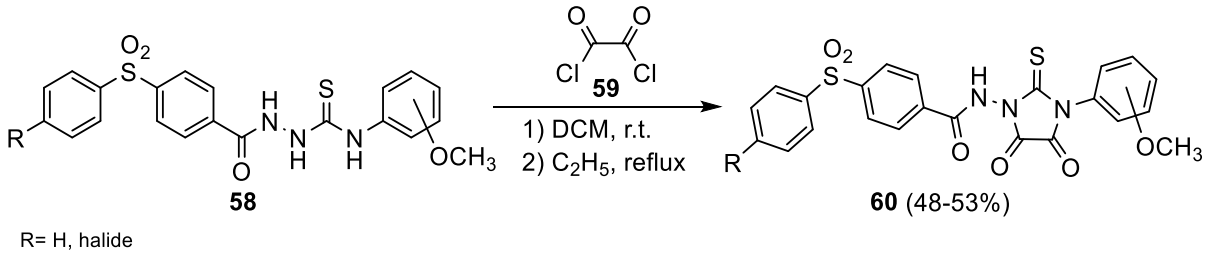

Scheme 13. Synthesis of antimicrobial imidazolidine derivatives **60**.

Synthesis and Biological Activity of Oxadiazole, Thiadiazole, and Triazole Derivatives

1,3,4-Oxadiazole derivatives **65a-l** can be obtained *via* a two steps synthesis as shown in Scheme 14. In the first reaction step, *N*-phenyl-5-(substituted)-1,3,4-oxadiazol-2-amines **64a-c** are formed by refluxing substituted carbothioamides **63a-c** using iodobenzene diacetate and aqueous sodium hydroxide in methanol. In a second reaction step, a reduction of substituted 2-chloroquinoline-3-carbaldehyde **61a-c** is followed by the chlorination to obtain substituted 2-chloro-3-(chloromethyl)quinoline **62a-c**. Refluxing of **64a-c** with **62a-c** in K_2CO_3 and dimethylformamide affords the target molecule **65a-l** in good yields. By screening the obtained quinoline-oxadiazole **65a-l** against microbial, antitubercular, and antimalarial activities, it was found that compounds **65a**, **65e**, **65j,** and **65k** exhibit good antituberculosis activities. The majority of the compounds show excellent activity against *P. Falciparum* strains as compared to quinine. While compound **65k** emerged as the promising antimicrobial member within varies, it shows better antitubercular activity, antimalarial activity, and lower toxicity.[41]

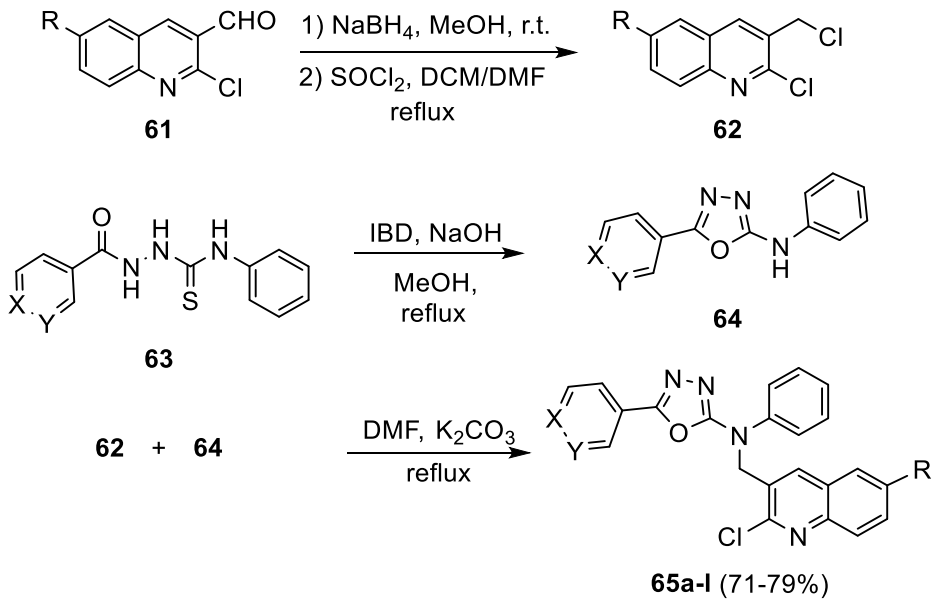

65a; R = H, X = N, Y = CH, **65b**; R = H, X = CH, Y = N, **65c**; R = H, X = CH, Y = CH, **65d**; R = CH_3, X = N, Y = CH, **65e**; R = CH_3, X = CH, Y = N, **65f**; R = CH_3, X = CH, Y = CH, **65g**; R = OCH_3, X = N, Y = CH, **65h**; R = OCH_3, X = CH, Y = N, **65i**; R = OCH_3, X = CH, Y = CH, **65j**; R = Cl, X = N, Y = CH, **65k**; R = Cl, X = CH, Y = N, **65l**; R = Cl, X = CH, Y = CH

Scheme 14. Synthesis of 1,3,4-oxadiazole derivatives **65a-l** *via* reaction with quinoline **62a-c**.

Furthermore, 2,2'-Terephthaloylbis(*N*-phenylhydrazinecarbothioamide) **66** was reacted with the corresponding 2-oxo-*N'*-arylpropanehydrazonoyl chlorides **67a-e** to form the respective bisthiadiazoles **69a-e** (Scheme 15). Similarly, 1,3,4-thiadiazole derivatives **72a–e** were synthesized *via* the reaction of ethyl 2-chloro-2-(2-arylhydrazono)acetates **70a-e** with compound **66** under the same reaction conditions (Scheme 15). The suggested mechanism for the formation of the products **69a-e** and **72a-e** was that the reaction of compound **66** with hydrazonoyl chlorides initially gives the intermediate **68a-e** and **71a-e** by a 1,3-addition then, *in situ* cyclization *via* loss of aniline to give the final product **69a-e** and **72a-e** (Scheme 15).[42]

In a screening of compounds **69a-e** and **72a-e** in a α-blocking activity test using α-sympatholytic activity in isolated vascular smooth muscle, all compounds showed antihypertensive α-blocking activities and they were arranged in descending order of activities as follows: **72b** > **72a** > **72c** > **66** > **72d** > **72e** > **69b** > **69c** > **69a** > **69e** > **69d**. The presence of a methyl group in position 4 of the aryl moiety at the thiazole ring correlates with a higher activity than that of a chlorine group. For thiadiazoles **72a–e**: **72b** (IC_{50} = 5.11 µg/mL) > **72a** (IC_{50} = 5.23 µg/mL) >**72d** (IC_{50} = 5.67 µg/mL). For thiadiazoles **69a–e**: **69b** (IC_{50} = 6.15 µg/mL) > **69a** (IC_{50} = 6.40 µg/mL) >**69d** (IC_{50} = 6.54 µg/mL).[42]

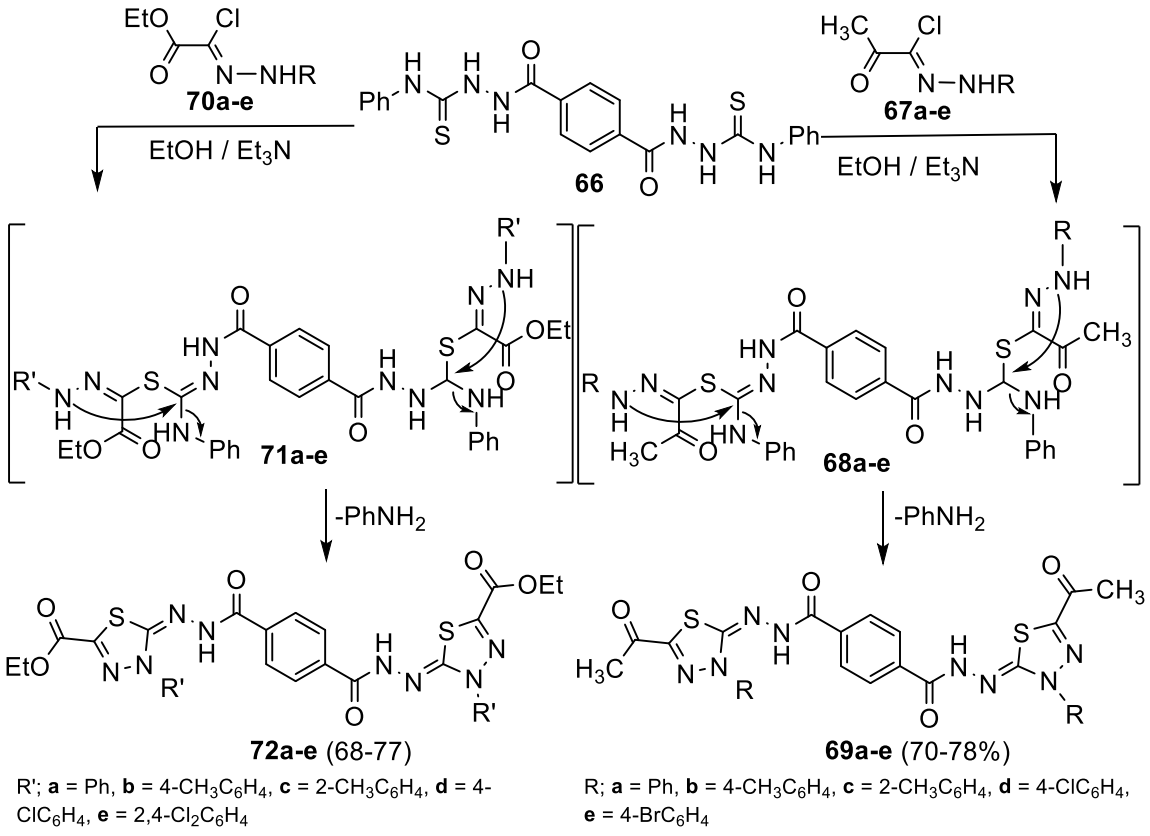

Scheme 15. Synthesis of different substituted bisthiadiazoles **69a-e** and **72a-e**.

ZUBRIENĖ *et al.* reported the syntheses of triazolthione **75** and triazolone **77** derivatives. A condensation reaction of carbothioamide **74** leads to the formation of 3-chloro-4-(2-oxo-4-(4-phenyl-5-thioxo-4,5-dihydro-1*H*-1,2,4-triazol-3-yl)pyrrolidin-1-yl)benzenesulfonamide **75**. Heating carboxamide **73** in alkaline medium followed by acidification with hydrochloric acid to pH=5, affords 4-((2-chloro-4-sulfamoylphenyl)amino)-3-(5-oxo-4-phenyl-4,5-dihydro-1*H*-1,2,4-triazol-3-yl)-butanoic acid **76**, which undergoes a rearrangement reaction in acidic medium to form the pyrrolidin-2-one ring to form triazolone **77** (Scheme 16).[43]

SX. G. KÜÇÜKGÜZEL *et al.* reported the synthesis of the three different bioactive *N*-containing five-membered rings **79**, **80,** and **81** *via* cyclization reactions of 1-(2',4'-difluoro-4-hydroxybiphenyl-3-carbonyl)-4-alkyl/arylthiosemicarbazides **78a-g** (Scheme 17).[44] By studying the biological activities of the products, it was found that they exhibit antimicrobial, antiviral, and anti-inflammatory activities. Compound **80d** showed antimicrobial activity against *Escherichia coli A1* and *Streptococcus pyogenes ATCC-176* at a concentration of 31.25 µg/mL, whereas **79b** exhibited activity against *Aspergillus variecolor* and *Trichophyton rubrum* at a concentration of 31.25 and 15.25 µg/mL, respectively. Additionally, compounds **79b**, **79d**, **79e**, **79g**, **80a,** and **80c** exhibited antiviral properties against coxsackievirus B4,

herpes simplex virus-1 TK-KOS, vaccinia virus, and sindbis virus at 16 μg/mL, respectively. The anti-inflammatory activity of **79a-g** was in the range from 36.3% to 73.0%, while for **80a-g** from 41.4% to 57.3% and for **81a-g** from 23.9% to 41.4%.[44]

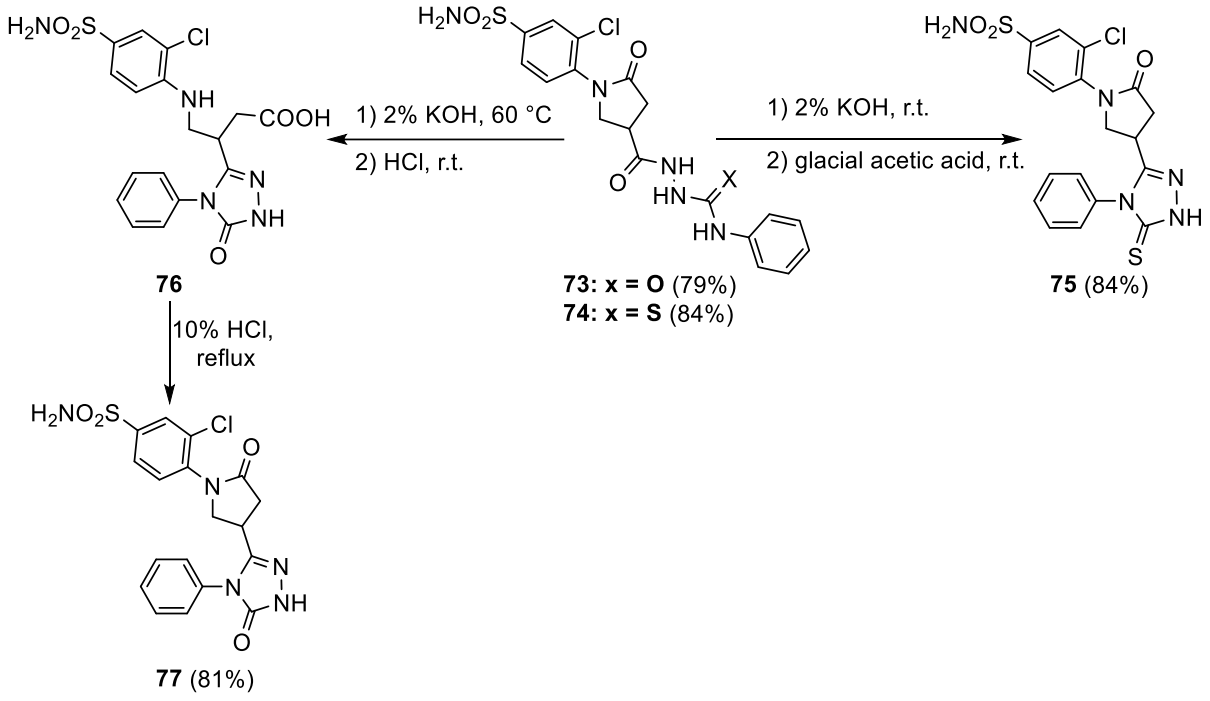

Scheme 16. Synthesis of triazolthione **75** and triazolone **77** derivatives.

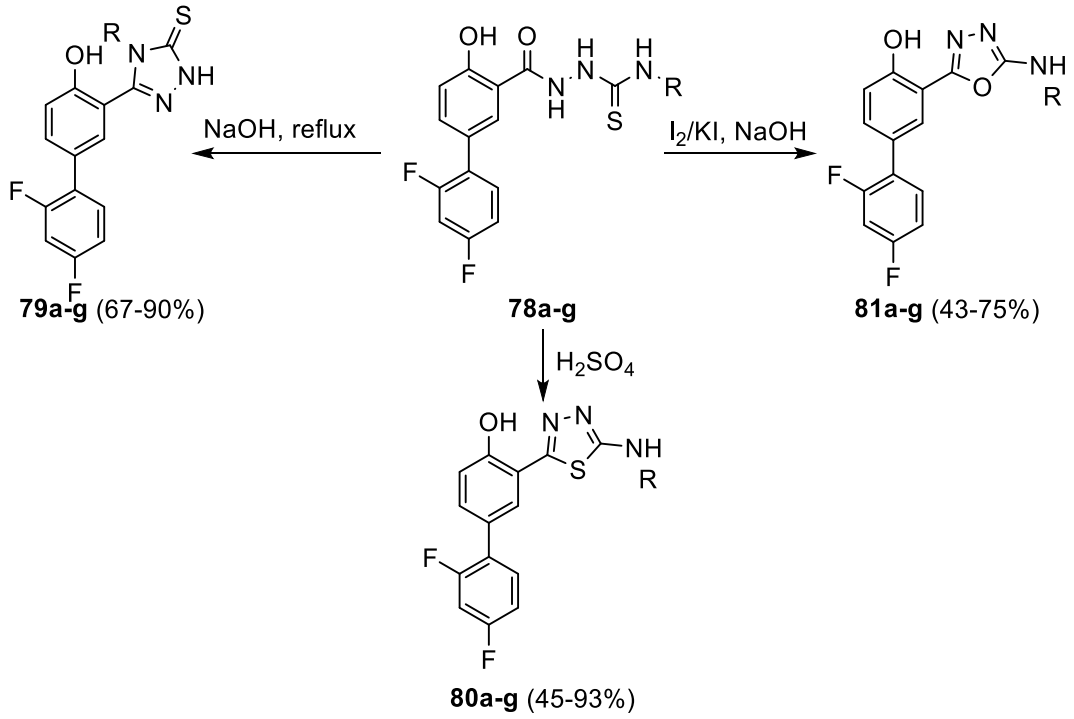

R'; **a** = CH_3, **b** = C_2H_5, **c** = C_3H_4, **d** = C_6H_5, **e** = 4-$CH_3C_6H_4$, **f** = 4-$OCH_3C_6H_4$, **g** = C_6H_{11}

Scheme 17. Synthesis of 1,2,4-triazoline-3-thiones **79a-g**, 1,3,4-thiadiazole **80a-g** and 1,3,4-oxadiazole **81a-g**.

1.2 4-Hydroxy-2-quinolones

Quinoline-2,4-diones **82** are interesting compounds due to their role in natural and synthetic chemistry and also their biological and pharmacological activities.[45-47] The synthetic methodology of these compounds, as well as their utility in the synthesis of fused *N*-containing five-membered ring systems, are discussed here. Quinolin-2,4-dione **82A** displays different tautomeric forms between the carbonyl groups, CH_2-3, and the NH-group of the quinoline moiety (**82A-C**, Figure 6).[48] X-ray structure analysis of numerous structures of that class have shown that 4-hydroxy-2-quinolones (form **82**, Figure 6) are the most frequently observed form.[48-49]

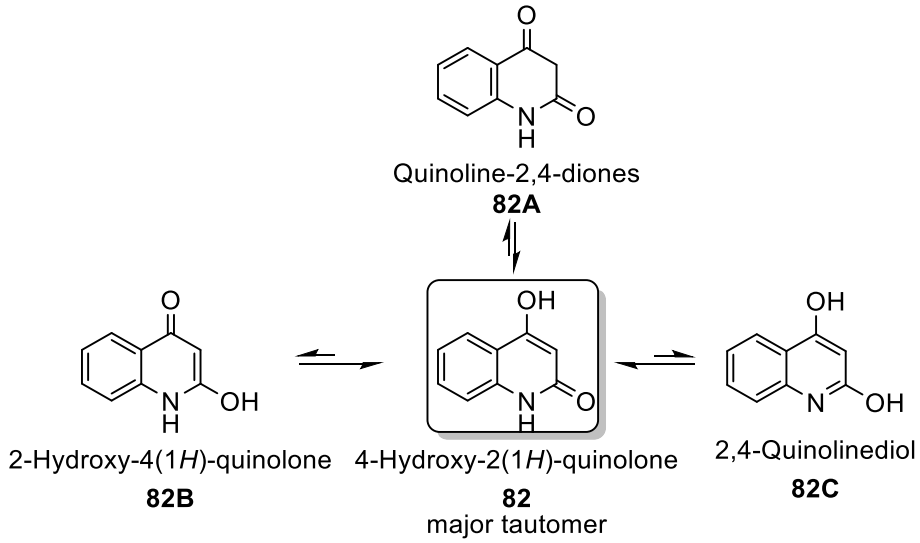

Figure 6: The tautomeric equilibrium of 4-hydroxy-2(1*H*)-quinolinone **82**.

The biological and pharmaceutical importance of quinones is based on their utility as drugs isolated from naturally occurring compounds. 2-Hydroxyquinoline and 4-hydroxyquinoline (4-quinolinol) were isolated from plants and they exist as 2(1*H*)-quinolone and 4(1*H*)-quinolone, respectively.[50]

The first generation of quinolone drugs was developed after observations related to nalidixic acid (**84**, Figure 7), which is a side product found during the synthesis of the antimalarial agent chloroquine.[51] *Ciprofloxacin* (**85**), as an example of a quinolone, shows substantial antimicrobial activity,[52] and Levofloxacin (**86**), an important antibiotic known as a class of fluoroquinolones and still used as a commercially available drug.[53] Figure 8 shows Skimmianine (**87**) and γ-Fagarine (**88**) as two examples of naturally occurring quinolinones which were proved to have anticancer activity.[54] Dictamnine (**89**), Kokusaginine (**90**), and Edulitine (**92**) are also important naturally-occurring compounds (Figure 8).[55]

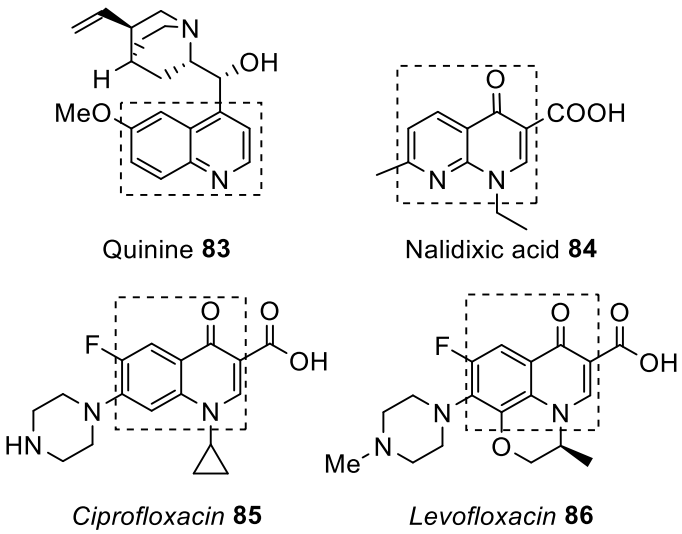

Figure 7: Structures of quinine (**83**), nalidixic acid (**84**), Ciprofloxacin (**85**), and Levofloxacin (**86**).

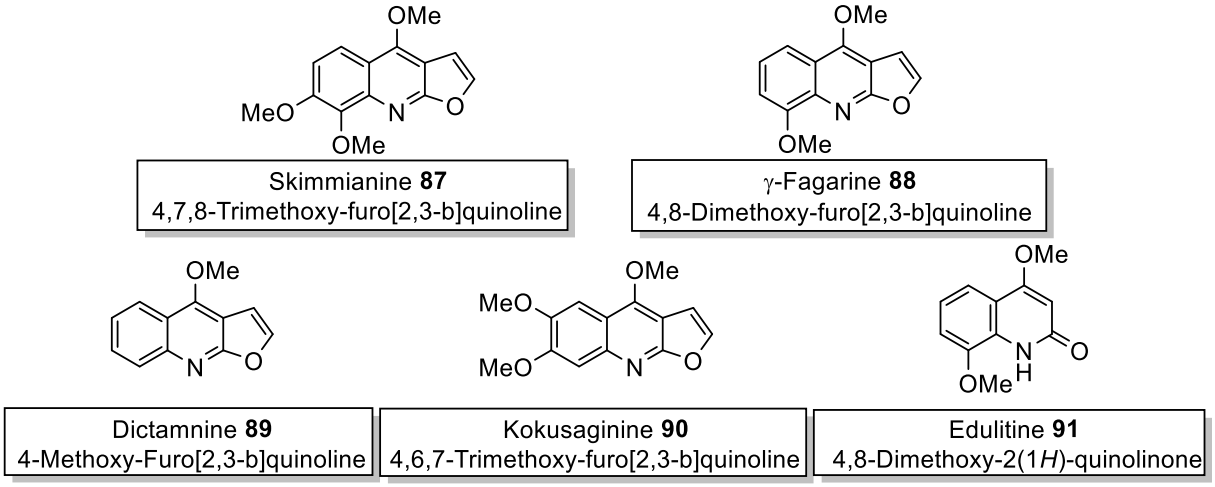

Figure 8: Examples of quinolinones as naturally occurring compounds.

The quinolindione structure is also present in some peptide-like natural products such as pipestelide C (**92**) which was isolated from a marine fungus (Figure 9).[56]

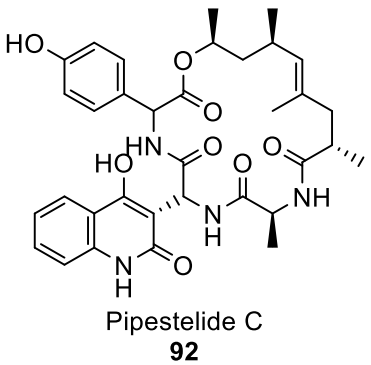

Figure 9: Naturally occurring dihydroxyquinolines: Pipestelide C (**92**).

1.2.1 Synthesis of 4-Hydroxy-2(1*H*)-Quinolones Derivatives

The GOULD-JACOBS synthesis is considered to be one of the oldest and the most popular methods for the preparation of quinolones.[57] It is based on the formation of Michael adducts **96** from heating aniline derivatives **93** with alkoxy methylene malonic ester or acyl malonic ester **94**. The fusion of the condensed products **96** in the alkaline medium gives the corresponding quinolone derivatives **97** (Scheme 18).[58]

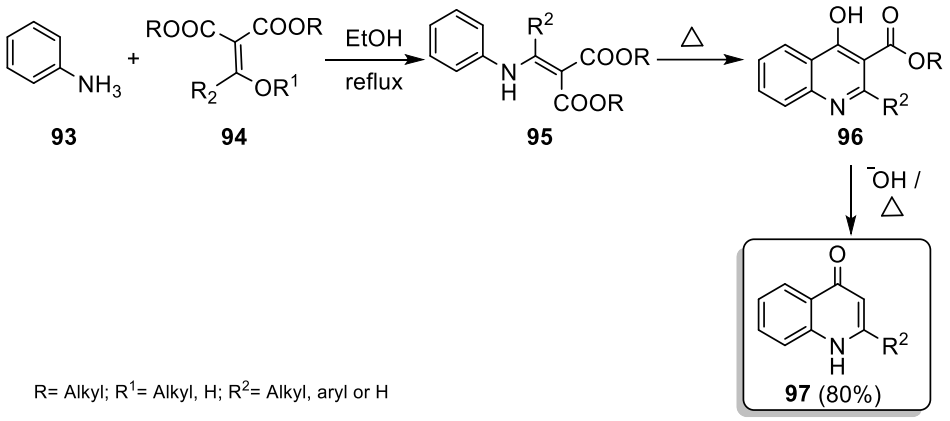

Scheme 18. Gould-Jacobs method for preparation of quinolones.

CHENG *et al.* reported the reaction of aniline (**93**) with excess diethyl malonate (**98**) under microwave irradiation (MW, 320 W) for 10 min to afford *N*,*N*'-diarylmalonamide derivatives **99**, which upon cyclization catalyzed by polyphosphoric acid (PPA) afforded 4-hydroxy-2-quinolone (**82**) (Scheme 19).[59]

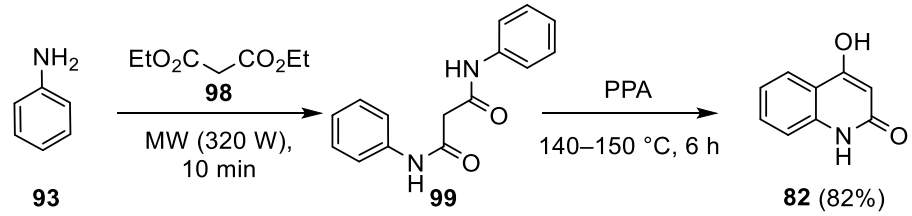

Scheme 19. The microwave-assisted reaction of anilines with diethyl malonate.

Reduction of ethyl 3-(2-nitrophenyl)-3-oxopropanoate (**100**) with hydrazine hydrate in the presence of Pd/C as catalyst followed by intramolecular cyclization leads to the formation of 4-hydroxy-1*H*-quinolin-2-one (**82**) in 87% yield (Scheme 20).[60]

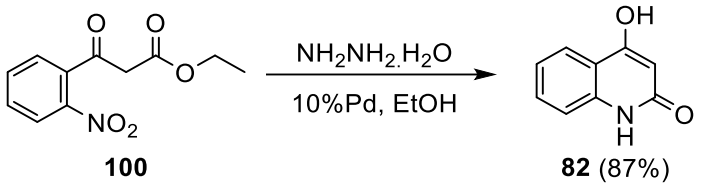

Scheme 20. Synthesis of 4-hydroxy-2-quinolone by Pd-catalyzed reduction.

1.2.2 4-Hydroxy-2(1*H*)-quinolones in Syntheses of Five-membered Heterocycles

Synthesis of Fused Pyrrole Derivatives

The WITTIG reaction of 3-aminoquinoline-2,4(1*H*,3*H*)-diones **101a-j** with ethyl-2-(*tri*-phosphinylylidene)acetate (**102**) were conducted in boiling xylene to afford fused pyrrolo[2,3-*c*]quinoline-2,4-diones **106a-j** (Scheme 21).[61] The reaction proceeds *via a* Michael addition forming compound **103**, followed by cyclization, accompanied by the elimination of EtOH, to obtain compound **104**. After the rearrangement of intermediates **104** to **105**, **106** was formed by the elimination of triphenylphosphine oxide ($OPPh_3$) (Scheme 21).[61]

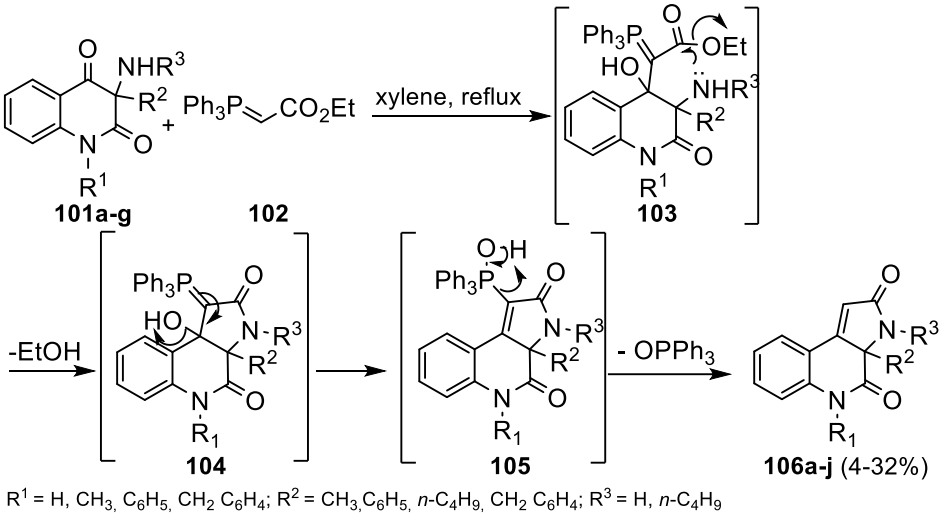

Scheme 21. Synthesis of pyrrolo[2,3-c]quinoline-2,4-diones **106a-j**.

Alternatively, heating equimolar amounts of 4-hydroxy-1-methylquinolin-2(1*H*)-one (**107**) and phenylhydrazine hydrochloride (**108**) in the presence of *p*-toluenesulfonic acid (*p*-TSA) gave 5-methyl-indolo[3,2-*c*]quinolin-6-one (**109**) (Scheme 22).[62]

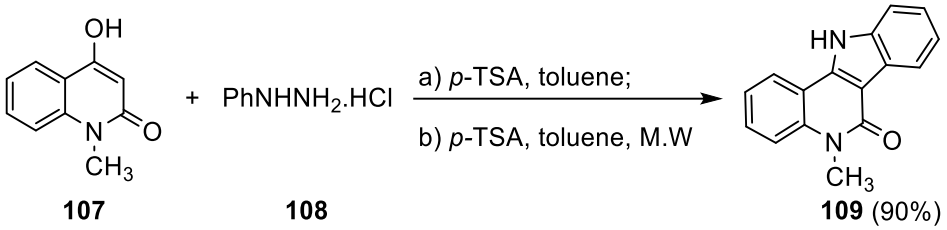

Scheme 22. Synthesis of fused quinolin-2-ones **109**.

Synthesis of Fused Oxazole and Thiazole Derivatives

STEINSCHIFTER *et al.* reported the formation of 2-styryl-5*H*-1,3-oxazolo[4,5-*c*]quinolin-4-ones derivatives **111a-e** by refluxing 4-hydroxy-3-(3-phenylacryloyl)-1*H*-quinolin-2-ones **110a-e** and hydroxylamine hydrochloride in pyridine (Scheme 23). The incorporation of the nitrogen atom can be explained by a Beckmann rearrangement of the intermediate oxime.[63] KATAGI *et al.* synthesized 1,2-oxazoloquinolones **112a-f** under different conditions by the reaction of **110a-f** with hydroxylamine hydrochloride in glacial acetic acid under reflux (Scheme 23).[64]

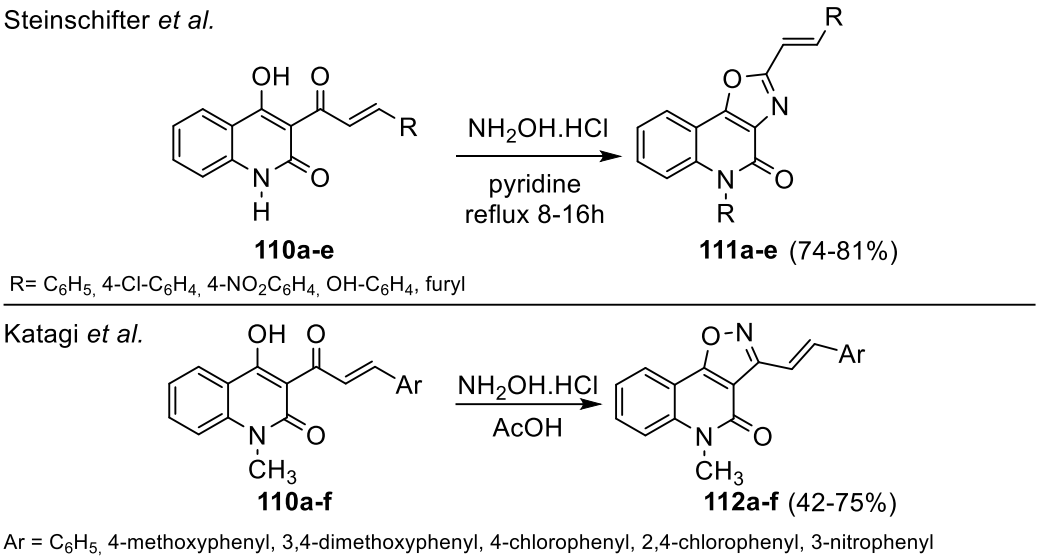

Scheme 23. Synthesis of 1,3-oxazolo[4,5-c]quinolin-4-ones **111a-e** and 3-(isoxazol-3-yl)-quinolinones **112a-f**.

Oxazoles that are fused between N^1-quinoline and C-2 can also be obtained by bromination of 1-allyl-4-hydroxy-*N*-isopropyl-2-oxo-1,2-dihydroquinoline-3-carboxamide (**113**) to give the corresponding bromo derivative **114** as shown in Scheme 24.[65]

Reactions of 3-thiocyanat-1*H*-quinoline-2,4-dione derivatives **115a-e** with sulfuric acid can afford 3a*H*,5*H*-thiazolo[5,4-*c*]quinoline-2,4-dione derivatives **116a-e** in good yield. In the presence of cyclohexylbenzene, these compounds can undergo thermal rearrangements, which afford the thiazoles **119a-e**. The initial ring-opening of the quinolinone skeleton gives the

isocyanate intermediate **117** which then tautomerizes to compound **118** to afford the corresponding quinazolinone **119a-e** *via* ring closure (Scheme 25).[66]

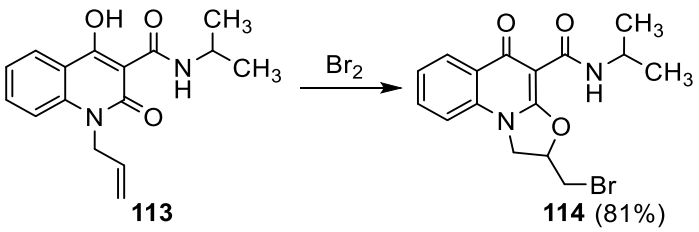

Scheme 24. Synthesis of oxazolo[3,2-*a*]quinoline-4-carboxamide **114**.

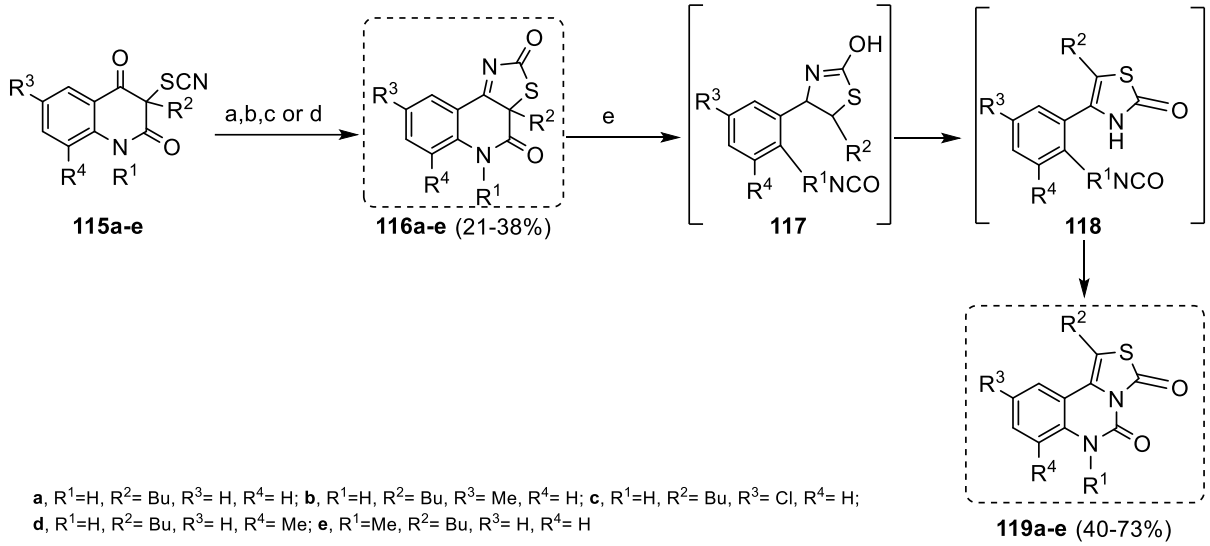

Scheme 25. Synthesis of thiazolo[5,4-c]quinoline-2,4-diones **119a-e**. a) sulfuric acid; b) mixture of conc. sulfuric acid and HOAc (9:l, v/v); c) mixture of conc. sulfuric acid and HOAc (9:l,v/v) and P_2O_5 (0.6 g/mmol). d) sulfuric acid and $AlCl_3$. e) cyclohexylbenzene.

Synthesis of Fused Pyrazole and 1,2,3-Triazoloquinolone Derivatives

To synthesize pyrazolo[4,3-*c*]quinoline-4-ones **124a-i**, first *N*-substituted 3-acetyl-4-hydroxyquinolones **121** are obtained by acetylation of 4-hydroxyquinolones **120** with acetyl chloride using pyridine as a base. Then, the acetyl compounds **121** are reacted with an excess of the appropriate arylhydrazines **122** by refluxing in 1-butanol to give the corresponding 3-acetylquinolone arylhydrazones **123a-i**. 1,3-Diphenyl-1,5-dihydropyrazolo-[4,3-*c*]-quinoline-4-ones (**124a-i**) were obtained upon boiling 3-acetylquinolone arylhydrazones **123a-i** in H_2SO_4/AcOH (Scheme 26).[67]

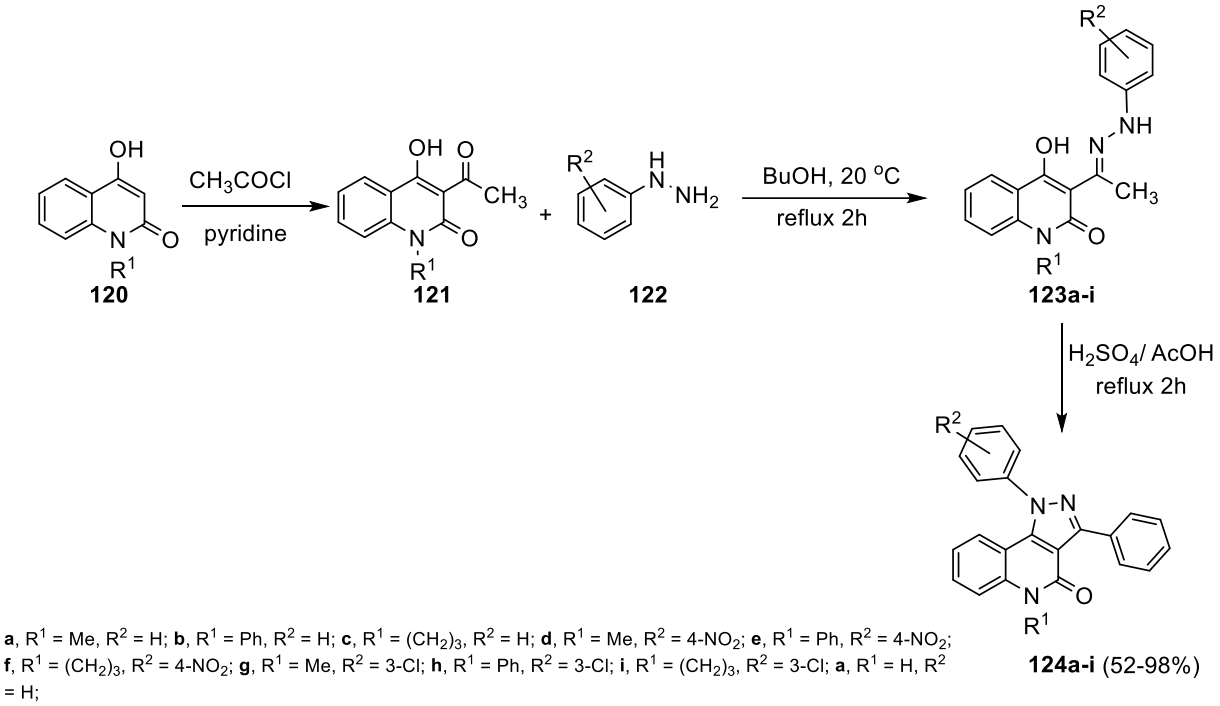

Scheme 26. Synthesis of pyrazolo[4,3-c]quinolin-4-ones **124a-i**.

ALY *et al.* synthesized a class of 1,2,3-triazoles derived from 2-quinolone **127a-d** *via* Cu-catalyzed [3+2]-cycloadditions of 4-azidoquinolin-2(1*H*)-ones **125a-d** with some ethyl propiolate **126** (Scheme 27). The mechanism of the formation of the target product is based on the nucleophilic addition of the acetylenic anion **128** to the formed azido-salt of **125** to form intermediate **129**. Rearrangement of **129** forms the anion **130**, which upon proton transfer gives **127** (Scheme 27).[68]

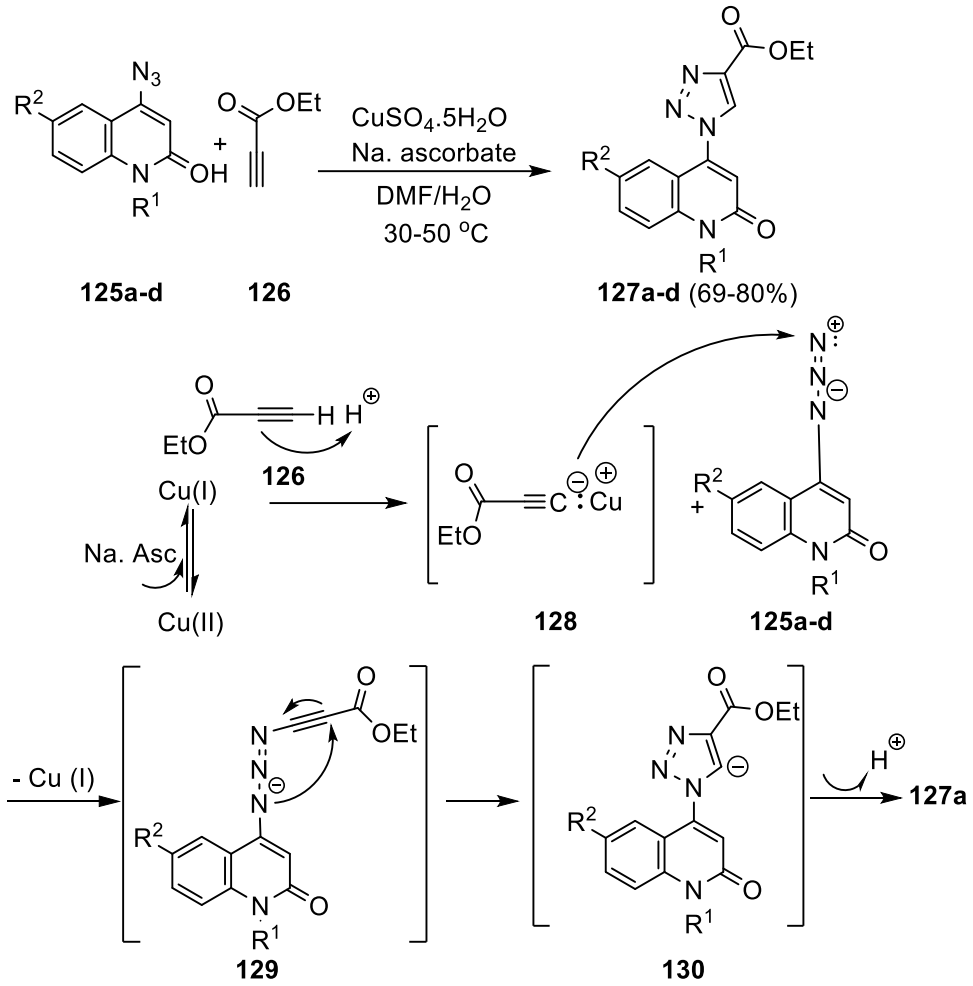

125,127: **a**, $R^1 = R^2 = H$; **b**, $R^1 = H$, $R^2 = Me$; **c**, $R^1 = H$, $R^2 = OMe$; **d**, $R^1 = Me$, $R^2 = H$

Scheme 27. Reaction of 4-azidoquinolin-2(1*H*)-ones **125a-d** with ethyl propiolate (**126**).

1.3 [2.2]Paracyclophane

1.3.1 Structure of [2.2]Paracyclophane

Cyclophanes are interesting molecules that have been studied extensively. In the preparation of poly(*p*-xylylene) from *p*-xylene, BROWN and FARTHING first isolated [2.2]paracyclophane (**131**).[69] [2.2]Paracyclophanes are strained molecules with strain energies of ca. 31 kcal mol^{-1}.[70] UV spectra of [2.2]paracyclophane (**131**) show strong cofacial π-orbital overlap of its two benzene rings, and its X-ray structure showed the benzyl-benzyl bonds are stretched with the bent and distorted benzene rings separated by a distance 2.78Å, as shown in Figure 10.[71] The distance between non-bridged carbon atoms on both benzene rings is approximately 3.09 Å and the angle between the upper benzene planes and the ethyl bridging bonds is 12.6°.[72-73]

[2.2]Paracyclophane (**131**) is considered to have a conjugated π-system of two benzene rings even though there are non-conjugated ethyl bridges. Electron density distribution studies and potential energy density distribution studies showed that there is a repulsive interaction between the two rings caused by the ethylene bridges. It was also mentioned that the transannular interaction is not optimal due to the ethylene bridges and distortions of the benzene rings into a boat conformation.[74] The orbital overlap of the two benzene rings in [2.2]paracyclophane (**131**) shows strong interactions that can be analyzed.[75]

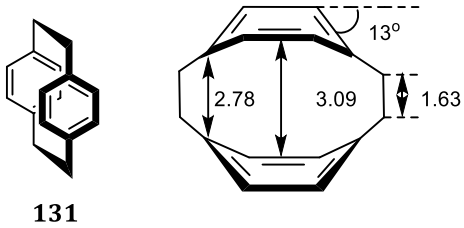

131

Figure 10: Structural parameters of [2.2]paracyclophane (**131**).

The nomenclature of these molecules following IUPAC rules is rather difficult. Thus, a new nomenclature system was invoked. According to VÖGTLE *et al.*, the term "phane" describes a structure that contains at least one aromatic or phenyl ring bridged by an alkane.[76] If the aromatic ring includes a benzene derivative, the class of cyclophanes is described. Hence, [2.2]paracyclophane (**131**) consists of two benzene rings bridged at para position *via* two ethanyl groups, CRAM and STEINBERG suggested the name for this molecule as 'paracyclophane' as the two benzene rings are connected through the para positions on the benzene rings (Figure 11).[77]

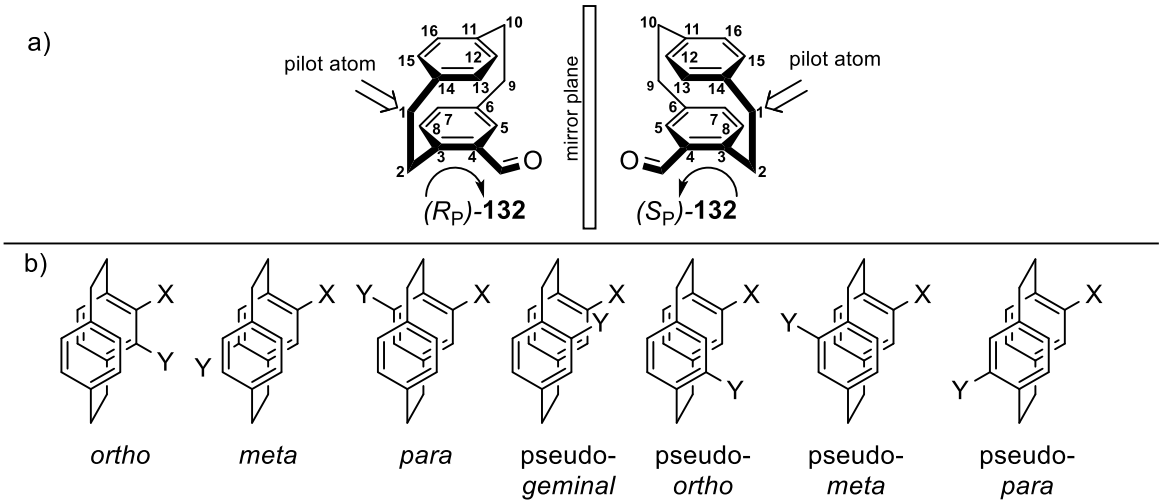

Figure 11: a) Nomenclature and chirality descriptors exemplified by 4-formyl[2.2]paracyclophane (**132**). b) Available aromatic substitution pattern of disubstituted [2.2]paracyclophane (**131**) with relative nomenclature.

The numbers in the brackets denote the number of carbon atoms bridging the benzene rings. Finally, in a disubstituted [2.2]paracyclophane, when both substituents are attached to different decks of [2.2]paracyclophane, *pseudo-* is used as a prefix and is followed by, *ortho, para, meta,* and *gem,* depending on where the other substituent is attached on the other deck. These four isomers, *pseudo-ortho, pseudo-para*, *pseudo-meta,* and *pseudo-gem* are shown in Figure 11.[76]

1.3.2 Heterocyclic [2.2]Paracyclophanes

Heterocyclic compounds based on the [2.2]paracyclophane (**131**) substructure are known since the 1960s, but there has been an increase of interest in the past few years. The motivation for most studies is to create heterocycles having either planar chirality,[78] or the capacity for long-distance electronic communication; [2.2]paracyclophane (**131**) offers both these possibilities. The application of heterocycles based on [2.2]paracyclophane (**131**), can be organized into five structural types (Figure 12): heterocyclic derivatives attached to the paracyclophanyl group (type **I**), heterocycles attached to the bridge (type **II**), heterocycles fused to the ethano bridge (type **III**), fused heterocycles fused to the benzene moiety (type **IV**), heterocycles between the two benzene rings of paracyclophane (type **V**).[79]

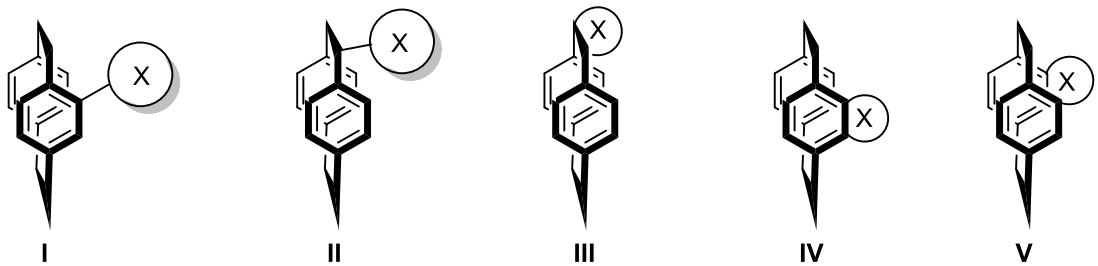

Figure 12: Five types of heterocycle-substituted [2.2]paracyclophanes **131**.

1.3.3 Chirality

Enantiomerically pure, planar chiral [2.2]paracyclophane derivatives can be synthesized on a large scale. To reduce the usage of expensive chiral (semi)preparative HPLC techniques, chiral resolution *via* derivatizing agents has been reported in some cases. Racemic 4-formyl[2.2]paracyclophane (**132**) can be easily enantioenriched by fractional crystallization of the diastereomeric mixture of imines **134** (Scheme 28).[80-82] The diastereomerically pure imine **134** is easily hydrolyzed on silica, yielding (S_P)-**132** in more than 98% *ee*. Although only the (S_P) isomer is isolated when using the amine (*R*)-**133**, it is also possible to obtain the (R_P) isomer, when (*S*)-**133** is used.[81]

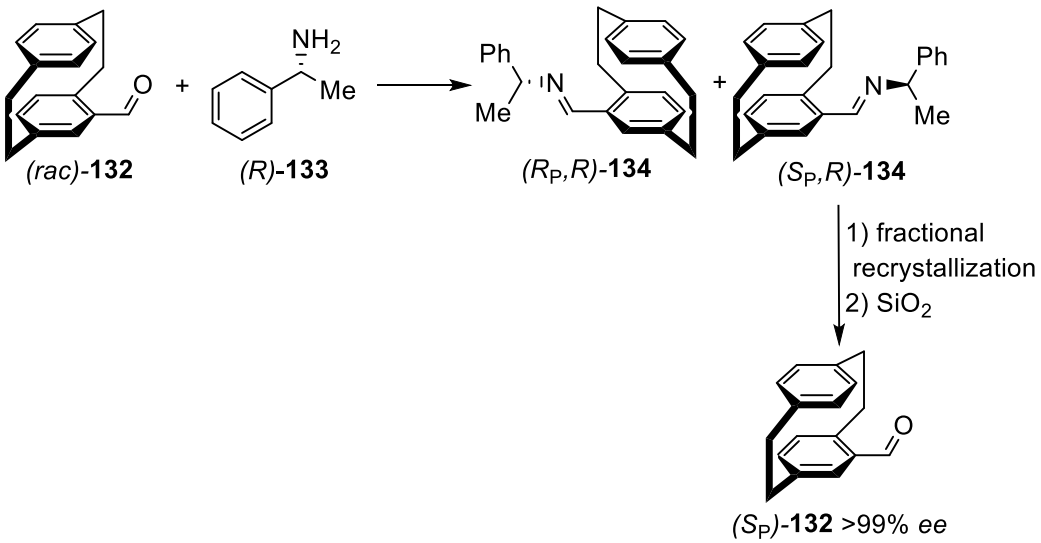

(rac)-**132** *(R)*-**133** *(R_P,R)*-**134** *(S_P,R)*-**134** *(S_P)*-**132** >99% *ee*

Scheme 28. Chiral resolution of 4-formyl[2.2]paracyclophane (**132**).

2. Objective

Since the chemistry of five-membered heterocyclic rings has great attention because of their synthetic challenges as well as biological and pharmaceutical importance.[1] Azoles, which are five-membered heterocyclic compounds that have nitrogen atom and an additional heteroatom (N, S, or O) in the ring,[3] are a very important compound class which has a vast biologically active nature.[9] Coincidently, thiosemicarbazides have a wide range of applications as antibacterial, antifungal, chemotherapeutic, and bioanalytical reagents. They are also ideal candidates for the synthesis of different types of five-membered heterocyclic rings. Additionally, [2.2]paracyclophane and its derivatives have been the subject of particular interest in stereoselective synthesis and their incorporation into more complex molecular frameworks since their discovery, more than six decades ago.[83-85] Most of the unique properties of these cyclophanes are the result of the rigid framework and the short distance between the two aromatic rings within the [2.2]paracyclophane unit. Azole-linked [2.2]paracyclophanes have been used very frequently for catalyst design and other applications.[86-112]

Consequently, this thesis aims to establish synthetic access to [2.2]paracyclophane-based derivatives which are attached to thiosemicarbazides. Moreover, the main goal is to synthesize a new different substituted *N*-containing five-membered heterocycles and investigate the prospective biological and/or optical activity of these compounds (Figure 13).

In the first project, the design and synthesis of thiosemicarbazides derivatives linked to [2.2]paracyclophanes will be established. After that, different classes of five-membered heterocycles were synthesized by applying various types of cyclization reactions. Additionally, donor-acceptor interaction of [2.2]paracyclophanyl-acylthiosemicarbazides (as donors) with different electron-poor molecules (as acceptors) were applied to obtained several novel five-membered heterocycles (Figure 13). Furthermore, the design and synthesis of the homochiral cyclophane molecules were also investigated.

In a second project, the cytotoxic activity of the synthesized compounds towards the NCI-60 panel of cancer cell lines was determined and the cellular mechanism of the most potent inhibitors was investigated. Moreover, docking studies for the most active compound was applied in comparison with a reference chosen suitable compounds.

Finally, the chemistry of 4-hydroxy-2-quinolones in the synthesis of important biologically active molecules was established by investigating a novel series of fused five-membered heterocyclic rings attached to 4-hydroxy-2-quinolones. The target compounds were obtained *via* donor-acceptor interaction between 4-hydroxy-2-quinolones as donors and different types of acceptors.

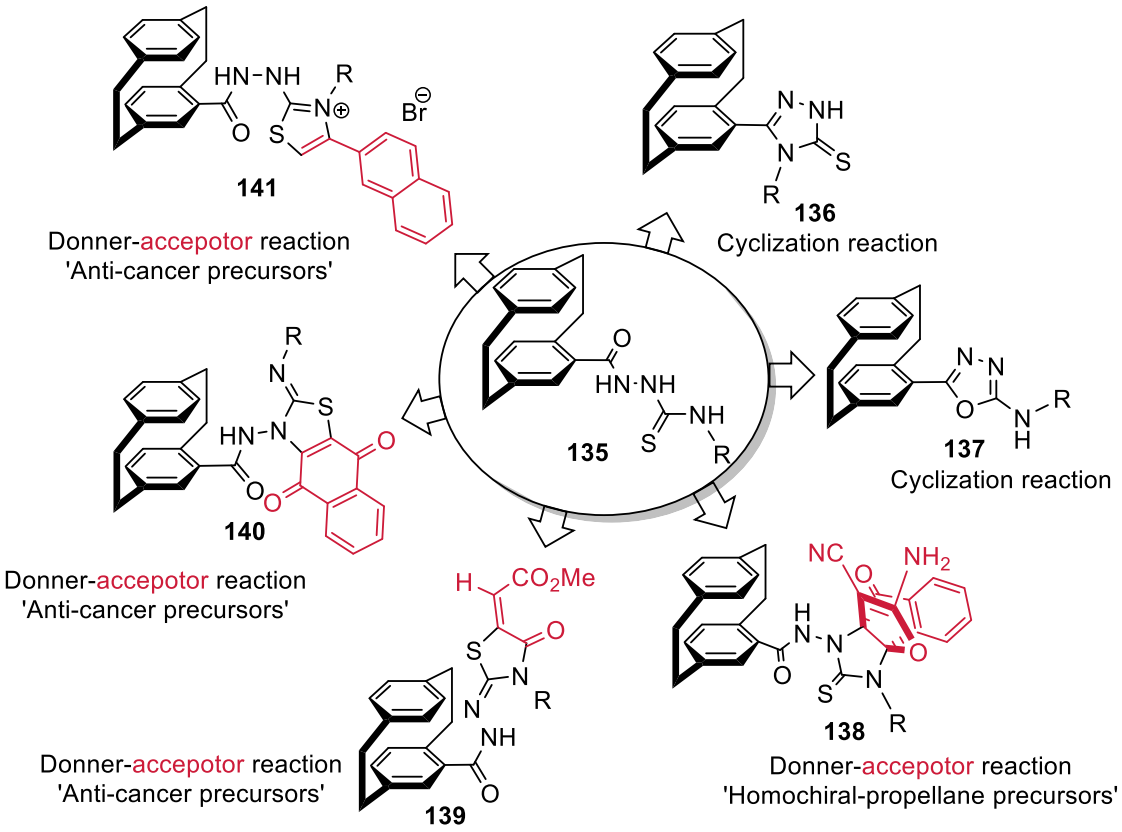

Figure 13: Objectives of this thesis.

3. Results and Discussion

The focus of this work lies on the syntheses and applications of five-membered, nitrogen-containing heterocyclic compounds, and summarizes the results of five different projects in this area. The synthesis of heteroyl-tetrasubstituted thiazoles will be discussed first, whereby new *N*-containing five-membered rings were being obtained in a fast and simple manner. The link between [2.2]paracyclophane and hydrazinecarbothioamides and the synthesis of substituted triazolthiones and oxadiazoles derivatives will be presented in the following chapter. In the third part, the synthesis of homochiral paracyclophane attached to [3.3.3]propellanes will be discussed. In the fourth part, different bio-active substituted thiazole rings attached to [2.2]paracyclophane will be shown. The last part addresses the syntheses of novel fused heterocyclic quinolones.

3.1. Facile Synthesis of Heteroyl-tetrasubstituted Thiazoles[1]

Because of the accessibility and capability of carbothioamides, and their analogs, to act as bifunctional nucleophiles,[113-118] they play an important role among other nitrogen and sulfur-containing compounds. Carbothioamides contain numerous nucleophilic centers and are used as building blocks for the syntheses of various heterocyclic rings.[119-121]

Tetracyanoethylene (TCNE, **143**) is utilized in a wide range of reactions, either as a building block or as a mediator of reactions.[122] The addition of nucleophiles to the TCNE double bond followed by a loss of cyanate fragments has been known to be the most common reaction.[123-125] However, the direct nucleophilic addition to the nitrile moiety may also occur.[126-127] In this work, different heterocyclic compound families including thiadiazoles, thiadiazines, thiadiazepines, and pyrazoles were prepared upon the reaction of TCNE with 2,4-disubstituted thiosemicarbazides.[128] For example the reaction of methyl-2,4-dioxobutanoate with TCNE affords methyl 3-acyl-4-cyano-5-(dicyanomethylene)-2-hydroxy-2,5-dihydro)-1*H*-pyrazole-2-carboxylate.[129] Thiosemicarbazides, which are carbothioamide derivatives, have several nucleophilic centers and are ideal candidates and valuable building blocks for the syntheses of different heterocyclic rings. In previous work, HASSAN *et al.* reported reactions between *N*-substituted-2-phenyl thiosemicarbazides **142a-c** and TCNE **143** that afford mesoionic-1,2,4-triazolium-3-thiolate derivatives **144a-c** in 67-76% yield

[1] Excerpts of this chapter were already published in
A. A. Hassan, A. A. Aly, N. K. Mohamed, L. E. A. El-Haleem, S. Bräse, M. Nieger, *Monatsh. Chem.* **2020**, *151*, 1425–1431.

(Scheme 29).[118] This unique reactivity was studied further in the present investigation. For this purpose, the preparation of electron-deficient analogs of **142a-c** with a lower nucleophilicity, namely *N*-substituted 2-heteroylhydrazinecarbothioamides **145a-f** was conducted. In my master thesis, I have already synthesized various substituted imidazoles,[130] thiazoles,[131] and thiadiazine[132] rings from the reactions of heteroylthiosemicarbazides **145a-f** with different acceptors such as 3-dioxo-2,3-dihydro-1*H*-inden-2-ylidene)propane-dinitrile,[130] dimethyl acetylenedi-carboxylate,[131] and 2,3-dichloro-1,4-naphthoquinone.[132] In the present project, the behavior of heteroylthiosemicarbazides **145a-f** towards TCNE **143** was investigated.

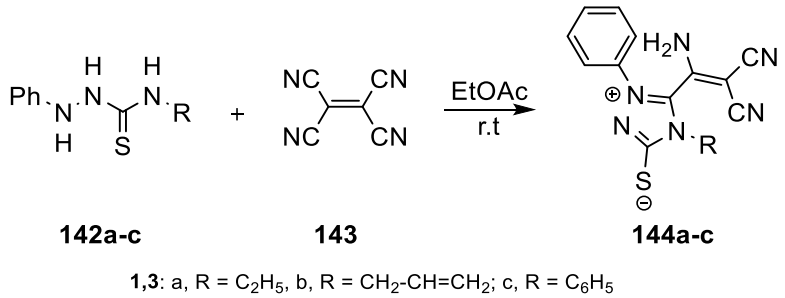

142a-c **143** **144a-c**

1,3: a, R = C_2H_5, b, R = CH_2-CH=CH_2; c, R = C_6H_5

Scheme 29. Reactions of disubstituted thiosemicarbazides **142a-c** with TCNE **143**.

The green color of the transient complex was also observed after adding equimolar amounts of TCNE **143** to a solution of **145a-f** in dry THF in the presence of air at room temperature, which gradually turns to brown, and then to a characteristic yellow color. This observation can be explained by the initial formation of an unstable CT-complex followed by the formation of *N*-(2-substituted imino)-4-amino-5-cyanothiazol-3(2*H*)-3-yl)-heteroyl-2-carboxamides **146a-f**, which were obtained as a yellow to orange crystals in 79-68% yield (Table 2).

The structural properties of **146a-f** were determined based on their spectroscopic properties, elemental analyses, and single-crystal X-ray crystallography. As an example, the molecular structure of **146a** was supported by the following findings: the molecular formula of **146a** ($C_{17}H_{14}N_6OS$) suggests that the product is built up from one molecule of **145a** and one molecule of TCNE (**143**) with the loss of one molecule of malononitrile and the abstraction of two hydrogen atoms from the starting material **145a**, giving rise to the ion m/z 350. The detailed description will be shown in chapter 5.2.1.

Table 2: Reactions of **145a-f** with TCNE **143** and formation of the products **146a-f**, yield of the synthetic products **146a-f** in different solvents.

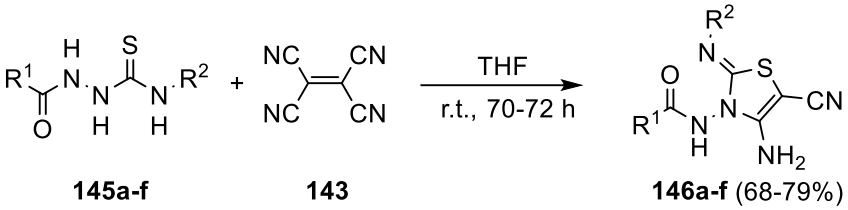

145a-f **143** **146a-f** (68-79%)

Entry	146a-f	R^1	R^2	Yield [%]				
				THF	CH_2Cl_2	benzene	CH_3CN	1,4-dioxane
1	**146a**	Pyridyl	Benzyl	79	36	33	40	56
2	**146b**	Pyridyl	Allyl	71	29	30	38	53
3	**146c**	Furan	Benzyl	74	34	31	39	54
4	**146d**	Furan	Allyl	68	28	27	37	51
5	**146e**	Thiophene	Benzyl	77	34	31	39	54
6	**146f**	Thiophene	Allyl	70	28	27	36	51

The structures of **146a-f** were confirmed by single-crystal X-ray crystallography. *N*-(2-Allyl imino)-4-amino-5-cyanothiazol-3(2*H*)-3-yl)-furan-2-carboxamide (**146d**) was crystallized from ethanol and measured by X-ray analysis in the triclinic space group P-1 (Figure 14).

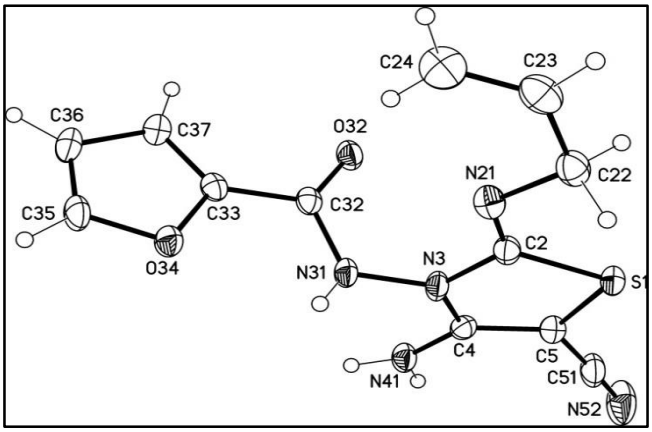

Figure 14: Molecular structure of **146d** (displacement parameters are drawn at 50% probability level).

The C(2)-S(1) and C(5)-S(1) bond lengths of 1.7684(12) Å and 1.7717(13)Å respectively due to C-S σ-bond. The C(2)-N(21) bond length of 1.2605 (17) Å and C(4)-C(5) bond length of 1.3730 (17) Å are close to those of C/C double bonds, the thiazole ring is planar (mean deviation from the thiazole plane 0.017 Å). The same structural features were assumed for

other derivatives based on the similarities in the corresponding NMR spectra (see chapter 5.2.1).

With the optimized reaction conditions in hand, increasing the amount of the starting material **145a-f** was not necessary to obtain the products **146a-f** in high yield. Tetra-substituted thiazole derivatives **146a-f** were produced by the addition of one equivalent of TCNE **143**. The use of various solvents such as methylene chloride, benzene, acetonitrile, and 1,4-dioxane has been studied, however, THF proved to be most suitable. Hight amounts of the products were obtained under standard ambient conditions, whereas the same reactions under inert atmosphere yielded only traces of the products. The mechanistic rationale for the formation of tetra-substituted thiazoles **146a-f** is given in Scheme 30.

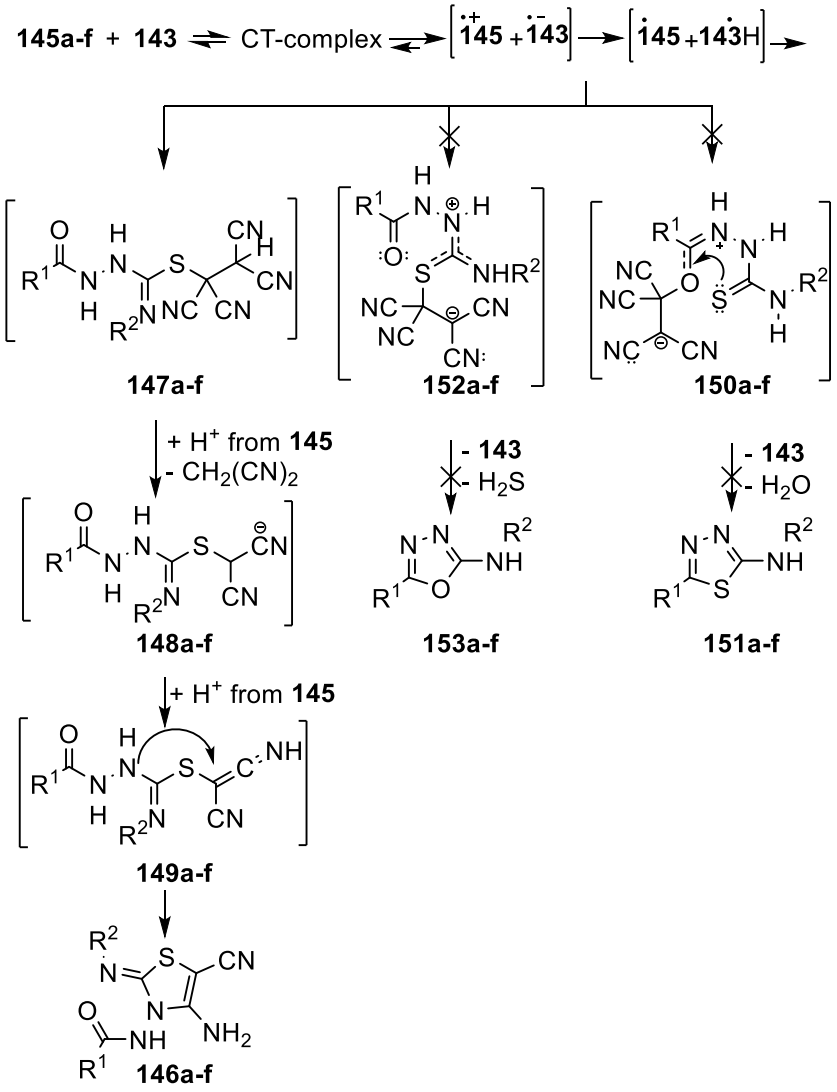

Scheme 30. Mechanistic rationale for the formation of compounds **146a-f**.

Charge transfer complexes may (but not necessarily have to) play an intermediate role. There are two suggested routes for the formation of the radicals **145**• and **143**•H. The first one is the

combination of the two radicals, which affords the intermediate **147a-f**. Elimination of one molecule of $CH_2(CN)_2$ followed by the abstraction of another hydrogen atom from **145** gives the intermediate **148a-f** which abstracts another proton of **145** to give the imine **149**. This is followed by cyclization of the imine **149** by an intramolecular nucleophilic attack of the hydrazide NH on the imine C=NH yielding the tetra-substituted thiazoles **146a-f**.

In the second route, the cyclization involves an intramolecular nucleophilic attack on either a thiocarbonyl or carbonyl group (Scheme 30). Since the previously mentioned reactions do not occur when adding **143** to **145a-f**, it can be concluded that TCNE (**143**) acts as a building block and not as a mediator in this reaction.

Overall, novel heteroyl-tetrasubstituted thiazole derivatives **146a-f** containing aliphatic and aromatic substituents were obtained *via* cyclization reactions of *N*-substituted 2-heteroylhydrazine-carbothioamides **145a-f** by reaction with TCNE (**143**). Heteroyl-hydrazinecarbothioamides are multi-dentate nucleophiles allowing for various modes of heterocyclization with TCNE and providing several electrophilic sites. These results encouraged investigations of a new series of hydrazinecarbothioamides which are presented in the following sections.

3.2. Insertion of [2.2]Paracyclophane into Hydrazinecarbothioamides

[2.2]Paracyclophanes are an intriguing class of compounds that have attracted growing attention since their first appearance in literature in 1949.[133] The cyclophane chemistry is a promising field, which describes the use of cyclophanes in stereoselective synthesis and their incorporation into more complex molecular frameworks, such as heterocycles and polymers.[69, 77, 84-85, 134-136] Much attention is focused on developing new methods for the synthesis of functionalized [2.2]paracyclophanes as precursors for polycyclic hydrocarbons, chiral templates, or auxiliaries.[133] [2.2]Paracyclophanes attached to *N*-heterocycles which possess an sp^2-nitrogen in *ortho*-position are of particular interest.[137] ALY *et al.* reported reactions of monosubstituted [2.2]paracyclophane derivatives and investigate its intriguing behavior.[138-142] Recently, they reported the synthesis of 4-acetyl[2.2]paracyclophanylidene thiosemicarbazone **155** from the reaction between 4-acetyl[2.2]paracyclophane **154** and thiosemicarbazide **27** (Scheme 31).[138]

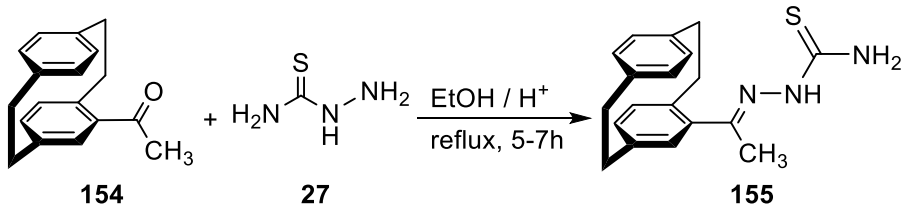

Scheme 31. Synthesis of paracyclophane thiosemicarbazone derivatives **155**.

The main goal for this project was to investigate a new route for the attachment of [2.2]paracyclophane **131** to hydrazinecarbothioamides derivatives and synthesize *N*-containing five-membered heterocycles with various substituents.

3.2.1. Synthesis of (4-[2.2]Paracyclophanyl)hydrazide[2]

Compounds comprising a −NH–NH–C=O moiety are known as hydrazide linkers. In particular, hydrazide-based compounds have shown antioxidant activity.[143-144] Hydrazides and carbohydrazides have been described as useful building blocks for the assembly of various heterocyclic rings.[145] A large number of aliphatic, acyclic, aromatic, and heterocyclic carbohydrazides,[146-149] of which their derivatives and related compounds are reported, present

[2] Excerpts of this chapter were already published in
A. A. Aly, S. Bräse, A. A. Hassan, N. K. Mohamed, L. E. A. El-Haleem, M. Nieger, *Molecules* **2020**, *25(15)*, 3315.

a wide range of biological activities.[150-151] Herein, the aim was to prepare [2.2]paracyclophane molecules linked by the carbohydrazide group. The strategy of preparing compound **159** starting from the commercially available hydrocarbon **131**. Compound **131** was first converted into the acid chloride **157**[152] by the procedure described in Scheme 32, which consisted first of the conversion of **131** into **156** with oxalyl chloride/aluminum trichloride. Heating **156**, leads to giving **157**. The resulting acid chloride **157** was then subjected to esterification using ethanol to produce compound **158** (Scheme 32).[152] Finally, the ester **158** was reacted with hydrazine hydrate yielded the corresponding racemic-carbohydrazide **159** with 80% yield. NMR and mass spectra support the proposed structure of the newly prepared compound **159** (see chapter 5.2.2.1). The results of an X-ray structure analysis shown in Figure 15 were also used to elucidate the structural features of compound **159**.

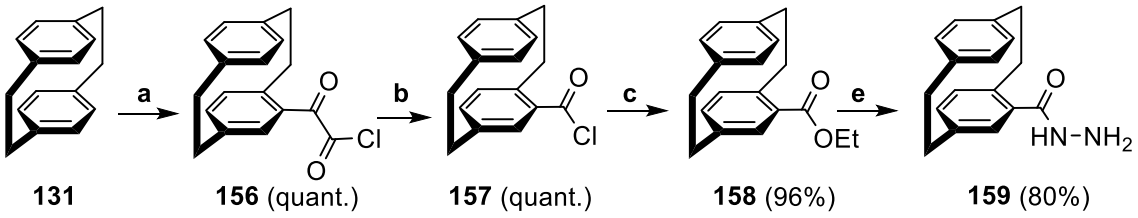

Scheme 32. Strategy of preparing the (4'-[2.2]paracyclophanyl)hydrazide **159**. Reagents and conditions: a) $(COCl)_2/AlCl_3$, -10 °C to 5 °C, 20 min;[152] b) PhCl, Δ, 40 h;[152] c) EtOH, reflux 24 h;[152] d) NH_2NH_2 as a solvent, Δ, 14 h.

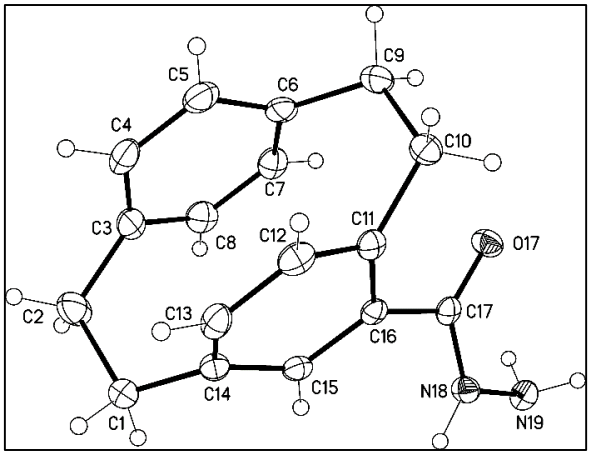

Figure 15: Molecular structure of compound **159** identified according to IUPAC nomenclature as 1,4(1,4)-dibenzenacyclohexaphane-1^2-carbohydrazide.

It was also reported that when two equivalents of 4-acetyl[2.2]paracyclophane (**154**) are reacted with one equivalent of thiocarbohydrazide **160**, bis-4-acetyl-[2.2]paracyclophanylidene-hydrazine-1-carbothiohydrazone (**161**) is formed in 88% yield (Scheme 33).[138]

This previous work gave the idea for the synthesis of compound 2-(4-[2.2]paracyclophanoyl-*N*-4-([2.2]paracyclophanylhydrazine carboxamide (**164**) and attempts to cyclize it (Scheme 35). First, [2.2]paracyclophane isocyanate (**163**) was prepared according to

a literature known procedure by converting the acid chloride **157** into **163** *via* the corresponding carbonylazide **162** in 95% yield (Scheme 34).[153] Heating of **162** under argon atmosphere and in toluene afforded the target molecule **163** in a 70% yield (Scheme 34).[153]

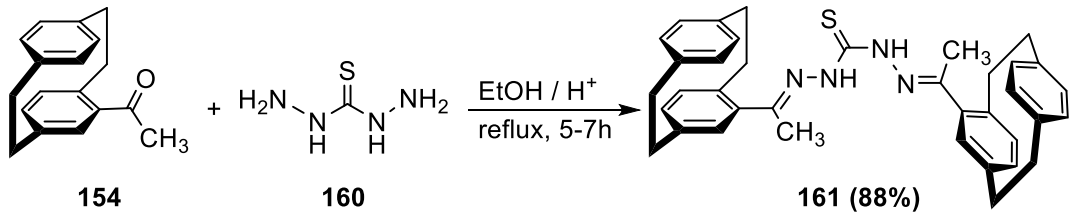

Scheme 33. Synthesis of bis-4-acetyl-[2.2]paracyclophanylidene-hydrazine-1-carbothiohydrazone (**161**).

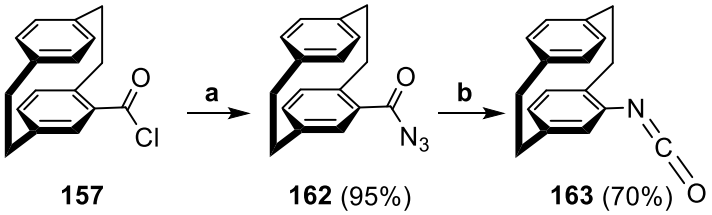

Scheme 34. Strategy of preparing (*rac*)-4-isocyanato[2.2]paracyclophane (**163**). Reagents and conditions: a) NaN_3, acetone/water, r.t., 2 h;[153] b) toluene, 80 °C, 1 h.[153]

Furthermore, refluxing of (4'-[2.2]paracyclophanyl)hydrazide (**159**) with 4-([2.2]paracyclophanyl)isothiocyanate (**163**) (Scheme 35) in ethanol/DMF afforded compound **164** in 70% yield. In the following experiment, boiling **164** in sodium hydroxide to obtain the cyclized compound 5-(4-[2.2]paracyclophane)-*N*-([2.2]paracyclophane)-1,3,4-oxadazol-2-amine (**165**) was not successful (Scheme 35).

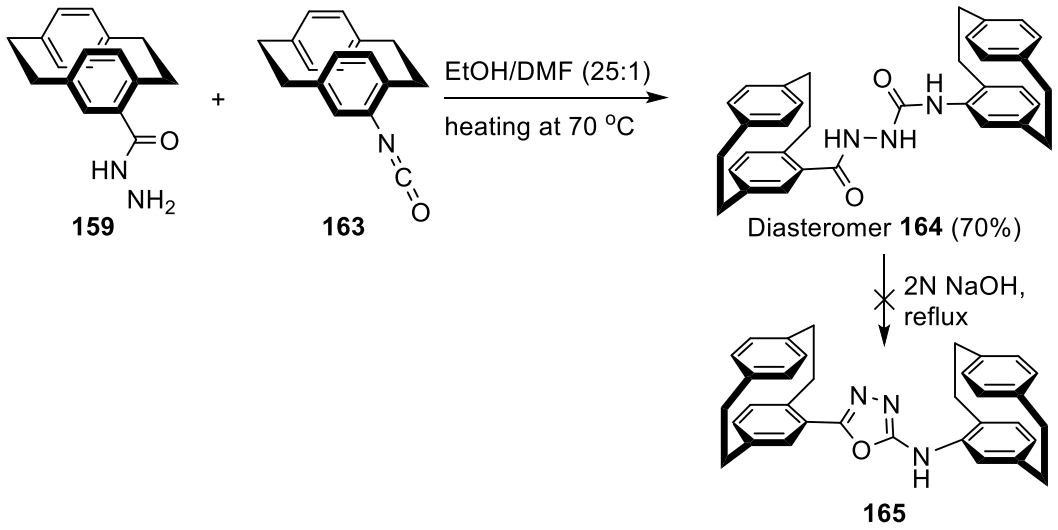

Scheme 35. Synthesis of the diastereomeric *N*-([2.2]paracyclophanylcarbamoyl)-4-([2.2]paracyclophanylcarboxamide (**164**).

3.2.2. Synthesis of Enantiopure *N*-([2.2]Paracyclophanylcarbamoyl)-4-([2.2]paracyclophanylcarboxamide)

Planar chiral [2.2]paracyclophane derivatives have received interest due to their stability towards light, oxidation, acids, and bases.[154-155] BRÄSE *et al.* reported a synthesis of chiral mono-substituted [2.2]paracyclophanes which can yield high enantioselectivities for chiral ligands.[156-160] In general, the planar chirality present in [2.2]paracyclophane derivatives was defined using R_p and S_p.[161] Because of the importance of chirality in the [2.2]paracyclophane moiety, a synthesis of the homochiral analog of the diastereomer **164** was investigated (Figure 16).

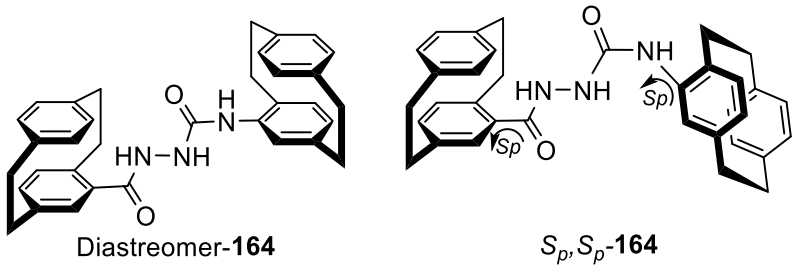

Figure 16: The structure of the diastereomeric and homochiral *N*-([2.2]paracyclophanylcarbamoyl)-4-([2.2]paracyclophanylcarboxamide (**164**).

To prepare the homochiral *N*-([2.2]paracyclophanylcarbamoyl)-4-([2.2]paracyclophanyl-carboxamide (**164**), the preparation of an enantiomerically pure formyl[2.2]paracyclophane (**132**) was performed first, as a convenient procedure for the enantiopure separation by chiral resolution was reported in the literature (Scheme 28, see chapter 1.3.3).[82] The *ee* ratio of (S_p,*S*)/(R_p/*R*) pair of enantiomers was measured by chiral HPLC. It was found that (S_p)-aldehyde **132** has 57.9% *ee* as shown in Figure 17.

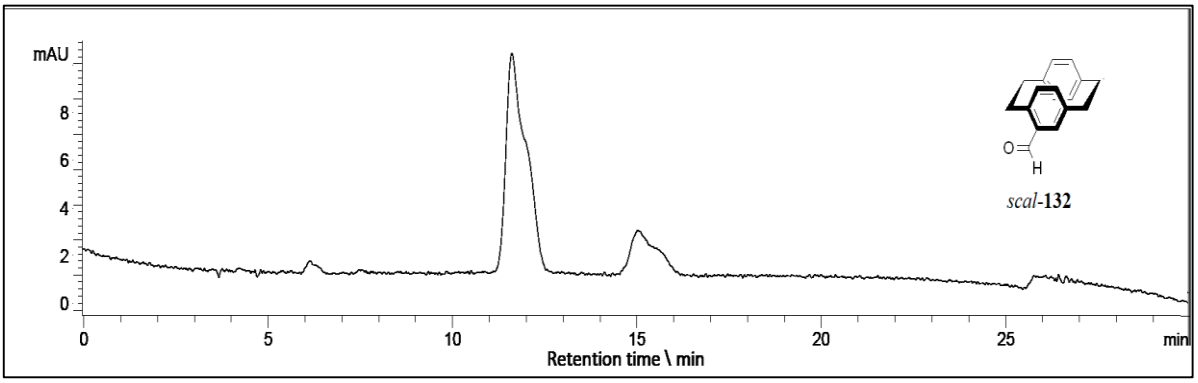

Figure 17: Analytical HPLC of 4-formyl[2.2]paracyclophane *scal*-**132**.

In the next reaction step, scalemic 4-formyl[2.2]paracyclophane *scal*-**132**[82] (57.9% ee, Figure 17) was oxidized to the corresponding acid *scal*-**166**.[162] Afterward, the reaction with thionyl chloride *scal*-**168** gave compound *scal*-**157** (Scheme 36),[153] and then the resulting acid chloride *scal*-**157** was quenched with ethanol to afford the ester *scal*-**158**.[152] Heating *scal*-**158** in excess of hydrazine hydrate gave the carbohydrazide *scal*-**159** (Scheme 36). Subsequently, isocyanate *scal*-**163** was prepared by repeating the previous steps in Scheme 34. Finally, compound *scal*-**164** was obtained *via* the reaction of carbohydrazide [2.2]paracyclophane *scal*-**159** and [2.2]paracyclophane isocyanate *scal*-**163**. By applying chiral HPLC separation on *scal*-**164**, the desired pure chiral (S_p,S_p)-*N*-([2.2]paracyclophanylcarbamoyl)-4-([2.2]paracyclophanyl-amide (S_p,S_p-**164**) was obtained (Figure 18).

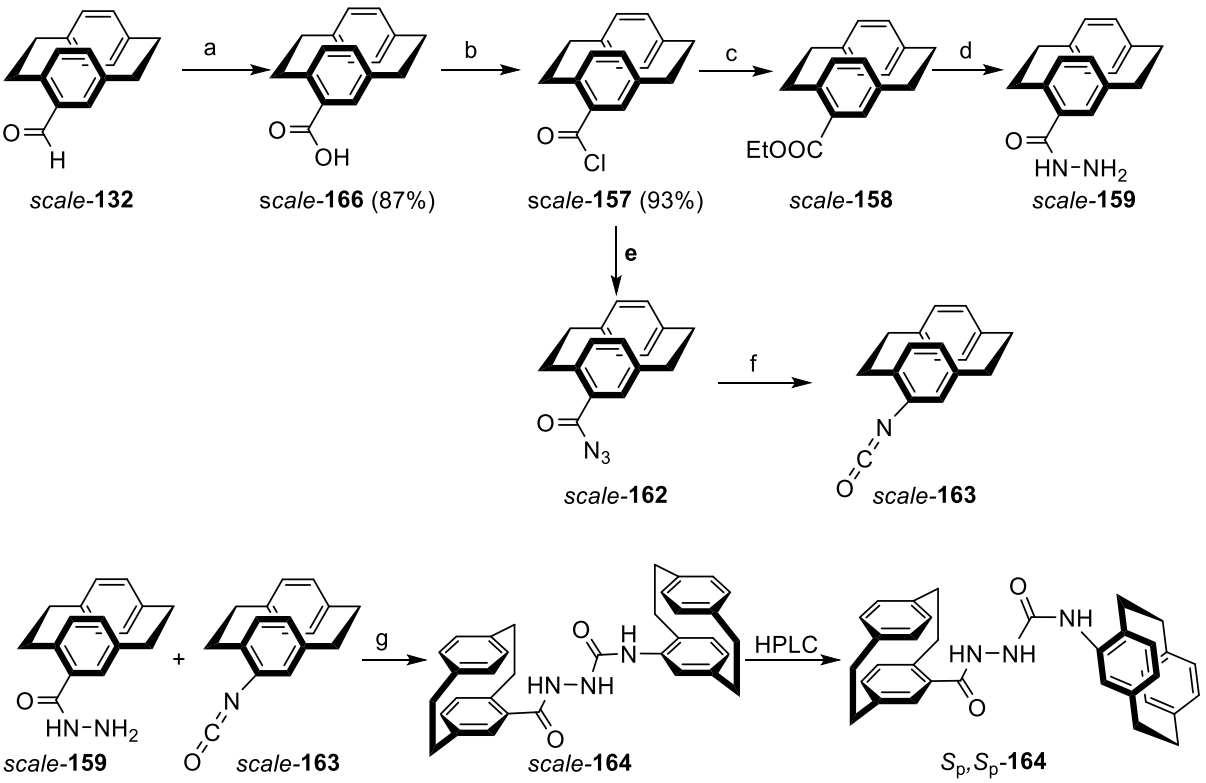

Scheme 36. Preparation of enantiomerically pure (S_p,S_p)-**164**. Reagents and conditions: a) aq. KOH, 100 °C, 22 h, then 35% H_2O_2, 10 °C, 20 min then 6 days, r.t..; b) $SOCl_2$/DMF, 80 °C; c) EtOH, reflux 24 h; d) NH_2NH_2, reflux, 14 h. e) NaN_3, acetone/water, r.t. 2 h; f) toluene, Ar, 80 °C, 1 h; g) EtOH/DMF, 70 °C, 4 h.

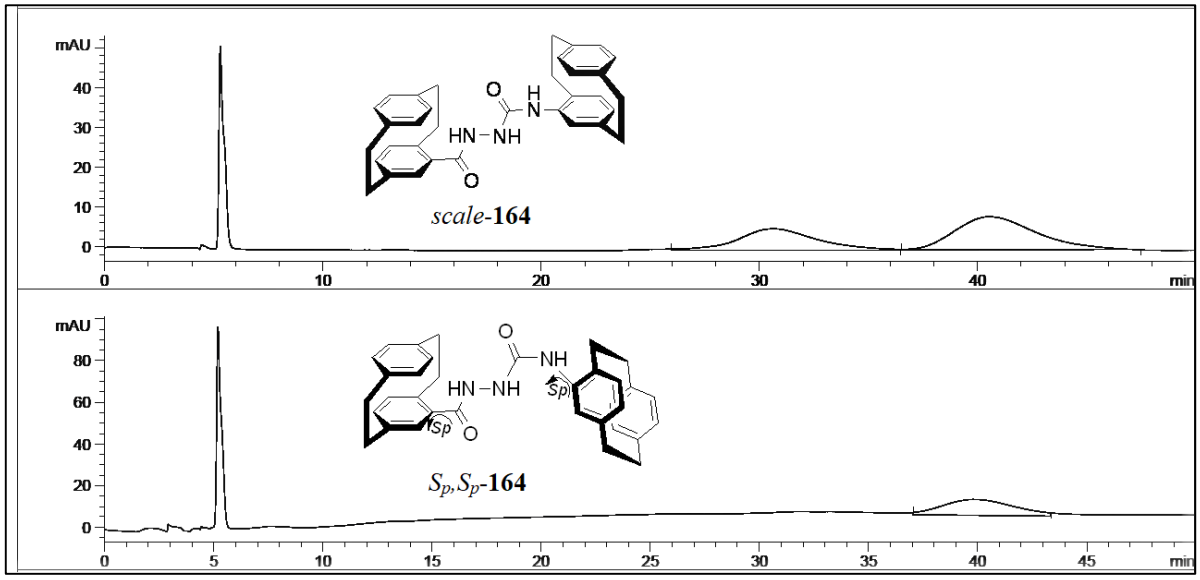

Figure 18: HPLC separation of (S_p,S_p)-*N*-([2.2]paracyclophanylcarbamoyl)-4-([2.2]paracyclophanylamide (**164**).

In summary, a protocol for the preparation of [2.2]paracyclophanyl)hydrazide **159** staring from the commercially available hydrocarbon [2.2]paracyclophane **131** was developed. It was also found that the diastereomer **164** can be synthesized successfully from the corresponding carbohydrazide **159** and isocyanate **163** in good yield (70%). Finally, by applying chiral HPLC separation on *scal*-**164**, the homochiral (S_p,S_p)-**164** was also successfully isolated.

3.2.3. Synthesis of [2.2]Paracyclophane Attached to *N*-Substituted Hydrazinecarbothioamide, Triazolthiones and Oxadiazoles

3.2.3.1. [2.2]Paracyclophanyl-*N*-substituted Hydrazinecarbothioamide

As mentioned before (see chapter 1.1.2.2), the reactivity of thiosemicarbazides makes them valuable building blocks for the synthesis of other heterocyclic motifs, especially five-membered rings. The focus of this study lies in the synthesis of a hydrazinecarbothioamide moiety attached to [2.2]paracyclophane. As they are less nucleophilic and more electron deficient than thiosemicarbazides, they are also ideal candidates and valuable building blocks for the synthesis of different heterocyclic rings, which rapidly cyclize.

To synthesize 2-(4'-[2.2]paracyclophanyl-4*H*-*N*-substituted-hydrazinecarbothioamides **135a-f**, carbohydrazide **159** was refluxed with different isothiocyanate derivatives (Table 3).

Table 3: Synthesis of the target 2-(4'-[2.2]paracyclophanyl-4*H*-*N*-substituted hydrazinecarbothioamides **135a-f**.

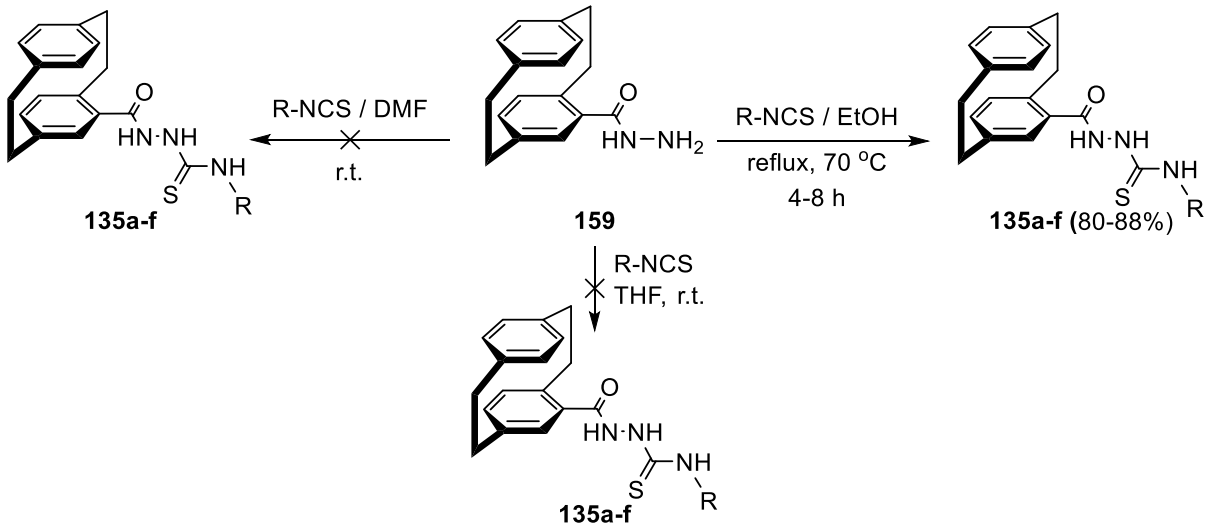

Entry	135a-f	R	Yield [%]			
			DMF	THF	DCM	EtOH
1	**135a**	3-Pyridyl	--	--	5	82
2	**135b**	Phenyl	--	--	4	88
3	**135c**	Allyl	--	--	2	86
4	**135d**	Ethyl	--	--	3	81
5	**135e**	Cyclopropyl	--	--	1	80
6	**135f**	Benzyl	--	--	2	85

In the first experiments with DMF as solvent neither at room temperature nor under reflux the target product **135a-f** was obtained. Therefore, THF and DCM were also tested as alternative solvents. In the case of DCM, traces of the target molecules (1-5%) were detected, while in THF no product formation was observed. Finally, experiments with boiling EtOH as a solvent

were successful, and the target products **135a-f** were obtained with an 80-88% yield (Table 3). Spectroscopic details are shown in chapter 5.2.2.2. The X-ray structure analysis of compounds **135b, c,** and **f** proved the proposed structures as shown in Figure 19. It should be noted that the determined dihedral angles between CS-NH-NH-CO are close to 90°.

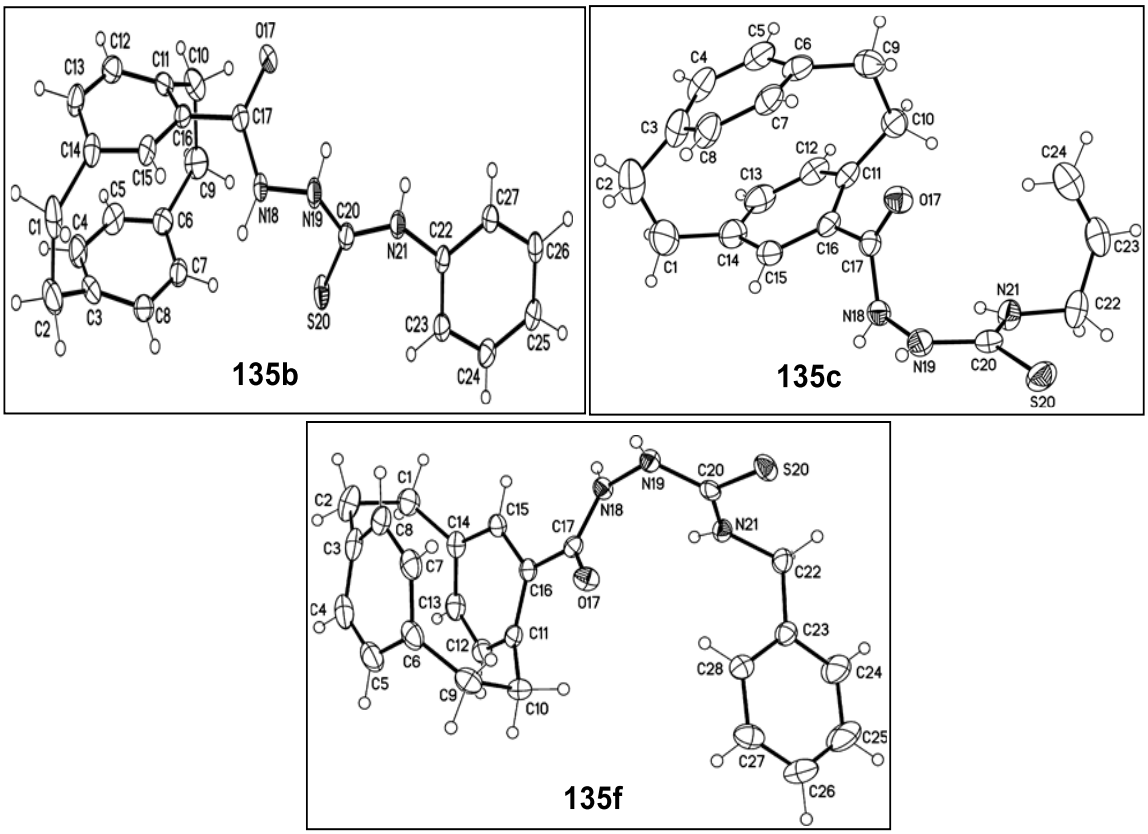

Figure 19: Molecular structure of compound **135b** identified according to IUPAC nomenclature as 2-(1,4(1,4)-dibenzenacyclohexaphane-1^2-carbonyl)-*N*-phenylhydrazine-1-carbothioamide (displacement parameters are drawn at 50% probability level), **135c** identified according to IUPAC nomenclature as 2-(1,4(1,4)-dibenzenacyclohexaphane-1^2-carbonyl)-*N*-vinylhydrazine-1-carbothioamide (displacement parameters are drawn at 50% probability level) and **135f** identified according to IUPAC nomenclature as 2-(1,4(1,4)-dibenzenacyclohexaphane-1^2-carbonyl)-*N*-benzylhydrazine-1-carbothioamide (displacement parameters are drawn at 50% probability level).

3.2.3.2. [2.2]Paracyclophanyl-substituted Triazolthiones and Oxadiazoles

Azole-linked [2.2]paracyclophanes have been used very frequently for catalyst design and other applications.[86-112] Although there are many examples of diazoles and triazoles, there are to the best of my knowledge no examples of 4-heterosubstituted analogs, which encouraged me to investigate the synthesis of a triazolthione and oxadiazole attached to the [2.2]paracyclophane unit by testing different cyclization methods from the literature for hydrazinecarbothioamides.

Triazolthione was derived from natural products by applying certain reactions to get the desired compounds,[163] and has also gained considerable importance in medicinal chemistry due to its

potential anticancer,[164-165] antimicrobial,[166] antioxidant, antitumor,[167] anti-tuberculosis,[168] anticonvulsant,[169] fungicidal,[170] antiepileptic,[171] and anti-inflammatory[172] properties. More recently, triazolthione compounds with an alkylated sulfur group have been published.[173-174] 1,2,4-Triazolthione derivatives have been successfully prepared by using various methods. The most prevalent method is the dehydrative cyclization of different hydrazinecarbothioamides in basic media[175] or acidic ionic liquid[176] followed by neutralization with acid or base, respectively. IDREES *et al.* reported a synthetic route towards 1,2,4-triazolthione derivatives by boiling thiosemicarbazide **167** in sodium hydroxide solution and ethanol. Cooling down to room temperature and acidification with diluted HOAc, afforded the target compound **168** (Scheme 37),[177] while HANIF *et al*. reported a synthetic route towards 1,2,4-triazoles **170** from refluxing potassium hydrazinecarbodithioate salt **169** in a diluted solution of hydrazine hydrate (Scheme 37).[178]

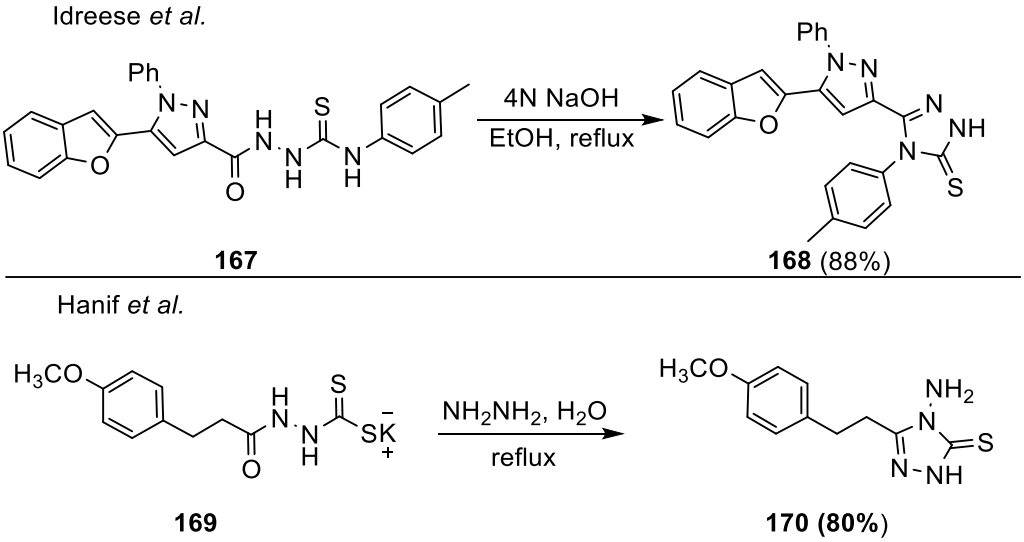

Scheme 37. Syntheses of substituted 1,2,4-triazoles **168** and **170**.

The synthesis of this nitrogen-containing heterophanes led to the idea that substituted 1,2,4-triazole-3-thiones **136a-f** could be obtained by boiling [2.2]paracyclophanyl-hydrazinecarbothioamide derivatives **135a-f** in sodium hydroxide for 2-4 h to obtain the target molecules **136a-f** (Table 4).

The structure of the newly synthesized compounds **136a-f** was supported by spectroscopic data (see chapter 5.2.2.3). To prove the structures of compounds **136a-f**, X-ray structure analyses were measured for compounds **136b** and **136c** as shown in Figure 20. Based on their spectroscopic similarities in NMR experiments, the same structures were presumed for other derivatives (see spectra in chapter 5.2.2.3).

Table 4: Preparation of 4-substituted 5-(4'-[2.2]paracyclophanyl)-2,4-dihydro-3*H*-1,2,4-triazole3-thiones **136a-f**.

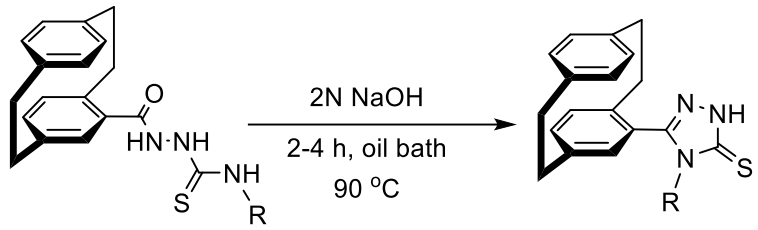

135a-f **136a-f** (70-80%)

Entry	136a-f	R	Yield [%]
1	**136a**	3-Pyridyl	76
2	**136b**	Phenyl	78
3	**136c**	Allyl	78
4	**136d**	Ethyl	72
5	**136e**	Cyclopropyl	72
6	**136f**	Benzyl	78

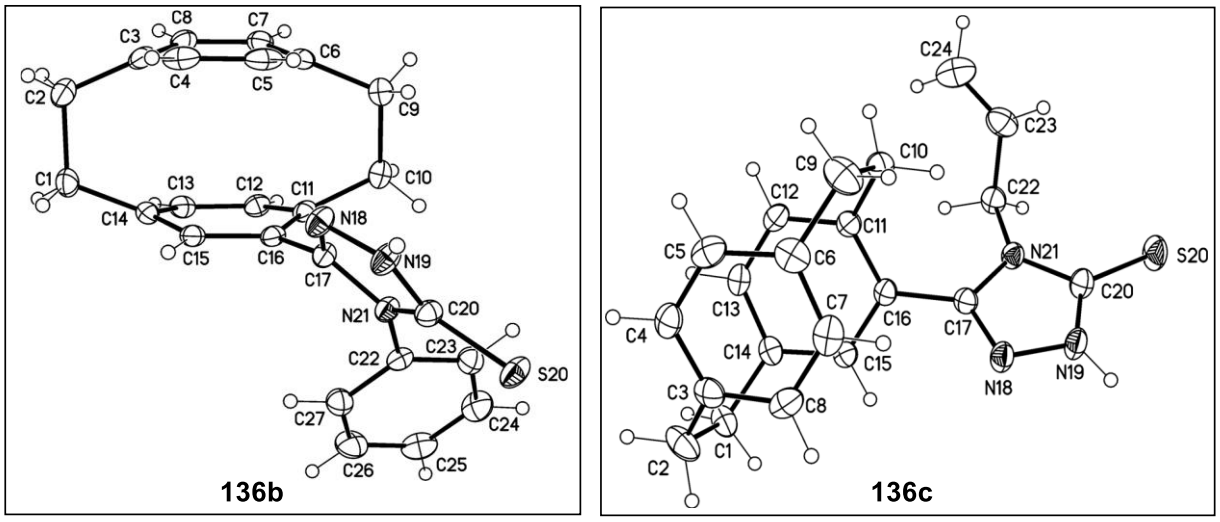

Figure 20: Molecular structure of compound **136b** identified according to IUPAC nomenclature as 5-(1,4(1,4)-dibenzenacyclohexaphane-1^2-yl)-4-phenyl-2,4-dihydro-3*H*-1,2,4-triazol-3-thione (displacement parameters are drawn at 50% probability level), and **136c** identified according to IUPAC nomenclature as 5-(1,4(1,4)-dibenzenacyclohexaphane-12-yl)-4-allyl-2,4-dihydro-3*H*-1,2,4-triazol-3-thione (solvent omitted for clarity; displacement parameters are drawn at 50% probability level).

Additionally, 1,3,4-oxadiazoles are an interesting class of azole compounds and are widely applied in the development of functional materials, such as electroluminescent and electron-transport materials.[179-180] Besides that, they play an important role in biological processes and exhibit antitumor,[181] antiviral,[182] and anti-inflammatory activities.[183] 1,3,4-Oxadiazoles are deployed for several purposes as a design element in medicinal chemistry.[184-185] For example, the heterocycle can adjust small molecule physicochemical and pharmacokinetic profiles because of its function as an aromatic ring spacer with relatively low lipophilicity.[184-185]

1,3,4-Oxadiazoles are resistant towards metabolism by hydrolytic esterase and peptidase enzymes and it can act as a bioisosteric hydrogen bond acceptor for carbonyl compounds such as ketones, esters, amides, and carbamates.

In the literature, several methods for the synthesis of 1,3,4-oxadiazoles were reported. The commonly used synthetic route towards 1,3,4-oxadiazoles includes acid hydrazide (or hydrazine) reactions with acid chlorides / carboxylic acids and direct cyclization of diacylhydrazines using a variety of dehydrating agents such as thionyl chloride,[186] phosphorous oxychloride,[187] phosphorous pentoxide,[188] and direct reactions of acids with (*N*-isocyanimino)triphenylphosphorane.[69, 189-191] To prepare the target products **137a-e**, **135a-e** were dissolved in THF with Et_3N. Stirring the reaction mixtures under gentle heating afforded the corresponding 2-substituted 1,3,4-oxadiazol-2-amines **137a-e** in moderate yields (Table 5).

Table 5: Internal cyclization of *N*-substituted 2-(4'-[2.2]paracyclophanyl-4*H*-hydrazine-carbothioamides **135a-e** into 2-substituted-amino-1,3,4-oxadiazoles **137a-e**.

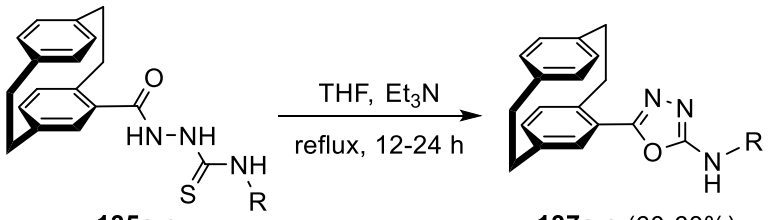

Entry	137a-e	R	Yield [%]			
			DMF	EtOAc	DCM	THF
1	**137a**	3-Pyridyl	--	4	8	66
2	**137b**	Phenyl	--	2	8	68
3	**137c**	Allyl	--	--	6	66
4	**137d**	Ethyl	--	--	5	60
5	**137e**	Cyclopropyl	--	--	6	63

Various solvents such as DMF, EtOAc, DCM and THF were tested. In the case of DMF, the reaction was not successful, while in EtOAc, product formation in yields lower than 5% was observed for the two derivatives with the aromatic substituents. In DCM, the target products could be obtained but in very low yields (5-8%) as shown in Table 5. A solution of THF/Et_3N proved to be the best conditions, leading to product formation in good yields (60-68%). The highest yields of the products were obtained in experiments at room temperature and without the necessity of an inert atmosphere. The structure of compounds **137a-e** was supported by

spectroscopic data (see chapter 5.2.2.4). Additionally, X-ray structure analysis for compounds **137b** and **137d** proved the suggested structures as shown in Figure 21.

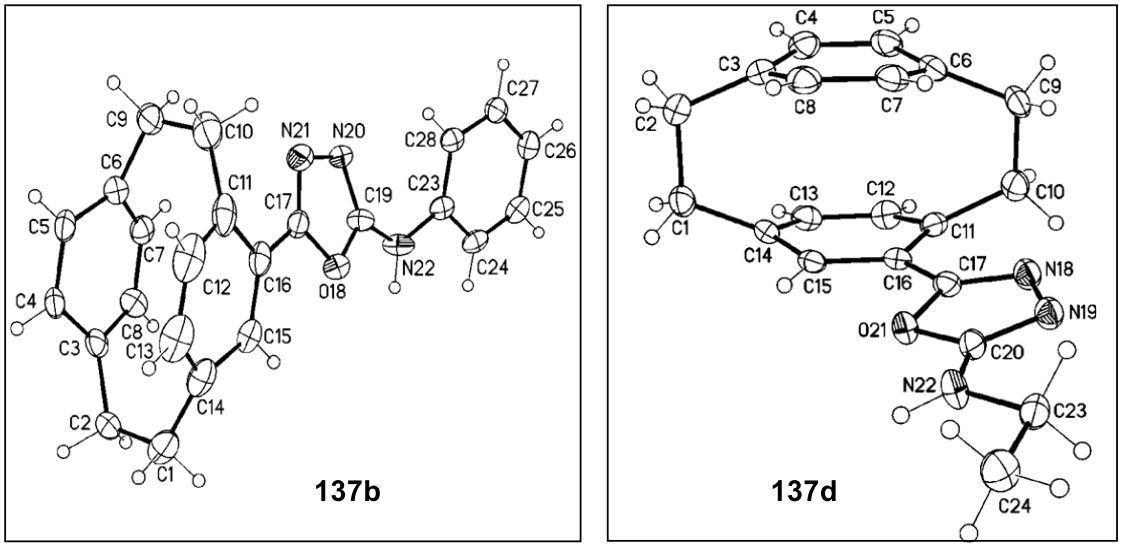

Figure 21: Molecular structure of compound **137b** identified according to IUPAC nomenclature as 5-(1,4(1,4)-dibenzenacyclohexaphane-1^2-yl)-*N*-phenyl-1,3,4-oxadiazol-2-amine (displacement parameters are drawn at 30% probability level), and **137d** identified according to IUPAC nomenclature as 5-(1,4(1,4)-dibenzenacyclohexaphane-12-yl)-*N*-ethyl-1,3,4-oxadiazol-2-amine (displacement parameters are drawn at 50% probability level).

In summary, the target compounds **135a-f**, a novel class of hydrazinecarbothioamides attached to [2.2]paracyclophane, were successfully obtained from the corresponding carbohydrazide **159** in very good yields (80-88%). Besides, the syntheses of novel substituted fived membered heterocyclic rings by cyclization reactions of the new series of the hydrazinecarbothioamides **135a-f** was achieved. By using the literature conditions, triazolethiones **136a-f** could be obtained in very good yields (70-80%). Suitable reaction conditions were also found for oxadiazoles derivatives **137a-e**, which were obtained in good yields (60-68%). X-ray crystal structure analysis supports all of the suggested structures.

3.3. Stereoselective Synthesis of Homochiral [2.2]Paracyclophanylindenofuranylimidazo-[3.3.3]propellanes[3]

3.3.1. [3.3.3]Propellanes

Propellanes are compounds containing a tricyclic system wherein all three rings are fused by a common carbon-carbon bond. In 1966, GINSBURG *et al.*[192] proposed the term propellane due to the characteristic propeller shape (Y-shaped) of these molecules. To distinguish between different ring sizes, the compounds are often named [m.n.o]propellanes, in which m, n, and o represent the number of non-shared carbon atoms in each of the three rings.[193-194] There are different types of propellane skeleton according to the numbers of atoms in the free chain around the C-C bridge bond which are classified into: [1.1.1]propellane, [2.2.2]propellane, [3.3.3]propellane, and so on. The first synthesized propellanes were reported in the 1930s during the investigations of the Diels−Alder reaction.[195-199] The first "propellane by design" was synthesized much later, in 1965.[200-201]

The propellane moieties are very important as they have a lot of applications including bioactive medicinal compounds[202] or polymers[203] which are used in the treatment of neurodegenerative diseases such as Parkinson's disease and Alzheimer's disease.[204] Some of the natural propellanes have been evaluated for their anticancer,[205] antibiotic,[206] antibacterial,[207] antifungal,[202] and platelet-activating factor antagonistic activities.[208-209] They have attracted more attention from many research groups owing to their challenging structures and various applications as well as being the main structural unit in some natural products. A very interesting class in propellane chemistry are nitrogen-containing propellanes and analogs, due to their presence in biologically active natural products and pharmaceuticals such as the periglaucine A (**171**), modhephene (**172**), and hasubanan alkaloids (**173**) (Figure 22).[210-211] Recently, the total synthesis of many different propellane-containing natural products has been reviewed.[212] Some modern synthetic approaches to form carbocyclic or heterocyclic propellanes include [4+2]cycloadditions,[213] manganese[214] or palladium[215] catalysis and nucleophilic substitutions of 1,1,2,2-tetrasubstituted alkenes.[216-217] Highly chemoselective and regioselective dioxa[3.3.3]propellanes have been synthesized *via* the reaction of the Knoevenagel adducts of acenaphthoquinone, malononitrile, and ninhydrin

[3] Excerpts of this chapter were already published in
A. A. Hassan, S. Bräse, A. A. Aly, N. K. Mohamed, L. E. A. El-Haleem, M. Nieger, *Monatshefte für Chemie*, **2021**, *in press*.

in presence of 3-oxo-3-arylpropionitriles in high yields.[218] The synthesis of oxo-thioxo[3.3.3]propellanes was also reported by YAVARI *et al.* during the dithiocarbamate reaction with the Knoevenagel adduct formed from ninhydrin and malononitrile.[219]

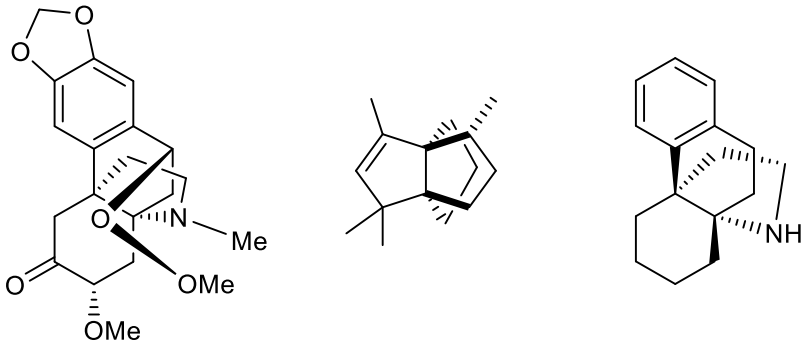

171 **172** **173**

Figure 22. Examples of naturally occurring and biologically active propellanes.

Propellane-type indanes bearing a rigid three dimensioned structure are very appealing as it is possible to introduce certain functional groups to the indandione moiety to point in the desired direction. In the light of the literature, HASSAN *et al.* reported a direct and concise synthetic method for the synthesis of furo-imidazo[3.3.3]propellanes by the reaction of dicyanomethylene-1,3-indanedione (CNIND), with *N*-substituted 2-(2,4-dinitrophenyl) hydrazinecarbothioamides[220] and with thiocarbohydrazides.[221] They also reported the synthesis of furo-imidazo[3.3.3]propellane derivatives by the reaction of substituted alkenylidene hydrazinecarbothioamide with CNIND. Their cytotoxicity was evaluated against the NCI-60 panel of cancer cell lines, and the DNA-binding mode was investigated.[222]

3.3.2. Synthesis of Paracyclophanylindenofuranylimidazo[3.3.3]propellanes

[2.2]Paracyclophanes have been reported to be valuable as a typical bioisostere for secondary affinity and selectivity-generating π2 systems.[223] Also, GMEINER *et al.* have found that indoloparacyclophanes can be used as double layered aryl bioisosteres of highly selective D4 receptor ligands.[224-225]

Therefore, the investigation of a new class of heterocyclic propellane compounds attached to [2.2]paracyclophane was pursued by applying donor-acceptor interactions for the starting materials **135a-f**. However, there are a variety of methods for the synthesis of different types of heterocyclic propellanes, all of which suffer from some disadvantages like multistep reaction processes, harsh reaction conditions, long reaction times, poor regioselectivity, and low yields.

These findings were prompted to consider the reaction of [2.2]paracyclophanyl-substituted hydrazinecarbothioamides **135a-e** with dicyanomethylene-1,3-indanedione (**174**, CNIND) for the construction of [2.2]paracyclophanylindenofuranylimidazo[3.3.3]propellanes (Table 6).

Table 6: Reaction of racemic paracyclophanyl-substituted hydrazinecarbothioamides **135a-e** with CNIND **174** and optimization of reaction conditions for the formation of **138a**.

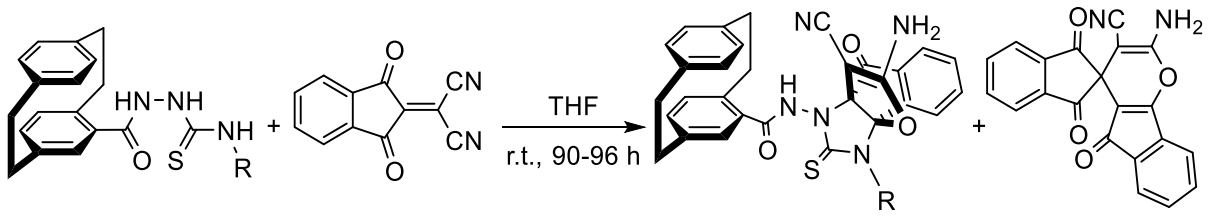

135a-e **174** **138a-e** (35-81%) **175** (9-12%)

Entry	169a-e	R	Solvent	Yield [%]
1	**169a**	3-Pyridyl	CH_2Cl_2	39
2	**169a**	3-Pyridyl	DMF	31
3	**169a**	3-Pyridyl	CH_3CN	41
4	**169a**	3-Pyridyl	Toluene	34
5	**169a**	3-Pyridyl	THF	81
6	**169b**	Phenyl	THF	40
7	**169c**	Allyl	THF	35
8	**169d**	Ethyl	THF	36
9	**169e**	Cyclopropyl	THF	38

Initially, the reaction was conducted at room temperature in DCM between [2.2]paracyclophanyl-*N*-pyridinyl-hydrazinecarbothioamide (**135a**) and CNIND (**174**), where the desired [2.2]paracyclophanylindenofuranylimidazo[3.3.3]propellane **138a** was isolated in 39% yield (Table 6). To optimize the yield, different solvents were tested (Table 6), whereby THF gave the best result with a yield of 81%.

An increased amount of the starting material **135a** was not required to obtain high yields of product **138a**. Additionally, if two equivalents of **174** and one equivalent of **135a** were added under the same optimized conditions, the yield of **138a** was reduced. These reaction conditions for the synthesis of [2.2]paracyclophanyl-*N*-pyridyl hydrazinecarbothioamides **138a** were also applied in the reactions of other substituted [2.2]paracyclophanyl-*N*-substituted hydrazine-carbothioamides **135a-e** with compound **174**, the yields were comparable to **138a** as shown in Table 6 for **138a-c**.

The structures of products **138a-e** were deduced from their ^{1}H NMR, ^{13}C NMR, and IR spectra as well as their mass spectra (see chapter 5.2.3). The ^{13}C NMR spectrum of **138a** shows

characteristic resonances representing the furan-C-2 and C-3 carbons at 168.3 and 51.4 ppm, respectively. Both are by the observed trends in δ values for carbon atoms in push-pull alkenes.[226-227] The mass spectra of **138a** show a molecular ion at *m/z* = 611 (35%) which explains the formation of the product by the reaction of **135a** and **174** without any loss from both molecules. Clear evidence for the structure of **138a** was obtained from single-crystal X-ray analysis (Figure 23). Based on their spectroscopic similarities in NMR, the same structure was assumed for the other derivatives **138a-e**.

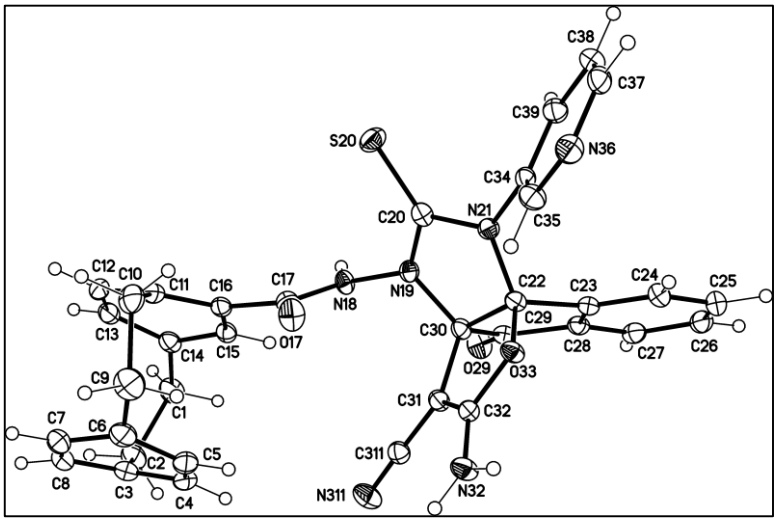

Figure 23: Molecular structure of **138a** (solvent omitted for clarity, displacement parameters are drawn at 50% probability level).

Compounds **135a-e** may react with the sulfur atom, and hydrazinecarbothioamide-NH's as nucleophilic sites (Scheme 38, route A-D). An alternative suggested reaction mechanism could be ruled out based on the ^{13}C NMR spectrum and the absence of a signal corresponding to a C=S group in **138a-e**. Without reference compounds, comparing the ^{1}H NMR or ^{13}C NMR chemical shifts for the alternative structures **180-182a-e** would not be easy, and spectroscopic data are not sufficient to confirm the exact structure. The relative stereochemistry of **138a** was unambiguously established by single-crystal X-ray diffraction, which clearly shows that it has the propellane system (Figure 23). The crystal structure of **138a** shows that the C22-C30 bond length = 1.5378 (16) Å has C-C single bond character and is shared by three different rings N19-C20-N21-C22-C30, C23-C28-O33-C22-C30, and C31-C32-C29-C23-C30. The bond length C(20)-S(20) = 1.6459 (13) Å and C(29)-O(29) = 1.2089 (16) Å belong to C=S and C=O character, respectively. The sums of angles around C(22: angles C30-C22-N21, C30-C22 C23, C30-C22 O33) and C(30: angles C22 C30 N19, C22-C30-C31, C22-C30 O33) are 317^{o} and 309°, respectively revealing that restrained around C(22) and C(30).

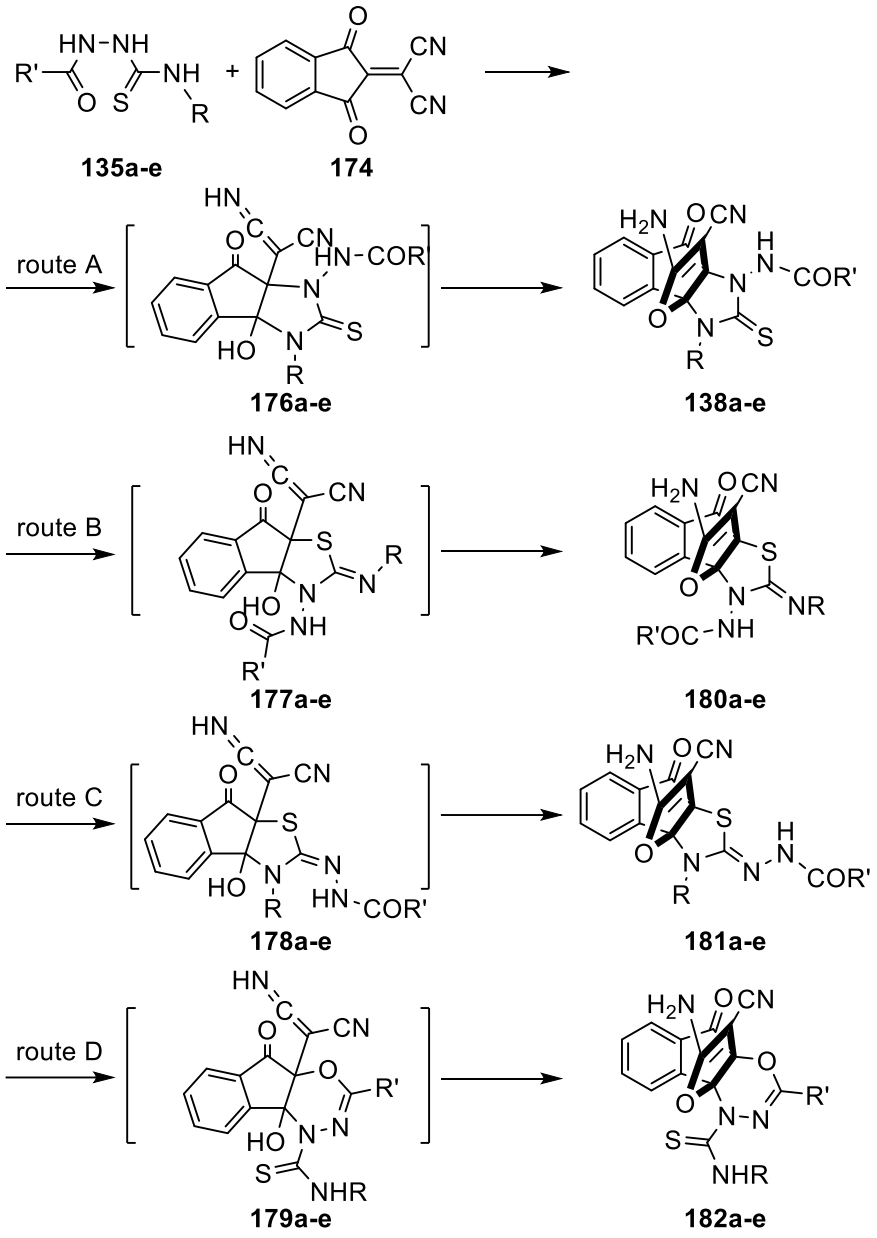

Scheme 38. Intermediates **A-D** and alternative products **138**, **180-182a-e**.

From the resulting spectral data as well as combustion analysis, separation of 2'-amino-1,3,5'-trioxo-1,3-dihydro-5'*H*-spiro[indene-2,4'-indeno[1,2-*b*]pyran]-3'-carbonitrile **175** as another product from the reaction between **135a-e** and **174** can be suggested, it was formed in yields varying from 9 to 12%. The spiro-product **175** was characterized by comparing its melting point and IR with an authentic sample.[228]

KUNDA and PRAMANIK have reported the synthesis of 2-amino-2',4-spiro(1',3'-indanedione)-5-oxo-4,5-dihydro-indeno[1,2-*b*]pyran-3'-carbonitrile **175** *via* several multistep reactions.[228] Single-crystal X-ray analysis provided clear evidence for the structure of **175** (Figure 24).

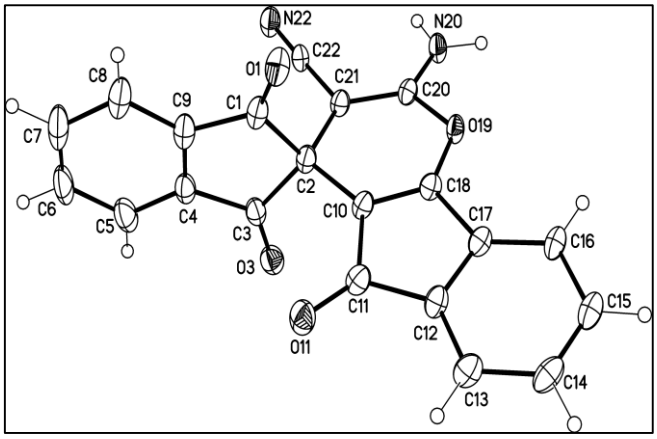

Figure 24: Molecular structure of one of the two crystallographic independent molecules of **175** (displacement parameters are drawn at 50% probability level).

This explains the mechanism for the formation of compound **175** by abstracting two hydrogens from **135a-e**, CNIND **175** is reduced to give **183** which may be derived to the carbanion of indanedione **184** and malononitrile **185**. Then, adduct **186** is formed after a nucleophilic attack of **184** on the C–C double bond of **183**. Finally, an intramolecular nucleophilic attack of the indene-OH to one of the cyano groups in compound **187** gives spiro-[1',3'-indanedione]-oxo-4,5-dihydro-indeno[1,2-*b*]pyran-3-carbonitrile (**175**) *via* intermediate **188**.

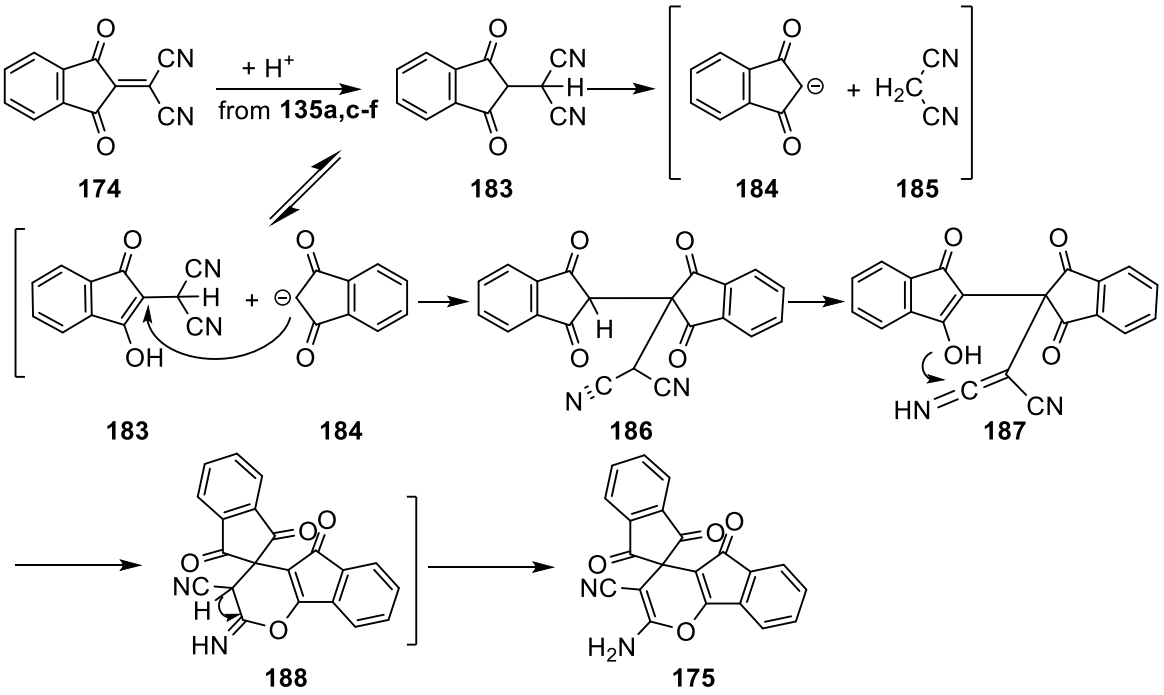

Scheme 39. The mechanism for the formation of compound **175**.

3.3.3. Synthesis of Homochiral [2.2]Paracyclophanylindenofuranylimidazo-[3.3.3]]propellanes

As mentioned above, planar chiral [2.2]paracyclophane derivatives have great importance in various applications.[154] Many research groups continue to pursue new, optically active compounds,[229] which inspired the synthesis of homochiral [2.2]paracyclophanyl-indenofuranylimidazo[3.3.3]propellanes. To prepare the homochiral propellanes (S_p)-**138a**, the synthesis of *scal*-**135a** was performed (see section 3.2.2) by refluxing carbohydrazide *scal*-**159** with pyridyl isothiocyanate in EtOH (Scheme 39). Repeating the previous reaction steps in Table 6, compound *scal*-**138a** was prepared in its non-enantiomerically pure forms. Upon applying chiral HPLC, enantiomerically pure chiral (S_p)-**138a** was obtained in very good yield (84%) as shown in Figure 25.

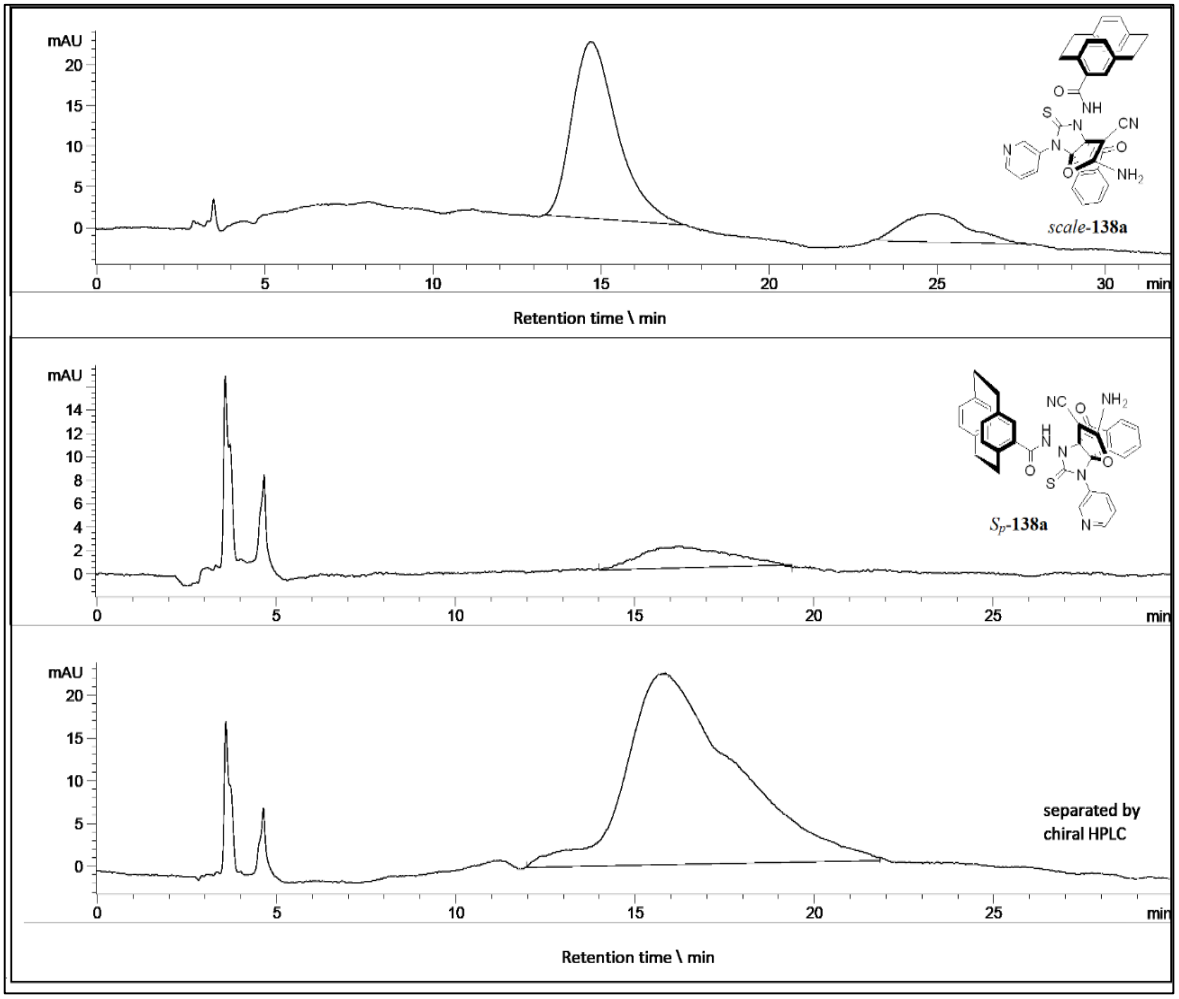

Figure 25: Analytical HPLC traces of *scal*- and (S_p)-**138a**.

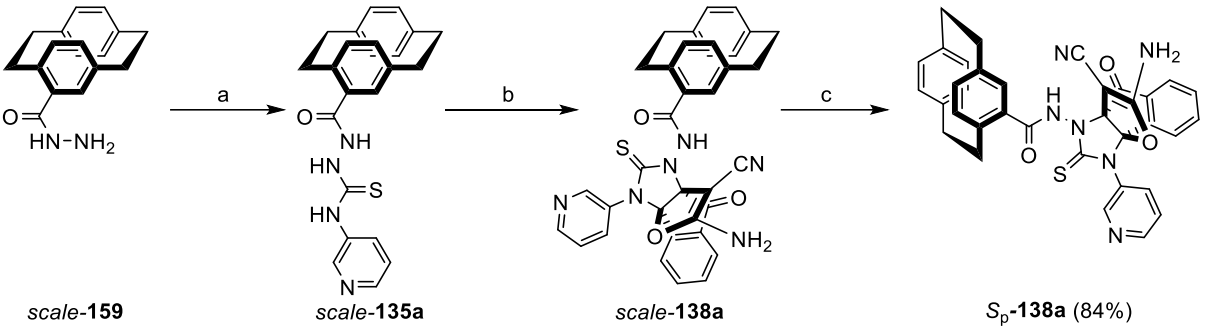

Scheme 39. Synthesis of *(S*p*)*-**138a**. Reagents and conditions: a) 3-isothiocyanatopyridine, EtOH, reflux 4 h; b) CNIND, THF, r.t. 90 h; c) chiral HPLC separation.

In summary, this section focused on the synthesis of new heterocyclic propellanes combined with [2.2]paracyclophane. By applying donor-acceptor interactions between hydrazinecarbothioamides **135a-e** and CNIND **174**, [2.2]paracyclophanylindenofuranylimidazo-[3.3.3]propellane **138a-e** could be obtained in good yield (35-81%). Also homochiral [2.2]paracyclophanylindenofuranylimidazo[3.3.3]propellane *S*p-**138a** was successfully synthesized with 84% yield.

3.4. Substituted Paracyclophanylthiazoles as Anti-cancer Agents

Cancer is one of the main causes of death, surpassed only by heart disease.[230] Although chemotherapeutic agents are effective in treating various cancer types in their early stages, efficacy against metastatic cancer forms is far from satisfactory.[230] Therefore, the development of novel anticancer drugs is the main goal of this research. Microtubules, composed of α,β-tubulin heterodimers, play an important role in cell mitosis, motility, and organelle distribution.[231] In the last decades, the discovery and development of novel small molecules, able to inhibit tubulin polymerization, were of interest to many researchers.[232] The recently discovered anti-tubulin polymerization activity of thiazole scaffolds, such as 2-aryl-thiazolidine-4-carboxylic acid amides (ATCAA) **I** which show potent cytotoxic activity against prostate cancer cells with an average IC_{50} in the range from 0.7 to 1.0 μM and average IC_{50} against melanoma cells were 1.8-2.6 μM (Figure 26).[233]

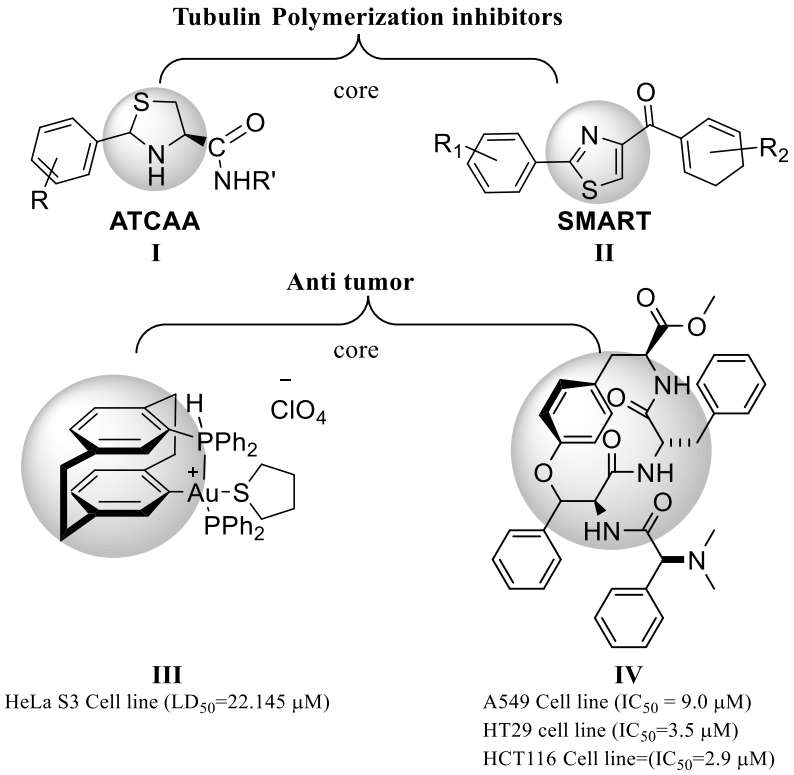

Figure 26: Structures of biologically active thiazole and paracyclophane derivatives.

Moreover, novel substituted methoxybenzoylaryl-thiazole (SMART) **II** compounds were found to inhibit melanoma and prostate cancer cell growth *in vitro* at nanomolar concentrations.[233] Preliminary studies showed that SMART as well as ATCAA compounds disrupt tubulin polymerization, therefore are capable of preventing the formation of functional microtubule and block cell mitosis.[230]

Gold (I) complexes of phosphino[2.2]paracyclophane ligands **III** clearly showed their cytotoxic activity in the HeLa S3 cell line (LD_{50} = 22.15 μM) which is compared with cisplatin (LD_{50} = 7.65 μM) in the same scale. Though their mechanisms of action are different and include necrosis, apoptosis, and DNA damage (Figure 26).[234]

3.4.1. Design, Synthesis, Molecular Docking and Mechanistic Studies of 2-(2-(4'-[2.2]Paracyclophonyl)-hydrazinylidene)-3-substituted-4-oxo-thiazolidin-5-ylidene)acetates[4]

3.4.1.1. Design and Synthesis

In recent years, several publications documented the structure-activity relationship of paracyclophane substituents among others derivative (**III**, **IV**) and that these derivatives exhibit cytotoxicity towards the human cancer cell lines A549 (IC_{50} = 9.0 μM), HT29 (IC_{50}=3.5 μM), and HCT116 (IC_{50}=2.9 μM).[235] Based on this data novel anti-cancer agents, that could potentially combine the anti-tubulin polymerization activity of thiazole scaffolds and the potential antitumor effect of the [2.2]paracyclophane scaffold was designed (Figure 27).

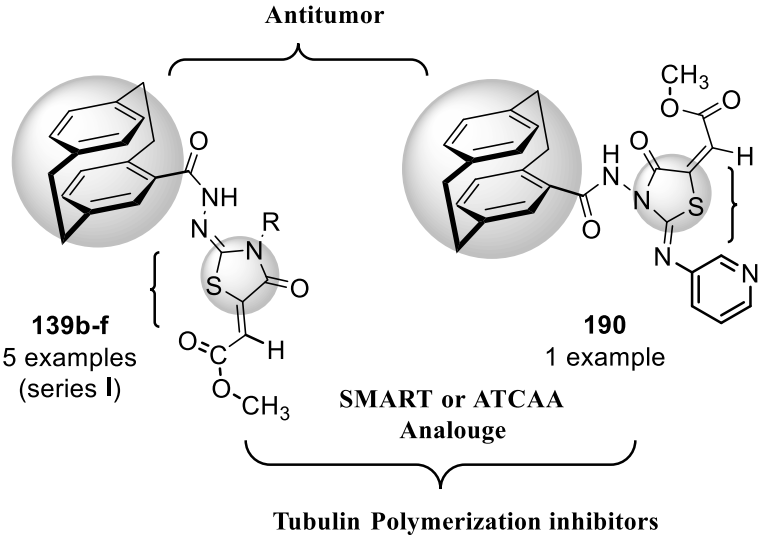

Figure 27: Design of the target compounds **139a-f**.

The main goal of this project involved the synthesis of new thiazole bearing [2.2]paracyclophanyl derivatives (series **I**) **139a-f** substituted with either electron-donating or withdrawing groups to study their respective electronic effects. The thiazolidinones **139b-f** and

[4] Excerpts of this chapter were already published in
A. A. Aly, S. Bräse, A. A. Hassan, N. K. Mohamed, L. E. A. El-Haleem, M. Nieger, N. M. Morsy, E. M. N. Abdelhafez, *Molecules* **2020**, *25*(13), 3089.

190 were obtained in the reactions of **135a-f** with dimethyl acetylenedicarboxylate (DMAD) (**189a**) in 67-78% yield (Table 7).

Table 7: Reactions of **135a-f** with dimethyl acetylenedicarboxylate (**189a**); synthesis of different regioisomeric thiazolidines **139b-f** or **190**.

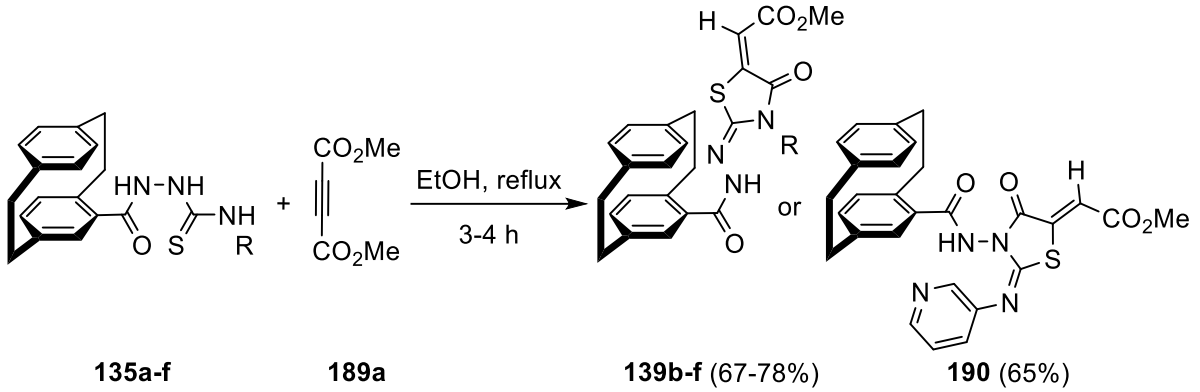

Entry	139b-f, 190	R	Yield [%]
1	**139b**	Phenyl	78
2	**139c**	Allyl	79
3	**139d**	Ethyl	69
4	**139e**	Cyclopropyl	67
5	**139f**	Benzyl	76
6	**190**	3-Pyridyl	65

Surprisingly, the reaction of 2-(4-[2.2]paracyclophanoyl)-*N*-(pyridine-3-yl)hydrazinecarbothioamide (**135a**) with **189** under the conditions mentioned above gave the regioisomer methyl 2((*E*-3-[4-[2.2]paracyclophanoylamido-4-oxo-2-(pyridine-3-ylimino)thiazolidin-5-ylidene)-acetate (**190**) in 65% yield (Table 7). The unusual reactivity of **135a** towards **189** might be attributed to the resonance structures of **135a** that could decrease the basicity of the N^3-H. Therefore, the reaction proceeds directly *via* the N^2-H, which would be of higher basicity (Figure 28).

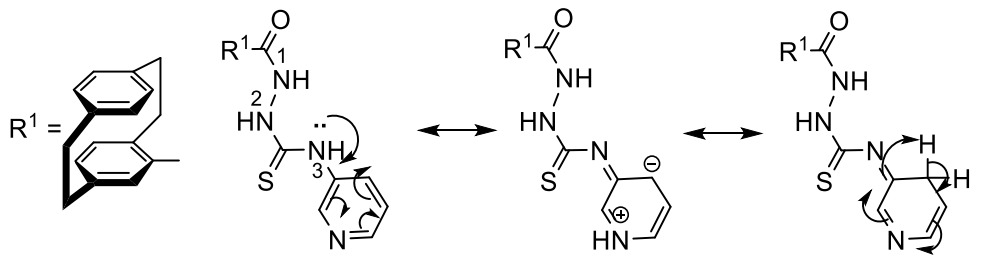

Figure 28: Resonance structures of compound **135a**.

The X-ray structure analysis of methyl (*E*)-2-((*E*)(2'-4-[2.2]paracyclophanyl)-hydrazinylidene)-3-benzyl-4-oxathiazolidin-5-ylidene)acetate (**139f**) confirm the proposed

structure (Figure 29). Based on their spectroscopic similarities with NMR, the same structure was assumed for the other derivatives **139b-e**. The structure of compound **190** was confirmed by NMR spectroscopy, mass spectrometry, and elemental analysis (see chapter 5.2.4.1). And finally, it was unambiguously provided by X-ray structure analysis (Figure 29).

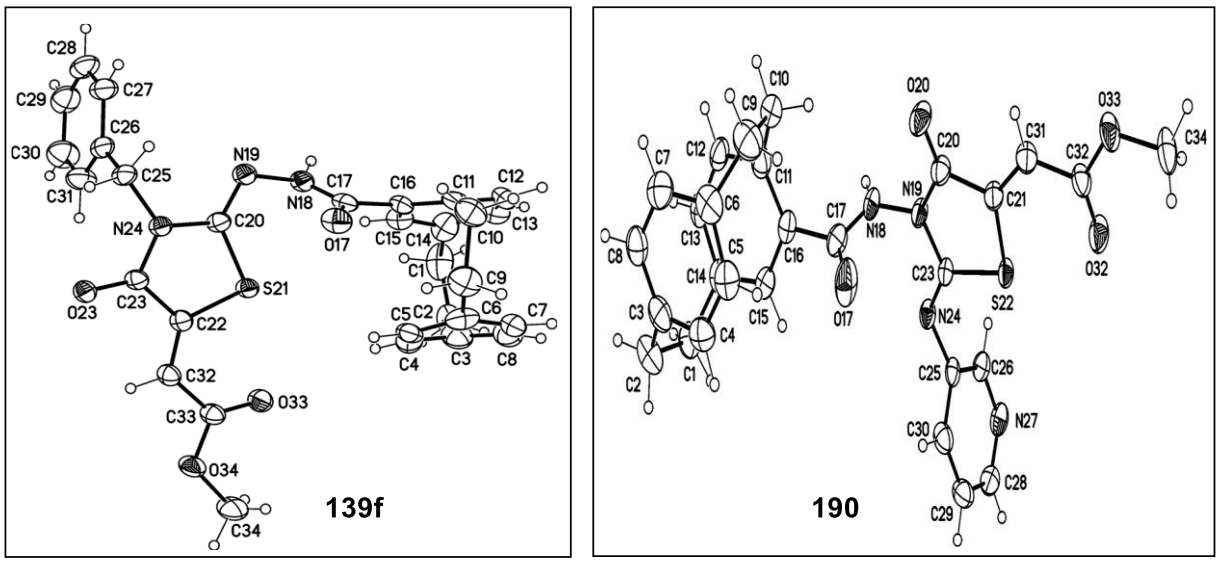

Figure 29: Molecular structure of compound **139f** identified according to IUPAC nomenclature as methyl (*E*)-2-((*E*)-2-(2-(1,4(1,4)-dibenzen-cyclohexaphane-12-carbonyl)hydrazinylidene)-3-benzyl-4-oxothiazolidin-5-ylidene)acetate (displacement parameters are drawn at 50% probability level) and **190** identified according to IUPAC nomenclature as methyl (*E*)-2-((*E*)-3-(1,4(1,4)-dibenzenacyclohexaphane-1^2-carboxamido)-4-oxo-2-(pyridin-3-ylimino)thiazolidin-5-ylidene)acetate (displacement parameters are drawn at 50% probability level).

3.4.1.2. Screening, Molecular Docking, and Mechanistic Study

The screening of compounds **159**, **135d-f**, **139b-f,** and **190** in biological activity assays was performed by the National Cancer Institute (NCI, USA). All experiments in the following section were conducted by Dr. E. M. N. Abdelhafez and molecular docking and mechanistic studies were performed in collaboration with Dr. E. M. N. Abdelhafez.

Anti-proliferative Investigation Against 60 Cancer Cell Lines at the National Cancer Institute

The evaluation of the activity against tumor cells of compounds **152**, **160d-f**, **184b-f,** and **185** was performed with a full panel of 60 cell lines derived from nine cancer types (leukemia, lung, colon, CNS, melanoma, ovarian, renal, prostate, and breast cancer),[236] by the National Cancer Institute (NCI, USA). The methodology of the NCI anticancer screening has been described in detail elsewhere (http://www.dtp.nci.nih.gov).[236] Briefly, tested compounds were added to the culture at a single concentration (10^{-5} M) and the cultures were incubated for 48 h. The endpoint was determined using a protein-binding dye, SRB. The results for tested compounds

are reported as the percentage of growth of the treated cells when compared with the untreated control cells. The percentage of growth was assessed spectrophotometrically versus controls that were not treated with test agents. All experiments have been repeated 3 times.

The open-chain structures compounds **159** and **135d-f**, are concluded to be not cytotoxic, as they showed moderate to weak activity on most of the tested cancer cell lines (Table 8). Furthermore, a screening of the thiazolidinones **139b-f** and **190** was done, whereby compound **139b** demonstrated pronounced cytotoxicity on the nine tested cancer cell lines. It is noticeable that compounds **139b, 139c, 139d,** and **139f** are the most potent tested derivatives on leukemia cell lines. They showed growth inhibition percentages higher than 100 percent which means they caused complete cancer cell death. It can be presumed that these compounds can stop the division and growth of cancer cells and can cause tumors to shrink in size. caused complete cell death of leukemia cells RPMI-8226 with inhibition percentages of 120.89, 147.00, 109.36, and 114.28%, respectively, and against SR with inhibition percentages of 115.60, 114.70, 98.21, and 113.40%, respectively. Compound **139d** showed remarkable activity against the other tested cell lines. Although **139e** showed moderate to weak activity against most of the tested cancer cell lines, compound **139f** exhibited significant inhibition against non-small cell lung cancer cell line NCI-H522, colon cancer cell lines HT29 and SW-620, melanoma cell line LOX IMVI, ovarian cancer cell line OVCAR-3, renal cancer cell line CAKI-1, prostate cancer cell line PC-3 and breast cancer cell lines BT-549, T-47D and MDA-MB-468 (Table 8). Furthermore, compounds **139c** and **190** displayed mild to moderate activities on most of the cancer panel cell lines (Table 8).

Table 8: Growth inhibition% of compounds **159**, **135d-f**, **139b-f**, and **190** (conc. 10^{-5} M) against different cell lines.

Panel/Cell Line		**152**	**135d**	**135e**	**135f**	**139b**	**139c**	**139d**	**139e**	**139b**	**190**
Leukemia	CCRF-CEM	0.98	0.36	0	58.62	87.04	77.08	66.08	41.43	96.17	31.27
	HL-60(TB)	0.93	0.18	0	23.33	83.60	8.16	11.64	26.38	**105.46**	48.64
	K-562	2.15	0	0	41.43	72.95	48.13	45.78	30.52	81.13	20.72
	MOLT-4	2.40	3.67	0	28.15	96.97	64.55	62.85	55.61	98.91	21.86
	RPMI-8226	4.02	0	0	40.09	**120.89**	**109.36**	**114.28**	49.83	**147.00**	83.01
	SR	0	0	0	21.51	**115.60**	98.21	**113.40**	39.13	**114.70**	74.18
Non-Small Cell Lung Cancer	A549/ATCC	3.47	0.23	0	34.09	30.92	5.20	3.	11.39	22.95	2.04
	EKVX	4.70	0.17	5.62	9.62	41.03	9.16	6.44	12.16	22.30	2.61
	HOP-62	0	0	0	25.81	97.00	0	0	0	22.76	4.
	HOP-92	12.99	5.93	2.83	21.43	24.66	18.59	18.43	16.16	24.50	8.14

	NCI-H226	0.38	0	0	14.87	26.22	12.45	7.31	9.41	35.20	7.48
	NCI-H23	1.33	0	2.32	21.29	59.57	11.85	0.40	9.32	22.64	9.18
	NCI-H322M	0	5.56	4.94	14.13	31.54	2.94	7.75	4.43	6.70	1.72
	NCI-H460	0	0	0	52.42	39.35	0	0	1.98	6.29	0.75
	NCI-H522	13.68	12.60	7.35	23.96	58.47	39.25	40.31	30.01	84.06	17.74
Colon Cancer	COLO 205	0	0	0	5.21	52.26	0	0	4.48	27.31	0
	HCC-2998	0	3.94	0	16.84	96.36	0	0	0	20.49	0
	HCT-116	0	9.23	7.52	35.53	95.95	46.02	50.54	24.59	50.48	6.35
	HCT-15	5.21	1.48	3.31	48.91	99.66	33.11	31.60	29.43	72.16	11.75
	HT29	5.65	2.97	0	12.49	**113.13**	53.99	54.76	23.99	87.62	7.71
	KM12	0.85	1.00	0	10.69	91.51	18.40	15.01	1.32	34.90	7.32
	SW-620	0	2.80	0	29.26	92.61	55.46	91.21	12.94	81.83	10.84
CNS Cancer	SF-268	2.74	1.34	4.59	14.91	27.49	0	2.18	2.56	14.95	3.08
	SF-295	0.50	0	6.78	32.30	.41	6.42	3.13	8.80	10.63	5.63
	SF-539	2.01	0.08	0	2.91	**122.50**	0.33	9.82	0	56.74	11.63
	SNB-19	---	0	0	29.70	60.06	15.31	14.43	11.26	43.08	16.64
	SNB-75	---	11.48	10.24	------	54.29	21.92	21.18	24.73	48.78	0.25
	U251	3.14	1.55	0	36.49	84.20	18.17	15.64	20.27	45.04	14.66
Melanoma	LOX IMVI	0	0	0	35.50	**127.77**	21.22	26.51	9.41	93.79	9.78
	MALME-3M	0	3.08	0	19.83	21.23	7.56	8.06	11.28	11.57	0
	M14	0	6.33	5.05	33.38	46.88	21.14	12.85	19.23	36.59	7.99
	MDA-MB-435	1.07	0	0	13.75	10.39	0	0.72	8.06	8.44	0
	SK-MEL-2	0	9.57	0	17.65	12.98	2.70	5.78	13.53	14.42	0
	SK-MEL-28	0	0	0	20.10	17.54	0	0	10.28	0	0.86
	SK-MEL-5	0	4.71	3.29	27.13	30.65	7.53	7.50	14.50	17.72	3.64
	UACC-257	7.20	4.47	0	4.87	30.75	8.89	7.26	16.33	19.02	0.83
	UACC-62	3.42	2.48	6.63	33.04	74.85	22.84	21.39	17.97	48.11	10.67
Ovarian Cancer	IGROV1	0	0	0	37.59	94.03	10.76	11.62	7.20	57.72	15.44
	OVCAR-3	0	0	1.36	36.27	**106.25**	13.56	7.09	15.87	79.71	4.51
	OVCAR-4	1.91	0	0	39.23	70.61	2.93	10.	10.51	55.43	7.76
	OVCAR-5	0	0	3.84	0	51.75	3.90	0	0	34.65	0.61
	OVCAR-8	0	1.52	0	23.03	59.27	11.78	7.42	13.28	28.	1.51
	NCI/ADR-RES	0	2.54	0	1.26	68.61	10.50	13.46	7.72	29.61	4.70
	SK-OV-3	0	0	0	0	0	0	0	0	0	0
Renal Cancer	786-0	**---**	0	0		**100.28**	8.77	9.45	14.62	50.45	8.52
	A498	0	---	----	18.59	50.75	12.10	6.63	3.39	53.92	3.59
	ACHN	0	0	0	24.94	30.67	12.21	10.45	17.78	34.18	11.02

	CAKI-1	6.77	5.52	5.14	17.12	94.65	5.23	0	24.49	84.43	4.78
	SN12C	3.45	0	4.72	32.64	77.51	13.14	4.97	17.07	38.76	8.87
	TK-10	0	7.32	0	0	84.83	0	6.50	0	4.53	0
	UO-31	0	14.64	16.30	16.77	41.51	24.62	21.03	21.73	54.96	21.86
Prostate Cancer	PC-3	3.57	10.57	8.89	35.36	**135.88**	51.62	43.28	18.95	82.23	18.19
	DU-145	0	0	0	53.46	49.13	0	0	6.20	16.79	0
Breast Cancer	MCF7	0	7.93	6.36	26.70	76.79	48.47	56.29	36.38	67.26	26.75
	MDA-MB-231/ATCC	0	0	0	21.04	67.47	2.27	3.95	3.50	43.16	10.64
	HS 578T	0	1.60	0	2.23	22.06	6.41	1.03	5.01	12.58	0
	BT-549	0	2.46	0	9.43	64.50	38.28	7.73	26.81	89.68	18.41
	T-47D	2.05	0	4.18	27.33	**138.25**	.25	5.77	23.00	**106.25**	31.13
	MDA-MB-468	0.58	0	0	16.40	**100.39**	23.68	12.74	29.74	78.91	18.03

Structure-Activity Relationship (SAR)

Notably, the newly prepared [2.2]paracyclophane/thiazole conjugates showed significant anti-cancer activity. The disparity among the different derivatives may be attributed to the type of substitution on the thiazole ring; either on the nitrogen atom (compounds **139b-f**) or at position 2 (compound **190**). It is presumed that increasing thiazole flexibility through inserting a phenyl or benzyl group (compound **139b** and **139f**, respectively) into the structure can improve binding to the target protein and hence leads to higher antiproliferative activities against all tested cell lines. Interestingly, the other [2.2]paracyclophane/thiazole derivative **190** bearing pyridinyl amine moiety at position 2 of the thiazole ring reduces the activity apparent by the lower cytotoxicity.

***In vitro* Five Dose Full NCI 60 Cell Panel Assay**

NCI selected compound **139b** for a five-dose investigation against 60 human tumor cell lines that were incubated at five different concentrations (0.01, 0.1, 1, 10, and 100 μM) (Figure 30). The results were used to form log concentration vs growth% inhibition curves and three response parameters (GI_{50}, TGI, and LC_{50}) were calculated for each cell line (Table 27, chapter 5.2.4.3). The GI_{50} value (growth inhibitory activity) corresponds to the compound concentration resulting in a 50 percent decrease in net cell growth, the TGI value (cytostatic activity) is the compound concentration resulting in total growth inhibition (TGI), and the LC_{50} value (cytotoxic activity) is the compound concentration resulting in net 50% loss of initial cells at the end of the incubation period of 48 h.

The requirement for a compound's selectivity depends on the ratio obtained by dividing the full MID panel (the average sensitivity of all cell lines towards the test agent) (μM) by their subpanel MID (μM). Ratios between 3 and 6 refer to moderate selectivity; ratios above 6 indicate high selectivity towards the corresponding cell line, while compounds not meeting either of these criteria are rated non-selective.

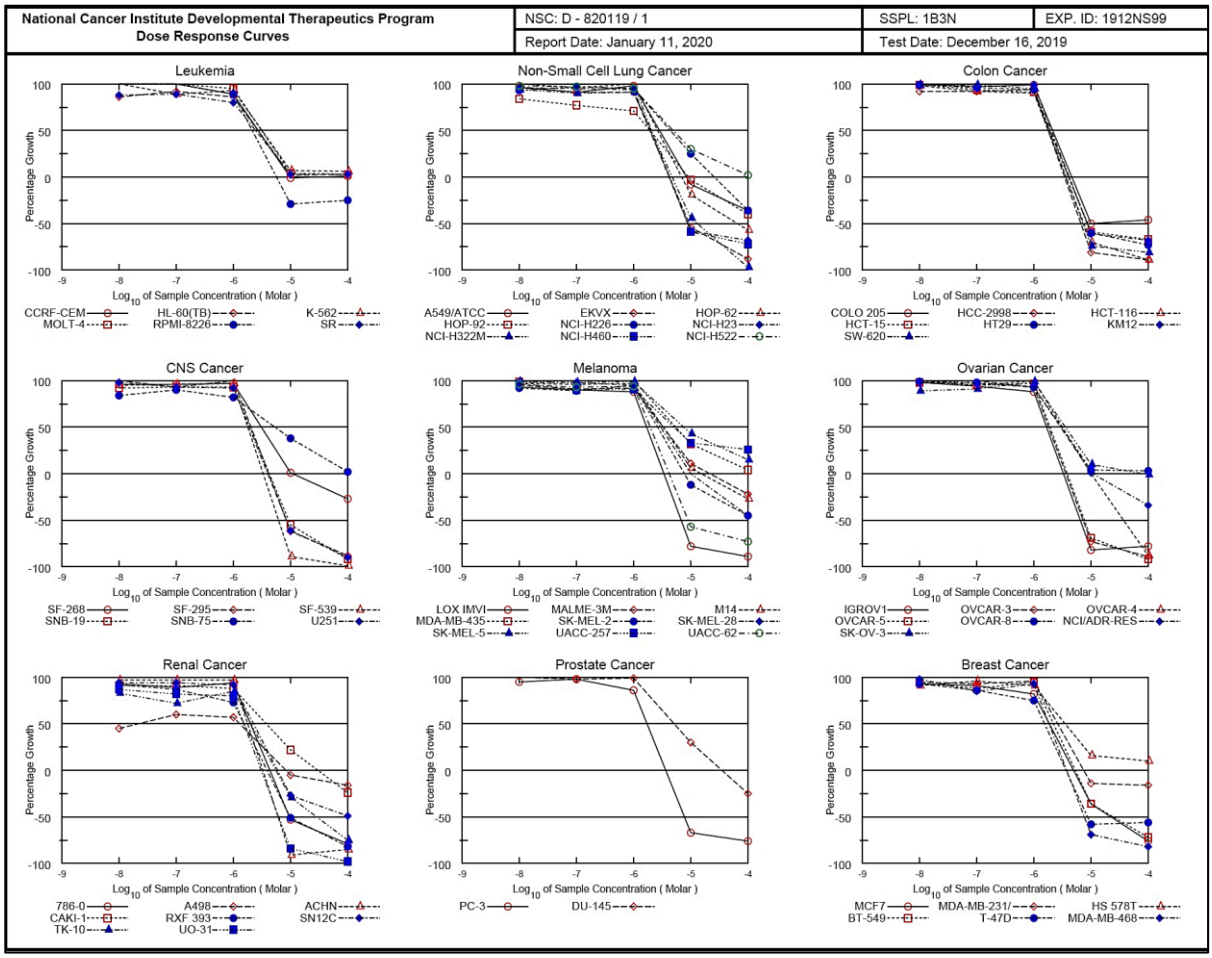

Figure 30: Dose-response curves of compound **139b** (Log_{10} of sample conc 0.01, 0.1, 1, 10, and 100 μM) against all nine different cancer cell line panels (leukemia, non-small cell lung, colon, CNS, melanoma, ovarian, renal, prostate and breast cancers). Results and images provided by NCI.

The compound under investigation (**139b**) showed remarkable anticancer activity against most of the tested cell lines representing nine different subpanels with GI_{50} range 1.52-7.56 μM (Table 27). The results indicate that **139b** shows high activity against renal cancer (RXF-393), melanoma (LOX IMIV), colon cancer (HCC-2998), non-small cell lung cancer (EKVX), and leukemia (RPMI-8226) with GI_{50} values of 1.52, 1.69, 1.78, 1.91 and 2.15 μM, respectively. An obvious sensitivity profile towards leukemia subpanel (GI_{50} values ranging from 2.15 to 3.15 μM), colon cancer subpanel (GI_{50} values ranging from 1.78 to 2.13 μM), breast cancer subpanel (GI_{50} values ranging from 1.54 to 1.87 μM), and ovarian cancer subpanel (GI_{50} values

ranging from 1.66 to 3.55 μM). In this context, compound **139b** was found to have a broad spectrum antitumor activity against the nine tumor subpanels tested with selectivity ratios ranging between 0.63-1.28 μM and 0.58-5.89 μM at the GI_{50} and TGI levels, respectively. Furthermore, it showed moderate selectivity toward prostate and colon cancer subpanels only with a selectivity ratio of 5.89 and 5.34 at the TGI level, respectively.

Evaluation of *In-vitro* Antiproliferative Activities Against Leukemia RPMI-8226 and SR

The antiproliferative investigation results against 60 cell lines at the NCI, which revealed the activity towards leukemia cancer, especially the leukemia cell lines RPMI-8226, and SR, encouraged the performance of further *in vitro* antiproliferative studies against those two cell lines. Compounds **139b-d, f,** and **190** were evaluated for their antiproliferative activity by performing MTT assays against a panel of two human tumor cell lines leukemia RPMI-8226 and SR with Colchicine as a reference. As shown in Table 9, the antiproliferative activities of the tested compounds were generally more pronounced against the two panels of leukemia cancer cells as compared with the reference. Compound **139b** exhibited the highest antiproliferation compared to the reference and the other tested compounds whereas it showed IC_{50} values of 1.61 and 1.11 μM better than Colchicine (i.e. the reference compound) of IC_{50} values of 4.05 and 1.81 μM against leukemia RPMI-8226 and SR, respectively. On the other hand, compound **139d** showed significant antiproliferative activity against the leukemia cell line RPMI-8226with an IC_{50} value of 3.17 μM, which is lower than the reference IC_{50} value of 4.05 μM. This may be attributed to the electron-withdrawing substitution of the phenyl and benzyl groups that both compounds **139b** and **139f** have, which might positively affect cell permeability. Compound **139f** showed to Colchicine comparable IC_{50} values of 4.62 and 2.02 μM.

Table 9: MTT assay for the antiproliferative IC_{50}± SEM (μM) activity of compound **139b-d**,**f**, **190,** and Colchicine. Results provided by Dr. E. M. N. Abdelhafez.

Compound	Cytotoxicity **IC_{50} (μM)**	
	RPMI-8226	L.SR
139b	1.61±0.04	1.11±0.03
139c	17.81±0.48	22.06±0.60
139d	3.17±0.08	5.04±0.13
139f	4.62±0.12	2.02±0.06
190	9.96±0.27	4.84±0.13
Colchicine	4.05±0.11	1.81±0.04

Evaluation of *in vitro* Tubulin Polymerization Inhibitory Activity

To investigate whether the antiproliferative activities of compounds **139b-d, f,** and **190** are based on interactions with tubulin, an ELISA assay for ß-tubulin was performed, which evaluates the ability to inhibit tubulin polymerization at the determined IC_{50} concentrations. The results revealed that all tested compounds (**139b-d,f,** and **190**) show tubulin polymerization inhibitory activity with Colchicine as reference (Table 10).

As in preceding experiments, compound **139b** showed the highest ability to inhibit tubulin polymerization with an IC_{50} value of 4.97 µM compared to the reference with an IC_{50} value of 3.76 µM and other tested compounds. Whereas compounds **139d** and **190** showed remarkable tubulin polymerization inhibition (with IC_{50} values of 6.61 and 8.38 µM) however, **139c** displayed relatively weak inhibition with IC_{50} value (14.79 µM). The results are in agreement with the previously mentioned results in tests for anti-proliferative activity.

Table 10: A) *In vitro* tubulin polymerization inhibitory activity for compounds **139b-d**,**f** and **190,** and Colchicine as a reference, B) Inhibition of tubulin polymerization displaying IC_{50}± SEM (µM) for compounds **139b-d**,**f,** and **190** and Colchicine as reference. Results provided by Dr. E. M. N. Abdelhafez.

A

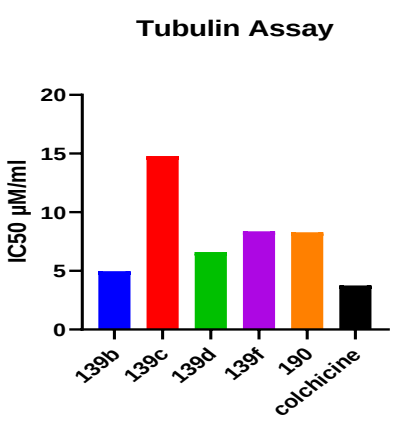

B

Compound	Tubulin polymerization inhibition IC_{50} (µM)
139b	4.97±0.11
139c	14.79±0.32
139d	6.61±0.14
139f	8.38±0.18
190	8.28±0.18
Colchicine	3.76±0.08

Cell Cycle Analysis

Cell growth can be controlled by interfering with the cell cycle control mechanisms. During one cell cycle, the G2/M checkpoint is a potential target for cancer therapy (see chapter 5.2.4.3), because of this checkpoint. Prevents DNA-damaged cells from entering mitosis and allows for the repair of DNA that was damaged in late S or G2 phases before mitosis (Table 11).

Induction of cell cycle arrest is a common mechanism proposed for the cytotoxic effects of anticancer-drugs containing [2.2]paracyclophane/thiazole derivatives. The cell cycle analysis indicated that leukemia SR cells treated with compound **139b** showed a significant growth arrest at the G2/M phase compared to control cells, where the S phase progression of SR cells was substantially delayed (Figure 31).

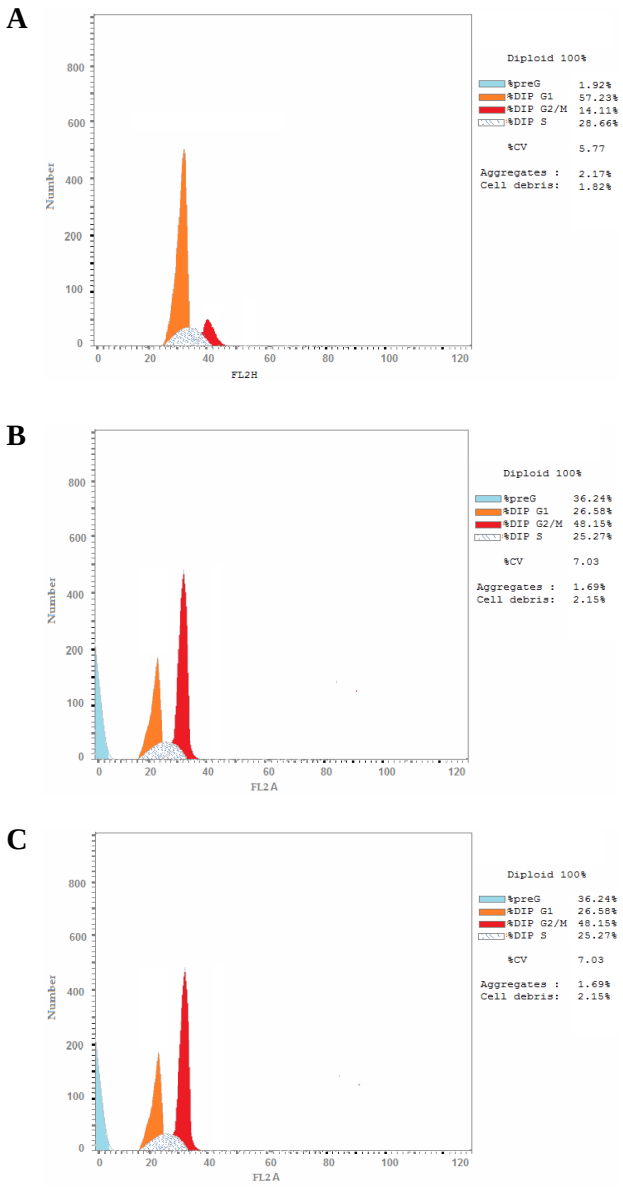

Figure 31: Cell cycle analysis of SR cells treated with Annexin PI at IC_{50}. Concentration representing growth arrest at the pre-G1 (G0) and G2/M phases. A) Untreated cells, B) Treated cells with Colchicine, C) Treated cells with **139b**. The test was repeated three times, **139b,** and the reference was incubated for 24 h (2 x 10^5 cells/well) at 37°C. Results provided by Dr. E. M. N. Abdelhafez.

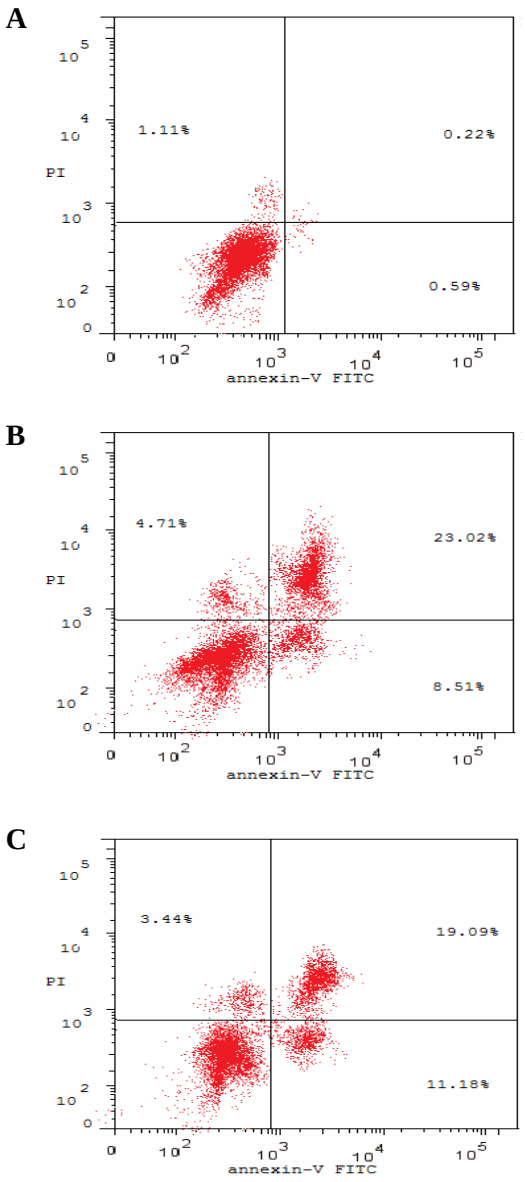

Figure 32: Contour diagram of Annexin V/PI Flow Cytometry against SR cancer cell line. A) Untreated cells, B) Treated cells with Colchicine, C) Treated cells with **139b**. The test was repeated three times. Incubation for 24 h was analyzed by flow cytometry after double staining the cells with Annexin V/PI. Results provided by Dr. E. M. N. Abdelhafez.

The results of Annexin V/PI flow cytometry of SR cells after treatment with **139b** at IC_{50} concentration (1.11 µM) showed an increase in the percentage of the necrotic cells in late apoptosis to 19% (upper right quadrant of the cytogram) (Figure 32). Hence, compound **139b** showed a considerable ability to dissipate cell membrane integrity. Whereas the lower right quadrant illustrating the early apoptotic cells which keep their membrane integrity indicates the ability of **139b** to initiate apoptosis.

Table 11: DNA content % using propidium iodide flow cytometry. Results provided by Dr. E. M. N. Abdelhafez.

Compound	DNA content %				
	%G0-G1	%S	%G2-M	%Pre G1	Comment
139b/SR	31.47	23.79	44.74 ± 0.1747***	33.71	cell growth arrest (G2/M)
Colchicine/SR	26.58	25.27	48.15 ± 1.000***	36.24	cell growth arrest (G2/M)
cont.SR	57.23	28.66	14.11 ± 0.1050	1.92	---

Compound 139b Induces Mitochondrial Depolarization and ROS Production

Mitochondria play an essential role in the propagation of apoptosis.[237] It is reported that, at an early stage, apoptotic stimuli are capable to modify the mitochondrial transmembrane potential ($\Delta\psi$mt). $\Delta\psi$mt was recorded by the fluorescence of the dye JC-1.20. Treatment SR cells with **139b** displayed a remarkable shift in fluorescence compared with control cells, explaining the depolarization of the mitochondrial membrane potential (Figure 33). The disruption of $\Delta\psi$mt is associated with the appearance of annexin-V positivity in the treated cells when they are in an early apoptotic stage. It is documented that the dissipation of $\Delta\psi$mt is characteristic of apoptosis and has been indicated with both microtubule-stabilizing and destabilizing agents in different cell types.[238] Induction of cell cycle arrest is a common mechanism proposed for the cytotoxic effects of anticancer drug-containing paracyclophane/thiazole derivatives. Mitochondrial membrane depolarization is associated with mitochondrial production of ROS.[239] Therefore, we investigated whether ROS production increased after treatment with the tested compounds.

The presented results in Figure 34, showed that **139b** induces the production of significant amounts of ROS (109.84%) in comparison to control cells and the Colchicine reference. This result is consistent with the dissipation of $\Delta\psi$mt described above.

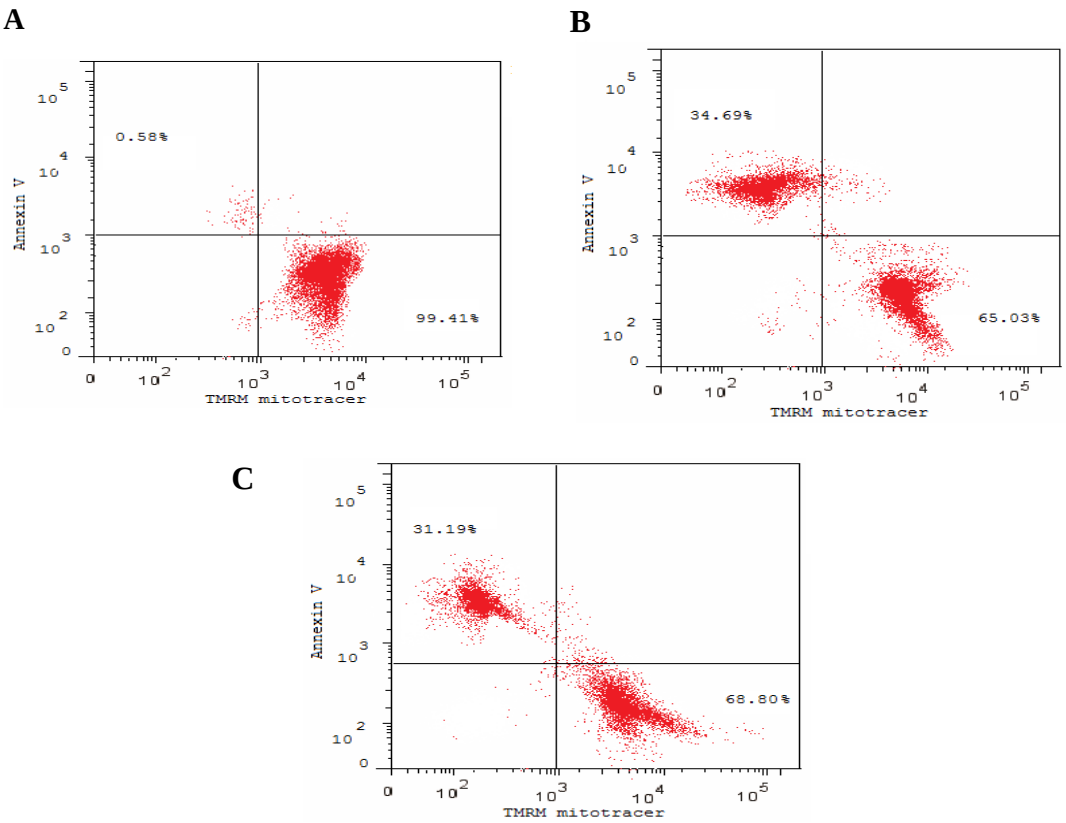

Figure 33: Contour diagram of Annexin V/PI Flow Cytometry illustrating induction of the loss of mitochondrial membrane potential ($\Delta\psi$mt) against SR cancer cell line; A) Untreated cells, B) Treated cells with Colchicine and C) Treated cells with **139b**. (B & C were performed on conc 20, 10, 5, 2.5, 1.2, 0.63, 0.31 ng/ml). The test is repeated three times and the substrate was incubated at 37 °C in dark within 15–30 min. Results and images provided by Dr. E. M. N. Abdelhafez.

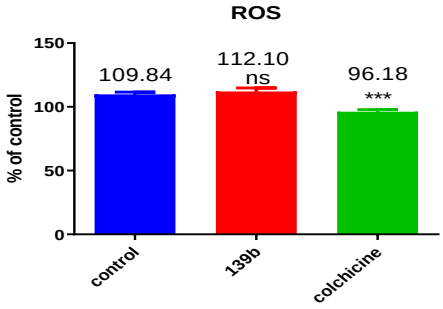

Figure 34: Mitochondrial production of ROS in SR cells with **139b** and Colchicine reference compared to control. Mean+/- standard deviation plotted for 3 replicates per condition Results Significantly different from control at ***p < 0.05. the substrate was incubated for 30 minutes at 37 °C protected from light. Results and images provided by Dr. E. M. N. Abdelhafez.

Effect of Compound 139b on Multidrug-Resistant Leukemia SR Cells

It was reported that in many cancer cells overexpression of P-glycoprotein (P-gp), which results in innate or acquired resistance to chemotherapy, was observed.[240] By comparing the activity of **139b** with the reference compound (Table 12) against multidrug-resistant (MDR) Leukemia SR cells to assess the ability of the drug to overcome Pgp-mediated MDR. Table 12 shows that compound **139b** (1.285 ng/mL, 1.15-fold change) has better resistance indices comparable to

control (1.121 ng/mL, 1-fold). The activity in the P-glycoprotein [241] overexpressing cell line demonstrated that **139b** is an important substrate drug.

Table 12: In vitro growth inhibitory effects of **139b** in comparison to Colchicine on multidrug-resistant leukemia cell line (MDR cell). Results provided by Dr. E. M. N. Abdelhafez.

Compound Code	IC_{50} ± SEM (ng/mL) (n =3)	
	Pgp-mediated MDR	Fold change
139b/**SR**	1.285 ± 0.06	1.15
Colchicine/**SR**	1.726 ± 0.05	1.54
cont. **SR**	1.121 ± 0.05	1

Effect of 139b on Caspase-3 Activation

Since caspase-3 plays an important role in the spreading of the apoptotic signal after cells have been exposed to antimitotic compounds,[242] the effect of compound **139b** on a caspase-3 activated enzyme in Leukemia SR cells was evaluated in ELISA assays, which were replicated three times. References as well as **139b** were incubated for 30 min at room temperature in the dark. The results revealed that **139b** is a potential caspase-3 activator recognizable by the 8.84-fold increase (471.2 ng/mL) in the level of active caspase 3 compared to the control which is even higher than for Colchicine with a concentration of 428.9 ng/mL (8.05-fold) (Table 13).

Table 13: Caspase-3 conc and fold change levels for compounds **139b** and Colchicine (pg/mL) ± SD on leukemia SR cell line. Results provided by Dr. E. M. N. Abdelhafez.

Compound	Caspase 3	
	Conc pg/mL	Fold change
1b/SR	471.2 ± 6.11	8.84
Colchicine/SR	428.9 ± 5.47	8.05
Control SR	53.28 ± 1.09	1

Effect of 139b on BAX and Bcl-2 Proteins

The proteins of the Bcl2 family[243] play a major role in controlling apoptosis through the regulation of mitochondrial processes and the release of mitochondrial proapoptotic molecules that play an important role in the cell death pathway.[244] Compound **139b** caused a 7.98-fold upregulation of the BAX protein (Table 14), while it clearly showed levels of the anti-apoptotic protein Bcl2 up to 0.59-folds compared to the control untreated cells (Figure 35).

Table 14: Bax and Bcl-2 conc and fold change levels for compounds **139b** and Colchicine (pg/mL) ± SD on leukemia SR cell line. Results provided by Dr. E. M. N. Abdelhafez.

Compound	BAX		Bcl2	
	Conc (pg/mL)	Fold Change	Conc (ng/mL)	Fold Change
139b/SR	359 ± 3.830 ***	7.98	5.045 ± 0.1918 ***	0.59
Colchicine/SR	341.8 ± 4.310 ***	7.60	4.101 ± 0.1441 ***	0.48
cont.SR	44.96 ± 1.270	1	8.569 ± 0.1565	1

Results Significantly different from control at ***p < 0.05.

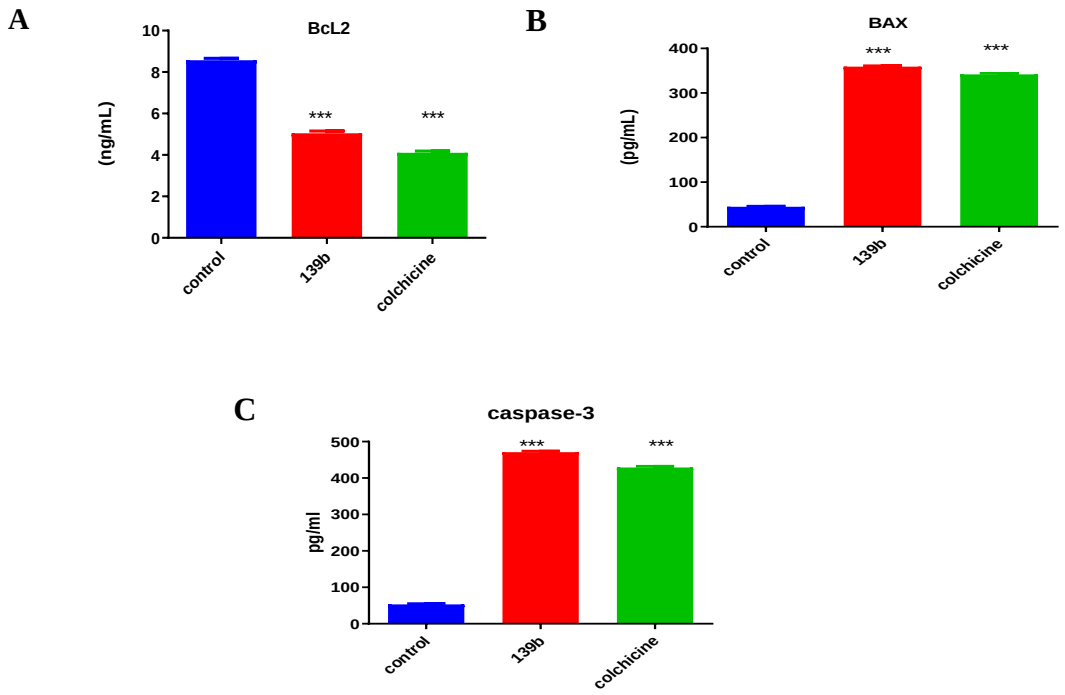

Figure 35:Concentrations of A: Bcl2 (conc; 32,16,8,4,2,1,0.5 ng/mL); B: BAX (conc; 2000, 1000, 500, 250, 125, 62.5, 31.25 pg/mL)and C: caspase-3 expression (2500, 1250, 625, 313, 156, 78, 39 pg/mL)) for **139b** and Colchicine on Leukemia SR cell line relative to control. Results provided by Dr. E. M. N. Abdelhafez.

Docking Studies

The molecular modeling of possible binding modes for the newly synthesized thiazole/paracyclophane hybrids **184b-d,f**, and **185** and Colchicine as a reference was done to predict the binding interactions with β-tubulin at the Colchicine binding site with structural data obtained from the protein data bank (PDB: 3HKC). The docking study was carried out using the Molecular Operating Environment (MOE®) version 2014.09 with Colchicine as a reference as a validation of the method. The theoretical predictions in the molecular docking study are in agreement with the experimentally observed tubulin polymerization inhibition of highly active derivatives such as **184b, 184c, 184d,** and **184f**. All derivatives were successfully docked into the Colchicine binding site of β-tubulin. The binding free energies from the major docked poses are listed in Table 15 and the most favorable poses of the tested compounds are

shown in Figure 36-41. Most of the tested compounds have high binding affinities to the enzyme as the binding free energy (*Δ*G) values range from −0.5 to −3.4 kcal/mol comparable to the reference Colchicine (*Δ*G = −0.6 to −2.3 kcal/mol). The docking result for the reference compound Colchicine is consistent with the mode of action of these thiazole/paracyclophane derivatives (Table 15).

Table 15: Energy scores for the complexes formed by the tested compounds **139a-d**,**f,** and the reference Colchicine in the active site of the β-tubulin enzyme (PDB: 3HKC). Results provided by Dr. E. M. N. Abdelhafez.

Compound	S Score	*Δ*G (kcal/mol)	Ligand-Receptor Interaction		
			Residue	Type	Length (Å)
Colchicine	−5.62	−3.4	GlU71	H-donor	3.16
		−0.5	Mg601	metal	2.61
139b	−7.05	−2.2	Mg601	Metal	2.00
		−0.6	ALA247	pi-H	4.17
139c	−6.94	−1.0	GLU71	H-donor	3.90
		−2.1	Mg601	metal	2.51
		−0.7	ARG 2	pi-H	4.69
139d	−6.43	−2.0	GLN11	H-acceptor	3.09
		−2.2	Mg601	metal	2.33
139f	−7.16	−0.9	ASP245	H-donor	3.27
		−2.3	ARG 2	H-acceptor	3.41
		−0.9	GLU71	pi-H	3.98
190	−6.29	−1.8	Mg601	metal	2.40
		−0.7	TYR224	pi-H	3.79
		−0.7	ALA247	pi-H	4.50

*Δ*G (Kcal/mole)[a]; The binding free energies.

The 2D diagram shows crucial interactions of ALA-247, TYR224, and Mg601 with the [2.2]paracyclophane ring, the thiazole ring, and the ester C=O functionality. Moreover, stabilization of the reference Colchicine within the active site is achieved through one strong hydrogen bond with the amino acid GLU71 and metal intercalation with Mg601. Docking results with the Colchicine binding site revealed that most of the tested compounds show good binding to the enzyme and make several interactions comparable to that of the reference Colchicine (Figure 36). Compounds **139b**, **139c**, **139d,** and **190** exhibits the same interaction as the reference with Mg601, additionally, both **139c** and **139f** showed hydrogen bonding interaction with GLU71 (Figure 37-41). On the other hand, compound **139c** possesses stronger interactions than the reference. It interacts with the same amino acids and with one additional H-Pi bond with ARG2 (Figure 38), however, compounds **139b** and **190** display extra H-Pi interaction with ALA247 (Figure 37-41). Compound **190** (Figure 41) shows no hydrogen

binding interactions with the amino acid residue GLU71, but an additional H-Pi interaction with TYR224.

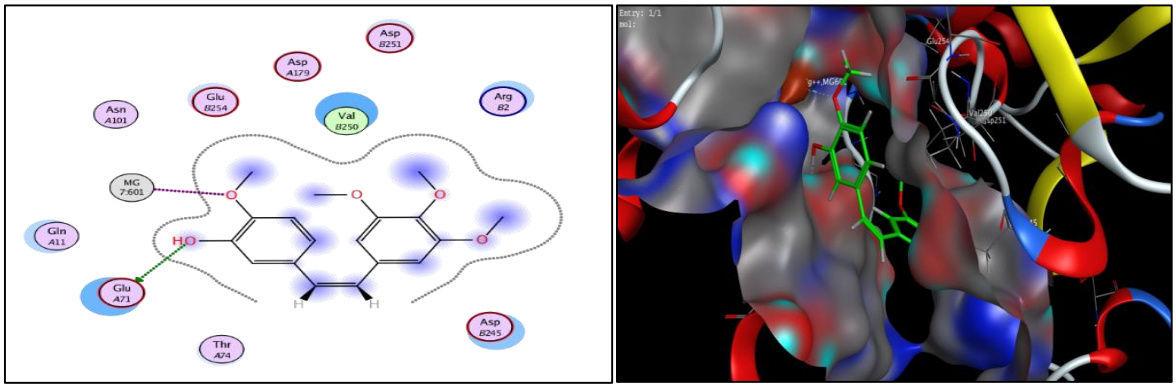

Figure 36: 2D and 3D diagrams illustrate the binding modes of the reference Colchicine interacted with the Colchicine binding site of β-tubulin. Results provided by Dr. E. M. N. Abdelhafez.

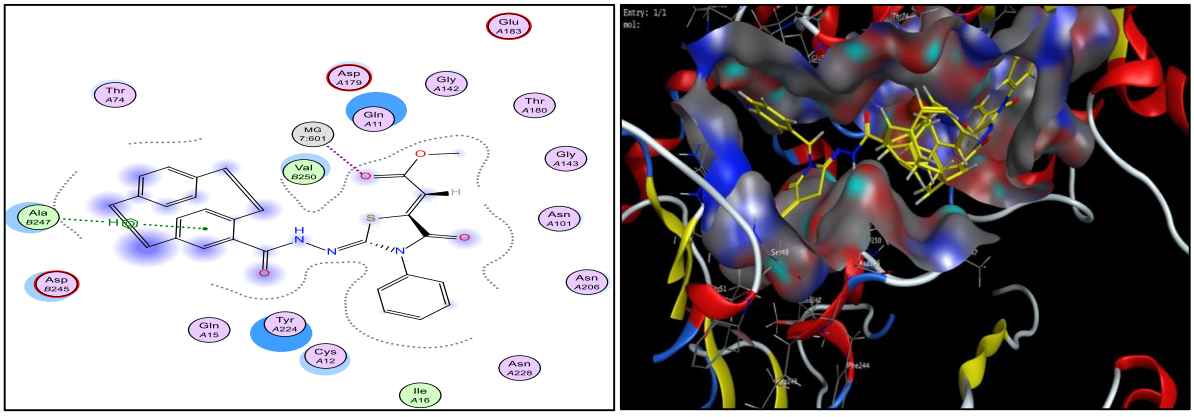

Figure 37: 2D and 3D diagrams illustrate the binding modes of **139b** interacted with the Colchicine binding site of β-tubulin. Results provided by Dr. E. M. N. Abdelhafez.

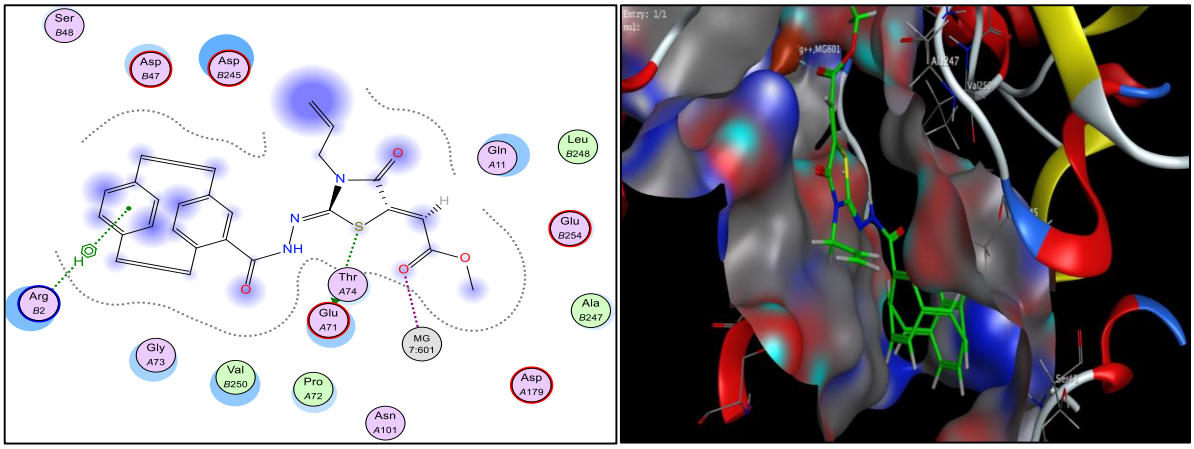

Figure 38: 2D and 3D diagrams illustrate the binding modes of **139c** interacted with the Colchicine binding site of β-tubulin. Results provided by Dr. E. M. N. Abdelhafez.

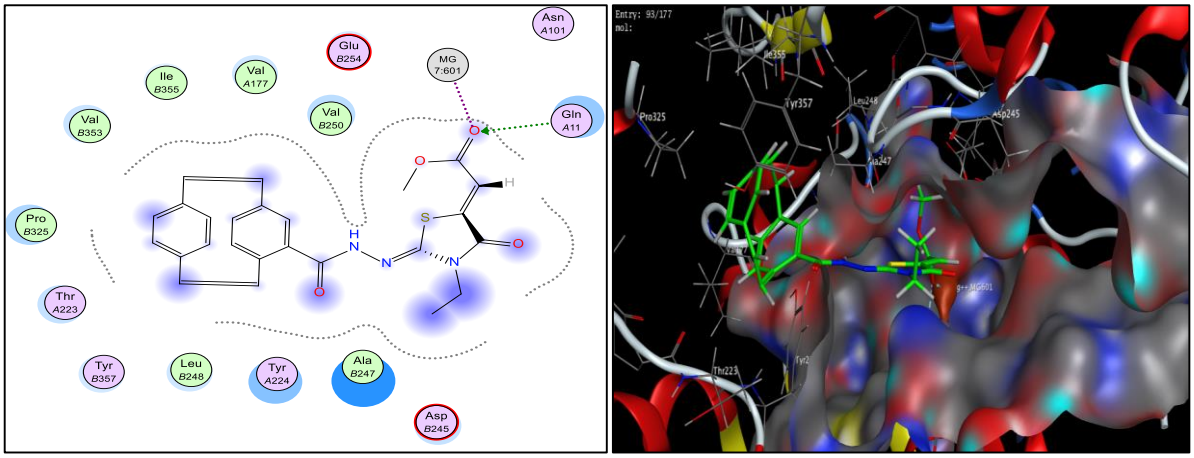

Figure 39: 2D and 3D diagrams illustrate the binding modes of **139d** interacted with the Colchicine binding site of β-tubulin. Results provided by Dr. E. M. N. Abdelhafez.

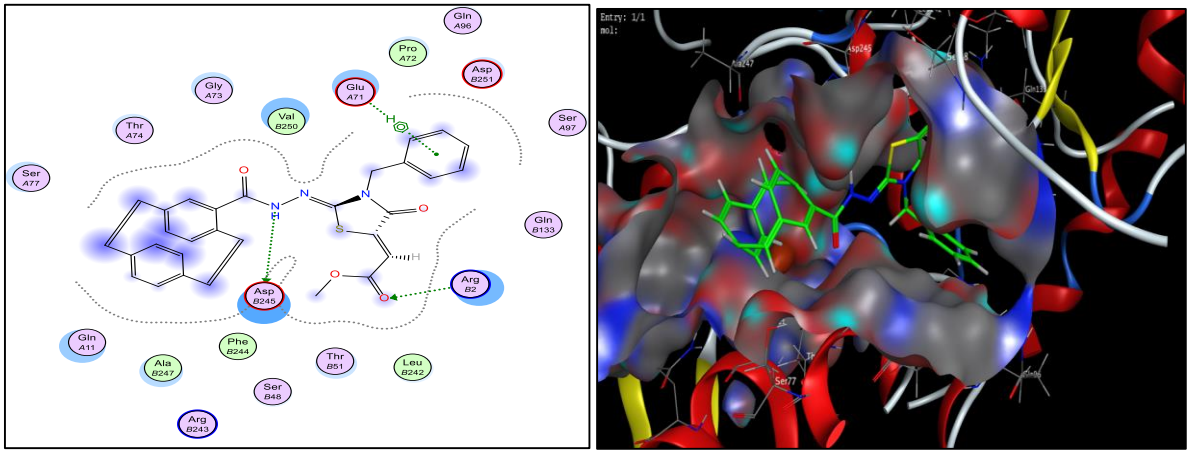

Figure 40: 2D and 3D diagrams illustrate the binding modes of **139f** interacted with the Colchicine binding site of β-tubulin. Results provided by Dr. E. M. N. Abdelhafez.

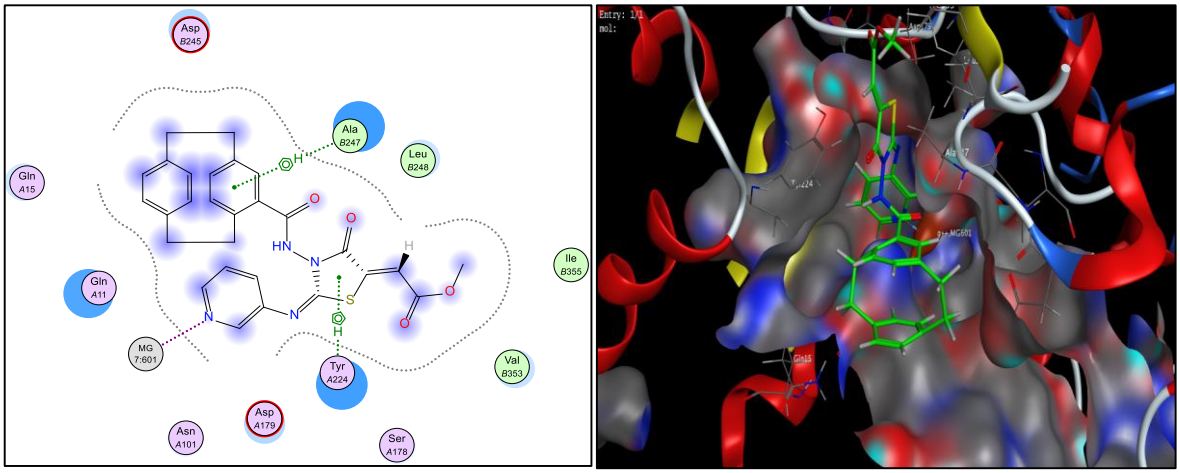

Figure 41: 2D and 3D diagrams illustrate the binding modes of **190** interacted with the Colchicine binding site of β-tubulin. Results provided by Dr. E. M. N. Abdelhafez.

In summary, the compounds methyl 2-(2-(4'-[2.2]paracyclophanyl)-hydrazinylidene)-3-substituted-4-oxothiazolidin-5-ylidene)acetates **139b-f** and methyl 2((*E*-3-[4-[2.2]para-cyclophanoylamido-4-oxo-2-(pyridine-3-ylimino)thiazolidin-5-ylidene)acetate (**190**) were synthesized successfully and screened against 60 cancer cell lines. Since these compounds showed moderate to high activity as anticancer agents, further investigations regarding the synthesis and biology of [2.2]paracyclophane-heterocyclic compounds will be performed to prove the hypothesis that paracyclophane/thiazole conjugates operate through tubulin polymerization inhibition. The obtained results indicated that compound **139b** could be considered a good pharmacophore for further medicinal study.

3.4.2. Design, Synthesis, Molecular Docking, and Mechanistic Studies of [2.2]Paracyclophanyldihydronaphtho[2,3-*d*]thiazoles and thiazolium Bromides [5]

3.4.2.1. Design and Synthesis

1,4-Naphthoquinones are common in various natural products [245-249] and present in a variety of biologically and pharmaceutically applicable compounds.[250] Derivatives of 1,4-naphthoquinone are used as antifungal,[251] antibacterial,[252], and antitumor agents.[253] The chemistry of quinone-annulated heterocycles is highly dependent on the substituents at the quinone moiety. Compounds such as daunorubicin (**I**) and mitoxantrone (**II**) (Figure 42) show potent anti-tumor activities (Figure 42).[254-255] Pterocaryquinone was isolated from *Pterocarya tonkinesis* and shows activity toward mouth cancer.[256] In the search for agents that have better and wider reactivity range, pharmacological properties, and low side effects, it seemed quite appealing to incorporate heterocyclic rings with at least two heteroatoms (e.g. thiazole).[257]
Various therapeutic agents with incorporated thiazole scaffolds such as compounds **III** and **IV** (Figure 42) have been widely investigated for their antitumor activity.[258-259] As previously described, compound **139b** in series **I** (Figure 42, see section 3.4.1) exhibits antiproliferative activity against different human tumor cell lines with GI_{50} values in the range 0.03-2.38 μM. Additionally, it confines viable cells in the G2/M phase and markedly inhibits *in vitro* CDK1 activity.[260] Deregulation of the cell cycle is one of the characteristics of tumor formation and progression.[261]

[5] Excerpts of this chapter were already published in
A. A. Aly, S. Bräse, A. A. Hassan, N. K. Mohamed, L. E. A. El-Haleem, M. Nieger, E. M. N. Abdelhafez, *Molecules,* **2020**, *25(25)*:5569
.

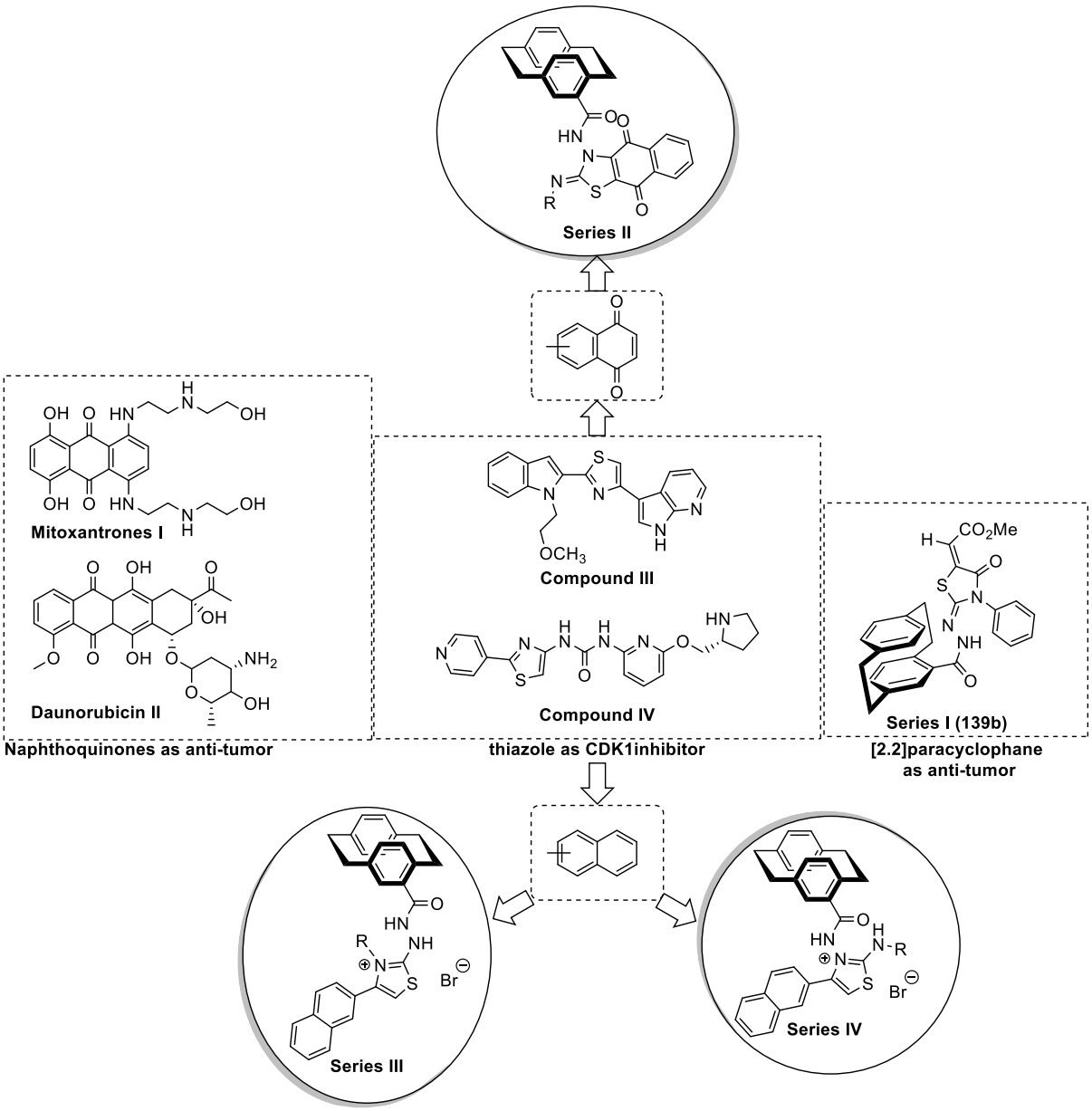

Figure 42: Reported antitumor 1,4-naphthoquinones (**I**, **II**), thiazoles derivatives (**III**, **IV**), [2.2]paracyclophane thiazoles derivatives series **I** (**139b**), and the new designed compounds series **II** (**140b-f**), series **III** (**141b-d,f**) and series **IV** (**196**).

Human kinases remain interesting targets in oncology, cyclin-dependent kinases (CDKs) are a class of serine/threonine protein kinases that regulates the temporal progression of cells through the cell cycle.[262] To date, 21 different CDKs (1−11a, 11b−20) have been identified in the human genome and they can be classified into two main categories based on their primary roles.[263-264] CDK1, CDK2, CDK4, and CDK6 have been found to regulate the cell cycle progression upon binding to cyclin proteins. CDK1 forms a complex with cyclin A/B and regulates phosphorylation of cytoskeleton proteins involved in mitosis.[258] CDK1/CyclinB1 is a potential therapeutic target using novel selective small molecule inhibitors of CDK1/CyclinB1.[258]

A series of naphthothiazoldiones have been synthesized by the reaction of *N*-substituted thioureas with 2,3-dichloro-1,4-naphthoquinone.[265-266] Moreover, naphthothiazole-5-carboxamides were obtained from naphthalimides[267] as well as *N*-substituted-2-(methylamino)naphthoquinones that reacted with S_2Cl_2 and DABCO (1,4-diazobicyclooctane) to give 2,3-dihydronaphtho[2,3-*d*][1,3]thiazole-4,9-diones. Despite continuous interest in 1,4-naphthoquinones fused with heterocycles, only a limited number of naphthoquinothiadiazines have been known so far. Moreover, in the previous section, it was shown that the [2.2]paracyclophane derivatives **139b-f** display anticancer activity with cytotoxicity of 0.63-1.28 and 0.58-5.89 µM at the GI_{50} and TGI levels. Enlightened by the aforementioned information and in continuation of the efforts in probing for novel effective anticancer agents, three series of novel thiazole/[2.2]paracyclophane conjugates (Figure 42) were designed, synthesized, and investigated concerning their potency as new CDK1 inhibitors. Series **II** was designed by fusing a naphthoquinone moiety with a thiazole ring to explore the binding affinity of these novel compounds to the target enzyme. Whereas series **III** & **IV** bear naphthyl moieties attached to the thiazole with variant substitutions at *N*-thiazole (series **III**) or position 2 of the thiazole (series **IV**). By introducing different substituents to the three synthesized series a versatile molecular skeleton was provided which allows for structure-activity relationship exploration studies (Figure 42).[268]

The syntheses of series **II** were started by applying the Eschenmoser coupling interaction (Table 16), the extrusion of sulfur from organic thiones, and related systems. It is a useful method for the formation of carbon-carbon bonds in high yield.[269] The reaction of thioamides with mono-haloketones and the preparation of several heterocyclic rings as well as natural products *via* Eschenmoser's method has been also reported.[270] That encouraged to apply the reaction of [2.2]paracyclophanylhydrazinecarbothioamides **135b-f** with 2,3-dichloro-1,4-naphthoquinone (DCNQ) (**191**) under Eschenmoser contraction condition (Ph_3P, Et_3N, and CH_3CN and reflux), the reaction proceeded to give the fused thiazoles **140b-f** in 55-70% yield (Table 16).

The structure of the obtained products **140b-f** was confirmed by IR, NMR, and mass spectra in addition to HRMS (see chapter 5.2.4.2). Red crystals of **140e** were obtained with which the structure was confirmed by X-ray analysis (Figure 43). By comparing the NMR spectra with those of the derivatives **140b-d,f** the same structure was assumed.

Table 16: Reaction of **135b-f** with 2,3-dichloro-1,4-napthoquinone (**191**) under Eschenmoser contraction condition; synthesis of fused thiazoles **140b-f**.

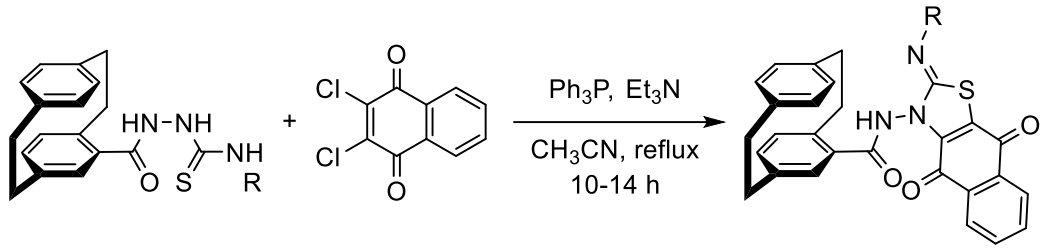

135b-f **191** **140b-f** (55-70%)

Entry	140b-f	R	Yield [%]
1	**140b**	Phenyl	70
2	**140c**	Allyl	67
3	**140d**	Ethyl	57
4	**140e**	Cyclopropyl	55
5	**140f**	Benzyl	65

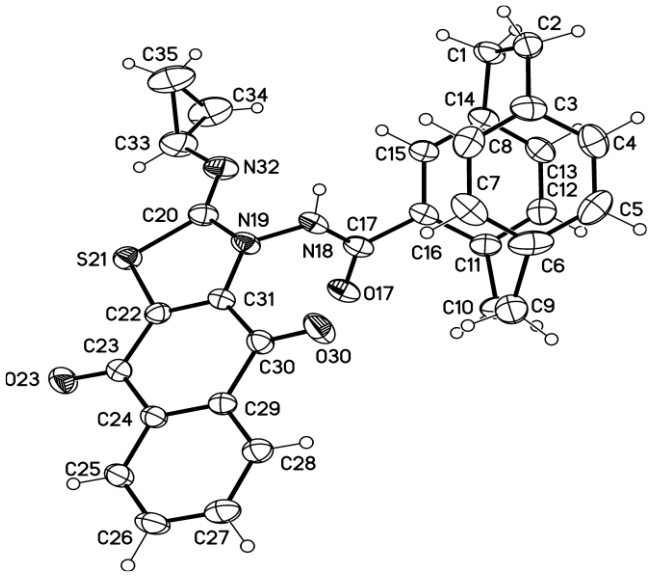

Figure 43: Molecular structure of compound **140e** identified according to IUPAC nomenclature as (*Z*)-*N*-(2-(cyclopropylimino)-4,9-dioxo-4,9-dihydronaphtho[2,3-*d*]thiazol-3(2*H*)-yl)-1,4(1,4)-dibenzenacyclohexaphane-12-carboxamide (minor disordered parts omitted for clarity, displacement parameters are drawn at 50% probability level).

The proposed mechanism for product formation shows an initial formation of zwitterion salt **192**. Subsequently, the sulfur lone pair in **135b-f** attacks the positively charged carbon in **192**, and by the elimination of Ph_3P, the intermediate **193** is obtained (Scheme 40). The neutralization and elimination of one HCl molecule in the presence of Et_3N then lead to intermediate **194**. Repeating the previous processes by nucleophilic attack of Ph_3P and elimination of the second molecule of HCl in the presence of Et_3N gives compounds **140b-f** (Scheme 40).

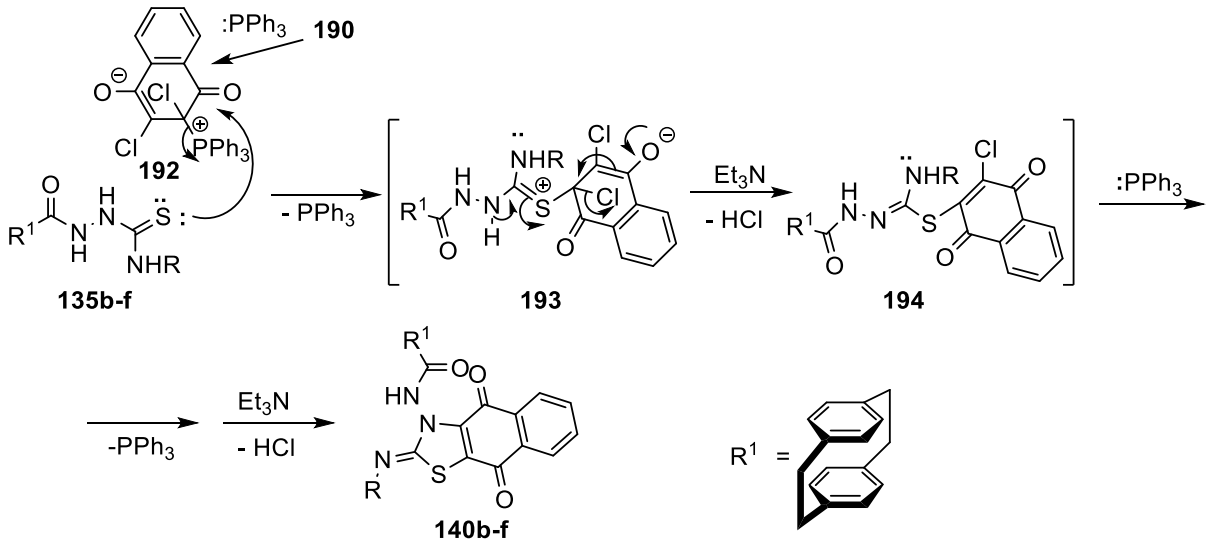

Scheme 40. Mechanism describes the formation of compounds **187b-f** under Eschenmoser contraction condition.

Furthermore, to prepare series **III** and **IV** compounds **135b-f** were reacted with 2-bromo-1-(naphthalene-1-yl)ethanone (BNE) (**195**) in ethyl acetate under standard ambient conditions, yielding compounds **141b-d,f**. Interestingly, the reaction of compound **135e** with **195** gave the regioisomer **196** in 60% yield (Table 17). The structure of compounds **141b-d,f,** and **196** were proven by NMR, mass, and IR spectral data (see chapter 5.2.4.2). The structures of **141c** and **196** were confirmed by X-ray structure analysis as shown in Figure 44.

Table 17: Reaction of **135b-f** with 2-bromo-2′-acetonaphthone (**195**); synthesis of thiazole derivatives **141b-d,f** or **196**.

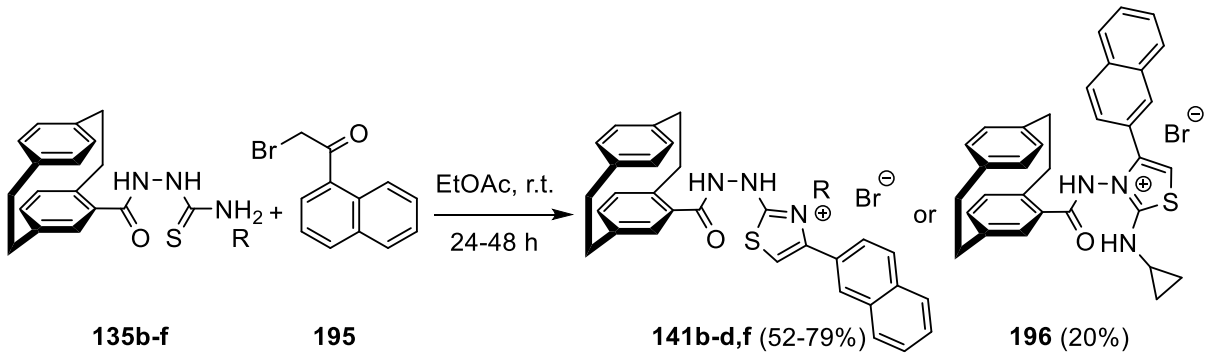

Entry	**141b-d,f** and **196**	R	Yield [%]
1	**141b**	Phenyl	79
2	**141c**	Allyl	52
3	**141d**	Ethyl	52
4	**141f**	Benzyl	61
5	**141**	Cyclopropyl	20

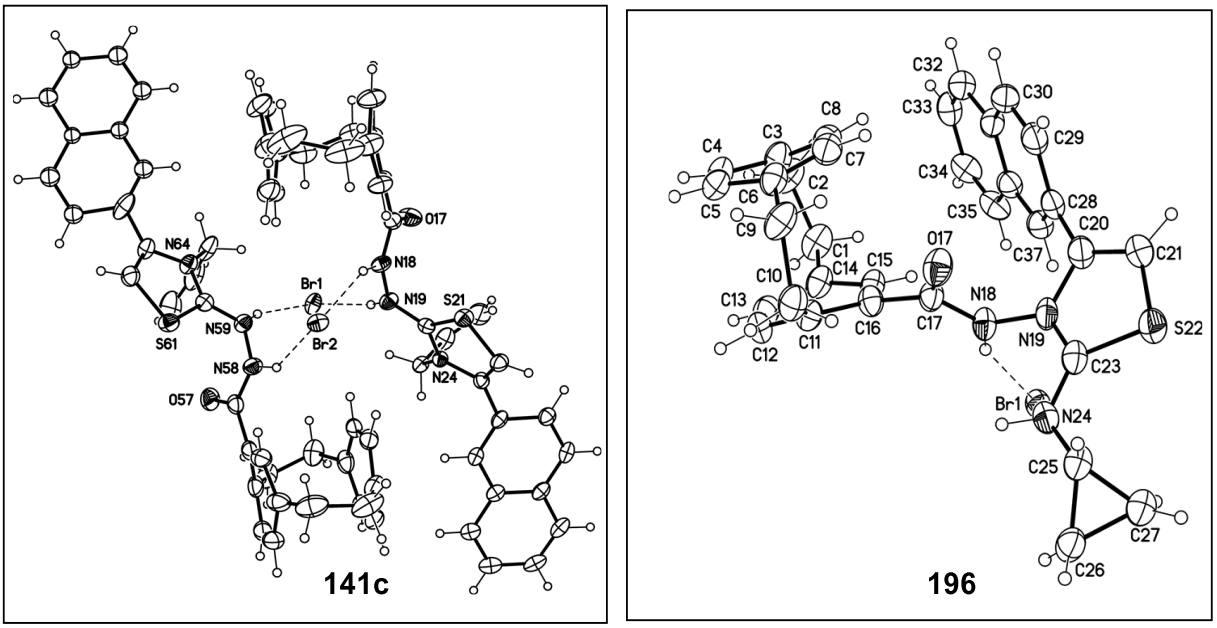

Figure 44: Molecular structure of the dimer of compound **141c** identified according to IUPAC nomenclature as 2-(2-(1,4(1,4)-dibenzenacyclohexaphane-1^2-carbonyl)hydrazineyl)-3-allyl-4-(naphthalen-2-yl)thiazol-3-ium bromide (displacement parameters are drawn at 50% probability level) and **196** identified according to IUPAC nomenclature as 3-(1,4(1,4)-dibenzenacyclohexaphane-1^2-carboxamido)-2-(cyclo-propylamino)-4-(naphthalen-2-yl)thiazol-3-ium bromide (minor disordered parts omitted for clarity, solvent omitted for clarity; displacement parameters are drawn at 30% probability level).

The mechanism which involves the formation of **141b-d,f** (Scheme 41) started with the initial addition of the sulfur lone pair to the electrophilic carbon of **195** to obtain the zwitterion salt **197**. Elimination of HBr from the intermediate **197** gives **198**. Two routes were then suggested, (a) in which cyclization process existed from the amine-*N*H^3 to the carbonyl carbon of **198** to give salt **199** which *via* neutralization gave intermediate **200** (Scheme 41). Then, the elimination of water from **200**, followed by salt formation with HBr gave the products **141bd,f** (Scheme 41). While route (b) depicts the other type of cyclization process that occurred *via* intermediate **198** by the hydrazinyl-*N*H^2 lone pair. By repeating the previously mentioned steps on route (a), compound **196** could be formed *via* intermediate **201** (Scheme 41).

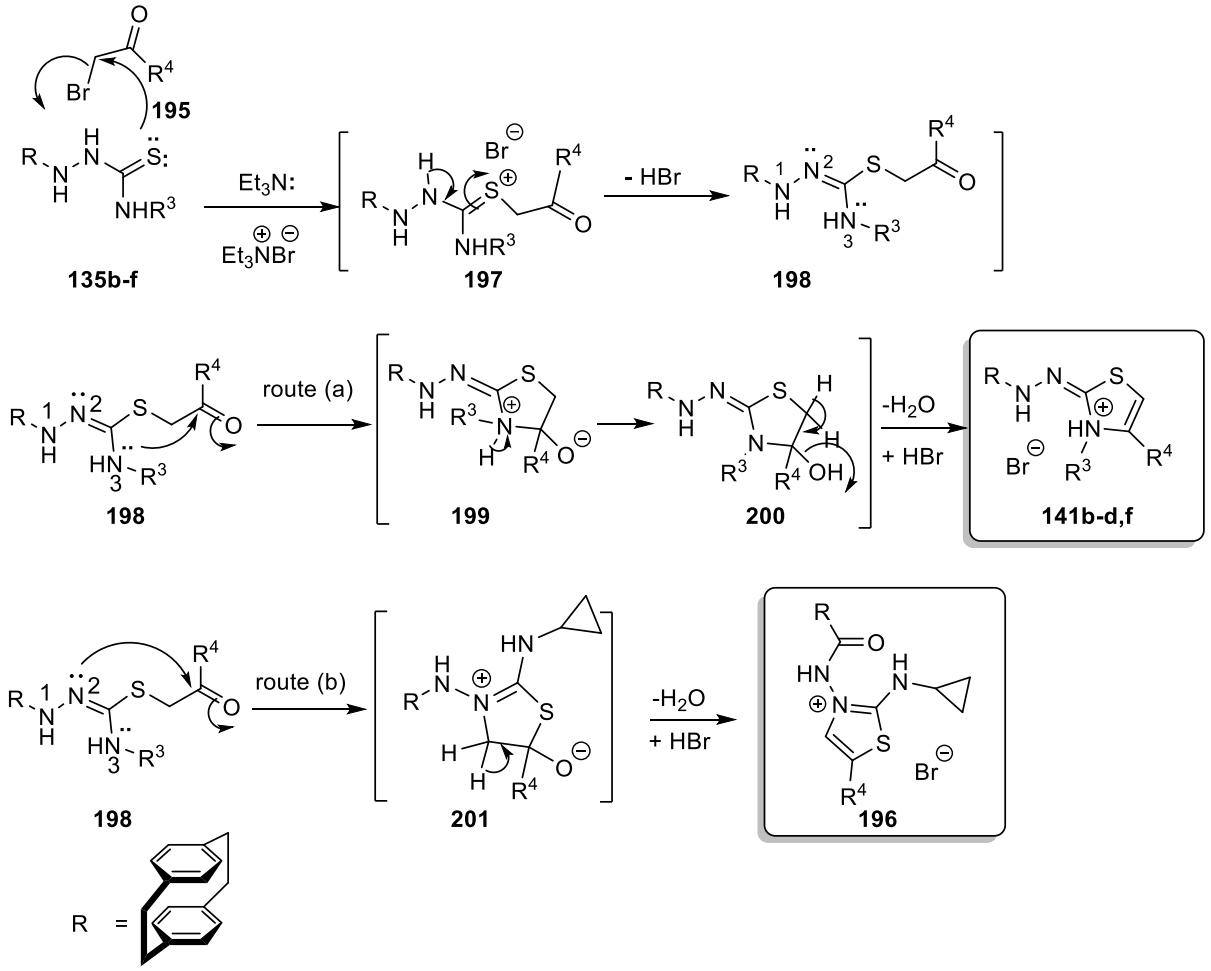

Scheme 41. Mechanism describes the formation of compounds **141b-d**,**f,** and **196**.

3.4.2.2. Screening, Molecular Docking, and Mechanistic Study

The bioactivity screening of compounds **140b-f**, **141b-d,f,** and **196** was done by the National Cancer Institute (NCI, USA).[236] Molecular docking and mechanistic study were performed in collaboration with Dr. E. M. N. Abdelhafez. All experiments in this section were also conducted by Dr. E. M. N. Abdelhafez.

Screening Against 60 Cancer Cell Lines at NCI

Compounds **140b-f**, **141b-d,f,** and **196** were added to the culture at a single concentration (10^{-5} M) and the cultures were incubated for 48 h. Endpoints were determined by adding a protein-binding dye, SRB. Results for each of the tested compounds were reported as the percentage of growth of the treated cells when compared to the untreated control cells. The percentage of growth was evaluated spectrophotometrically versus controls not treated with test agents. All experiments were repeated three times. The results provided NCI of naphtho-thiazole/[2.2]paracyclophane conjugates recorded in Table 18 indicate that the five compounds **140b-f** displayed very potent anticancer activity with complete cell death (% of growth

inhibition ≥ 100%) on most of the tested cancer cell lines. Interestingly, compounds **140c** and **140d** showed complete cell death on all nine cancer cell panels with cell growth inhibition percentages in a range of 103.65-198.49% and 103.66-197.05%, respectively. Additionally, compound **140e** lead to complete cell death on three cancer cell panels (Colon cancer, CNS cancer, and Melanoma) with cell growth inhibition percentages in the range of 109.10-193.24%. Compounds **140b**, **140f** as well as **141c** caused complete cell death on only one panel (Melanoma) with cell growth inhibition percentages in the range of 110.14-172.49% while they exhibited moderate cytotoxic activity toward the other tested cell lines. On the other hand, compounds **141b**, **141d**, and **141f** shower lower activity. Compound **141d** had significant cytotoxicity against melanoma SK-MEL-5 and breast cancer T-47D with inhibition (%) of 83.18 and 75.60%, respectively. However, it showed moderate activity against the leukemia cell line RPMI-8226 and the colon cancer cell line HCT-15 with cell growth inhibition (%) of 62.22% and 59.89% respectively. Moreover, Compound **141f** showed moderate inhibition against the leukemia K-562 cell line, the colon cancer cell line HCT-15, and the prostate cancer cell line PC-3 with inhibition percentages of 54.53%, 63.36%, and 54.49%, respectively. Meanwhile, compound **141b** displayed weak cell growth inhibition activity against most of the tested cancer cell lines.

Based on the results displayed in Table 18, it can be deduced that the replacement of the naphthyl group by naphthoquinone group in compounds **140b-f** causes the outstanding anticancer activity. This could be attributed to the increase of the binding to the target protein due to the presence of two additional oxygen groups in quinone moiety and this encouraged further investigations of the compounds in a molecular docking study.

Table 18: Growth inhibition of compounds **140b-f** and **141b-d**,**f** at (conc. 10^{-5} M) against different cell lines. Results provided by NCI.

Panel/ Cell Line		**140b**	**140c**	**140d**	**140e**	**140f**	**141b**	**141c**	**141d**	**141f**
Leukemia	CCRF-CEM	20.15	**103.65**	**116.03**	77.39	59.23	7.77	58.83	48.46	49.02
	HL-60(TB)	8.41	**120.12**	**118.34**	97.61	72.97	3.67	50.76	46.34	17.11
	K-562	22.24	**112.34**	**128.49**	74.12	51.17	14.31	65.03	58.59	54.53
	MOLT-4	16.68	**115.46**	**132.80**	91.47	78.95	11.35	54.75	43.07	32.30
	RPMI-8226	24.80	**127.65**	**133.56**	80.48	41.03	9.83	74.17	62.22	37.81
	SR	38.87	**108.54**	**103.66**	70.59	51.66	11.99	60.88	45.35	53.27
Non-Small Cell Lung Cancer	A549/ATCC	35.96	76.74	**138.85**	32.30	20.00	2.64	43.90	28.88	12.65
	EKVX	29.59	**120.17**	**161.32**	32.49	11.57	7.32	41.82	31.03	21.69
	HOP-62	33.63	80.49	**158.60**	45.90	22.46	6.03	24.84	19.99	22.55
	HOP-92	-7.25	78.49	**109.79**	4.51	-27.44	3.02	40.36	28.25	11.28

	NCI-H226	48.81	51.50	26.96	35.15	33.73	5.88	24.77	21.36	13.23
	NCI-H23	69.39	**134.07**	**132.12**	90.37	68.04	2.21	44.16	39.27	21.82
	NCI-H322M	0.21	32.21	19.52	3.95	-5.53	1.65	2.44	4.81	5.69
	NCI-H460	28.14	87.28	90.38	46.08	25.07	-0.23	47.70	29.96	39.19
	NCI-H522	31.97	**120.20**	**134.81**	62.67	47.13	7.64	23.62	22.73	18.21
Colon Cancer	COLO 205	-2.11	80.85	57.45	3.67	-5.94	-3.93	55.51	39.55	15.44
	HCC-2998	13.21	**133.50**	**137.87**	38.63	-1.21	-12.31	10.89	-0.89	2.86
	HCT-116	39.13	**132.42**	**150.92**	**109.10**	44.14	8.46	72.90	59.89	63.36
	HCT-15	48.69	**168.35**	**168.11**	97.21	44.66	-0.25	50.52	33.91	57.16
	HT29	8.23	73.95	50.97	-7.76	0.35	5.99	69.86	50.14	26.49
	KM12	21.19	93.96	**129.88**	64.80	25.15	-3.08	43.43	17.79	18.15
	SW-620	24.10	**159.75**	**156.56**	81.66	22.49	4.29	27.07	18.93	20.05
CNS Cancer	SF-268	32.26	91.21	110.65	54.82	41.37	15.04	37.67	29.00	19.26
	SF-295	12.21	30.80	69.03	20.44	5.24	9.26	54.00	36.89	14.92
	SF-539	7.45	**198.29**	**194.41**	94.83	12.52	-8.64	22.07	18.69	4.73
	SNB-19	39.25	95.41	**174.30**	66.30	25.88	1.20	33.22	17.91	9.35
	SNB-75	63.66	**194.63**	**198.23**	**110.40**	66.13	20.65	46.73	41.79	27.60
	U251	17.35	99.78	**181.45**	67.40	29.29	8.65	46.10	26.06	42.13
Melanoma	LOX IMVI	37.84	**180.28**	**183.86**	99.49	64.25	4.55	40.06	22.40	39.20
	MALME-3M	**169.26**	**188.59**	**187.38**	**164.33**	94.48	-13.76	23.30	14.64	0.23
	M14	95.86	**193.88**	**193.47**	**121.83**	80.70	-2.71	24.45	14.96	13.94
	MDA-MB-435	**172.49**	**193.49**	**197.05**	**193.24**	**185.53**	-2.78	32.55	24.57	7.06
	SK-MEL-2	24.77	**117.29**	**140.56**	50.50	22.73	-2.05	14.41	21.90	0.55
	SK-MEL-28	7.59	**135.36**	**181.24**	59.83	8.64	-2.49	27.78	18.01	8.15
	SK-MEL-5	60.33	**198.49**	**196.93**	**177.60**	48.69	3.12	**110.14**	83.18	44.92
	UACC-257	37.58	**172.55**	**190.50**	**128.61**	47.42	-1.20	51.31	33.52	5.58
	UACC-62	29.18	**136.03**	**154.04**	**112.39**	33.59	5.12	47.31	46.24	34.09
Ovarian Cancer	IGROV1	51.23	**120.49**	**139.81**	65.42	46.96	-0.96	18.70	19.70	12.89
	OVCAR-3	35.24	**126.39**	**118.83**	98.89	48.92	3.35	46.79	39.78	30.37
	OVCAR-4	30.63	**196.31**	**198.41**	59.51	52.34	10.84	66.51	59.08	29.10
	OVCAR-5	-10.49	**165.70**	**177.37**	-11.35	-18.38	-6.60	-3.27	-6.38	-5.03
	OVCAR-8	37.77	94.40	182.60	96.21	53.68	2.18	34.51	22.47	11.63
	NCI/ADR-RES	29.79	112.75	122.75	82.21	35.70	0.82	32.84	28.33	8.21
	SK-OV-3	23.68	44.32	38.03	40.91	27.13	4.34	17.91	21.63	19.80
Renal Cancer	786-0	19.04	**121.83**	**190.37**	31.40	17.33	0.60	29.94	22.26	12.69
	A498	6.32	44.03	48.42	10.55	13.32	26.71	37.26	27.25	13.08
	ACHN	57.35	**195.25**	**190.19**	74.36	57.98	-6.42	27.66	15.91	11.65
	CAKI-1	67.87	79.67	91.15	69.16	56.64	9.75	39.11	32.21	42.98
	RXF 393	29.32	**126.32**	**187.24**	46.32	39.72	-0.91	25.92	26.73	13.75
	SN12C	29.81	**196.64**	**191.17**	69.12	38.18	7.24	25.74	18.58	19.77
	TK-10	-8.43	41.72	11.39	-14.71	-23.73	-0.99	20.32	20.52	8.81
	UO-31	66.37	**135.24**	**173.08**	78.47	61.82	32.71	57.68	49.11	42.83
	PC-3	33.67	99.63	**102.79**	69.33	42.21	14.03	62.23	51.20	54.49

Prostate Cancer	DU-145	28.33	**190.66**	**191.42**	66.79	11.20	-4.41	25.02	12.24	7.12
Breast Cancer	MCF7	54.39	**162.80**	**163.07**	88.50	59.97	16.30	64.10	47.06	35.02
	MDA-MB-231/ATCC	60.00	**106.76**	**107.49**	84.61	59.61	-4.46	7.06	4.91	10.63
	HS 578T	21.13	**109.43**	**108.98**	53.83	27.78	15.85	41.31	38.71	21.79
	BT-549	32.10	**199.09**	**197.40**	62.82	22.75	7.56	46.06	39.07	17.13
	T-47D	28.91	**103.21**	**119.84**	79.61	64.88	11.05	79.21	75.60	46.29
	MDA-MB-468	-5.28	**130.08**	**133.70**	67.59	20.05	-5.95	60.86	56.41	32.25

In vitro Five-dose Full NCI 60 Cell Panel Assay

Compounds **140c**, **140d**, and **140e** have achieved complete growth inhibition on different cancer cell lines and were selected for advanced five-dose testing against the full panel of 60 human tumor cell lines (Figure 45-47). All the 60 cell lines, representing nine tumor subpanels, were incubated at five different concentrations (0.01, 0.1, 1, 10, and 100 mM). The results were used to create log concentration versus percentage growth inhibition curves and three response parameters (GI_{50}, TGI, and LC_{50}) were calculated for each cell line.

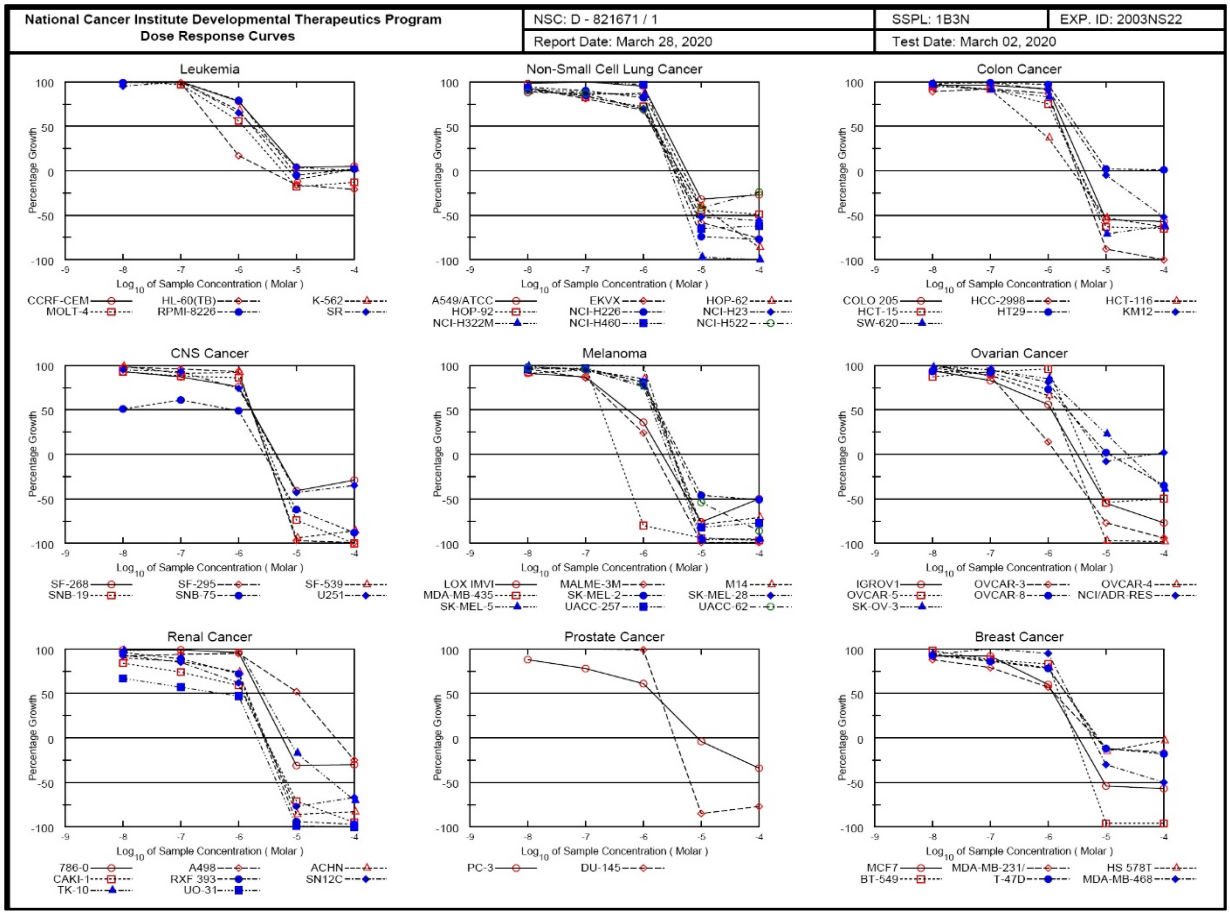

Figure 45: Dose-Response Curves for all cell lines for compound **140c**. Results provided by NCI.

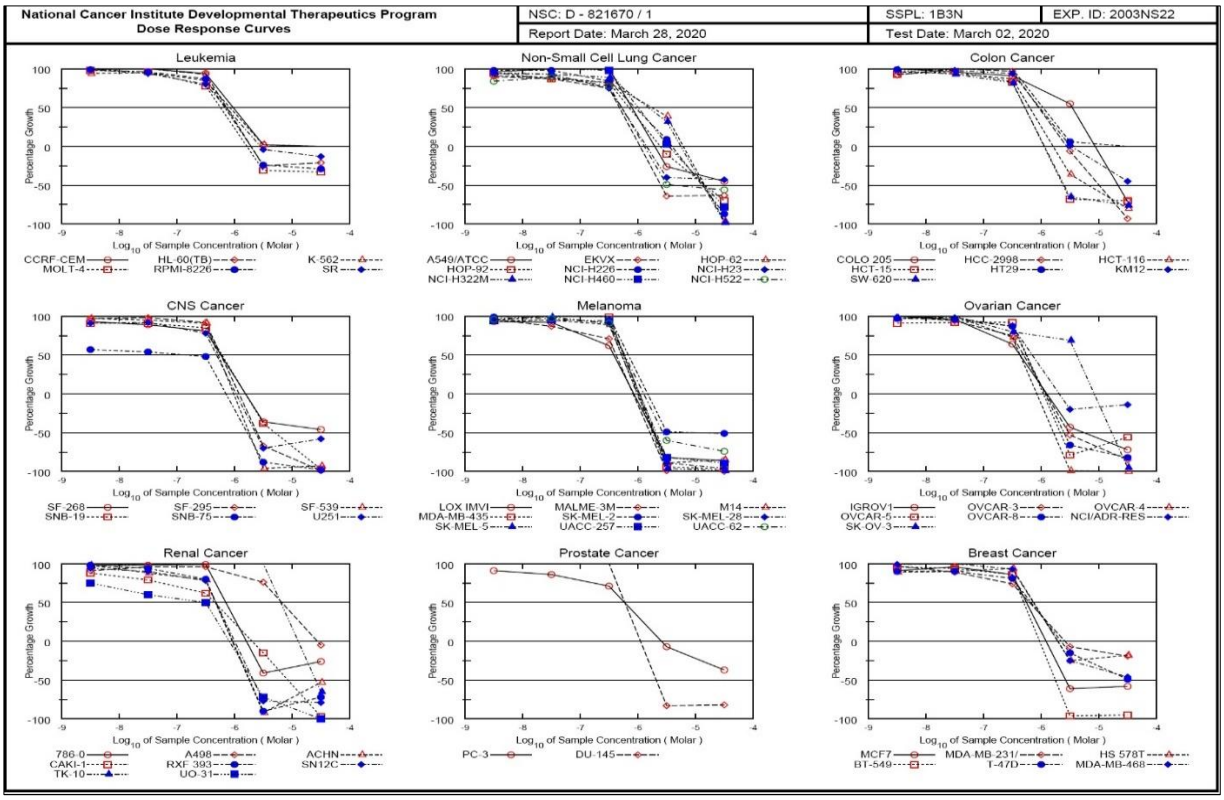

Figure 46: Dose-Response Curves for all cell lines for compound **140d**. Results provided by NCI.

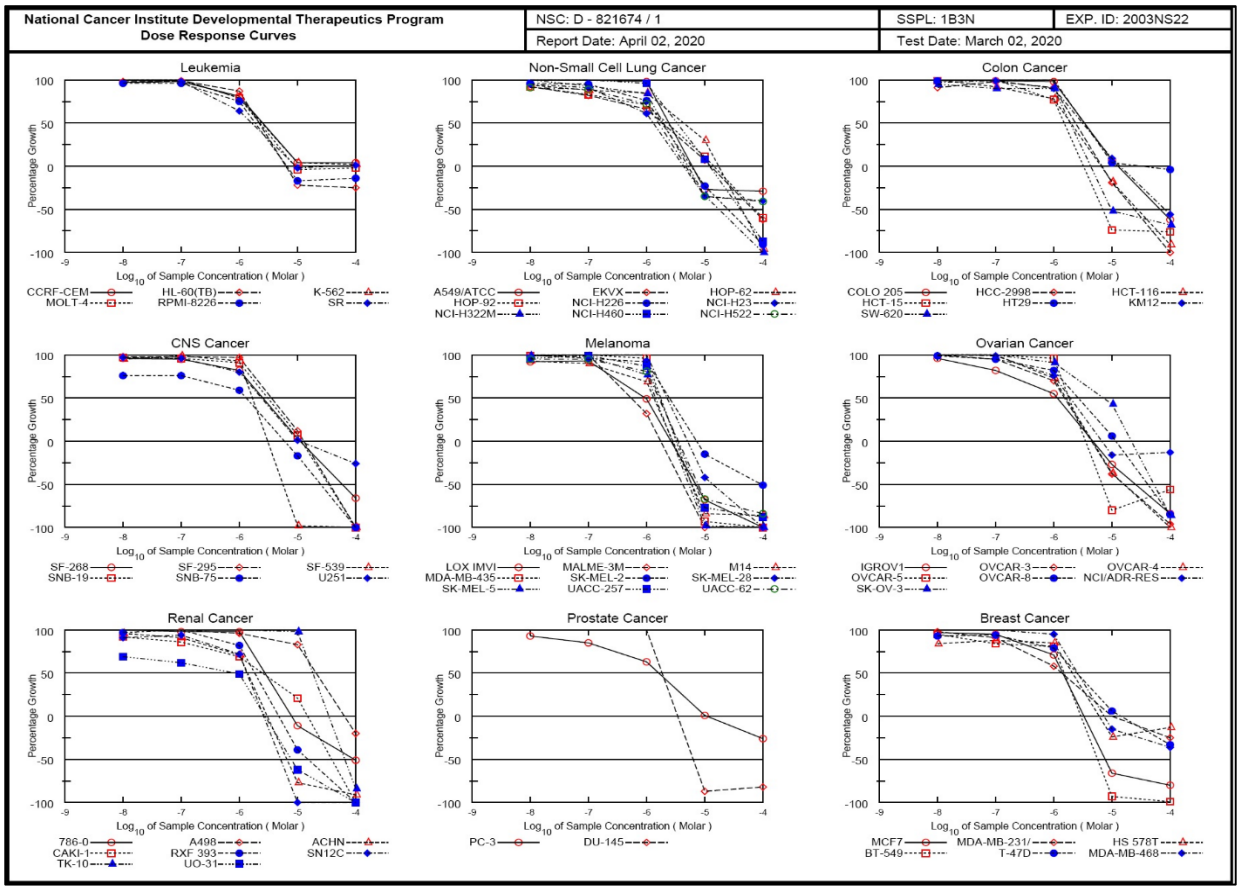

Figure 47: Dose-Response Curves for all cell lines for compound **140e**. Results provided by NCI.

From the results in Table 28 and 29 (see chapter 5.2.4.3), it is clear that compound **140d** exhibits remarkable anticancer activity against most of the tested cell lines representing nine different subpanels. Compound **140d** showed high activity against most of the tested cell lines with GI_{50} ranging from 1.85 to 9.98 µM (Table 28). Compound **140d** was found to have broad-spectrum antitumor activity against the nine tumor subpanels tested with selectivity ratios ranging between 0.73 and 1.14 at the GI_{50} level (Table 28). Furthermore, compound **140e** exhibited remarkable anticancer activity against most of the tested cell lines representing nine different subpanels and showed high activity against most of the tested cell lines with GI_{50} ranging from 1.31 to 9.66 µM (Table 28). Compound **140e** was found to have broad-spectrum antitumor activity against the tested nine tumor subpanels with selectivity ratios ranging between 0.98 and 1.43 at the GI_{50} level. On the other hand, compound **140c** was found to have broad-spectrum cell growth inhibition activity against major of the tested tumor subpanels with GI_{50} values ranging from 1.13 to 5.77 µM, selectivity ratio ranging from 0.78 to 1.32 (Table 28). It can be deduced that compound **140c**, **140d**, and **140e** were found to be broad-spectrum antitumor agents against different tested tumor subpanels with no selectivity towards the tested cell lines.

Evaluation of *In-vitro* Antiproliferative Activities Against Melanoma SK-MEL-5

The synthesized compounds **140c**, **140e**, **140f**, **141b-d,f**, **196** as well as the reference Dinaciclib were tested for their antiproliferative activity by treating melanoma SK-MEL-5 cells at a concentration of 50 µM for 4 days and adding 3-(4,5-dimethylthiazol-2-yl)-2,5-diphenyltetrazolium bromide (MTT) to determine the antiproliferation activity of the target compounds. GraphPad Prism software (GraphPad Software, San Diego, CA, USA) was used to calculate the median inhibition concentration (IC_{50}) for the tested compounds (Figure 48). The difference in the results was considered significant when the values of P are less than 0.05. As shown in Table 19, the three most active [2.2]paracyclophane/thiazole conjugates bearing naphthoquinone moiety **140c**, **140e**, and **140f** exhibited potent to remarkable proliferation inhibition of cancer cells with IC_{50} of 0.81, 4.18, and 9.11 µM compared to Dinaciclib with IC_{50} of 5.97 µM. On the other hand, all other compounds bearing naphthyl moiety instead showed moderate activity against the growth of the cancer cell lines. From these results, we can conclude that the presence of a naphthoquinone moiety improves the binding to target proteins in addition to substitution with benzyl, allyl, or cyclopropyl groups. Especially these substitutions are increasing the flexibility of the compound (as in compounds **140c** and **140e**), which enhances the anti-proliferative potency of these compounds against melanoma

SK-MEL-5. According to the screening results, it was decided to perform further molecular docking studies as well to examine the cytotoxic behavior of compounds **140c** and **140e** on normal cells. It is interesting to mention that proliferation inhibitory results were positively correlated with the anticancer results obtained from NCI.

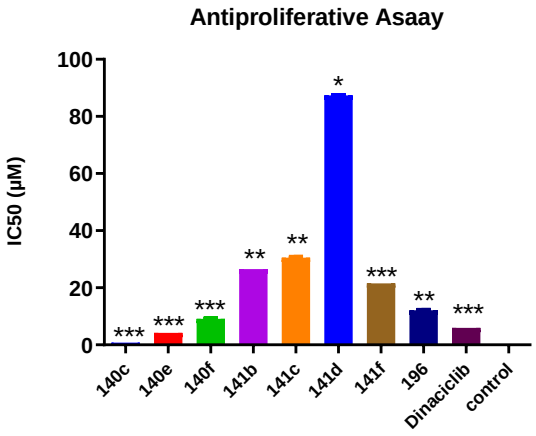

Figure 48: MTT assay of **140c,e-f**, **141b-d,f**, **196,** and Dinaciclib on SK-MEL-5 line relative to control. Results provided by Dr. E. M. N. Abdelhafez.

Table 19: Antiproliferative activity of the target compounds **140c**, **140e**, **140f**, **141b-d,f** and **196**. Results provided by Dr. E. M. N. Abdelhafez.

Compound	**Cytotoxicity IC_{50} (µM) [a] ± SEM**
140c	0.81±0.03***
140e	4.18±0.18***
140f	9.11±0.39***
141b	26.5±1.13**
141c	30.8±1.32**
141d	87.3±3.73*
141f	21.5±0.92**
196	12.1±0.52***
Dinaciclib	5.97±0.25***
Control	0

[a] IC_{50} = compound concentration required to inhibit tumor cell proliferation by 50%. All data were obtained by triplet testing. Data are expressed as the mean ± SEM from the dose-response curves of at least three independent experiments. Results Significantly different from control at ***$p < 0.05$.

According to the screening results and to better explore the SAR of the compounds, besides the biochemical assay (IC_{50}) on the SK-MEL-5 cancer cell line, we also evaluated the compound's cellular antiproliferative activity against the WI38 cell line - normal lung cells of a 3-month-gestation aborted female fetus - to monitor the general cytotoxicity as well (Table 20). Independently, compounds **140c** and **140e** showed the smallest IC_{50} values among the tested compounds against SK-MEL-5 leukemia cancer cells, thereby, **140c** and **140e** were

selected for further investigation for its antiproliferation on normal healthy unaffected cell lines by MTT assay (Table 20).

Table 20: Antiproliferative IC_{50}± SEM (µM) activity of compound **140c**, **140e**, and Dinaciclib.

Compound	Cytotoxicity IC_{50}± SEM (µM)
	WI38
140c	32.59±1.44
140e	39.86±1.76
Dinaciclib	22.01±0.97

The data given are mean values derived from at least three replicates ± SEM.

Compounds **140c** and **140e** achieved IC_{50} values of 32.59 and 39.86 µM, respectively on the selected normal WI38 cell line which are higher values than the reference Dinaciclib IC_{50} = 22.01 µM. The obtained results indicate the relative safety of the tested compounds on normal cells, also they showed a good selectivity window between normal cells and cancer cells.

Selectivity Profiling of Compound 140c

Given the fact that **140c** exhibited the best *in vitro* biochemical activity against the SK-MEL-5 cell line, antiproliferative efficacy in cancer cell lines and to investigate the antiproliferative activities of **140c** related to interaction with CDK that may play critical roles in the regulation of cell cycle or/and transcription. Moreover, kinase inhibitors should possess both a high affinity towards the targeted kinase as well as high selectivity versus other protein kinases. Compound **140c** was chosen for further selectivity evaluations. First, **140c** was subjected to examine selectivity among 8 different available CDK isoforms (CDK1,2,3,4,5,6,7,9) in comparison to the reference Dinaciclib using Kinase-Glo® MAX kit and incubate tested compounds at 30°C for 45 min (Figure 49).

A

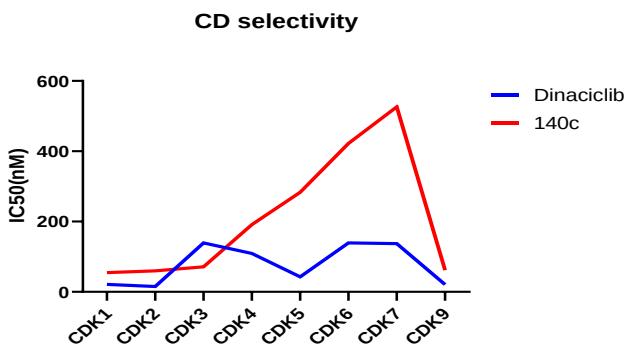

B

CDK target	IC_{50}(nM)± SEM	
	140c	**Dinaciclib**
CDK1	54.8	21.3
CDK2	59.8	15.3
CDK3	71.4	139
CDK4	191	109
CDK5	283	42.6
CDK6	422	139
CDK7	526	137
CDK9	61.6	20.6

Figure 49: Selectivity profiling of compound **140c** and Dinaciclib. (A, B) Biochemical testing of **140c** against CDK isoforms on the SK-MEL-5 line. All data were obtained by triplet testing. Results provided by Dr. E. M. N. Abdelhafez.

Interestingly, **140c** potently inhibited CDK kinase showing IC_{50} values in nanomolar values. Moreover, it exhibited selectivity toward CDK1, 2, and 9 with IC_{50} values of 54.8, 59.8, and 61.6 nM in comparison to Dinaciclib with IC_{50} of 21.3, 15.3, and 20.6 nM indicating more than 10-fold selectivity over CDK3, 4, 5,6, 7. It is noteworthy, that compound **140c** revealed the best selectivity toward CDK1/CyclinB1 with the smallest IC_{50} of 54.8 nM.

Inhibition of Phospho-CDK1 / CDC2 Cell-Based Phosphorylation in SK-MEL-5 Cancer Cell

As it is understood, kinase inhibitors should possess both high affinities towards the targeted kinase as well as high selectivity compared to other protein kinases. Thereby, the cellular mode of action of the most potent tested inhibitor **140c** was investigated using Anti-CDC2 (Phospho-Tyr15) Antibody *via* in an Elisa assay to show the capability of **140c** to down-regulate CDK1 phosphorylated substrate and loss of cyclin expression in treated cells. The Anti-CDC2 (Phospho-Tyr15) antibody is a rabbit polyclonal antibody. Treatment of SK-MEL-5 cells with **140c** for a period of 24 h showed a reduction of phosphorylation at Tyr15 (Figure 50).

A

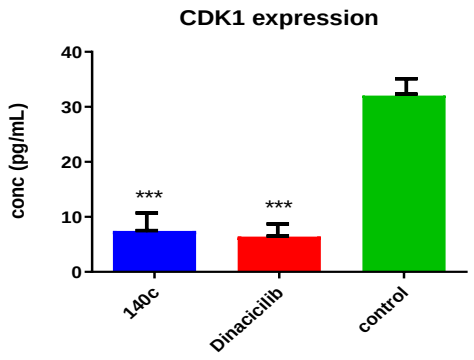

B

Compound	CDK1/CDC2 Phospho-Tyr15	
	conc (pg/mL)	Fold change
140c	7.45±0.4***	76.74157
Dinaciclib	6.42±0.07***	80.01873
control	32.04±3.1	0

Figure 50: Effect of **140c** and Dinaciclib on CDK1/CDC2 Phospho-Tyr15 regulation in the SK-MEL-5 cell line. A) Enzyme-Linked Immunosorbent Assay (ELISA) for immunogen phosphor-peptide for **140c** and Dinaciclib and non-phospho peptide for control group using Anti-CDC2 (Phospho-Tyr15) Antibody. B) CDK1/CDC2 Phospho-Tyr15 inhibition (conc. (pg/mL) ± SEM) of compound **140c** and Dinaciclib. All data were obtained by triplet testing. Results Significantly different from control at ***$p < 0.05$. Results provided by Dr. E. M. N. Abdelhafez.

Figure 50 illustrates that compound **140c** revealed a significant downregulation of Phospho-Tyr15 with a level (7.45 pg/mL) which is close to the reference inhibitor (6.42 pg/mL) in comparison to the control group (32.04 pg/mL). **140c** caused CDK1 Phospho-Tyr15 down expression level about 76.74-fold change comparable to the reference (80.02-fold change) relative to the control (Figure 50) that confirmed cellular CDK1 inhibition.

Cell Cycle Analysis

Cell cycle analysis was carried out for the most potent compound **140c** against the SK-MEL-5 melanoma cancer cell line. The assay was carried out using Cytometers which are Becton Dickinson Immuno-Cytometry Systems, Beckman/Coulter Inc., DACO/Cytomation, and PARTEC GmbH. The results of Annexin V/PI flow cytometry of SK-MEL-5 cells were repeated three times after treatment with concentrations in the IC_{50} value (0.81 µM) of **140c**. The results showed that the percentage of cells of SK-MEL-5 in the G0/G1 phase of the cell cycle was 56.29% of the control, which is remarkably different from Dinaciclib with 41.43% and even further decreased to 37.26% upon treatment with **140c** (Table 21). G2/M phase exhibited a noteworthy percent increase reached to 36.36% when treated with **140c** because of cell accumulation at this phase. Moreover, it is recognizable that the apoptotic cell percentage for phase Pre G1 was raised from 1.61% for untreated control to 36.41% and 32.84% in comparison to treated cells with compound **187c** and Dinaciclib, respectively, (upper right quadrant of the cytogram) (Figure 51).

Table 21: DNA content (%) using propidium iodide flow cytometry. Results provided by Dr. E. M. N. Abdelhafez.

Phase	**Phase %**		
	140c	**Dinaciclib**	**control**
%G0-G1	37.26	41.43	56.29
%S	26.38	29.17	31.96
%G2-M	36.36***	29.4***	11.75
%Pre G1	36.41***	32.84***	1.61

*Results Significantly different from control at ***p < 0.05.*

The obtained results indicated that the late apoptosis percent is greater than that of early apoptosis, which is considered as a good sign for irreversible apoptosis (Figure 52 and 53). According to the above-mentioned results, it is clear that compound **140c** exhibited pre G1 apoptosis and cell cycle arrest at the G2/M phase. Additionally, results revealed that the tested compound is not cytotoxic but antiproliferative, causing programmed cell death and cell cycle arrest.[271]

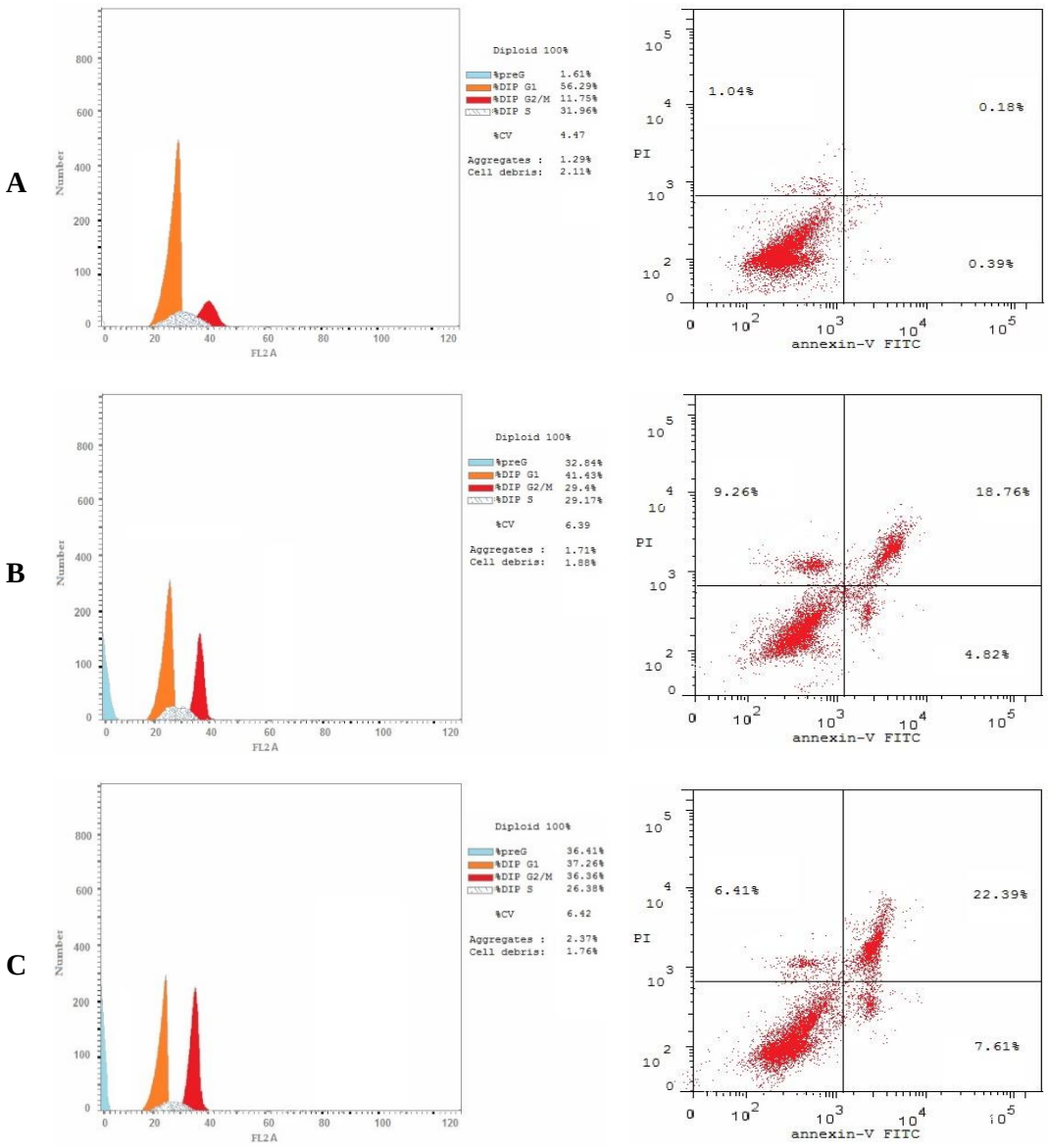

Figure 51: Cell cycle analysis and Apoptosis induction analysis against SK-MEL-5 using Annexin V/PI at IC_{50}. Concentrations representing growth arrest at the pre-G1 (G0) and G2/M phases. A) Untreated cells, B) Treated cells with Dinaciclib C) Treated cells with **140c**. The test is repeated three times and **140c** & reference were incubated for 24hr (2 x 10^5 cells/well) at 37 °C. Results provided by Dr. E. M. N. Abdelhafez.

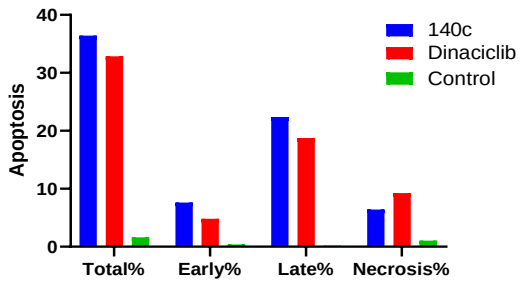

Figure 52: Percentage of apoptosis and necrosis for compound **140c** on SK-MEL-5 melanoma cell line. Results provided by Dr. E. M. N. Abdelhafez.

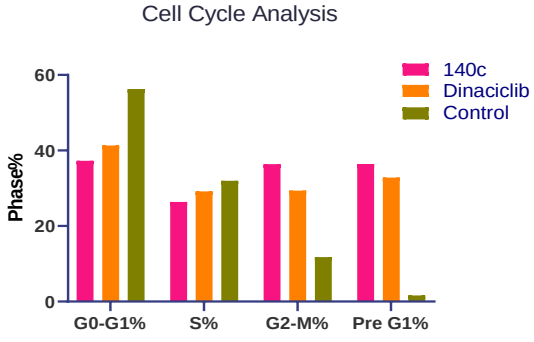

Figure 53: Cell cycle analysis on SK-MEL-5 melanoma cell line treated with compound **140c**. Results provided by Dr. E. M. N. Abdelhafez.

Caspase-3 Activation Assay

Caspase-3 is essential for apoptotic signal spreading after exposure to antimitotic compounds,[242] the effect of [2.2]paracyclophane/thiazole conjugate **140c** on caspase-3 activated enzyme was evaluated in ELISA assays and replicated three times. **140c** was evaluated against the melanoma cancer cell line SK-MEL at concentrations of 2500, 1250, 625, 313, 156, 78, 39 pg/ml. Table 22 displays the results which demonstrate that compound **140c** possesses a remarkable overexpression of caspase-3 proteins (519.4 pg/mL) which is higher compared to the reference Dinaciclib (476.7 pg/mL). Compound **140c** caused overexpression of caspase-3 proteins about 8.66-fold higher than the reference (7.95-fold) relative to control (Figure 54). Hence, it could be deduced from the above results that the apoptosis may be attributed to overexpression of caspase-3 which is induced by the tested compounds.

Table 22: Caspase-3 conc (pg/mL) ± SEM and fold change levels for **140c** and Dinaciclib on the SK-MEL-5 cell line. Results provided by Dr. E. M. N. Abdelhafez.

Compound	**Caspase 3**	
	Conc pg/mL	**Fold change**
140c/SK-MEL-5	519.4±5.8***	8.66
Dinacilib/SK-MEL-5	476.7±8.4***	7.95
Cont.SK-MEL-5	59.95±2.1	1

*Results Significantly different from control at ***p < 0.05.*

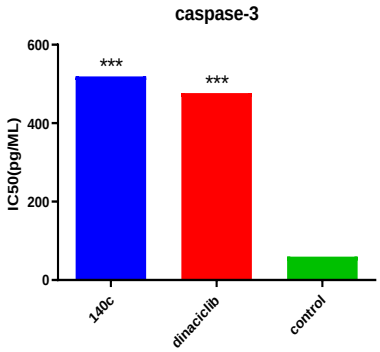

Figure 54: Caspase-3 levels of **140c** and Dinaciclib on the SK-MEL-5 line relative to control. Results provided by Dr. E. M. N. Abdelhafez.

Docking Studies

Docking experiments were performed using the MOE 2014 software. Target compounds **140b-f**, **141b-d,f,** and **196** were constructed into the builder interface of the MOE program, the energy was minimized until an RMSD (root mean square deviations) gradient of 0.01 kcal/mol and RMS (Root Mean Square) distance of 0.1 Å with MMFF94X (Merck molecular force

field 94x) force-field and the partial charges was automatically calculated. X-ray crystallographic structures of the ligand-enzyme complexes were downloaded from a protein data bank (www.rcsb.org); CDK1/CyclinB1 enzyme (pdb: 4YC3).[272] Enzymes were prepared for docking studies by deleting the ligand, adding hydrogen atoms, checking the atom connection, and type with automatic correction. Then the potential of the receptor was fixed and docking of the designed compounds into the 3d structure of the catalytic site of CDK1/CyclinB1 enzyme was done. The obtained poses were studied and the poses which showed the best ligand-enzyme interactions were selected and stored for energy calculations. Table 23 lists the docking energy scores for the synthesized compounds and Dinaciclib (the reference drug), and the detailed 2D and 3D interactions formed from the tested compounds with the amino acid residues in the empty pocket of the enzyme (Figure 55-65).

All of the synthesized compounds showed binding affinity to the enzyme with binding free energies (*Δ*G) in the range of 10.2 to -3.1 kcal/mol relative to that of Dinaciclib (-0.7 to -2.5 kcal/mol, Table 23) supporting that CDK1/CyclinB1 inhibition is a reasonable mechanism explaining the anti-tumor activity observed with those compounds. It is obvious from these results that there are significant binding interactions with CDK1/CyclinB1 for compounds **140b-f** which are containing naphthoquinone scaffold showing specific interactions of the two oxygen atoms with amino acid residues GLU181 and VAL186 (Figure 56-60). This supports the higher anti-tumor activity of **140b-f** compared to the other derivatives **142b-d,f,** and **196** which are lacking two oxygen atoms. There is no significant difference between energy scores of all the tested compounds and Dinaciclib, so energy scores could not be used in explaining differences in activity observed. A detailed study of the binding interactions might explain such differences. In series, **II**, the [2.2]paracyclophane/thiazoles-naphthoquinones conjugates, compounds **140b-f** with the highest anti-tumor activity, showed the highest affinity to CDK1/CyclinB1 receptor. The binding is supported by the formation of two hydrogen bonds with GLU181, two hydrogen bonds with VAL186 and HIS337, and two hydrophobic interactions with ALA185 and PRO340 (Figure 56-60, Table 23). Moreover, **140b** and **140c** showed additional hydrogen bonds with HIS337 revealing a strong binding that stabilizes the ligand in the enzyme (Figure 56 and 57). Compound **140b** as well as the reference exhibited hydrogen bond interaction with VAL336 (Figure 55 and 56). On the other hand, series **III** and **IV**, [2.2]paracyclophane/thiazoles-naphthyl conjugates **141b-d,f** and **196**, showed a lower amount of interaction with the CDK1 active site, which is by the anti-tumor data of this group (Figure 61-65, Table 23). This could be explained by the lack of two oxygen atoms in the naphthyl moiety. Interestingly, all members of series **III** and **IV** kept binding with the GLU181

residue like the compounds in series **II**. However, only in **141c**,**d**, and **196** remained hydrogen bonding with VAL186 as well as a hydrophobic bonding with PRO340 amino acid residue (Figure 62, 63 and 65, respectively). Furthermore, **141c** and **141d** revealed new hydrogen bonds with PHE338 amino acid residue (Figure 62 and 63).

Table 23: Molecular docking data for compounds **140b-f**, **141b-d**,**f**, **196**, and Dinaciclib in CDK1 active site (PDB ID 4YC3). Results provided by Dr. E. M. N. Abdelhafez.

Code	S_score	Interaction with amino acid residue	Distance (Å)	Binding Energy (kcal/mol)
Dinaciclib	-6.7067	hydrogen bonding (H-donor) with VAL336	3.17	-2.5
		hydrogen bonding (H-donor) with TYR223	3.11	-1.2
		hydrophobic interaction (Pi-H) with PRO339	4.13	-1.0
140b	-3.4359	hydrogen bonding (H-donor) with GLU181	2.76	5.2
		hydrogen bonding (H-acceptor) with VAL186	3.01	-1.0
		hydrogen bonding (H-acceptor) with HIS337	3.02	-0.7
		hydrogen bonding (H-acceptor) with GLU181	3.09	-1.1
		hydrophobic interaction (Pi-H) with ALA185	3.50	-0.9
		hydrophobic interaction (Pi-H) with PRO301	4.70	-0.6
		hydrophobic interaction (Pi-H) with PRO340	3.44	-1.0
140c	-4.5662	hydrogen bonding(H-donor) with GLU181	2.67	8.7
		hydrogen bonding (H-acceptor) with VAL186	2.99	-1.0
		hydrogen bonding (H-acceptor) with HIS337	3.04	-0.7
		hydrogen bonding (H-acceptor) with GLU181	3.14	-1.1
		hydrophobic interaction (Pi-H) with ALA185	3.50	-0.8
		hydrophobic interaction (Pi-H) with PRO340	3.41	-0.9
140d	-4.5192	hydrogen bonding (H-donor) with Glu١٨١	2.91	1.9
		hydrogen bonding (H-acceptor) with VAL186	3.07	-0.9
		hydrogen bonding (H-acceptor) with GLU181	2.94	-1.0
		hydrophobic interaction (Pi-H) with ALA185	3.62	-1.1
		hydrophobic interaction (Pi-H) with PRO340	3.39	-0.7
140e	-5.0874	hydrogen bonding (H-donor) with GLU181	2.59	7.6
		hydrogen bonding (H-acceptor) with VAL186	2.87	-1.0
		hydrogen bonding (H-acceptor) with VAL181	3.24	-1.0
		hydrophobic interaction (Pi-H) with ALA185	3.53	-1.0
		hydrophobic interaction (Pi-H) with PRO301	4.68	-0.6
		hydrophobic interaction (Pi-H) with VAL336	3.64	-1.1
		hydrophobic interaction (Pi-H) with PRO340	3.38	-0.9
140f	-2.8405	hydrogen bonding (H-donor) with VAL336	2.65	-1.7
		hydrogen bonding (H-donor) with GLU181	2.62	10.2
		hydrogen bonding (H-acceptor) with VAL186	3.01	-1.0
		hydrogen bonding (H-acceptor) with GLU181	3.23	-0.9
		hydrophobic interaction (Pi-H) with ALA185	3.63	-0.9
		hydrophobic interaction (Pi-H) with LEU300	4.03	-1.1
141b	-5.5781	hydrogen bonding (H-donor) with GLU181	3.28	0.1
		hydrophobic interaction (Pi-H) with PRO339	3.59	-0.6
141c	-6.9592	hydrogen bonding (H-donor) with PHE338	3.28	-0.8
		hydrogen bonding (H-donor) with GLU181	2.92	1.7
		hydrophobic interaction (Pi-H) with VAL 186	4.07	-0.6
		hydrophobic interaction (Pi-H) with PRO340	3.52	-0.6
141d	-6.9227	hydrogen bonding (H-donor) with PHE338	2.79	-2.5
		hydrogen bonding (H-donor) with GLU181	2.79	5.3
		hydrophobic interaction (Pi-H) with VAL186	3.92	-3.1
		hydrophobic interaction (Pi-H) with PRO339	3.71	-0.6
141f	-5.8622	hydrogen bonding (H-donor) with GLU181	2.70	7.6
		hydrophobic interaction (Pi-H) with ALA185	3.55	-0.8

		hydrophobic interaction (Pi-H) with LEU300	4.05	-0.9
		hydrophobic interaction (Pi-H) with VAL336	3.73	-1.2
		hydrophobic interaction (Pi-H) with PRO339	4.13	-0.8
		hydrophobic interaction (Pi-H) with PRO340	3.56	-0.8
196	-6.7288	hydrogen bonding (H-donor) with GLU181	2.68	8.8
		hydrophobic interaction (Pi-H) with ALA185	3.54	-0.6
		hydrophobic interaction (Pi-H) with VAL186	3.94	-1.3
		hydrophobic interaction (Pi-H) with PRO301	4.56	-0.7
		hydrophobic interaction (Pi-H) with VAL336	3.77	-1.4
		hydrophobic interaction (Pi-H) with PRO340	3.65	-0.8

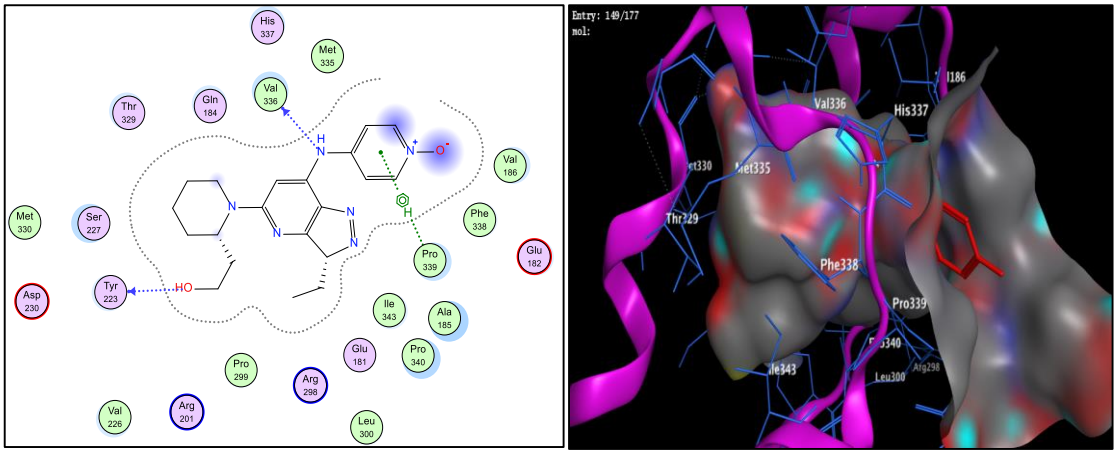

Figure 55: 2D & 3d representation of docking and ligand interactions of Dinaciclib in the 4YC3 receptor. Results provided by Dr. E. M. N. Abdelhafez.

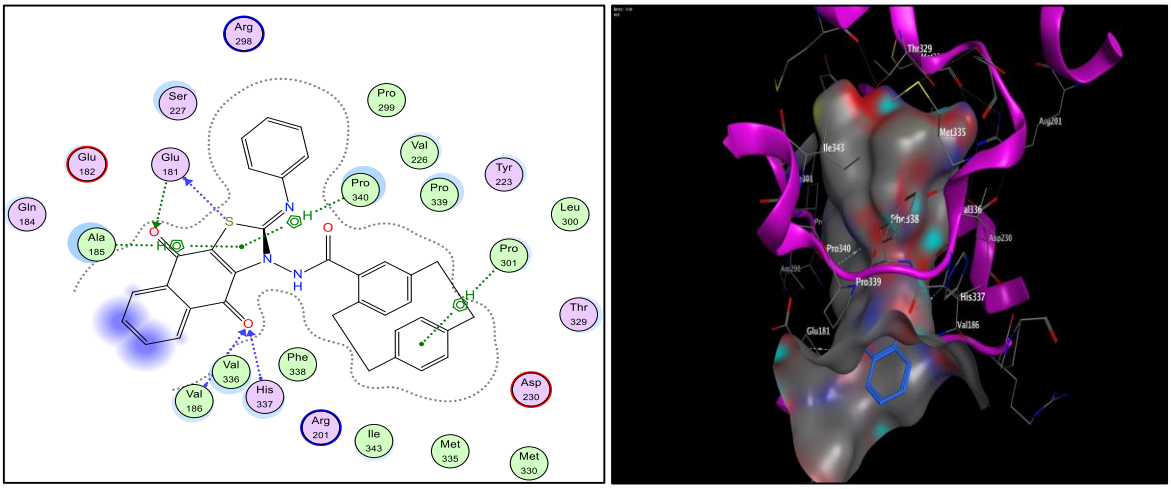

Figure 56: 2D & 3d representation of docking and ligand interactions of **140b** in the 4YC3 receptor. Results provided by Dr. E. M. N. Abdelhafez.

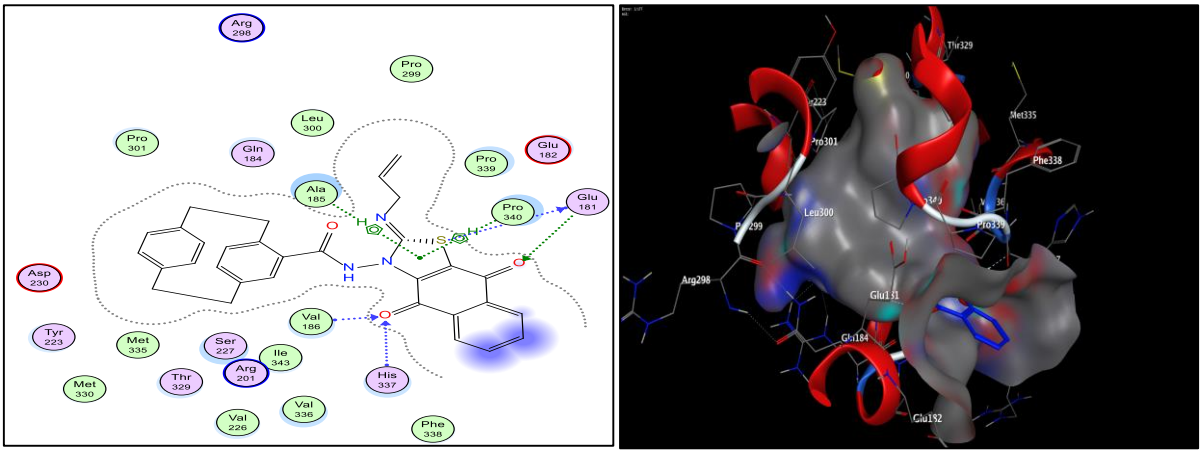

Figure 57: 2D & 3d representation of docking and ligand interactions of **140c** in the 4YC3 receptor. Results provided by Dr. E. M. N. Abdelhafez.

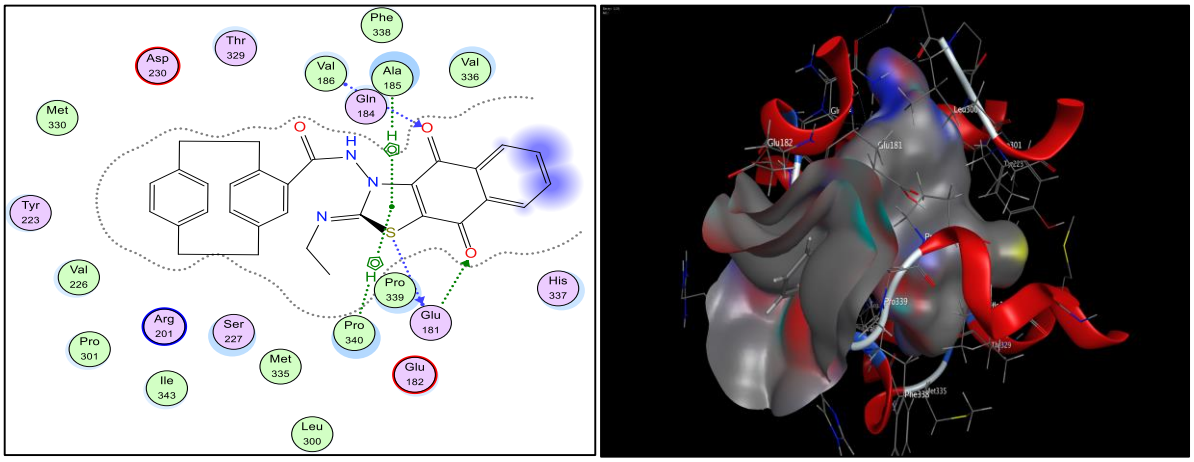

Figure 58: 2D & 3d representation of docking and ligand interactions of **140d** in the 4YC3 receptor. Results provided by Dr. E. M. N. Abdelhafez.

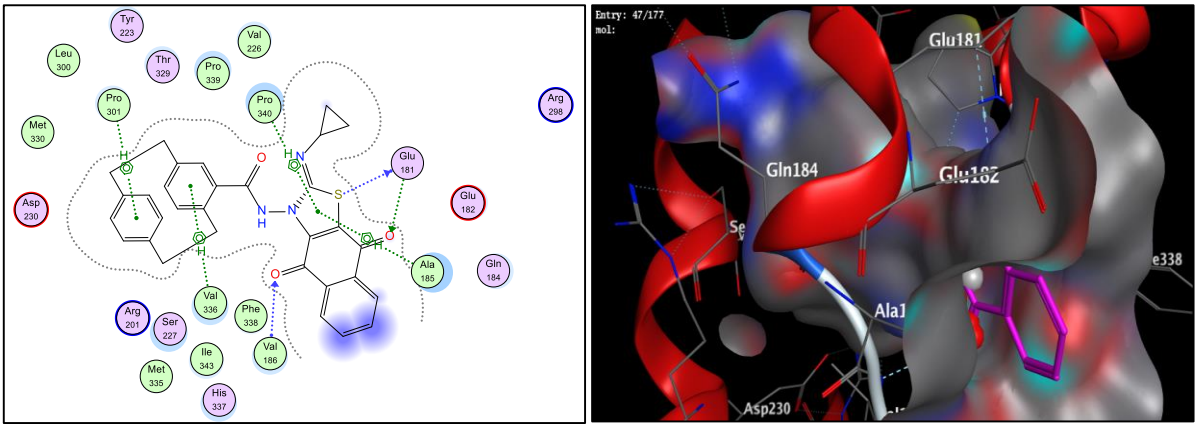

Figure 59: 2D & 3d representation of docking and ligand interactions of **140e** in the 4YC3 receptor. Results provided by Dr. E. M. N. Abdelhafez.

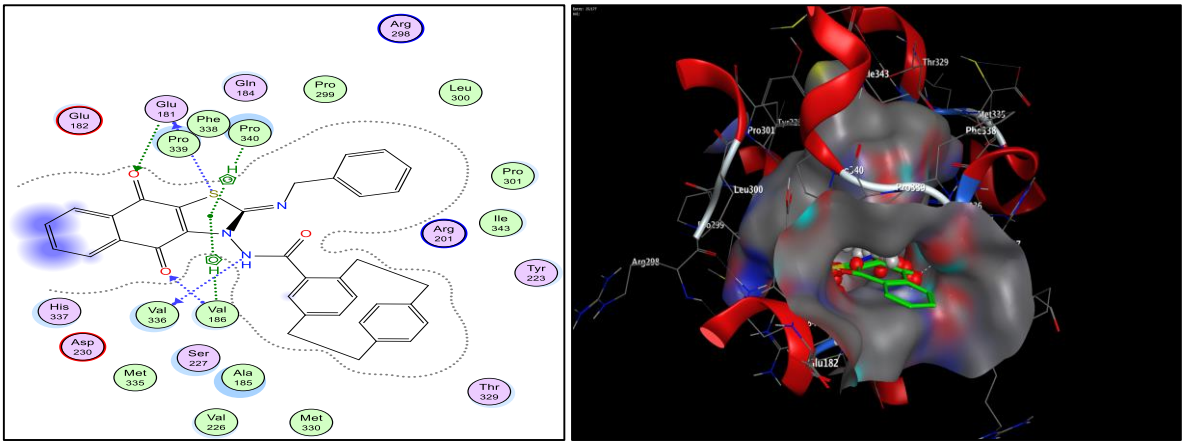

Figure 60: 2D & 3d representation of docking and ligand interactions of **140f** in the 4YC3 receptor. Results provided by Dr. E. M. N. Abdelhafez.

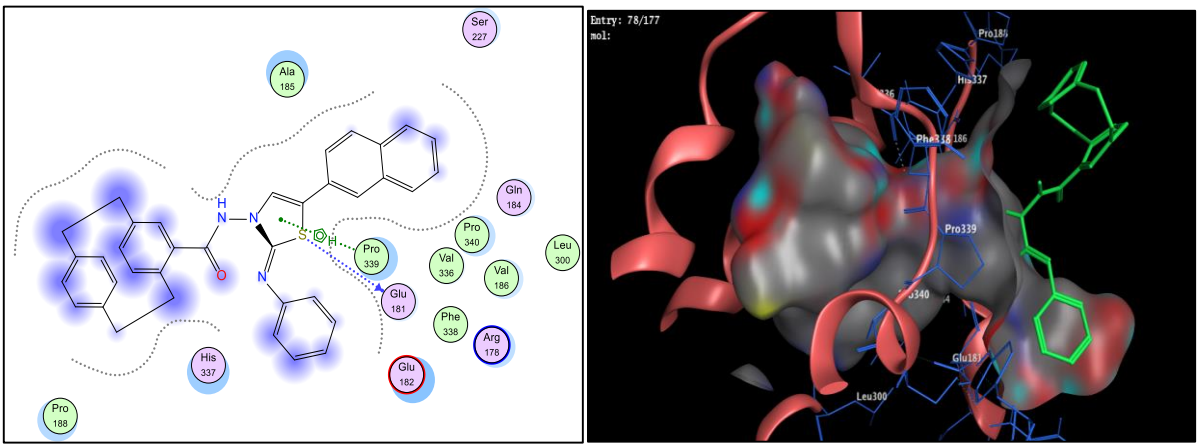

Figure 61: 2D & 3d representation of docking and ligand interactions of **141b** in the 4YC3 receptor. Results provided by Dr. E. M. N. Abdelhafez.

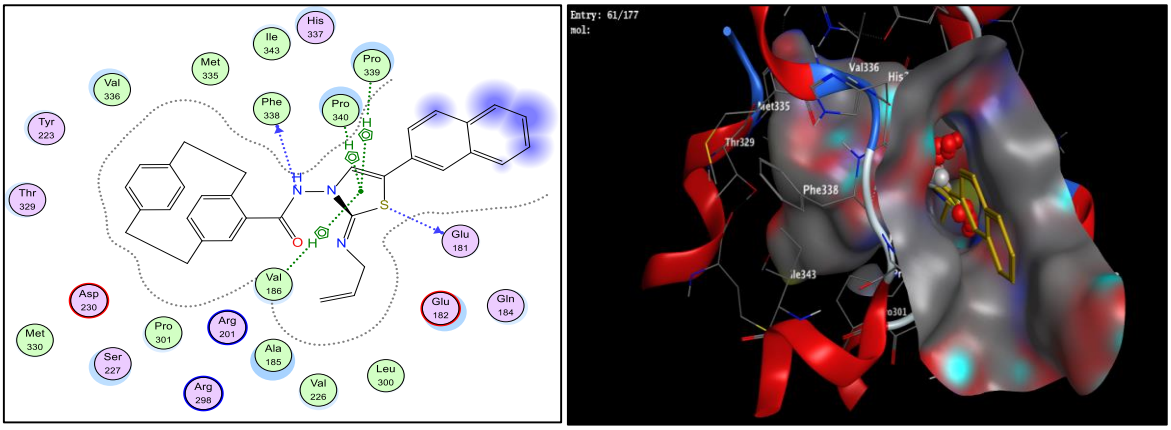

Figure 62: 2D & 3d representation of docking and ligand interactions of **141c** in the 4YC3 receptor. Results provided by Dr. E. M. N. Abdelhafez.

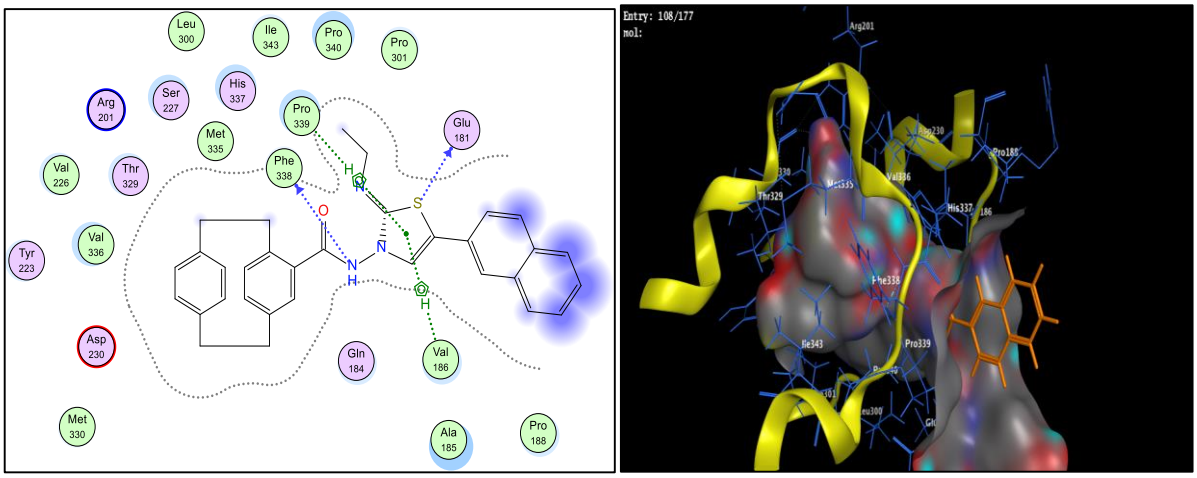

Figure 63: 2D & 3d representation of docking and ligand interactions of **141d** in the 4YC3 receptor. Results provided by Dr. E. M. N. Abdelhafez.

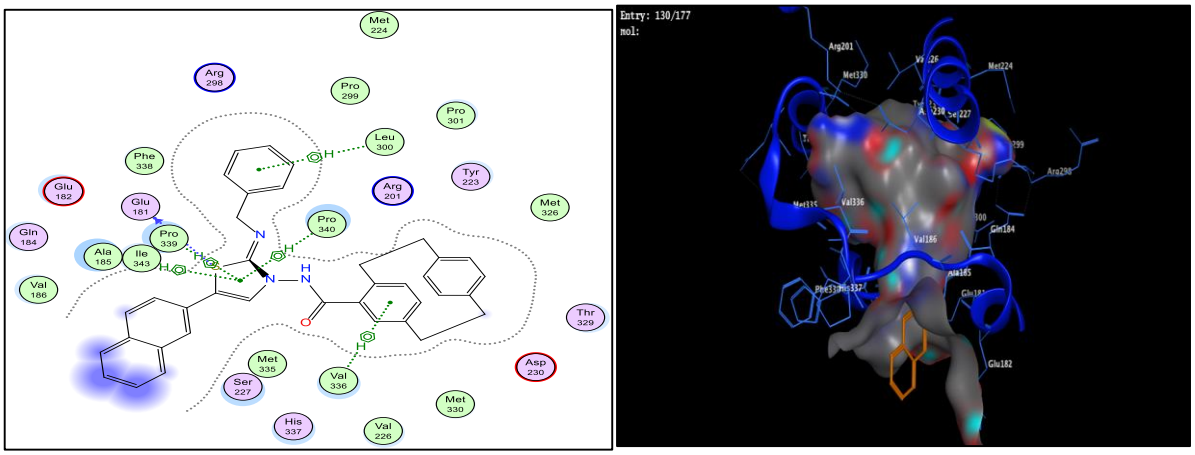

Figure 64: 2D & 3d representation of docking and ligand interactions of **141f** in the 4YC3 receptor. Results provided by Dr. E. M. N. Abdelhafez.

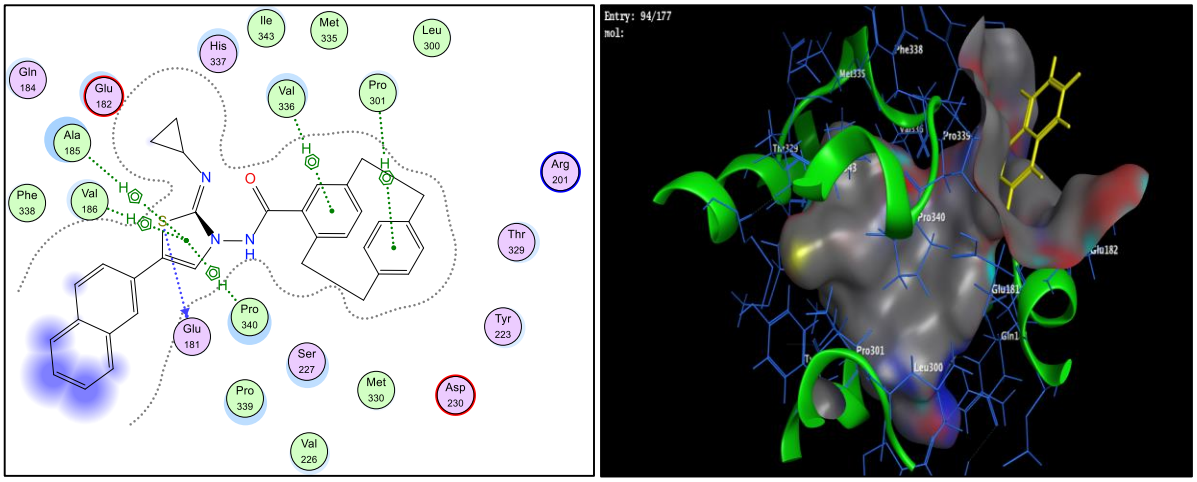

Figure 65: 2D & 3d representation of docking and ligand interactions of **196** in the 4YC3 receptor. Results provided by Dr. E. M. N. Abdelhafez.

In summary, three novel series of bioactive molecules containing three bioactive entities 1,4-dihydronaphthoquinone, thiazole, and [2.2]paracyclophane in hybrid structures were synthesized and characterized. One-dose anticancer test results indicate that compounds **140b-f** exhibit the highest ability to inhibit the proliferation of the tested cancer cell lines. *In vitro* five-dose full NCI 60 cell panel assay revealed that compounds **140c-e** exhibit a broad-spectrum of anti-tumor activity against the nine tumor subpanels tested without pronounced selectivity. Compounds **140b-f** exhibit potent inhibition of melanoma SK-MEL-5 cancer cell growth compared to Dinaciclib as a reference. Compound **140c** showed the smallest IC_{50} value of 54.8 nM on the target enzyme CDK1 in comparison to Dinaciclib as a reference. Accordingly, compound **140c** was investigated extensively and showed downregulation of Phospho-Tyr15 with a level (7.45 pg/mL) comparable to that of the reference. Furthermore, the effect of compound **140c** on the caspase-3 level was evaluated and an 8.66-fold increase was detected. The effect of compound **140c** on the cell cycle arrest was also examined. Moreover, a molecular docking study was performed to explain and confirm the mechanism of action. These results led to the discovery of promising novel hybrids of thiazole and paracyclophanes, that should be investigated further as potential anticancer agents.

3.5. Synthesis of Novel Fused Heterocycles Attached to 4-Hydroxy-2-quinolones

In the following, the results of investigations of novel fused five-membered heterocycles attached to 4-hydroxy-2-quinolones will be presented and discussed.

Furoquinolones are an interesting class of 2-quinolones, that occur naturally in compounds such as *Skimmianine* and γ-Fagarine, which were found to show anti-cancer activity (see chapter 1.2, Figure 8). [54-55]

Alkyl quinolones (AQs) are a species-specific class of quorum-sensing molecules that have been found in *P. aeruginosa*[273-274] and related bacteria such as *P. putida* and *Burkholderia spp.*[275] More than 55 distinct AQs (Figure 66, assigned as PQS (**202**)) are produced through the PqsABCDE biosynthetic pathway in *P. aeruginosa*. With the majority of the diversity resulting from unsaturation, different alkyl chain lengths, and modification of the ring-substituted nitrogen.[275-276] An insight into the evolutionary basis of AQ diversity has emerged from *Burkholderia thailandensis*, where AQ analogs (Figure 66, assigned as HHQ (**203**) and HQNO (**204**)) are shown to act synergistically as bacterial growth inhibitors.[277-278]

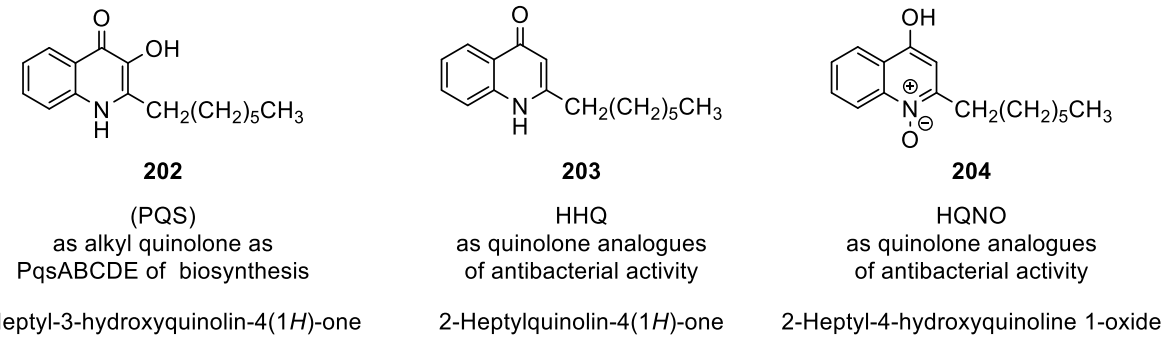

Figure 66: An example of QS of PqsABCDE biosynthesis and two examples of quinolone analogs as antibacterial reagents.

Some quinolone derivatives were developed as antibiotics for humans in clinical use,[279] that exert their influence by inhibiting two topoisomerase enzymes of type II, topoisomerase IV, and DNA gyrase.[280] DNA topoisomerases are found in both prokaryotic and eukaryotic cells and are targeted for chemotherapeutic interventions in anti-cancer and anti-bacterial therapies.[281] Synthesis of the zwitterionic 4-hydroxycoumarin derivatives was investigated through a unique reaction of 4-hydroxycoumarins with *p*-benzoquinone and pyridine in dry acetone. Recently, ALY *et al.* reported various compounds derived from 4-hydroxy-2-quinolone.[68, 282-287] A class of 1,2,3-triazoles derived from 2-quinolone has been synthesized *via* Cu-catalyzed [3+2]-cycloadditions (Meldal–Sharpless 'click'-reactions) of

4-azidoquinolin-2(1*H*)-ones with ethyl propiolate. they also synthesized fused naphthofuro[3,2-*c*]quinoline-6,7,12-triones and pyrano[3,2-*c*]quinoline-6,7,8,13-tetraones, that have shown potential as Externally Regulated Kinases (ERK) inhibitors.[286]

The aforementioned biological and pharmaceutical activities of 4-hydroxy-2-quinolones make them valuable in drug development and research. Consequently, shedding new light on these heterocycles is very important. In general, quinolones and their fused analogs are highly demanded possible pharmaceutical applications. Therefore, it is necessary to develop simple and mild methods for synthesizing quinolone derivatives. Furthermore, the reactivity of 1,6-disubstituted 4-hydroxy-quinoline-2-ones **82a-f** towards 3,4,5,6-tetrachloro-1,2-benzoquinone (**205**), 2,3-dichloropyrazine (**212**) and *E*-dibenzoylethene (**219**) was tested.

3.5.1. Reaction of 4-Hydroxy-quinoline-2-ones with 3,4,5,6-Tetrachloro-1,2-benzoquinone[6]

New benzofuroquinolone derivatives that might show biological activity and be suitable pharmaceutical applications were investigated. First, the reaction of 4-hydroxy-2(1*H*)-quinolinones **82a-f** with 3,4,5,6-tetrachloro-1,2-benzoquinone (*o*-CHL) (**205**) was conducted. 4-Hydroxy-2(1*H*)-quinolinones **82a-f** were reacted with 3,4,5,6-tetrachloro-1,2-benzoquinone (**205**) in THF under reflux for 10-15 h which yielded the corresponding 7,8-dichloro-benzofuro[3,2-*c*]quinoline-6,9,10(5*H*)-triones **206a-f** (Table 24).

The structures of the products **206a-f** were determined by analyzing the IR, mass, and NMR spectra as well as elemental analyses (see chapter 5.2.5). For example, the structure of **206f** was confirmed by NMR analysis. The methyl group protons were assigned to the observed signal at δ_H = 2.41 ppm and the methyl carbon to the signal at δ_C = 20.3 ppm. Methyl protons also give a weak signal in the COSY-NMR spectrum and the methyl carbon gives a weak cross signal to a broadened singlet at δ_H = 7.69 ppm in the HMBC spectrum. This signal can be assigned to H-1 and a broadened doublet at δ_H = 7.64 ppm which is assigned to H-3. The broadening of these signals reflects the weak coupling between them. Another HMBC correlation signal indicates the coupling of H-4 C-2 carbon (δ_C = 137.6). Also, C-11b (δ_C = 108.7) gives a cross-signal in the HMBC spectrum with the signal assigned to an NH proton at δ_H = 11.98 ppm. Compound **207** may be formed as a regioisomer of **206** (Figure 67),

[6] Excerpts of this chapter were already published in
A. A. Aly, A. A. Hassan, N. K. Mohamed, L. E. A. El-Haleem and S. Bräse, *J. Chem. Res.*, **2020**, *44*(7-8), 388-392.

but this was excluded by NMR spectra since there was a good HMBC correlation between C-11a and C-10. For example, in compound **206f**, a good correlation was observed between the carbon at δ_C = 166.5 and the carbon δ_C = 174.5 ppm. A third alternative structure **208** (Figure 67) which might be formed was also ruled out since there was no correlation between the carbonyl-7 and C-6a detected.

Table 24: Synthesis of 7,8-dichloro-benzofuro[3,2-*c*]quinoline-6,9,10(5*H*)-triones **206a-f**.

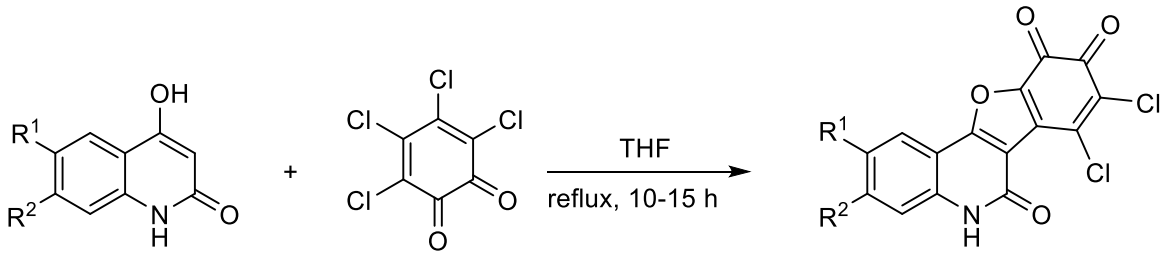

82a-f **205** **206a-f** (70-78%)

Entry	206a-f	R^1	R^2	Yield [%]
1	**206a**	H	H	74
2	**206b**	Cl	H	70
3	**206c**	H	Cl	66
4	**206d**	Br	H	75
5	**206e**	H	CH_3	76
6	**206f**	CH_3	H	78

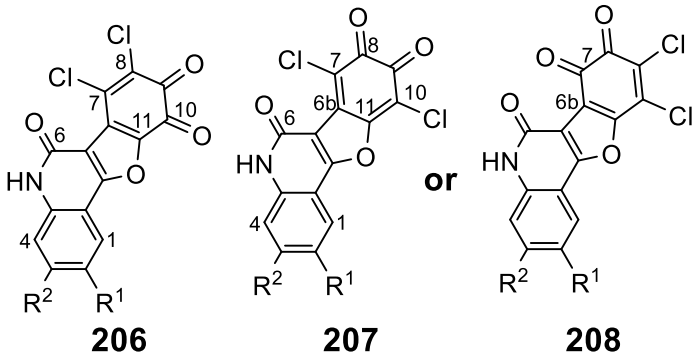

206 **207** **208**

Figure 67: The structures of the three possible regioisomers **206**-**208**.

The mechanism of the reaction involves a Michael addition at C-3 of the quinolone **82** to the α-carbon of its quinone **205** to obtain the zwitterion **209** (Scheme 42) *via* a 1,6-addition. After that, the elimination of HCl gives the intermediate **210**, which can also exist in the corresponding enolate **211** (Scheme 42). Then, a nucleophilic attack by the oxygen lone-pair of the vinylic carbon leads to cyclization after the elimination of another HCl molecule to provide the products **203a-f** (Scheme 42).

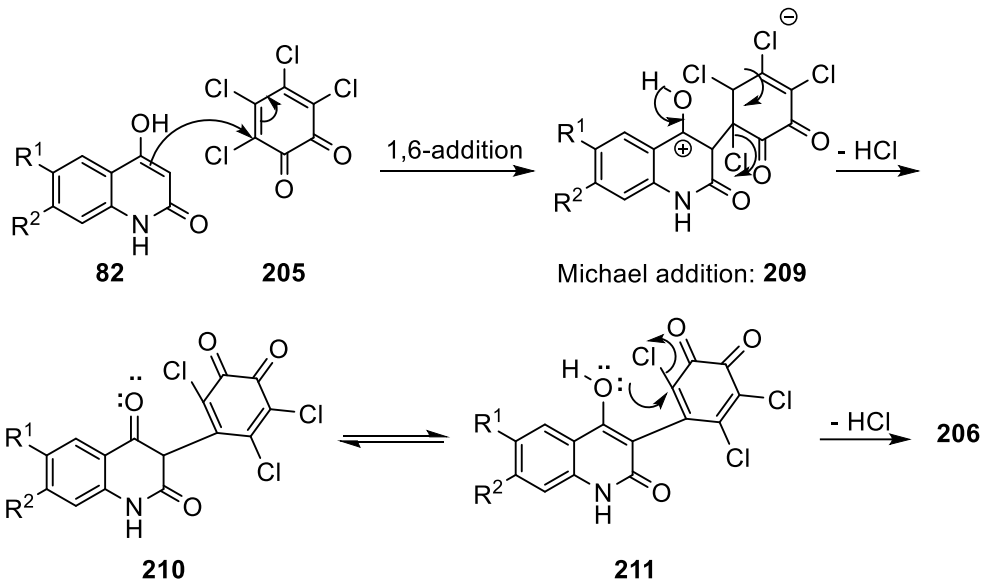

Scheme 42. Mechanism describing the formation of compounds **206a-f**.

3.5.2. The Reaction of 4-Hydroxy-quinoline-2-ones with 2,3-Dichloropyrazine[7]

The furopyrazine scaffold with an amino- and carboxy-terminus was reported. These substituents lead to a conformationally restricted dipeptidomimetic scaffold.[288] New quinolones fused with furopyrazine were prepared by mixing equimolar amounts of 2,3-dichloropyrazine (DCP) (**212**) and 1,6-disubstituted-4-hydroxyquinoline-2-ones **82a-f** and refluxing in DMF with catalytic amounts of Et_3N. Substrates **213a-f** were obtained as single products (Table 25). Structure elucidation of compounds **213a-f** was carried out by IR and NMR spectroscopy as well as mass spectrometry and elemental analyses (see chapter 5.2.5).

The formed products were identified as pyrazino[2′,3′:4,5]furo[3,2-*c*]quinolin-6(5*H*)-ones **213a-f**. For example, the elemental analysis and mass spectra for **213a** proved its molecular formula to be $C_{22}H_{10}N_4O_4$, which can be explained by adding two moles of **82a** to one mole of **212** followed by the elimination of two moles of HCl. The previously expected structure **214** was ruled out, as there is no proton for the azomethine in the ^{1}H NMR spectrum (Figure 68). Either the *syn*-form **213a′** or the *anti*-form **213a** has to show symmetric carbon signals in the ^{13}C NMR spectrum. Using Spartan 18: geometries program[289] the structures are geometry-optimized at the 6-31G* level with B3LYP. The energy difference between the

[7] Excerpts of this chapter were already published in
A. A. Aly, A. A. Hassan, N. K. Mohamed, L. E. A. El-Haleem, S. Bräse, M. Polamo, M. Nieger and A. B. Brown, *Molecules*, **2019**, *24*, 3782.

calculated *anti*-**213a** and the *syn*-**213a'** shows that *anti*-**213a** is thermally more stable than *syn*-**213a'** by 2.029 kcal/mol.

Table 25: Reactions of 2-quinolinones **82a-f** with 2,3-dichloropyrazine (**212**); synthesis of pyrazino-[2′,3′:4,5]furo[3,2-*c*]quinolin-6(5*H*)-ones **213a-f**.

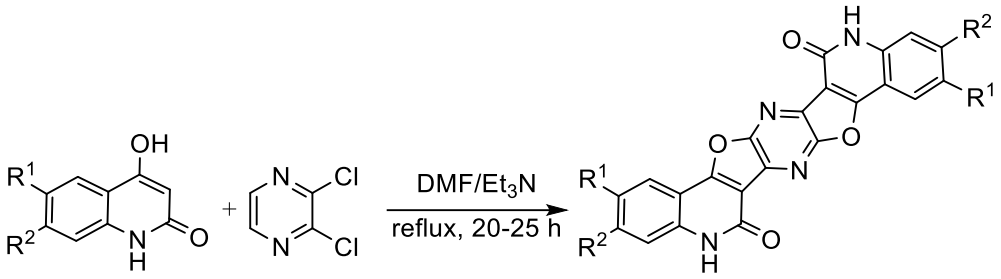

82a-f **212** **213a-f** (60-70%)

Entry	213a-f	R^1	R^2	Yield [%]
1	**213a**	H	H	65
2	**213b**	Cl	H	67
3	**213c**	H	Cl	64
4	**213d**	Br	H	70
5	**213e**	H	CH_3	68
6	**213f**	CH_3	H	66

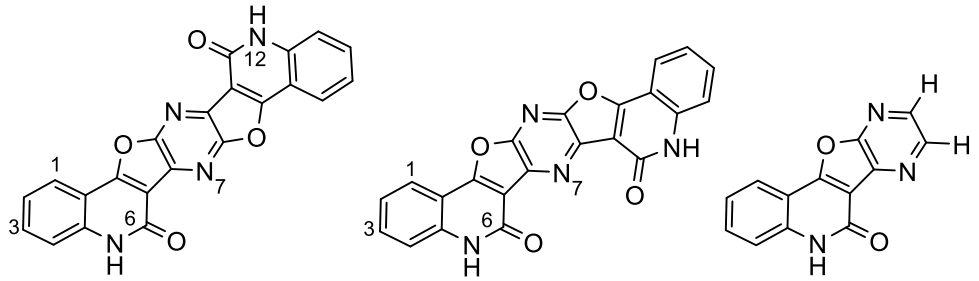

***Anti*-213a** **S*yn*-213a'** **214**

Figure 68: Alternative structures of compound **213a**.

Compounds **213a-f** are products of a reaction between 2,3-dichloropyrazine (**212**) and two equivalents of 4-hydroxy-2-quinolinone (**82**). The reaction leads to the replacement of both chlorine and hydrogen atoms of **212** with either an α-carbon or *pseudo*-phenolic oxygen of **82**. Both positions included in **82** were formally nucleophilic. However, the α-carbon normally reacted first. It was not clear whether there was any direct reaction of **212** with the four nucleophiles. In systems in which all the chlorine and hydrogen atoms of **212** were replaced, the reaction of C-5 and C-6 (the hydrogen-bearing carbons) involved a reaction with an oxidant (e.g., a molecular halogen), sometimes followed by an organometallic coupling.[290-291] Moreover, pyrazines bearing leaving groups readily undergo replacement of those leaving

groups, by either S_NAr or by addition of the nucleophile, ring-opening, and ring closure (ANRORC) mechanisms.[292-294] If the activation of pyrazine occurred by an electrophile, the nucleophile can act as weak as *o*-phenylenediamine.[295] If **212** does not undergo four-fold nucleophilic substitution, the likeliest scenario seems to be a *two*-fold displacement followed by a two-fold oxidative cyclization, presumably driven by air. If the chlorides were the leaving groups, only one can first undergo *ipso*-substitution, as other nucleophiles must attack the other side of the ring. The S_NAr process can only result in *ipso*-substitution when the ANRORC process proceeds at the *pseudo-meta* position (Scheme 43). The proposed mechanism for the formation of **213a-f** is shown in Scheme 44. Here, the nucleophile attacks **82** at its α-carbon. If one substitution gives an *ipso*-displacement and the other gives *pseudo-meta*-displacement, the observed *anti*-regiochemistry is expected and the order of the two substitutions does not matter.

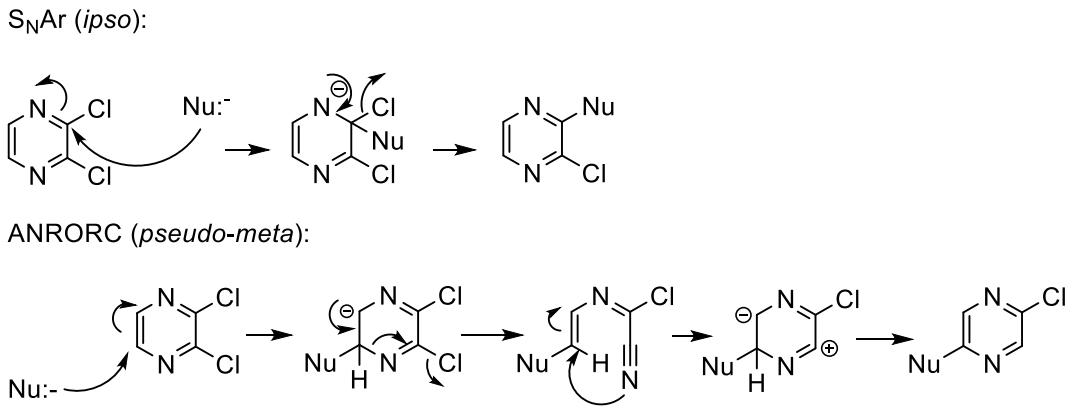

Scheme 43. S_NAr versus ANRORC substitutions on **212**.

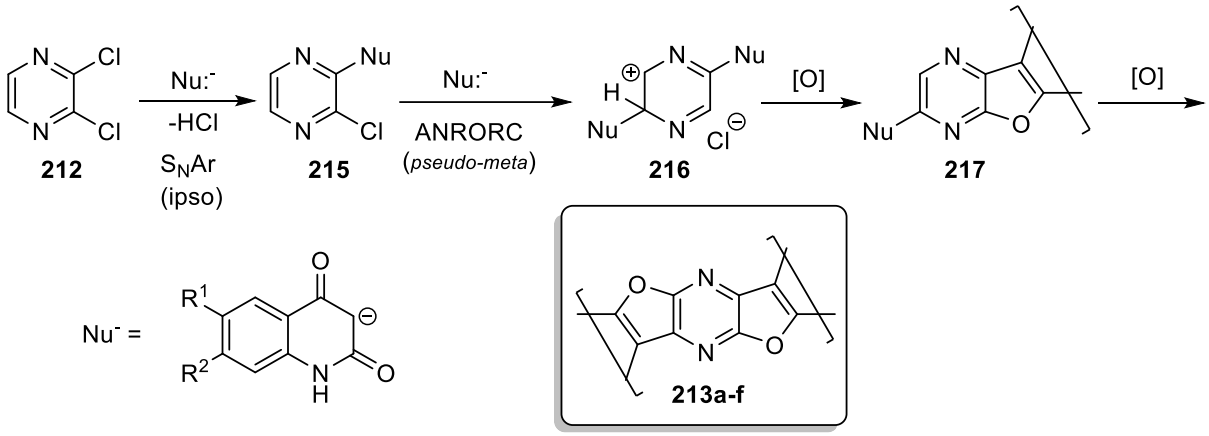

Scheme 44. The proposed rationale for the formation of **213**.

3.5.3. The Reaction of 4-Hydroxy-quinoline-2-ones with *E*-dibenzoylethene

The reaction of 4-hydroxy-quinoline-2-ones **82** with alkynes was studied previously[285] by reacting **82a** with diethyl acetylenedicarboxylate (**189b**) in absolute ethanol, containing catalytic amounts of Et_3N. Pyrano[3,2-*c*]quinoline-4-carboxylate **218** was obtained in good yield (Scheme 45). As the goal is to synthesize new fused five-membered heterocycles and not six-membered rings, reactions of 4-hydroxy-quinoline-2-ones **82a-f** with alkene derivatives were investigated.

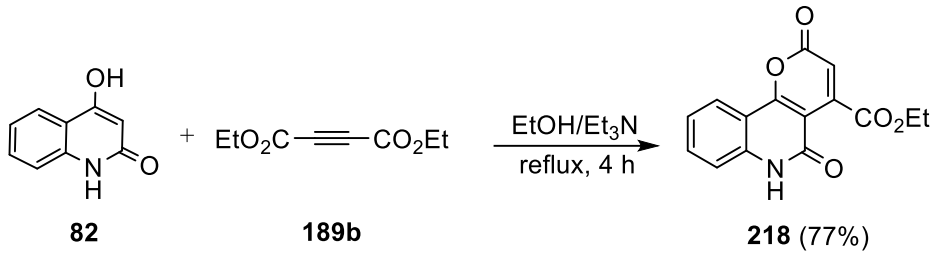

82 **189b** **218** (77%)

Scheme 45. **The** reaction of 4-hydroxy-quinoline-2-ones **82** with diethyl acetylenedicarboxylate **189b**.

Single products were obtained from the reaction of *E*-dibenzoylethene (DBE) (**219**) with **82a-f** in pyridine/Et_3N (Table 26, **220a-f**). The targeted fused furoquinolones **221a-f** were not successfully synthesized under these conditions. Instead compounds **220a-f** bearing open chains were the only products obtained by this reaction. In the future, different reaction conditions will be screened to synthesize **221a-f**. The structure elucidation for **220a-f** relies intensively on NMR spectroscopy. For example, the ^{1}H NMR spectrum of **220f** shows a singlet signal at δ = 11.35 ppm and a broad signal at δ = 10.77 ppm (see chapter 5.2.5). The integrals indicate two phenyl rings and one quinolone and, consequently, they rule out the alternative structures **222f'** and **222f''** (Figure 69).

The structures of products **220a-f** were deduced from the corresponding NMR and IR spectra as well as by mass spectrometry (see chapter 5.2.5). The structure of compound **220f** was furthermore proved by X-ray structure analysis as shown in Figure 70.

Table 26: Reactions of 2-quinolones **82a-f** with *E*-dibenzoylethene (**219**); synthesis of 2-(4-hydroxy-2-oxo-1,2-dihydroquinolin-3-yl)-1,4-diphenyl-butane-1,4-diones **220a-f**.

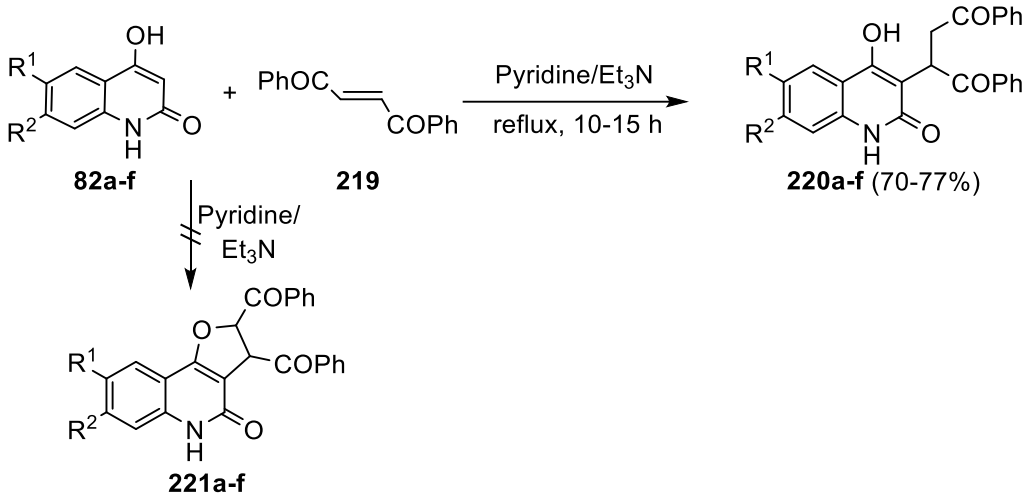

Entry	220a-f	R^1	R^2	Yield [%]
1	**220a**	H	H	75
2	**220b**	Cl	H	72
3	**220c**	H	Cl	70
4	**220d**	Br	H	76
5	**220e**	H	CH_3	77
6	**220f**	CH_3	H	74

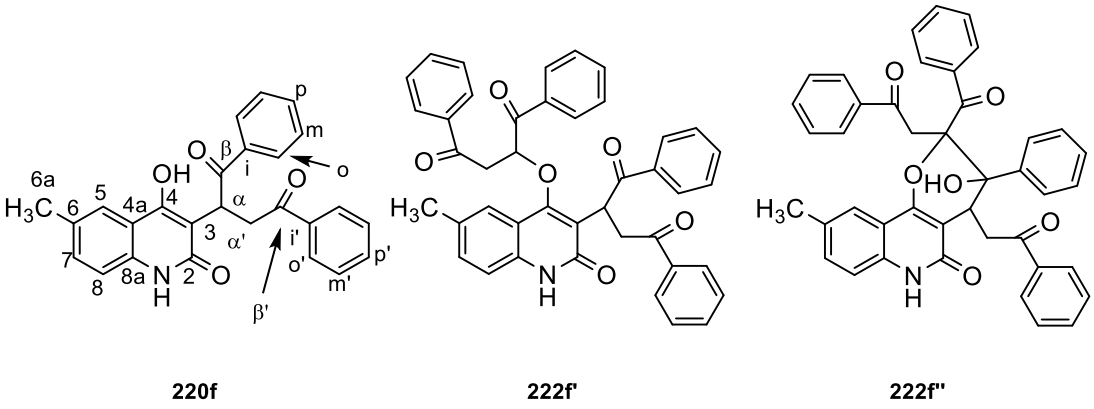

Figure 69: Different suggested structures of **214f**, **216f'**, and **216f''**.

Surprisingly, in an attempt to prepare 4-hydroxy-2-quinolone **82g** from 2-hydroxyaniline (**223**) and diethyl malonate (**98**) in PPA according to the procedure described in the literature,[296] compound **224** was obtained in 80% yield (Scheme 46). Similarly, by applying the same conditions, the reaction of **224** with **219** produced compound **225** in 85% yield.

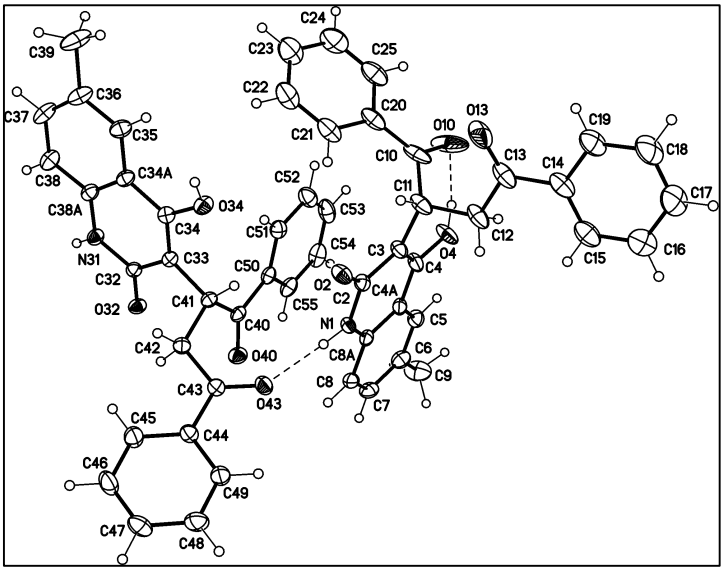

Figure 70: Molecular structure of the dimer of compound **220f** (displacement parameters are drawn at the 50% probability level, both crystallographic independent molecules shown).

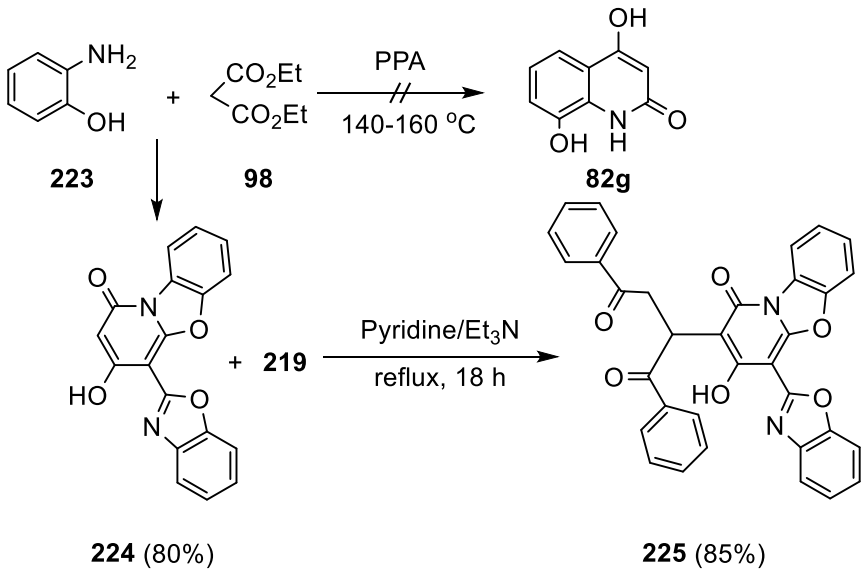

Scheme 46. Formation of compound **224** and its reaction with compound **219**.

The suggested mechanism for the formation of compound **224** is shown in Scheme 47. First, the reaction of **223** with **98** presumably starts with an *N*-acylation to form intermediate **226**. The expected formation of **82g** would then involve ring closure in the fashion of a Friedel-Crafts acylation. The pathway leading to **227** on the other hand requires a Claisen condensation between **226** and a second molecule of **98** to give intermediate **227**. One of the pendant esters of **227** react intramolecularly with the NH and OH groups and form the benzoxazole subunit of intermediate **228**. Lastly, the reaction of the remaining ester group of **228** with a second molecule of **223** affords the other benzoxazole unit of **224**.

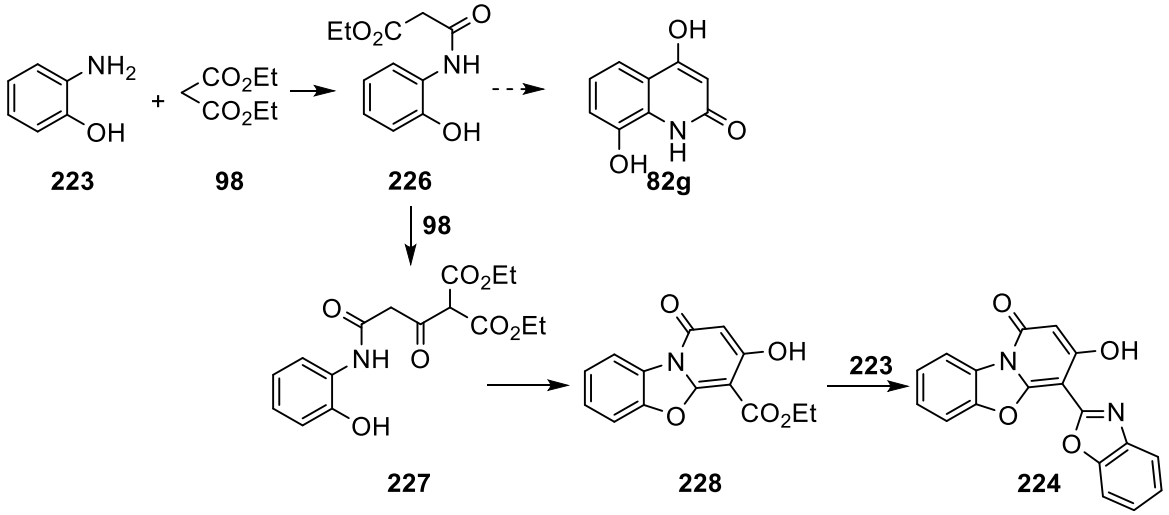

Scheme 47. The proposed rationale for the formation of **224**.

The structure of product **225** was deduced from the corresponding NMR and IR spectra as well as by mass spectrometry (see chapter 5.2.5). Additionally, the structure of compound **225** was confirmed by X-ray crystallography (Figure 71).

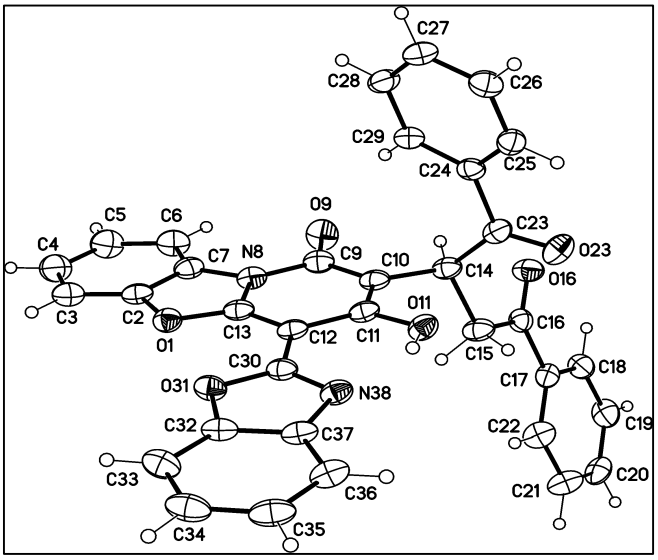

Figure 71: Molecular structure of compound **225** assigned as 2-(4-hydroxy-6-methyl-2-oxo-1,2-dihydroquinolin-3-yl)-1,4-diphenylbutane-1,4-dione (displacement parameters are drawn at 50% probability level).

In summary, the reaction of 1,6-disubstituted-4-hydroxy-quinolin-2-ones **82a-f** with 3,4,5,6-tetrachloro-1,2-benzoquinone (*o*-CHL) (**205**) afforded a series of novel 7,8-dichloro-benzofuro[3,2-*c*]quinoline-6,9,10(5*H*)-triones (**206a-f**). Then, reactions of 2,3-dichloropyrazine (**212**) with **82a-f** provided 5,12-dihydropyrazino[2,3-*c*:5,6-*c*′]difuro[2,3-*c*:4,5-*c*′]diquinoline-6,14(5H,12*H*)-diones **213a-f**, *via* an apparent S_NAr/ANRORC sequence. Finally, the reaction of the same quinolones **82a-f** with *E*-dibenzoylethene (**219**) led to conjugate addition without

cyclization and afforded **220a-f**. However, the reaction of 2-hydroxyaniline **223** with diethyl malonate **98** unexpectedly led to 4-(benzo-[*d*]oxazol-2-yl)-3-hydroxy-1*H*-[4,5]oxazolo-[3,2-*a*]pyridine-1-one **224**, which also underwent conjugate addition to dibenzoylethene to give 2-(4-hydroxy-6-methyl-2-oxo-1,2-dihydroquinolin-3-yl)-1,4-diphenylbutane-1,4-dione **225**.

4. Summary and Outlook

This work aimed to investigate new synthetic routes towards novel five-membered heterocycles attached to [2.2]paracyclophane or fused with 4-hydroxy-quinoline-2-ones and determine the biological activity and chirality.

4.1. Tetrasubstituted Thiazoles

In the first part of the work, the transformation of *N*-substituted 2-(pyridyl-, furan-, or thiophene-) thiosemicarbazides **145a-f** to *N*-(2-substituted imino)-4-amino-5-cyanothiazol-3(2*H*)-3-yl)-(pyridyl-, furan-, or thiophene-)-2-carboxamides **146a-f** was achieved *via* the reaction with tetracyanoethylene (TCNE, **143**). In this transformation, TCNE was used as a building block. Optimization of reaction conditions was done, the best results were achieved in experiments at r.t. with THF as the solvent providing the target products **146a-f** (6 examples) in 68-79% yield (Figure 72).

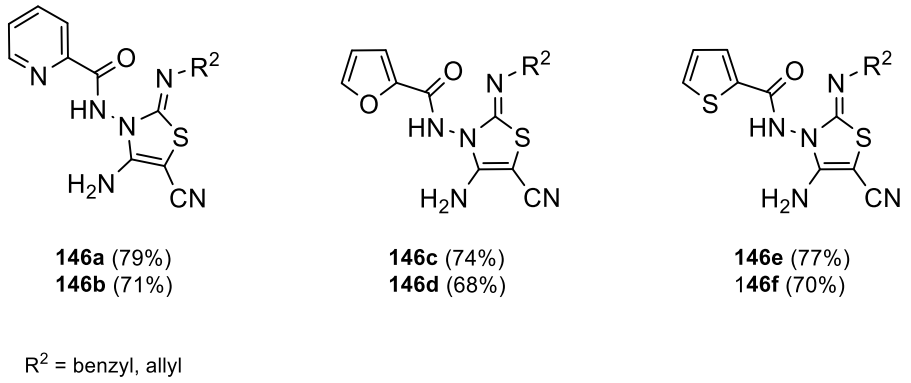

Figure 72: Overview of the synthesized tetrasubstituted thiazoles.

4.1.1. Outlook for Tetrasubstituted Thiazoles

Heteroylhydrazinecarbothioamides are multi-dentate nucleophiles which allow for various modes of heterocyclization with different types of acceptors and were already investigated during my master thesis to produce substituted imidazoles,[130] thiazoles,[131] and thiadiazines.[132] Now TCNE was applied to produce tetrasubstituted thiazoles **146a-f**. No further investigation is needed, but the investigation of the prospective biological activities of these compounds is planned.

4.2. [2.2]Paracyclophane-based Hydrazinecarbothioamides

The second part of the thesis focused on the syntheses of novel derivatives with [2.2]paracyclophane backbones. First, a new synthesis route towards (4-[2.2]paracyclophanyl)-hydrazide **159** (Scheme 49) was investigated. Compound **159** was successfully prepared in 80% yield by boiling the corresponding ester **158** directly in an excess of hydrazine hydrate. Then, hydrazide **159** was applied in two different synthesis routes. In the first route, it was reacted with the prepared [2.2]paracyclophane isocyanate **163** under the suitable condition to produce the target product 2-(4-[2.2]paracyclophanoyl-*N*-4-([2.2]paracyclophanylhydrazine carboxamide **164** in 70% yield. Furthermore, the homochiral analog for the diastereomer-**164** was successfully prepared by starting with the scalemic 4-formyl[2.2]paracyclophane *scal*-**132**,[82] which undergoes multistep reaction yielding carbohydrazide *scal*-**159** as well as isocyanate *scal*-**163**, which then undergoes the same condition to afforded *scal*-**164**. The desired pure chiral (S_p,S_p)-**164** was obtained in 50% yield by applying HPLC-based chiral separation.

The second route was designed to synthesize the staring material for all of the upcoming work, by reacting (4-[2.2]paracyclophanyl)hydrazide **159** with different derivatives of isothiocyanate to afford the corresponding [2.2]paracyclophanyl-*N*-substituted hydrazinecarbothioamides **135a-f**. To optimize the yield, different reaction conditions were tested, whereas the highest yields (80-88%) were achieved in ethanol at r.t. (Scheme 49).

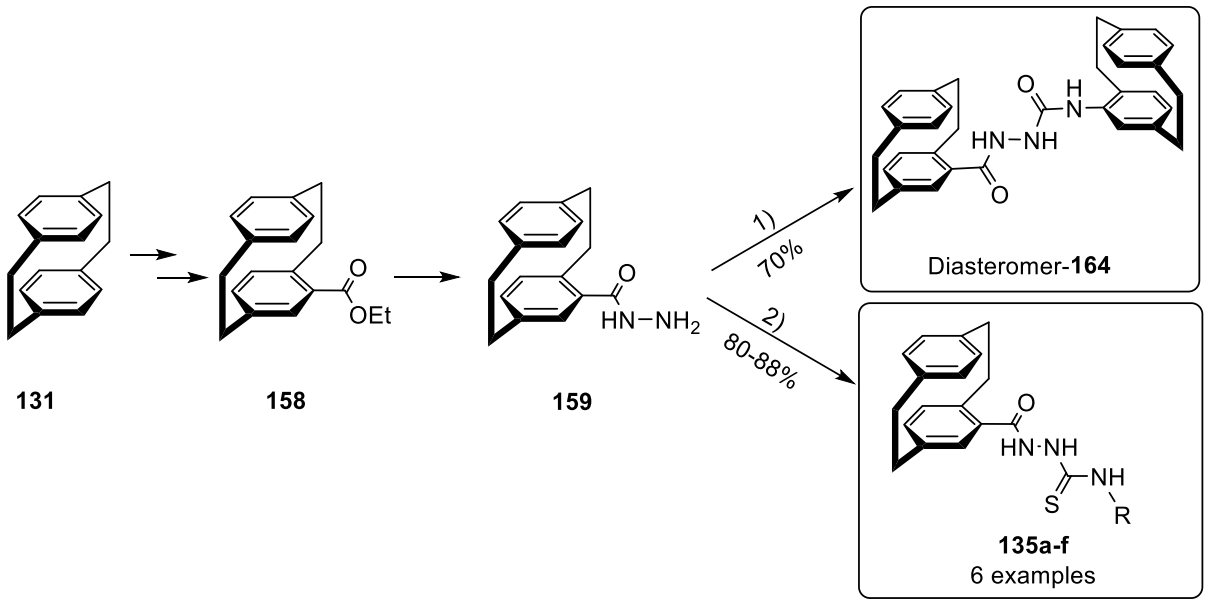

Scheme 49. Schematic routes of the synthesis of (4-[2.2]paracyclophanyl)hydrazide **159**, diastereomer-**164**, and [2.2]paracyclophanyl-*N*-substituted hydrazinecarbothioamide **135a-f**. Reaction conditions: 1) [2.2]PC-NCO, EtOH:DMF (25:1)/ heating at 70 °C. 2) R-NCS / EtOH, reflux, 70 °C, 4-8 h.

Azole-linked [2.2]paracyclophanes have been frequently used in catalyst design and other applications.[86-112] Various azole-linked [2.2]paracyclophanes were successfully obtained by applying cyclization reaction conditions on [2.2]paracyclophanyl-*N*-substituted hydrazine-carbothioamides **135a-f**. 1,2,4-Triazole-3-thiones **136a-f** could be obtained by boiling [2.2]paracyclophanylhydrazinecarbothioamide derivatives **135a-f** in sodium hydroxide for 2-4h, a white precipitate from the target molecule 4-substituted 5-(4'-[2.2]paracyclophanyl)-2,4-dihydro-3*H*-1,2,4-triazole-3-thiones **136a-f** in good yields (Scheme 48). However, also 1,3,4-oxadiazoles **137a-e** were synthesized in moderate yields by boiling **135a-e** in THF/Et_3N for about 12-24 h (Scheme 48).

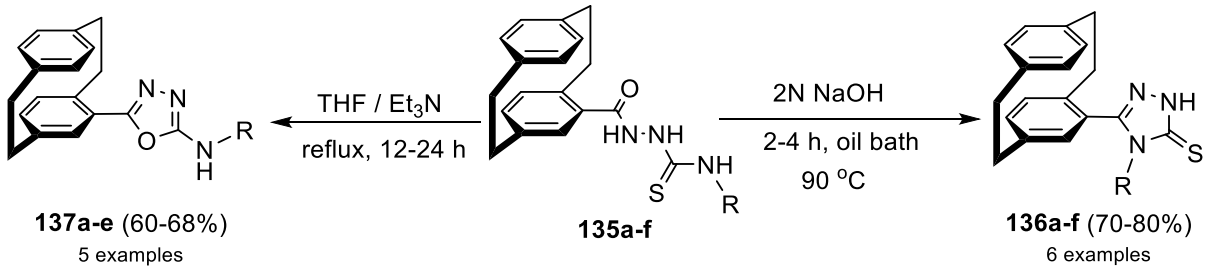

Scheme 48. Synthesis of 1,2,4-triazole-3-thiones **136a-f** and 1,3,4-oxadiazoles **137a-e**.

4.2.1. Outlook for [2.2]Paracyclophane-based Hydrazinecarbothioamides

For the [2.2]paracyclophanyl-*N*-substituted hydrazinecarbothioamide series **135a-f**, more derivatives will be prepared. It also planned to synthesize pseudo-*ortho* and pseudo-*para* analogs with hydrazinecarbothioamides linked and chiral derivatives from the pseudo-*ortho* and pseudo-*para* analogs will also be prepared.

Furthermore, thioglycosides have received considerable attention, because they are widely employed as biological inhibitors.[297-300] The synthesis of thioglycosides attached to [2.2]paracyclophane can be investigated by reacting 1,2,4-triazole-3-thiones **136a-f** with 1-bromide sugars (**225**) to afford the corresponding [2.2]paracyclophane-based thioglycosides **226a-f** (Scheme 49).

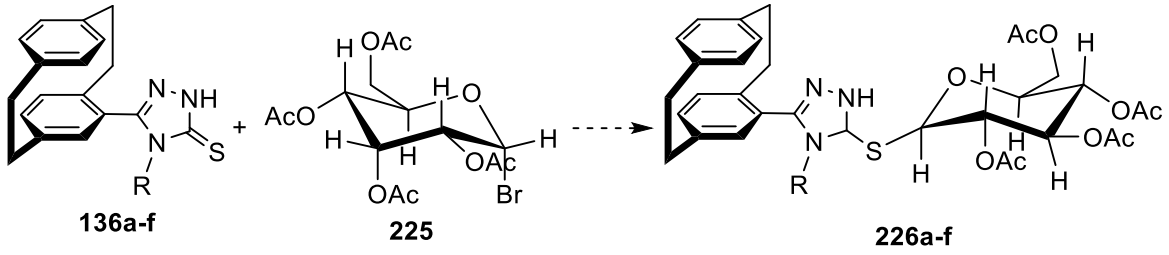

Scheme 49. Schematic plan to synthesize [2.2]paracyclophane-based thioglycosides **226a-f**.

4.3. Homochiral Paracyclophanyl-based [3.3.3]Propellanes

Novel derivatives of [3.3.3]propellanes attached to [2.2]paracyclophane were successfully synthesized in good yields by applying donor-acceptor reactions to the [2.2]paracyclophanyl-substituted hydrazinecarbothioamides **135a-e** with CNIND (**174**) in THF. The reactions yielded the corresponding [2.2]paracyclophanylindenofuranylimidazo[3.3.3]propellanes **138a-e** and the spiro-**175** were obtained as a side product (Scheme 50). The main goal was to prepare the homochiral derivatives from the [2.2]paracyclophanylindenofuranylimidazo-[3.3.3]propellanes **138a-e**, by using the scalemic carbohydrazide **159** and repeating the previous steps, compound *scal*-**138a** was synthesized. Enantiomerically pure chiral (S_p)-**138a** was obtained in very good yield (84%) *via* chiral HPLC separation.

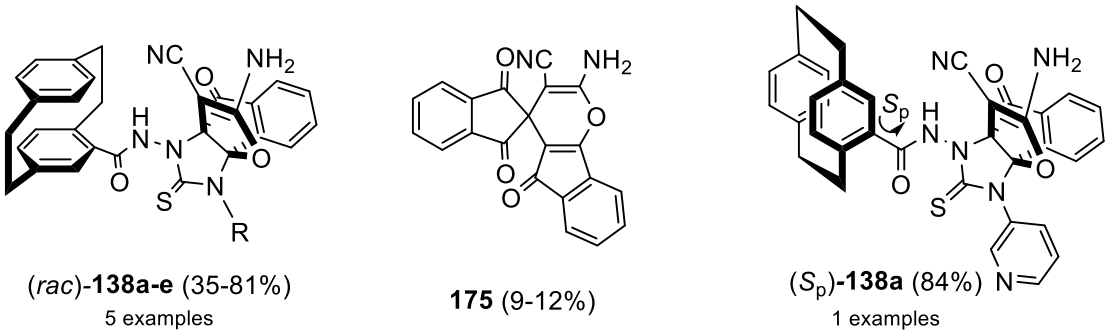

Scheme 50. Overview of isolated products(*rac*)-**138a-e**, **175**, and (S_p)-**138a.**

4.3.1. Outlook for Homochiral [2.2]Paracyclophanyl-based [3.3.3]Propellanes

As only one example for homochiral [2.2]paracyclophanylindenofuranylimidazo-[3.3.3]propellanes **138a** was successfully prepared, its necessary to synthesize more derivatives which correspond to the racemic compounds **138a-e**. Thereupon, the biological activities of these compounds will be studied.

[2.2]Paracyclophanylindenofuranylimidazo[3.3.3]propellanes **138a-f** are very interesting molecules as they contain a lot of functional groups that can make them act as donor and acceptor in the same time, dependent on the type of reaction. In the future, different reactions with compounds **138a-f** will be tested, to investigate under which conditions these compounds act as electron-withdrawing molecules or as electron-donating molecules, respectively (Figure 73).

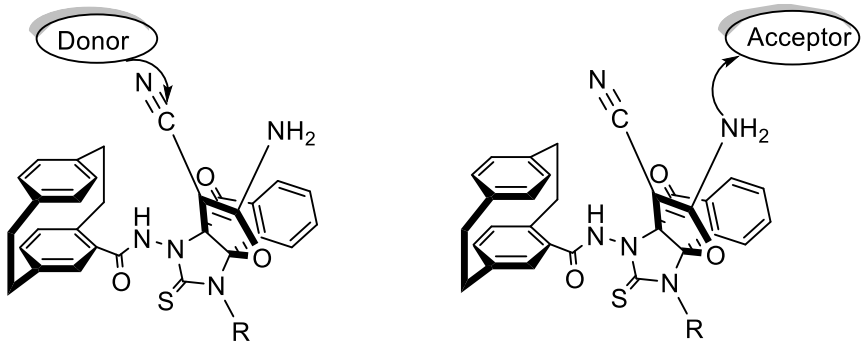

Figure 73: Multi-functionalized groups in [2.2]paracyclophanylindenofuranylimidazo[3.3.3]propellanes **138a-f**.

4.4. [2.2]Paracyclophanylthiazoles as Anti-cancer Agents

To develop new anti-tumor agents gathering both thiazole and [2.2]paracyclophane, the series **I**, **II**, **III**, **IV** shown in Figure 74 were designed. The biological activities against tumor cells of these compounds were evaluated for a full panel of 60 cell lines derived from nine cancer types [236] by the National Cancer Institute (NCI, USA). Molecular docking and mechanistic studies were performed in collaboration with Dr. E. M. N. Abdelhafez.

For the series **I**, [2.2]paracyclophanyl-substituted hydrazinecarbothioamides **135a-f** were reacted with dimethyl acetylenedicarboxylate (**189a**) in methanol to afford the expected thiazolidinones **139b-f** together with **190** in 67-78% yields (Figure 74).

The screening of compounds **139b-f** revealed that compound **139b** caused complete cell death on the nine tested cancer cell lines. Consequently, compound **139b** was selected by NCI for five dose investigations against the full panel of 60 human tumor cell lines. It showed a broad-spectrum antitumor activity against the nine tumor subpanels tested with selectivity ratios ranging between 0.63-1.28 and 0.58-5.89 at the GI_{50} and TGI levels

, respectively. By testing the ability of compounds **139b-f** and **190** to inhibit tubulin polymerization inhibitory at their IC_{50} concentrations using ELISA assays for β-tubulin, compound **139b** showed the highest ability to inhibit tubulin polymerization with an IC_{50} value of 4.97. Furthermore, it was found that **139b** induced the production of significant amounts of ROS (109.84%) compared to control cells and Colchicine reference. Results also revealed that **139b** is a potential caspase-3 activator and slightly increases the level of active caspase-3 with conc 471.2 ng/mL (8.84 fold) compared to Colchicine with conc 428.9 ng/mL (8.05 fold). A molecular docking study was performed to explain and confirm the mechanism of action. All of these results indicate that compound **139b** could be considered a good pharmacophore in further medicinal studies.

Afterward, the design and syntheses of compounds **140b-f** (series **II**), **141b-d,f** (series **III**) and **196** (series **IV**) were investigated. To synthesize compounds **140b-f**, **135b-f** were reacted with 2,3-dichloro-1,4-naphthoquinone (**191**) under Eschenmoser contraction conditions to give fused thiazoles **140b-f** in 55-70% yield (Figure 74). While **141b-d,f,** and **196** were synthesized by reactions of **135a-f** with 2-bromo-1-(naphthalene-1-yl)ethanone (**195**) in ethyl acetate to give compounds **141b-d,f** in good yield (52-79%). However, reactions of compound **135e** with **195** gave the regioisomer **196** in 60% yield (Figure 74).

In subsequent experiments, compounds **140c**, **140d,** and **140e** were shown to induce complete cell death of different cancer cell lines and were therefore selected for advanced five-dose testing against the full panel of 60 human tumor cell lines. Compounds **140c**, **140d,** and **140e** were found to be a broad-spectrum antitumor agent against different tested tumor subpanels with no selectivity toward the tested cell lines. It can be deduced that the replacement of the naphthyl group by naphthoquinone group in compounds **140b-f** gives rise to the anti-cancer activity, which could be attributed to an increased binding to the target protein due to the presence of two additional oxygen groups in the quinone moiety.

In course of the evaluation of the *in vitro* antiproliferative activities against the melanoma SK-MEL-5 cell line, it was found that the three most active [2.2]paracyclophane/thiazole conjugates bearing naphthoquinone moiety **140c**, **140e**, and **140f** exhibited potent to remarkable proliferation inhibition of cancer cell with IC_{50} values of 0.81, 4.18 and 9.11 µM compared to Dinaciclib with IC_{50} of 5.97 µM. These results encouraged further investigations of **140c** and **140e** for their antiproliferation on healthy cell lines in MTT assays, in which compounds **140c** and **140e** achieved IC_{50} values of 32.59 and 39.86 µM, respectively on the WI38 cell line which are higher than that of the reference Dinaciclib (IC_{50} = 22.01 µM). The obtained results indicate the relative safety of the tested compounds on normal cells, also they showed a good selectivity window between normal cells and cancer cells.

Consequently, compound **140c** was investigated extensively and it showed a marked downregulation of phospho-Tyr15 with a level (7.45 pg/mL) comparable to that of the reference. Furthermore, the effect of compound **140c** on caspase-3 was evaluated to find increasing in its level by 8.66 folds. The effect of compound **140c** on the cell cycle arrest was also examined. Moreover, a molecular docking study was performed to explain and confirm the mechanism of action.

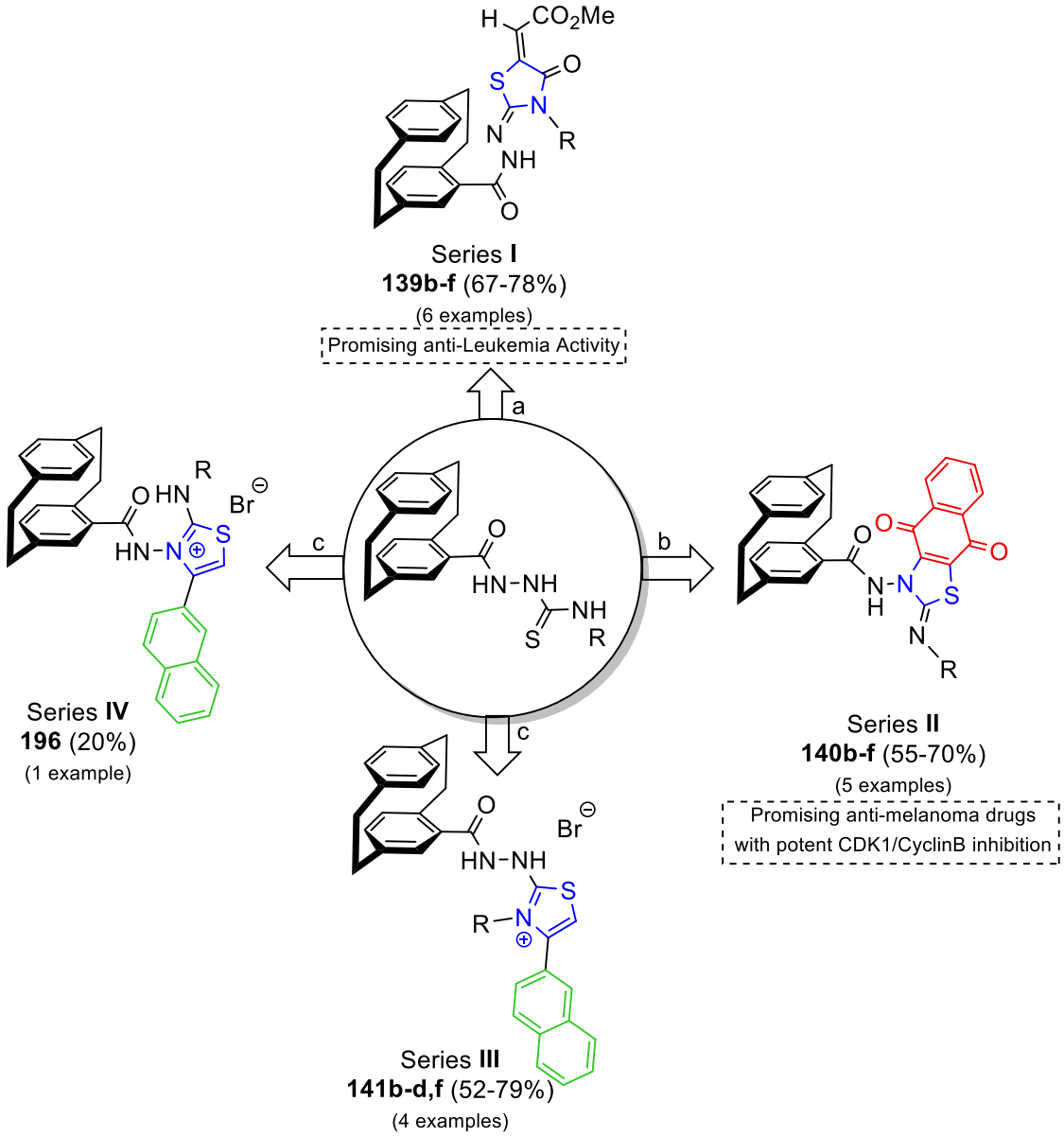

Figure 74: Designed [2.2]paracyclophanylthiazoles as anti-cancer Drugs. Reagents and conditions: a) DMAD, MeOH, reflux, 3-4 h; b) DCNQ, Ph_3P, Et_3N, CH_3CN, reflux, 10-14 h; 2-bromo-2′-acetonaphthone, EtOAC, r.t., 24-48 h.

4.4.1. Outlook for [2.2]Paracyclophanylthiazoles as Anti-cancer Agents

These combined results led to the discovery of novel promising thiazole/[2.2]paracyclophanes hybrids as interesting starting points in medicinal chemistry that warrants further research and development as potential cancer candidates.

4.5. Fused Heterocycles Based on 4-Hydroxy-2-quinolones

In this section, the aim was to investigate new fused five-membered heterocyclic rings based on 4-hydroxy-2-quinolones. The reactivity of 1,6-disubstituted-4-hydroxy-2(1*H*)-quinolinones

82a-f towards 3,4,5,6-tetrachloro-1,2-benzoquinone (**205**), 2,3-dichloropyrazine (**212**), and *E*-dibenzoylethene (**219**) was tested.

First, 4-hydroxy-2(1*H*)-quinolinones **82a-f** were reacted with 3,4,5,6-tetrachloro-1,2-benzoquinone (**205**) in THF under reflux for 10-15 h (Figure 75), yielded the corresponding 7,8-dichloro-benzofuro[3,2-*c*]quinoline-6,9,10(5*H*)-triones **206a-f** in a good yield (70-78%). Afterward, by focusing on the preparation of new furopyrazines fused with quinolones (Figure 75), refluxing of one mole of 2,3-dichloropyrazine (**212**) and two mole of 1,6-disubstituted-4-hydroxyquinoline-2-ones **82a-f**, in DMF/Et_3N, pyrazino[2′,3′:4,5]furo-[3,2-*c*]quinolin-6(5*H*)-ones **213a-f** was obtained as single products with a good yield (60-70%). The formation of **213a-f** was obtained by either S_NAr or by ANRORC mechanisms. Furthermore, the reaction of 4-hydroxy-quinoline-2-ones **82a-f** with alkenes was studied by reacting *E*-dibenzoylethene (**219**) with **82a-f** in pyridine/Et_3N (Figure 75). The compounds **220a-f** were obtained as single products with a good yield, while the targeted compounds were not formed under these conditions. Interestingly, on preparing 4-hydroxy-2-quinolone **82g** from 2-hydroxyaniline (**223**), the novel quinolones **224** was obtained in 80% yield (Figure 75). Under the same reaction conditions, **224** with **219** reacted to compound **225** in 85% yield.

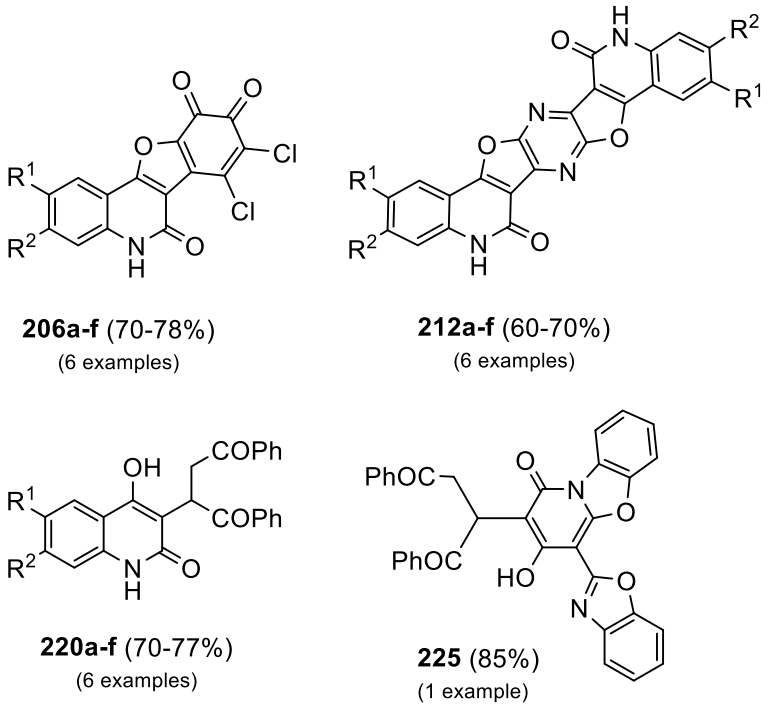

Figure 75: Overview of isolated products from the reaction of 4-hydroxy-quinoline-2-ones **82a-f** with different types of the acceptor.

4.5.1. An Outlook of Fused Heterocycles Based on 4-Hydroxy-2-quinolones

As new fused five-membered heterocycles were synthesized successfully, future work will aim to find reaction conditions under which the fused furo-quinolones **221a-f** are formed. Also, a novel series of derivatives of quinolone **224** will be synthesized by using different *ortho*-substituted anilines, like 2-aminoaniline or 2-aminobenzenethiol, and applying different methods for the formation of new heterocycles.

5. Experimental Section

5.1. General Remarks

Parts of the general information are standardized descriptions and were taken from a previous group member.[301] Literal excerpts thereof are marked with an asterisk *.

5.1.1. Nomenclature of [2.2]Paracyclophanes

*The IUPAC nomenclature for cyclophanes, in general, is rather confusing and difficult to understand. Therefore VÖGTLE *et al.* developed a specific cyclophane nomenclature, which is based on a core-substituent ranking.[76] This is exemplified in Figure 76 for 4-formyl[2.2]paracyclophane. The core structure is named according to the length of the aliphatic bridges in squared brackets (e.g. [n.m]) and the benzene substitution patterns (*ortho*, *meta*, or *para*).

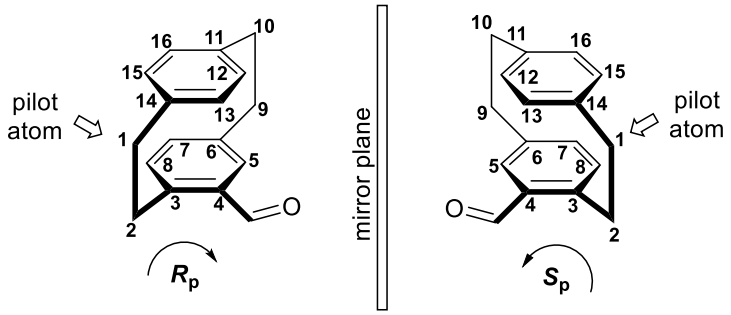

Figure 76: Nomenclature illustrated on the enantiomers of 4-formyl[2.2]paracyclophane.

[2.2]Paracyclophane possesses a D_{2h} symmetry, which is broken by the first substituent, resulting in two planar chiral enantiomers. They cannot be drawn in a racemic fashion. By definition, the arene bearing the substituent is set to a chirality plane, and the first atom of the cyclophane structure outside the plane and closest to the chirality center is defined as the "*pilot atom*". If both arenes are substituted, the substituent with higher priority according to the Cahn-Ingold-Prelog (CIP) nomenclature is preferred.[302] The stereo descriptor is determined by the sense of rotation viewed from the pilot atom. An unambiguous numeration (Figure 76) is required to describe the positions of the substituents correctly. The numbering of the arenes follows the sense of rotation determined by CIP. To indicate the stereochemistry of the planar chirality, a subscripted *p* is added. As it is impossible to draw PC in a racemic manner, only one arbitrary enantiomer/diastereomer is shown in each case for the racemic products.

5.1.2. Devices and Analytical Instruments

Nuclear Magnetic Resonance Spectroscopy (NMR)

*The NMR spectra of the compounds described herein were recorded on a Bruker Avance 300 NMR instrument at 300 MHz for ^{1}H NMR and 75 MHz for ^{13}C NMR, a Bruker Avance 400 NMR instrument at 400 MHz for ^{1}H NMR and 101 MHz for ^{13}C NMR, a Bruker Avance 500 NMR instrument at 500 MHz for ^{1}H NMR and 125 MHz for ^{13}C NMR.

The NMR spectra were recorded at room temperature in deuterated solvents acquired from Eurisotop. The chemical shift δ is expressed in parts per million [ppm] and the references used were the ^{1}H and ^{13}C peaks of the solvents themselves: d_1-chloroform ($CDCl_3$): 7.26 ppm for ^{1}H NMR and 77.0 ppm for ^{13}C NMR, d_6-dimethyl sulfoxide ($(CD_3)_2SO$-d_6): 2.50 ppm for ^{1}H NMR and 39.4 ppm for ^{13}C NMR and d_6-acetone (Acetone-d_6): 2.05 ppm for ^{1}H NMR and 29.8 and 206.2 ppm for ^{13}C NMR.

For the characterization of centrosymmetric signals, the signal's median point was chosen, for multiplets the signal range was given. The following abbreviations were used to describe the proton splitting pattern: d = doublet, t = triplet, m = multiplet, dd = doublet of doublet, ddd = doublet of doublet of doublet, dt = doublet of triplet. Absolute values of the coupling constants "*J*" are given in Hertz [Hz] in absolute value and decreasing order. The following abbreviations were used to distinguish between signals: H^{Ar} = aromatic-CH, H^{Pc} = [2.2]paracyclophane-CH_2. Signals of the ^{13}C NMR spectra were assigned with the help of distortionless enhancement by polarization transfer spectra DEPT90 and DEPT135 and were specified in the following way: + = primary or tertiary carbon atoms (positive DEPT signal), – = secondary carbon atoms (negative DEPT signal), C_q = quaternary carbon atoms (no DEPT signal).

In some cases, the signals were assigned using ^{1}H-^{1}H COSY (correlation spectroscopy), ^{1}H-^{13}C-HSQC (Heteronuclear Single Quantum Coherence) and ^{1}H-^{13}C-HMBC (Heteronuclear Multiple Quantum Correlation) techniques.

Infrared Spectroscopy (IR)

*The infrared spectra were recorded with a Bruker Alpha ATR instrument. Solids were measured by attenuated total reflection (ATR) method. The positions of the respective transmittance bands are given in wavenumbers $\bar{\upsilon}$ [cm^{-1}] and were measured in the range from 3600 cm^{-1} to 500 cm^{-1}.

Characterization of the transmittance bands was done in a sequence of transmission strength T with the following abbreviations: vs (very strong, 0−9% T), s (strong, 10−39% T), m (medium, 40−69% T), w (weak, 70−89% T), vw (very weak, 90−100% T) and br (broad).

Mass Spectrometry (MS)

*Fast atom bombardment (FAB) experiments were conducted using a Finnigan, MAT 90 (70 eV) instrument, with 3-nitrobenzyl alcohol (3-NBA) as matrix and reference for high resolution. For the interpretation of the spectra, molecular peaks $[M]^+$, peaks of protonated molecules $[M+H]^+$, and characteristic fragment peaks are indicated with their mass-to-charge ratio (*m/z*). In the case of high-resolution measurements, the tolerated error is 0.0005 m/z.

Electrospray ionization-mass spectrometry (ESI) experiments were recorded on a Q-Exactive (Orbitrap) mass spectrometer (Thermo Fisher Scientific, San Jose, CA, USA) equipped with a HESI II probe to record high resolution. The tolerated error is 5 ppm of the molecular mass. Again, the spectra were interpreted by molecular peaks $[M]^+$, peaks of protonated molecules $[M+H]^+$, and characteristic fragment peaks and indicated with their mass-to-charge ratio (*m/z*).

High-resolution mass spectrometry (HRMS) the measurements were either recorded with the Finnigan MAT 95 (FAB) or with the ThermoFisher QExactive Plus (ESI). The following abbreviations were used: calc. = expected value (calculated); found = value found in the analysis.

Elemental Analysis (EA)

*Elemental analyses were performed on an Elementar vario MICRO instrument. The weight scale used was a Sartorius M2P. Calculated (calc.) and found percentage by mass values for carbon, hydrogen, nitrogen, and sulfur are indicated in fractions of 100%.

Melting Points (Mp)

Melting points were taken in open capillaries on an OptiMelt MPA100 device from the company Stanford Research System or on a Gallenkamp melting point apparatus (Weiss-Gallenkamp, Loughborough, UK) and are uncorrected.

Thin Layer Chromatography (TLC)

*For the analytical thin layer chromatography, TLC silica plates coated with fluorescence indicator from Merck (silica gel 60 F254, thickness 0.2 mm) were used. UV-active compounds

were detected at 254 nm and 366 nm excitation wavelength with a Heraeus UV-lamp, model Fluotest.

Weight Scale

For weightings of solids and liquids, a Radwag Wagi model AS 220.X2 was used.

High-Performance Liquid Chromatography (HPLC)

Purification of diastereomeric mixtures such as *N*-([2.2]paracyclophanylcarbamoyl)-4-([2.2] paracyclophanylcarboxamide **157** and *N*-((3*aS*,8*bR*)-2-amino-3-cyano-4-oxo-9-(pyridin-3-yl)-10-thioxo-4*H*-3*a*,8*b*-(epiminomethanoimino)indeno[1,2-*b*]furan-11-yl)[2.2]paracyclophan-amide **169a** were conducted using preparative HPLC setups: JASCO HPLC System (LC-NetII/ADC) equipped with two PU-2087 Plus pumps, a CO-2060 Plus thermostat, a MD-2010 Plus diode array detector and a CHF-122SC fraction collector of ADVANTEC. For the purification, a Daicel Chiralpak (AZ-H 20 × 250 mm, the particle size of 5 µm) was used with HPLC-grade acetonitrile as a mobile phase. Detection was conducted at 256 nm.

Analysis of the enantiomeric excess was conducted using an AGILENT HPLC 1100 series system with a G1322A degasser, a G1211A pump, a G1313A autosampler, a G1316A column oven, and a G1315B diode array system. Chiralpak OD-H (4.6 × 250 mm, 5 µm particle size) columns were used with HPLC-grade *n*-hexane/isopropanol as a mobile phase.

Optical Rotations

Optical Rotations for each chiral, non-racemic compound was measured by using Perkin-Elmer 241 Polarimeter, it was calculated according to the following equation:

$$[\alpha]_{\lambda}^{T} = \frac{\alpha}{c.1} \quad [\mathrm{ml \cdot dm^{-1} g^{-1}}]$$

α: measured rotational angle [°]
c: sample concentration [g/ml]
l: cuvette length [dm]
T: temperature [K]
λ: wavelength of the polarized light [nm]

The measurement was conducted at 20 °C with the sodium *D* line with a wavelength of λ=589.3 nm: $[\alpha]_{D}^{20}$

5.1.3. Solvents and Reagents

*Solvents of technical quality were purified by distillation or with the solvent purification system MB SPS5 from MBRAUN before use. Solvents of *p.a.* (*per analysis*) quality were commercially acquired from Sigma Aldrich, Carl Roth, Acros Organics, or Thermo Fisher Scientific and, unless otherwise stated, used without further purification. Dry solvents were either purchased from Carl Roth, Acros Organics, or Sigma Aldrich (< 50 ppm H_2O over molecular sieves). All reagents were commercially acquired from abcr, Acros Organics, Alfa Aesar, Sigma Aldrich, TCI, Chempur, Carbolution, or Synchemie. Unless otherwise stated, all chemicals were used without further purification.

5.1.4. Experimental Procedure

*Air- and moisture-sensitive reactions were carried out under argon atmosphere in oven-dried glassware using standard Schlenk techniques. Solid compounds were ground using a mortar and pestle before use, liquid reagents and solvents were injected with plastic syringes and stainless-steel cannula of different sizes unless otherwise specified.

Reactions at low temperature were cooled using flat dewars produced by Isotherm, Karlsruhe, filled with a water/ice mixture for 0 °C, water/ice/sodium chloride for –20 °C, or isopropanol/dry ice mixture for –78 °C. For reactions at high temperature, the reaction flask was equipped with a reflux condenser and connected to the argon line.

Solvents were evaporated under reduced pressure at 40 °C using a rotary evaporator. Unless otherwise stated, solutions of inorganic salts are saturated aqueous solutions.

Reaction Monitoring

The progress of the reaction in the liquid phase was monitored by TLC. UV active compounds were detected with a UV-lamp at 254 nm and 366 nm excitation wavelength. When required, a solution of Seebach reagent (2.5% phosphor molybdic acid, 1.0% Cerium(IV) sulfate tetrahydrate and 6.0% sulfuric acid in H_2O, dipping solution) or potassium permanganate (1.5 g $KMnO_4$, 10 g K_2CO_3 and 1.25 ml 10% NaOH in 200 ml H_2O, dipping solution) and heated with a heat gun.

Product Purification

Unless otherwise stated, the crude compounds were purified *via* column chromatography. For the stationary phase of the column, silica gel, produced by Merck (silica gel 60, 0.040 × 0.063 mm, 260 – 400 mesh ASTM), and sea sand by Riedel de-Haën (baked out and washed with hydrochloric acid) were used. Solvents used were commercially acquired in HPLC-grade or *p. a.* grade and individually measured volumetrically before mixing.

5.2. Synthetic Methods and Characterization Data

5.2.1. Analytical Data of Tetrasubstituted Thiazoles

N-substituted 2-heteroylhydrazinecarbothioamides **145a-f** were prepared according to the literature.[303-304]

General Procedures (GP1)

A solution of *N*-substituted 2-heteroylhydrazinecarbothioamides (**145a-f**, 1.00 mmol, 1.00 equiv.) in dry THF (25 mL) was added dropwise to tetracyanoethylene (TCNE) (**143**, 0.128 g, 1.00 mmol, 1.00 equiv.) in dry THF (20 mL) under stirring at room temperature. The reaction mixture was stirred for 70-72 h at room temperature which caused a spontaneous change of color from green to brown and finally to yellow with consuming all the starting materials and completion of the reaction. After removal of the solvent under reduced pressure, the crude residue was purified by column chromatography to afford **146a-f**.

(*Z*)-*N*-(4-Amino-2-(benzylimino)-5-cyanothiazol-3(2*H*)-yl)picolinamide (146a)

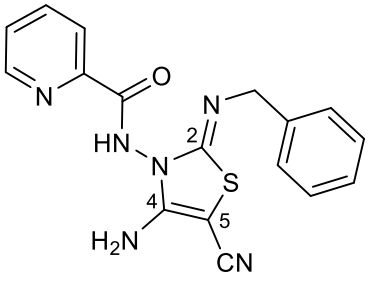

According to **GP1**, *N*-benzyl-2-picolinoylhydrazine-1-carbothioamide (**145a**, 0.286 g, 1.00 mmol, 1.00 equiv.) was reacted with TCNE (**143**, 0.128 g, 1.00 mmol, 1.00 equiv.) in dry THF (20 mL) for 72 h. The crude product was purified by column chromatography (cyclohexane/ethyl acetate; 20:1) to yield 0.275 g (79%, 785 µmol) of the title compound as a yellow solid.

R_f = 0.27(cyclohexane/ethyl acetate; 20:1). – **Mp**: 124–125 °C. – **^{1}H NMR** (400 MHz, DMSO-d_6) δ = 11.30 (s, 1H, N*H*), 8.76–8.66 (m, 1H, H^{Ar}), 8.10–7.99 (m, 2H, H^{Ar}), 7.70–7.66 (m, 1H, H^{Ar}), 7.45 (s, 2H, NH_2), 7.35–7.12 (m, 5H, H^{Ar}), 4.21 (s, 2H, CH_2) ppm. – **^{13}C NMR** (101 MHz, DMSO-d_6) δ = 163.9 (C_q, *C*O), 161.7 (C_q, *C*4), 153.6 (C_q, *C*2), 150.6 (C_q, C^{Ar}), 148.8 (+, CH^{Ar}), 139.5 (+, CH^{Ar}), 138.0 (C_q, C^{Ar}), 128.3 (+, 2 × CH^{Ar}), 127.7 (+, CH^{Ar}), 127.3 (+, 2 × CH^{Ar}), 126.7 (+, CH^{Ar}), 123.0 (+, CH^{Ar}), 116.8 (C_q, *C*N), 57.7 (C_q, *C*5), 55.83 (–, CH_2) ppm. – **IR** (ATR) = 3330 (m), 3234 (m), 3190 (s), 3060 (w), 2180 (vs), 1704 (m), 1639 (vs), 1571 (vs), 1482 (vs), 1462 (vs), 1340 (s), 1085 (s), 999 (s), 810 (m), 721 (vs), 693 (vs), 601 (vs), 577 (vs) cm^{-1}. – **MS** (FAB, 3-NBA): *m/z* (%) =351 (100) $[M+H]^+$, 350 (97) $[M]^+$. – **EA** ($C_{17}H_{14}N_6OS$) calc.: C, 58.27; H, 4.03; N, 23.98; S, 9.15. found: C, 58.33; H, 4.10; N, 24.04; S, 9.22.

(*Z*)-*N*-(2-(Allylimino)-4-amino-5-cyanothiazol-3(2*H*)-yl)picolinamide (146b)

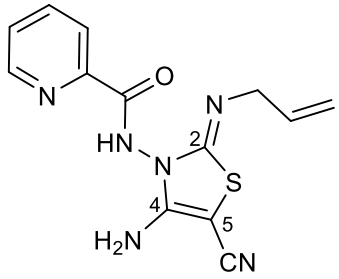

According to **GP1**, *N*-allyl-2-picolinoylhydrazine-1-carbothioamide (**145b**, 0.236 g, 1.00 mmol, 1.00 equiv.) was reacted with TCNE (**143**, 0.128 g, 1.00 mmol, 1.00 equiv.) in dry THF (20 mL) for 72 h. The crude product was purified by column chromatography (cyclohexane/ethyl acetate; 20:1) to yield 0.213 g (71%, 709 µmol) of the title compound as a yellow solid.

R_f = 0.29 (cyclohexane/ethyl acetate; 20:1). – **Mp**: 170–171 °C. – **^{1}H NMR** (400 MHz, DMSO-d_6) δ = 11.25 (s, 1H, N*H*), 8.83–8.62 (m, 1H, H^{Ar}), 8.21–7.92 (m, 2H, H^{Ar}), 7.72–7.66 (m, 1H, H^{Ar}), 7.43 (s, 2H, NH_2), 5.85–5.76 (m, 1H, CH^{allyl}), 5.40–4.87 (m, 2H, CH_2^{allyl}), 3.66–3.62 (m, 2H, CH_2^{allyl}) ppm. – **^{13}C NMR** (101 MHz, DMSO-d_6) δ = 164.1 (C_q, *C*O), 153.6 (C_q, *C*4) 150.3 (C_q, C^{Ar}), 148.9 (+, *C*H^{Ar}), 148.8 (C_q, *C*2), 138.1 (+, *C*H^{Ar}), 135.3 (+, *C*H^{allyl}), 127.8 (+, *C*H^{Ar}), 123.1 (+, *C*H^{Ar}), 116.9 (–, *C*H$_2^{allyl}$), 115.4 (C_q, *C*N), 55.0 (C_q, *C*5), 43.6 (–, *C*H$_2^{allyl}$) ppm. – **IR** (ATR) = 3335 (w), 3293 (w), 3187 (m), 2193 (s), 1704 (m), 1635 (vs), 1587 (vs), 1485 (vs), 1434 (vs), 1340 (s), 1282 (s), 1038 (s), 996 (vs), 921 (vs), 748 (vs), 599 (vs), 555 (vs), 533 (vs), 441 (vs) cm–1. – **MS** (FAB, 3-NBA): *m/z* (%) = 301 (100) $[M+H]^+$, 300 (50) $[M]^+$. – **EA** ($C_{13}H_{12}N_6OS$) calc.: C, 51.99; H, 4.03; N, 27.98; S, 10.68. found: C, 52.05; H, 4.11; N, 28.04; S, 10.73.

(*Z*)-*N*-(4-Amino-2-(benzylimino)-5-cyanothiazol-3(2*H*)-yl)furan-2-carboxamide (146c)

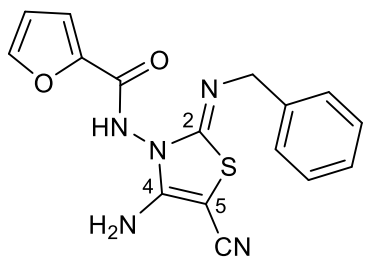

According to **GP1**, *N*-benzyl-2-(furan-2-carbonyl)hydrazine-1-carbothioamide (**145c**, 0.275 g, 1.00 mmol, 1.00 equiv.) was reacted with TCNE (**143**, 0.128 g, 1.00 mmol, 1.00 equiv.) in dry THF (20 mL) for 70 h. The crude product was purified by column chromatography (cyclohexane/ethyl acetate; 20:1) to yield 0.25 g (74%, 737 μmol) of the title compound as an orange solid.

R_f = 0.44 (cyclohexane/ethyl acetate; 20:1). – **Mp**: 180–181 °C. – **^{1}H NMR** (400 MHz, DMSO-d_6) δ = 11.10 (s, 1H, N*H*), 7.98–7.88 (m, 1H, H^{Ar}), 7.75 (s, 2H, NH_2), 7.69–7.30 (m, 5H, H^{Ar}), 7.28–7.10 (m, 2H, H^{Ar}), 4.32 (s, 2H, CH_2) ppm. – **^{13}C NMR** (101 MHz, DMSO-d_6) δ = 157.3 (C_q, *C*O), 153.3 (C_q, *C*4), 145.5 (C_q, C^{Ar}), 139.2 (+, CH^{Ar}), 146.3 (C_q, *C*2), 139.0 (C_q, C^{Ar}), 128.1 (+, 2 × CH^{Ar}), 127.1 (+, 2 × CH^{Ar}), 126.5 (+, CH^{Ar}), 116.4 (C_q, *C*N), 116.1 (+, CH^{Ar}), 113.1 (+, CH^{Ar}), 57.6 (C_q, *C*5), 55.8 (–, CH_2) ppm. – **IR** (ATR) = 3347 (w), 3298 (w), 3187 (m), 2919 (w), 2851 (w), 2190 (s), 1691 (s), 1639 (vs), 1582 (vs), 1494 (vs), 1462 (vs), 1451 (vs), 1340 (s), 1282 (vs), 1152 (vs), 1071 (vs), 857 (s), 768 (vs), 724 (vs), 696 (vs), 592 (vs), 429 (vs) cm^{-1}. – **MS** (FAB, 3-NBA): *m/z* (%) = 340 (100) $[M+H]^+$, 339 (60) $[M]^+$. – **EA** ($C_{16}H_{13}N_5O_2S$) calc.: C, 56.63; H, 3.86; N, 20.64; S, 9.45. found: C, 56.70; H, 3.92; N, 20.69; S, 9.51.

(*Z*)-*N*-(2-(Allylimino)-4-amino-5-cyanothiazol-3(2*H*)-yl)furan-2-carboxamide (146d)

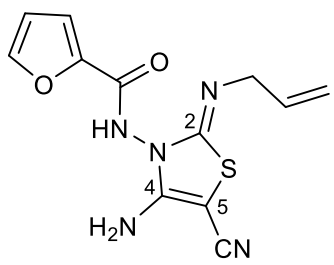

According to **GP1**, *N*-allyl-2-(furan-2-carbonyl)hydrazine-1-carbothioamide (**145d**, 0.225 g, 1.00 mmol, 1.00 equiv.) was reacted with TCNE (**143**, 0.128 g, 1.00 mmol, 1.00 equiv.) in dry THF (20 mL) for 70 h. The crude product was purified by column chromatography (cyclohexane/ethyl acetate; 20:1) to yield 0.196 g (68%, 677 µmol) of the title compound as a yellow solid.

R_f = 0.42 (cyclohexane/ethyl acetate; 20:1). – **Mp**: 130–131 °C. – **^{1}H NMR** (400 MHz, DMSO-*d*$_6$) δ = 11.20 (s, 1H, N*H*), 8.28–8.02 (m, 1H, *H*^{Ar}), 7.58–7.30 (m, 2H, *H*^{Ar}), 7.25 (s, 2H, N*H*$_2$), 5.95–5.73 (m, 1H, C*H*^{allyl}), 5.47–4.80 (m, 2H, C*H*$_2^{allyl}$), 3.96–3.61 (m, 2H, C*H*$_2^{allyl}$) ppm. – **^{13}C NMR** (101 MHz, DMSO-*d*$_6$) δ = 158.3 (C$_q$, *C*O), 154.3 (C$_q$, *C*4), 145.3 (C$_q$, *C*^{Ar}), 139.3 (+, *C*H^{Ar}), 147.3 (C$_q$, *C*2), 133.3 (+, *C*H^{allyl}), 117.2 (–, *C*H$_2^{allyl}$), 116.7 (C$_q$, *C*N), 116.2 (+, *C*H^{Ar}), 114.1 (+, *C*H^{Ar}), 56.8 (C$_q$, *C*5), 48.6 (–, *C*H$_2^{allyl}$) ppm. – **IR** (ATR) = 3531 (w), 3320 (w), 3123 (w), 2956 (w), 2922 (w), 2859 (w), 2203 (w), 1645 (s), 1584 (s), 1470 (s), 1387 (s), 1286 (s), 1169 (s), 1075 (vs), 1014 (vs), 931 (s), 884 (s), 761 (vs), 514 (vs), 455 (vs) cm^{-1}. – **MS** (FAB, 3-NBA): *m/z* (%) = 290 (100) [M+H]$^+$, 289 (65) [M]$^+$. – **EA** ($C_{12}H_{11}N_5O_2S$) calc.: C, 49.82; H, 3.83; N, 24.21; S, 11.08. found: C, 49.88; H, 3.89; N, 24.26; S, 11.17.

(*Z*)-*N*-(4-Amino-2-(benzylimino)-5-cyanothiazol-3(2*H*)-yl)thiophene-2-carboxamide (146e)

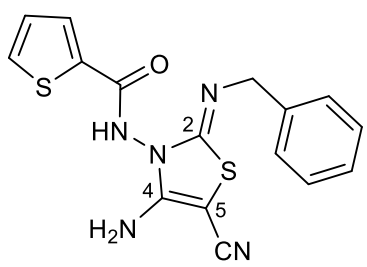

According to **GP1**, *N*-benzyl-2-(thiophene-2-carbonyl)-hydrazine-1-carbothioamide (**145e**, 0.291 g, 1.00 mmol, 1.00 equiv.) was reacted with TCNE (**143**, 0.128 g, 1.00 mmol, 1.00 equiv.) in dry THF (20 mL) for 70 h. The crude product was purified by column chromatography (cyclohexane/ethyl acetate; 20:1) to yield 0.275 g (77%, 774 µmol) of the title compound as an orange solid.

R_f = 0.51 (cyclohexane/ethyl acetate; 20:1). – **Mp**: 140–141 °C. – **^{1}H NMR** (400 MHz, DMSO-d_6) δ = 11.25 (s, 1H, N*H*), 8.01–7.78 (m, 3H, H^{Ar}), 7.55 (s, 2H, NH_2), 7.42–7.02 (m, 5H, H^{Ar}), 4.29 (s, 2H, H_2) ppm. – **^{13}C NMR** (101 MHz, DMSO-d_6) δ = 161.1 (C_q, *C*O), 153.3 (C_q, *C*4), 150.6 (C_q, *C*2), 139.3 (C_q, C^{Ar}), 135.9 (C_q, C^{Ar}), 132.6 (+, CH^{Ar}), 130.5 (+, CH^{Ar}), 128.1 (+, 2 × CH^{Ar}), 127.1 (+, 2 × CH^{Ar}), 127.0 (+, CH^{Ar}), 126.5 (+, CH^{Ar}), 116.4 (C_q, *C*N), 63.4 (C_q, *C*5), 55.8 (–, CH_2) ppm. – **IR** (ATR) = 3588 (w), 3485 (w), 3398 (w), 2925 (w), 2846 (vw), 2225 (s), 2210 (vs), 1655 (m), 1602 (s), 1502 (vs), 1363 (m), 1252 (m), 1105 (m), 1068 (m), 967 (m), 766 (w), 714 (m), 666 (s), 555 (s), 533 (vs) cm^{-1}. – **MS** (FAB, 3-NBA): *m/z* (%) = 356 (100) $[M+H]^+$, 355 (80) $[M]^+$. – **EA** ($C_{16}H_{13}N_5OS_2$) calc.: C, 54.07; H, 3.69; N, 19.70; S, 18.04. found: C, 54.12; H, 3.74; N, 19.74; S, 18.10.

(*Z*)-*N*-(2-(Allylimino)-4-amino-5-cyanothiazol-3(2*H*)-yl)thiophene-2-carboxamide (146f)

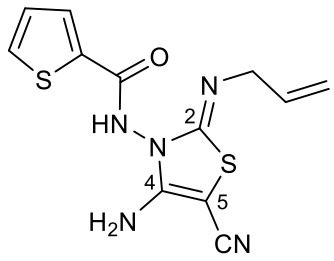

According to **GP1**, *N*-allyl-2-(thiophene-2-carbonyl)hydrazine-1-carbothioamide (**145f**, 0.241 g, 1.00 mmol, 1.00 equiv.) was reacted with TCNE (**143**, 0.128 g, 1.00 mmol, 1.00 equiv.) in dry THF (20 mL) for 70 h. The crude product was purified by column chromatography (cyclohexane/ethyl acetate; 20:1) to yield 0.213 g (70%, 697 µmol) of the title compound as a yellowish-orange solid.

R*f* = 0.53 (cyclohexane/ethyl acetate; 20:1). – **Mp**: 152–153°C. – **^{1}H NMR** (400 MHz, DMSO-*d*$_6$) δ = 11.20 (br, 1H, N*H*), 8.10–7.82 (m, 3H, *H*^{Ar}), 7.55 (s, 2H, N*H*$_2$), 5.90–5.74 (m, 1H, C*H*^{allyl}), 5.21–4.99 (m, 2H, C*H*$_2^{allyl}$), 3.81–3.68 (m, 2H, C*H*$_2^{allyl}$) ppm. – **^{13}C NMR** (101 MHz, DMSO-*d*$_6$) δ = 160.1 (C$_q$, *C*O), 154.4 (C$_q$, *C*4), 138.3 (C$_q$, *C*^{Ar}), 137.2 (C$_q$, *C*2), 133.7 (+, *C*H^{Ar}), 132.2 (+, *C*H^{Ar}), 131.3 (+, *C*H^{allyl}), 129.3 (+, *C*H^{Ar}), 117.4 (–, *C*H$_2^{allyl}$), 114.6 (C$_q$, *C*N) 58.3 (C$_q$, *C*5), 49.6 (–, *C*H$_2^{allyl}$) ppm. – **IR** (ATR) = 3398 (w), 3310 (w), 3131 (w), 3082 (w), 2925 (w), 2868 (w), 2186 (w), 1639 (vs), 1584 (vs), 1527 (vs), 1502 (vs), 1415 (vs), 1354 (vs), 1275 (vs), 1033 (vs), 918 (vs), 851 (vs), 717 (vs) cm^{-1}. – **MS** (FAB, 3-NBA): *m/z* (%) = 306 (100) [M+H]$^+$, 305 (60) [M]$^+$. – **EA** ($C_{12}H_{11}N_5OS_2$) calc.: C, 47.20; H, 3.63; N, 22.93; S, 21.00. found: C, 47.25; H, 3.69; N, 22.98; S, 21.08.

Analytical Data of [2.2]Paracyclophane-based Hydrazinecarbo-thioamides

5.2.2.1. *N*-([2.2]Paracyclophanylcarbamoyl)-4-([2.2]paracyclophanylcarboxamide

(*rac*)-Ethyl [2.2]paracyclophane-4-carboxylate (158)

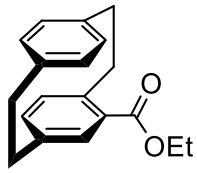

Anhydrous aluminum chloride (0.230 g, 1.73 mmol, 1.73 equiv.) was suspended in 10 mL of dichloromethane. After cooling to –10 °C, a solution of oxalic acid dichloride (0.221 g, 1.75 mmol, 1.75 equiv.) in 5 mL of dichloromethane was added dropwise over 10 min. After stirring for further 10 min at this temperature, the suspension was treated with solid [2.2]paracyclophane (**131)** (0.208 mg, 1.00 mmol, 1.00 equiv.) (red color, exothermic). After a further 10 minutes at –10 °C, the reaction mixture was poured onto 10 g of ice. Thereafter, the mixture was extracted with dichloromethane (3 x 10 mL). The combined organic phases were dried over sodium sulfate and concentrated under reduced pressure to obtain 0.294 g (98%, 984 μmol) of 4-acetyl chloro-[[2.2]paracyclophane] (**156)** as pale yellow crystals. Then, **156** (0.294 g, 1.00 mmol, 1.00 equiv.) was dissolved in 10 ml of chlorobenzene and heated to reflux for 3 h. The chlorobenzene was distilled off under reduced pressure, 0.294 g (quant.) of 4-[[2.2]paracyclophanoyl] chloride **157** were obtained as pale yellow crystals. The formed **157** was then dissolved in 50 mL of ethanol and heated to reflux for 1 h. The solvent was removed under reduced pressure and the crude product was purified by column chromatography on silica gel (cyclohexane/ethyl acetate; 4:1) to yield 0.294 g of the title compound (97%, 1.05 mmol) as a white solid.

R_f = 0.67 (cyclohexane/ethyl acetate; 4:1). – **^{1}H NMR** (300 MHz,$CDCl_3$-*d*) δ = 7.13 (t, *J* = 2.2 Hz, 1H, H^{Ar}), 6.65 (dt, *J* = 7.8, 2.2 Hz, 1H, H^{Ar}), 6.60–6.40 (m, 5H, H^{Ar}), 4.39 (qd, *J* = 7.2, 2.4 Hz, 2H, CH_2), 4.20–4.01 (m, 1H, H^{Pc}), 3.27–2.94 (m, 6H, H^{Pc}), 2.94–2.76 (m, 1H, H^{Pc}), 1.44 (td, *J* = 7.1, 2.4 Hz, 3H, CH_3) ppm. The analytical data matches that of the literature.[152]

(*rac*)-4-[2.2]Paracyclophanyl)hydrazide (159)

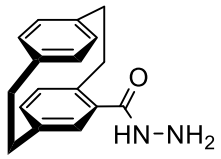

Under an argon atmosphere, a mixture of ethyl [2.2]paracyclophane-4-carboxylate (**158**) (0.280 g, 1.00 mmol, 1.00 equiv.) was dissolved in 10 mL of hydrazine hydrate and refluxed for 14 h. The reaction mixture was then cooled to room temperature until a precipitate was formed (24 h). The precipitate was then filtered and washed with 60 mL of water (three times) followed by 20 ml of heptane and then dried under reduced pressure. The title compound was obtained as a white solid and recrystallized from ethanol to yield 0.220 g (83%, 826 μmol).

R_f = 0.12 (cyclohexane/ethyl acetate; 6:1). – **Mp**: 230–232 °C. – **^{1}H NMR** (400 MHz, DMSO-d_6) δ = 9.09 (s, 1H, N*H*), 6.66 (d, *J* = 1.9 Hz, 1H, H^{Ar}), 6.60 (d, *J* = 7.7 Hz, 1H, H^{Ar}), 6.57 (dd, *J* = 7.7, 1.9 Hz, 1H, H^{Ar}), 6.53 (d, *J* = 1.3 Hz, 2H, H^{Ar}), 6.47 (d, *J* = 7.7 Hz, 1H, H^{Ar}), 6.42 (d, *J* = 7.8 Hz, 1H, H^{Ar}), 4.46 (br, 2H, NH_2), 3.08 (dddd, *J* = 12.7, 9.9, 6.4, 3.1 Hz, 3H, H^{Pc}), 3.04–2.85 (m, 4H, H^{Pc}), 2.81 (ddd, *J* = 12.5, 9.5, 6.3 Hz, 1H, H^{Pc}) ppm. – **^{13}C NMR** (101 MHz, DMSO-d_6) δ = 167.8 (C_q, *C*O), 139.3 (C_q, C^{Ar}), 139.3 (C_q, C^{Ar}), 139.0 (C_q, C^{Ar}), 138.8 (C_q, C^{Ar}), 135.5 (+, *C*H^{Ar}), 134.5 (+, *C*H^{Ar}), 133.7 (+, *C*H^{Ar}), 132.5 (+, *C*H^{Ar}), 132.4 (+, *C*H^{Ar}), 131.6 (+, *C*H^{Ar}), 131.43 (+, *C*H^{Ar}), 131.4 (C_q, C^{Ar}), 34.8 (–, *C*H_2), 34.7 (–, *C*H_2), 34.5 (–, *C*H_2), 34.2 (–, *C*H_2) ppm. – **IR** (ATR) $\tilde{\nu}$ = 3292 (m), 3196 (w), 2952 (w), 2928 (m), 2849 (w), 1657 (s), 1632 (vs), 1592 (w), 1557 (w), 1497 (vs), 1470 (s), 1445 (s), 1408 (w), 1309 (m), 1290 (w), 1092 (w), 983 (s), 950 (m), 928 (w), 899 (m), 874 (w), 826 (s), 796 (m), 721 (s), 701 (w), 679 (s), 653 (s), 626 (vs) cm^{-1}. – **MS** (FAB, 3-NBA): *m/z* (%) = 267 (20) [M+H]$^+$, 266 (100) [M]$^+$. – **HRMS** (FAB, 3-NBA, $C_{17}H_{18}O_1N_2$, [M+H]$^+$) calc.: 266.1419, found: 266.1418.

(*rac*)-4-Isocyanato[2.2]paracyclophane (163)

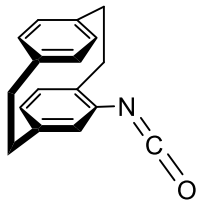

To a suspension of 4-[[2.2]paracyclophanoyl] chloride (**157**, 0.271 g, 1.00 mmol, 1.00 equiv.) in acetone (10 mL) was slowly added a solution of sodium azide (0.650 g, 10.0 mmol, 10.0 equiv.) in water (10 mL) over 10 min. The reaction mixture was warmed to 50 °C and stirring continued at this temperature for 5 h. For work-up, ice-cold water (50 mL) was added, then the precipitate was filtered off and air-dried to give 4-(azidocarbonyl)[2.2]paracyclophane (**162**, 0.260 g, 95%) as colorless amorphous material. The crude product (**162**, 0.260 g, 0.94 mmol, 1.00 equiv.) was dissolved in anhydrous toluene (10 mL) under N_2 and the mixture was refluxed for 1 h. The solvent was evaporated under reduced pressure and the crude pale yellow residue was purified by column chromatography using a mixture of cyclohexane/ethyl acetate (4:1) on silica gel yielding 4-isocyanato[2.2]paracyclophane (**163**, 0.100 g, 43%, 401 μmol) as a colorless crystalline solid.

R_f = 0.36 (cyclohexane/ethyl acetate; 4:1). – **^{1}H NMR** (400 MHz, DMSO-d_6) δ = 7.31 (d, J = 2.0 Hz, 1H, H^{Ar}), 6.73 (dd, J = 7.8, 2.0 Hz, 1H, H^{Ar}), 6.65–6.57 (m, 3H, H^{Ar}), 6.56–6.49 (m, 2H, H^{Ar}), 4.23 (ddd, J = 12.9, 9.0, 2.6 Hz, 1H, H^{Pc}), 3.25–3.14 (m, 4H, H^{Pc}), 3.13–3.00 (m, 2H, H^{Pc}), 2.91 (ddd, J = 12.9, 9.9, 7.3 Hz, 1H, H^{Pc}) ppm. The analytical data matches that of the literature.[153]

(*rac*)-*N*-([2.2]Paracyclophanylcarbamoyl)-4-([2.2]paracyclophanylcarboxamide (164)

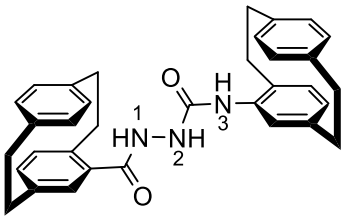

In a 100 ml round-bottomed flask, a mixture of carbohydrazide-[2.2]paracyclophane (**159**, 0.266 g, 1.00 mmol, 1.00 equiv.) and [2.2]paracyclophane isocyanate (**163**, 0.249 g, 1.00 mmol, 1.00 equiv.) in a mixture of absolute EtOH: DMF (25:1 by volume in mL) was heated in an oil bath at 70 °C for 4 h. The formed precipitate was filtered and washed with heptane several times (3 x 10 mL), after this 0.360 g (70%, 698 μmol) of the title compound was obtained as a white solid.

R_f = 0.13 (cyclohexane/ethyl acetate; 4:1). – **Mp**: 310–312 °C. – **^{1}H NMR** (400 MHz, DMSO-d_6) δ = 9.72 (d, J = 2.4 Hz, 1H, NH^1), 8.39 (dd, J = 4.1, 2.5 Hz, 1H, NH^2), 7.99 (s, 1H, NH^3), 6.93–6.87 (m, 2H, H^{Ar}), 6.76–6.71 (m, 2H, H^{Ar}), 6.65–6.63 (m, 1H, H^{Ar}), 6.55–6.48 (m, 5H, H^{Ar}), 6.44–6.31 (m, 4H, H^{Ar}), 3.79 (ddd, J = 12.6, 9.0, 3.4 Hz, 1H, H^{Pc}), 3.17–3.09 (m, 2H, H^{Pc}), 3.09–2.99 (m, 4H, H^{Pc}), 2.99–2.90 (m, 6H, H^{Pc}), 2.90–2.67 (m, 3H, H^{Pc}) ppm. – **^{13}C NMR** (101 MHz, DMSO-d_6) δ = 168.8 (C_q, CO), 156.3 (C_q, CO), 140.7 (C_q, C^{Ar}), 140.3 (C_q, C^{Ar}), 140.2 (C_q, C^{Ar}), 140.1 (C_q, C^{Ar}), 139.9 (C_q, C^{Ar}), 139.7 (C_q, C^{Ar}), 139.6 (C_q, C^{Ar}), 139.4 (C_q, C^{Ar}), 139.1 (+, CH^{Ar}), 138.1 (+, CH^{Ar}), 136.4 (+, CH^{Ar}), 135.4 (+, CH^{Ar}), 133.5 (+, CH^{Ar}), 133.3 (+, CH^{Ar}), 133.2 (+, CH^{Ar}), 133.1 (+, CH^{Ar}), 132.9 (+, CH^{Ar}), 132.8 (+, CH^{Ar}), 132.3 (+, CH^{Ar}), 132.2 (+, CH^{Ar}), 131.9 (+, CH^{Ar}), 128.8 (C_q, C^{Ar}), 127.7 (C_q, C^{Ar}), 126.2 (+, CH^{Ar}), 35.5 (–, CH$_2$), 35.2 (–, 2 × CH$_2$), 34.9 (–, 2 × CH$_2$), 34.7 (–, CH$_2$), 33.5 (–, CH$_2$), 33.2 (–, CH$_2$) ppm. – **IR** (ATR) $\tilde{\nu}$ = 3428 (vw), 3104 (w), 2978 (w), 2864 (w), 2853 (w), 1642 (vs), 1572 (vs), 1561 (vs), 1541 (vs), 1499 (vs), 1422 (vs), 1234 (vs), 1207 (vs), 718 (vs), 656 (vs), 625 (vs), 584 (vs), 514 (vs), 503 (vs), 492 (vs), 411 (vs), 377 (vs) cm^{-1}. – **MS** (FAB, 3-NBA): *m/z* (%) = 516 (50) [M+H]$^+$, 515 (29) [M]$^+$. – **HRMS** (FAB, 3-NBA, $C_{34}H_{34}O_2N_3$, [M+H]$^+$) calc.: 516.2651, found: 516.2652.

(*rac*)-4-Formyl[2.2]paracyclophane (132)

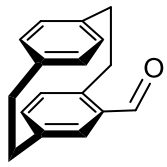

To a solution of [2.2]paracyclophane (**131**, 5.00 g, 24.0 mmol, 1.00 equiv.) in 600 ml of dichloromethane at 0 °C was added 15.4 ml of titanium tetrachloride (9.11 g, 5.26 mL, 48.0 mmol, 2.00 equiv.) followed by the addition of 1,1-dichloromethylether (2.90 g, 2.28 mL, 25.2 mmol, 1.05 equiv.). After stirring for 15 min at 0 °C, the mixture was stirred for 16 h at room temperature. The mixture changes color from clear to yellow to black. The black reaction mixture was poured on ice and stirred for 2 h, again changing its color to yellow. The organic layer was separated and the aqueous layer was extracted with dichloromethane (3 × 50 mL). The combined organic layers were washed with brine (100 mL), dried over Na_2SO_4 and the solvent was removed under reduced pressure. The crude compound was filtered over a silica pad (dichloromethane as eluent) to remove residual titanium salts and recrystallized from *n*-hexane to yield the title compound (5.10 g, 90%, 21.6 mmol) as a white solid.

R_f = 0.41 (cyclohexane/ethyl acetate; 20.1). – **^{1}H NMR** (400 MHz, $CDCl_3$) δ = 9.95 (s, 1H, C*H*O), 7.02 (d, *J* = 1.9 Hz, 1H, H^{Ar}), 6.73 (dd, *J* = 7.8, 1.9 Hz, 1H, H^{Ar}), 6.61–6.55 (m, 2H, H^{Ar}), 6.50 (dd, *J* = 7.8, 1.9 Hz, 1H, H^{Ar}), 6.43 (dd, *J* = 7.8, 1.8 Hz, 1H, H^{Ar}), 6.38 (dd, *J* = 7.8, 1.8 Hz, 1H, H^{Ar}), 4.11 (ddd, *J* = 13.0, 9.9, 1.7 Hz, 1H, H^{Pc}), 3.35–3.14 (m, 3H, H^{Pc}), 3.14–2.89 (m, 4H, H^{Pc}) ppm. The analytical data is consistent with the literature.[82]

(S_p)-4-Formyl[2.2]paracyclophane (132)

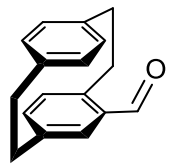

A solution of (*rac*)-4-formyl[2.2]paracyclophane (**132**, 1.72 g, 7.30 mmol, 1.00 equiv.), and €-phenylethylamine (**159**, 0.88 g, 7.30 mmol, 1.00 equiv.) in 60 mL toluene was heated to reflux for 16 h. After cooling to room temperature, the solvent was removed under reduced pressure and the residue was repeatedly recrystallized from *n*-hexane until clear cubic crystals were formed. (S_p,*R*)-4-(*N*-1-(Phenylethyl)methaniminyl)-[2.2]paracyclophane **160** (0.32 g, 26% based on 0.50 equiv. of (S_p)-starting material) was obtained as clear crystals. Afterward, to a solution of (S_p,*R*)-**160** (0.22 g, 0.95 mmol, 1.00 equiv.) in dichloromethane, 5 g of silica was added and the suspension was stirred at room temperature for 30 min. The solvent was removed under reduced pressure and the resulting solid was purified by short column chromatography on silica gel (dichloromethane as eluent) to yield 0.23 g of the title compound (quant.) as a white solid. The *ee* ratio of (S_p,*S*)/(R_p/*R*) pair of enantiomers was determined by Analytical Chiral HPLC (Chiralcel® OD-H, *n*-hexane/*i*PrOH, 90:10, 1.0 mL/min, λ =256 nm): t_{R1} = 11.6 min (78.9.6%), t_{R2} = 15.0 min (21.0%). *ee* = 57.9%.

The analytical data is consistent with the literature, see above for (*rac*)-**132**.

(S$_p$*,S*$_p$*)-N*-([2.2]Paracyclophanylcarbamoyl)-4-([2.2]paracyclophanylcarboxamide (164)

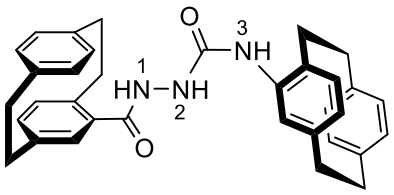

In a 100 mL round-bottomed flask, a mixture of carbohydrazide [2.2]paracyclophane (*scale*-**159**, 160 mg, 0.60 mmol, 1.00 equiv.) and [2.2]paracyclophane isocyanate (*scale*-**163**, 150 mg, 0.60 mmol, 1.00 equiv.) in a mixture of absolute EtOH: DMF (25:1 by volume in mL) was heated in an oil bath at 70 °C for 4 h. The formed precipitate was filtered and washed with heptane several times (3 x 20 mL). By applying the chiral-HPLC separation on *scal*-**164**, the title compound was obtained with a yield of 0.26 g (50%) as a white solid. The *ee* ratio of (S_p,*S*)/(R_p/*R*) pair of enantiomers was determined by Analytical Chiral HPLC (Chiralcel® OD-H, *n*-hexane/*i*PrOH, 90:10, 1.0 mL/min, λ =256 nm): t_{R1} = 30.5 min (38.0%), t_{R2} = 61.9 min (21.0%). *ee* = 23.9%. Separation of enantiomers was done by Semipreparative Chiral HPLC (Chiralcel® AZ-H, acetonitrile, 25.0 mL/min, λ =256 nm): t_R = 39.9 min (100%).

R$_f$ = 0.13 (cyclohexane/ethyl acetate; 4:1), $[\alpha]_D$= + 41.8 (c 0.004, CH_2Cl_2). – **Mp**: 310–312 °C. – **^{1}H NMR** (400 MHz, DMSO-d_6) δ = 9.73 (s, 1H, NH^1), 8.40 (s, 1H, NH^2), 8.00 (s, 1H, NH^3), 7.07–6.85 (m, 2H, H^{Ar}), 6.84–6.74 (m, 2H, H^{Ar}), 6.65 (dd, *J* = 7.7, 1.8 Hz, 1H, H^{Ar}), 6.58–6.45 (m, 6H, H^{Ar}), 6.40 (d, *J* = 0.7 Hz, 2H, H^{Ar}), 6.33 (dd, *J* = 7.8, 1.8 Hz, 1H, H^{Ar}), 3.84–3.77 (m, 1H, H^{Pc}), 3.16–3.08 (m, 2H, H^{Pc}), 3.06–2.91 (m, 10H, H^{Pc}), 2.89–2.69 (m, 3H, H^{Pc}) ppm. – **^{13}C NMR** (101 MHz, DMSO-d_6) δ = 168.6 (C_q, *C*O), 156.2 (C_q, *C*O), 140.6 (C_q, C^{Ar}), 140.2 (C_q, C^{Ar}), 139.9 (C_q, 2 × C^{Ar}), 139.5 (C_q, C^{Ar}), 139.4 (C_q, C^{Ar}), 139.0 (C_q, C^{Ar}), 138.5 (C_q, C^{Ar}), 136.2 (+, CH^{Ar}), 135.5 (+, CH^{Ar}), 135.3 (+, CH^{Ar}), 133.6 (+, CH^{Ar}), 133.5 (+, 2 × CH^{Ar}), 133.1 (+, CH^{Ar}), 132.9 (+, 2 × CH^{Ar}), 132.4 (+, CH^{Ar}), 132.3 (+, CH^{Ar}), 132.1 (+, CH^{Ar}), 128.8 (C_q, C^{Ar}), 127.2 (C_q, C^{Ar}), 125.9 (+, 2 × CH^{Ar}), 35.3 (–, CH_2), 35.2 (–, CH_2), 35.1 (–, CH_2), 35.0 (–, CH_2), 34.9 (–, CH_2), 33.5 (–, CH_2), 33.4 (–, CH_2), 33.2 (–, CH_2) ppm. – **IR** (ATR) $\tilde{\nu}$ = 3428 (vw), 3104 (w), 2978 (w), 2864 (w), 2853 (w), 1642 (vs), 1572 (vs), 1561 (vs), 1541 (vs), 1499 (vs), 1422 (vs), 1234 (vs), 1207 (vs), 718 (vs), 656 (vs), 625 (vs), 584 (vs), 514 (vs), 503 (vs), 492 (vs), 411 (vs), 377 (vs) cm^{-1}. – **MS** (FAB, 3-NBA): *m/z* (%) = 516 (80) $[M+H]^+$, 515 (30) $[M]^+$. – **HRMS** (FAB, 3-NBA, $C_{34}H_{34}O_2N_3$, $[M+H]^+$) calc.: 516.2651, found: 516.2652.

5.2.2.2. [2.2]Paracyclophanyl-*N*-Substituted Hydrazinecarbothioamide

General Procedures (GP2)

A mixture of carbohydrazide-[2.2]paracyclophane (**159**, 1.00 equiv.) and the isothiocyanate (1.00 equiv.) in 60 mL ethanol was refluxed for 4–8 h. The reaction mixture was poured into a beaker and was allowed to stand until a precipitate was formed. Then the precipitate was filtered and washed with heptane several times (3 × 100 mL). The crude product was recrystallized from EtOH/acetonitrile (50 mL/50mL).

(*rac*)-2'(4'-[2.2]Paracyclophanyl)-*1 yridine*din-3-yl)hydrazi2e-1-carbothioamide *9* (135a).

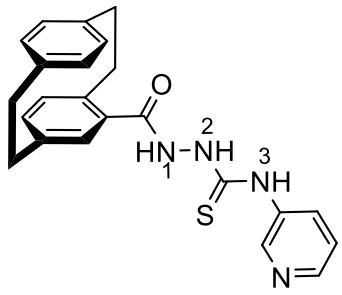

According to **GP2**, carbohydrazide-[2.2]paracyclophane (**159**, 1.00 g, 3.75 mmol, 1.00 equiv.) was reacted with 3-isothiocyanato-pyridine (0.511 g, 0.42 mL, 3.75 mmol, 1.00 equiv.) in dry EtOH (60 mL) for 6 h. A precipitate of the title compound was obtained as a white solid (1.240 g, 82%, 3.08 mmol).

R_f = 0.42 (dichloromethane/methanol; 10:1). – **Mp**: 152–154 °C. – **^{1}H NMR** (400 MHz, DMSO-d_6) δ = 9.93 (s, 1H, NH^2), 9.72 (s, 1H, NH^1), 8.57 (s, 1H, NH^3), 8.34 (dd, J = 4.8, 1.5 Hz, 1H, H^{Ar}), 7.90–7.40 (m, 2H, H^{Ar}), 7.38 (dd, J = 8.2, 4.7 Hz, 1H, H^{Ar}), 7.12–6.87 (m, 2H, H^{Ar}), 6.84–6.57 (m, 2H, H^{Ar}), 6.58–6.48 (m, 2H, H^{Ar}), 6.46 (d, J = 7.8 Hz, 1H, H^{Ar}), 3.75–3.34 (m, 1H, H^{Pc}), 3.27–3.05 (m, 3H, H^{Pc}), 3.05–2.90 (m, 3H, H^{Pc}), 2.90–2.77 (m, 1H, H^{Pc}) ppm. – **^{13}C NMR** (101 MHz, DMSO-d_6) δ = 181.5 (C_q, CS), 167.7 (C_q, CO), 147.0 (+, CH^{Ar}), 145.7 (+, CH^{Ar}), 140.2 (C_q, C^{Ar}), 139.4 (C_q, C^{Ar}), 139.2 (C_q, C^{Ar}), 138.9 (C_q, C^{Ar}), 136.1 (C_q, C^{Ar}), 135.7 (+, 2 × CH^{Ar}), 135.2 (+, CH^{Ar}), 133.4 (+, CH^{Ar}), 132.5 (+, CH^{Ar}), 132.4 (+, CH^{Ar}), 132.3 (+, 2 × CH^{Ar}), 131.4 (C_q, C^{Ar}), 122.9 (+, CH^{Ar}), 38.8 (–, CH$_2$), 34.7 (–, CH$_2$), 34.6 (–, CH$_2$), 34.4 (–, CH$_2$) ppm. – **IR** (ATR) $\tilde{\nu}$ = 3296 (w), 3206 (w), 3091 (w), 2925 (w), 2839 (vw), 1645 (w), 1604 (m), 1557 (s), 1456 (s), 1279 (m), 1129 (vs), 795 (w), 725 (m), 613 (vs), 514 (w) cm^{-1}. – **MS** (FAB, 3-NBA): *m/z* (%) = 403 (55) [M+H]$^+$, 402 (30) [M]$^+$. – **HRMS** (FAB, 3-NBA, $C_{23}H_{23}O_1N_4{}^{32}S_1$, [M+H]$^+$) calc.: 403.1593, found: 403.1591.

(*rac*)-2'(4'-[2.2]Paracyclophanyl)-*N*-phenylhydrazinecarbothioamide (**135b**)

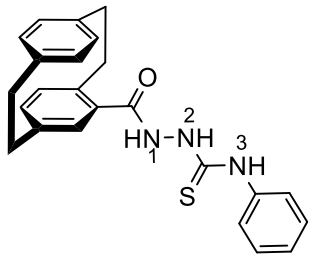

According to **GP2**, carbohydrazide-[2.2]paracyclophane (**159**, 1.00 g, 3.75 mmol, 1.00 equiv.) was reacted with phenyl isothiocyanate (0.507 g, 0.45 mL, 3.75 mmol, 1.00 equiv.) in dry EtOH (60 mL) for 4 h. A precipitate of the title compound was obtained as a white solid (1.330 g, 88%, 3.31 mmol).

R_f = 0.17 (cyclohexane/ethyl acetate; 4:1). – **Mp**: 190–92 °C. – **^{1}H NMR** (400 MHz, DMSO-d_6) δ = 9.86 (s, 1H, NH^2), 9.63 (s, 1H, NH^1), 7.55 (d, J = 7.8 Hz, 1H, H^{Ar}), 7.50 (s, 1H, NH^3), 7.33 (t, J = 7.9 Hz, 2H, H^{Ar}), 7.14 (t, J = 7.6 Hz, 2H, H^{Ar}), 6.95 (s, 1H, H^{Ar}), 6.63 (dd, J = 7.8, 1.8 Hz, 2H, H^{Ar}), 6.52 (d, J = 8.0 Hz, 3H, H^{Ar}), 6.47 (d, J = 7.8 Hz, 1H, H^{Ar}), 3.76 (s, 1H, H^{Pc}), 3.33–2.79 (m, 7H, H^{Pc}) ppm. – **^{13}C NMR** (101 MHz, DMSO-d_6) δ = 181.2 (C_q, *C*S), 171.8 (C_q, *C*O), 140.1 (+, *C*H^{Ar}), 140.0 (C_q, C^{Ar}), 139.5 (C_q, C^{Ar}), 139.4 (C_q, C^{Ar}), 139.3 (C_q, C^{Ar}), 139.0 (+, 2 × *C*H^{Ar}), 135.7 (+, 2 × *C*H^{Ar}), 135.1 (+, *C*H^{Ar}), 132.6 (+, *C*H^{Ar}), 132.5 (+, 2 × *C*H^{Ar}), 132.4 (+, 2 × *C*H^{Ar}), 131.6 (+, *C*H^{Ar}), 129.0 (C_q, C^{Ar}), 128.2 (C_q, C^{Ar}), 34.8 (–, *C*H$_2$), 34.7 (–, *C*H$_2$), 34.5 (–, *C*H$_2$), 34.4 (–, *C*H$_2$) ppm. – **IR** (ATR) $\tilde{\nu}$ = 3241 (m), 3233 (m), 3109 (m), 2925 (m), 2846 (w), 1646 (w), 1608 (m), 1591 (m), 1560 (vs), 1487 (vs), 1436 (vs), 1360 (vs), 1316 (vs), 1235 (vs), 1024 (m), 898 (m), 747 (vs), 714 (vs), 687 (vs), 640 (s), 506 (vs), 483 (vs), 402 (s) cm^{-1}. – **MS** (FAB, 3-NBA): *m/z* (%) = 402 (85) [M+H]$^+$, 401 (20) [M]$^+$. – **HRMS** (FAB, 3-NBA, $C_{24}H_{24}O_1N_3{}^{32}S_1$, [M+H]$^+$) calc.: 402.1635, found: 402.1633.

(*rac*)-*N*-Allyl-2'(4'-[2.2]paracyclophanyl)hydrazine-1-carbothioamide (135c)

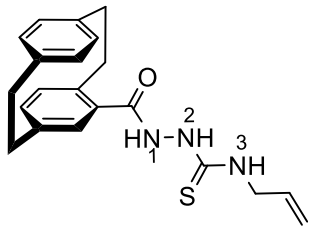

According to **GP2**, carbohydrazide-[2.2]paracyclophane (**159**, 1.00 g, 3.75 mmol, 1.00 equiv.) was reacted with ally isothiocyanate (0.37 g, 0.372 mL, 3.75 mmol, 1.00 equiv.) in dry EtOH (60 mL) for 6 h. A precipitate of the title compound was obtained as a white solid (1.180 g, 86%, 3.23 mmol).

R_f = 0.54 (cyclohexane/ethyl acetate; 1:1). – **Mp**: 162–164 °C. – **^{1}H NMR** (400 MHz, DMSO-d_6) δ = 9.01 (s, 1H, NH^2), 8.65 (s, 1H, NH^1), 7.74 (s, 1H, NH^3), 6.96 (d, J = 2.0 Hz, 1H, H^{Ar}), 6.72 (t, J = 7.8, 2H, H^{Ar}), 6.66–6.22 (m, 4H, H^{Ar}), 5.97–5.87 (m, 1H, CH^{allyl}), 5.26–5.04 (m, 2H, CH_2^{allyl}), 4.32–4.24 (m, 2H, CH_2^{allyl}), 3.84–3.74 (m, 1H, H^{Pc}), 3.28–2.78 (m, 7H, H^{Pc}) ppm. – **^{13}C NMR** (101 MHz, DMSO-d_6) δ = 182.7 (C_q, *C*S), 167.7 (C_q, *C*O), 140.1 (C_q, C^{Ar}), 139.5 (C_q, C^{Ar}), 139.3 (C_q, C^{Ar}), 139.0 (C_q, C^{Ar}), 135.7 (+, *C*H^{Ar}), 135.2 (+, *C*H^{Ar}), 135.1 (+, *C*H^{Ar}), 134.8 (+, *C*H^{allyl}), 132.6 (+, *C*H^{Ar}), 132.5 (+, *C*H^{Ar}), 132.3 (+, *C*H^{Ar}), 131.5 (+, *C*H^{Ar}), 128.9 (C_q, C^{Ar}), 115.0 (–, *C*H$_2^{allyl}$), 56.0 (–, *C*H$_2^{allyl}$), 34.8 (–, *C*H$_2$), 34.7 (–, *C*H$_2$), 34.5 (–, 2 × *C*H$_2$) ppm. – **IR** (ATR) $\tilde{\nu}$ = 3360 (s), 3247 (w), 3132 (w), 2962 (w), 2929 (m), 2856 (w), 1660 (s), 1479 (m), 1412 (m), 1266 (s), 1230 (m), 1188 (vs), 1129 (m), 958 (s), 921 (s), 898 (m), 824 (w), 810 (m), 720 (m), 687 (m), 633 (vs), 603 (s), 513 (s), 506 (s), 442 (s) cm^{-1}. – **MS** (FAB, 3-NBA): *m/z* (%) = 366 (100) $[M+H]^+$, 365 (30) $[M]^+$. – **HRMS** (FAB, 3-NBA, $C_{21}H_{24}O_1N_3{}^{32}S_1$, $[M+H]^+$) calc.: 366.1640, found: 366.1638.

(*rac*)-2'(4'-[2.2]Paracyclophanyl)-*N*-ethylhydrazine-1-carbothioamide (**135d**)

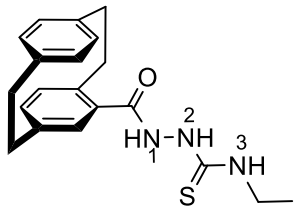

According to **GP2**, carbohydrazide-[2.2]paracyclophane (**159**, 1.00 g, 3.75 mmol, 1.00 equiv.) was reacted with ethyl isothiocyanate (0.327 g, 0.33 mL, 3.75 mmol, 1.00 equiv.) in dry EtOH (60 mL) for 6 h. A precipitate of the title compound was obtained as a white solid (1.080 g, 81%, 3.06 mmol).

R_f = 0.54 (cyclohexane/ethyl acetate; 1:1). – **Mp**: 130–132 °C. – **^{1}H NMR** (400 MHz, DMSO-d_6) δ = 9.65 (s, 1H, NH^2), 9.22 (s, 1H, NH^1), 7.81 (s, 1H, NH^3), 6.91 (d, J = 1.8 Hz, 1H, H^{Ar}), 6.63 (dd, J = 7.7, 1.9 Hz, 2H, H^{Ar}), 6.51 (d, J = 9.6 Hz, 3H, H^{Ar}), 6.44 (d, J = 7.8 Hz, 1H, H^{Ar}), 3.72–3.65 (m, 1H, H^{Pc}), 3.60–3.26 (m, 2H, CH_2^{ethyl}), 3.26–2.68 (m, 7H, H^{Pc}), 1.06 (t, J = 7.0 Hz, 3H, CH_3^{ethyl}) ppm. – **^{13}C NMR** (101 MHz, DMSO-d_6) δ = 181.7 (C_q, *C*S), 167.6 (C_q, *C*O), 140.1 (C_q, C^{Ar}), 139.5 (C_q, C^{Ar}), 139.2 (C_q, C^{Ar}), 139.0 (C_q, C^{Ar}), 135.7 (+, 2 × *C*H^{Ar}), 135.1 (+, *C*H^{Ar}), 132.7 (+, *C*H^{Ar}), 132.6 (+, *C*H^{Ar}), 132.5 (+, *C*H^{Ar}), 132.4 (+, *C*H^{Ar}), 131.5 (C_q, C^{Ar}), 56.0 (–, *C*H_2^{ethyl}), 35.0 (–, *C*H_2), 34.9 (–, *C*H_2), 34.6 (–, 2 × *C*H_2), 14.7 (+, *C*H_3^{ethyl}) ppm. – **IR** (ATR) $\tilde{\nu}$ = 3357 (w), 3286 (w), 3190 (w), 3182 (w), 3152 (w), 3068 (w), 3041 (w), 3010 (w), 2973 (w), 2928 (m), 1667 (vs), 1543 (vs), 1500 (s), 1480 (m), 1453 (m), 1431 (m), 1375 (w), 1273 (m), 1237 (vs), 1188 (vs), 1156 (m), 1068 (s), 938 (w), 899 (w), 834 (m), 820 (s), 799 (s), 718 (m), 628 (s), 599 (s), 567 (s), 541 (s), 509 (vs), 462 (m), 450 (s), 416 (m) cm^{-1}. – **MS** (FAB, 3-NBA): *m/z* (%) = 354 (100) $[M+H]^+$, 353 (20) $[M]^+$. – **HRMS** (FAB, 3-NBA, $C_{20}H_{24}O_1N_3{}^{32}S_1$, $[M+H]^+$) calc.: 354.1640, found: 354.1640.

(*rac*)-2'(4'-[2.2]Paracyclophanyl)-*N*-cyclopropylhydrazine-1-carbothioamide (135e)

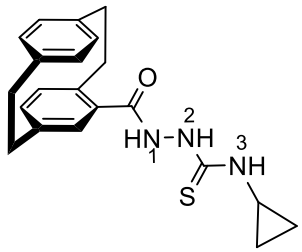

According to **GP2**, carbohydrazide-[2.2]paracyclophane (**159**, 1.00 g, 3.75 mmol, 1.00 equiv.) was reacted with cyclopropyl isothiocyanate (0.37 g, 0.35 mL, 3.75 mmol, 1.00 equiv.) in dry EtOH (60 mL) for 6 h. A precipitate of the title compound was obtained with as a white solid (1.100 g, 80%, 3.01 mmol).

R_f = 0.49 (cyclohexane/ethyl acetate; 1:1). – **Mp**: 158–160 °C. – **^{1}H NMR** (400 MHz, DMSO-d_6) δ = 9.66 (s, 1H, NH^2), 9.34 (s, 1H, NH^1), 6.90 (s, 1H, NH^3), 6.61 (dd, J = 7.7, 1.8 Hz, 2H, H^{Ar}), 6.55–6.46 (m, 4H, H^{Ar}), 6.43 (d, J = 7.8 Hz, 1H, H^{Ar}), 3.74–3.43 (m, 1H, H^{Pc}), 3.38 (d, J = 7.8 Hz, 2H, H^{Pc}), 3.09–2.95 (m, 2H, H^{Pc}), 2.94–2.80 (m, 3H, H^{Pc}), 1.23–1.06 (m, 1H, C$H^{cyclo.}$), 1.05–1.03 (m, 2H, C$H_2^{cyclo.}$), 0.63–0.56 (m, 2H, C$H_2^{cyclo.}$) ppm. – **^{13}C NMR** (101 MHz, DMSO-d_6) δ = 190.6 (C_q, CS), 167.2 (C_q, CO), 140.0 (C_q, C^{Ar}), 139.4 (C_q, C^{Ar}), 139.2 (C_q, C^{Ar}), 138.9 (C_q, C^{Ar}), 135.6 (+, 2 × CH^{Ar}), 135.0 (+, CH^{Ar}), 132.5 (+, CH^{Ar}), 132.4 (+, CH^{Ar}), 132.3 (+, 2 × CH^{Ar}), 131.6 (C_q, C^{Ar}), 34.7 (–, CH$_2$), 34.6 (–, CH$_2$), 34.5 (–, CH$_2$), 34.4 (–, CH$_2$), 27.1 (+, CH$^{cyclo.}$), 6.7 (–, CH$_2^{cyclo.}$), 6.5 (–, CH$_2^{cyclo.}$) ppm. – **IR** (ATR) $\tilde{\nu}$ = 3208 (s), 3094 (w), 2948 (w), 2919 (m), 2850 (w), 1701 (s), 1672 (m), 1500 (vs), 1394 (m), 1296 (vs), 1259 (vs), 1204 (vs), 1126 (m), 1048 (s), 1031 (s), 939 (w), 899 (m), 820 (w), 796 (m), 722 (m), 623 (vs), 514 (vs) cm^{-1}. – **MS** (FAB, 3-NBA): *m/z* (%) = 366 (85) $[M+H]^+$, 365 (25) $[M]^+$. – **HRMS** (FAB, 3-NBA, $C_{21}H_{24}O_1N_3{}^{32}S_1$, $[M+H]^+$) calc.: 366.1640, found: 366.1639.

(*rac*)-2'(4'-[2.2]Paracyclophanyl)-*N*-benzylhydrazine-1-carbothioamide (135f)

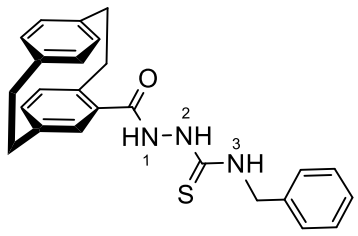

According to **GP2**, carbohydrazide-[2.2]paracyclophane (**159**, 1.00 g, 3.75 mmol, 1.00 equiv.) was reacted with benzyl isothiocyanate (0.560 g, 0.50 mL, 3.75 mmol, 1.00 equiv.) in dry EtOH (60 mL) for 2 h. A precipitate of the title compound was obtained as a white solid (1.330 g, 85%, 3.20 mmol).

R_f = 0.60 (dichloromethane/methanol; 10:1). – **Mp**: 172–174 °C. – **^{1}H NMR** (400 MHz, DMSO-d_6) δ = 9.76 (s, 1H, NH^2), 9.41 (s, 1H, NH^1), 8.34 (s, 1H, NH^3), 7.34–7.32 (m, 2H, H^{Ar}), 7.31–7.28 (m, 2H, H^{Ar}), 7.22–7.20 (m, 1H, H^{Ar}), 6.93 (s, 1H, H^{Ar}), 6.64–6.61 (m, 2H, H^{Ar}), 6.53–6.40 (m, 4H, H^{Ar}), 4.81–4.74 (m, 2H, CH_2), 3.70–3.68 (m, 1H, H^{Pc}), 3.14–2.78 (m, 7H, H^{Pc}) ppm. – **^{13}C NMR** (101 MHz, DMSO-d_6) δ = 182.9 (C_q, *C*S), 168.3 (C_q, *C*O), 140.6 (+, *C*H^{Ar}), 140.0 (C_q, C^{Ar}), 139.9 (C_q, C^{Ar}), 139.7 (C_q, C^{Ar}), 139.4 (C_q, C^{Ar}), 136.2 (+, 2 × *C*H^{Ar}), 135.7 (+, *C*H^{Ar}), 133.1 (C_q, C^{Ar}), 133.0 (+, 2 × *C*H^{Ar}), 132.9 (+, 2 × *C*H^{Ar}), 131.9 (C_q, C^{Ar}), 128.5 (+, 2 × *C*H^{Ar}), 127.5 (+, *C*H^{Ar}), 127.1 (+, *C*H^{Ar}), 47.2 (–, *C*H_2), 35.3 (–, *C*H_2), 35.2 (–, *C*H_2), 35.0 (–, 2 × *C*H_2) ppm. – **IR** (ATR) $\tilde{\nu}$ = 3346 (s), 3199 (m), 3081 (w), 3030 (w), 3007 (w), 2953 (w), 2928 (w), 2853 (w), 1653 (s), 1547 (vs), 1519 (s), 1451 (m), 1434 (m), 1409 (w), 1337 (m), 1272 (vs), 1249 (w), 1225 (s), 1186 (s), 1180 (s), 1129 (m), 1091 (w), 1054 (w), 1027 (w), 960 (s), 942 (w), 897 (m), 834 (w), 812 (w), 789 (m), 725 (vs), 691 (vs), 630 (vs), 507 (vs), 449 (vs), 419 (m) cm^{-1}. – **MS** (FAB, 3-NBA): *m/z* (%) = 416 (70) $[M+H]^+$, 415 (25) $[M]^+$. – **HRMS** (FAB, 3-NBA, $C_{25}H_{26}O_1N_3{}^{32}S_1$, $[M+H]^+$) calc.: 416.1797, found: 416.1799.

5.2.2.3. [2.2]Paracyclophanyl-substituted triazolthiones

General Procedures (GP3)

A stirring mixture of hydrazinecarbothioamide derivatives **135a**–**f** (1.00 mmol, 1.00 equiv.) and 10 ml of sodium hydroxide (1.00 mmol, as a 2 N solution) was refluxed for 2–4 h. After cooling, the solution was acidified with 10 mL of hydrochloric acid (6 M) and the formed precipitate was filtered. The precipitate was then recrystallized from ethanol (50 mL).

(*rac*)-5'(4'-[2.2]Paracyclophanyl)-1*H*-imidazo[1,5-*a*]pyridin-3-yl)-2,4-dihydro-3*H*-1,2,4-triazole-3-thione (136a)

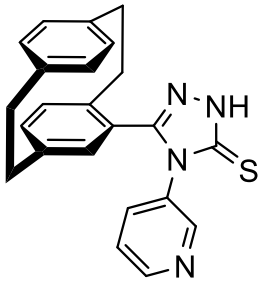

According to **GP3**, 2'(4'-[2.2]paracyclophanyl)-1*H*-imidazo[1,5-*a*]pyridin-3-yl)-hydrazine-1-carbothioamide (**135a**, 0.402 g, 1.00 mmol, 1.00 equiv.) was refluxed with NaOH for 2 h. A precipitate of the title compound was obtained as a white solid (0.290 g,76%, 754 µmol).

R_f = 0.40 (dichloromethane/methanol; 10:1). – **Mp**: 170–172 °C. – **^{1}H NMR** (400 MHz, DMSO-d_6) δ = 14.16 (s, 1H, N*H*), 8.55–8.28 (m, 2H, H^{Ar}), 7.71–7.17 (m, 2H, H^{Ar}), 6.96–6.94 (m, 1H, H^{Ar}), 6.74–6.65 (m, 2H, H^{Ar}), 6.59–6.33 (m, 4H, H^{Ar}), 3.16–2.91 (m, 6H, H^{Pc}), 2.88–2.78 (m, 2H, H^{Pc}) ppm. – **^{13}C NMR** (101 MHz, DMSO-d_6) δ = 167.9 (C_q, *C*S), 151.4 (C_q, C^{Ar}), 149.3 (+, *C*H^{Ar}), 148.7 (+, *C*H^{Ar}), 140.0 (C_q, C^{Ar}), 139.5 (C_q, C^{Ar}), 139.2 (C_q, C^{Ar}), 139.1 (C_q, C^{Ar}), 136.5 (C_q, C^{Ar}), 135.9 (+, *C*H^{Ar}), 135.1 (+, *C*H^{Ar}), 133.6 (+, *C*H^{Ar}), 133.1 (+, *C*H^{Ar}), 132.5 (+, *C*H^{Ar}), 132.0 (+, *C*H^{Ar}), 131.1 (+, *C*H^{Ar}), 130.9 (C_q, C^{Ar}), 124.9 (+, *C*H^{Ar}), 123.6 (+, *C*H^{Ar}), 34.7 (–, *C*H$_2$), 34.6 (–, *C*H$_2$), 34.4 (–, *C*H$_2$), 33.4 (–, *C*H$_2$) ppm. – **IR** (ATR) $\tilde{\nu}$ = 3160 (w), 3111 (w), 3078 (m), 3024 (m), 2975 (m), 2924 (s), 2890 (m), 2850 (s), 2776 (m), 2715 (w), 1646 (m), 1591 (m), 1547 (vs), 1483 (vs), 1470 (vs), 1432 (vs), 1360 (s), 1313 (vs), 1237 (vs), 1205 (vs), 799 (s), 718 (vs), 705 (vs), 673 (s), 618 (vs), 579 (m), 513 (vs) cm^{-1}. – **MS** (FAB, 3-NBA): *m/z* (%) = 385 (60) [M+H]$^+$, 384 (25) [M]$^+$. – **HRMS** (FAB, 3-NBA, $C_{23}H_{21}N_4{}^{32}S_1$, [M+H]$^+$) calc.: 385.1487, found: 385.1488.

(*rac*)-4-Phenyl-5'(4'-[2.2]paracyclophanyl)-2,4-dihydro-3*H*-1,2,4-triazole-3-thione (136b)

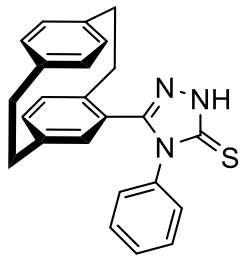

According to **GP3**, 2'(4'-[2.2]paracyclophanyl)-*N*-phenylhydrazine-carbothioamide (**135b**, 0.402 g, 1.00 mmol, 1.00 equiv.) was refluxed with NaOH for 2 h. A precipitate of the title compound was obtained as a white solid (0.300 g, 78%, 782 μmol).

R$_f$ = 0.29 (cyclohexane/ethyl acetate; 4:1). – **Mp**: 150–152 °C. – **^{1}H NMR** (400 MHz, DMSO-d_6) δ = 14.20 (s, 1H, N*H*), 7.31–7.27 (m, 3H, H^{Ar}), 7.07–7.03 (m, 2H, H^{Ar}), 673–6.69 (m, 1H, H^{Ar}), 6.63 (d, J = 2.0 Hz, 1H, H^{Ar}), 6.58–6.49 (m, 3H, H^{Ar}), 6.36–6.30 (m, 2H, H^{Ar}), 3.10–2.89 (m, 6H, H^{Pc}), 2.86–2.77 (m, 2H, H^{Pc}) ppm. – **^{13}C NMR** (101 MHz, DMSO-d_6) δ = 167.8 (C_q, *C*S), 151.7 (C_q, C^{Ar}), 139.7 (C_q, C^{Ar}), 139.2 (C_q, C^{Ar}), 139.1 (C_q, C^{Ar}), 139.0 (C_q, C^{Ar}), 135.7 (C_q, C^{Ar}), 135.0 (+, CH^{Ar}), 134.1 (+, CH^{Ar}), 133.5 (+, CH^{Ar}), 132.9 (+, 2 × CH^{Ar}), 132.0 (+, CH^{Ar}), 131.0 (+, CH^{Ar}), 128.8 (C_q, C^{Ar}), 128.6 (+, 2 × CH^{Ar}), 128.4 (+, 2 × CH^{Ar}), 125.3 (+, CH^{Ar}), 34.8 (–, CH_2), 34.7 (–, CH_2), 34.4 (–, CH_2), 33.6 (–, CH_2) ppm. – **IR** (ATR) $\tilde{\nu}$ = 3099 (w), 3040 (w), 2924 (s), 2850 (w), 2762 (w), 1594 (w), 1545 (w), 1499 (vs), 1422 (s), 1375 (w), 1333 (vs), 1309 (s), 1235 (s), 990 (m), 907 (w), 847 (s), 768 (s), 735 (s), 717 (s), 694 (vs), 612 (vs), 578 (m), 514 (vs), 492 (m) cm^{-1}. – **MS** (FAB, 3-NBA): *m/z* (%) = 38٤ (١٠0) $[M+H]^+$, 38٣ (٣5) $[M]^+$. – **HRMS** (FAB, 3-NBA, $C_{24}H_{22}N_3{}^{32}S_1$, $[M+H]^+$) calc.: 384.1534, found: 384.1526.

(*rac*)-4-Allyl-5'(4'-[2.2]paracyclophanyl)-2,4-dihydro-3*H*-1,2,4-triazole-3-thione (136c).

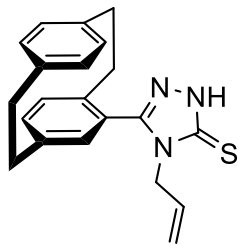

According to **GP3**, *N*-allyl-2'(4'-[2.2]paracyclo-phanyl)hydrazine-1-carbothioamide (**135c**, 0.365 g, 1.00 mmol, 1.00 equiv.) was refluxed with NaOH for 4 h. A precipitate of the title compound was obtained as a white solid (0.270 g,78%, 777 µmol).

R_f = 0.34 (cyclohexane/ethyl acetate; 4:1). – **Mp**: 142–144 °C. – **^{1}H NMR** (400 MHz, DMSO-d_6) δ = 14.05 (s, 1H, N*H*), 6.75 (dd, *J* = 7.8, 1.9 Hz, 1H, H^{Ar}), 6.69–6.58 (m, 5H, H^{Ar}), 6.38 (dd, *J* = 7.9, 1.8 Hz, 1H, H^{Ar}), 5.55–5.48 (m, 1H, CH^{allyl}), 4.90–4.52 (m, 2H, CH_2^{allyl}), 4.51–4.20 (m, 2H, CH_2^{allyl}), 3.13–2.90 (m, 7H, H^{Pc}), 2.82–2.77 (m, 1H, H^{Pc}) ppm. – **^{13}C NMR** (101 MHz, DMSO-d_6) δ = 166.9 (C_q, *C*S), 151.6 (C_q, C^{Ar}), 140.4 (C_q, C^{Ar}), 139.4 (C_q, C^{Ar}), 139.0 (C_q, C^{Ar}), 138.9 (C_q, C^{Ar}), 135.9 (+, CH^{allyl}), 135.5 (C_q, C^{Ar}), 133.5 (+, CH^{Ar}), 133.1 (+, CH^{Ar}), 133.0 (+, CH^{Ar}), 132.3 (+, CH^{Ar}), 131.5 (+, CH^{Ar}), 131.2 (+, CH^{Ar}), 125.3 (+, CH^{Ar}), 117.5 (–, CH_2^{allyl}), 45.4 (–, CH_2^{allyl}), 34.9 (–, CH_2), 34.8 (–, CH_2), 34.5 (–, CH_2), 33.5 (–, CH_2) ppm. – **IR** (ATR) $\tilde{\nu}$ = 3318 (vw), 3180 (w), 3123 (w), 3030 (w), 2929 (m), 2849 (w), 1547 (m), 1494 (vs), 1435 (s), 1360 (s), 1268 (s), 983 (m), 921 (s), 905 (vs), 847 (m), 776 (m), 732 (s), 681 (m), 647 (s), 608 (vs), 514 (vs) cm^{-1}. – **MS** (FAB, 3-NBA): *m/z* (%) = 348 (65) $[M+H]^+$, 347 (20) $[M]^+$. – **HRMS** (FAB, 3-NBA, $C_{21}H_{22}N_3{}^{32}S_1$, $[M+H]^+$) calc.: 347.1456, found: 347.1457.

(*rac*)-4-Ethyl-5'(4'-[2.2]paracyclophanyl)-2,4-dihydro-3*H*-1,2,4-triazole-3-thione (136d)

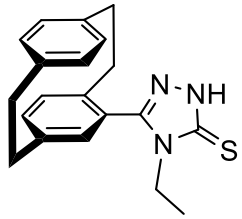

According to **GP3**, 2'(4'-[2.2]paracyclophanyl)-*N*-ethylhydrazine-1-carbothioamide (**135d**, 0.353 g, 1.00 mmol, 1.00 equiv.) was refluxed with NaOH for 4 h. A precipitate of the title compound was obtained as a white solid (0.240 g,72%, 715 μmol).

R_f = 0.29 (cyclohexane/ethyl acetate; 4:1). – **Mp**: 138–140 °C. – **^{1}H NMR** (400 MHz, DMSO-d_6) δ = 13.98 (s, 1H, N*H*), 6.74 (dd, *J* = 7.8, 1.8 Hz, 1H, H^{Ar}), 6.71–6.57 (m, 5H, H^{Ar}), 6.38 (dd, *J* = 7.9, 1.8 Hz, 1H, H^{Ar}), 3.86–3.58 (m, 2H, CH_2^{ethyl}), 3.12–2.97 (m, 5H, H^{Pc}), 2.96–2.91 (m, 2H, H^{Pc}), 2.79–2.72 (m, 1H, H^{Pc}), 0.81 (t, *J* = 7.1 Hz, 3H, CH_3^{ethyl}) ppm. – **^{13}C NMR** (101 MHz, DMSO-d_6) δ = 166.1 (C_q, *C*S), 151.1 (C_q, C^{Ar}), 140.4 (C_q, C^{Ar}), 139.2 (C_q, C^{Ar}), 138.7 (C_q, C^{Ar}), 138.6 (C_q, C^{Ar}), 135.8 (+, CH^{Ar}), 135.3 (+, CH^{Ar}), 133.2 (+, CH^{Ar}), 132.8 (+, 2 × CH^{Ar}), 132.1 (+, CH^{Ar}), 131.3 (+, CH^{Ar}), 125.0 (C_q, C^{Ar}), 38.4 (–, CH_2^{ethyl}), 34.7 (–, CH_2), 34.6 (–, CH_2), 34.3 (–, CH_2), 33.1 (–, CH_2), 13.0 (+, CH_3^{ethyl}) ppm. – **IR** (ATR) $\tilde{\nu}$ = 3122 (w), 2953 (w), 2932 (w), 1550 (w), 1500 (w), 1363 (vw), 1283 (w), 1142 (s), 1075 (vs), 980 (w), 946 (w), 905 (w), 850 (w), 789 (w), 769 (w), 605 (w), 516 (w), 455 (vs), 443 (s), 415 (m) cm^{-1}. – **MS** (FAB, 3-NBA): *m/z* (%) = 336 (95) $[M+H]^+$, 335 (40) $[M]^+$. – **HRMS** (FAB, 3-NBA, $C_{20}H_{22}N_3{}^{32}S_1$, $[M+H]^+$) calc.: 336.1534, found: 336.1534.

(*rac*)-4-Cyclopropyl-5'(4'-[2.2]paracyclophanyl)-2,4-dihydro-3*H*-1,2,4-triazole-3-thione (136e)

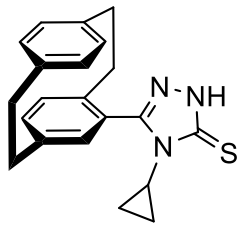

According to **GP3**, 2'(4'-[2.2]paracyclophanyl)-*N*-cyclopropylhydrazine-1-carbothioamide (**135e**, 0.365 g, 1.00 mmol, 1.00 equiv.) was refluxed with NaOH for 4 h. A precipitate of the title compound was obtained as a white solid (0.250 g, 72%, 719 μmol).

R_f = 0.23 (cyclohexane/ethyl acetate; 4:1). – **Mp**: 167–169 °C. – **^{1}H NMR** (400 MHz, DMSO-d_6) δ = 14.27 (s, 1H, N*H*), 6.75–6.70 (m, 1H, H^{Ar}), 6.67 (d, J = 1.8 Hz, 1H, H^{Ar}), 6.62–6.55 (m, 4H, H^{Ar}), 6.36 (dd, J = 7.8, 1.7 Hz, 1H, H^{Ar}), 3.13–2.98 (m, 8H, H^{Pc}), 2.91–2.86 (m, 1H, C$H^{cyclo.}$), 0.79–0.52 (m, 2H, C$H_2^{cyclo.}$), 0.45–0.05 (m, 2H, C$H_2^{cyclo.}$). – **^{13}C NMR** (101 MHz, DMSO-d_6) δ = 167.6 (C_q, *C*S), 152.6 (C_q, C^{Ar}), 139.3 (C_q, C^{Ar}), 139.2 (C_q, C^{Ar}), 139.0 (C_q, C^{Ar}), 138.9 (C_q, C^{Ar}), 134.7 (+, *C*H^{Ar}), 134.6 (+, *C*H^{Ar}), 133.0 (+, *C*H^{Ar}), 132.9 (+, *C*H^{Ar}), 132.8 (+, *C*H^{Ar}), 132.0 (+, *C*H^{Ar}), 131.0 (+, *C*H^{Ar}), 126.8 (C_q, C^{Ar}), 34.8 (–, *C*H$_2$), 34.7 (–, *C*H$_2$), 34.5 (–, *C*H$_2$), 33.4 (–, *C*H$_2$), 25.9 (+, *C*H$^{cyclo.}$), 8.3 (–, *C*H$_2^{cyclo.}$), 8.2 (–, *C*H$_2^{cyclo.}$) ppm. – **IR** (ATR) $\tilde{\nu}$ = 3091 (m), 3017 (m), 2922 (s), 1497 (vs), 1462 (m), 1429 (vs), 1411 (m), 1361 (s), 1313 (vs), 1271 (s), 1238 (m), 1213 (w), 1095 (m), 1060 (m), 1031 (s), 992 (s), 888 (m), 843 (m), 833 (s), 754 (m), 727 (vs), 714 (m), 652 (s), 629 (s), 596 (s), 513 (vs), 483 (m), 402 (w) cm^{-1}. – **MS** (FAB, 3-NBA): *m/z* (%) = 348 (100) $[M+H]^+$, 347 (55) $[M]^+$. – **HRMS** (FAB, 3-NBA, $C_{21}H_{22}N_3{}^{32}S_1$, $[M+H]^+$) calc.: 348.1534, found: 348.1599.

(*rac*)-4-Benzyl-5'(4'-[2.2]paracyclophanyl)-2,4-dihydro-3*H*-1,2,4-triazole-3-thione (136f)

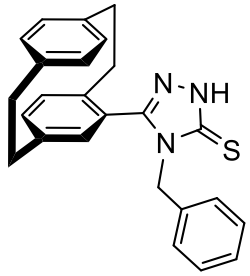

According to **GP3**, 2'(4'-[2.2]paracyclophanyl)-*N*-benzylhydrazine-1-carbothioamide (**135f**, 0.415 g, 1.00 mmol, 1.00 equiv.) was refluxed with NaOH for 2 h. A precipitate of the title compound was obtained as a white solid (0.310 g,78%, 780 μmol).

R$_f$ = 0.34 (cyclohexane/ethyl acetate; 4:1). – **Mp**: 185–187 °C. – **^{1}H NMR** (400 MHz, DMSO-d_6) δ = 14.13 (s, 1H, N*H*), 7.12–7.07 (m, 3H, H^{Ar}), 6.78–6.76 (m, 2H, H^{Ar}), 6.74–6.65 (m, 2H, H^{Ar}), 6.61–6.54 (m, 3H, H^{Ar}), 6.30–6.36 (m, 2H, H^{Ar}), 4.98 (s, 2H, CH_2), 3.06–2.89 (m, 6H, H^{Pc}), 2.73–2.66 (m, 2H, H^{Pc}) ppm. – **^{13}C NMR** (101 MHz, DMSO-d_6) δ = 167.4 (C_q, *C*S), 151.8 (C_q, C^{Ar}), 140.4 (C_q, C^{Ar}), 140.2 (C_q, C^{Ar}), 139.4 (C_q, C^{Ar}), 139.1 (C_q, C^{Ar}), 137.2 (C_q, C^{Ar}), 136.1 (+, 2 × CH^{Ar}), 135.7 (+, CH^{Ar}), 135.5 (+, CH^{Ar}), 133.5 (+, 2 × CH^{Ar}), 133.1 (+, CH^{Ar}), 133.0 (+, CH^{Ar}), 128.8 (+, CH^{Ar}), 128.6 (+, 2 × CH^{Ar}), 128.4 (C_q, C^{Ar}), 125.3 (+, CH^{Ar}), 46.4 (–, CH_2), 35.5 (–, CH_2), 34.9 (–, CH_2), 34.6 (–, CH_2), 33.3 (–, CH_2) ppm. – **IR** (ATR) $\tilde{\nu}$ = 3662 (vw), 3578 (vw), 3303 (w), 3080 (vw), 2863 (vw), 1731 (vw), 1640 (vw), 1149 (m), 1061 (vs), 942 (m), 793 (w), 562 (vw), 547 (vw), 453 (s), 445 (s), 435 (s), 414 (w) cm^{-1}. – **MS** (FAB, 3-NBA): *m/z* (%) = 398 (100) $[M+H]^+$, 397 (65) $[M]^+$. – **HRMS** (FAB, 3-NBA, $C_{25}H_{24}N_3{}^{32}S_1$, $[M+H]^+$) calc.: 398.1691, found: 398.1692.

5.2.2.4. [2.2]Paracyclophanyl-substituted oxadiazoles

General Procedures (GP4)

To a stirring mixture of hydrazinecarbothioamide derivatives **135a**–**e** (1.00 mmol, 1.00 equiv.) in 50 mL tetrahydrofuran (THF), 0.5 mL of Et_3N was added and the reaction mixture was refluxed for 12–24 h (the reaction was monitored by thin-layer chromatography). After removal of the solvent under reduced pressure, the crude residue was purified by column chromatography on silica gel to afford compounds **137a-e**.

(*rac*)-5'(4'-[2.2]Paracyclophanyl)-*1H*-1,2,4-triazol-*yridine*din-4-yl)-1,3,4-oxadiazol-2-amine (137a)

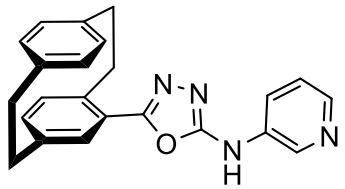

According to **GP4**, 2'(4'-[2.2]paracyclophanyl)-*1 yridine*din-3-yl)hydrazine-1-carbothioamide (**135a**, 0.402 g, 1.00 mmol, 1.00 equiv.) was refluxed in THF/Et_3N for 24 h. The crude product was purified *via* column chromatography (dichloromethane/methanol; 10:1) and the title compound was obtained as a yellow solid (0.240 g, 66%, 65.1 μmol).

R_f = 0.40 (dichloromethane/methanol; 10:1). – **Mp**: 212–214 °C. – **^{1}H NMR** (400 MHz, $CDCl_3$) δ = 9.06 (br, 1H, N*H*), 8.68 (d, *J* = 6.1 Hz, 2H, H^{Ar}), 7.75–7.72 (m, 1H, H^{Ar}), 7.28–7.26 (m, 1H, H^{Ar}), 6.99–6.93 (m, 2H, H^{Ar}), 6.90–6.73 (m, 5H, H^{Ar}), 3.21–3.12 (m, 4H, H^{Pc}), 3.10–3.01 (m, 3H, H^{Pc}), 2.99–2.93 (m, 1H, H^{Pc}) ppm. – **^{13}C NMR** (101 MHz, $CDCl_3$) δ = 167.1 (C_q, C^{Ar}), 159.9 (C_q, C^{Ar}), 140.4 (+, 2 × CH^{Ar}), 139.9 (C_q, C^{Ar}), 139.8 (C_q, C^{Ar}), 139.3 (C_q, C^{Ar}), 138.7 (C_q, C^{Ar}), 137.2 (C_q, C^{Ar}), 136.3 (+, CH^{Ar}), 135.1 (+, CH^{Ar}), 133.1 (+, CH^{Ar}), 132.5 (+, CH^{Ar}), 132.2 (+, CH^{Ar}), 130.9 (+, CH^{Ar}), 130.6 (+, CH^{Ar}), 130.0 (+, CH^{Ar}), 125.0 (C_q, C^{Ar}), 124.2 (+, CH^{Ar}), 35.5 (–, CH_2), 35.3 (–, CH_2), 35.1 (–, CH_2), 34.3 (–, CH_2) ppm. – **IR** (ATR) $\tilde{\nu}$ = 3421 (vw), 3377 (w), 3060 (w), 2949 (w), 2925 (w), 2849 (w), 1748 (w), 1704 (vs), 1649 (vs), 1605 (s), 1587 (vs), 1551 (m), 1466 (s), 1436 (s), 1397 (s), 1281 (vs), 1258 (vs), 1181 (vs), 1135 (s), 1109 (m), 1092 (m), 1044 (s), 1007 (m), 857 (m), 836 (m), 772 (s), 749 (s), 694 (vs), 636 (s), 585 (s), 552 (s), 510 (vs) cm^{-1}. – **MS** (FAB, 3-NBA): *m/z* (%) = 369 (100) $[M+H]^+$, 368 (25) $[M]^+$. – **HRMS** (FAB, 3-NBA, $C_{23}H_{21}O_1N_4$, $[M+H]^+$) calc.: 369.1715, found: 369.1714.

(*rac*)-5'(4'-[2.2]Paracyclophanyl)-*N*-phenyl-1,3,4-oxadiazol-2-amine (137b)

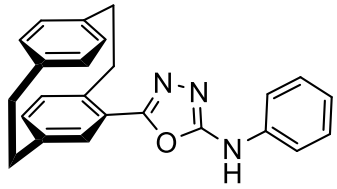

According to **GP4**, 2'(4'-[2.2]paracyclophanyl)-*N*-phenyl-hydrazinecarbothioamide (**135b**, 0.401 g, 1.00 mmol, 1.00 equiv.) was refluxed in THF/Et_3N for 20 h. The crude product was purified *via* column chromatography (dichloromethane/methanol; 10:1) and the title compound was obtained as a yellow solid (0.250 g, 68%, 68.0 µmol).

R_f = 0.40 (dichloromethane/methanol; 10:1). – **Mp**: 192–194 °C. – **^{1}H NMR** (400 MHz, Acetone-d_6) δ = 10.03 (s, 1H, N*H*), 7.80–7.77 (m, 1H, H^{Ar}), 7.48–7.38 (m, 2H, H^{Ar}), 7.10–7.03 (m, 2H, H^{Ar}), 6.99–6.96 (m, 1H, H^{Ar}), 6.92–6.73 (m, 2H, H^{Ar}), 6.70–6.45 (m, 4H, H^{Ar}), 3.23–3.13 (m, 3H, H^{Pc}), 3.12–3.01 (m, 4H, H^{Pc}), 3.00–2.94 (m, 1H, H^{Pc}) ppm. – **^{13}C NMR** (101 MHz, Acetone-d_6) δ = 162.7 (C_q, C^{Ar}), 160.0 (C_q, C^{Ar}), 141.3 (C_q, C^{Ar}), 141.1 (C_q, C^{Ar}), 140.5 (C_q, C^{Ar}), 140.2 (C_q, C^{Ar}), 139.6 (C_q, C^{Ar}), 137.1 (+, CH^{Ar}), 135.4 (+, CH^{Ar}), 134.0 (+, CH^{Ar}), 133.9 (+, CH^{Ar}), 133.6 (+, CH^{Ar}), 133.0 (+, CH^{Ar}), 132.9 (+, CH^{Ar}), 131.3 (+, CH^{Ar}), 130.3 (+, CH^{Ar}), 129.9 (+, CH^{Ar}), 125.8 (C_q, C^{Ar}), 122.8 (+, CH^{Ar}), 121.6, (+, CH^{Ar}), 35.9 (–, CH_2), 35.7 (–, CH_2), 35.5 (–, CH_2), 34.7 (–, CH_2) ppm. – **IR** (ATR) $\tilde{\nu}$ = 3377 (w), 3060 (w), 2949 (w), 2925 (w), 2849 (w), 1748 (w), 1704 (vs), 1649 (vs), 1605 (s), 1587 (vs), 1466 (s), 1436 (s), 1281 (vs), 1258 (vs), 1181 (vs), 1135 (s), 1109 (m), 1092 (m), 1044 (s), 857 (m), 772 (s), 749 (s), 694 (vs), 636 (s), 585 (s), 510 (vs) cm^{-1}. – **MS** (FAB, 3-NBA): *m/z* (%) = 368 (75) $[M+H]^+$, 367 (٣5) $[M]^+$. – **HRMS** (FAB, 3-NBA, $C_{24}H_{22}O_1N_3$, $[M+H]^+$) calc.: 368.1763, found: 368.1761.

(*rac*)-*N*-Allyl-5'(4'-[2.2]paracyclophanyl)-1,3,4-oxadiazol-2-amine (137c)

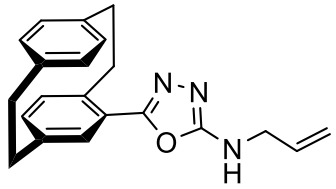

According to **GP4**, *N*-allyl-2'(4'-[2.2]paracyclophanyl)hydrazine-1-carbothioamide (**135c**, 0.365 g, 1.00 mmol, 1.00 equiv.) was refluxed in THF/Et_3N for 14 h. The crude product was purified *via* column chromatography (dichloromethane/methanol; 10:1) and the title compound was obtained as a yellow solid (0.220 g, 66%, 66.4 µmol).

R_f = 0.46 (dichloromethane/methanol; 10:1). – **Mp**: 206–208 °C. – **^{1}H NMR** (400 MHz, Acetone-d_6) δ = 6.91 (s, 1H, N*H*), 6.70–6.55 (m, 5H, H^{Ar}), 6.44–6.37 (m, 2H, H^{Ar}), 6.10–6.02 (m, 1H, CH^{allyl}), 5.38–5.17 (m, 2H, CH_2^{allyl}), 4.07–4.05 (m, 2H, CH_2^{allyl}), 3.18–3.10 (m, 3H, H^{Pc}), 3.08–2.96 (m, 4H, H^{Pc}), 2.95–2.89 (m, 1H, H^{Pc}) ppm. – **^{13}C NMR** (101 MHz, Acetone-d_6) δ = 164.3 (C_q, C^{Ar}), 160.0 (C_q, C^{Ar}), 141.3 (C_q, C^{Ar}), 140.6 (C_q, C^{Ar}), 140.3 (C_q, C^{Ar}), 139.8 (C_q, C^{Ar}), 137.1 (+, CH^{Ar}), 135.7 (+, CH^{Ar}), 135.1 (+, CH^{Ar}), 134.2 (+, CH^{Ar}), 134.1 (+, CH^{allyl}), 133.1 (+, CH^{Ar}), 132.9 (+, CH^{Ar}), 131.3 (+, CH^{Ar}), 126.5 (C_q, C^{Ar}), 116.5 (–, CH$_2^{allyl}$), 46.4 (–, CH$_2^{allyl}$), 36.1 (–, CH$_2$), 35.8 (–, CH$_2$), 35.6 (–, CH$_2$), 34.8 (–, CH$_2$) ppm. – **IR** (ATR) $\tilde{\nu}$ = 3214 (w), 3156 (w), 3013 (w), 2946 (m), 2925 (m), 2888 (m), 2856 (w), 1717 (w), 1653 (vs), 1623 (vs), 1595 (s), 1557 (s), 1337 (s), 1271 (s), 1035 (vs), 967 (vs), 925 (vs), 844 (vs), 795 (s), 724 (vs), 630 (vs), 577 (s), 514 (vs) cm^{-1}. – **MS** (FAB, 3-NBA): *m/z* (%) = 332 (100) [M+H]$^+$, 331 (50) [M]$^+$. – **HRMS** (FAB, 3-NBA, $C_{21}H_{22}O_1N_3$, [M+H]$^+$) calc.: 332.1763, found: 332.1764.

(*rac*)-*N*-Ethyl-5'(4'-[2.2]paracyclophanyl)-1,3,4-oxadiazol-2-amine (137d)

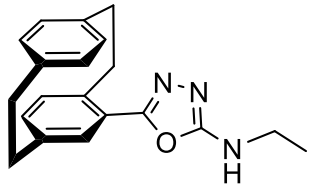

According to **GP4**, 2'(4'-[2.2]paracyclophanyl)-*N*-ethylhydrazine-1-carbothioamide (**135d**, 0.353 g, 1.00 mmol, 1.00 equiv.) was refluxed in THF/Et_3N for 12 h. The crude product was purified *via* column chromatography (cyclohexane/ethyl acetate; 1:1) and the title compound was obtained as a yellow solid (0.190 g, 60%, 595 μmol).

R_f = 0.30 (cyclohexane/ethyl acetate; 1:1). – **Mp**: 212–214 °C. – **^{1}H NMR** (400 MHz, DMSO-d_6) δ = 6.83 (s, 1H, N*H*), 6.69–6.63 (m, 2H, H^{Ar}), 6.59–6.54 (m, 3H, H^{Ar}), 6.41 (d, J = 8.1 Hz, 1H, H^{Ar}), 6.31 (d, J = 7.9 Hz, 1H, H^{Ar}), 4.03–3.82 (m, 2H, CH_2^{ethyl}), 3.14–2.89 (m, 6H, H^{Pc}), 2.94–2.89 (m, 2H, H^{Pc}), 1.23 (t, J = 7.2 Hz, 3H, CH_3^{ethyl}) ppm. – **^{13}C NMR** (101 MHz, DMSO-d_6) δ = 163.1 (C_q, C^{Ar}), 158.1 (C_q, C^{Ar}), 140.1 (C_q, C^{Ar}), 139.2 (C_q, C^{Ar}), 139.1 (C_q, C^{Ar}), 138.3 (C_q, C^{Ar}), 136.1 (+, CH^{Ar}), 134.1 (+, CH^{Ar}), 133.2 (+, CH^{Ar}), 133.0 (+, CH^{Ar}), 131.9 (+, CH^{Ar}), 131.6 (+, CH^{Ar}), 130.1 (+, CH^{Ar}), 125.0 (C_q, C^{Ar}), 37.5 (–, CH$_2^{ethyl}$), 34.8 (–, CH$_2$), 34.7 (–, CH$_2$), 34.5 (–, CH$_2$), 33.8 (–, CH$_2$), 14.6 (+, CH$_3^{ethyl}$) ppm. – **IR** (ATR) $\tilde{\nu}$ = 3357 (vw), 3210 (w), 3153 (w), 3013 (w), 2956 (m), 2929 (s), 2851 (w), 1730 (vs), 1642 (vs), 1618 (vs), 1595 (vs), 1557 (s), 1435 (vs), 1259 (vs), 1251 (vs), 1200 (vs), 1173 (vs), 1164 (vs), 1147 (vs), 1128 (vs), 1034 (vs), 898 (s), 846 (s), 796 (s), 742 (s), 721 (vs), 704 (vs), 635 (vs), 516 (vs) cm^{-1} – **MS** (FAB, 3-NBA): *m/z* (%) = 320 (95) $[M+H]^+$, 319 (40) $[M]^+$. – **HRMS** (FAB, 3-NBA, $C_{20}H_{22}O_1N_3$, $[M+H]^+$) calc.: 320.1763, found: 320.1762.

(*rac*)-*N*-Cyclopropyl-5'(4''-[2.2]paracyclophanyl)-1,3,4-oxadiazol-2-amine (137e).

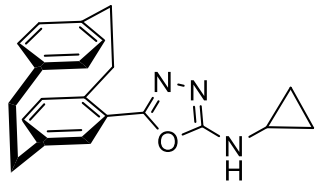

According to **GP4**, 2'(4''-[2.2]paracyclophanyl)-*N*-cyclopropyl-hydrazine-1-carbothioamide (**135e**, 0.365 g, 1.00 mmol, 1.00 equiv.) was refluxed in THF/Et_3N for 16 h. The crude product was purified *via* column chromatography (cyclohexane/ethyl acetate; 1:1) and the title compound was obtained as a violet solid (0.210 g, 63%, 63.4 µmol).

R_f = 0.28 (cyclohexane/ethyl acetate; 1:1). – **Mp**: 222–224 °C. – **^{1}H NMR** (400 MHz, Methanol-d_4) δ = 6.91 (s, 1H, N*H*), 6.67–6.59 (m, 2H, H^{Ar}), 6.58–6.51 (m, 3H, H^{Ar}), 6.45–6.35 (m, 2H, H^{Ar}), 3.18–3.11 (m, 3H H^{Pc}), 3.09–3.01 (m, 3H, H^{Pc}), 2.98–2.91 (m, 2H, H^{Pc}), 2.75–2.69 (m, 1H, C$H^{cyclo.}$), 0.84–0.79 (m, 2H, C$H_2^{cyclo.}$), 0.67–0.63 (m, 2H, C$H_2^{cyclo.}$) ppm. – **^{13}C NMR** (101 MHz, Methanol-d_4) δ = 165.6 (C_q, C^{Ar}), 160.9 (C_q, C^{Ar}), 141.9 (C_q, C^{Ar}), 140.09 (C_q, C^{Ar}), 140.8 (C_q, C^{Ar}), 140.5 (C_q, C^{Ar}), 137.5 (+, CH^{Ar}), 136.0 (+, CH^{Ar}), 134.4 (+, CH^{Ar}), 134.3 (+, CH^{Ar}), 133.3 (+, CH^{Ar}), 133.2 (+, CH^{Ar}), 131.6 (+, CH^{Ar}), 126.0 (C_q, C^{Ar}), 36.3 (–, CH$_2$), 36.1 (–, CH$_2$), 36.0 (–, CH$_2$), 35.4 (–, CH$_2$), 25.2 (+, CH$^{cyclo.}$), 7.4 (–, 2 × CH$_2^{cyclo.}$) ppm. – **IR** (ATR) $\tilde{\nu}$ = 3284 (vw), 3177 (w), 3143 (w), 3006 (w), 2956 (m), 2929 (m), 2851 (w), 1734 (s), 1633 (vs), 1611 (vs), 1595 (vs), 1555 (vs), 1435 (s), 1367 (s), 1258 (vs), 1201 (vs), 1074 (vs), 1040 (vs), 1020 (s), 966 (s), 846 (s), 793 (s), 724 (vs), 704 (vs), 671 (s), 635 (vs), 516 (vs) cm^{-1}. – **MS** (FAB, 3-NBA): *m/z* (%) = 332 (100) [M+H]$^+$, 331 (55) [M]$^+$. – **HRMS** (FAB, 3-NBA, $C_{21}H_{22}O_1N_3$, [M+H]$^+$) calc.: 332.1763, found: 332.1762.

5.2.3. Analytical Data of [2.2]Paracyclophanyl-based [3.3.3]Propellanes

General Procedures (GP5)

A solution of *N*-substituted [2.2]paracyclophanylhydrazinecarbothioamides (**135a-e**, 1.00 mmol, 1.00 equiv.) in dry tetrahydrofuran (THF) (20 mL) was added dropwise to a solution of dicyanomethylene-1,3-indanedione (CNIND) (**174**, 0.208 g, 1.00 mmol, 1.00 equiv.) in dry THF (15 mL). The reaction mixture was stirred at room temperature for 90-96 h (reaction was monitored by thin-layer chromatography). After removal of the solvent under reduced pressure, the crude residue was purified by column chromatography to give two compounds, **138a–e** and **175**.

(*rac*)-*N*-((3*aS*,8bR)-2-Amino-3-cyano-4-oxo-1 yridinedin-3-yl)-10-thi5xo-4*H*-3*a*,8*b*- 6 (epimino-methanoimino)indeno[1,2-*b*]furan-11-yl)[2.2]paracyclophanamide (138a)**

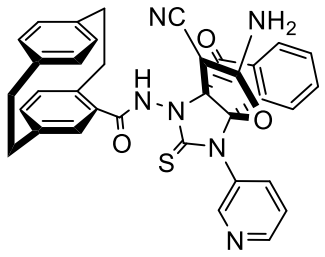

According to **GP5**, 2'(4'-[2.2]paracyclophanyl)-*1 yridine*din-3-yl)-hydrazine-1-carbothioamide (**135a**, 0.402 g, 1.00 mmol, 1.00 equiv.) was refluxed with CNIND (**174**, 0.208 g, 1.00 mmol, 1.00 equiv.) in dry THF (35 mL) for 90 h. The crude product was purified *via* column chromatography (dichloromethane/methanol; 10:1) and the title compound was obtained as a white solid (0.495 g, 81%, 811 μmol). *5*

R*f* = 0.35 (dichloromethane/methanol; 10:1). – **Mp**: 244–246 °C. – **^{1}H NMR** (500 MHz, DMSO-d_6) δ = 11.00 (s, 1H, N*H*), 8.76 (dd, *J* = 4.7, 1.6 Hz, 1H, H^{Ar}), 8.55 (d, *J* = 2.5 Hz, 1H, H^{Ar}), 8.34 (s, 2H, H^{Ar}), 8.07–8.04 (m, 1H, H^{Ar}), 7.82–7.76 (m, 3H, H^{Ar}), 7.67–6.64 (m, 1H, H^{Ar}), 7.07–6.96 (m, 1H, H^{Ar}), 6.85 (s, 2H, NH_2), 6.68–6.39 (m, 5H, H^{Ar}), 3.83–3.80 (m, 1H, H^{Pc}), 3.24–3.09 (m, 3H, H^{Pc}), 3.02–2.87 (m, 4H, H^{Pc}) ppm. – **^{13}C NMR** (126 MHz, DMSO-d_6) δ = 189.5 (C_q, *C*O), 182.4 (C_q, *C*S), 168.3 (C_q, C^{Ar}), 166.8 (C_q, *C*O), 150.6 (+, CH^{Ar}), 150.5 (C_q, C^{Ar}), 142.5 (C_q, C^{Ar}), 141.0 (C_q, C^{Ar}), 140.0 (C_q, C^{Ar}), 139.8 (C_q, C^{Ar}), 139.4 (+, CH^{Ar}), 138.0 (+, CH^{Ar}), 137.5 (+, CH^{Ar}), 136.1 (C_q, C^{Ar}), 136.0 (+, CH^{Ar}), 135.9 (+, CH^{Ar}), 133.3 (+, CH^{Ar}), 133.1 (C_q, C^{Ar}), 133.0 (+, 2 × CH^{Ar}), 132.9 (+, CH^{Ar}), 132.8 (+, CH^{Ar}), 132.6 (C_q, C^{Ar}), 132.5 (+, CH^{Ar}), 126.4 (+, CH^{Ar}), 125.1 (+, CH^{Ar}), 124.9 (+, CH^{Ar}), 116.4 (C_q, *C*N), 103.7 (C_q, C^{Ar}), 78.4 (C_q, C^{Ar}), 51.7 (C_q, C^{Ar}), 35.2 (–, CH_2), 35.1 (–, CH_2), 35.0 (–, CH_2), 34.6 (–, CH_2) ppm. – **IR** (ATR) $\tilde{\nu}$ = 3116 (w), 3084 (w), 2973 (w), 2948 (w), 2921 (w), 2854 (w), 2200 (w), 1730 (m), 1677 (w), 1649 (vs), 1584 (m), 1479 (w), 1434 (m), 1422 (s), 1337 (s), 1307 (vs), 1266 (vs), 1196 (s), 1050 (s), 993 (s), 958 (s), 898 (m), 857 (m), 803 (vs), 761 (s), 713 (s), 687 (s), 656 (s), 633 (vs), 528 (s), 516 (vs), 432 (vs) cm^{-1}. – **MS** (FAB, 3-NBA): *m/z*

(%) = 611 (35) $[M+H]^+$, 610 (20) $[M]^+$. – **HRMS** (FAB, 3-NBA, $C_{35}H_{27}O_3N_6{}^{32}S_1$, $[M+H]^+$) calc.: 611.1865, found: 611.1864.

(*rac*)-*N*-((3*aS,8*bR**)-2-Amino-3-cyano-4-oxo-9-phenyl-10-thioxo-4*H*-3*a*,8*b*-(epiminomethano-imino)indeno[1,2-*b*]furan-11-yl)[2.2]paracyclophanamide (138b)**

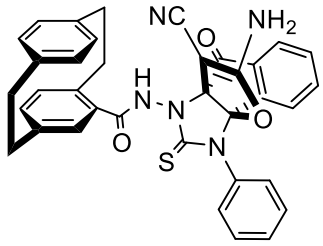

According to **GP5**, 2'(4'-[2.2]paracyclophanyl)-*N*-phenyl-hydrazinecarbothioamide (**135b**, 0.401 g, 1.00 mmol, 1.00 equiv.) was refluxed with CNIND (**174**, 0.208 g, 1.00 mmol, 1.00 equiv.) in dry THF (35 mL) for 90 h. The crude product was purified *via* column chromatography (cyclohexane/ethyl acetate; 4:1) and the title compound was obtained as a white solid (0.245 g, 40%, 402 μmol).

R_f = 0.33 (cyclohexane/ethyl acetate; 4:1). – **Mp**: 230–232 °C. – **^{1}H NMR** (500 MHz, DMSO-d_6) δ = 10.64 (s, 1H, N*H*), 8.76–8.23 (m, 2H, H^{Ar}), 8.13–7.77 (m, 3H, H^{Ar}), 7.67–7.54 (m, 2H, H^{Ar}), 7.41–7.31 (m, 2H, H^{Ar}), 7.05–6.96 (m, 1H, H^{Ar}), 6.94 (s, 2H, NH_2), 6.75–6.66 (m, 2H, H^{Ar}), 6.60–6.35 (m, 4H, H^{Ar}), 3.96–3.77 (m, 1H, H^{Pc}), 3.25–3.08 (m, 3H, H^{Pc}), 3.06–2.86 (m, 4H, H^{Pc}) ppm. – **^{13}C NMR** (126 MHz, DMSO-d_6) δ = 192.0 (C_q, *C*O), 182.3 (C_q, *C*S), 168.3 (C_q, C^{Ar}), 160.0 (C_q, *C*O), 158.7 (+, *C*H^{Ar}), 153.3 (C_q, C^{Ar}), 140.7 (C_q, C^{Ar}), 140.0 (C_q, C^{Ar}), 139.7 (C_q, C^{Ar}), 139.6 (C_q, C^{Ar}), 139.4 (+, *C*H^{Ar}), 139.3 (+, *C*H^{Ar}), 136.7 (C_q, C^{Ar}), 135.2 (+, *C*H^{Ar}), 133.7 (+, *C*H^{Ar}), 133.5 (+, *C*H^{Ar}), 133.1 (+, *C*H^{Ar}), 133.0 (C_q, C^{Ar}), 132.9 (+, *C*H^{Ar}), 132.7 (+, *C*H^{Ar}), 132.4 (+, *C*H^{Ar}), 132.3 (+, *C*H^{Ar}), 130.8 (+, *C*H^{Ar}), 130.0 (C_q, C^{Ar}), 129.6 (+, 2 × *C*H^{Ar}), 124.9 (+, *C*H^{Ar}), 122.3 (+, *C*H^{Ar}), 117.5 (C_q, *C*N), 104.0 (C_q, C^{Ar}), 79.1 (C_q, C^{Ar}), 51.5 (C_q, C^{Ar}), 35.3 (–, *C*H_2), 35.0 (–, *C*H_2), 34.9 (–, *C*H_2), 34.3 (–, *C*H_2) ppm. – **IR** (ATR) $\tilde{\nu}$ = 3521 (vw), 3381 (w), 3200 (w), 2979 (w), 2919 (w), 2836 (w), 2206 (m), 1731 (m), 1674 (s), 1645 (vs), 1582 (s), 1493 (m), 1434 (s), 1370 (s), 1324 (vs), 1307 (vs), 1262 (vs), 1190 (m), 1160 (m), 994 (s), 969 (s), 813 (s), 795 (s), 768 (s), 747 (s), 707 (s), 691 (vs), 619 (vs), 592 (vs), 577 (s), 533 (s), 517 (vs), 489 (s), 462 (s), 422 (vs) cm^{-1}. – **MS** (FAB, 3-NBA): *m/z* (%) = 610 (35) [M+H]$^+$, 609 (25) [M]$^+$. – **HRMS** (FAB, 3-NBA, $C_{36}H_{28}O_3N_5{}^{32}S_1$, [M+H]$^+$) calc.: 610.1913, found: 610.1875.

(*rac*)-*N*-((3*aS,8*bR**)-9-Allyl-2-amino-3-cyano-4-oxo-10-thioxo-4*H*-3*a*,8*b*-(epiminomethano-imino)indeno[1,2-*b*]furan-11-yl)[2.2]paracyclophanamide (138c)**

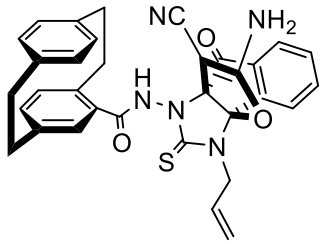

According to **GP5**, *N*-allyl-2'(4'-[2.2]paracyclophanyl)hydrazine-1-carbothioamide (**135c**, 0.365 g, 1.00 mmol, 1.00 equiv.) was refluxed with CNIND (**174**, 0.208 g, 1.00 mmol, 1.00 equiv.) in dry THF (35 mL) for 96 h. The crude product was purified *via* column chromatography (dichloromethane/methanol; 10:1). and the title compound was obtained as a white solid (0.200 g, 35%, 349 μmol).

R*f* = 0.36 (dichloromethane/methanol; 10:1). – **Mp**: 195–197 °C. – **^{1}H NMR** (500 MHz, Acetone-*d*$_6$) δ = 10.85 (s, 1H, N*H*), 7.88–7.82 (m, 1H, *H*^{Ar}), 7.71–7.66 (m, 1H, *H*^{Ar}), 7.60–7.46 (m, 2H, *H*^{Ar}) 7.29 (s, 2H, *H*^{Ar}), 6.87 (s, 2H, N*H*$_2$), 6.66–6.62 (m, 1H, *H*^{Ar}), 6.57–6.52 (m, 4H, *H*^{Ar}), 5.89–5.86 (m, 1H, C*H*^{allyl}), 5.63–5.01 (m, 2H, C*H*$_2^{allyl}$), 4.43–4.25 (m, 2H, C*H*$_2^{allyl}$), 3.88–3.73 (m, 1H, *H*^{Pc}), 3.19–3.14 (m, 3H, *H*^{Pc}), 3.09–2.99 (m, 4H, *H*^{Pc}) ppm. – **^{13}C NMR** (126 MHz, Acetone-*d*$_6$) δ = 192.6 (C$_q$, *C*O), 186.9 (C$_q$, *C*S), 168.1 (C$_q$, *C*^{Ar}), 164.1 (C$_q$, *C*O), 145.5 (C$_q$, *C*^{Ar}), 140.3 (C$_q$, *C*^{Ar}), 139.6 (C$_q$, *C*^{Ar}), 137.2 (C$_q$, *C*^{Ar}), 136.4 (C$_q$, *C*^{Ar}), 136.2 (+, *C*H^{Ar}), 135.3 (+, *C*H^{allyl}), 135.0 (+, *C*H^{Ar}), 133.3 (+, *C*H^{Ar}), 133.1 (+, *C*H^{Ar}), 132.9 (C$_q$, *C*^{Ar}), 132.6 (+, *C*H^{Ar}), 132.4 (+, *C*H^{Ar}), 132.3 (+, *C*H^{Ar}), 132.1 (C$_q$, *C*^{Ar}), 125.6 (+, *C*H^{Ar}), 125.1 (+, *C*H^{Ar}), 124.4 (+, *C*H^{Ar}), 124.2 (+, *C*H^{Ar}), 116.9 (C$_q$, *C*N), 115.4 (–, *C*H$_2^{allyl}$), 106.6 (C$_q$, *C*^{Ar}), 67.2 (C$_q$, *C*^{Ar}), 55.5 (C$_q$, *C*^{Ar}), 46.9 (–, *C*H$_2^{allyl}$), 35.6 (–, *C*H$_2$), 35.3 (–, *C*H$_2$), 35.2 (–, *C*H$_2$), 35.1 (–, *C*H$_2$) ppm. – **IR** (ATR) $\tilde{\nu}$ = 3319 (w), 3306 (w), 3274 (w), 3077 (w), 2924 (w), 2191 (w), 1731 (vs), 1653 (vs), 1595 (vs), 1587 (vs), 1463 (m), 1434 (s), 1339 (m), 1255 (vs), 1198 (s), 1153 (m), 1035 (vs), 1010 (vs), 993 (s), 958 (vs), 901 (s), 798 (vs), 759 (s), 640 (vs), 577 (vs), 533 (vs), 514 (vs), 453 (vs) cm^{-1}. – **MS** (FAB, 3-NBA): *m/z* (%) = 574 (20) [M+H]$^+$, 573 (10) [M]$^+$. – **HRMS** (FAB, 3-NBA, $C_{33}H_{28}O_3N_5{}^{32}S_1$, [M+H]$^+$) calc.: 574.1907, found: 574.1890.

(*rac*)-*N*-((3*aS,8*bR**)-2-Amino-3-cyano-9-ethyl-4-oxo-10-thioxo-4*H*-3*a*,8*b*-(epiminomethano-imino)indeno[1,2-*b*]furan-11-yl)[2.2]paracyclophanamide (138d)**

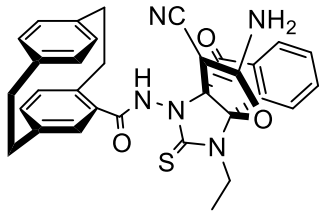

According to **GP5**, 2'(4'-[2.2]paracyclophanyl)-*N*-ethylhydrazine-1-carbothioamide (**135d**, 0.353 g, 1.00 mmol, 1.00 equiv.) was refluxed with CNIND (**174**, 0.208 g, 1.00 mmol, 1.00 equiv.) in dry THF (35 mL) for 96 h. The crude product was purified *via* column chromatography (cyclohexane/ethyl acetate; 1:1) and the title compound was obtained as a white solid (0.200 g, 36%, 356 µmol).

R_f = 0.26 (cyclohexane/ethyl acetate; 1:1). – **Mp**: 202–204 °C. – **^{1}H NMR** (500 MHz, DMSO-d_6, ppm) δ = 10.74 (s, 1H, N*H*), 8.25 (d, J = 7.8 Hz, 1H, H^{Ar}), 8.17–8.12 (m, 2H, H^{Ar}), 8.07–7.95 (m, 2H, H^{Ar}), 7.89–7.86 (m, 1H, H^{Ar}), 6.93 (s, 2H, NH_2), 6.68–6.62 (m, 1H, H^{Ar}), 6.56–6.39 (m, 4H, H^{Ar}), 4.10 (q, J = 7.2 Hz, 2H, CH_2^{ethyl}), 3.82–3.77 (m, 1H, H^{Pc}), 3.18–3.07 (m, 3H, H^{Pc}), 3.03–2.90 (m, 3H, H^{Pc}), 2.87–2.82 (m, 1H, H^{Pc}), 1.23 (t, J = 7.1 Hz, 3H, CH_3^{ethyl}) ppm. – **^{13}C NMR** (126 MHz, DMSO-d_6) δ = 189.4 (C_q, *C*O), 186.9 (C_q, *C*S), 168.0 (C_q, C^{Ar}), 161.4 (C_q, *C*O), 142.6 (C_q, C^{Ar}), 140.6 (C_q, C^{Ar}), 139.6 (C_q, C^{Ar}), 139.2 (C_q, C^{Ar}), 138.8 (C_q, C^{Ar}), 137.8 (+, *C*H^{Ar}), 136.1 (+, *C*H^{Ar}), 136.0 (+, *C*H^{Ar}), 135.3 (+, *C*H^{Ar}), 134.6 (+, *C*H^{Ar}), 132.6 (C_q, C^{Ar}), 132.4 (C_q, C^{Ar}), 132.2 (+, *C*H^{Ar}), 130.1 (+, *C*H^{Ar}), 129.8 (+, *C*H^{Ar}), 125.7 (+, *C*H^{Ar}), 123.9 (+, *C*H^{Ar}), 119.3 (+, *C*H^{Ar}), 117.3 (C_q, *C*N), 102.8 (C_q, C^{Ar}), 76.8 (C_q, C^{Ar}), 55.0 (–, *C*H_2^{ethyl}), 51.5 (C_q, C^{Ar}), 34.8 (–, *C*H_2), 34.7 (–, *C*H_2), 34.6 (–, *C*H_2), 34.5 (–, *C*H_2), 13.7 (+, *C*H_3^{ethyl}) ppm. – **IR** (ATR) $\tilde{\nu}$ = 3391 (w), 3357 (w), 3308 (w), 3244 (w), 3187 (w), 3006 (vw), 2929 (w), 2888 (vw), 2198 (s), 1732 (s), 1686 (m), 1659 (vs), 1581 (s), 1448 (s), 1392 (s), 1360 (m), 1334 (m), 1278 (vs), 1265 (vs), 1038 (m), 956 (m), 735 (m), 696 (m), 605 (m), 516 (w), 469 (w) cm^{-1}. – **MS** (FAB, 3-NBA): *m/z* (%) = 562 (100) $[M+H]^+$, 561 (60) $[M]^+$. – **HRMS** (FAB, 3-NBA, $C_{32}H_{28}O_3N_5{}^{32}S_1$, $[M+H]^+$) calc.: 562.1913, found: 562.1904.

(*rac*)-*N*-((3*aS,8*bR**)-2-Amino-3-cyano-9-cyclopropyl-4-oxo-10-thioxo-4*H*-3*a*,8*b*-(epiminomethano-imino)indeno[1,2-*b*]furan-11-yl)[2.2]paracyclophanamide (138e)**

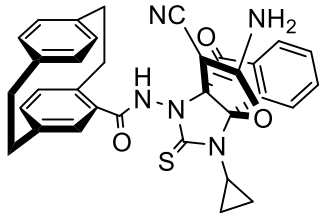

According to **GP5**, 2'(4'-[2.2]paracyclophanyl)-*N*-cyclopropyl-hydrazine-1-carbothioamide (**135e**, 0.365 g, 1.00 mmol, 1.00 equiv.) was refluxed with CNIND (**174**, 0.208 g, 1.00 mmol, 1.00 equiv.) in dry THF (35 mL) for 96 h. The crude product was purified *via* column chromatography (dichloromethane/methanol; 10:1) and the title compound was obtained as a white solid (0.215 g, 3^%, 375 µmol).

R_f = 0.35 (dichloromethane/methanol; 10:1). – **Mp**: 208–210 °C. – **^{1}H NMR** (500 MHz, DMSO-d_6) δ = 10.14 (s, 1H, N*H*), 8.27 (d, *J* = 7.8 Hz, 1H, H^{Ar}), 8.05–7.98 (m, 1H, H^{Ar}), 7.95–7.90 (m, 1H, H^{Ar}), 7.87–7.80 (m, 1H, H^{Ar}), 7.72–7.58 (m, 1H, H^{Ar}), 6.60 (s, 2H, NH_2), 6.79–6.58 (m, 2H, H^{Ar}), 6.56–6.38 (m, 4H, H^{Ar}), 3.54–3.51 (m, 1H, H^{Pc}), 3.18–3.08 (m, 2H, H^{Pc}), 3.04–2.89 (m, 4H, H^{Pc}), 2.85–2.79 (m, 1H, H^{Pc}), 1.76–1.69 (m, 1H, C$H^{cyclo.}$), 1.31–1.23 (m, 2H, C$H_2^{cyclo.}$), 1.03–0.84 (m, 2H, C$H_2^{cyclo.}$) ppm. – **^{13}C NMR** (126 MHz, DMSO-d_6) δ = 192.6 (C_q, *C*O), 178.3 (C_q, *C*S), 167.6 (C_q, C^{Ar}), 166.9 (C_q, *C*O), 146.4 (C_q, C^{Ar}), 139.8 (C_q, C^{Ar}), 139.7 (C_q, C^{Ar}), 139.5 (C_q, C^{Ar}), 139.4 (C_q, C^{Ar}), 138.1 (+, *C*H^{Ar}), 136.9 (+, *C*H^{Ar}), 136.1 (+, *C*H^{Ar}), 135.4 (+, *C*H^{Ar}), 135.0 (+, *C*H^{Ar}), 133.6 (+, *C*H^{Ar}), 132.9 (+, *C*H^{Ar}), 132.5 (C_q, C^{Ar}), 132.2 (C_q, C^{Ar}), 127.0 (+, *C*H^{Ar}), 126.2 (+, *C*H^{Ar}), 124.7 (+, *C*H^{Ar}), 124.4 (+, *C*H^{Ar}), 116.0 (C_q, *C*N), 107.4 (C_q, C^{Ar}), 68.7 (C_q, C^{Ar}), 49.5 (C_q, C^{Ar}), 35.4 (–, *C*H$_2$), 35.3 (–, *C*H$_2$), 35.2 (–, *C*H$_2$), 35.0 (–, *C*H$_2$), 27.9 (+, *C*H$^{cyclo.}$), 9.4 (–, *C*H$_2^{cyclo.}$), 7.9 (–, *C*H$_2^{cyclo.}$) ppm. – **IR** (ATR) $\tilde{\nu}$ = 3400 (w), 3251 (w), 3177 (w), 3030 (w), 2925 (s), 2851 (m), 2191 (w), 1732 (vs), 1659 (vs), 1587 (vs), 1497 (m), 1436 (s), 1337 (s), 1268 (vs), 1156 (vs), 1061 (vs), 1030 (vs), 936 (vs), 778 (vs), 670 (vs), 623 (vs), 562 (vs), 510 (vs) cm^{-1}. – **MS** (FAB, 3-NBA): *m/z* (%) = 574 (20) [M+H]$^+$, 573 (15) [M]$^+$. – **HRMS** (FAB, 3-NBA, $C_{33}H_{28}O_3N_5{}^{32}S_1$, [M+H]$^+$) calc.: 574.1913, found: 574.1910.

2'-Amino-1,',5'-trioxo-1,3-dihydr'-5'*H*-spiro[indene-',4'-indeno[1,2-*b*]pyran'-3'-carbonitrile (175)

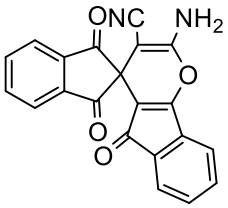

According to **GP5**, the title compound was obtained as a side product from the reaction of **135a-e** (1.00 mmol, 1.00 equiv.) and CNIND (**174**, 1.00 mmol, 1.00 equiv.) in dry THF (35 mL) as a yellow solid with a yield varying from 9 to 12%.

R_f = 0.58 (dichloromethane/methanol; 10:1). – **Mp**: 252–254 °C. – **^{1}H NMR** (400 MHz, DMSO-d_6) δ = 8.09–8.06 (m, 6H, H^{Ar}), 7.54 (t, J = 7.5 Hz, 1H, H^{Ar}), 7.41 (t, J = 7.2 Hz, 1H, H^{Ar}), 7.33 (s, 2H, NH_2). – **IR** (ATR) $\tilde{\nu}$ = 3357 (w), 3293 (w), 3230 (w), 3189 (m), 2200 (w), 1707 (vs), 1674 (vs), 1638 (s), 1585 (vs), 1378 (vs), 1333 (vs), 1259 (vs), 1217 (s), 1180 (m), 1135 (s), 1105 (m), 1072 (s), 963 (s), 915 (vs), 878 (m), 830 (m), 778 (s), 761 (vs), 722 (vs), 662 (s), 630 (s), 595 (vs), 523 (vs) cm^{-1}. The analytical data is consistent with literature.[228]

2'(4'-[2.2]Paracyclophanyl)-*1*-*yridine*din-3-yl)hydrazi*6*e-1-carbothioamide (*scale*-135a)

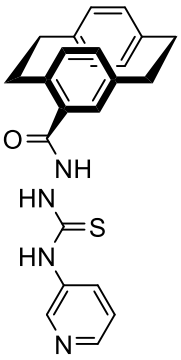

According to **GP5**, carbohydrazide-[2.2]paracyclophane (*scale*-**159**, 1.00 g, 3.75 mmol, 1.00 equiv.) was reacted with 3-isothiocyanatopyridine (0.511 g, 0.42 mL, 3.75 mmol, 1.00 equiv.) in dry EtOH (60 mL) for 6 h. A precipitate of the title compound was obtained as a white solid (1.240 g, 82%, 3.08 mmol).

$\mathbf{R}_f$ = 0.42 (dichloromethane/methanol; 10:1). See the above analysis for *rac*-**135**.

(S_p)-*N*-((3*aS*,8*bR*)-2-Amino-3-cyano-4-oxo-1 yridinedin-3-yl)-10-thio6xo-4*H*-3*a*,8*b*- 4 (epimino-methanoimino)indeno[1,2-*b*]furan-11-yl)[2.2]paracyclophanamide (S_p-138a)

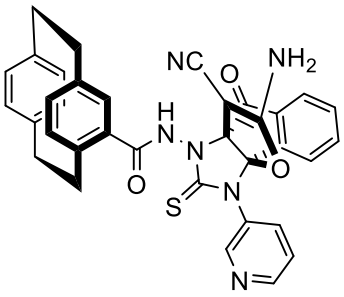

According to **GP5**, 2'(4'-[2.2]paracyclophanyl)-*1 yridine*din-3- 6 yl)hydrazine-1-carbothioamide (*scale*-**135a**, 0.402 g, 1.00 mmol, 1.00 equiv.) was refluxed with CNIND (**174**, 0.208 g, 1.00 mmol, 1.00 equiv.) in dry THF (35 mL) for 90 h. The crude product was purified *via* column chromatography (dichloromethane/methanol; 10:1) and *scal*-**138a** was obtained as a white solid compound (0.520 g, 84%, 843 μmol). The *ee* ratio of (S_p,*S*)/(R_p/*R*) pair of enantiomers was determined by Analytical Chiral HPLC (Chiralcel® OD-H, *n*-hexane/*i*PrOH, 90:10, 1.0 mL/min, λ =256 nm): t_{R1} = 17.1 min (62.1%), t_{R2} = 24.4 min (37.8%). *ee* = 37.7%. Separation of enantiomers was done by Semipreparative Chiral HPLC (Chiralcel® AZ-H, acetonitrile, 25.0 mL/min, λ =256 nm): t_R = 16.2 min (100%).

R_f = 0.35 (dichloromethane/methanol; 10:1), $[\alpha]_D$ = + 114 (c 0.004, CH_2Cl_2). – **Mp**: 245–247 °C. – **^{1}H NMR** (500 MHz, DMSO-d_6) δ = 11.04 (s, 1H, N*H*), 8.77 (dd, *J* = 4.7, 1.6 Hz, 1H, H^{Ar}), 8.54 (d, *J* = 2.5 Hz, 1H, H^{Ar}), 8.32 (s, 2H, H^{Ar}), 8.07–8.03 (m, 1H, H^{Ar}), 7.83–7.76 (m, 3H, H^{Ar}), 7.68–6.64 (m, 1H, H^{Ar}), 7.05–6.95 (m, 1H, H^{Ar}), 6.88 (s, 2H, NH_2), 6.68–6.39 (m, 5H, H^{Ar}), 3.83–3.79 (m, 1H, H^{Pc}), 3.23–3.09 (m, 3H, H^{Pc}), 3.05–2.88 (m, 4H, H^{Pc}) ppm. – **^{13}C NMR** (126 MHz, DMSO-d_6) δ = 189.6 (C_q, *C*O), 182.3 (C_q, *C*S), 168.4 (C_q, C^{Ar}), 166.8 (C_q, *C*O), 150.6 (+, *C*H^{Ar}), 150.4 (C_q, C^{Ar}), 142.5 (C_q, C^{Ar}), 141.1 (C_q, C^{Ar}), 140.0 (C_q, C^{Ar}), 139.8 (C_q, C^{Ar}), 139.4 (+, *C*H^{Ar}), 138.1 (+, *C*H^{Ar}), 137.6 (+, *C*H^{Ar}), 136.3 (C_q, C^{Ar}), 136.0 (+, *C*H^{Ar}), 135.3 (+, *C*H^{Ar}), 133.3 (+, *C*H^{Ar}), 133.1 (C_q, C^{Ar}), 133.0 (+, 2 × *C*H^{Ar}), 132.9 (+, *C*H^{Ar}), 132.8 (+, *C*H^{Ar}), 132.6 (C_q, C^{Ar}), 132.3 (+, *C*H^{Ar}), 126.3 (+, *C*H^{Ar}), 125.4 (+, *C*H^{Ar}), 124.9 (+, *C*H^{Ar}), 116.4 (C_q, *C*N), 103.7 (C_q, C^{Ar}), 78.3 (C_q, C^{Ar}), 51.7 (C_q, C^{Ar}), 35.2 (–, *C*H_2), 35.1 (–, *C*H_2), 35.0 (–, *C*H_2), 34.4 (–, *C*H_2) ppm. – **IR** (ATR) $\tilde{\nu}$ = 3116 (w), 3084 (w), 2973 (w), 2948 (w), 2921 (w), 2854 (w), 2200 (w), 1730 (m), 1677 (w), 1649 (vs), 1584 (m), 1479 (w), 1434 (m), 1422 (s), 1337 (s), 1307 (vs), 1266 (vs), 1196 (s), 1050 (s), 993 (s), 958 (s), 898 (m), 857 (m), 803 (vs), 761 (s), 713 (s), 687 (s), 656 (s), 633 (vs), 528 (s), 516 (vs), 432 (vs) cm^{-1}. – **MS** (FAB, 3-NBA): *m/z* (%) = 611 (35) [M+H]$^+$, 610 (20) [M]$^+$. – **HRMS** (FAB, 3-NBA, $C_{35}H_{27}O_3N_6{}^{32}S_1$, [M+H]$^+$) calc.: 611.1865, found: 611.1864.

5.2.4. Analytical Data of [2.2]Paracyclophanylthiazoles as Anti-cancer Agents

5.2.4.1. 2-(2'(4'-[2.2]Paracyclophonyl)-hydrazineylidene)-3-substituted-4-oxothia-zolidin-5-ylidene)acetates

General Procedures (GP6)

A mixture of *N*-substituted [2.2]paracyclophanylhydrazinecarbothioamides (**135a-f**, 1.00 mmol, 1.00 equiv.) and dimethyl acetylenedicarboxylate (DMAD) (**189a**, 0.142 g, 1.00 mmol, 1.00 equiv.) in absolute methanol (40 mL) was refluxed for 3–4 h (the reaction was monitored by thin-layer chromatography). After removal of the solvent under reduced pressure, the crude product was purified by column chromatography to afford **139b**–**f** and **190**.

(*rac*)-Methyl-((*E*'-2-(2-(4'-[2.2]paracyclophanyl)hydrazinylidene)-4-oxo-3-phenyl-thiazolidin-5-ylidene)acetate (139b)

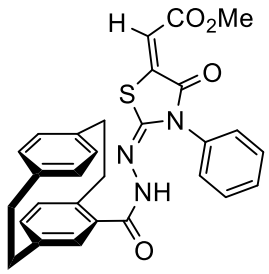

According to **GP6**, 2-(4'-[2.2]paracyclophanyl)-*N*-phenylhydrazine-carbothioamide (**135a**, 0.401 g, 1.00 mmol, 1.00 equiv.) was refluxed with DMAD (**189a**, 0.142 g, 1.00 mmol, 1.00 equiv.) in MeOH (40 mL) for 4 h. The crude product was purified *via* column chromatography (cyclohexane/ethyl acetate; 4:1) and the title compound was obtained as a yellow solid (0.400 g, 7^%, 782 µmol).

R$_f$ = 0.20 (cyclohexane/ethyl acetate; 4:1). – **Mp**: 202–204 °C. – **^{1}H NMR** (400 MHz, DMSO-d_6) δ = 10.77 (s, 1H, N*H*), 7.57 (d, *J* = 7.5 Hz, 2H, *H*^{Ar}), 7.52–7.41 (m, 2H, *H*^{Ar}), 7.16–7.00 (m, 1H, *H*^{Ar}), 7.05–6.97 (m, 1H, *H*^{Ar}), 6.86 (s, 1H, *H*^{vinyl}), 6.80–6.67 (m, 2H, *H*^{Ar}), 6.65–6.41 (m, 4H, *H*^{Ar}), 3.87 (s, 3H, C*H*$_3$), 3.14–3.09 (m, 3H, *H*^{Pc}), 3.05–2.94 (m, 2H, *H*^{Pc}), 2.93–2.81 (m, 3H, *H*^{Pc}) ppm. – **^{13}C NMR** (101 MHz, DMSO-d_6) δ = 165.8 (C$_q$, *C*O), 165.5 (C$_q$, *C*O), 165.4 (C$_q$, *C*O), 140.9 (C$_q$, *C*=N), 139.6 (C$_q$, *C*=C), 139.5 (C$_q$, *C*^{Ar}), 139.3 (C$_q$, *C*^{Ar}), 139.0 (C$_q$, *C*^{Ar}), 138.9 (C$_q$, *C*^{Ar}), 137.6 (C$_q$, *C*^{Ar}), 135.8 (+, *C*H^{Ar}), 135.6 (+, *C*H^{Ar}), 134.0 (+, *C*H^{Ar}), 132.6 (+, *C*H^{Ar}), 132.4 (+, *C*H^{Ar}), 132.2 (+, *C*H^{Ar}), 132.1 (+, *C*H^{Ar}), 131.2 (+, *C*H^{Ar}), 129.6 (+, *C*H^{Ar}), 129.5 (+, *C*H^{Ar}), 129.0 (+, *C*H^{Ar}), 128.1 (+, *C*H^{Ar}), 125.3 (C$_q$, *C*^{Ar}), 117.5 (+, *C*H^{vinyl}), 52.8 (+, *C*H$_3$), 34.7 (–, *C*H$_2$), 34.5 (–, *C*H$_2$), 34.3 (–, *C*H$_2$), 34.1 (–, *C*H$_2$) ppm. – **IR** (ATR) $\tilde{\nu}$ = 3378 (w), 3063 (vw), 2927 (w), 2846 (w), 1748 (w), 1704 (vs), 1649 (vs), 1587 (m), 1465 (s), 1397 (m), 1279 (vs), 1181 (vs), 1135 (m), 1045 (m), 1007 (w), 857 (w), 836 (w), 772 (m), 754 (w), 715 (w), 698 (m), 636 (w), 586 (w), 552 (w), 510 (m) cm^{-1}. – **MS** (FAB, 3-NBA): *m/z*

(%) = 512 (15) $[M+H]^+$, 511 (10) $[M]^+$. – **HRMS** (FAB, 3-NBA, $C_{29}H_{26}O_4N_3{}^{32}S_1$, $[M+H]^+$) calc.: 512.1644, found: 512.1645.

(*rac*)-Methyl-(*E*)-2-((*E*)-'-allyl-2-(2-(4'-[2.2]paracyclophanyl)hydrazinylidene)-4-oxo-thiazolidin-5-ylidene)acetate (139c)

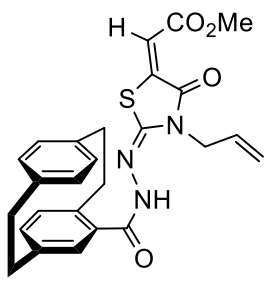

According to **GP6**, *N*-allyl-2-(4'-[2.2]paracyclophanyl)hydrazine-1-carbothioamide (**135c**, 0.365 g, 1.00 mmol, 1.00 equiv.) was refluxed with DMAD (**189a**, 0.142 g, 1.00 mmol, 1.00 equiv.) in MeOH (40 mL) for 3 h. The crude product was purified *via* column chromatography (cyclohexane/ethyl acetate; 4:1) and the title compound was obtained as a yellow solid (0.370 g, 79%, 778 µmol).

R_f = 0.17 (cyclohexane/ethyl acetate; 4:1). – **Mp**: 241–243 °C. – **^{1}H NMR** (400 MHz, Acetone-d_6) δ = 9.78 (s, 1H, N*H*), 7.08–6.88 (m, 2H, H^{Ar}), 6.82 (s, 1H, H^{vinyl}), 6.79–6.68 (m, 2H, H^{Ar}), 6.63–6.57 (m, 2H, H^{Ar}), 6.50 (d, J = 8.1 Hz, 1H, H^{Ar}), 6.03–5.94 (m, 1H, CH^{Allyl}), 5.38–5.13 (m, 2H, CH_2^{Allyl}), 4.55–4.43 (m, 2H, CH_2^{Allyl}), 4.28–4.15 (m, 1H, H^{Pc}), 3.87 (s, 3H, CH_3), 3.26–3.10 (m, 3H, H^{Pc}), 3.09–2.99 (m, 3H, H^{Pc}), 2.96–2.87 (m, 1H, H^{Pc}) ppm. – **^{13}C NMR** (101 MHz, Acetone-d_6) δ = 166.5 (C_q, *C*O), 166.2 (C_q, *C*O), 162.0 (C_q, *C*O), 141.6 (C_q, *C*=N), 140.6 (C_q, *C*=C), 140.2 (C_q, C^{Ar}), 139.8 (C_q, C^{Ar}), 139.1 (C_q, C^{Ar}), 136.6 (C_q, C^{Ar}), 136.4 (+, *C*H^{Ar}), 135.9 (+, *C*H^{Ar}), 133.3 (+, *C*H^{Ar}), 133.2 (+, *C*H^{Ar}), 133.1 (+, *C*H^{Ar}), 133.0 (+, *C*H^{Ar}), 132.8 (+, *C*H^{Ar}), 132.2 (+, *C*H^{Allyl}), 131.3 (C_q, C^{Ar}), 118.0 (–, *C*H_2^{Allyl}), 116.7 (+, *C*H^{vinyl}), 54.2 (+, *C*H$_3$), 52.5 (–, *C*H_2^{Allyl}), 35.6 (–, *C*H$_2$), 35.3 (–, *C*H$_2$), 35.2 (–, *C*H$_2$), 35.1 (–, *C*H$_2$) ppm. – **IR** (ATR) $\tilde{\nu}$ = 3421 (vw), 3303 (w), 3063 (w), 2945 (w), 2925 (w), 2851 (w), 1697 (s), 1655 (s), 1602 (vs), 1538 (m), 1432 (m), 1381 (s), 1320 (vs), 1193 (vs), 1135 (s), 1016 (m), 990 (w), 932 (w), 904 (w), 860 (w), 836 (w), 759 (w), 718 (m), 633 (w), 511 (m) cm^{-1}. – **MS** (FAB, 3-NBA): *m/z* (%) = 476 (55) $[M+H]^+$, 475 (20) $[M]^+$. – **HRMS** (FAB, 3-NBA, $C_{26}H_{26}N_3O_4{}^{32}S_1$, $[M+H]^+$) calc.: 476.1644, found: 476.1646.

(*rac*)-Methyl-(*E*)-2-((*E*)-2-(2-(4'-[2.2]paracyclophanyl)hydrazinylidene)-3-ethyl-4-oxo-thiazolidin-5-ylidene)acetate (139d)

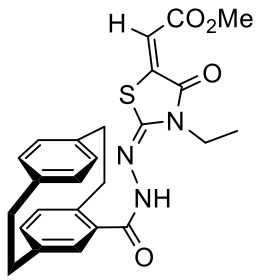

According to **GP6**, 2-(4'-[2.2]paracyclophanyl)-*N*-ethylhydrazine-1-carbothioamide (**135d**, 0.353 g, 1.00 mmol, 1.00 equiv.) was refluxed with DMAD (**189a**, 0.142 g, 1.00 mmol, 1.00 equiv.) in MeOH (40 mL) for 3 h. The crude product was purified *via* column chromatography (cyclohexane/ethyl acetate; 4:1) and the title compound was obtained as a yellow solid (0.320 g, 69%, 690 μmol).

R_f = 0.14 (cyclohexane/ethyl acetate; 4:1). – **Mp**: 220–222 °C. – **^{1}H NMR** (400 MHz, DMSO-d_6) δ = 10.83 (s, 1H, N*H*), 6.80 (s, 1H, H^{vinyl}), 6.67 (d, J = 7.8 Hz, 3H, H^{Ar}), 6.57 (s, 2H, H^{Ar}), 6.45 (d, J = 7.8 Hz, 2H, H^{Ar}), 3.95–2.89 (m, 2H, CH_2^{ethyl}), 3.78 (s, 3H, CH_3), 3.67–3.59 (m, 1H, H^{Pc}), 3.16–3.05 (m, 4H, H^{Pc}), 3.02–2.96 (m, 2H, H^{Pc}), 2.94–2.87 (m, 1H, H^{Pc}), 1.26 (t, J = 7.1 Hz, 3H, CH_3^{ethyl}) ppm. – **^{13}C NMR** (101 MHz, DMSO-d_6) δ = 165.9 (C_q, *C*O), 164.8 (C_q, *C*O), 163.4 (C_q, *C*O), 155.0 (C_q, *C*=N), 141.0 (C_q, *C*=C), 139.6 (C_q, C^{Ar}), 139.5 (C_q, C^{Ar}), 139.2 (C_q, C^{Ar}), 139.1 (C_q, C^{Ar}), 135.8 (+, 2 × *C*H^{Ar}), 135.2 (C_q, C^{Ar}), 132.6 (+, 2 × *C*H^{Ar}), 132.4 (+, *C*H^{Ar}), 132.3 (+, *C*H^{Ar}), 131.4 (+, *C*H^{Ar}), 114.9 (+, *C*H^{vinyl}), 52.7 (+, *C*H$_3$), 38.1 (–, *C*H$_2^{ethyl}$), 34.9 (–, *C*H$_2$), 34.7 (–, *C*H$_2$), 34.5 (–, *C*H$_2$), 34.4 (–, *C*H$_2$), 12.5 (+, *C*H$_3^{ethyl}$) ppm. – **IR** (ATR) $\tilde{\nu}$ = 3163 (vw), 3030 (vw), 2929 (w), 2815 (w), 2628 (vw), 1694 (s), 1649 (m), 1606 (vs), 1545 (s), 1432 (m), 1391 (s), 1320 (vs), 1289 (s), 1242 (s), 1197 (vs), 1183 (vs), 1133 (s), 1109 (m), 1055 (m), 921 (w), 866 (w), 837 (m), 762 (m), 718 (m), 707 (w), 637 (m), 514 (m) cm^{-1}. – **MS** (FAB, 3-NBA): *m/z* (%) = 464 (100) [M+H]$^+$, 463 (30) [M]$^+$. – **HRMS** (FAB, 3-NBA, $C_{25}H_{26}N_3O_4{}^{32}S_1$, [M+H]$^+$) calc.: 464.1644, found: 464.1643.

(*rac*)-Methyl-(*E*)-2-((E)-2-(2-(4'-[2.2]paracyclophanyl)hydrazinylidene)-3-cyclopropyl-4-oxothiazolidin-5-ylidene)acetate (139e)

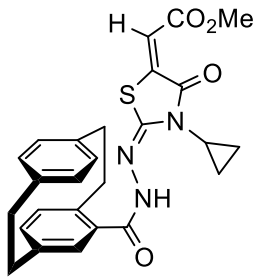

According to **GP6**, 2-(4'-[2.2]paracyclophanyl)-*N*-cyclopropyl-hydrazine-1-carbothioamide (**135e**, 0.365 g, 1.00 mmol, 1.00 equiv.) was refluxed with DMAD (**189a**, 0.142 g, 1.00 mmol, 1.00 equiv.) in MeOH (40 mL) for 3 h. The crude product was purified *via* column chromatography (cyclohexane/ethyl acetate; 4:1) and the title compound was obtained as a yellow solid (0.320 g, 67%, 673 µmol).

R*f* = 0.55 (cyclohexane/ethyl acetate; 1:1). – **Mp**: 180–182 °C. – **^{1}H NMR** (400 MHz, DMSO-d_6) δ = 10.80 (s, 1H, N*H*), 6.85 (s, 1H, H^{vinyl}), 6.75 (s, 1H, H^{Ar}), 6.70–6.65 (m, 2H, H^{Ar}), 6.63–6.52 (m, 3H, H^{Ar}), 6.46 (d, J = 7.8 Hz, 1H, H^{Ar}), 3.76 (s, 3H, CH_3), 3.74–3.34 (m, 1H, H^{Pc}), 3.22–3.05 (m, 3H, H^{Pc}), 3.03–2.96 (m, 2H, H^{Pc}), 2.98–2.84 (m, 2H, H^{Pc}), 1.08–1.04 (m, 1H, C$H^{Cyclo.}$), 1.03–0.98 (m, 4H, 2 × C$H_2^{Cyclo.}$) ppm. – **^{13}C NMR** (101 MHz, DMSO-d_6) δ = 165.9 (C_q, *C*O), 164.9 (C_q, *C*O), 164.1 (C_q, *C*O), 157.3 (C_q, *C*=N), 141.3 (C_q, *C*=C), 139.6 (C_q, C^{Ar}), 139.2 (C_q, C^{Ar}), 139.1 (C_q, C^{Ar}), 135.8 (C_q, C^{Ar}), 135.1 (+, *C*H^{Ar}), 133.0 (+, *C*H^{Ar}), 132.6 (+, 2 × *C*H^{Ar}), 132.4 (+, 2 × *C*H^{Ar}), 132.3(C_q, C^{Ar}), 131.4 (+, *C*H^{Ar}), 114.5 (+, *C*H^{vinyl}), 52.6 (+, *C*H$_3$), 34.9 (–, *C*H$_2$), 34.7 (–, *C*H$_2$), 34.5 (–, *C*H$_2$), 34.4 (–, *C*H$_2$), 25.7 (+, *C*H$^{Cyclo.}$), 6.7 (–, 2 × *C*H$_2^{Cyclo.}$) ppm. – **IR** (ATR) $\tilde{\nu}$ = 3315 (vw), 3187 (vw), 3013 (w), 2927 (m), 2851 (w), 1714 (s), 1697 (s), 1653 (s), 1606 (vs), 1545 (s), 1436 (m), 1383 (vs), 1322 (vs), 1254 (vs), 1200 (vs), 1180 (vs), 1014 (w), 840 (m), 758 (m), 717 (s), 626 (m), 511 (m) cm^{-1}. – **MS** (FAB, 3-NBA): *m/z* (%) = 476 (100) $[M+H]^+$, 475 (15) $[M]^+$. – **HRMS** (FAB, 3-NBA, $C_{26}H_{26}N_3O_4{}^{32}S_1$, $[M+H]^+$) calc.: 476.1644, found: 476.1643.

(*rac*)-Methyl-(*E*)-2-((*E*)-2-(2-(4'-[2.2]paracyclophanyl)hydrazinylidene)-3-benzyl-4-oxo-thiazolidin-5-ylidene)acetate (**139f**)

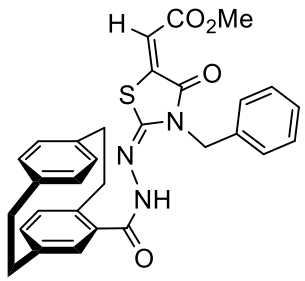

According to **GP6**, 2-(4'-[2.2]paracyclophanyl)-*N*-benzylhydrazine-1-carbothioamide (**135f**, 0.415 g, 1.00 mmol, 1.00 equiv.) was refluxed with DMAD (**189a**, 0.142 g, 1.00 mmol, 1.00 equiv.) in MeOH (40 mL) for 3 h. The crude product was purified *via* column chromatography (cyclohexane/ethyl acetate; 4:1) and the title compound was obtained as a yellow solid (0.400 g, 76%, 761 µmol).

R$_f$ = 0.20 (cyclohexane/ethyl acetate; 4:1). – **Mp**: 175–177 °C. – **^{1}H NMR** (400 MHz, DMSO-d_6) δ = 10.88 (s, 1H, N*H*), 7.43–7.31 (m, 3H, H^{Ar}), 7.28–7.23 (m, 1H, H^{Ar}), 6.99 (d, J = 4.8 Hz, 1H, H^{Ar}), 6.93 (s, 1H, H^{vinyl}), 6.88–6.82 (m, 1H, H^{Ar}), 6.71–6.55 (m, 2H, H^{Ar}), 6.45 (d, J = 10.3 Hz, 2H, H^{Ar}), 6.28 (d, J = 2.5 Hz, 2H, H^{Ar}), 5.44 (s, 2H, CH_2), 3.83 (s, 3H, CH_3), 3.68–3.62 (m, 2H, H^{Pc}), 3.18–3.05 (m, 2H, H^{Pc}), 3.02–2.82 (m, 4H, H^{Pc}) ppm. – **^{13}C NMR** (101 MHz, DMSO-d_6) δ = 166.0 (C_q, *C*O), 165.6 (C_q, *C*O), 161.5 (C_q, *C*O), 146.2 (C_q, *C*=N), 140.2 (C_q, *C*=C), 139.6 (C_q, C^{Ar}), 139.3 (C_q, C^{Ar}), 139.2 (C_q, C^{Ar}), 139.1 (C_q, C^{Ar}), 139.0 (C_q, C^{Ar}), 138.9 (+, *C*H^{Ar}), 138.6 (+, *C*H^{Ar}), 138.4 (+, *C*H^{Ar}), 137.8 (+, *C*H^{Ar}), 136.0 (+, *C*H^{Ar}), 135.9 (+, *C*H^{Ar}), 135.8 (+, *C*H^{Ar}), 132.5 (+, *C*H^{Ar}), 132.3 (+, *C*H^{Ar}), 132.2 (+, *C*H^{Ar}), 131.4 (+, *C*H^{Ar}), 128.5 (+, *C*H^{Ar}), 127.3 (C_q, C^{Ar}), 116.6 (+, *C*H^{vinyl}), 52.6 (+, *C*H$_3$), 51.3 (–, *C*H$_2$), 34.8 (–, *C*H$_2$), 34.6 (–, *C*H$_2$), 34.5 (–, *C*H$_2$), 34.4 (–, *C*H$_2$) ppm. – **IR** (ATR) $\tilde{\nu}$ = 3391 (w), 3288 (w), 3063 (vw), 2927 (w), 2849 (w), 1749 (s), 1718 (m), 1696 (s), 1660 (vs), 1626 (s), 1595 (vs), 1492 (w), 1435 (vs), 1411 (w), 1394 (m), 1371 (w), 1356 (m), 1322 (s), 1259 (s), 1234 (s), 1207 (vs), 1186 (vs), 1173 (vs), 1145 (vs), 1064 (w), 1018 (m), 996 (w), 874 (w), 841 (m), 824 (w), 756 (m), 731 (s), 720 (s), 697 (s), 635 (m), 513 (m), 439 (m) cm^{-1}. – **MS** (FAB, 3-NBA): *m/z* (%) = 526 (60) $[M+H]^+$, 525 (35) $[M]^+$. – **HRMS** (FAB, 3-NBA, $C_{30}H_{28}N_3O_4{}^{32}S_1$, $[M+H]^+$) calc.: 526.1801, found: 526.1799.

(*rac*)-Methyl-(*E*)-2-((*E*)-3-[2.2]paracyclophanyl)amido-4-oxo-2-(pyridin-3-ylimino)-thiazolidin-5-ylidene)acetate (**190**)

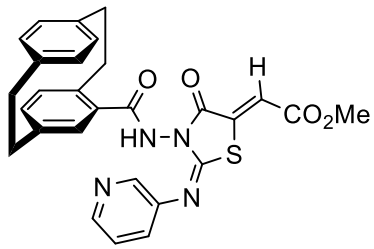

According to **GP6**, 2-(4'-[2.2]paracyclophanyl)-*N*-(pyridin-3-yl)hydrazine-1-carbothioamide (**135a**, 0.402 g, 1.00 mmol, 1.00 equiv.) was refluxed with DMAD (**189a**, 0.142 g, 1.00 mmol, 1.00 equiv.) in MeOH (40 mL) for 4 h. The crude product was purified *via* column chromatography (cyclohexane/ethyl acetate; 1:1) and the title compound was obtained as a yellow solid (0.340 g, 65%, 663 μmol).

R*f* = 0.17 (cyclohexane/ethyl acetate; 1:1). – **Mp**: 262–264 °C. – **^{1}H NMR** (400 MHz, Acetone-d_6) δ = 10.12 (s, 1H, N*H*), 8.43–8.28 (m, 2H, H^{Ar}), 7.48–7.44 (m, 2H, H^{Ar}), 7.05–6.98 (m, 2H, H^{Ar}), 6.86–6.74 (m, 2H, H^{Ar}), 6.65–6.62 (m, 1H, H^{Ar}), 6.57 (s, 1H, H^{vinyl}), 6.54–6.43 (m, 2H, H^{Ar}), 4.00–3.90 (m, 1H, H^{Pc}), 3.82 (s, 3H, CH_3), 3.20–2.91 (m, 7H, H^{Pc}) ppm. – **^{13}C NMR** (101 MHz, Acetone-d_6) δ = 167.0 (C_q, *C*O), 166.6 (C_q, *C*O), 162.5 (C_q, *C*O), 151.3 (C_q, *C*=N), 147.5 (+, *C*H^{Ar}), 144.3 (+, *C*H^{Ar}), 143.1 (C_q, C^{Ar}), 141.1 (C_q, *C*=C), 140.7 (C_q, C^{Ar}), 140.2 (C_q, C^{Ar}), 138.9 (C_q, C^{Ar}), 137.1 (C_q, C^{Ar}), 137.0 (+, 3 × *C*H^{Ar}), 133.7 (+, 2 × *C*H^{Ar}), 133.4 (+, *C*H^{Ar}), 133.2 (+, *C*H^{Ar}), 132.6 (C_q, C^{Ar}), 128.8 (+, *C*H^{Ar}), 125.0 (+, *C*H^{Ar}), 118.6 (+, *C*H^{vinyl}), 53.3 (+, *C*H$_3$), 35.8 (–, *C*H$_2$), 35.7 (–, *C*H$_2$), 35.6 (–, *C*H$_2$), 35.5 (–, *C*H$_2$) ppm. – **IR** (ATR) $\tilde{\nu}$ = 3193 (w), 3072 (w), 2924 (m), 2851 (w), 1724 (s), 1693 (vs), 1602 (vs), 1480 (m), 1428 (vs), 1374 (vs), 1323 (vs), 1241 (vs), 1201 (vs), 1177 (vs), 1013 (w), 904 (w), 861 (w), 756 (m), 718 (m), 703 (vs), 625 (m), 511 (m) cm^{-1}. – **MS** (FAB, 3-NBA): *m/z* (%) = 513 (100) [M+H]$^+$, 512 (15) [M]$^+$. – **HRMS** (FAB, 3-NBA, $C_{28}H_{25}O_4N_4{}^{32}S_1$, [M+H]$^+$) calc.: 513.1597, found: 513.1597.

5.2.4.2. [2.2]Paracyclophanyl-dihydronaphtho[2,3-*d*]thiazoles and -Thiazoleium bromides

General Procedures (GP7)

2,3-Dichloro-1,4-naphthoquinone (DCNQ) (**191**, 0.227 g, 1.00 mmol, 1.00 equiv.) was added to a stirred solution of *N*-substituted [2.2]paracyclophanylhydrazinecarbothioamides (**135b-f**, 1.00 mmol, 1.00 equiv.) in anhydrous CH_3CN (25 mL). The resulting solution was stirred at room temperature for 16 h. After *S*-alkylation was completed, the solvent was removed under reduced pressure and the dried salt was dissolved in anhydrous CH_3CN, after which Et_3N (1.10 mmol, 1.10 equiv.) and triphenylphosphine (1.10 mmol, 1.10 equiv.) were added. The resulting mixture was left under reflux for 8-10 h. The reaction mixture was then left to cool to room temperature, where after H_2O (50 mL) was added. The resulting solution was extracted with CH_2Cl_2 (3 × 50 mL). The organic extracts were dried over anhydrous $CaCl_2$, filtered, and the solvent was removed under reduced pressure. The crude was purified by Column chromatography using cyclohexane/ethyl acetate as eluent to afford **140b–f**.

***(rac)-(Z)-N*-(4,9-Dioxo-2-(phenylimino)-4,9-dihydronaphtho[2,3-*d*]thiazol-3(2*H*)-yl)-4'-[2.2]paracyclophanylamide (140b)**

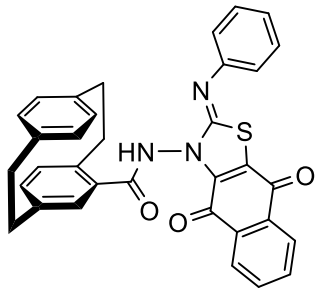

According to **GP7**, 2-(4'-[2.2]paracyclophanyl)-*N*-phenyl-hydrazinecarbothioamide (**135a**, 0.401 g, 1.00 mmol, 1.00 equiv.) was reacted with DCNQ (**191**, 0.227 g, 1.00 mmol, 1.00 equiv.) in CH_3CN for 10 h. The crude product was purified *via* column chromatography (cyclohexane/ethyl acetate; 4:1) and the title compound was obtained as a red solid (0.390 g, 70%, 702 μmol).

$\mathbf{R_f}$ = 0.36 (cyclohexane/ethyl acetate; 4:1). – **^{1}H NMR** (400 MHz, Acetone-d_6) δ = 10.41 (s, 1H, N*H*), 8.20–8.09 (m, 2H, H^{Ar}), 7.92–7.87 (m, 2H, H^{Ar}), 7.48–7.42 (m, 1H, H^{Ar}), 7.23–7.05 (m, 4H, H^{Ar}), 6.85–6.77 (m, 2H, H^{Ar}), 6.70–6.56 (m, 5H, H^{Ar}), 3.87–3.79 (m, 1H, H^{Pc}), 3.27–3.20 (m, 1H, H^{Pc}), 3.14–3.05 (m, 3H, H^{Pc}), 2.98–2.85 (m, 3H, H^{Pc}) ppm. – **^{13}C NMR** (101 MHz, Acetone-d_6) δ = 177.4 (C_q, *C*O), 174.2 (C_q, *C*O), 167.9 (C_q, *C*O), 154.3 (C_q, *C*=N), 150.5 (C_q, C^{Ar}), 142.1 (C_q, C^{Ar}), 141.8 (C_q, C^{Ar}), 141.1 (C_q, C^{Ar}), 140.9 (C_q, C^{Ar}), 140.7 (C_q, C^{Ar}), 140.2 (C_q, C^{Ar}), 140.1 (C_q, C^{Ar}), 137.2 (+, *C*H^{Ar}), 136.9 (+, *C*H^{Ar}), 135.2 (+, *C*H^{Ar}), 134.9 (+, *C*H^{Ar}), 133.9 (+, *C*H^{Ar}), 133.7 (C_q, C^{Ar}), 133.6 (+, *C*H^{Ar}), 133.3 (+, *C*H^{Ar}), 133.1 (+, *C*H^{Ar}), 132.9 (+, *C*H^{Ar}), 132.8 (+, *C*H^{Ar}), 132.7 (+, *C*H^{Ar}), 130.7 (+, *C*H^{Ar}), 127.7 (+, *C*H^{Ar}), 126.7 (+, *C*H^{Ar}), 125.4 (+, *C*H^{Ar}), 121.5 (+, *C*H^{Ar}), 108.3 (C_q, C^{Ar}), 35.8 (–, *C*H$_2$), 35.6 (–, *C*H$_2$),

35.5 (–, *C*H_2), 35.3 (–, *C*H_2) ppm. – **IR** (ATR) $\tilde{\nu}$ = 3404 (vw), 3244 (w), 3099 (vw), 2922 (s), 2851 (m), 1734 (w), 1669 (vs), 1632 (vs), 1587 (vs), 1562 (vs), 1486 (s), 1327 (s), 1262 (vs), 1196 (vs), 1153 (vs), 1062 (vs), 904 (s), 854 (vs), 765 (vs), 703 (vs), 697 (vs), 683 (vs), 588 (s), 510 (vs), 455 (vs) cm^{-1}. – **MS** (FAB, 3-NBA): *m/z* (%) = 556 (35) $[M+H]^+$, 555 (10) $[M]^+$. – **HRMS** (FAB, 3-NBA, $C_{34}H_{26}O_3N_3{}^{32}S_1$, $[M+H]^+$) calc.: 556.1695, found: 556.1694.

(*rac*)-(*Z*)-*N*-(2-(Allylimino)-4,9-dioxo-4,9-dihydronaphtho[2,3-*d*]thiazol-3(2*H*)-yl)4'-[2.2]paracyclophanylamide (140c)

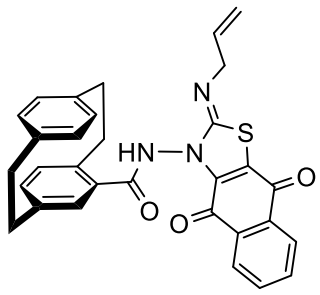

According to **GP7**, *N*-allyl-2-(4'-[2.2]paracyclophanyl)hydrazine-1-carbothioamide (**135c**, 0.365 g, 1.00 mmol, 1.00 equiv.) was reacted with DCNQ (**191**, 0.227 g, 1.00 mmol, 1.00 equiv.) in CH_3CN for 8 h. The crude product was purified *via* column chromatography (cyclohexane/ethyl acetate; 4:1) and the title compound was obtained as a red solid (0.350 g, 67%, 674 μmol).

R_f = 0.28 (cyclohexane/ethyl acetate; 4:1). – **^{1}H NMR** (400 MHz, DMSO-d_6) δ = 11.28 (s, 1H, N*H*), 8.42–7.76 (m, 4H, H^{Ar}), 7.03–6.70 (m, 2H, H^{Ar}), 6.64–6.35 (m, 5H, H^{Ar}), 6.06–5.65 (m, 1H, CH^{Allyl}), 5.43–4.97 (m, 2H, CH_2^{Allyl}), 4.05–3.78 (m, 2H, CH_2^{Allyl}), 3.65–3.54 (m, 1H, H^{Pc}), 3.18–2.73 (m, 7H, H^{Pc}) ppm. – **^{13}C NMR** (101 MHz, DMSO-d_6) δ = 178.6 (C_q, *C*O), 176.0 (C_q, *C*O), 174.6 (C_q, *C*O), 166.6 (C_q, *C*=N), 139.4 (C_q, C^{Ar}), 139.3 (C_q, C^{Ar}), 139.1 (C_q, C^{Ar}), 138.8 (C_q, C^{Ar}), 135.6 (C_q, C^{Ar}), 135.4 (C_q, C^{Ar}), 134.4 (+, *C*H^{Ar}), 134.2 (+, *C*H^{Ar}), 134.0 (+, *C*H^{Ar}), 133.6 (+, *C*H^{Ar}), 132.5 (+, 2 × *C*H^{Ar}), 132.3 (C_q, C^{Ar}), 131.8 (+, *C*H^{Allyl}), 131.3 (C_q, C^{Ar}), 131.2 (+, *C*H^{Ar}), 131.1 (+, *C*H^{Ar}), 126.7 (+, *C*H^{Ar}), 126.5 (+, *C*H^{Ar}), 126.0 (+, *C*H^{Ar}), 116.4 (–, *C*H$_2^{Allyl}$), 115.3 (C_q, C^{Ar}), 45.8 (–, *C*H$_2^{Allyl}$), 34.6 (–, *C*H$_2$), 34.5 (–, *C*H$_2$), 34.4 (–, *C*H$_2$), 34.3 (–, *C*H$_2$) ppm. – **IR** (ATR) $\tilde{\nu}$ = 3461 (vw), 3310 (w), 3123 (vw), 3013 (w), 2922 (w), 2849 (w), 1674 (m), 1650 (s), 1589 (vs), 1564 (s), 1497 (m), 1407 (w), 1255 (vs), 1214 (vs), 1125 (s), 840 (s), 786 (s), 703 (vs), 635 (s), 511 (vs), 431 (m) cm^{-1}. – **MS** (FAB, 3-NBA): *m/z* (%) = 520 (60) [M+H]$^+$, 519 (30) [M]$^+$. – **HRMS** (FAB, 3-NBA, $C_{31}H_{26}O_3N_3{}^{32}S_1$, [M+H]$^+$) calc.: 520.1695, found: 520.1693.

(*rac*)-(*Z*)-*N*-(2-(Ethylimino)-4,9-dioxo-4,9-dihydronaphtho[2,3-*d*]thiazol-3(2*H*)-yl)4'-[2.2]paracyclophanylamide (140d)

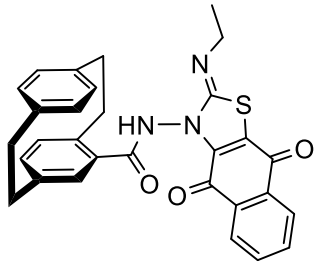

According to **GP7**, 2-(4'-[2.2]paracyclophanyl)-*N*-ethylhydrazine-1-carbothioamide (**135d**, 0.353 g, 1.00 mmol, 1.00 equiv.) was reacted with DCNQ (**191**, 0.227 g, 1.00 mmol, 1.00 equiv.) in CH_3CN for 8 h. The crude product was purified *via* column chromatography (cyclohexane/ethyl acetate; 4:1) and the title compound was obtained as a red solid (0.290 g, 57%, 571 µmol).

R_f = 0.25 (cyclohexane/ethyl acetate; 4:1). – **^{1}H NMR** (400 MHz, Acetone-d_6) δ = 10.17 (s, 1H, N*H*), 8.10–7.84 (m, 4H, H^{Ar}), 7.16–6.85 (m, 1H, H^{Ar}), 6.74–6.54 (m, 4H, H^{Ar}), 6.52–6.39 (m, 2H, H^{Ar}), 3.21–3.16 (m, 2H, H^{Pc}), 3.13–2.97 (m, 6H, H^{Pc}) 1.58–1.16 (m, 2H, CH_2^{ethyl}), 0.99 (t, *J* = 7.2 Hz, 3H, CH_3^{ethyl}) ppm. – **^{13}C NMR** (101 MHz, Acetone-d_6) δ = 179.9 (C_q, *C*O), 177.3 (C_q, *C*O), 175.9 (C_q, *C*O), 141.1 (C_q, *C*=N), 140.9 (C_q, C^{Ar}), 140.8 (C_q, C^{Ar}), 140.2 (C_q, C^{Ar}), 140.1 (C_q, C^{Ar}), 136.6 (+, CH^{Ar}), 135.4 (C_q, 2 × C^{Ar}), 135.0 (+, CH^{Ar}), 134.8 (+, CH^{Ar}), 133.9 (+, CH^{Ar}), 133.8 (+, 2 × CH^{Ar}), 133.2 (C_q, C^{Ar}), 133.1 (+, CH^{Ar}), 132.9 (+, CH^{Ar}), 132.8 (+, CH^{Ar}), 128.0 (C_q, C^{Ar}), 127.6 (+, CH^{Ar}), 127.2 (+, CH^{Ar}), 126.7 (C_q, C^{Ar}), 50.1 (–, CH_2^{ethyl}), 36.0 (–, CH_2), 35.9 (–, CH_2), 35.8 (–, CH_2), 35.7 (–, CH_2), 14.2 (+, CH_3^{ethyl}) ppm. – **IR** (ATR) $\tilde{\nu}$ = 3451 (vw), 3320 (w), 3156 (w), 2929 (w), 2851 (w), 1674 (m), 1647 (vs), 1589 (vs), 1497 (m), 1255 (vs), 1215 (vs), 1122 (s), 844 (m), 790 (m), 703 (vs), 635 (s), 511 (vs) cm^{-1}. – **MS** (FAB, 3-NBA): *m/z* (%) = 508 (50) $[M+H]^+$, 507 (20) $[M]^+$. – **HRMS** (FAB, 3-NBA, $C_{30}H_{26}O_3N_3{}^{32}S_1$, $[M+H]^+$) calc.: 508.1695, found: 508.1693.

(*rac*)-(*Z*)-*N*-(2-(Cyclopropylimino)-4,9-dioxo-4,9-dihydronaphtho[2,3-*d*]thiazol-3(2*H*)-yl)-4'-[2.2]paracyclophanylamide (140e)

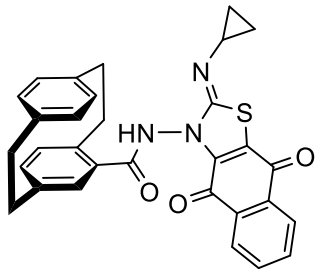

According to **GP7**, 2-(4'-[2.2]paracyclophanyl)-*N*-cyclopropyl-hydrazine-1-carbothioamide (**135e**, 0.365 g, 1.00 mmol, 1.00 equiv.) was reacted with DCNQ (**191**, 0.227 g, 1.00 mmol, 1.00 equiv.) in CH_3CN for 8 h. The crude product was purified *via* column chromatography (cyclohexane/ethyl acetate; 4:1) and the title compound was obtained as a red solid (0.285 g, 55%, 548 μmol).

R_f = 0.27 (cyclohexane/ethyl acetate; 4:1). – **^{1}H NMR** (400 MHz, $CDCl_3$-*d*) δ = 10.12 (s, 1H, N*H*), 8.13–8.05 (m, 2H, H^{Ar}), 7.76–7.69 (m, 2H, H^{Ar}), 7.12–6.91 (m, 1H, H^{Ar}), 6.76–6.43 (m, 6H, H^{Ar}), 3.83–3.68 (m, 1H, H^{Pc}), 3.21–3.09 (m, 2H, H^{Pc}), 3.08–2.80 (m, 5H, H^{Pc}) 2.58–2.42 (m, 1H, C$H^{Cyclo.}$), 1.74–0.47 (m, 4H, 2 × C$H_2^{Cyclo.}$) ppm. – **^{13}C NMR** (101 MHz, $CDCl_3$-*d*) δ = 179.5 (C_q, *C*O), 176.8 (C_q, *C*O), 173.6 (C_q, *C*O), 167.8 (C_q, *C*=N), 141.1 (C_q, C^{Ar}), 140.3 (C_q, C^{Ar}), 139.3 (C_q, C^{Ar}), 136.4 (C_q, C^{Ar}), 135.8 (C_q, C^{Ar}), 134.9 (C_q, C^{Ar}), 134.4 (+, *C*H^{Ar}), 134.2 (C_q, C^{Ar}), 133.9 (+, *C*H^{Ar}), 133.8 (+, *C*H^{Ar}), 133.2 (+, *C*H^{Ar}), 132.7 (+, *C*H^{Ar}), 132.3 (C_q, C^{Ar}), 132.0 (+, *C*H^{Ar}), 131.6 (+, *C*H^{Ar}), 127.7 (+, *C*H^{Ar}), 127.3 (+, *C*H^{Ar}), 127.1 (+, *C*H^{Ar}), 126.6 (+, *C*H^{Ar}), 126.3 (C_q, C^{Ar}), 35.6 (–, *C*H_2), 35.4 (–, *C*H_2), 35.2 (–, *C*H_2), 34.9 (–, *C*H_2), 26.0 (+, *C*H$^{Cyclo.}$), 7.9 (–, *C*$H_2^{Cyclo.}$), 7.5 (–, *C*$H_2^{Cyclo.}$) ppm. – **IR** (ATR) $\tilde{\nu}$ = 3458 (w), 3293 (w), 3116 (w), 3006 (w), 2919 (w), 2846 (w), 1664 (s), 1646 (vs), 1587 (vs), 1561 (vs), 1327 (s), 1259 (vs), 1218 (vs), 1156 (s), 1021 (m), 846 (s), 788 (s), 703 (vs), 636 (vs), 510 (vs) cm^{-1}. – **MS** (FAB, 3-NBA): *m/z* (%) = 520 (60) $[M+H]^+$, 519 (15) $[M]^+$. – **HRMS** (FAB, 3-NBA, $C_{31}H_{26}O_3N_3{}^{32}S_1$, $[M+H]^+$) calc.: 520.1695, found: 520.1693.

(*rac*)-(*Z*)-*N*-(2-(Benzylimino)-4,9-dioxo-4,9-dihydronaphtho[2,3-*d*]thiazol-3(2*H*)-yl)-4'-[2.2]paracyclophanylamide (140f)

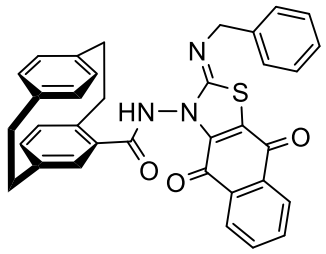

According to **GP7**, 2-(4'-[2.2]paracyclophanyl)-*N*-benzyl-hydrazine-1-carbothioamide (**135f**, 0.415 g, 1.00 mmol, 1.00 equiv.) was reacted with DCNQ (**191**, 0.227 g, 1.00 mmol, 1.00 equiv.) in CH_3CN for 10 h. The crude product was purified *via* column chromatography (cyclohexane/ethyl acetate; 4:1) and the title compound was obtained as a red solid (0.370 g, 65%,649 µmol).

R_f = 0.30 (cyclohexane/ethyl acetate; 4:1). – **^{1}H NMR** (400 MHz, DMSO-*d*$_6$) δ = 11.26 (s, 1H, N*H*), 8.10–8.01 (m, 2H, H^{Ar}), 7.90–7.84 (m, 2H, H^{Ar}), 748–7.02 (m, 5H, H^{Ar}), 6.78–6.37 (m, 7H, H^{Ar}), 4.12 (s, 2H, CH_2), 3.19–3.03 (m, 3H, H^{Pc}), 3.02–2.82 (m, 5H, H^{Pc}) ppm. – **^{13}C NMR** (101 MHz, DMSO-*d*$_6$) δ = 178.8 (C_q, *C*O), 176.2 (C_q, *C*O), 174.7 (C_q, *C*O), 173.0 (C_q, *C*=N), 140.5 (C_q, C^{Ar}), 139.5 (C_q, C^{Ar}), 139.0 (C_q, C^{Ar}), 138.9 (C_q, C^{Ar}), 138.2 (C_q, C^{Ar}), 135.7 (C_q, C^{Ar}), 135.6 (C_q, C^{Ar}), 134.6 (C_q, C^{Ar}), 134.5 (+, CH^{Ar}), 134.2 (+, CH^{Ar}), 132.7 (+, CH^{Ar}), 132.5 (+, CH^{Ar}), 132.4 (C_q, C^{Ar}), 132.0 (+, CH^{Ar}), 131.6 (+, CH^{Ar}), 131.5 (+, CH^{Ar}), 131.4 (+, CH^{Ar}), 131.3 (+, CH^{Ar}), 128.2 (+, CH^{Ar}), 128.1 (+, CH^{Ar}), 127.8 (+, CH^{Ar}), 127.3 (+, CH^{Ar}), 127.2 (+, CH^{Ar}), 127.0 (+, CH^{Ar}), 126.6 (+, CH^{Ar}), 126.1 (C_q, C^{Ar}), 57.3 (–, CH_2), 34.8 (–, CH_2), 34.6 (–, CH_2), 34.5 (–, CH_2), 34.4 (–, CH_2) ppm. – **IR** (ATR) $\tilde{\nu}$ = 3303 (w), 3063 (w), 2922 (w), 2856 (w), 1674 (s), 1659 (s), 1589 (vs), 1575 (s), 1507 (m), 1354 (s), 1310 (s), 1264 (vs), 1214 (vs), 1132 (s), 840 (s), 742 (s), 698 (vs), 640 (vs), 596 (m), 511 (vs) cm^{-1}. – **MS** (FAB, 3-NBA): *m/z* (%) = 570 (65) $[M+H]^+$, 569 (25) $[M]^+$. – **HRMS** (FAB, 3-NBA, $C_{35}H_{28}O_3N_3{}^{32}S_1$, $[M+H]^+$) calc.: 570.1851, found: 570.1854.

General Procedures (GP8)

A solution of *N*-substituted [2.2]paracyclophanylhydrazinecarbothioamides (**135b-f**, 1.00 mmol, 1.00 equiv.) dissolved in ethyl acetate (50 mL), was added to a solution of 2-bromo-1-(naphthalene-1-yl)ethanone (BNE) (**195**, 0.249 g, 1.00 mmol, 1.00 equiv.) dissolved in ethyl acetate (20 mL). The resulting solution was stirred at room temperature for about 24-48 h (the reaction was monitored by thin-layer chromatography). The formed precipitate was filtered and washed with EtOAc several times (3 x 20 mL) to afford compounds **141b-d,f,** and **196**.

(*rac*)-2-(2-(4'-[2.2]Paracyclophonyl)hydrazinyl)-4-(naphthalen-2-yl)-3-phenylthiazol-3-ium bromide (141b)

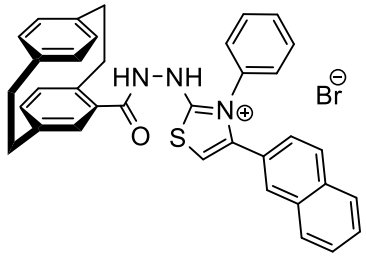

According to **GP8**, 2-(4'-[2.2]Paracyclophanyl)-*N*-phenyl-hydrazinecarbothioamide (**135a**, 0.401 g, 1.00 mmol, 1.00 equiv.) was reacted with BNE (**195**, 0.249 g, 1.00 mmol, 1.00 equiv.) in EtOAc for 24 h. A precipitate of the title compound was obtained as a white solid (0.500 g, 79%, 790 µmol).

R$_f$ = 0.47 (cyclohexane/ethyl acetate; 4:1). – **^{1}H NMR** (400 MHz, DMSO-*d*$_6$) δ = 12.05 (s, 1H, N*H*), 8.55 (s, 1H, *H*^{Ar}), 8.27–8.12 (m, 3H, *H*^{Ar}), 7.91–7.85 (m, 1H, *H*^{Ar}), 7.76–7.69 (m, 2H, *H*^{Ar}), 7.64–7.53 (m, 5H, *H*^{Ar}), 7.52 (s, 1H, *H*^{Ar}), 7.45 (s, 1H, N*H*), 6.64–6.57 (m, 1H, *H*^{Ar}), 6.51–6.27 (m, 6H, *H*^{Ar}), 3.53–3.42 (m, 1H, *H*^{Pc}), 3.24–2.86 (m, 3H, *H*^{Pc}), 2.82–2.61 (m, 4H, *H*^{Pc}) ppm. – **^{13}C NMR** (101 MHz, DMSO-*d*$_6$) δ = 165.6 (C$_q$, *C*O), 142.0 (C$_q$, *C*^{Ar}), 141.4 (C$_q$, *C*^{Ar}), 139.3 (C$_q$, *C*^{Ar}), 139.0 (C$_q$, *C*^{Ar}), 138.4 (C$_q$, *C*^{Ar}), 138.3 (C$_q$, *C*^{Ar}), 138.2 (C$_q$, *C*^{Ar}), 136.5 (C$_q$, *C*^{Ar}), 135.8 (C$_q$, *C*^{Ar}), 133.6 (+, *C*H^{Ar}), 132.7 (+, *C*H^{Ar}), 132.4 (+, *C*H^{Ar}), 132.3 (C$_q$, *C*^{Ar}), 132.2 (+, *C*H^{Ar}), 131.5 (+, *C*H^{Ar}), 131.3 (+, *C*H^{Ar}), 130.4 (+, 2 × *C*H^{Ar}), 130.3 (+, *C*H^{Ar}), 129.9 (+, *C*H^{Ar}), 129.4 (C$_q$, *C*^{Ar}), 128.6 (+, *C*H^{Ar}), 128.5 (+, *C*H^{Ar}), 129.6 (+, *C*H^{Ar}), 128.9 (+, *C*H^{Ar}), 128.3 (+, *C*H^{Ar}), 127.9 (+, *C*H^{Ar}), 127.3 (+, *C*H^{Ar}), 126.4 (+, *C*H^{Ar}), 124.5 (+, *C*H^{Ar}), 123.5 (+, *C*H^{Ar}), 34.4 (–, *C*H$_2$), 34.2 (–, *C*H$_2$), 34.1 (–, *C*H$_2$), 34.0 (–, *C*H$_2$) ppm. – **IR** (ATR) $\tilde{\nu}$ = 3264 (vw), 3058 (w), 2952 (w), 2857 (w), 2793 (w), 1701 (vs), 1694 (vs), 1601 (m), 1560 (vs), 1497 (m), 1435 (s), 1374 (m), 1261 (vs), 1239 (m), 1156 (w), 1048 (s), 819 (s), 766 (s), 754 (vs), 622 (vs) cm^{-1}. – **MS** (ESI): *m/z* (%) = 552 [M]$^+$ (100). – **HRMS** (ESI, [C$_{36}$H$_{30}$ON$_3$^{32}S$_1$]$^+$, [M]$^+$) calc.: 552.2104, found: 552.2085.

(*rac*)-3-Allyl-2-(2-(4'-[2.2]paracyclophonyl)hydrazineyl)-4-(naphthalen-2-yl)-thiazol-3-ium bromide (141c)

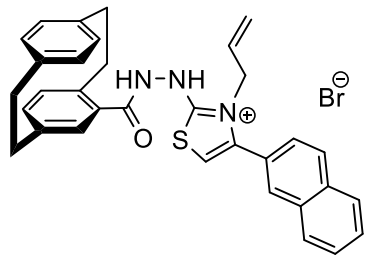

According to **GP8**, *N*-allyl-2-(4'-[2.2]paracyclophanyl)-hydrazine-1-carbothioamide (**135c**, 0.365 g, 1.00 mmol, 1.00 equiv.) was reacted with BNE (**195**, 0.249 g, 1.00 mmol, 1.00 equiv.) in EtOAc for 48 h. A precipitate of the title compound was obtained as a white solid (0.430 g, 72%, 721 µmol).

R_f = 0.15 (cyclohexane/ethyl acetate; 4:1). – **^{1}H NMR** (400 MHz, DMSO-d_6) δ = 11.23 (s, 1H, N*H*), 8.20 (s, 1H, H^{Ar}), 8.12–8.02 (m, 3H, H^{Ar}), 7.70–7.63 (m, 3H, H^{Ar}), 7.35 (s, 1H, H^{Ar}), 6.95 (s, 1H, N*H*), 6.79–6.63 (m, 3H, H^{Ar}), 6.62–6.51 (m, 4H, H^{Ar}), 5.89–5.80 (m, 1H, CH^{Allyl}), 5.32–5.00 (m, 2H, CH_2^{Allyl}), 4.84–4.70 (m, 2H, CH_2^{Allyl}), 3.73–3.67 (m, 1H, H^{Pc}), 3.22–3.08 (m, 3H, H^{Pc}), 3.06–2.92 (m, 4H, H^{Pc}) ppm. – **^{13}C NMR** (101 MHz, DMSO-d_6) δ = 173.8 (C_q, *C*O), 168.2 (C_q, C^{Ar}), 143.4 (C_q, C^{Ar}), 141.5 (C_q, C^{Ar}), 141.1 (C_q, C^{Ar}), 140.4 (C_q, C^{Ar}), 140.3 (C_q, C^{Ar}), 137.3 (C_q, C^{Ar}), 137.2 (C_q, C^{Ar}), 134.4 (+, *C*H^{Ar}), 133.9 (+, *C*H^{Ar}), 133.8 (+, *C*H^{Ar}), 133.7 (C_q, C^{Ar}), 133.5 (+, *C*H^{Allyl}), 133.4 (+, *C*H^{Ar}), 132.4 (+, *C*H^{Ar}), 132.2 (+, *C*H^{Ar}), 131.1 (+, *C*H^{Ar}), 130.9 (+, *C*H^{Ar}), 129.7 (+, *C*H^{Ar}), 129.5 (+, *C*H^{Ar}), 128.9 (+, 2 × *C*H^{Ar}), 128.3 (+, *C*H^{Ar}), 127.2 (+, *C*H^{Ar}), 126.6 (C_q, C^{Ar}), 118.9 (–, *C*H$_2^{Allyl}$), 108.3 (+, *C*H^{Ar}), 50.4 (–, *C*H$_2^{Allyl}$), 36.0 (–, *C*H$_2$), 35.8 (–, *C*H$_2$), 35.6 (–, *C*H$_2$), 35.5 (–, *C*H$_2$) ppm. – **IR** (ATR) $\tilde{\nu}$ = 3255 (vw), 3029 (w), 3003 (w), 2866 (w), 2819 (m), 2588 (w), 1683 (vs), 1608 (s), 1591 (vs), 1581 (vs), 1562 (m), 1449 (vs), 1374 (m), 1272 (vs), 1157 (s), 902 (s), 829 (vs), 762 (vs), 717 (s), 687 (s), 622 (s), 596 (vs), 565 (s), 510 (s), 479 (vs) cm^{-1}. – **MS** (ESI): *m/z* (%) = 516 [M]$^+$ (100). – **HRMS** (ESI, [$C_{33}H_{30}ON_3{}^{32}S_1$]$^+$, [M]$^+$) calc.: 516.2104, found: 516.2091.

(*rac*)-2-(2-(4'-[2.2]Paracyclophonyl)hydrazineyl)-3-ethyl-4-(naphthalen-2-yl)-thiazol-3-ium bromide (141d)

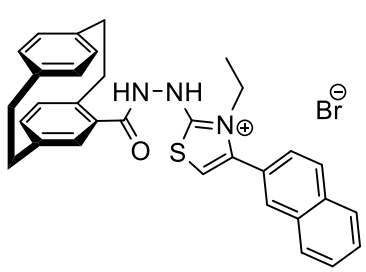

According to **GP8**, 2-(4'-[2.2]paracyclophanyl)-*N*-ethyl-hydrazine-1-carbothioamide (**135d**, 0.353 g, 1.00 mmol, 1.00 equiv.) was reacted with BNE (**195**, 0.249 g, 1.00 mmol, 1.00 equiv.) in EtOAc for 28 h. A precipitate of the title compound was obtained as a white solid (0.305 g, 52%, 522 µmol).

R$_f$ = 0.13 (cyclohexane/ethyl acetate; 4:1). – **^{1}H NMR** (400 MHz, DMSO-d_6) δ = 11.20 (s, 1H, N*H*), 8.25 (s, 1H, H^{Ar}), 8.15–8.06 (m, 3H, H^{Ar}), 7.75–7.66 (m, 3H, H^{Ar}), 7.27 (s, 1H, H^{Ar}), 6.95 (s, 1H, N*H*), 6.77 (dd, *J* = 7.8, 1.8 Hz, 1H, H^{Ar}), 6.66–6.53 (m, 6H, H^{Ar}), 4.10 (q, *J* = 7.2 Hz, 2H, CH_2^{ethyl}), 3.73–3.68 (m, 1H, H^{Pc}), 3.22–3.08 (m, 4H, H^{Pc}), 3.06–2.93 (m, 3H, H^{Pc}), 1.23 (t, *J* = 7.1 Hz, 3H, CH_3^{ethyl}) ppm. – **^{13}C NMR** (101 MHz, DMSO-d_6) δ = 173.3 (C_q, *C*O), 167.5 (C_q, C^{Ar}), 142.2 (C_q, C^{Ar}), 140.5 (C_q, C^{Ar}), 140.2 (C_q, C^{Ar}), 139.5 (C_q, C^{Ar}), 139.4 (C_q, C^{Ar}), 136.4 (C_q, C^{Ar}), 136.3 (C_q, C^{Ar}), 133.5 (+, *C*H^{Ar}), 133.0 (+, *C*H^{Ar}), 132.9 (+, *C*H^{Ar}), 132.7 (+, *C*H^{Ar}), 132.6 (C_q, C^{Ar}), 132.5 (+, *C*H^{Ar}), 131.5 (+, *C*H^{Ar}), 131.4 (+, *C*H^{Ar}), 130.3 (+, *C*H^{Ar}), 128.9 (+, *C*H^{Ar}), 128.6 (+, *C*H^{Ar}), 128.0 (+, *C*H^{Ar}), 127.9 (C_q, C^{Ar}), 127.4 (+, *C*H^{Ar}), 126.5 (+, *C*H^{Ar}), 125.9 (+, *C*H^{Ar}), 107.3 (+, *C*H^{Ar}), 43.1 (–, *C*H_2^{ethyl}), 35.1 (–, *C*H_2), 34.9 (–, *C*H_2), 34.7 (–, *C*H_2), 34.6 (–, *C*H_2), 13.1 (+, *C*H_3^{ethyl}) ppm. – **IR** (ATR) $\tilde{\nu}$ = 3264 (vw), 3012 (w), 2927 (m), 2744 (m), 1683 (vs), 1591 (vs), 1584 (vs), 1453 (vs), 1435 (m), 1272 (vs), 1157 (m), 904 (m), 826 (s), 755 (vs), 717 (s), 684 (m), 615 (m), 578 (s), 511 (s), 479 (vs) cm^{-1}. – **MS** (ESI): *m/z* (%) = 504 [M]$^+$ (100). – **HRMS** (ESI, [$C_{32}H_{30}ON_3{}^{32}S_1$]$^+$, [M]$^+$) calc.: 504.2104, found: 504.2088.

(*rac*)-2-(2-(4'-[2.2]Paracyclophonyl)hydrazineyl)-3-benzyl-4-(naphthalen-2-yl)-thiazol-3-ium bromide (141f)

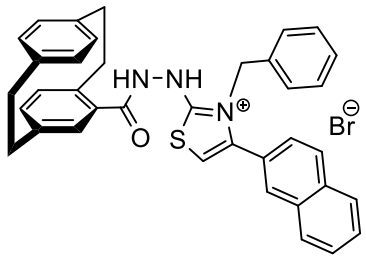

According to **GP8**, 2-(4'-[2.2]paracyclophanyl)-*N*-benzyl-hydrazine-1-carbothioamide (**135f**, 0.415 g, 1.00 mmol, 1.00 equiv.) was reacted with BNE (**195**, 0.249 g, 1.00 mmol, 1.00 equiv.) in EtOAc for 24 h. A precipitate of the title compound was obtained as a white solid (0.460 g, 71%, 711 µmol).

R*f* = 0.22 (cyclohexane/ethyl acetate; 4:1). – **^{1}H NMR** (400 MHz, DMSO-d_6, ppm) δ = 11.04 (s, 1H, N*H*), 8.03–7.89 (m, 4H, H^{Ar}), 7.65–7.50 (m, 3H, H^{Ar}), 7.34–7.28 (m, 3H, H^{Ar}), 7.21 (s, 1H, H^{Ar}), 7.06 (d, J = 8.2 Hz, 2H, H^{Ar}), 6.92 (s, 1H, N*H*), 6.74 (dd, J = 7.8, 1.8 Hz, 1H, H^{Ar}), 6.70–6.53 (m, 6H, H^{Ar}), 5.38 (s, 2H, CH_2), 3.75–3.69 (m, 1H, H^{Pc}), 3.21–3.07 (m, 4H, H^{Pc}), 3.05–2.93 (m, 3H, H^{Pc}) ppm. – **^{13}C NMR** (101 MHz, DMSO-d_6) δ = 172.8 (C_q, *C*O), 166.8 (C_q, C^{Ar}), 142.2 (C_q, C^{Ar}), 140.4 (C_q, C^{Ar}), 140.1 (C_q, C^{Ar}), 139.5 (C_q, C^{Ar}), 139.4 (C_q, C^{Ar}), 136.3 (C_q, C^{Ar}), 136.1 (C_q, C^{Ar}), 134.5 (C_q, C^{Ar}), 133.3 (+, CH^{Ar}), 133.0 (+, CH^{Ar}), 132.9 (+, CH^{Ar}), 132.7 (+, CH^{Ar}), 132.5 (C_q, C^{Ar}), 132.4 (C_q, C^{Ar}), 131.9 (+, CH^{Ar}), 131.6 (+, CH^{Ar}), 129.9 (+, CH^{Ar}), 129.0 (+, CH^{Ar}), 128.6 (+, CH^{Ar}), 128.5 (+, CH^{Ar}), 128.1 (+, CH^{Ar}), 127.9 (+, CH^{Ar}), 127.8 (+, CH^{Ar}), 127.3 (+, CH^{Ar}), 126.8 (+, CH^{Ar}), 126.6 (+, 2 × CH^{Ar}), 126.2 (+, CH^{Ar}), 126.1 (+, CH^{Ar}), 106.2 (+, CH^{Ar}), 50.2 (–, CH_2), 35.1 (–, CH_2), 34.9 (–, CH_2), 34.7 (–, CH_2), 34.6 (–, CH_2) ppm. – **IR** (ATR) $\tilde{\nu}$ = 3364 (vw), 3087 (w), 3046 (w), 2925 (m), 2731 (w), 1687 (m), 1595 (s), 1581 (s), 1497 (m), 1455 (s), 1380 (w), 1268 (s), 1156 (s), 1122 (m), 904 (m), 822 (vs), 748 (vs), 698 (vs), 625 (s), 588 (s), 513 (vs), 479 (vs), 450 (s) cm^{-1}. – **MS** (ESI): *m/z* (%) = 566 $[M]^+$ (100). – **HRMS** (ESI, $[C_{37}H_{32}ON_3{}^{32}S_1]^+$, $[M]^+$) calc.: 566.2261, found: 566.2246.

3-(4'-[2.2]Paracyclophanyl)amido-2-(cyclopropylamino)-4-(naphthalen-2-yl)thiazol-3-ium bromide **(196)**

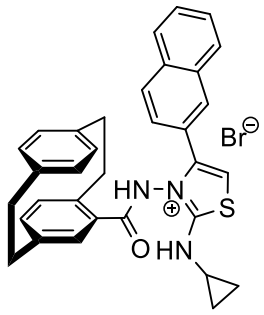

According to **GP8**, 2-(4'-[2.2]paracyclophanyl)-*N*-cyclopropyl-hydrazine-1-carbothioamide (**135e**, 0.365 g, 1.00 mmol, 1.00 equiv.) was reacted with BNE (**195**, 0.249 g, 1.00 mmol, 1.00 equiv.) in EtOAc for 28 h. A precipitate of the title compound was obtained as a white solid (0.355 g, 60%, 595 µmol).

R_f = 0.16 (cyclohexane/ethyl acetate; 4:1). – **^{1}H NMR** (400 MHz, DMSO-d_6) δ = 11.79 (s, 1H, N*H*), 8.45 (s, 1H, H^{Ar}), 8.28–8.01 (m, 3H, H^{Ar}), 7.89–7.61 (m, 3H, H^{Ar}), 7.47 (s, 1H, H^{Ar}), 6.92–6.60 (m, 3H, H^{Ar}), 6.52–6.26 (m, 4H, H^{Ar}), 5.36 (s, 1H, N*H*), 3.72–3.66 (m, 1H, H^{Pc}), 3.20–2.96 (m, 5H, H^{Pc}), 2.87–2.76 (m, 2H, H^{Pc}), 2.74–2.64 (m, 1H, C$H^{Cyclo.}$), 1.04–0.95 (m, 2H, C$H_2^{Cyclo.}$), 0.81–0.75 (m, 2H, C$H_2^{Cyclo.}$) ppm. – **^{13}C NMR** (101 MHz, DMSO-d_6) δ = 172.0 (C_q, *C*O), 166.1 (C_q, C^{Ar}), 142.4 (C_q, C^{Ar}), 142.3 (C_q, C^{Ar}), 139.7 (C_q, C^{Ar}), 139.5 (C_q, C^{Ar}), 138.8 (C_q, C^{Ar}), 137.1 (C_q, C^{Ar}), 136.6 (C_q, C^{Ar}), 136.4 (+, CH^{Ar}), 134.1 (+, CH^{Ar}), 133.2 (+, CH^{Ar}), 132.9 (+, CH^{Ar}), 132.7 (C_q, C^{Ar}), 131.8 (+, CH^{Ar}), 130.3 (+, CH^{Ar}), 129.9 (+, CH^{Ar}), 129.1 (+, CH^{Ar}), 128.8 (+, CH^{Ar}), 128.4 (+, CH^{Ar}), 127.9 (+, CH^{Ar}), 127.4 (C_q, C^{Ar}), 126.9 (+, CH^{Ar}), 126.3 (+, CH^{Ar}), 126.1 (+, CH^{Ar}), 104.3 (+, CH^{Ar}), 35.0 (–, CH_2), 34.8 (–, CH_2), 34.6 (–, CH_2), 34.5 (–, CH_2), 28.2 (+, C$H^{Cyclo.}$), 7.3 (–, C$H_2^{Cyclo.}$), 7.2 (–, C$H_2^{Cyclo.}$) ppm. – **IR** (ATR) $\tilde{\nu}$ = 3364 (vw), 3080 (w), 2922 (m), 2849 (m), 2775 (w), 1686 (s), 1615 (vs), 1599 (vs), 1581 (vs), 1446 (s), 1343 (m), 1268 (s), 1064 (s), 938 (w), 904 (m), 824 (vs), 817 (vs), 755 (vs), 718 (s), 626 (s), 511 (vs), 480 (vs) cm^{-1}. – **MS** (ESI): *m/z* (%) = 516 $[M]^+$ (65). – **HRMS** (ESI, $[C_{33}H_{30}ON_3{}^{32}S_1]^+$, $[M]^+$) calc.: 516.2104, found: 516.2155.

5.2.4.3. Biology Results

One-Dose Antiproliferative Assay at the National Cancer Institute (NCI), USA

Figure 77: One dose mean graph for Compound **159**.

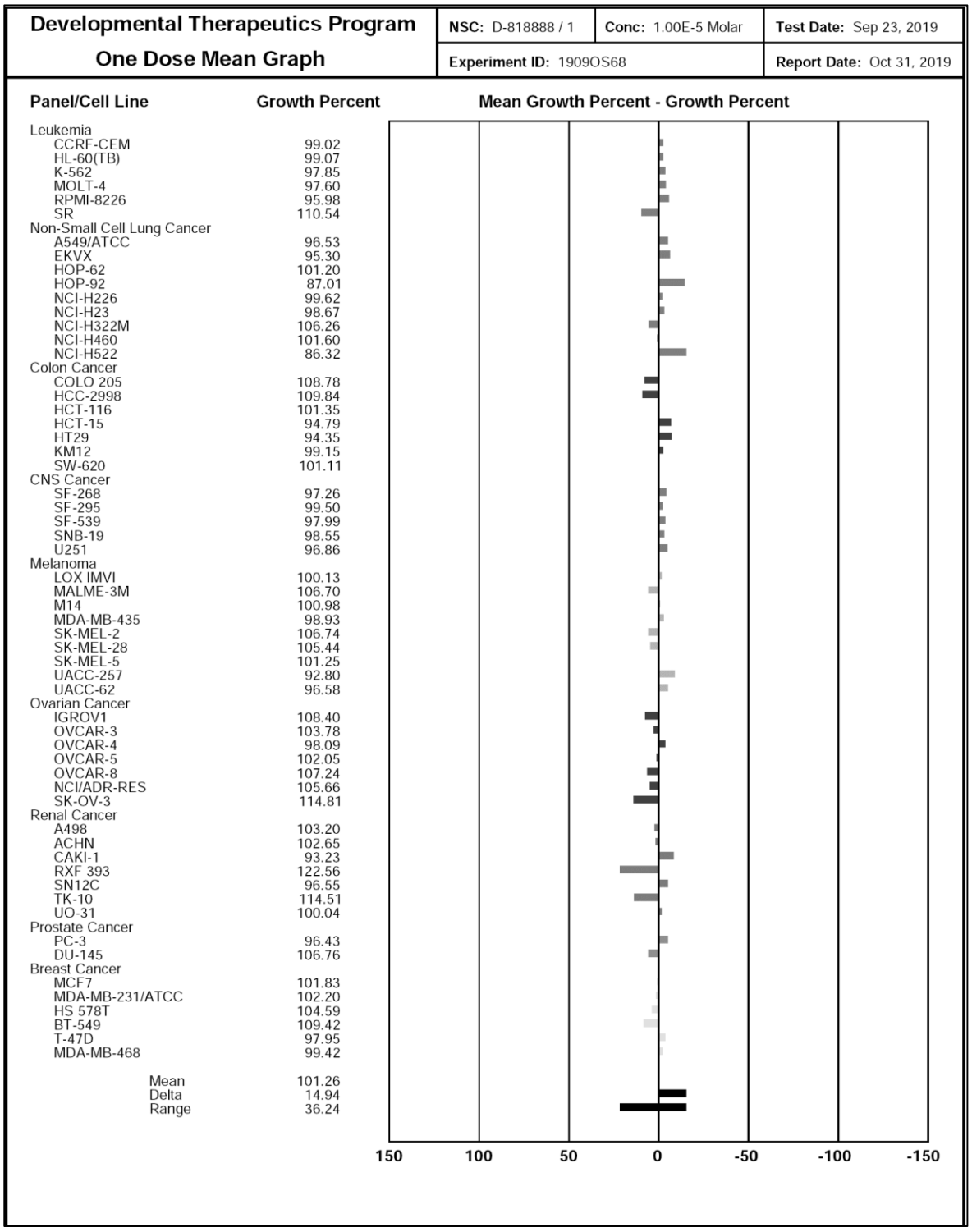

Figure 78: One dose mean graph for Compound **135a**.

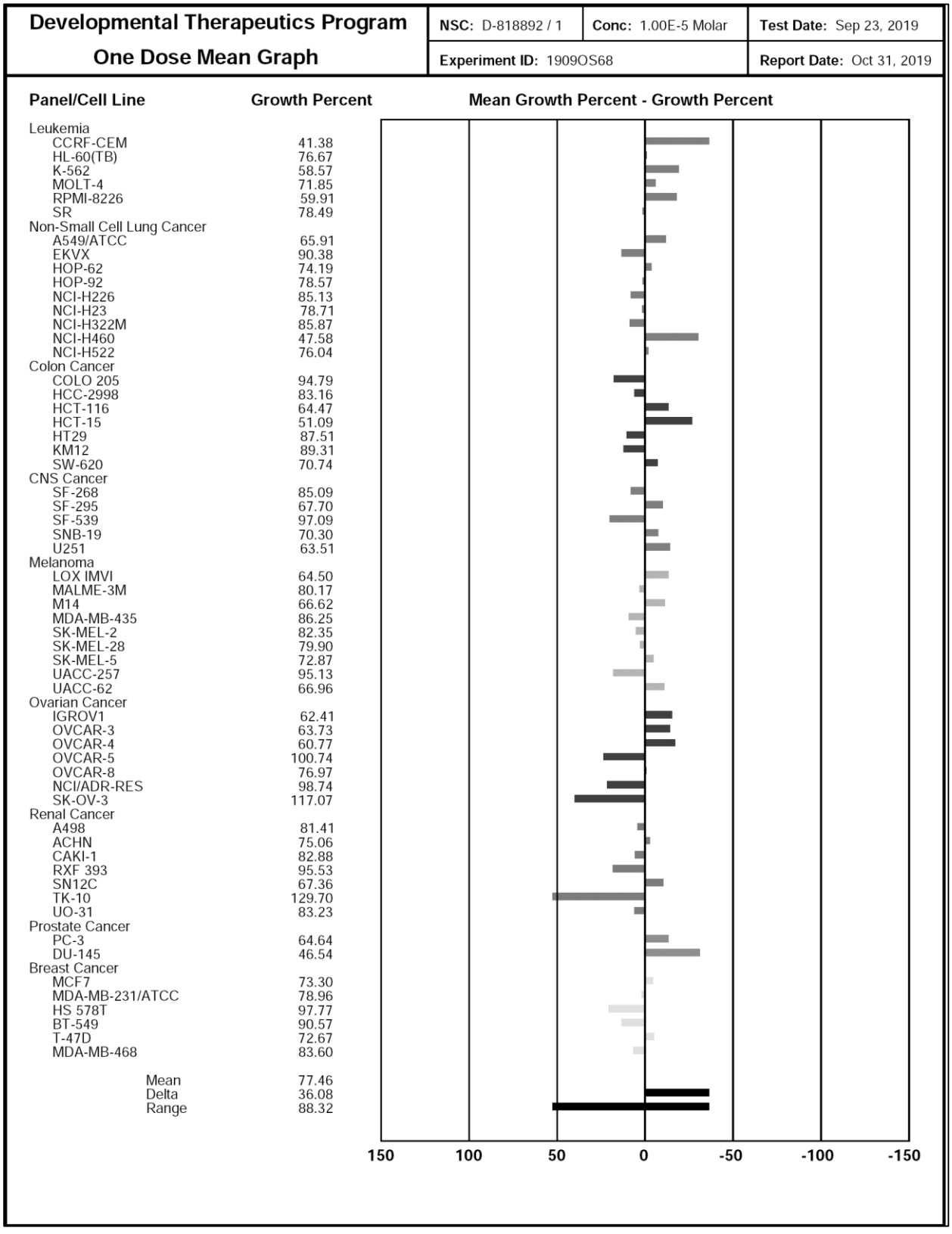

Developmental Therapeutics Program
One Dose Mean Graph

NSC: D-818892 / 1	Conc: 1.00E-5 Molar	Test Date: Sep 23, 2019
Experiment ID: 1909OS68		Report Date: Oct 31, 2019

Panel/Cell Line	Growth Percent
Leukemia	
CCRF-CEM	41.38
HL-60(TB)	76.67
K-562	58.57
MOLT-4	71.85
RPMI-8226	59.91
SR	78.49
Non-Small Cell Lung Cancer	
A549/ATCC	65.91
EKVX	90.38
HOP-62	74.19
HOP-92	78.57
NCI-H226	85.13
NCI-H23	78.71
NCI-H322M	85.87
NCI-H460	47.58
NCI-H522	76.04
Colon Cancer	
COLO 205	94.79
HCC-2998	83.16
HCT-116	64.47
HCT-15	51.09
HT29	87.51
KM12	89.31
SW-620	70.74
CNS Cancer	
SF-268	85.09
SF-295	67.70
SF-539	97.09
SNB-19	70.30
U251	63.51
Melanoma	
LOX IMVI	64.50
MALME-3M	80.17
M14	66.62
MDA-MB-435	86.25
SK-MEL-2	82.35
SK-MEL-28	79.90
SK-MEL-5	72.87
UACC-257	95.13
UACC-62	66.96
Ovarian Cancer	
IGROV1	62.41
OVCAR-3	63.73
OVCAR-4	60.77
OVCAR-5	100.74
OVCAR-8	76.97
NCI/ADR-RES	98.74
SK-OV-3	117.07
Renal Cancer	
A498	81.41
ACHN	75.06
CAKI-1	82.88
RXF 393	95.53
SN12C	67.36
TK-10	129.70
UO-31	83.23
Prostate Cancer	
PC-3	64.64
DU-145	46.54
Breast Cancer	
MCF7	73.30
MDA-MB-231/ATCC	78.96
HS 578T	97.77
BT-549	90.57
T-47D	72.67
MDA-MB-468	83.60
Mean	77.46
Delta	36.08
Range	88.32

Mean Growth Percent - Growth Percent

150 100 50 0 -50 -100 -150

Figure 79: One dose mean graph for Compound **135d**.

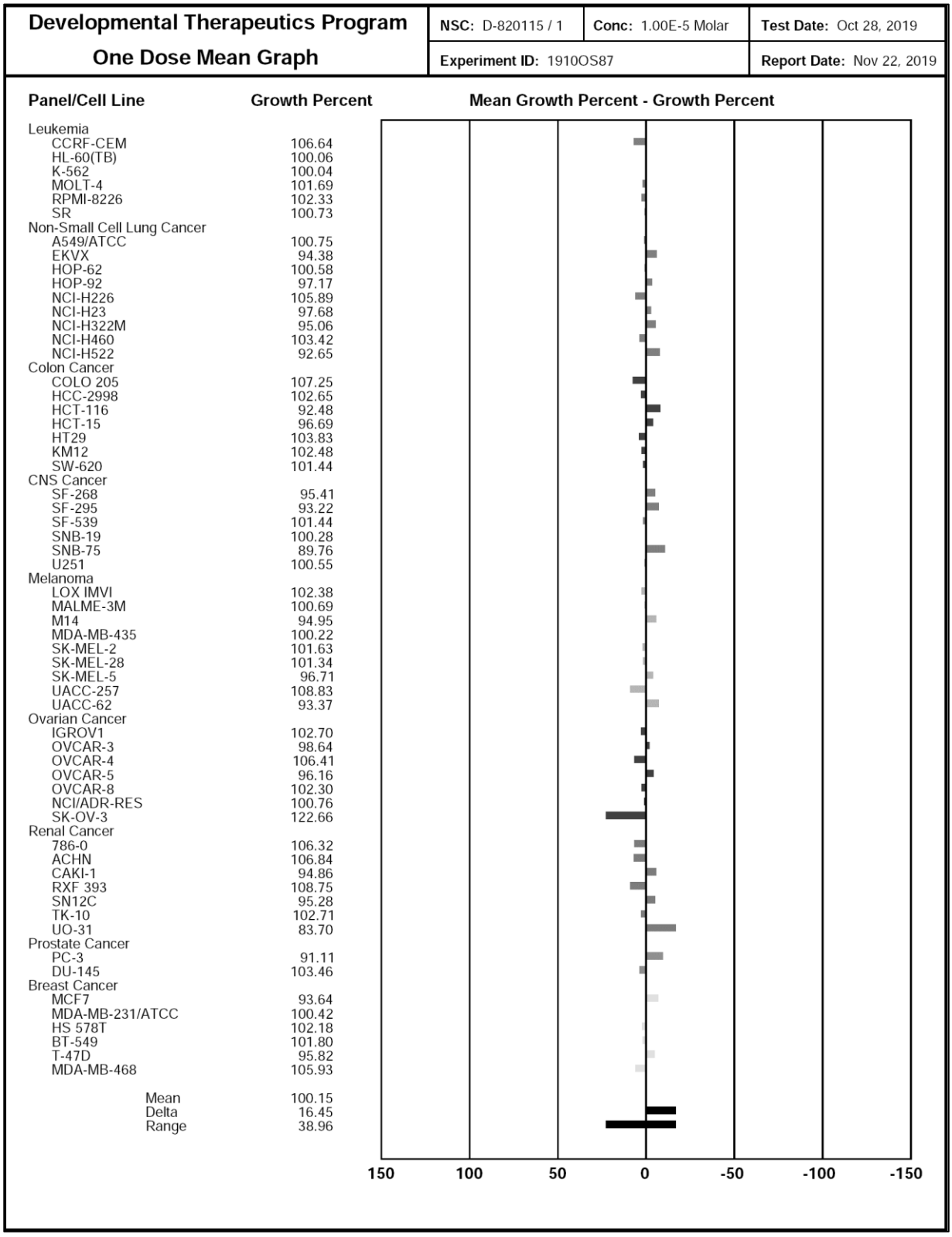

Figure 80: One dose mean graph for Compound **135e.**

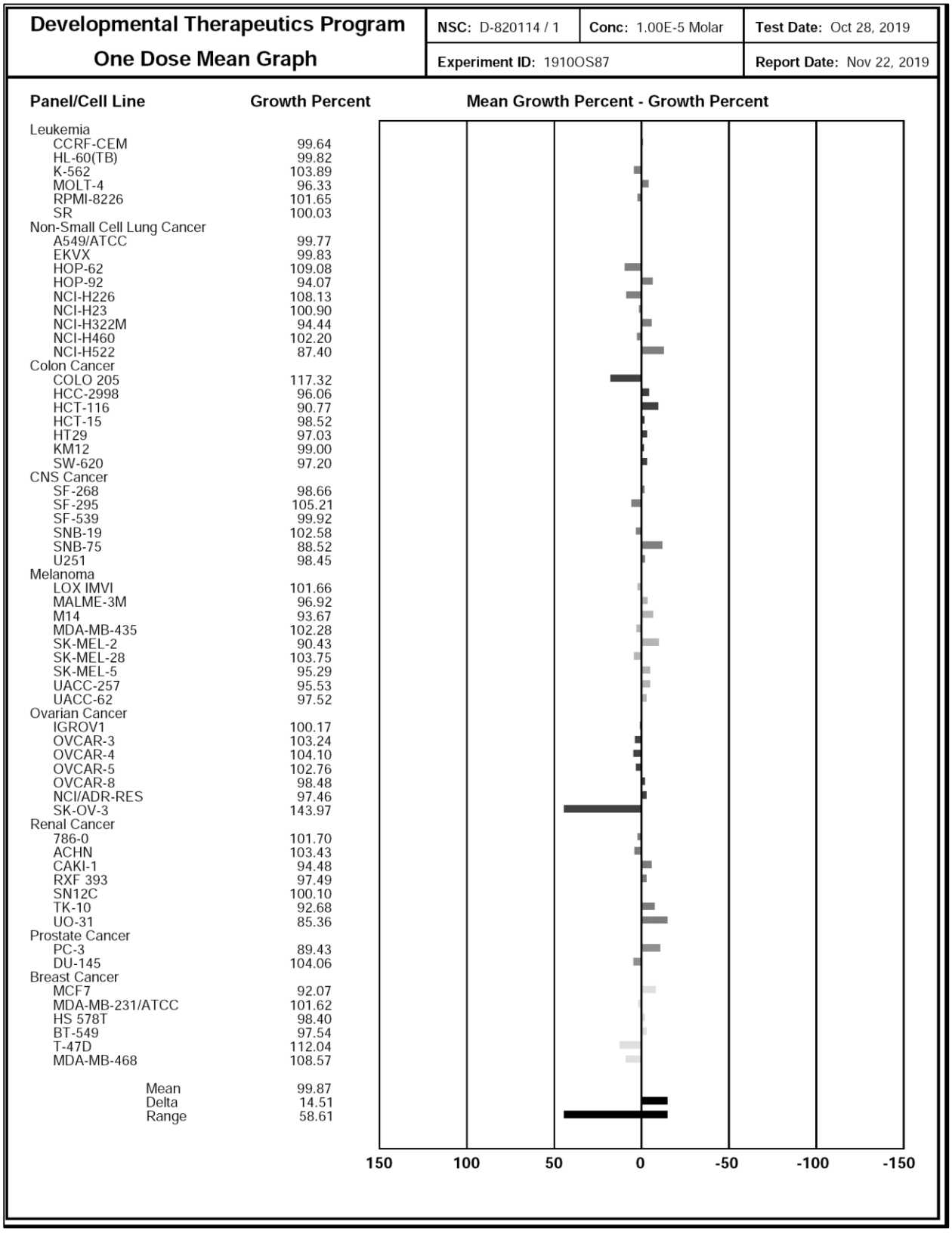

Figure 81: One dose mean graph for Compound **139b**.

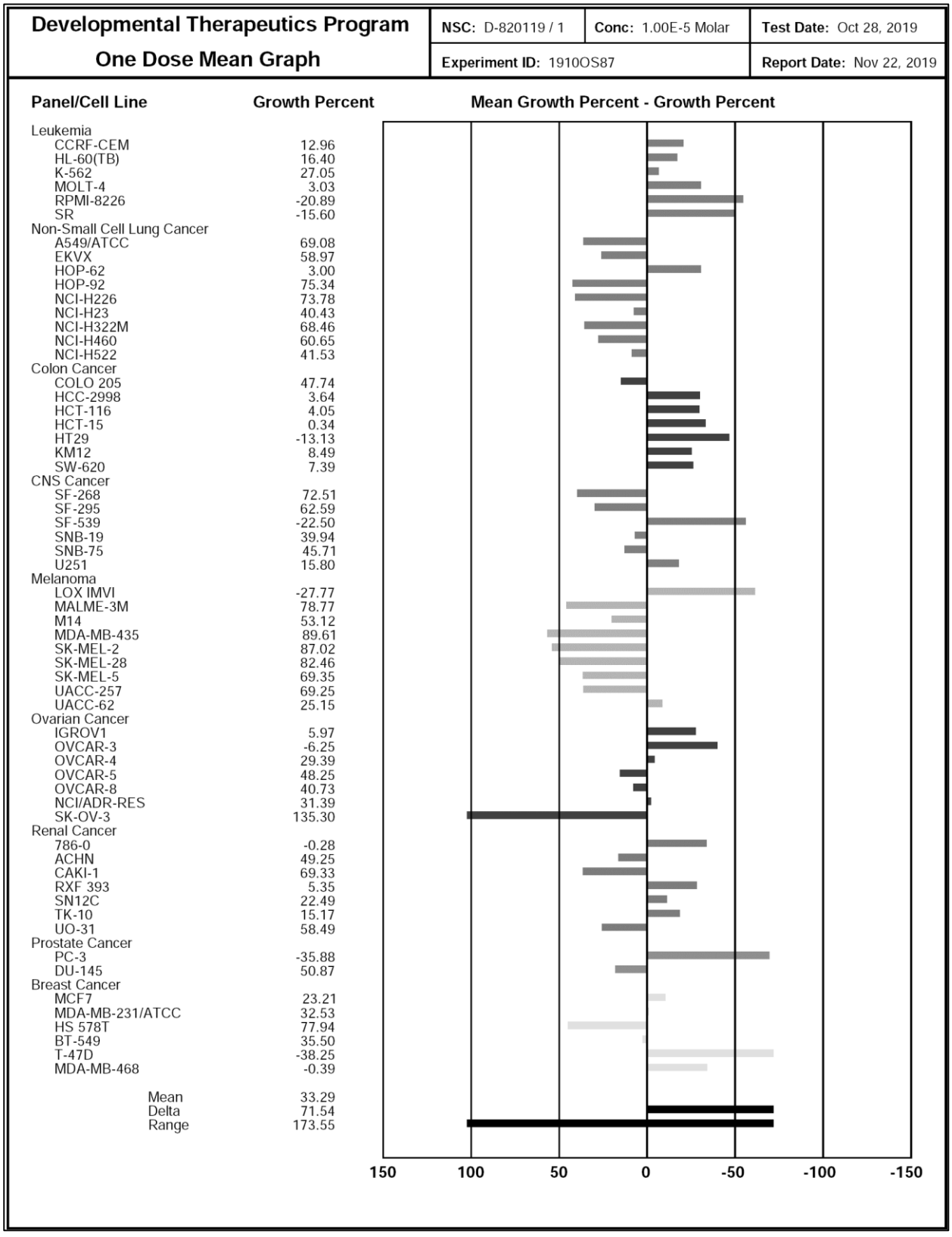

Figure 82: One dose mean graph for Compound **139c**.

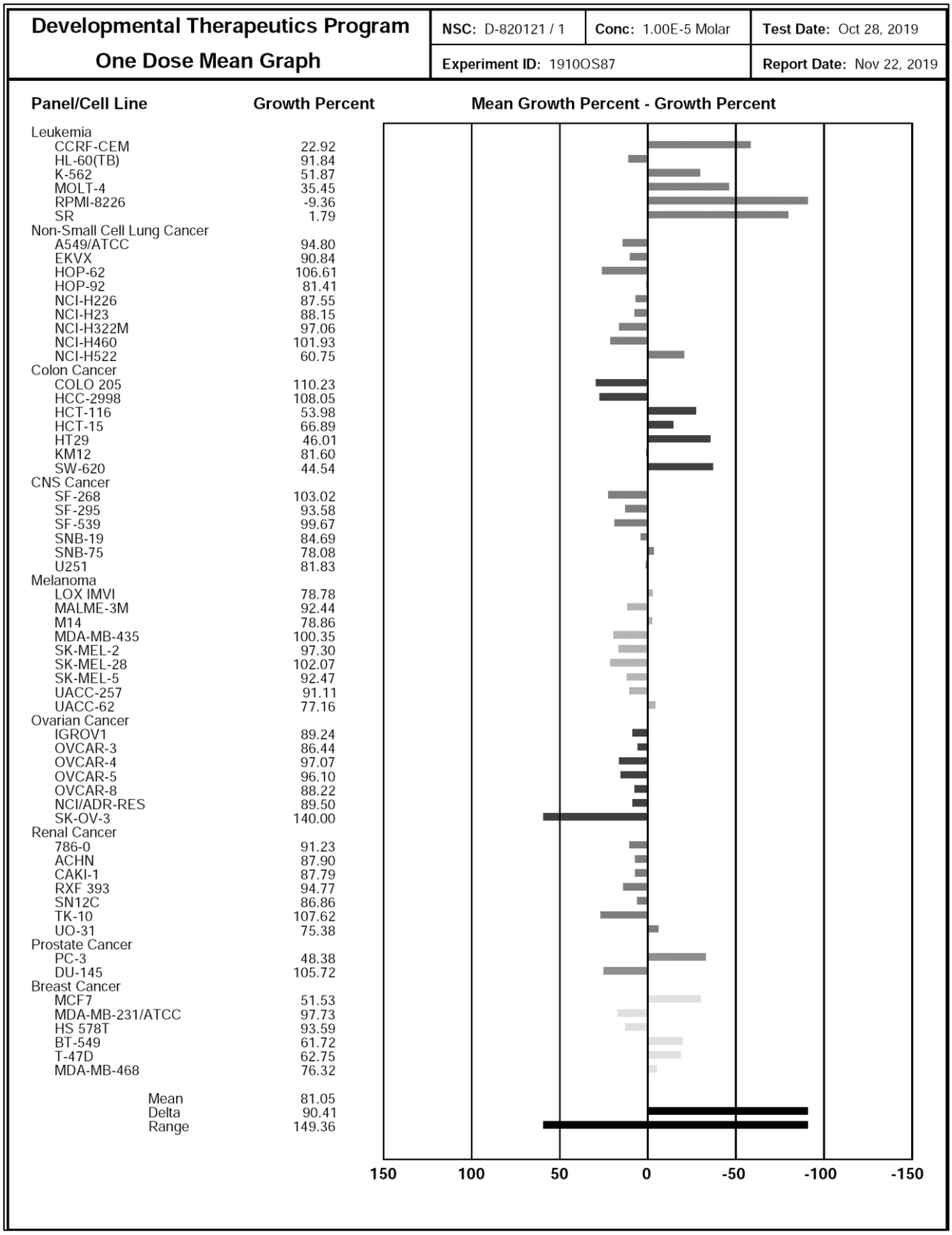

Figure 83: One dose mean graph for Compound **139d**.

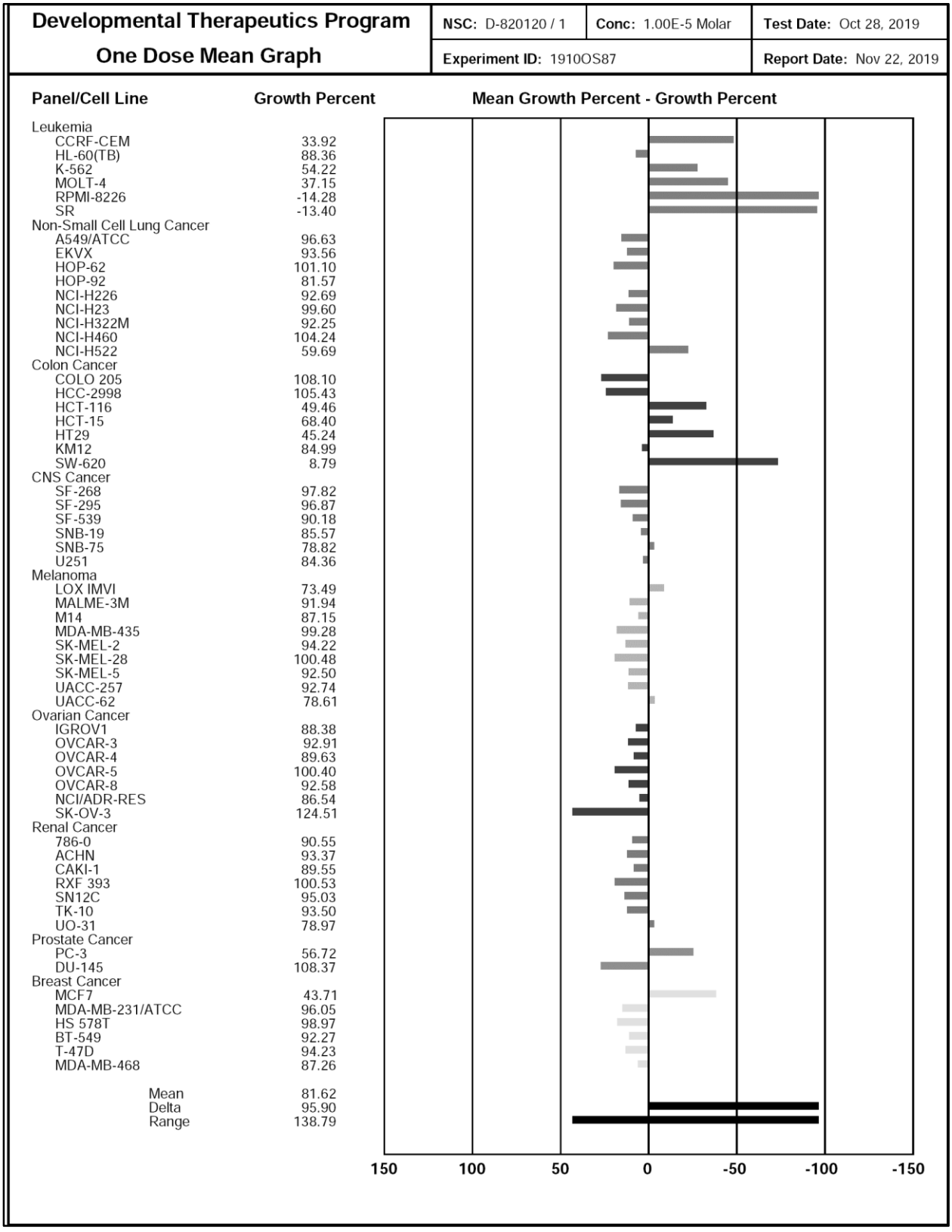

Figure 84: One dose mean graph for Compound **139e**.

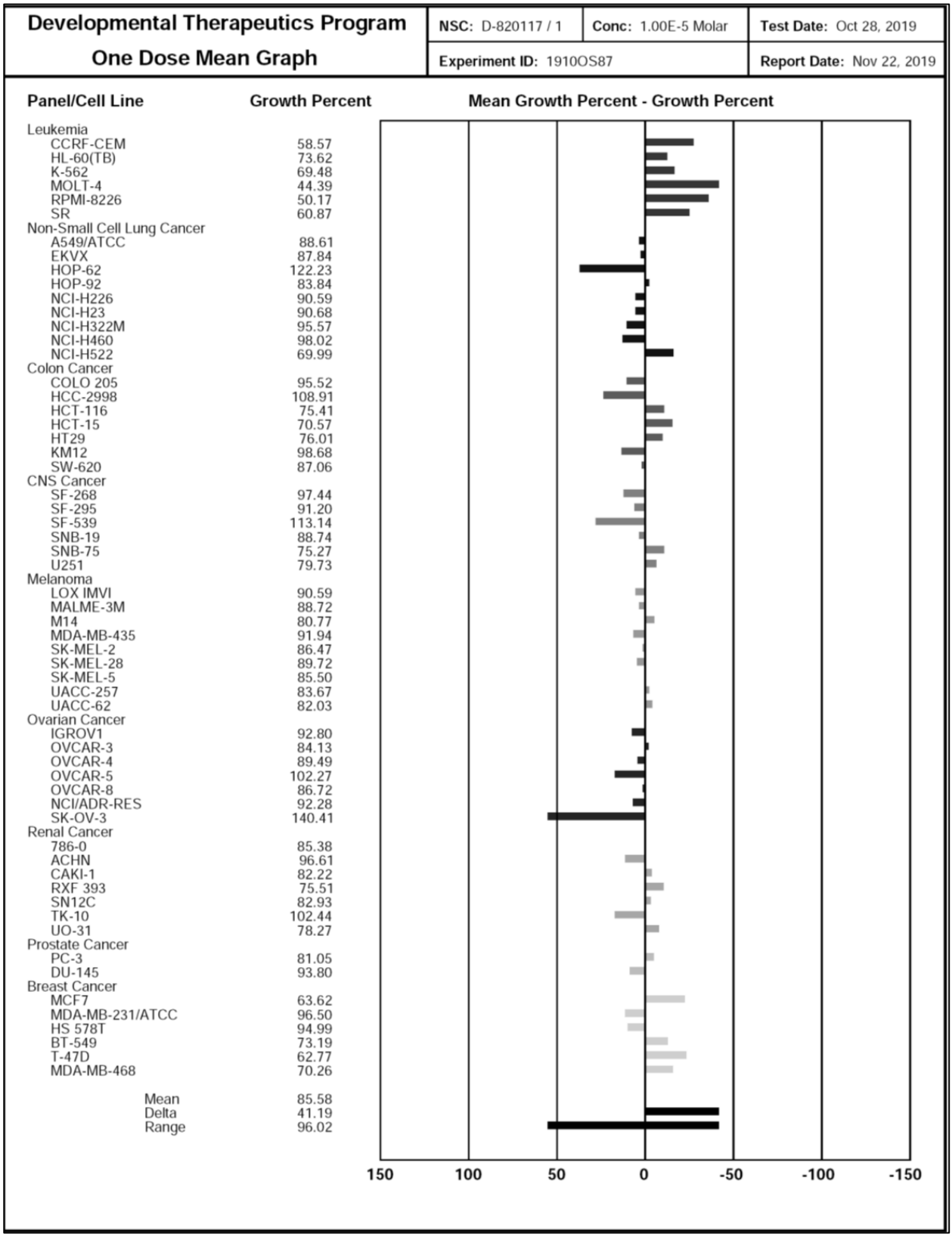

Figure 85: One dose mean graph for Compound **139f**.

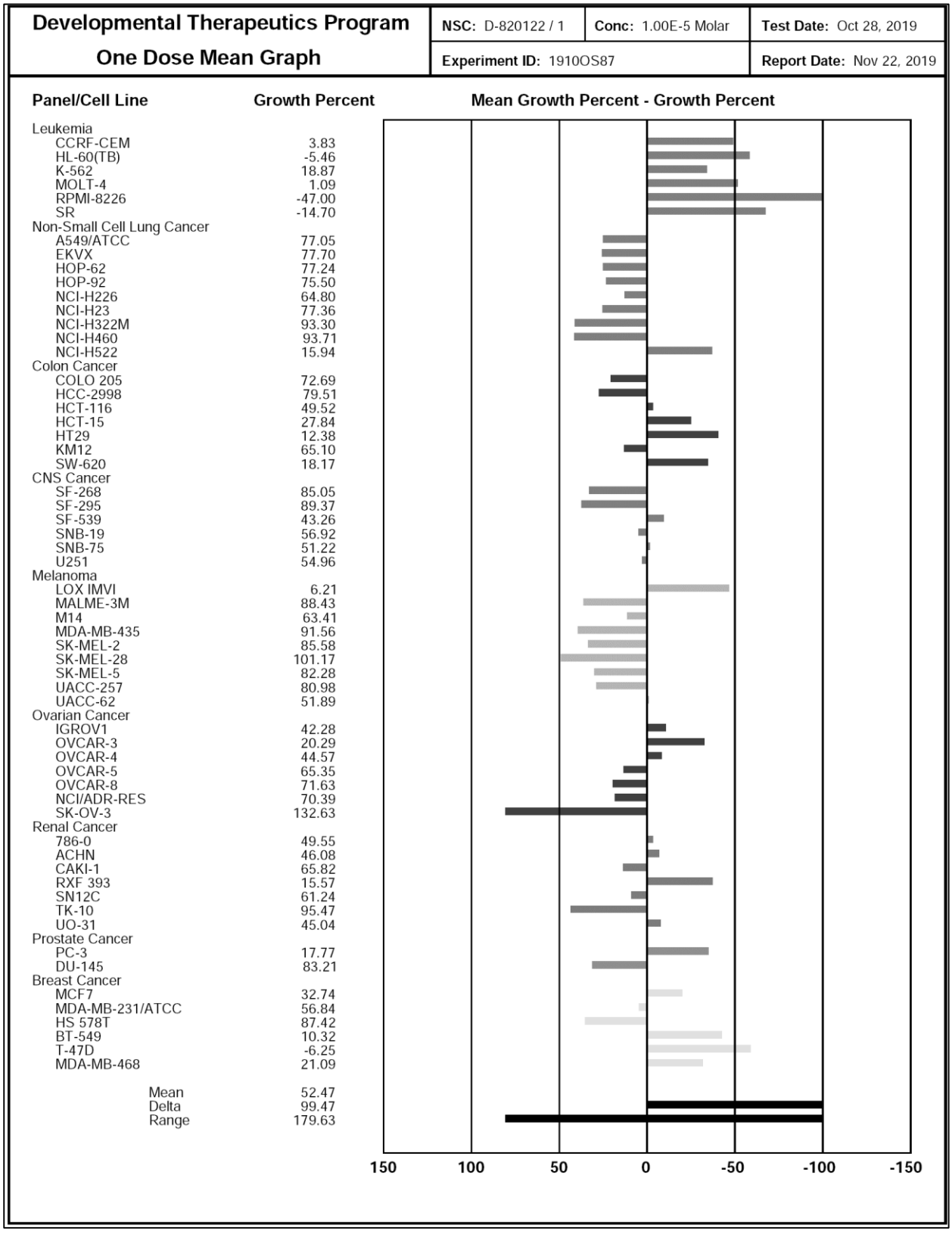

Figure 86: One dose mean graph for Compound **190**.

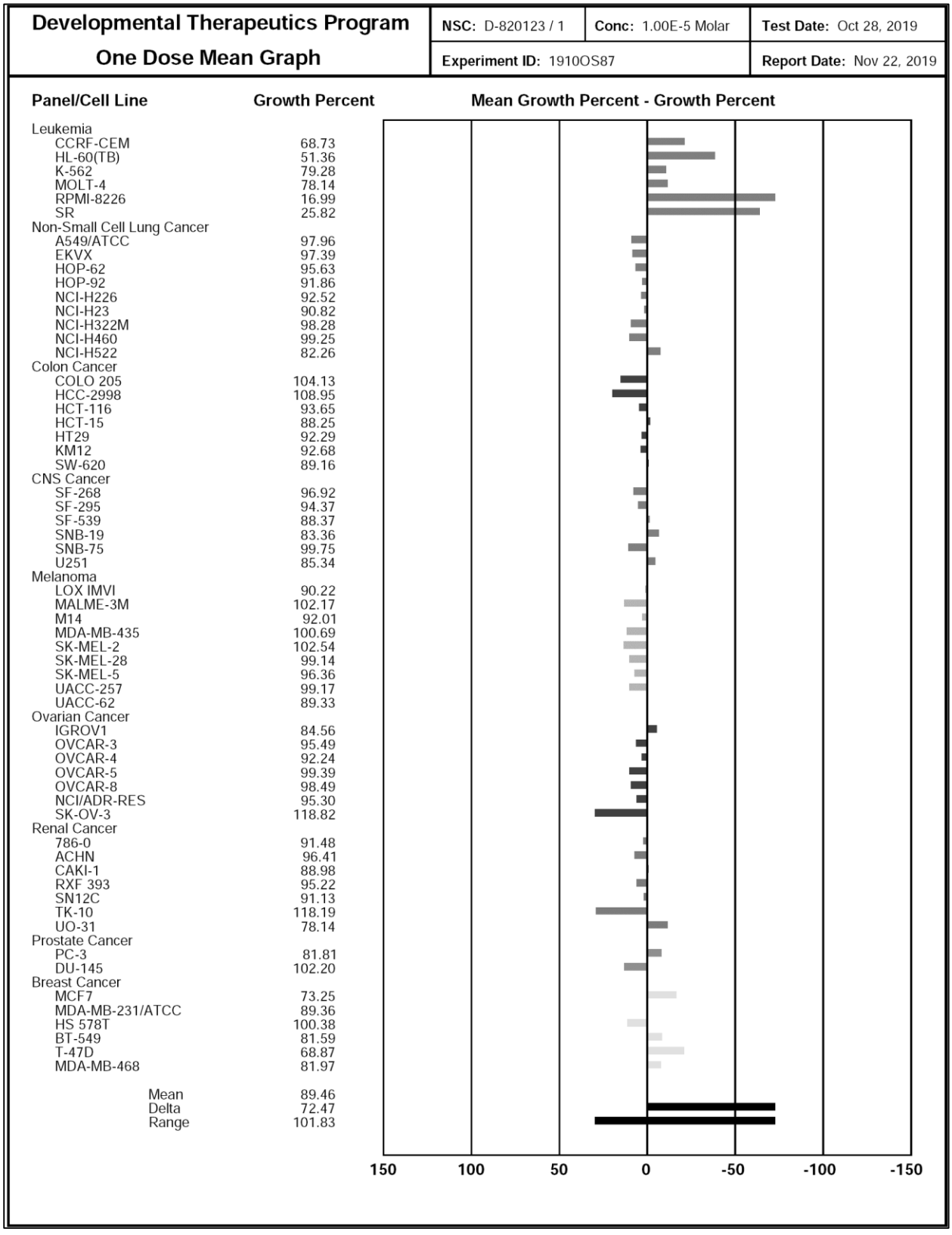

Figure 87: One dose mean graph for Compound **140b**.

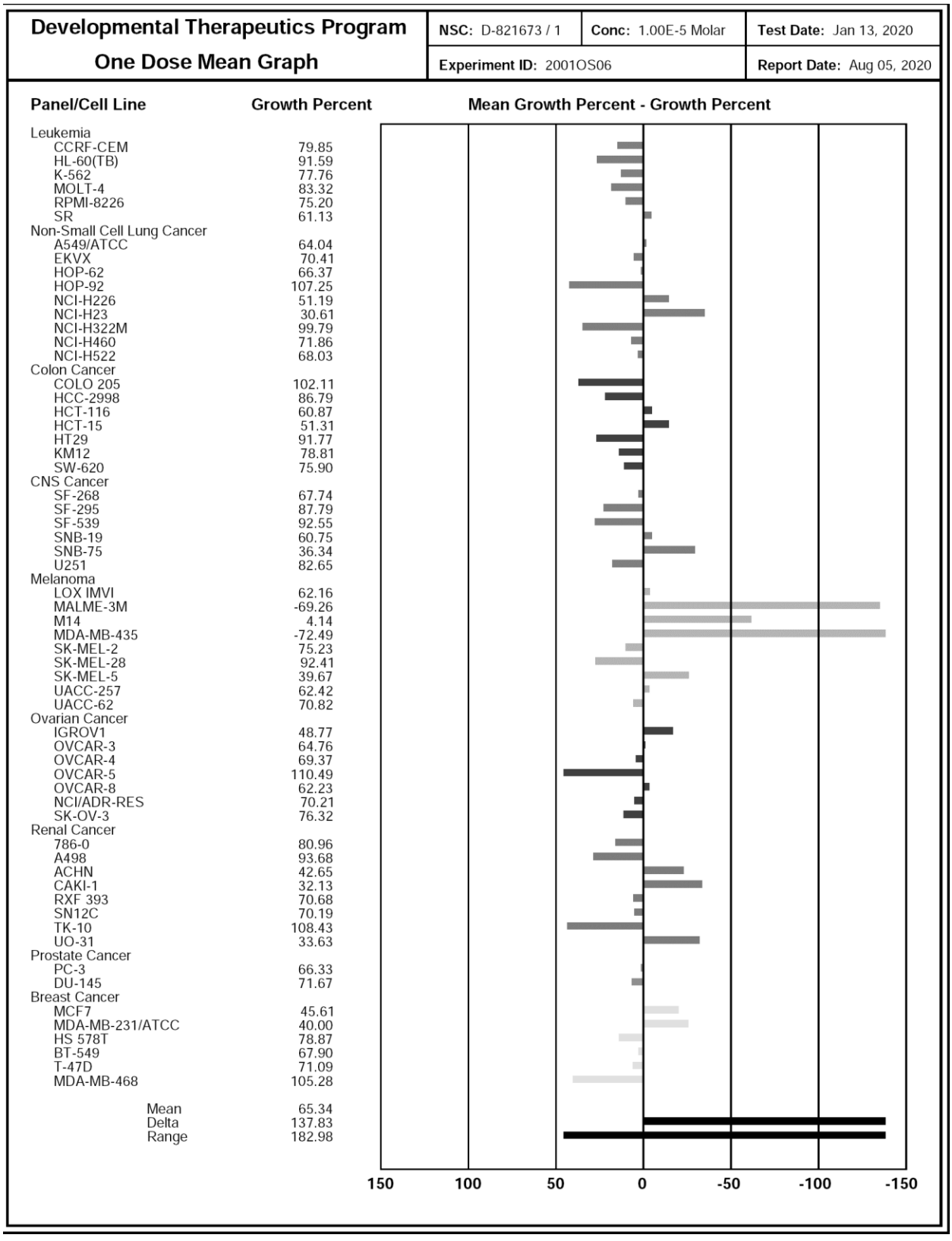

Figure 88: One dose mean graph for Compound **140c**.

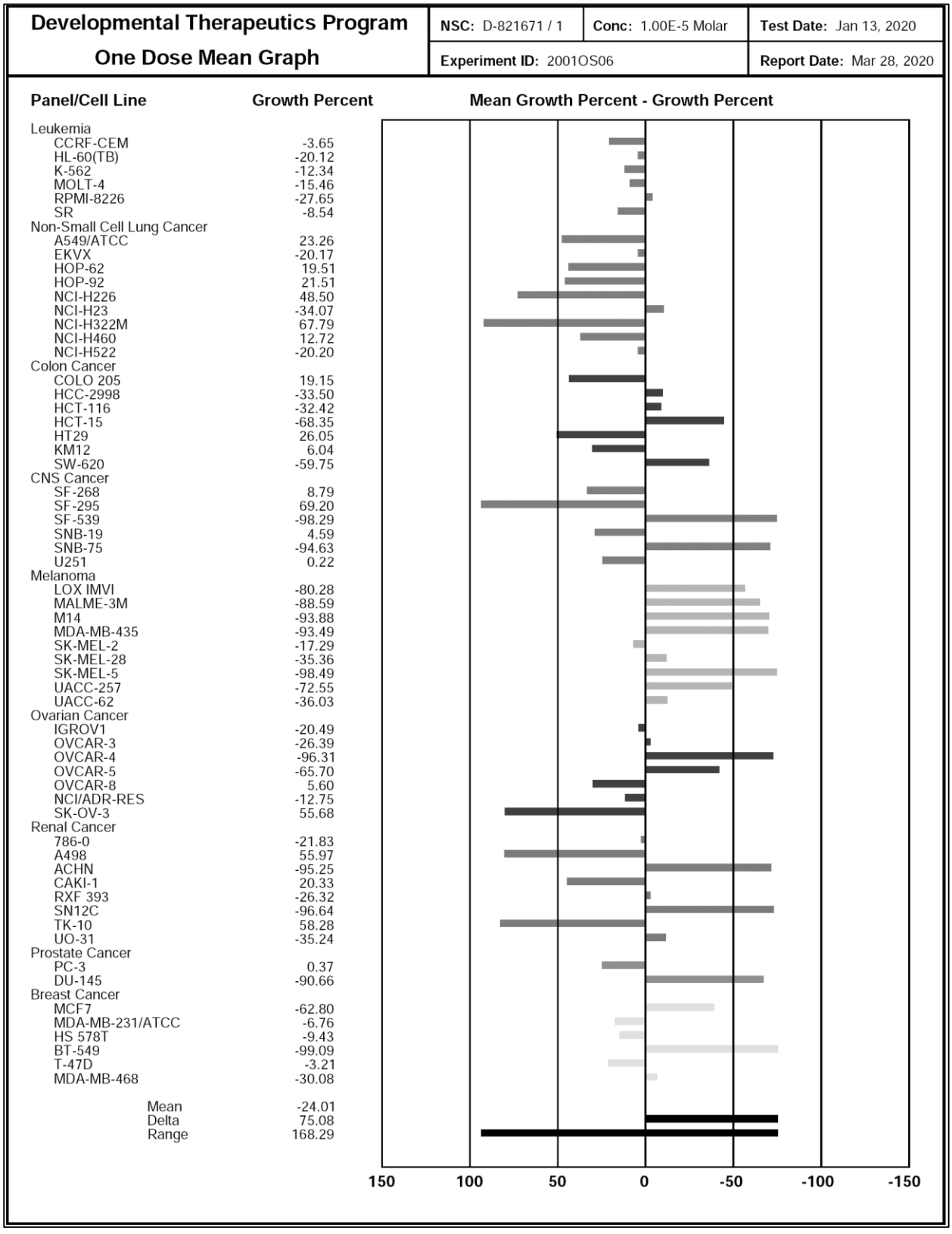

Figure 89: One dose mean graph for Compound **140d**.

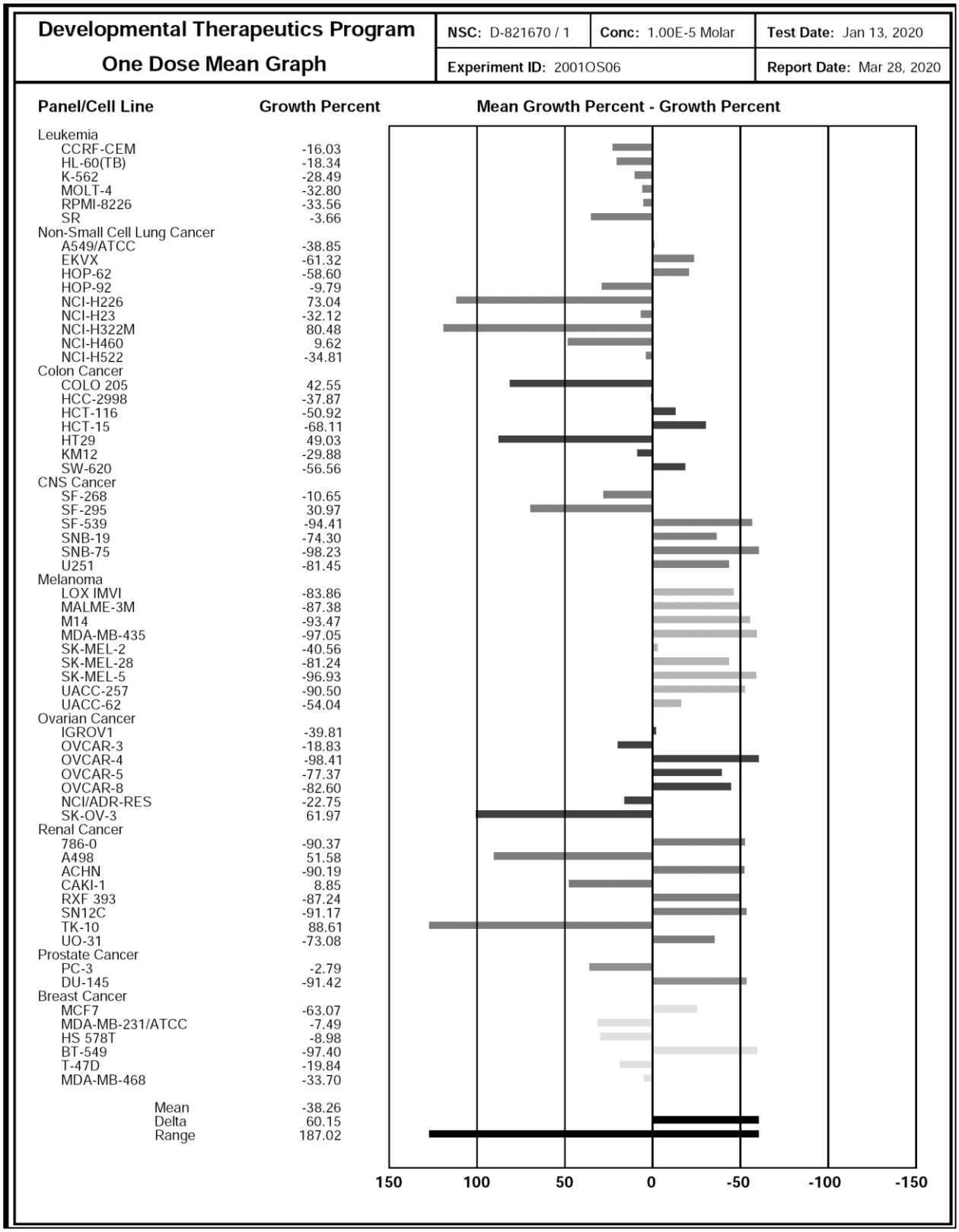

Figure 90: One dose mean graph for Compound **140e**.

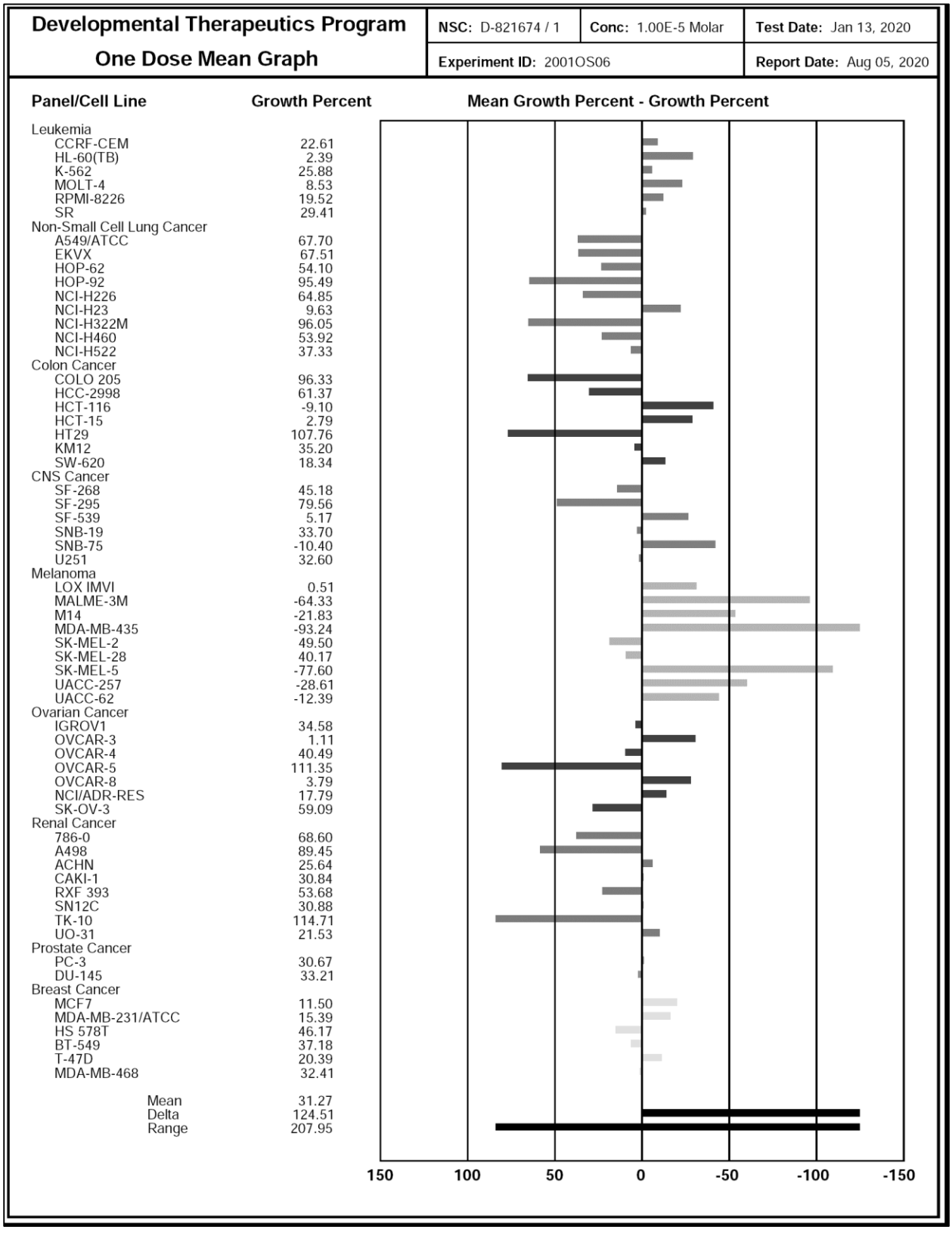

Figure 91: One dose mean graph for Compound **140f**.

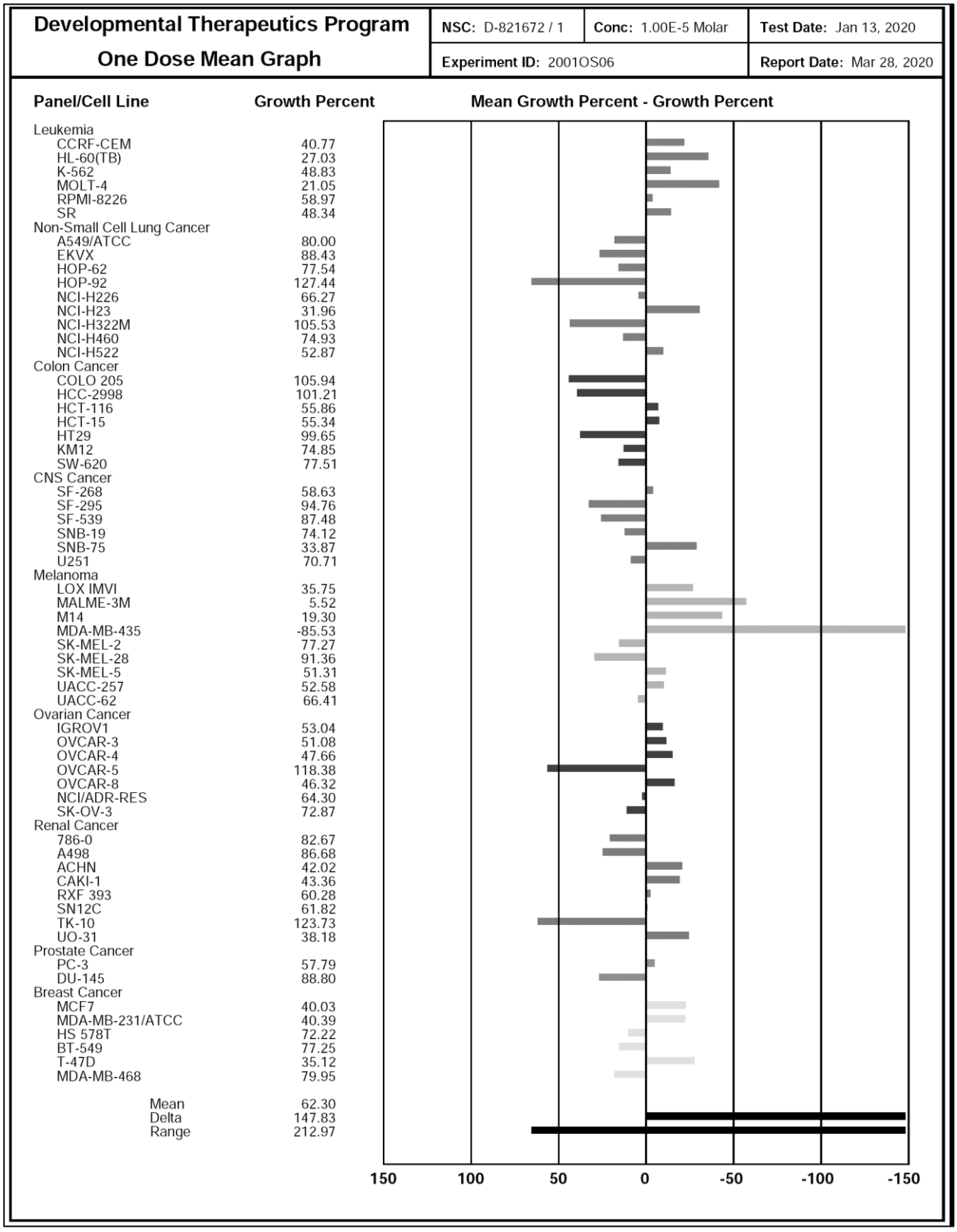

Figure 92: One dose mean graph for Compound **141b**.

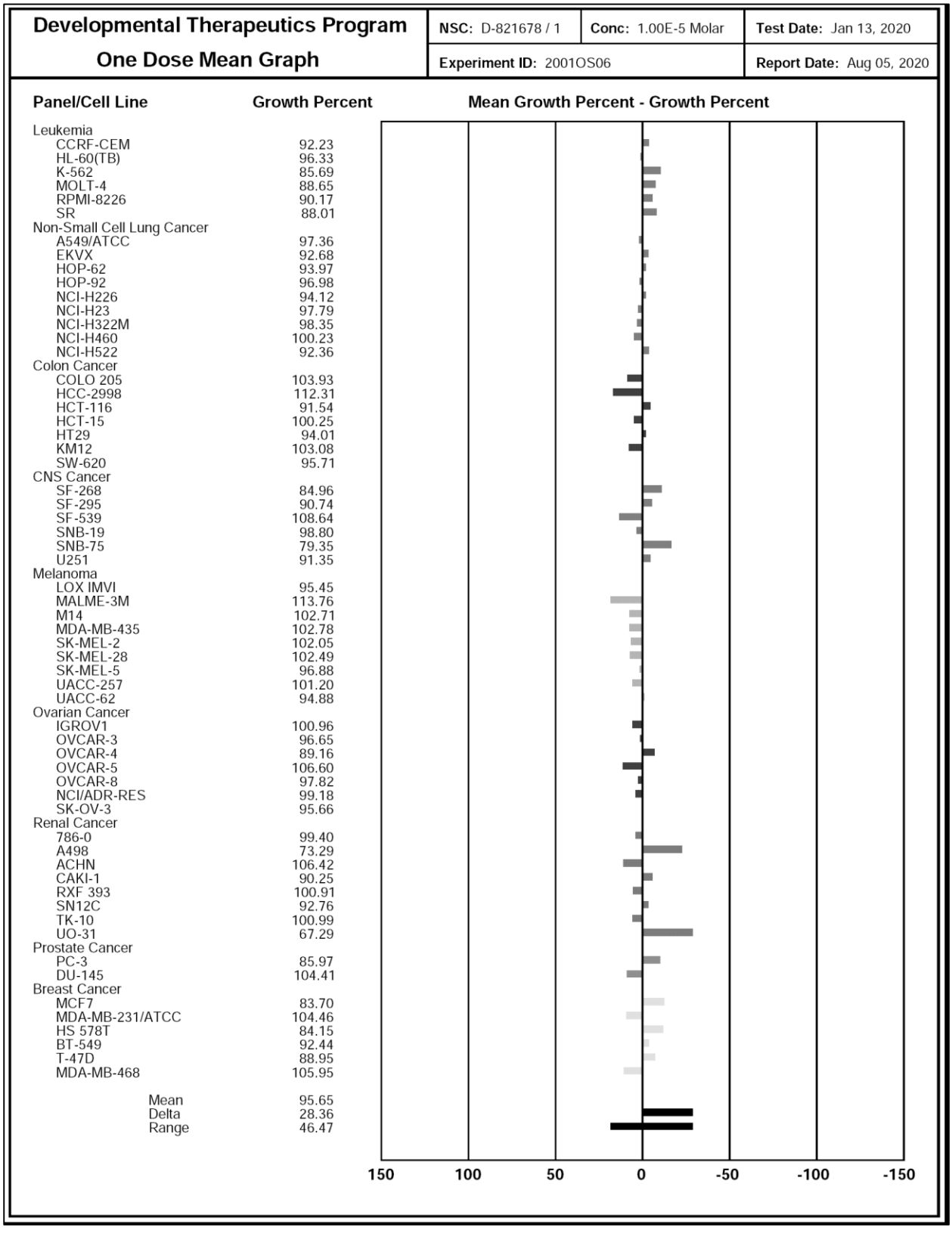

Figure 93: One dose mean graph for Compound **141c**.

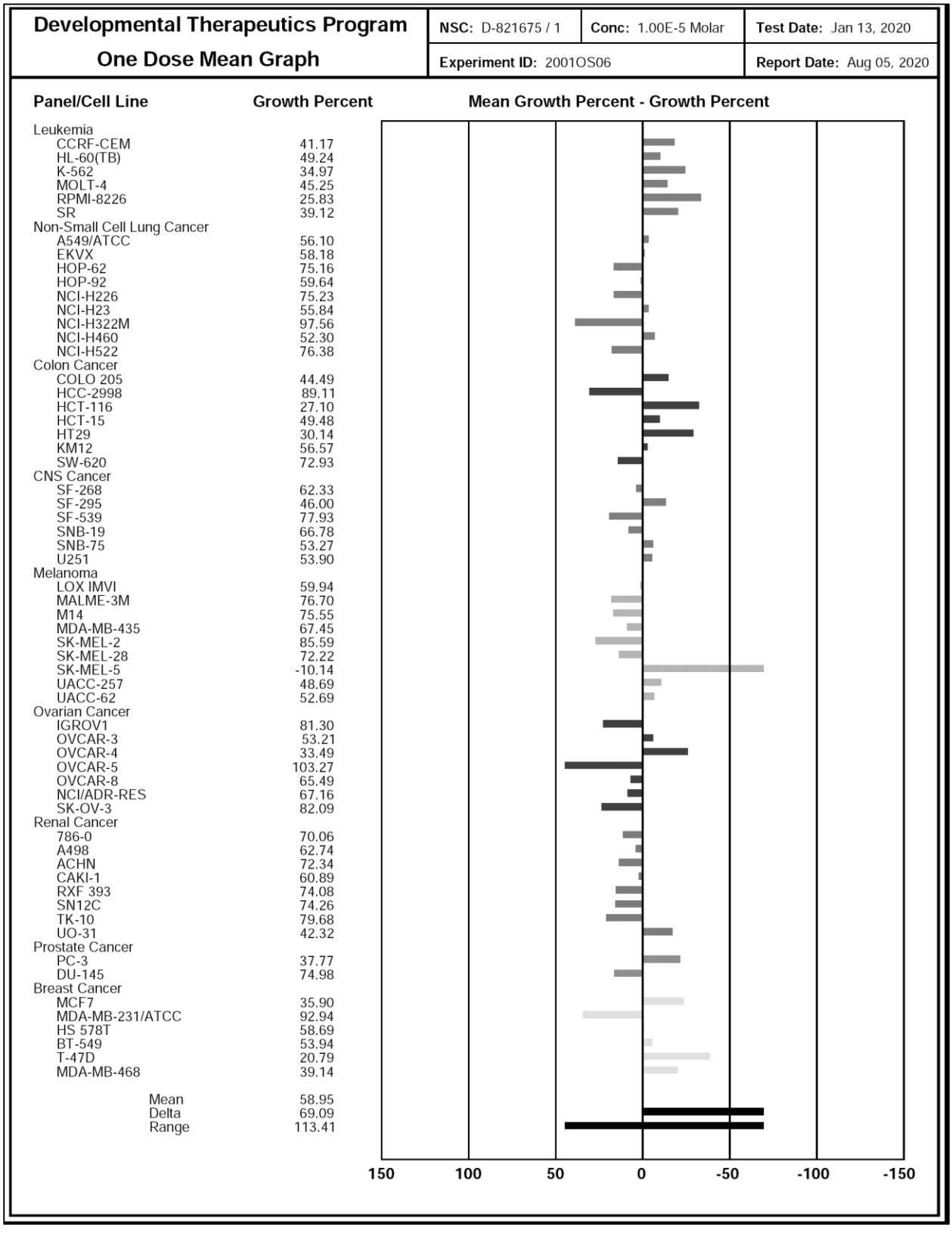

Compound 141d

Figure 94: One dose mean graph for Compound **141d**.

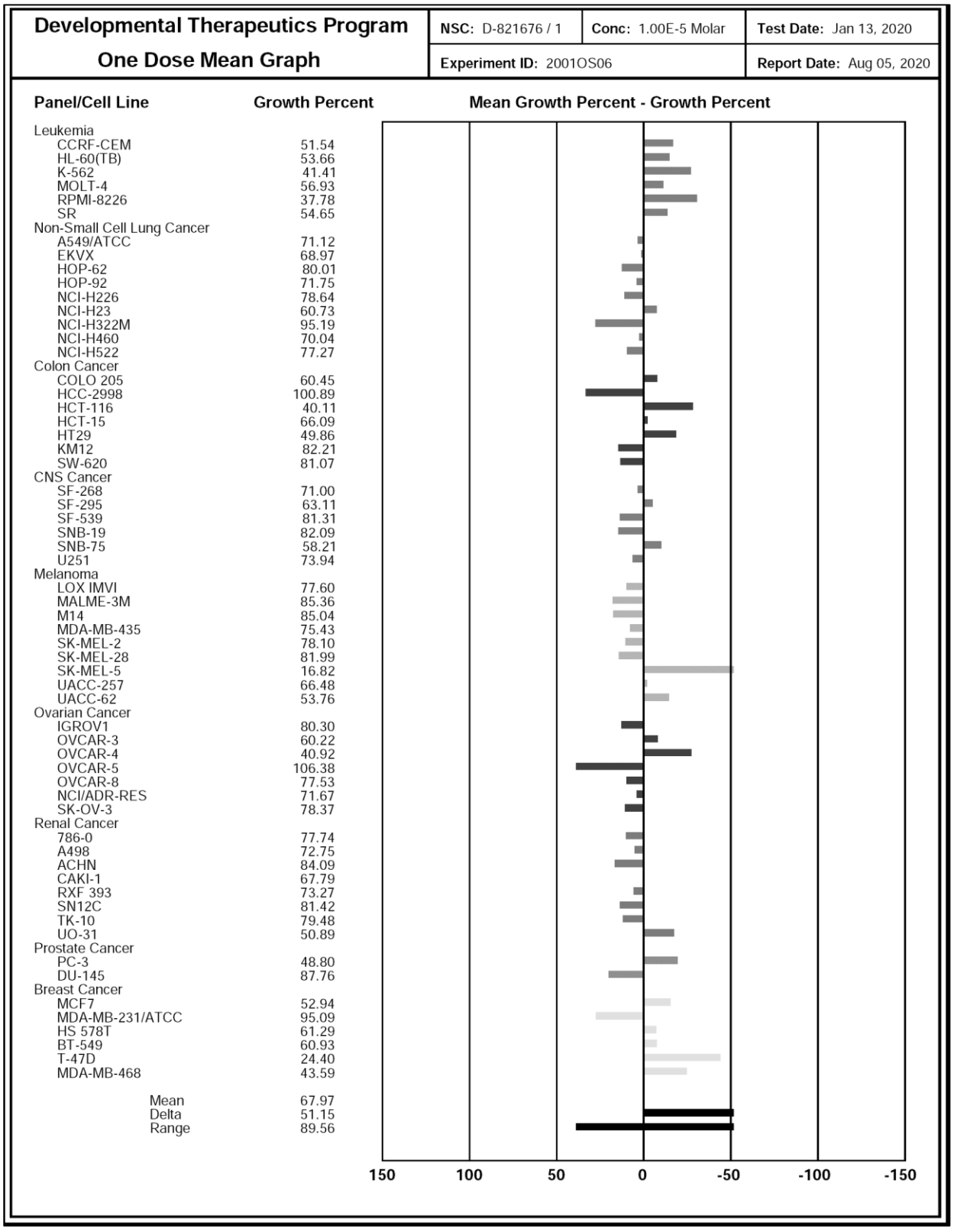

Figure 95: One dose mean graph for Compound **141f**.

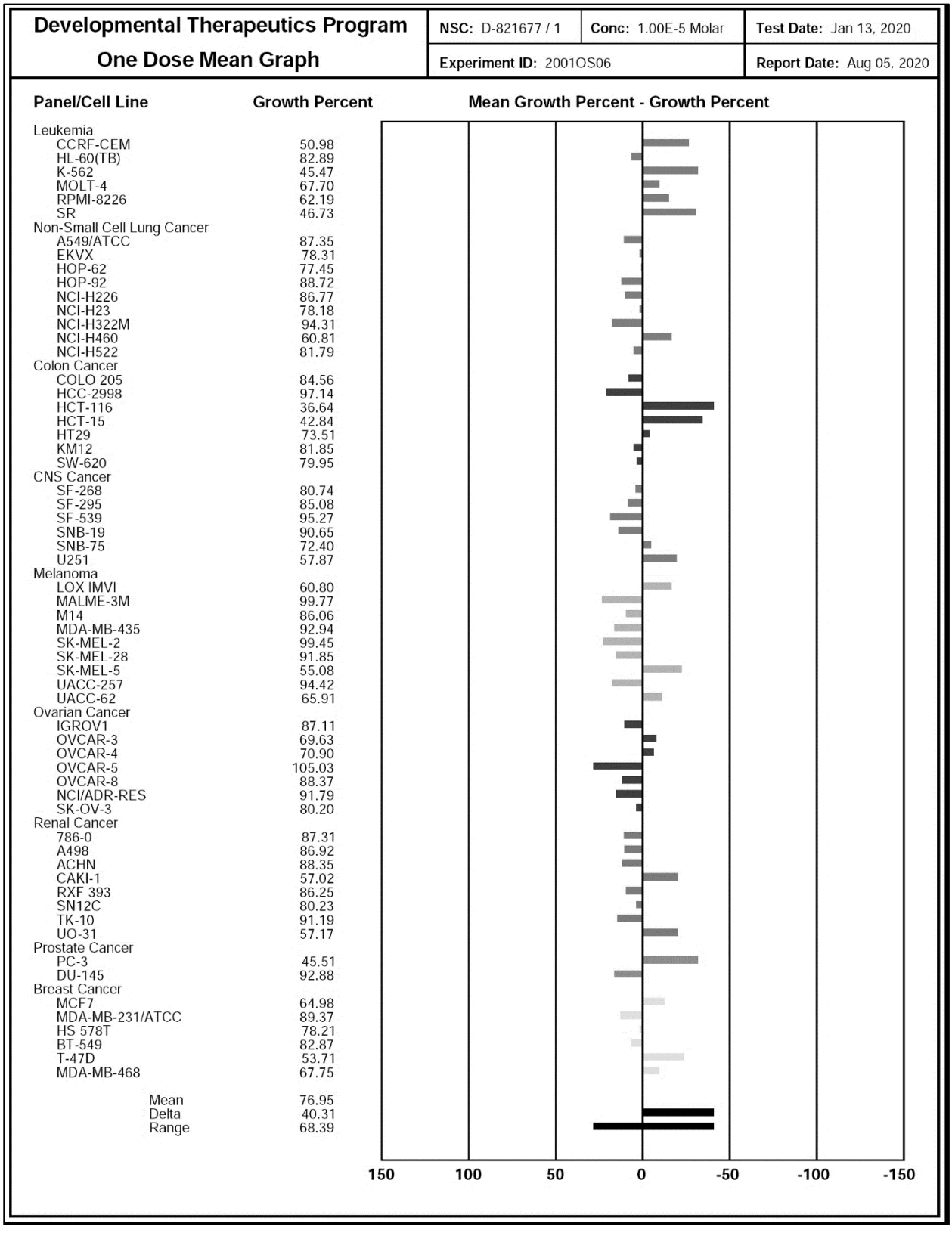

In vitro Testing Results at the National Cancer Institute (NCI), USA

Figure 96: *In vitro* testing results for Compound **139b**.

National Cancer Institute Developmental Therapeutics Program
In-Vitro Testing Results

NSC : D - 820119 / 1	Experiment ID : 1912NS99	Test Type : 08	Units : Molar
Report Date : January 11, 2020	Test Date : December 16, 2019	QNS :	MC :
COMI : LE91	Stain Reagent : SRB Dual-Pass Related	SSPL : 1B3N	

			Log10 Concentration												
	Time		Mean Optical Densities					Percent Growth							
Panel/Cell Line	Zero	Ctrl	-8.0	-7.0	-6.0	-5.0	-4.0	-8.0	-7.0	-6.0	-5.0	-4.0	GI50	TGI	LC50
Leukemia															
CCRF-CEM	0.487	2.914	2.974	2.922	2.652	0.481	0.510	102	100	89	-1	1	2.71E-6	.	> 1.00E-4
HL-60(TB)	0.406	2.183	1.932	2.036	1.936	0.447	0.457	86	92	86	2	3	2.70E-6	> 1.00E-4	> 1.00E-4
K-562	0.188	2.367	2.372	2.130	2.210	0.338	0.320	100	89	93	7	6	3.15E-6	> 1.00E-4	> 1.00E-4
MOLT-4	0.547	2.770	2.824	2.852	2.657	0.636	0.608	102	104	95	4	3	3.12E-6	> 1.00E-4	> 1.00E-4
RPMI-8226	0.785	2.894	2.888	2.888	2.671	0.558	0.588	100	100	89	-29	-25	2.15E-6	5.69E-6	> 1.00E-4
SR	0.274	1.603	1.443	1.460	1.338	0.316	0.316	88	89	80	3	3	2.46E-6	> 1.00E-4	> 1.00E-4
Non-Small Cell Lung Cancer															
A549/ATCC	0.451	2.507	2.425	2.330	2.466	0.414	0.288	96	91	98	-8	-36	2.83E-6	8.37E-6	> 1.00E-4
EKVX	0.739	2.159	2.111	2.027	2.028	0.340	0.090	97	91	91	-54	-88	1.91E-6	4.23E-6	9.38E-6
HOP-62	0.765	2.634	2.633	2.553	2.663	0.621	0.330	100	96	102	-19	-57	2.68E-6	6.97E-6	6.60E-5
HOP-92	1.240	1.907	1.803	1.754	1.712	1.205	0.747	84	77	71	-3	-40	1.91E-6	9.14E-6	> 1.00E-4
NCI-H226	0.851	1.538	1.487	1.519	1.505	1.021	0.545	93	97	95	25	-36	4.38E-6	2.55E-5	> 1.00E-4
NCI-H23	0.613	1.933	1.880	1.862	1.856	0.257	0.197	96	95	94	-58	-68	1.95E-6	4.15E-6	8.85E-6
NCI-H322M	0.736	2.158	2.073	2.021	2.030	0.416	0.024	94	90	91	-44	-97	2.02E-6	4.75E-6	1.32E-5
NCI-H460	0.403	3.139	3.175	3.169	3.162	0.167	0.115	101	101	101	-59	-72	2.08E-6	4.29E-6	8.82E-6
NCI-H522	1.646	3.296	3.263	3.254	3.219	2.135	1.683	98	97	95	30	2	4.89E-6	> 1.00E-4	> 1.00E-4
Colon Cancer															
COLO 205	0.438	1.938	2.017	1.890	1.924	0.219	0.236	105	97	99	-50	-46	2.13E-6	4.61E-6	.
HCC-2998	0.812	2.712	2.557	2.559	2.594	0.158	0.088	92	92	94	-81	-89	1.78E-6	3.45E-6	6.68E-6
HCT-116	0.279	2.366	2.314	2.208	2.166	0.084	0.030	98	92	90	-70	-89	1.79E-6	3.66E-6	7.51E-6
HCT-15	0.280	1.739	1.718	1.648	1.601	0.116	0.092	99	94	91	-59	-67	1.87E-6	4.05E-6	8.76E-6
HT29	0.402	2.477	2.462	2.389	2.357	0.159	0.109	99	96	94	-60	-73	1.93E-6	4.07E-6	8.56E-6
KM12	0.607	3.019	3.088	3.020	2.999	0.236	0.196	103	100	99	-61	-68	2.03E-6	4.15E-6	8.51E-6
SW-620	0.319	2.444	2.426	2.423	2.344	0.084	0.062	99	99	95	-74	-81	1.85E-6	3.66E-6	7.23E-6
CNS Cancer															
SF-268	0.931	2.967	2.884	2.884	2.898	0.961	0.681	96	96	97	1	-27	3.09E-6	1.12E-5	> 1.00E-4
SF-295	0.443	2.128	2.153	2.009	2.153	0.171	0.053	102	93	101	-62	-88	2.07E-6	4.19E-6	8.50E-6
SF-539	0.878	2.905	2.811	2.817	2.840	0.099	0.009	95	96	97	-89	-99	1.79E-6	3.32E-6	6.18E-6
SNB-19	0.591	2.168	2.040	2.056	2.057	0.267	0.049	92	93	93	-55	-92	1.95E-6	4.25E-6	9.26E-6
SNB-75	2.041	3.178	2.993	3.059	2.976	2.478	2.060	84	90	82	38	2	5.44E-6	> 1.00E-4	> 1.00E-4
U251	0.464	2.379	2.345	2.254	2.235	0.181	0.047	98	93	92	-61	-90	1.89E-6	4.00E-6	8.47E-6
Melanoma															
LOX IMVI	0.303	2.024	1.902	1.849	1.812	0.066	0.035	93	90	88	-78	-89	1.69E-6	3.37E-6	6.75E-6
MALME-3M	0.604	1.414	1.370	1.341	1.345	0.693	0.471	95	91	92	11	-22	3.27E-6	2.14E-5	> 1.00E-4
M14	0.497	2.107	2.054	2.041	2.051	0.595	0.365	97	96	97	6	-27	3.27E-6	1.54E-5	> 1.00E-4
MDA-MB-435	0.791	3.214	3.198	3.203	3.203	1.571	0.885	99	100	100	32	4	5.44E-6	> 1.00E-4	> 1.00E-4
SK-MEL-2	1.053	2.159	2.074	2.034	2.108	0.929	0.578	92	89	95	-12	-45	2.65E-6	7.76E-6	> 1.00E-4
SK-MEL-28	0.642	2.000	1.975	1.966	1.936	0.639	0.355	98	98	95	.	-45	2.97E-6	9.87E-6	> 1.00E-4
SK-MEL-5	0.996	3.323	3.299	3.288	3.305	2.002	1.342	99	98	99	43	15	7.56E-6	> 1.00E-4	> 1.00E-4
UACC-257	1.150	2.795	2.749	2.635	2.642	1.701	1.581	97	90	91	33	26	5.14E-6	> 1.00E-4	> 1.00E-4
UACC-62	0.905	3.021	2.934	2.863	2.896	0.392	0.247	96	93	94	-57	-73	1.96E-6	4.21E-6	9.02E-6
Ovarian Cancer															
IGROV1	0.436	1.986	1.951	1.885	1.793	0.077	0.097	98	94	88	-82	-78	1.66E-6	3.27E-6	6.44E-6
OVCAR-3	0.529	1.850	1.893	1.858	1.751	0.141	0.060	103	101	93	-73	-89	1.80E-6	3.61E-6	7.23E-6
OVCAR-4	0.815	1.931	1.968	1.878	1.940	0.811	0.100	103	95	101	.	-88	3.17E-6	9.88E-6	3.69E-5
OVCAR-5	0.564	1.338	1.321	1.300	1.315	0.175	0.044	98	95	97	-69	-92	1.92E-6	3.84E-6	7.68E-6
OVCAR-8	0.646	2.901	2.881	2.856	2.755	0.744	0.723	99	98	93	4	3	3.08E-6	> 1.00E-4	> 1.00E-4
NCI/ADR-RES	0.454	1.544	1.521	1.508	1.465	0.465	0.298	98	97	93	1	-34	2.92E-6	1.06E-5	> 1.00E-4
SK-OV-3	0.661	1.881	1.748	1.777	1.865	0.786	0.652	89	91	99	10	-1	3.55E-6	7.53E-5	> 1.00E-4
Renal Cancer															
786-0	0.498	2.127	2.007	1.951	2.037	0.236	0.103	93	89	94	-53	-79	2.00E-6	4.38E-6	9.58E-6
A498	1.944	2.497	2.192	2.275	2.261	1.850	1.639	45	60	57	-5	-16	.	8.36E-6	> 1.00E-4
ACHN	0.301	1.222	1.198	1.198	1.195	0.029	0.044	97	97	97	-91	-85	1.78E-6	3.29E-6	6.08E-6
CAKI-1	1.105	3.076	2.897	2.890	2.839	1.533	0.843	91	91	88	22	-24	3.74E-6	3.00E-5	> 1.00E-4
RXF 393	1.595	2.363	2.305	2.264	2.153	0.778	0.285	92	87	73	-51	-82	1.52E-6	3.86E-6	9.78E-6
SN12C	0.525	2.199	2.104	2.104	2.072	0.383	0.266	94	94	92	-27	-49	2.27E-6	5.94E-6	> 1.00E-4
TK-10	1.057	2.023	1.854	1.752	1.877	0.755	0.269	83	72	85	-29	-75	2.03E-6	5.60E-6	2.92E-5
UO-31	0.658	1.965	1.797	1.734	1.710	0.105	0.012	87	82	80	-84	-98	1.53E-6	3.08E-6	6.20E-6
Prostate Cancer															
PC-3	0.525	2.132	2.058	2.094	1.903	0.172	0.127	95	98	86	-67	-76	1.71E-6	3.63E-6	7.70E-6
DU-145	0.888	3.006	3.007	2.969	2.981	1.522	0.669	100	98	99	30	-25	5.11E-6	3.53E-5	> 1.00E-4
Breast Cancer															
MCF7	0.517	2.575	2.438	2.389	2.203	0.331	0.126	93	91	82	-36	-76	1.87E-6	4.95E-6	2.25E-5
MDA-MB-231/ATCC	0.686	1.678	1.624	1.610	1.643	0.590	0.573	95	93	96	-14	-16	2.63E-6	7.46E-6	> 1.00E-4
HS 578T	1.444	2.516	2.418	2.470	2.415	1.613	1.554	91	96	91	16	10	3.49E-6	> 1.00E-4	> 1.00E-4
BT-549	0.928	2.081	2.007	1.941	2.028	0.598	0.257	94	88	95	-36	-72	2.22E-6	5.35E-6	2.47E-5
T-47D	0.994	2.332	2.241	2.147	1.996	0.416	0.437	93	86	75	-58	-56	1.54E-6	3.65E-6	8.68E-6
MDA-MB-468	0.779	1.544	1.527	1.429	1.489	0.240	0.138	98	85	93	-69	-82	1.84E-6	3.74E-6	7.61E-6

Figure 97: Log 10 concentration of compound **139b**.

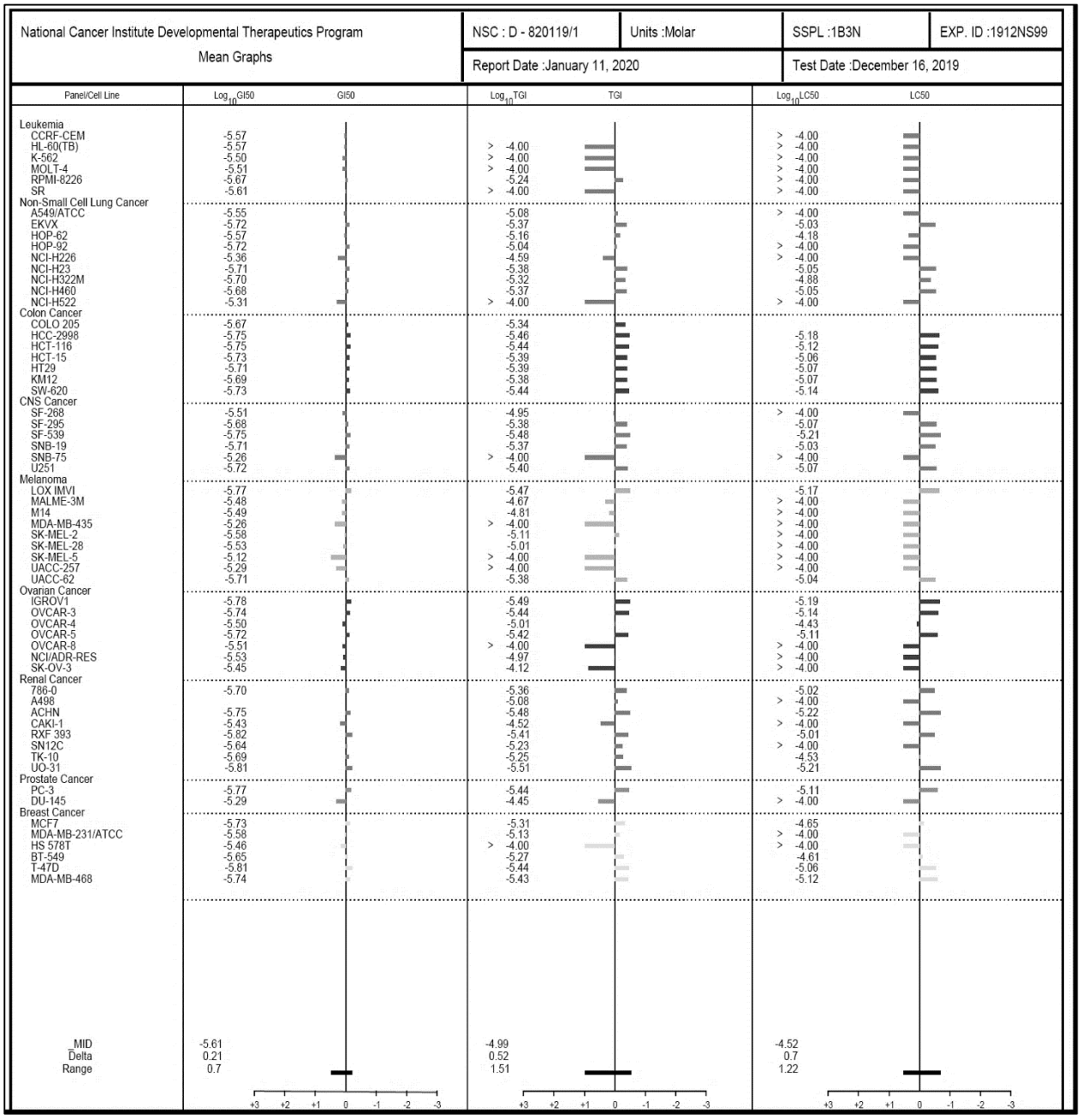

Figure 98: *In vitro* testing results for Compound **140c**.

National Cancer Institute Developmental Therapeutics Program
In-Vitro Testing Results

NSC : D - 821671 / 1	Experiment ID : 2003NS22	Test Type : 08	Units : Molar
Report Date : March 28, 2020	Test Date : March 02, 2020	QNS :	MC :
COMI : LE 155	Stain Reagent : SRB Dual-Pass Related	SSPL : 1B3N	

		Log10 Concentration													
	Time	Mean Optical Densities						Percent Growth							
Panel/Cell Line	Zero	Ctrl	-8.0	-7.0	-6.0	-5.0	-4.0	-8.0	-7.0	-6.0	-5.0	-4.0	GI50	TGI	LC50
Leukemia															
CCRF-CEM	0.510	2.658	2.693	2.672	2.191	0.587	0.623	102	101	78	4	5	2.39E-6	> 1.00E-4	> 1.00E-4
HL-60(TB)	0.825	3.183	3.200	3.161	1.224	0.693	0.654	101	99	17	-16	-21	3.95E-7	3.26E-6	> 1.00E-4
K-562	0.235	2.239	2.266	2.311	1.593	0.211	0.273	101	104	68	-10	2	1.69E-6	.	> 1.00E-4
MOLT-4	0.763	3.141	3.136	3.080	2.106	0.627	0.668	100	97	56	-18	-13	1.22E-6	5.76E-6	> 1.00E-4
RPMI-8226	0.711	2.867	2.845	2.893	2.410	0.676	0.763	99	101	79	-5	2	2.21E-6	.	> 1.00E-4
SR	0.391	1.744	1.672	1.749	1.275	0.451	0.396	95	100	65	4	.	1.78E-6	> 1.00E-4	> 1.00E-4
Non-Small Cell Lung Cancer															
A549/ATCC	0.425	2.293	2.253	2.359	2.198	0.290	0.310	98	104	95	-32	-27	2.26E-6	5.61E-6	> 1.00E-4
EKVX	0.561	2.078	1.966	1.791	1.596	0.234	0.135	93	81	68	-58	-76	1.39E-6	3.46E-6	8.60E-6
HOP-62	1.398	2.939	2.773	2.718	2.742	0.840	0.193	89	86	87	-40	-86	1.96E-6	4.85E-6	1.65E-5
HOP-92	1.117	1.845	1.793	1.720	1.645	0.625	0.574	93	83	72	-44	-49	1.56E-6	4.19E-6	> 1.00E-4
NCI-H226	0.785	2.033	1.955	1.903	1.812	0.202	0.177	94	90	82	-74	-77	1.61E-6	3.35E-6	6.99E-6
NCI-H23	0.897	2.486	2.350	2.230	2.007	0.435	0.392	91	84	70	-52	-56	1.46E-6	3.76E-6	9.72E-6
NCI-H322M	0.676	1.772	1.686	1.637	1.602	0.019	-0.002	92	88	85	-97	-100	1.55E-6	2.92E-6	5.50E-6
NCI-H460	0.317	2.930	2.968	2.996	2.840	0.112	0.121	101	103	97	-65	-62	1.94E-6	3.97E-6	8.11E-6
NCI-H522	0.874	2.183	2.023	2.018	1.778	0.508	0.666	88	87	69	-42	-24	1.49E-6	4.19E-6	> 1.00E-4
Colon Cancer															
COLO 205	0.722	2.900	2.815	2.819	2.732	0.327	0.311	96	96	92	-55	-57	1.94E-6	4.24E-6	9.28E-6
HCC-2998	0.774	2.533	2.347	2.385	2.299	0.093	-0.001	89	92	87	-88	-100	1.62E-6	3.14E-6	6.06E-6
HCT-116	0.304	2.842	2.780	2.624	1.244	0.144	0.114	98	91	37	-53	-63	5.77E-7	2.58E-6	9.31E-6
HCT-15	0.260	2.399	2.292	2.235	1.868	0.097	0.090	95	92	75	-63	-65	1.52E-6	3.50E-6	8.07E-6
HT29	0.396	2.543	2.491	2.518	2.468	0.430	0.412	98	99	97	2	1	3.09E-6	> 1.00E-4	> 1.00E-4
KM12	0.643	3.135	3.139	3.108	2.922	0.609	0.309	100	99	91	-5	-52	2.68E-6	8.80E-6	9.05E-5
SW-620	0.360	2.637	2.540	2.422	2.243	0.105	0.138	96	91	83	-71	-62	1.63E-6	3.45E-6	7.30E-6
CNS Cancer															
SF-268	0.756	2.524	2.400	2.302	2.107	0.446	0.533	93	87	76	-41	-29	1.68E-6	4.48E-6	> 1.00E-4
SF-295	0.953	3.229	3.190	3.141	3.060	0.031	0.012	98	96	93	-97	-99	1.68E-6	3.08E-6	5.66E-6
SF-539	0.702	2.401	2.390	2.249	2.270	0.041	0.099	99	91	92	-94	-86	1.69E-6	3.12E-6	5.79E-6
SNB-19	0.901	2.530	2.412	2.338	2.299	0.232	-0.014	93	88	86	-74	-100	1.67E-6	3.44E-6	7.05E-6
SNB-75	1.913	2.894	2.412	2.513	2.395	0.726	0.232	51	61	49	-62	-88	8.43E-7	2.76E-6	7.79E-6
U251	0.417	2.043	1.954	1.921	1.616	0.238	0.272	95	93	74	-43	-35	1.60E-6	4.28E-6	> 1.00E-4
Melanoma															
LOX IMVI	0.342	2.445	2.262	2.165	1.102	0.082	0.171	91	87	36	-76	-50	5.32E-7	2.10E-6	5.86E-6
MALME-3M	0.733	1.265	1.243	1.189	0.863	0.006	0.008	96	86	24	-99	-99	3.83E-7	1.58E-6	4.00E-6
M14	0.498	2.251	2.097	2.165	1.989	0.104	0.142	91	95	85	-79	-71	1.63E-6	3.30E-6	6.65E-6
MDA-MB-435	0.572	2.542	2.535	2.592	0.112	0.034	0.015	100	103	-80	-94	-97	1.94E-7	3.63E-7	6.82E-7
SK-MEL-2	1.118	2.596	2.574	2.537	2.311	0.600	0.553	98	96	81	-46	-51	1.74E-6	4.32E-6	7.27E-5
SK-MEL-28	0.802	2.118	2.161	2.205	2.171	0.049	0.029	103	107	104	-94	-96	1.87E-6	3.35E-6	6.00E-6
SK-MEL-5	0.878	3.175	3.157	3.055	2.620	0.031	0.045	99	95	76	-96	-95	1.41E-6	2.75E-6	5.37E-6
UACC-257	1.032	2.464	2.403	2.420	2.191	0.190	0.236	96	97	81	-82	-77	1.55E-6	3.15E-6	6.39E-6
UACC-62	1.131	2.967	2.918	2.869	2.560	0.525	0.157	97	95	78	-54	-86	1.63E-6	3.91E-6	9.38E-6
Ovarian Cancer															
IGROV1	0.483	1.984	1.898	1.725	1.324	0.219	0.112	94	83	56	-55	-77	1.13E-6	3.21E-6	9.08E-6
OVCAR-3	0.492	1.714	1.728	1.571	0.664	0.112	0.029	101	88	14	-77	-94	3.28E-7	1.43E-6	5.03E-6
OVCAR-4	1.065	1.998	1.968	1.896	1.685	0.036	0.021	97	89	66	-97	-98	1.26E-6	2.56E-6	5.18E-6
OVCAR-5	0.797	2.041	1.878	1.950	1.994	0.368	0.398	87	93	96	-54	-50	2.03E-6	4.37E-6	9.42E-6
OVCAR-8	0.451	2.377	2.242	2.226	1.866	0.486	0.294	93	92	73	2	-35	2.13E-6	1.12E-5	> 1.00E-4
NCI/ADR-RES	0.567	2.184	2.180	2.104	1.880	0.522	0.597	100	95	81	-8	2	2.24E-6	.	> 1.00E-4
SK-OV-3	1.041	2.044	2.026	1.990	1.899	1.272	0.632	98	95	85	23	-39	3.70E-6	2.34E-5	> 1.00E-4
Renal Cancer															
786-0	1.016	3.077	3.047	3.067	2.993	0.701	0.711	99	99	96	-31	-30	2.30E-6	5.70E-6	> 1.00E-4
A498	1.819	2.610	2.548	2.561	2.574	2.229	1.360	92	94	95	52	-25	1.05E-5	4.70E-5	> 1.00E-4
ACHN	0.368	1.804	1.664	1.608	1.437	0.051	0.064	90	86	74	-86	-83	1.42E-6	2.91E-6	5.96E-6
CAKI-1	0.530	1.911	1.693	1.549	1.351	0.155	0.025	84	74	59	-71	-95	1.18E-6	2.86E-6	6.92E-6
RXF 393	0.962	1.803	1.770	1.708	1.567	0.058	0.026	96	89	72	-94	-97	1.35E-6	2.71E-6	5.43E-6
SN12C	0.763	2.720	2.573	2.434	1.971	0.178	0.253	93	85	62	-77	-67	1.22E-6	2.79E-6	6.42E-6
TK-10	1.162	1.919	1.905	2.253	2.492	0.962	0.343	98	144	176	-17	-70	4.48E-6	8.14E-6	4.13E-5
UO-31	0.618	1.662	1.320	1.214	1.108	0.004	-0.010	67	57	47	-99	-100	4.96E-7	2.09E-6	4.60E-6
Prostate Cancer															
PC-3	0.560	1.738	1.601	1.481	1.283	0.540	0.371	88	78	61	-4	-34	1.49E-6	8.81E-6	> 1.00E-4
DU-145	0.439	2.029	2.114	2.065	2.014	0.066	0.102	105	102	99	-85	-77	1.85E-6	3.45E-6	6.46E-6
Breast Cancer															
MCF7	0.368	2.366	2.206	2.206	1.576	0.168	0.159	92	92	60	-54	-57	1.23E-6	3.36E-6	9.17E-6
MDA-MB-231/ATCC	0.661	1.705	1.580	1.485	1.257	0.581	0.558	88	79	57	-12	-16	1.27E-6	6.69E-6	> 1.00E-4
HS 578T	1.398	2.514	2.447	2.367	2.282	1.189	1.362	94	87	79	-15	-3	2.04E-6	6.93E-6	> 1.00E-4
BT-549	1.363	2.471	2.453	2.337	2.281	0.058	0.054	98	88	83	-96	-96	1.53E-6	2.91E-6	5.54E-6
T-47D	1.004	2.375	2.272	2.188	2.067	0.880	0.821	93	86	78	-12	-18	2.03E-6	7.29E-6	> 1.00E-4
MDA-MB-468	0.883	2.186	2.108	2.189	2.120	0.615	0.443	94	100	95	-30	-50	2.28E-6	5.72E-6	> 1.00E-4

Figure 99: Log 10 concentration of compound **140c**.

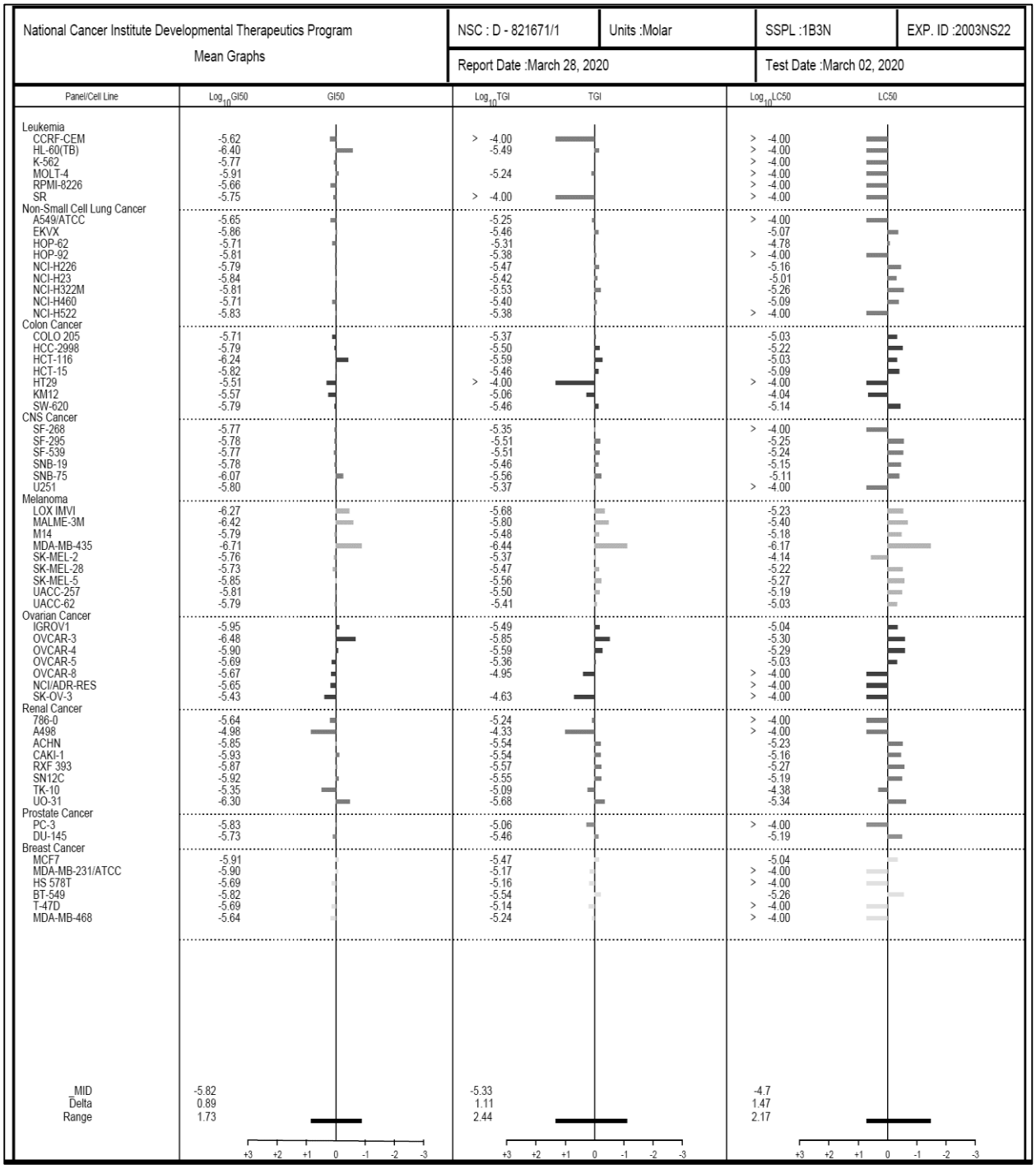

Figure 100: *In vitro* testing results for Compound **140d**.

National Cancer Institute Developmental Therapeutics Program
In-Vitro Testing Results

NSC : D - 821670 / 1	Experiment ID : 2003NS22	Test Type : 08	Units : Molar
Report Date : March 28, 2020	Test Date : March 02, 2020	QNS :	MC :
COMI : LE142	Stain Reagent : SRB Dual-Pass Related	SSPL : 1B3N	

			Log10 Concentration												
	Time		Mean Optical Densities					Percent Growth							
Panel/Cell Line	Zero	Ctrl	-8.5	-7.5	-6.5	-5.5	-4.5	-8.5	-7.5	-6.5	-5.5	-4.5	GI50	TGI	LC50
Leukemia															
CCRF-CEM	0.510	2.658	2.684	2.733	2.525	0.551	0.513	101	103	94	2	.	9.98E-7	> 3.33E-5	> 3.33E-5
HL-60(TB)	0.825	3.183	3.154	3.177	3.012	0.622	0.650	99	100	93	-25	-21	7.70E-7	2.05E-6	> 3.33E-5
K-562	0.235	2.239	2.127	2.138	1.935	0.279	0.238	94	95	85	2	.	8.79E-7	> 3.33E-5	> 3.33E-5
MOLT-4	0.763	3.141	3.098	3.043	2.613	0.525	0.514	98	96	78	-31	-33	5.99E-7	1.72E-6	> 3.33E-5
RPMI-8226	0.711	2.867	2.841	2.789	2.591	0.537	0.507	99	96	87	-24	-29	7.17E-7	2.01E-6	> 3.33E-5
SR	0.391	1.744	1.730	1.665	1.476	0.374	0.342	99	94	80	-4	-13	7.57E-7	2.95E-6	> 3.33E-5
Non-Small Cell Lung Cancer															
A549/ATCC	0.425	2.293	2.221	2.332	2.306	0.313	0.233	96	102	101	-26	-45	8.35E-7	2.07E-6	> 3.33E-5
EKVX	0.561	2.078	1.923	1.879	1.691	0.202	0.209	90	87	75	-64	-63	5.01E-7	1.15E-6	2.64E-6
HOP-62	1.398	2.939	2.805	2.765	2.668	1.998	0.061	91	89	82	39	-96	1.85E-6	6.48E-6	1.53E-5
HOP-92	1.117	1.845	1.810	1.754	1.713	1.008	0.339	95	87	82	-10	-70	7.41E-7	2.60E-6	1.56E-5
NCI-H226	0.785	2.033	2.007	2.012	1.831	0.892	0.103	98	98	84	9	-87	9.36E-7	4.09E-6	1.37E-5
NCI-H23	0.897	2.486	2.396	2.379	2.089	0.541	0.510	94	93	75	-40	-43	5.50E-7	1.50E-6	> 3.33E-5
NCI-H322M	0.676	1.772	1.712	1.697	1.646	1.030	0.016	95	93	89	32	-98	1.61E-6	5.90E-6	1.43E-5
NCI-H460	0.317	2.930	2.962	3.018	2.867	0.390	0.070	101	103	98	3	-78	1.06E-6	3.60E-6	1.50E-5
NCI-H522	0.874	2.183	1.979	2.038	1.890	0.446	0.384	84	89	78	-49	-56	5.51E-7	1.37E-6	4.64E-6
Colon Cancer															
COLO 205	0.722	2.900	2.893	2.813	2.709	1.915	0.208	100	96	91	55	-71	3.63E-6	9.06E-6	2.26E-5
HCC-2998	0.774	2.533	2.394	2.612	2.473	0.728	0.052	92	104	97	-6	-93	9.48E-7	2.91E-6	1.06E-5
HCT-116	0.304	2.842	2.750	2.701	2.520	0.194	0.061	96	94	87	-36	-80	6.67E-7	1.70E-6	6.89E-6
HCT-15	0.260	2.399	2.248	2.334	2.028	0.084	0.079	93	97	83	-68	-70	5.49E-7	1.18E-6	2.54E-6
HT29	0.396	2.543	2.518	2.590	2.566	0.533	0.396	99	102	101	6	.	1.15E-6	3.18E-5	> 3.33E-5
KM12	0.643	3.135	3.098	3.093	2.997	0.676	0.354	99	98	94	1	-45	9.99E-7	3.56E-6	> 3.33E-5
SW-620	0.360	2.637	2.601	2.471	2.234	0.125	0.086	98	93	82	-65	-76	5.51E-7	1.20E-6	2.62E-6
CNS Cancer															
SF-268	0.756	2.524	2.399	2.329	2.190	0.487	0.412	93	89	81	-36	-46	6.15E-7	1.65E-6	> 3.33E-5
SF-295	0.953	3.229	3.163	3.177	3.058	0.314	0.012	97	98	92	-67	-99	6.15E-7	1.27E-6	2.60E-6
SF-539	0.702	2.401	2.354	2.309	2.255	0.029	0.048	97	95	91	-96	-93	5.54E-7	1.02E-6	1.89E-6
SNB-19	0.901	2.530	2.381	2.391	2.293	0.558	0.029	91	91	85	-38	-97	6.45E-7	1.64E-6	5.31E-6
SNB-75	1.913	2.894	2.471	2.439	2.380	0.223	0.031	57	54	48	-88	-98	1.32E-7	7.46E-7	1.74E-6
U251	0.417	2.043	1.893	1.916	1.678	0.125	0.176	91	92	78	-70	-58	5.12E-7	1.12E-6	2.43E-6
Melanoma															
LOX IMVI	0.342	2.445	2.302	2.267	1.655	0.063	0.049	93	92	62	-82	-86	4.06E-7	9.04E-7	2.01E-6
MALME-3M	0.733	1.265	1.245	1.197	1.110	0.008	-0.005	96	87	71	-99	-100	4.42E-7	8.70E-7	1.71E-6
M14	0.498	2.251	2.136	2.160	2.066	0.055	0.075	93	95	89	-89	-85	5.54E-7	1.06E-6	2.01E-6
MDA-MB-435	0.572	2.542	2.447	2.595	2.526	0.034	0.016	95	103	99	-94	-97	5.98E-7	1.09E-6	1.97E-6
SK-MEL-2	1.118	2.596	2.577	2.619	2.633	0.571	0.546	99	102	102	-49	-51	7.39E-7	1.58E-6	9.60E-6
SK-MEL-28	0.802	2.118	2.159	2.235	2.296	0.092	0.030	103	109	113	-89	-96	6.87E-7	1.21E-6	2.15E-6
SK-MEL-5	0.878	3.175	3.113	3.150	2.966	0.034	0.011	97	99	91	-96	-99	5.51E-7	1.02E-6	1.89E-6
UACC-257	1.032	2.464	2.379	2.394	2.378	0.190	0.109	94	95	94	-82	-89	5.93E-7	1.14E-6	2.20E-6
UACC-62	1.131	2.967	2.885	2.917	2.807	0.448	0.299	96	97	91	-60	-74	6.23E-7	1.33E-6	2.84E-6
Ovarian Cancer															
IGROV1	0.483	1.984	2.032	1.931	1.438	0.275	0.135	103	96	64	-43	-72	4.46E-7	1.31E-6	5.78E-6
OVCAR-3	0.492	1.714	1.729	1.645	1.408	0.232	0.072	101	94	75	-53	-85	5.22E-7	1.28E-6	3.16E-6
OVCAR-4	1.065	1.998	1.971	2.020	1.748	0.013	0.004	97	102	73	-99	-100	4.54E-7	8.87E-7	1.73E-6
OVCAR-5	0.797	2.041	1.926	1.946	1.941	0.169	0.349	91	92	92	-79	-56	5.86E-7	1.15E-6	2.26E-6
OVCAR-8	0.451	2.377	2.311	2.295	2.125	0.155	0.081	97	96	87	-66	-82	5.81E-7	1.24E-6	2.63E-6
NCI/ADR-RES	0.567	2.184	2.170	2.154	1.979	0.455	0.486	99	98	87	-20	-14	7.43E-7	2.17E-6	> 3.33E-5
SK-OV-3	1.041	2.044	2.012	2.070	1.842	1.734	0.048	97	103	80	69	-95	4.35E-6	8.75E-6	1.76E-5
Renal Cancer															
786-0	1.016	3.077	3.031	3.046	3.063	0.599	0.755	98	98	99	-41	-26	7.48E-7	1.70E-6	> 3.33E-5
A498	1.819	2.610	2.541	2.576	2.580	2.417	1.731	91	96	96	76	-5	6.93E-6	2.90E-5	> 3.33E-5
ACHN	0.368	1.804	1.770	1.632	1.503	0.030	0.173	98	88	79	-92	-53	4.92E-7	9.65E-7	1.89E-6
CAKI-1	0.530	1.911	1.751	1.620	1.389	0.452	0.019	88	79	62	-15	-97	4.80E-7	2.14E-6	8.98E-6
RXF 393	0.962	1.803	1.787	1.755	1.639	0.095	0.266	98	94	80	-90	-72	5.02E-7	9.86E-7	1.94E-6
SN12C	0.763	2.720	2.605	2.516	2.293	0.178	0.157	94	90	78	-77	-79	5.06E-7	1.07E-6	2.24E-6
TK-10	1.162	1.919	1.893	2.112	2.435	2.380	0.404	97	126	168	161	-65	1.03E-5	1.71E-5	2.85E-5
UO-31	0.618	1.662	1.398	1.248	1.142	0.176	-0.014	75	60	50	-72	-100	3.34E-7	8.60E-7	2.21E-6
Prostate Cancer															
PC-3	0.560	1.738	1.629	1.573	1.399	0.519	0.352	91	86	71	-7	-37	6.20E-7	2.69E-6	> 3.33E-5
DU-145	0.439	2.029	2.079	2.144	2.060	0.076	0.080	103	107	102	-83	-82	6.37E-7	1.19E-6	2.22E-6
Breast Cancer															
MCF7	0.368	2.366	2.179	2.278	2.078	0.145	0.155	91	96	86	-61	-58	5.83E-7	1.28E-6	2.82E-6
MDA-MB-231/ATCC	0.661	1.705	1.671	1.595	1.431	0.612	0.533	97	89	74	-7	-19	6.52E-7	2.69E-6	> 3.33E-5
HS 578T	1.398	2.514	2.391	2.400	2.450	1.048	1.150	89	90	94	-25	-18	7.82E-7	2.05E-6	> 3.33E-5
BT-549	1.363	2.471	2.428	2.403	2.311	0.049	0.074	96	94	86	-96	-95	5.22E-7	9.83E-7	1.85E-6
T-47D	1.004	2.375	2.232	2.245	2.115	0.849	0.514	90	90	81	-15	-49	6.98E-7	2.30E-6	> 3.33E-5
MDA-MB-468	0.883	2.186	2.175	2.184	2.089	0.662	0.479	99	100	93	-25	-46	7.66E-7	2.04E-6	> 3.33E-5

Figure 101: Log 10 concentration of compound **140d**.

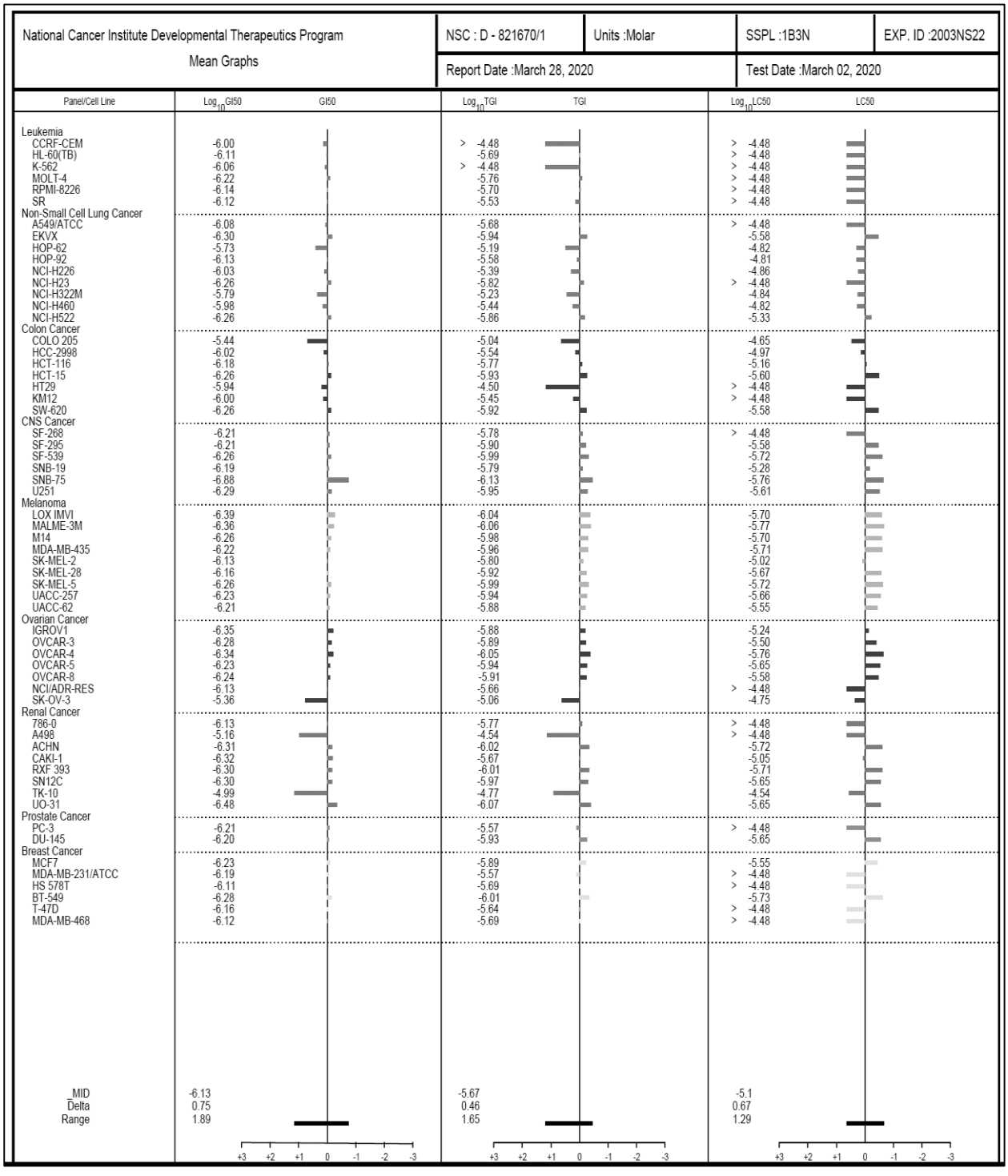

Figure 102: *In vitro* testing results for Compound **140e**.

National Cancer Institute Developmental Therapeutics Program
In-Vitro Testing Results

NSC : D - 821674 / 1	Experiment ID : 2003NS22	Test Type : 08	Units : Molar
Report Date : April 02, 2020	Test Date : March 02, 2020	QNS :	MC :
COMI : LE 146	Stain Reagent : SRB Dual-Pass Related	SSPL : 1B3N	

		Log10 Concentration												
	Time	Mean Optical Densities						Percent Growth						
Panel/Cell Line	Zero	Ctrl	-8.0	-7.0	-6.0	-5.0	-4.0	-8.0	-7.0	-6.0	-5.0	-4.0	GI50	TGI	LC50
Leukemia															
CCRF-CEM	0.510	2.691	2.630	2.639	2.283	0.590	0.602	97	98	81	4	4	2.53E-6	> 1.00E-4	> 1.00E-4
HL-60(TB)	0.825	3.183	3.125	3.148	2.871	0.642	0.618	98	99	87	-22	-25	2.18E-6	6.26E-6	> 1.00E-4
K-562	0.235	2.184	2.183	2.210	1.773	0.315	0.273	100	101	79	4	2	2.43E-6	> 1.00E-4	> 1.00E-4
MOLT-4	0.763	3.137	3.161	3.175	2.632	0.731	0.749	101	102	79	-4	-2	2.22E-6	8.89E-6	> 1.00E-4
RPMI-8226	0.711	2.827	2.751	2.749	2.295	0.587	0.610	96	96	75	-17	-14	1.86E-6	6.47E-6	> 1.00E-4
SR	0.391	1.715	1.751	1.686	1.241	0.383	0.405	103	98	64	-2	1	1.64E-6	.	> 1.00E-4
Non-Small Cell Lung Cancer															
A549/ATCC	0.425	2.366	2.391	2.502	2.329	0.310	0.303	101	107	98	-27	-29	2.42E-6	6.07E-6	> 1.00E-4
EKVX	0.561	2.124	1.997	1.837	1.596	0.664	0.211	92	82	66	7	-62	1.87E-6	1.25E-5	6.60E-5
HOP-62	1.398	3.018	2.921	2.826	2.776	1.877	0.052	94	88	85	30	-96	4.28E-6	1.72E-5	4.29E-5
HOP-92	1.117	1.906	1.841	1.775	1.680	1.206	0.449	92	83	71	11	-60	2.26E-6	1.44E-5	7.28E-5
NCI-H226	0.785	2.010	1.955	1.946	1.710	0.604	0.074	96	95	76	-23	-91	1.81E-6	5.83E-6	2.50E-5
NCI-H23	0.897	2.667	2.579	2.508	1.981	0.583	0.540	95	91	61	-35	-40	1.31E-6	4.32E-6	> 1.00E-4
NCI-H322M	0.676	1.848	1.854	1.771	1.655	0.445	-0.036	101	93	84	-34	-100	1.93E-6	5.13E-6	1.74E-5
NCI-H460	0.317	2.879	2.947	2.919	2.775	0.533	0.041	103	102	96	8	-87	3.35E-6	1.22E-5	4.09E-5
NCI-H522	0.874	2.268	2.141	2.122	1.874	0.567	0.515	91	89	72	-35	-41	1.60E-6	4.69E-6	> 1.00E-4
Colon Cancer															
COLO 205	0.722	2.950	3.030	2.931	2.898	0.882	0.271	104	99	98	7	-62	3.36E-6	1.27E-5	6.62E-5
HCC-2998	0.774	2.528	2.373	2.489	2.364	0.625	-0.018	91	98	91	-19	-100	2.34E-6	6.67E-6	2.40E-5
HCT-116	0.304	2.858	2.862	2.658	2.286	0.249	0.027	100	92	78	-18	-91	1.94E-6	6.45E-6	2.73E-5
HCT-15	0.260	2.347	2.327	2.380	1.865	0.069	0.062	99	102	77	-74	-76	1.51E-6	3.24E-6	6.96E-6
HT29	0.396	2.555	2.534	2.646	2.560	0.477	0.379	99	104	100	4	-4	3.32E-6	2.87E-5	> 1.00E-4
KM12	0.643	3.093	3.023	3.070	2.856	0.857	0.286	97	99	90	9	-56	3.12E-6	1.37E-5	8.18E-5
SW-620	0.360	2.619	2.511	2.403	2.397	0.174	0.116	95	90	90	-52	-68	1.92E-6	4.32E-6	9.71E-6
CNS Cancer															
SF-268	0.756	2.512	2.449	2.422	2.194	0.808	0.260	96	95	82	3	-66	2.54E-6	1.10E-5	5.91E-5
SF-295	0.953	3.260	3.215	3.218	3.186	1.225	-0.043	98	98	97	12	-100	3.55E-6	1.27E-5	3.57E-5
SF-539	0.702	2.407	2.330	2.390	2.284	0.012	0.001	95	99	93	-98	-100	1.67E-6	3.06E-6	5.58E-6
SNB-19	0.901	2.515	2.470	2.451	2.370	1.021	-0.063	97	96	91	7	-100	3.09E-6	1.17E-5	3.42E-5
SNB-75	1.913	2.863	2.631	2.632	2.476	1.596	-0.020	76	76	59	-17	-100	1.32E-6	6.04E-6	2.51E-5
U251	0.417	2.108	2.064	2.037	1.772	0.438	0.308	97	96	80	1	-26	2.41E-6	1.11E-5	> 1.00E-4
Melanoma															
LOX IMVI	0.342	2.434	2.259	2.297	1.374	0.108	-0.037	92	93	49	-68	-100	9.66E-7	2.62E-6	6.98E-6
MALME-3M	0.733	1.338	1.331	1.369	0.928	-0.012	-0.057	99	105	32	-100	-100	5.70E-7	1.75E-6	4.19E-6
M14	0.498	2.275	2.142	2.095	1.724	0.082	0.071	93	90	69	-84	-86	1.33E-6	2.83E-6	6.03E-6
MDA-MB-435	0.572	2.578	2.566	2.656	2.508	0.041	-0.045	99	104	96	-93	-100	1.76E-6	3.23E-6	5.93E-6
SK-MEL-2	1.118	2.690	2.693	2.624	2.564	0.951	0.546	100	96	92	-15	-51	2.47E-6	7.25E-6	9.29E-5
SK-MEL-28	0.802	2.155	2.218	2.299	2.237	0.468	-0.024	105	111	106	-42	-100	2.40E-6	5.22E-6	1.39E-5
SK-MEL-5	0.878	3.159	3.136	3.110	2.640	0.018	-0.046	99	98	77	-98	-100	1.43E-6	2.76E-6	5.32E-6
UACC-257	1.032	2.529	2.463	2.514	2.338	0.242	0.128	96	99	87	-77	-88	1.69E-6	3.41E-6	6.88E-6
UACC-62	1.131	3.034	2.942	2.942	2.675	0.371	0.186	95	95	81	-67	-84	1.62E-6	3.52E-6	7.66E-6
Ovarian Cancer															
IGROV1	0.483	2.061	1.991	1.780	1.355	0.355	0.079	96	82	55	-27	-84	1.16E-6	4.74E-6	2.58E-5
OVCAR-3	0.492	1.683	1.682	1.622	1.325	0.303	0.022	100	95	70	-38	-96	1.53E-6	4.42E-6	1.59E-5
OVCAR-4	1.065	1.968	2.027	1.965	1.723	0.666	-0.044	107	100	73	-37	-100	1.61E-6	4.58E-6	1.59E-5
OVCAR-5	0.797	2.042	2.041	2.070	1.996	0.163	0.352	100	102	96	-80	-56	1.83E-6	3.53E-6	6.79E-6
OVCAR-8	0.451	2.338	2.311	2.237	1.994	0.562	0.066	99	95	82	6	-85	2.62E-6	1.16E-5	4.10E-5
NCI/ADR-RES	0.567	2.195	2.204	2.182	1.806	0.479	0.495	101	99	76	-16	-13	1.93E-6	6.77E-6	> 1.00E-4
SK-OV-3	1.041	2.127	2.147	2.124	2.029	1.504	0.143	102	100	91	43	-86	7.03E-6	2.14E-5	5.23E-5
Renal Cancer															
786-0	1.016	3.147	3.143	3.104	3.097	0.905	0.501	100	98	98	-11	-51	2.75E-6	7.93E-6	9.61E-5
A498	1.819	2.582	2.581	2.617	2.548	2.449	1.448	100	105	96	83	-20	2.07E-5	6.34E-5	> 1.00E-4
ACHN	0.368	1.829	1.771	1.699	1.407	0.086	0.034	96	91	71	-77	-91	1.39E-6	3.03E-6	6.60E-6
CAKI-1	0.530	1.953	1.843	1.753	1.509	0.831	-0.019	92	86	69	21	-100	2.48E-6	1.49E-5	3.87E-5
RXF 393	0.962	1.743	1.716	1.754	1.606	0.584	-0.029	97	101	82	-39	-100	1.85E-6	4.75E-6	1.50E-5
SN12C	0.763	2.699	2.521	2.585	2.148	-0.005	-0.051	91	94	72	-100	-100	1.33E-6	2.61E-6	5.11E-6
TK-10	1.162	2.014	2.083	2.425	2.647	1.998	0.192	108	148	174	98	-84	1.84E-5	3.47E-5	6.54E-5
UO-31	0.618	1.756	1.409	1.326	1.177	0.237	-0.059	69	62	49	-62	-100	8.50E-7	2.77E-6	7.85E-6
Prostate Cancer															
PC-3	0.560	1.756	1.672	1.572	1.313	0.569	0.412	93	85	63	1	-26	1.62E-6	1.07E-5	> 1.00E-4
DU-145	0.439	1.975	2.057	2.032	1.977	0.058	0.077	105	104	100	-87	-82	1.85E-6	3.43E-6	6.36E-6
Breast Cancer															
MCF7	0.368	2.302	2.246	2.204	1.737	0.125	0.073	97	95	71	-66	-80	1.42E-6	3.29E-6	7.62E-6
MDA-MB-231/ATCC	0.661	1.660	1.639	1.568	1.241	0.658	0.497	98	91	58	.	-25	1.37E-6	9.82E-6	> 1.00E-4
HS 578T	1.398	2.565	2.379	2.430	2.386	1.065	1.210	84	88	85	-24	-13	2.09E-6	6.03E-6	> 1.00E-4
BT-549	1.363	2.576	2.515	2.385	2.342	0.092	0.015	95	84	81	-93	-99	1.50E-6	2.91E-6	5.64E-6
T-47D	1.004	2.401	2.306	2.317	2.105	1.090	0.672	93	94	79	6	-33	2.49E-6	1.44E-5	> 1.00E-4
MDA-MB-468	0.883	2.247	2.273	2.288	2.173	0.752	0.569	102	103	95	-15	-36	2.55E-6	7.32E-6	> 1.00E-4

Figure 103: Activity (Log 10 concentration) of compound **140e**.

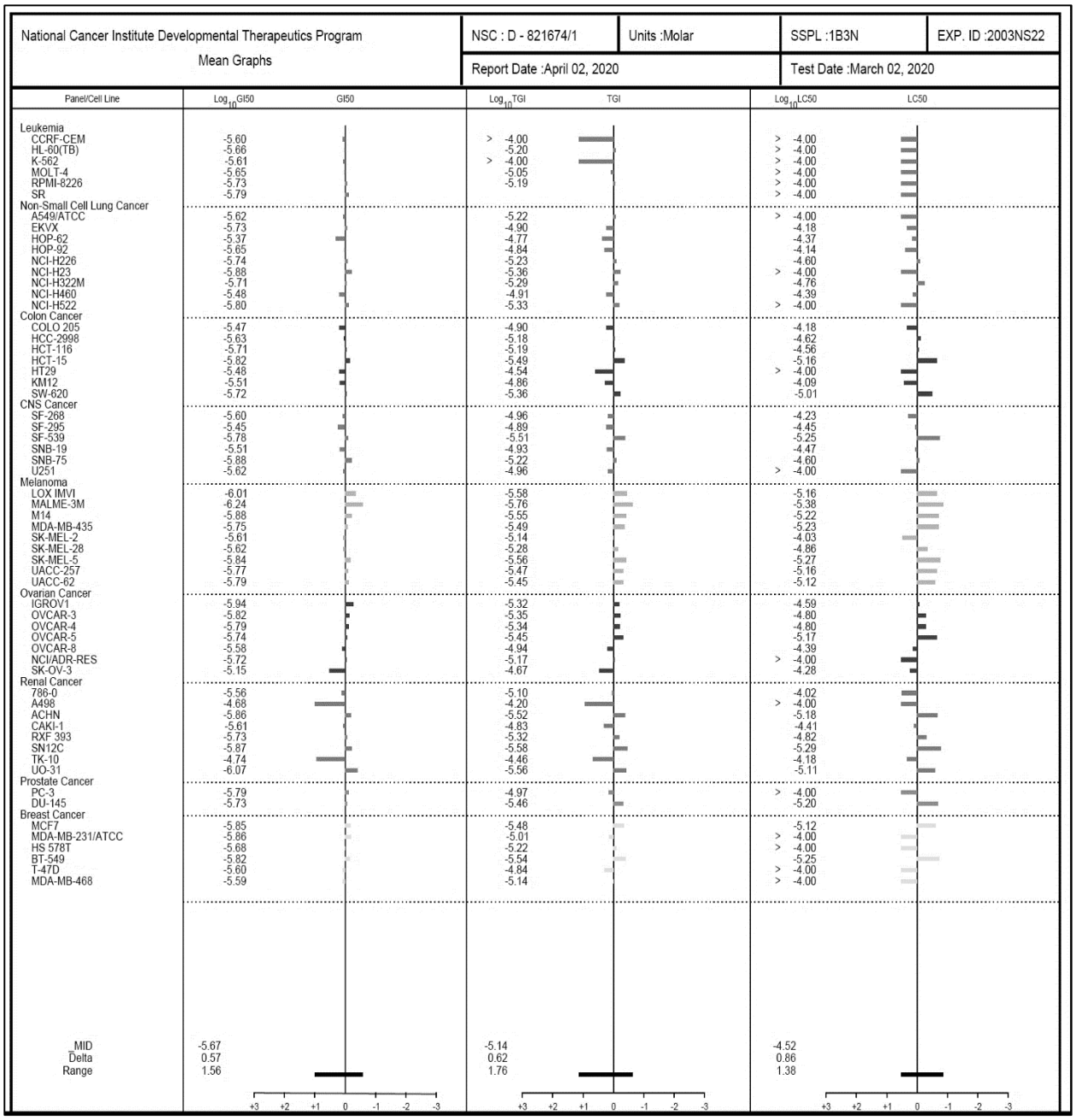

Tables

Table 27: Results of in vitro five doses (conc 0.01, 0.1, 1, 10 and 100 μM) testing of nine human cancer types and selectivity for compound **139b**. Results provided by NCI.

Panel	Cell line	GI50			TGI			LC50
		Conc./cell line (μM)	Subpanel MID[b]	Selectivity ratio (MID[a]: MID[b])	Conc./cell line (μM)	Subpanel MID[d]	Selectivity ratio (MID[c]: MID[d])	
Leukemia	CCRF-CEM	2.71	2.72	0.88	-	81.14	3.85	> 100
	HL-60(TB)	2.70			> 100			> 100
	K-562	3.15			> 100			> 100
	MOLT-4	3.12			> 100			> 100
	RPMI-8226	2.15			5.69			> 100
	SR	2.46			> 100			> 100
Non-Small Cell Lung Cancer	A549/ATCC	2.83	2.74	0.87	8.	16.05	1.31	> 100
	EKVX	1.91			4.23			9.38
	HOP-62	2.68			6.97			6.60
	HOP-92	1.91			9.14			> 100
	NCI-H226	4.38			2.55			> 100
	NCI-H23	1.95			4.15			8.85
	NCI-H322M	2.02			4.75			1.32
	NCI-H460	2.08			4.29			8.82
	NCI-H522	4.89			> 100			> 100
Colon Cancer	COLO 205	2.13	1.91	1.24	4.61	3.95	5.34	
	HCC-2998	1.78			3.45			6.68
	HCT-116	1.79			3.66			7.51
	HCT-15	1.87			4.05			8.76
	HT29	1.93			4.07			8.56
	KM12	2.03			4.15			8.51
	SW-620	1.85			3.66			7.23
CNS Cancer	SF-268	3.09	2.71	0.88	1.12	19.48	1.08	> 100
	SF-295	2.07			4.19			8.50
	SF-539	1.79			3.32			6.18
	SNB-19	1.95			4.25			9.26
	SNB-75	5.44			> 100			> 100
	U251	1.89			4.00			8.47
Melanoma	LOX IMVI	1.69	3.77	0.63	3.	36.54	0.58	6.75
	MALME-3M	3.27			2.14			> 100
	M14	3.27			1.54			> 100
	MDA-MB-435	5.44			100			> 100
	SK-MEL-2	2.65			7.76			> 100
	SK-MEL-28	2.97			9.87			> 100
	SK-MEL-5	7.56			> 100			> 100
	UACC-257	5.14			> 100			> 100
	UACC-62	1.96			4.21			9.02
Ovarian Cancer	IGROV1	1.66	2.59	0.92	3.27	18.46	1.14	6.44
	OVCAR-3	1.80			3.61			7.23
	OVCAR-4	3.17			9.88			3.69

	OVCAR-5	1.92			3.84			7.68
	OVCAR-8	3.08			> 100			> 100
	NCI/ADR-RES	2.92			1.06			> 100
	SK-OV-3	3.55			7.53			> 100
Renal Cancer	786-0	2.00	1.86	1.28	4.38	16.64	1.27	9.58
	A498	--			8.36			> 100
	ACHN	1.78			3.29			6.08
	RXF393	3.74			3.86			> 100
	CAKI-1	1.52			3.00			9.78
	SN12C	2.27			5.94			> 100
	TK-10	2.03			5.60			2.92
	UO-31	1.53			3.08			6.20
Prostate Cancer	PC-3	1.71	3.41	0.69	3.63	3.58	5.89	7.70
	DU-145	5.11			3.53			> 100
Breast Cancer	MCF7	1.87	2.27	1.05	4.95	24.28	0.87	2.25
	MDA-MB-231/ATCC	2.63			7.46			> 100
	HS 578T	3.49			> 100			> 100
	BT-549	2.22			5.35			2.47
	T-47D	1.54			3.65			8.68
	MDA-MB-468	1.84			3.74			7.61
MID[a]	2.38			**MID[c]**	21.08			

MID^{a,c} = Average sensitivity of all cell lines in mM; MID^{b,d} = Average sensitivity of all cell lines of a particular subpanel in mM.

Table 28:Results of in vitro five doses testing of nine human cancer types and selectivity (GI_{50}) for compounds **140c**, **140d,** and **140e**. Results provided by NCI.

Panel	Cell line	**140c**			**140d**			**140e**		
		GI_{50}			GI_{50}			GI_{50}		
		Conc. Per cell line	Sub-panel MID[b]	Selectivity ratio (MID[a]: MID[b])	Conc. Per cell line	Sub-panel MID[b]	Selectivity ratio (MID[a]: MID[b])	Conc. Per cell line	Sub-panel MID[b]	Selectivity ratio (MID[a]: MID[b])
leukemia	CCRF-CEM	2.39	2.21	0.99	9.98	7.87	0.73	2.53	2.14	1.16
	HL-60(TB)	3.95			7.70			2.18		
	K-562	1.69			8.79			2.43		
	MOLT-4	1.22			5.99			2.22		
	RPMI-8226	2.21			7.17			1.86		
	SR	1.78			7.57			1.64		
Non-Small Cell Lung Cancer	A549/ATCC	2.26	1.69	1.03	8.35	5.07	1.14	2.42	2.31	1.07
	EKVX	1.39			5.01			1.87		
	HOP-62	1.96			1.85			4.28		
	HOP-92	1.56			7.41			2.26		
	NCI-H226	1.61			9.36			1.81		
	NCI-H23	1.46			5.50			1.31		
	NCI-H322M	1.55			1.61			1.93		
	NCI-H460	1.94			1.06			3.35		
	NCI-H522	1.49			5.51			1.60		
Colon Cancer	COLO 205	1.94	2.61	0.84	3.63	5.99	0.96	3.36	2.50	0.99
	HCC-2998	1.62			9.48			2.34		
	HCT-116	5.77			6.67			1.94		
	HCT-15	1.52			5.49			1.51		
	HT29	3.09			1.15			3.32		

	KM12	2.68			9.99			3.12		
	SW-620	1.63			5.51			1.92		
CNS Cancer	SF-268	1.68	2.79	0.78	6.15	5.12	1.13	2.54	2.43	1.02
	SF-295	1.68			6.15			3.55		
	SF-539	1.69			5.54			1.67		
	SNB-19	1.67			6.45			3.09		
	SNB-75	8.43			1.32			1.32		
	U251	1.60			5.12			2.41		
Melanoma	LOX IMVI	5.32	2.32	0.95	4.06	5.77	1.00	9.66	3.12	0.79
	MALME-3M	3.83			4.42			5.70		
	M14	1.63			5.54			1.33		
	MDA-MB-435	1.94			5.98			1.76		
	SK-MEL-2	1.74			7.39			2.47		
	SK-MEL-28	1.87			6.87			2.40		
	SK-MEL-5	1.41			5.51			1.43		
	UACC-257	1.55			5.93			1.69		
	UACC-62	1.63			6.23			1.62		
Ovarian Cancer	IGROV1	1.13	2.25	0.98	4.46	5.38	1.07	1.16	2.53	0.98
	OVCAR-3	3.28			5.22			1.53		
	OVCAR-4	1.26			4.54			1.61		
	OVCAR-5	2.03			5.86			1.83		
	OVCAR-8	2.13			5.81			2.62		
	NCI/ADR-RES	2.24			7.43			1.93		
	SK-OV-3	3.70			4.35			7.03		
Renal Cancer	786-0	2.30	2.25	0.98	7.48	4.82	1.20	2.75	2.53	0.98
	A498	1.05			6.93			2.07		
	ACHN	1.42			4.92			1.39		
	CAKI-1	1.18			4.80			2.48		
	RXF393	1.35			5.02			1.85		
	SN12C	1.22			5.06			1.33		
	TK-10	4.48			1.03			1.84		
	UO-31	4.96			3.34			8.50		
Prostate Cancer	PC-3	1.49	1.67	1.32	6.20	6.29	0.92	1.62	1.74	1.43
	DU-145	1.85			6.37			1.85		
Breast Cancer	MCF7	1.23	1.73	1.27	5.83	6.67	0.87	1.42	1.90	1.31
	MDA-MB-231/ATCC	1.27			6.52			1.37		
	HS 578T	2.04			7.82			2.09		
	BT-549	1.53			5.22			1.50		
	T-47D	2.03			6.98			2.49		
	MDA-MB-468	2.28			7.66			2.55		
MID[a]	2.20				5.77			2.48		

MID[a,c] = Average sensitivity of all cell lines in µM.
MID[b,d] = Average sensitivity of all cell lines of a particular subpanel in µM

Table 29: Results of in vitro five doses testing of nine human cancer types and selectivity (TGI and LC_{50}) for compounds **140c**, **140d,** and **140e**. Results provided by NCI.

Panel	**Cell line**	**140c**		**140d**		**140e**	
		TGI	LC50	TGI	LC50	TGI	LC50
leukemia	CCRF-CEM	>100	>100	3.33	>3.33	>100	>100
	HL-60(TB)	3.26	>100	2.05	>3.33	6.26	>100
	K-562	--	>100	3.33	>3.33	>100	>100
	MOLT-4	5.76	>100	1.72	>3.33	8.89	>100
	RPMI-8226	--	>100	2.01	>3.33	6.47	>100
	SR	>100	>100	2.95	>3.33	--	>100
Non-Small Cell Lung Cancer	A549/ATCC	5.61	>100	2.07	>3.33	6.07	>100
	EKVX	3.46	8.60	1.15	2.64	1.25	
	HOP-62	4.85	1.65	6.48	1.53	1.72	

	HOP-92	4.19	>100	2.60	1.56	1.44	
	NCI-H226	3.35	6.99	4.09	1.37	5.83	
	NCI-H23	3.76	9.72	1.50	>3.33	4.32	>100
	NCI-H322M	2.92	5.50	5.90	1.43	5.13	
	NCI-H460	3.97	8.11	3.60	1.50	1.22	
	NCI-H522	4.19	>100	1.37	4.64	4.69	>100
Colon Cancer	COLO 205	4.24	9.28	9.06	2.26	1.27	6.62
	HCC-2998	3.14	6.06	2.91	1.06	6.67	2.40
	HCT-116	2.58	9.31	1.70	6.89	6.45	2.73
	HCT-15	3.50	8.07	1.18	2.54	3.24	6.96
	HT29	>100	>100	3.18	>3.33	2.87	>100
	KM12	8.80	9.05	3.56	>3.33	1.37	8.18
	SW-620	3.45	7.30	1.20	2.62	4.32	9.71
CNS Cancer	SF-268	4.48	>100	1.65	>3.33	1.10	5.91
	SF-295	3.08	5.66	1.27	2.60	1.27	3.57
	SF-539	3.12	5.79	1.02	1.89	3.06	5.58
	SNB-19	3.44	7.05	1.64	5.31	1.17	3.42
	SNB-75	2.76	7.79	7.46	1.74	6.04	2.51
	U251	4.28	>100	1.12	2.43	1.11	>100
Melanoma	LOX IMVI	2.10	5.86	9.04	2.01	2.62	6.98
	MALME-3M	1.58	4.00	8.70	1.71	1.75	4.19
	M14	3.30	6.65	1.06	2.01	2.83	6.03
	MDA-MB-435	3.63	6.82	1.09	1.97	3.23	5.93
	SK-MEL-2	4.32	7.27	1.58	9.60	7.25	9.29
	SK-MEL-28	3.35	6.00	1.21	2.15	5.22	1.39
	SK-MEL-5	2.75	5.37	1.02	1.89	2.76	5.32
	UACC-257	3.15	6.39	1.14	2.20	3.41	6.88
	UACC-62	3.91	9.38	1.33	2.84	3.52	7.66
Ovarian Cancer	IGROV1	3.21	9.08	1.31	5.78	4.74	2.58
	OVCAR-3	1.43	5.03	1.28	3.16	4.42	1.59
	OVCAR-4	2.56	5.18	8.87	1.73	4.58	1.59
	OVCAR-5	4.37	9.42	1.15	2.26	3.53	6.79
	OVCAR-8	1.12	>100	1.24	2.63	1.16	4.10
	NCI/ADR-RES	--	>100	2.17	>3.33	6.77	>100
	SK-OV-3	2.34	>100	8.75	1.76	2.14	5.23
Renal Cancer	786-0	5.70	>100	1.70	>3.33	7.93	9.61
	A498	4.70	>100	2.90	>3.33	6.34	>100
	ACHN	2.91	5.96	9.65	1.89	3.03	6.60
	CAKI-1	2.86	6.92	2.14	8.98	1.49	3.87
	RXF393	2.71	5.43	9.86	1.94	4.75	1.50
	SN12C	2.79	6.42	1.07	2.24	2.61	5.11
	TK-10	8.14	4.13	1.71	2.85	3.47	6.54
	UO-31	2.09	4.60	8.60	2.21	2.77	7.85
Prostate Cancer	PC-3	8.81	>100	2.69	>3.33	1.07	>100
	DU-145	3.45	6.46	1.19	2.22	3.43	6.36
Breast Cancer	MCF7	3.36	9.17	1.28	2.82	3.29	7.62
	MDA-MB-231/ATCC	6.69	>100	2.69	>3.33	9.82	>100
	HS 578T	6.93	>100	2.05	>3.33	6.03	>100
	BT-549	2.91	5.54	9.83	1.85	2.91	5.64
	T-47D	7.29	>100	2.30	>3.33	1.44	>100
	MDA-MB-468	5.72	>100	2.04	>3.33	7.32	>100

Materials and Methods

A. NCI screening assay

As mentioned, the methodology of the NCI procedure for primary anticancer assays was detailed on their site (http://www.dtp.nci.nih.gov). But briefly, the protocol is performed at 60 human tumor cell lines panel derived from different nine neoplastic diseases. NCI-60 testing is performed in two parts: first, a single concentration is tested in all 60 cell lines at a single dose of 10-5 molar or 15 μg/mL by the protocol of the Drug Evaluation Branch, National Cancer Institute, Bethesda, USA. If the results obtained meet selection criteria, then the compound is tested again in all 60 cell lines in 5 x 10 folds of dilution with the top dose being 10-4 molar or 150 μg/ml.

B. MTT- Cytotoxicity assay method

The MTT method of monitoring *in vitro* cytotoxicity was well suited for the use with multiwell plates. For best results, cells in the log phase of growth were employed and the final cell number was not more than 106 cells/cm^2. Each test included a blank containing exclusively medium without cells.[305]

1. Cultures were removed from the incubator into a laminar flow hood or other sterile work areas.
2. Each vial of MTT [M-5655] was reconstituted to be used with 3 ml of the medium or balanced salt solution without phenol red and serum, reconstituted MTT was added in an amount equal to 10% of the culture medium volume.
3. Cultures were returned to the incubator for 2-4 h depending on cell type and maximum cell density (an incubation period of 2 h was generally adequate but may be lengthened for low cell densities or cells with lower metabolic activity). the incubation times were consistent when making comparisons.
4. After the incubation period, cultures were removed from the incubator and the resulting formazan crystals were dissolved by adding an amount of MTT Solubilization Solution [M-8910] equal to the original culture medium volume.
5. Gentle mixing was done in a gyratory shaker to enhance dissolution. Occasionally, especially in dense cultures, pipetting up and down [trituration] was required to completely dissolve the MTT formazan crystals.
6. The absorbance was measured spectrophotometrically at a wavelength of 570 nm. The background absorbance of multi-well plates was measured at 690 nm and subtracted from

the 450 nm measurement. Tests performed in multi-well plates were read by using the appropriate type of plate reader or the contents of individual wells were transferred to appropriate size cuvettes for spectrophotometric measurements.

C. Analysis of cell cycle by flow cytometry

Cytometers were Becton Dickinson Immunocytometry Systems, Beckman/Coulter Inc., DACO/Cytomation, and PARTEC GmbH.[306]

1. The software used to deconvolute the DNA content frequency histograms to estimate the proportions of cells in the respective phases of the cycle is available from Phoenix Flow Systems and Verity Software House.
2. A centrifuge was done to can accommodate 5 ml tubes.
3. PI staining solution: 0.1% (v/v) Triton X-100, 10 mg/mL PI (Molecular Probes, Inc.) and 100 mg/mL of DNase-free RNase A in PBS.
4. PBS (phosphate buffered saline, e.g. Dulbecco PBS): 136.9 mM NaCl, 2.7 mM KCl, 8.1 mM Na_2HPO_4, 0.9 mM $CaCl_2$, 0.45mM $MgCl_2$.
5. DAPI staining solution: 0.1% (v/v) Triton X-100 and 1 mg/mL DAPI (Molecular Probes, Inc.) in PBS.
6. Monoclonal or polyclonal antibodies (Abs) applicable to cell-cycle analysis, including cyclin Abs (provided, e.g., by DACO Corporation, Sigma Chemical Co., Upstate Biotechnology Incorporated, B.D. Biosciences/PharMingen, and Santa Cruz Biotechnology, Inc.).
7. Cell permeabilizing solution was prepared by mixing 0.25% Triton X-100, 0.01% sodium azide in PBS.
8. The rinsing solution was prepared by mixing 1% bovine serum albumin (BSA), 0.01% sodium azide in PBS.
9. DNA denaturation buffer: 0.1 mM Na-EDTA in 1 mM Na-cacodylate; adjust pH to 6.0. To make 0.2 M stock solution of cacodylate buffer, 42.8 g of $Na(CH_3)_2\ As_2{\cdot}3H_2O$ was dissolved in 100 ml H_2O, by taken 50 ml of this solution, and then 29.6 ml of 0.2 M HCl was added, volume was adjusted to 200 ml with H_2O.
10. Diluting buffer by adding 0.1% Triton X-100, 0.5% (w/v) BSA in PBS.
11. 0.2 M phosphate buffer was prepared by mixing of 81 ml of 0.2 M Na_2HPO_4 with 19 ml of 0.2 M KH_2PO_4 (pH 7.4).

D. Tubulin polymerization inhibitory activity

Tubulin polymerization inhibitory activity was measured using kits pre-coated with a biotin-conjugated antibody specific to TUBb that is bound to TUBb provided after the addition of samples or standards. Avidin protein conjugated to horseradish peroxidase (HRP) was provided to bind the biotin-labeled antibody.[307] This complex gave a characteristic color change upon substrate addition *via* HRP enzyme-substrate reaction. The color change was measured spectrophotometrically at a wavelength of 450 nm ± 10 nm. The decrease in color intensity was interpreted as a sign of tubulin inhibition. The results were calculated as the concentration of TUBb available for antibody reaction, and the percent inhibition of TUBb was calculated for each sample as a percent of control. *In vitro* kinetics of microtubule assembly was measured using an ELISA kit for TUBb (Cloud-Clone. Corp.) on an SR cell line. Briefly, growing cells from Leukemia SR cell lines were trypsinized, counted, and seeded at the appropriate densities into 96-well microtiter plates. Afterward, the cells were incubated in a humidified atmosphere at 37^{o}C for 24 h. The standards, the compounds to be tested, and the control Colchicine were diluted to designated concentrations. On the 96-well microtiter plates, standard or sample was added to each well in 100 µL and incubated at 37^{o}C for 2 h. The solution was aspirated, and 100 µL of prepared detection reagent A was added to each well. Incubation was done at 37^{o}C for 2 h. After washing with 100 ml of prepared detection reagent B, incubation was continued at 37^{o}C for 30 min. Five washing steps with 100 µL of prepared detection reagent B were performed, then 90 ml of 3,3′,5,5′-tetramethylbenzidine (TMB) substrate solution was added, and incubated at 37^{o}C for 15-25 min. 50 ml of stop solution was added. Optical density (O.D.) was measured at 450 nm using a microplate reader (Spectramax Plus 96 well plate spectrophotometer).

Results for each compound were reported, at 10 mM concentration, as the percent of inhibition of the treated cells compared to that of the untreated control cells.

E. Multidrug resistance Assay

Before adding to the wells, the SABC working solution and TMB substrate were equilibrated for at least 30 min at room temperature (32 °C). When diluting samples and reagents, they must be mixed completely and evenly. It is recommended plotting a standard curve for each test.

1. Standard, tested samples, and control wells were set to zero on the pre-coated plate respectively, and their positions were recorded. Each standard and sample was measured

in duplicate. The plate was washed two times before adding standard, sample, and control (zero) to wells!

2. Standard solutions of 0.1 ml of 20 ng/mL, 10 ng/mL, 5 ng/mL, 2.5 ng/mL, 1.25 ng/mL, 0.625 ng/mL, 0.312 ng/mL was aliquoted into the standard wells.
3. 0.1 ml Of sample / standard dilution buffer was added into the control (zero) well.
4. 0.1 ml Of properly diluted sample (rat serum, plasma, tissue homogenates, and other biological fluids.) was added into test sample wells. The plate was sealed with a cover and incubated at 37°C for 90 min.
5. The cover was removed and the plate content was discarded, the plate was clapped on the absorbent filter papers or other absorbent material. The wells were not let to be dry at any time and the plate was not washed!
6. 0.1 ml of Biotin-detection antibody working solution was added into the above wells (standard, test sample & zero wells). The solution was added at the bottom of each well without touching the sidewall. The plate was sealed with a cover and incubated at 37°C for 60 min.
7. The cover was removed, and the plate was washed 3 times with wash buffer. 0.1 ml Of SABC working solution was added into each well, the plate was covered and incubated at 37°C for 30 min. the cover was removed and the plate was washed 5 times with washed buffer, and the wash buffer was let to stay in the wells for 1-2 min each time.
8. 90 μL Of TMB substrate was added into each well, the plate was covered and incubated at 37°C in dark within 15-30 min. The shades of blue were seen in the first 3-4 wells (with most concentrated Abcb1 standard solutions), the other wells showed no obvious color. 50 μL Of stop solution was added into each well and mix thoroughly. The color changes into yellow immediately.
9. The O.D. absorbance was read at 450 nm in a microplate reader immediately after adding the stop solution.

F. Caspase Assay

Caspase assay was performed according to the following procedures:[308]

1. All reagents were allowed to reach room temperature before use. All liquid reagents were gently mixed before use (Note: A standard curve must be run with each assay).
2. The number of 8-well strips needed for the assay was determined and inserted in the frames for use.

3. 100 µL Of the standard diluent buffer was added to the zero standard wells. Well(s) which reserved for chromogen blank was lifted empty.
4. 100 µL of standards and controls or diluted samples were added to the appropriate microtiter wells. The sample dilution chosen was optimized for each experimental system. Mixing by a gentle tap on the side of the plate.
5. Wells was covered with a plate cover and incubated for 2 hours at room temperature.
6. Thoroughly, the solution was aspirated or decanted from wells and the liquid was discarded. Wells was washed 4 times.
7. A solution of 100 µL of Caspase-3 (Active) Detection Antibody was pipette into each well except the chromogen blank(s), then mixing the solution by tap gently on the side of the plate.
8. The plate was covered with plate cover and incubated for 1 h at room temperature.
9. Thoroughly, the solution was aspirated or decanted from wells and the liquid was discarded.
10. Wells was washed 4 times (All washing
11. must be performed with the *Wash Buffer Concentrate (25X)* provided).
12. 100 µL of Anti-Rabbit IgG HRP Working Solution was added to each well except the chromogen blank(s). The working dilution was prepared as described in Preparing IgG HRP.
13. The wells were covered with the plate cover and incubated for 30 minutes at room temperature.
14. Thoroughly, the solution was aspirated or decanted from wells and the liquid was discarded.
15. 100 µL of stabilized chromogen was added to each well. The liquid in the wells was turned blue.
16. Incubation occurred for 30 min at room temperature and in the dark. Note: the plate was not covered with aluminum foil or metalized Mylar®. The incubation time for the chromogen substrate was often determined by the microtiter plate reader used. Many plate readers can record a maximum optical density (O.D.) of 2.0. The O.D. values were monitored and the substrate reaction stopped before the O.D. of the positive wells exceeded the limits of the instrument. The O.D. values at 450 nm were read after the Stop Solution was added to each well.
17. 100 µL of stop solution was added to each well and mixing by tap the side of the plate gently. The solution was changed from blue to yellow.

18. The absorbance of each well was read at 450 nm having blanked the plate reader against a chromogen blank composed of 100 µL of stabilized chromogen and stop solution each. The plate was read within 2 hours after adding the stop solution.
19. A curve fitting software was used to generate the standard curve. A four-parameter algorithm was provided with the best standard curve fit.
20. The concentrations for unknown samples were read and controlled from the standard curve. Multiply value(s) obtained for sample(s) by the appropriate dilution factor to correct for the dilution in step 3. Samples producing signals greater than that of the highest standard was diluted in standard diluent buffer and reanalyzed.

G. BAX assay

All reagents were brought, except the human Bax-α Standard, to room temperature for at least 30 minutes prior use.

The human Bax-α Standard solution was not left at room temperature for more than 10 minutes.

All standards, controls, and samples were run in duplicate.[309]

1. The number of wells that used was determined by referring to the assay layout sheet.
2. Desiccated back into the pouch and seal the Ziploc. Unused wells were stored at 4 °C.
3. 100 µL of assay buffer was Pipet into the S0 (0 pg/mL standard) wells.
4. 100 µL of standards #1 through #6 was Pipet into the appropriate wells.
5. 100 µL of the samples was Pipet into the appropriate wells.
6. A gentle mix was done for the contents by tap the plate.
7. The plate was sealed and incubated at room temperature on a plate shaker for 1 hour at ~500 rpm.
8. The contents of the wells were removed and the wells were washed by adding 400 µL of wash solution to every well, the wash for the wells was repeated 4 more times for a total of 5 washes. After the final wash, the wells firmly were aspirated, then the plate was taped on a lint-free paper towel to remove any remaining wash buffer.
9. 100 µL of yellow antibody was Pipet into each well, except for the blank.
10. The plate was sealed and incubated at room temperature on a plate shaker for 1 hour at ~500 rpm.
11. The contents of the wells were removed and the wells were washed by adding 400 µL of wash solution to every well.
12. The washing step was repeated for 4 more times for a total of 5 washes.

13. After the final wash, the wells were aspirated then the plate was taped on a lint-free paper towel to remove any remaining wash buffer.
14. 100 µL of the blue conjugate was added to each well, except for the blank.
15. The plate was sealed and incubated at room temperature on a plate shaker for 30 minutes at ~500 rpm.
16. The contents of the wells were removed and washed by adding 400 µL of wash solution to every well.
17. The washing step was repeated for 4 more times for a total of 5 washes.
18. After the final wash, the wells were aspirated then the plate was taped on a lint-free paper towel to remove any remaining wash buffer.
19. 100 µL of substrate solution was Pipet into each well.
20. Incubation for 30 minutes was done at room temperature on a plate shaker at ~500 rpm.
21. 100 µL of stop solution was added to each well.
22. The plate reader was blanked against the blank wells, the optical density was read at 450 nm with correction between 570 and 590 nm.

H. *BcL2 Assay*

The assay was performed as the following protocol:[310]

1. All reagents were mixed thoroughly without foaming before use.
2. The microwells were washed twice with approximately 300 µL wash buffer (PBS with 1% Tween 20) per well with a thorough aspiration of microwell contents between washes.
3. After the last wash, the content of the well was removed and the microwell strips were taped on an absorbent pad to remove excess wash buffer. The microwell strips were used immediately after washing.
4. 100 µL of sample diluent was added in duplicate to all standard wells and the blank wells. Standard (1:2 dilution) was prepared in duplicate ranging from 32 ng/mL to 0.5 ng/mL.100 µL of sample diluent was added in duplicate, to the blank wells, then, 80 µL of sample diluent was added in duplicate to the sample wells.
5. 20 µL of each sample was added in duplicate to the designated wells.
6. 50 µL of diluted biotin conjugate was added to all wells, including the blank wells. A plate cover was used and incubated at room temperature, on a microplate shaker at 100 rpm for 2 hours.
7. The plate cover was removed and the content of the well was removed, microwell strips were washed 3 times as described in step 2.

8. 100 µL of diluted streptavidin-HRP was added to all wells, including the blank wells.
9. A plate cover was used and incubated at room temperature, on a microplate shaker at 100 rpm for 1 hour.
10. The plate cover was removed and the content of the well was removed, microwell strips were washed 3 times as described in step 2.
11. 100 µl of mixed TMB substrate solution was pipette to all wells, including the blanks.
12. The microwell strips were incubated at room temperature (18 °C to 25 °C) for about 15 minutes, on a rotator set at 100 rpm. The point, at which the substrate reaction was stopped, was determined by the ELISA reader.
13. The enzyme reaction was stopped by quickly pipetting 100 µL of stop solution into each well, including the blank wells. The stopped solution was spread quickly and uniformly throughout the microwells to completely inactivate the enzyme. The results were read immediately after the stop solution was added.
14. The absorbance of each microwell was read on a spectrophotometer using 450 nm as the primary wavelength.

I. Assessment of Mitochondrial Changes

The assay was done as follows:[311]

Cells were grown (adherent or suspension) in an appropriate media to obtain at least 3 x 104 cells per assayed conditions; positive, negative, and experimental controls, and test compound(s). Cell loss was account for during the processing. Negative control – unlabeled cells not exposed to ROS Inducer or treatment, positive control – cells incubated with 1X ROS Label only.

Experimental control–labeled cells treated with 1X ROS Inducer:

1. The suspended cells were harvest by centrifugation at 300 x g (300 times of the grams) for 5 min at room temperature. This setting was used throughout the entire protocol for both cell types.
2. Adherent cells were fully detached (e.g. trypsinize and quench with media) and harvest by centrifugation. The cell pellets resuspended in culture media with 1X ROS Label.
3. A single-cell suspension was ensured by gently pipetting up and down and incubated for 30 minutes at 37°C protected from light.
4. Upon completion, the cells were spin down and the media was removed. The cells were treated with the target compounds for the desired period directly in culture media, ROS Assay Buffer supplemented with 10% FBS, or culture media without phenol red. The

appropriate controls were included. If using ROS Inducer as an experimental control, the stock was diluted to 1X, and treat the cells for 1 hour before analyses.

5. The cell concentration was Adjusted so at least 1 $x10^4$ cells should be analyzed per experimental condition. The cells were gently pipetted up/down to ensure single-cell suspension and analyze on the flow cytometer in the FL-1 channel. Forward and side scatter gates were established from negative control cells to exclude debris and cellular aggregates. Mean fluorescence intensity in Ex/Em = 495/529 nm was quantified and compared between untreated cells and cells treated with test compounds, or between different cell types.

J. Detection of ROS in Suspension and Adherent Cells by Microplate Assay:[312]

4. 2.5 x 10^4 Adherent cells were seeded per well in a 96-well plate to obtain ~ 70-80% confluency on the day of the experiment.
5. Cells were allowed to adhere overnight. Suspended cells were grown so that approximately 1.5 x 10^5 cells per well are available. The next day, the media was removed and the adherent cells were washed in 100 µL of ROS Assay Buffer. Suspension cells were collected by centrifugation and washed once in PBS.
6. 100 µL of 1X ROS Label diluted in ROS Assay Buffer per well was added into adherent cells or resuspend the pelleted cells at 1.5 x 106 cells/mL, Incubated for 45 min at 37°C in the dark.
7. For adherent cells: the ROS Label was removed, 100 µL of ROS Assay Buffer or PBS was added and measured fluorescence immediately, or the cells were treated with 100 µL of diluted test compounds for the desired period. Appropriate controls were included as well as blank wells (media or buffer only). For suspension cells: the cells were washed by centrifugation in ROS Assay Buffer, the same cell concentration was maintained.
8. 100.000 labeled cells per well were seeded in 100 µL volume and the ROS was measured or the cells were treated with tested compounds in ROS Assay Buffer supplemented with 10% FBS or media without phenol red for the appropriate time.
9. Fluorescence was measured at Ex/Em= 495/529 nm in endpoint mode in the presence of compounds and controls. Change in fluorescence was determined after background subtraction.

K. CDK inhibitory assay[313]

1. Assay Protocol for CDK1/cyclinB

All samples and controls were tested in duplicate.

1. 5x Kinase assay buffer 1, ATP, and 10x CDK substrate peptide 1 were prepared.
2. The master mixture (25 µl per well): N wells x (6 µl 5x Kinase assay buffer 1 + 1 µl ATP (500 µM) + 5 µl 10x CDK substrate peptide 1 + 13 µl distilled water) was prepared, 25 µl was added to every well.
3. 5 µl of Inhibitor solution of each well labeled as “Test Inhibitor” was added. For the “Positive Control" and “Blank”, 5 µl of the same solution was added without inhibitor (Inhibitor buffer).
4. 3 ml of 1x Kinase assay buffer 1 was prepared by mixing 600 µl of 5x Kinase assay buffer 1 with 2400 µl water.
5. To the wells designated as "Blank", 20 µl of 1x Kinase assay buffer 1 was added.
6. CDK1/CyclinB1 enzyme was thawed on ice. Upon the first thaw, spin was done to a tube containing an enzyme to recover the full content of the tube. The amount of CDK1/CyclinB1 required for the assay was calculated and the enzyme was diluted to ~1.0 ng/µl with 1x Kinase assay buffer 1. The remaining undiluted enzyme was stored in aliquots at -80°C.
7. A reaction was initiated by adding 20 µl of diluted CDK1/CyclinB1 enzyme to the wells designated “Positive Control” and "Test Inhibitor Control", the mixture was incubated at 30°C for 45 minutes.
8. Kinase-Glo Max reagent was thawed.

2. Assay Protocol for CDK2

All samples and controls were tested in duplicate.

1. 5x Kinase assay buffer 1, ATP, and 10 x CDK substrate peptide 1 was thawed.
2. The master mixture (25 µl per well): N wells x (6 µl 5 x Kinase assay buffer 1 + 1 µl ATP (500 µM) + 5 µl 10x CDK substrate peptide 1 + 13 µl distilled water) was prepared, 25 µl was added to every well.
3. 5 µl of Inhibitor solution of each well-labeled was added as “Test Inhibitor”. For the “Positive Control" and “Blank”, 5 µl of the same solution was added without inhibitor (Inhibitor buffer).
4. 3 ml of 1x Kinase assay buffer 1 was prepared by mixing 600 µl of 5x Kinase assay buffer 1 with 2400 µl water.
5. To the wells designated as "Blank", 20 µl of 1x Kinase assay buffer 1 was added.
6. CDK2/CyclinA2 enzyme was thawed on ice. Upon the first thaw, spin was done to a tube containing an enzyme to recover the full content of the tube. The amount of

CDK2/CyclinA2 required for the assay was calculated and the enzyme was diluted to ~2.5 ng/µl with 1x Kinase assay buffer 1. The remaining undiluted enzyme was stored in aliquots at -80°C.

3. Assay Protocol for CDK3

1. 100 µl 10 mM ATP to 1.25 ml 6 µM substrate peptide was added. The mixture was diluted with dH_20 to 2.5 ml to make 2X ATP/substrate cocktail ([ATP]=400 µM, [substrate]=3 µm).
2. The enzyme was transferred from –80°C to ice and allowed to thaw on ice.
3. Microcentrifuge was done briefly at 4°C to bring the liquid to the bottom of the vial, then, it returned immediately to ice.
4. 1 ml 10X kinase buffer [1 ml 10X Kinase Buffer 250 mM Tris-HCl pH 7.5, 100 mM $MgCl_2$, 1 mM Na_3VO_4, 50 mM b-glycerophosphate, 20 mM dithiothreitol (DTT)] was added to 1.5 ml dH_2O to make 2.5 ml 4X reaction buffer.
5. The enzyme was diluted in 1.25 ml of 4X reaction buffer to make 4X reaction cocktail ([enzyme]=4.0 ng/µl in 4X reaction cocktail).
6. 12.5 µl of the 4X reaction cocktail was added to 12.5 µl/well of a prediluted compound of interest (usually around 10 µM) and incubated for 5 minutes at room temperature.
7. 25 µl of 2X ATP/substrate cocktail was added to 25 µl/well preincubated reaction cocktail/compound.
8. The reaction plate was incubated at room temperature for 30 minutes.
9. 50 µl/well Stop Buffer (50 mM EDTA, pH 8) was added to stop the reaction.
10. 25 µl of each reaction was transferred to a 96-well streptavidin-coated plate containing 75 µl dH_2O/well and incubated at room temperature for 60 minutes, then, wash three times with 200 µl/well PBS/T.
11. The primary antibody, Phospho-Rb (Ser807/811) Antibody #9308, 1:1000 in PBS/T was diluted with 1% BSA. 100 µl/well primary antibody was added.
12. The mixture was incubated at 37°C for 120 minutes and washed three times with 200 µl/well PBS/T.
13. Europium labeled anti-rabbit antibody 1:1000 in PBS/T was diluted with 1% BSA. 100 µl/well diluted antibody was added.
14. The mixture was incubated at room temperature for 30 minutes and washed five times with 200 µl/well PBS/T.
15. 100 µl/well DELFIA® Enhancement Solution was added. And incubated at room temperature for 5 minutes.

16. 615 nm fluorescence emission was Detected with appropriate Time-Resolved Plate Reader.

4. Assay Protocol for CDK4

All samples and controls should be tested in duplicate.

1. 5x Kinase assay buffer 1, ATP, and 10x CDK4 substrate peptide was thawed.
2. The master mixture was prepared (25 µl per well): N wells x (6 µl 5x Kinase assay buffer 1 + 1 µl ATP (500 µM) + 5 µl 10x CDK4 substrate peptide + 13 µl distilled water), 25 µl was added to every well.
3. 5 µl of inhibitor solution of each labeled well was added as “Test Inhibitor”. For the “Positive Control" and “Blank”, 5 µl of the same solution was added without inhibitor (Inhibitor buffer).
4. 3 ml Of 1x Kinase assay buffer 1 was prepared by mixing 600 µl of 5x Kinase assay buffer 1 with 2400 µl water.
5. To the wells designated as "Blank", 20 µl of 1x Kinase assay buffer 1 was added.
6. CDK4/CyclinD3 enzyme was thawed on ice. Upon the first thaw, spin was done for a tube containing an enzyme to recover the full content of the tube. The amount of CDK4/CyclinD3 required for the assay was calculated and the enzyme was diluted to ~10 ng/µl with 1x Kinase assay buffer 1. remaining undiluted enzyme was stored in aliquots at -80°C.
7. The reaction was initiated by adding 20 µl of diluted CDK4/CyclinD3 enzyme to the wells designated “Positive Control” and "Test Inhibitor Control", and then incubated at 30°C for 60 minutes.
8. Kinase-Glo® Max Luminescence Kinase Assay reagent was thawed.
9. After the 60 minutes’ reaction, 50 µl of Kinase-Glo® Max reagent was added to each well. The plate was covered with aluminum foil and incubated at room temperature for 10 ~ 15 minutes.
10. Luminescence was measured using the microplate reader. “Blank” value was subtracted from all readings.

5. Assay Protocol for CDK5

1. 5x Kinase assay buffer 1, ATP, and 10x CDK substrate peptide 1 was thawed.
2. The master mixture was prepared (25 µl per well): N wells x (6 µl 5x Kinase assay buffer 1 + 1 µl ATP (500 µM) + 5 µl 10x CDK substrate peptide 1 + 13 µl distilled water), 25 µl was added to every well.

3. 5 µl of Inhibitor solution of each well was added, labeled as “Test Inhibitor”. For the “Positive Control" and “Blank”, 5 µl of the same solution was added without inhibitor (Inhibitor buffer).
4. 3 ml of 1x Kinase assay buffer 1 was prepared by mixing 600 µl of 5x Kinase assay buffer 1 with 2400 µl water.
5. To the wells designated as "Blank", 20 µl of 1x Kinase assay buffer 1 was added.
6. CDK5/p25 enzyme was thawed on ice. Upon the first thaw, spin was done for a tube containing an enzyme to recover the full content of the tube. The amount of CDK5/p25 required for the assay was calculated and the enzyme was diluted to ~0.75 ng/µl with 1x Kinase assay buffer 1. The remaining undiluted enzyme was stored in aliquots at -80°C.
7. The reaction was initiated by adding 20 µl of diluted CDK5/p25 enzyme to the wells designated “Positive Control” and "Test Inhibitor Control", then Incubated at 30°C for 45 minutes.
8. Kinase-Glo Max reagent was thawed.
9. After the 45-minute reaction, 50 µl of Kinase-Glo Max reagent was added to each well. The plate was covered with aluminum foil and incubated at room temperature for 15 minutes.
10. Luminescence was measured using the microplate reader. “Blank” value was subtracted from all readings.

6. Assay Protocol for CDK6

• Enzyme, substrate, ATP, and inhibitors were diluted in Kinase Buffer.
• To the wells of 384 low volume plate, the following was added:
- 1 µl of inhibitor or (5% DMSO)
- 2 µl of enzyme
- 2 µl of substrate/ATP mix
• Incubation at room temperature for 60 minutes.
• 5 µl of ADP-Glo™ Reagent
• Incubation at room temperature for 40 minutes.
• 10 µl of Kinase Detection Reagent
• Incubation at room temperature for 30 minutes.
• Luminescence was recorded (Integration time 0.5-1second).

7. Assay Protocol for CDK7

1. 5x Kinase assay buffer 1, ATP, and 10x CDK substrate peptide 2 was thawed.

2. The master mixture was prepared (12.5 µl per well): N wells x (3 µl 5x Kinase assay buffer 1 + 0.5 µl ATP (500 µM) + 1.25 µl CDK substrate peptide 2 (1 mg/ml) + 7.75 µl distilled water), 12.5 µl was added to every well.
3. 2.5 µl of Inhibitor solution was added of each well labeled as “Test Inhibitor”. For the “Positive Control" and “Blank”, 2.5 µl of 10% DMSO in water was added (Inhibitor buffer).
4. 3 ml of 1x Kinase assay buffer 1 was prepared by mixing 600 µl of 5x Kinase assay buffer 1 with 2400 µl water.
5. To the wells designated as "Blank", 10 µl of 1x Kinase assay buffer 1 was added.
6. CDK7/Cyclin H/MAT1 enzyme was thawed on ice. Upon the first thaw, spin was done for a tube containing the enzyme to recover the full content of the tube. The amount of CDK7/Cyclin H/MAT1 that was required for the assay was calculated and the enzyme was diluted to ~10 ng/µl with 1x Kinase assay buffer 1.
7. The reaction was initiated by adding 10 µl of diluted CDK7/Cyclin H/MAT1 enzyme to the wells designated “Positive Control” and "Test Inhibitor Control", then Incubated at 30°C for 60 minutes.
8. ADP-Glo reagent was thawed.
9. After the 60-minute reaction, 25 µl of ADP-Glo reagent was added to each well. The plate was covered with aluminum foil and incubated at room temperature for 45 minutes.
10. Kinase-Detection reagent was thawed.
11. After the 45 minutes’ incubation, 50 µl of Kinase Detection reagent was added to each well. The plate was covered with aluminum foil and incubated at room temperature for another 45 minutes.
12. Luminescence was measured using the microplate reader. “Blank” value was subtracted from all readings.

8. Assay Protocol for CDK9

1. 5x Kinase assay buffer 1, ATP, and 5x CDK substrate peptide 2 was thawed.
2. The master mixture was prepared (25 µl per well): N wells x (6 µl 5x Kinase assay buffer 1 + 1 µl ATP (500 µM) + 10 µl 5x CDK substrate peptide 2 + 8 µl distilled water). 25 µl was added to every well.
3. 5 µl of Inhibitor solution of each well was added labeled as “Test Inhibitor”. For the “Positive Control" and “Blank”, 5 µl of the same solution was added without inhibitor (Inhibitor buffer).

4. 3 ml Of 1x Kinase assay buffer 1 was prepared by mixing 600 µl of 5x Kinase assay buffer 1 with 2400 µl water.
5. To the wells designated as "Blank", 20 µl of 1x Kinase assay buffer 1 was added.
6. CDK9/CyclinT enzyme was thawed on ice. Upon the first thaw, spin was done for a tube containing an enzyme to recover the full content of the tube. The amount of CDK9/CyclinT required for the assay was calculated and the enzyme was diluted to ~5 ng/µl with 1x Kinase assay buffer 1.
7. The reaction was initiated by adding 20 µl of diluted CDK9/CyclinT enzyme to the wells designated “Positive Control” and "Test Inhibitor Control", then Incubated at 30°C for 45 minutes.
8. Kinase-Glo Max reagent was thawed.
9. After the 45-minute reaction, 50 µl of Kinase-Glo Max reagent was added to each well. The plate was covered with aluminum foil and incubated at room temperature for 15 minutes.
10. Luminescence was measured using the microplate reader. “Blank” value was subtracted from all readings.

9. Inhibition of Phospho-CDK1 / CDC2 Cell-Based Phosphorylation in SK-MEL-5 cancer cell

The assay was performed according to the following protocol

1. 200 µl of 20,000 adherent cells were seeded in culture medium in each well of a 96-well plate. The plates included in the kit were sterile and treated for cell culture. For suspension cells and loosely attached cells, the plates were coated with 100 µl of 10 µg/ml Poly-L-Lysine (not included) to each well of a 96-well plate for 30 minutes at 37°C before adding cells.
2. The cells were incubated overnight at 37°C, 5% CO_2, and then treated as desired.
3. The cell culture medium was removed and rinse with 200 µl of 1x TBS, twice.
4. The cells were fixed by incubating with 100 µl of Fixing Solution for 20 minutes at room temperature. The 4% formaldehyde was used for adherent cells and 8% formaldehyde was used for suspension cells and loosely attached cells. During the incubation, the plates were sealed with Parafilm.
5. The Fixing Solution was removed and the plate was washed 3 times with 200 µl 1x Wash Buffer for five minutes each time with gentle shaking on the orbital shaker. The plate was stored at 4°C for a week.

6. 100 µl Quenching Buffer was added and incubated for 20 minutes at room temperature.
7. The plate was washed 3 times with 1x Wash Buffer for 5 minutes at a time, with gentle shaking on the shaker.
8. 200 µl of Blocking Buffer was added and incubated for 1 hour at room temperature, washed 3 times with 200 µl of 1x Wash Buffer for 5 minutes at a time, with gentle shaking on the shaker.
9. 50 µl of 1x primary antibodies (Anti-CDC2 (Phospho-Tyr15) Antibody, Anti-CDC2 Antibody and/or Anti-GAPDH Antibody) was added to the corresponding wells, covered with Parafilm and incubated for 16 hours (overnight) at 4°C, washed 3 times with 200 µl of 1x Wash Buffer for 5 minutes at a time, with gentle shaking on the shaker.
10. 50 µl of 1x secondary antibodies (HRP-Conjugated Anti- Rabbit IgG Antibody and/or HRP-Conjugated Anti-Mouse IgG Antibody) was added to corresponding wells and incubated for 1.5 hours at room temperature with gentle shaking on the shaker.
11. Washed 3 times with 200 µl of 1x Wash Buffer for 5 minutes at a time, with gentle shaking on the shaker.
12. 50 µl of Ready-to-Use Substrate was added to each well and incubated for 30 minutes at room temperature in the dark with gentle shaking on the shaker. Note: Ready-to-Use Substrate is a light-sensitive reagent. Keep away from light.
13. 50 µl of Stop Solution was added to each well and read OD at 450 nm immediately using the microplate reader.

L. Docking Studies

The automated docking simulation study was performed using Molecular Operating Environment (MOE®) version 2014.09, at Assiut University Faculty of Pharmacy, Chemical Computing Group Inc., and Montreal, Canada. The X-ray crystallographic structure of the target kinase (PDB: ID 4YC3) was obtained from the Protein data bank. The target compounds were constructed into a 3D model using the builder interface of the MOE program. After checking their structures and the formal charges on atoms by the 2D depiction, the following steps were carried out:[314-315]

- The target compounds were subjected to a conformational search.

• All conformers were subjected to energy minimization, all the minimizations were performed with MOE until an RMSD gradient of 0.01 Kcal/mole and an RMS distance of 0.1 Å with MMFF94X force-field and the partial charges were automatically calculated.

The enzyme was prepared for docking studies by:

• Hydrogen atoms were added to the system with their standard geometry.

• The atoms connection and type were checked for any errors with automatic correction.

• Selection of the receptor and its atoms potential were fixed.

• The MOE® Alpha Site Finder was used for the active site search in the enzyme structure using all default items. Dummy atoms were created from the obtained alpha Spheres.

5.2.5. Analytical Data of Fused Heterocycles Based on 4-Hydroxy-2-quinolones

1,6-Disubstituted-quinoline-2,4-(1*H*,3*H*)-diones **82a–f** were prepared according to the literature.[296, 316]

General Procedures (GP9)

A suspension of 1,6-disubstituted quinoline-2,4-(1*H*,3*H*)-diones (**82a-f**, 1.00 mmol, 1.00 equiv.) in THF (50 mL) was added to a solution of 3,4,5,6-tetrachloro-1,2-benzoquinone (*o*-CHL) (**205**, 0.25 g, 1.00 mmol, 1.00 equiv.) in THF (15 mL). The reaction mixture was gently heated under reflux for 10-15 h until the starting material had disappeared (monitored by TLC). The resulting precipitates were filtered and washed with THF several times (3 x 20 mL) to afford compounds **206a-f**.

7,8-Dichlorobenzofuro[3,2-*c*]quinolin-6,9,10(5*H*)-trione (206a)

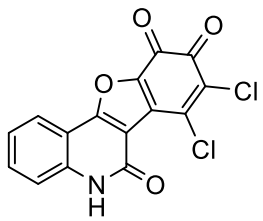

According to **GP9**, 4-hydroxyquinolin-2(1*H*)-one (**82a**, 0.161 g, 1.00 mmol, 1.00 equiv.) was refluxed with *o*-CHL (**205**, 0.245 g, 1.00 mmol, 1.00 equiv.) in THF for 10 h. A precipitate of the title compound was obtained as a pale brown solid (0.250 g, 75%, 748 μmol).

R$_f$ = 0.15 (cyclohexane/ethyl acetate; 1:1). – **Mp**: > 350 °C. – **^{1}H NMR** (400 MHz, DMSO-*d*$_6$) δ = 12.20 (s, 1H, N*H*), 7.78–7.76 (m, 2H, *H*^{Ar}), 7.37–7.34 (m, 2H, *H*^{Ar}) ppm. – **^{13}C NMR** (101 MHz, DMSO-*d*$_6$) δ = 177.8 (C$_q$, *C*O), 174.0 (C$_q$, *C*O), 163.5 (C$_q$, *C*^{Ar}), 157.2 (C$_q$, *C*O), 151.0 (C$_q$, *C*^{Ar}), 148.8 (C$_q$, *C*^{Ar}), 144.0 (C$_q$, *C*^{Ar}), 140.6 (C$_q$, *C*^{Ar}), 130.6 (C$_q$, *C*^{Ar}), 128.0 (+, *C*H^{Ar}), 127.4 (+, *C*H^{Ar}), 125.6 (+, *C*H^{Ar}), 124.4 (+, *C*H^{Ar}), 110.0 (C$_q$, *C*^{Ar}), 108.0 (C$_q$, *C*^{Ar}) ppm. – **IR** (ATR) $\tilde{\nu}$ = 3328 (vw), 3187 (vw), 2927 (m), 2851 (w), 1720 (s), 1665 (s), 1600 (vs), 1585 (s), 1436 (m), 1383 (vs), 1322 (vs), 1254 (vs), 1200 (vs), 1180 (vs), 840 (m), 758 (m), 717 (s), 626 (m) cm^{-1}. – **MS** (FAB, 3-NBA): *m/z* (%) = 335 (55) [M+H]$^+$, 334 (20) [M]$^+$. – **EA** ($C_{15}H_5Cl_2NO_4$) calc.: C, 53.92; H, 1.51; N, 4.19. found: C, 54.10; H, 1.55; N, 4.30.

2,7,8-Trichlorobenzofuro[3,2-*c*]quinolin-6,9,10(5*H*)-trione (206b)

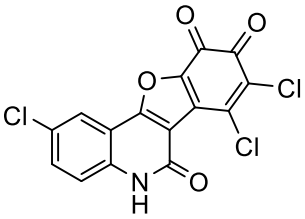

According to **GP9**, 6-chloro-4-hydroxyquinolin-2(1H)-one (**82b**, 0.195 g, 1.00 mmol, 1.00 equiv.) was refluxed with *o*-CHL (**205**, 0.245 g, 1.00 mmol, 1.00 equiv.) in THF for 15 h. A precipitate of the title compound was obtained as a pale brown solid (0.258 g, 70%, 700 µmol).

R_f = 0.13 (cyclohexane/ethyl acetate; 1:1). – **Mp**: > 350 °C. – **^{1}H NMR** (400 MHz, DMSO-d_6) δ = 11.90 (s, 1H, N*H*), 7.78 (d, *J* = 0.8 Hz, 1H, H^{Ar}), 7.56-7.54 ppm (m, 2H, H^{Ar}) ppm. – **^{13}C NMR** (101 MHz, DMSO-d_6) δ = 179.8 (C_q, *C*O), 174.8 (C_q, *C*O), 166.5 (C_q, C^{Ar}), 156.5 (C_q, *C*O), 152.0 (C_q, C^{Ar}), 150.0 (C_q, C^{Ar}), 136.9 (C_q, C^{Ar}), 133.0 (C_q, C^{Ar}), 131.0 (C_q, C^{Ar}), 128.6 (C_q, C^{Ar}), 128.0 (+, *C*H^{Ar}), 127.4 (+, *C*H^{Ar}), 126.0 (+, *C*H^{Ar}), 110.0 (C_q, C^{Ar}), 108.0 (C_q, C^{Ar}) ppm. – **IR** (ATR) $\tilde{\nu}$ = 3328 (vw), 3187 (vw), 2927 (m), 2851 (w), 1723 (s), 1666 (s), 1601 (vs), 1585 (s), 1436 (m), 1385 (vs), 1321 (vs), 1254 (vs), 1205 (vs), 1182 (vs), 840 (m), 751 (m), 720 (s), 626 (m) cm^{-1}. – **MS** (FAB, 3-NBA): *m/z* (%) = 369 (40) $[M+H]^+$, 368 (60) $[M]^+$. – **EA** ($C_{15}H_4Cl_3NO_4$) calc.: C, 48.88; H, 1.09; N, 3.80. found: C, 48.74; H, 1.12; N, 3.70.

3,7,8-Trichlorobenzofuro[3,2-*c*]quinolin-6,9,10(5*H*)-trione (206c)

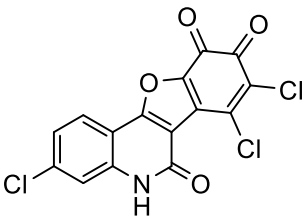

According to **GP9**, 7-chloro-4-hydroxyquinolin-2(1*H*)-one (**82c**, 0.19 g, 1.00 mmol, 1.00 equiv.) was refluxed with *o*-CHL (**205**, 0.245 g, 1.00 mmol, 1.00 equiv.) in THF for 15 h. A precipitate of the title compound was obtained as a pale brown solid (0.243 g, 66%, 659 µmol).

R_f = 0.13 (cyclohexane/ethyl acetate; 1:1). – **Mp**: > 350 °C. – **^{1}H NMR** (400 MHz, DMSO-d_6) δ = 11.80 (s, 1H, N*H*), 7.74-7.72 (m, 1H, H^{Ar}), 7.55-7.52 (m, 2H, H^{Ar}) ppm. – **^{13}C NMR** (101 MHz, DMSO-d_6) δ = 179.0 (C_q, *C*O), 173.2 (C_q, *C*O), 164.8 (C_q, C^{Ar}), 158.5 (C_q, *C*O), 151.0 (C_q, C^{Ar}), 150.4 (C_q, C^{Ar}), 136.4 (C_q, C^{Ar}), 133.0 (C_q, C^{Ar}), 130.4 (C_q, C^{Ar}), 128.6 (C_q, C^{Ar}), 128.06 (+, *C*H^{Ar}), 127.2 (+, *C*H^{Ar}), 124.6 (+, *C*H^{Ar}), 111.0 (C_q, C^{Ar}), 108.0 (C_q, C^{Ar}) ppm. – **IR** (ATR) $\tilde{\nu}$ = 3330 (vw), 3188 (vw), 2923 (m), 2852 (w), 1722 (s), 1670 (s), 1590 (vs), 1580 (s), 1434 (m), 1386 (vs), 1322 (vs), 1254 (vs), 1205 (vs), 1184 (vs), 840 (m), 752 (m), 723 (s), 626 (m) cm^{-1}. – **MS** (FAB, 3-NBA): *m/z* (%) = 369 (34) $[M+H]^+$, 368 (52) $[M]^+$. – **EA** ($C_{15}H_4Cl_3NO_4$) calc.: C, 48.88; H, 1.09; N, 3.80 found: C, 48.70; H, 1.00; N, 3.60.

2-Bromo-7,8-dichlorobenzofuro[3,2-*c*]quinolin-6,9,10(5*H*)-trione (206d)

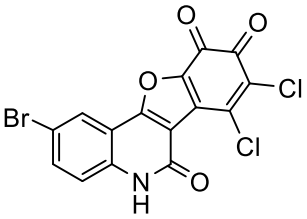

According to **GP9**, 7-bromo-4-hydroxyquinolin-2(1*H*)-one (**82d**, 0.240 g, 1.00 mmol, 1.00 equiv.) was refluxed with *o*-CHL (**205**, 0.245 g, 1.00 mmol, 1.00 equiv.) in THF for 10 h. A precipitate of the title compound was obtained as a brown solid (0.310 g, 75%, 751 µmol).

R_f = 0.12 (cyclohexane/ethyl acetate; 1:1). – **Mp**: > 350 °C. – **^{1}H NMR** (400 MHz, DMSO-d_6) δ = 12.10 (s, 1H, N*H*), 7.66 (d, *J* = 1.2 Hz, 1H, H^{Ar}), 7.45-7.40 (m, 2H, H^{Ar}) ppm. – **^{13}C NMR** (101 MHz, DMSO-d_6) δ = 179.2 (C_q, *C*O), 174.1 (C_q, *C*O), 166.2 (C_q, C^{Ar}), 160.0 (C_q, *C*O), 156.0 (C_q, C^{Ar}), 149.0 (C_q, C^{Ar}), 135.0 (C_q, C^{Ar}), 133.0 (C_q, C^{Ar}), 131.0 (C_q, C^{Ar}), 128.6 (C_q, C^{Ar}), 128.0 (+, *C*H^{Ar}), 126.0 (+, *C*H^{Ar}), 124.8 (+, *C*H^{Ar}), 110.0 (C_q, C^{Ar}), 108.0 (C_q, C^{Ar}) ppm. – **IR** (ATR) $\tilde{\nu}$ = 3328 (vw), 3189 (vw), 2921 (m), 2853 (w), 1720 (s), 1665 (s), 1585 (vs), 1580 (s), 1439 (m), 1386 (vs), 1322 (vs), 1254 (vs), 1204 (vs), 1185 (vs), 840 (m), 750 (m), 723 (s), 620 (m) cm^{-1}. – **MS** (FAB, 3-NBA): *m/z* (%) = 414 (52) $[M+H]^+$, 413 (64) $[M]^+$. – **EA** ($C_{15}H_4BrCl_2NO_4$) calc.: C, 43.62; H, 0.98; N, 3.39. found: C, 43.50; H, 1.08; N, 3.50.

7,8-Dichloro-3-methyl-benzofuro[3,2-*c*]quinolin-6,9,10(5*H*)-trione (206e)

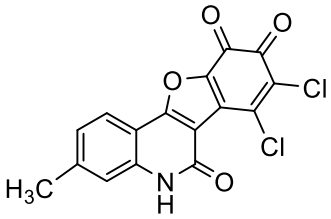

According to **GP9**, 4-hydroxy-7-methylquinolin-2(1*H*)-one (**82e**, 0.175 g, 1.00 mmol, 1.00 equiv.) was refluxed with *o*-CHL (**205**, 0.245 g, 1.00 mmol, 1.00 equiv.) in THF for 12 h. A precipitate of the title compound was obtained as a brown solid (0.312 g, 76%, 755 µmol).

R_f = 0.14 (cyclohexane/ethyl acetate; 1:1). – **Mp**: > 350 °C. – **^{1}H NMR** (400 MHz, DMSO-d_6) δ = 11.98 (s, 1H, N*H*), 7.76 (dd, *J* = 1.0, 0.7 Hz, 1H, H^{Ar}), 7.60-7.54 (m, 2H, H^{Ar}), 2.35 (s, 3H, CH_3) ppm. – **^{13}C NMR** (101 MHz, DMSO-d_6) δ = 178.8 (C_q, *C*O), 174.0 (C_q, *C*O), 166.6 (C_q, C^{Ar}), 156.2 (C_q, *C*O), 153.0 (C_q, C^{Ar}), 146.7 (C_q, C^{Ar}), 141.5 (C_q, C^{Ar}), 141.0 (C_q, C^{Ar}), 137.0 (C_q, C^{Ar}), 135.4 (C_q, C^{Ar}), 132.2 (+, *C*H^{Ar}), 128.2 (+, *C*H^{Ar}), 122.4 (+, *C*H^{Ar}), 112.0 (C_q, C^{Ar}), 110.0 (C_q, C^{Ar}), 20.3 (+, *C*H_3) ppm. – **IR** (ATR) $\tilde{\nu}$ = 3310 (vw), 3190 (vw), 2920 (m), 2850 (w), 1725 (s), 1709 (s), 1600 (vs), 1580 (s), 1440 (m), 1390 (vs), 1320 (vs), 1254 (vs), 1202 (vs), 1180 (vs), 841 (m), 753 (m), 723 (s), 620 (m) cm^{-1}. – **MS** (FAB, 3-NBA): *m/z* (%) = 349 (56) $[M+H]^+$, 348 (50) $[M]^+$. – **EA** ($C_{16}H_7Cl_2NO_4$) calc.: C, 55.20; H, 2.03; N, 4.02. found: C, 55.35; H, 2.10; N, 4.10.

7,8-Dichloro-2-methyl-benzofuro[3,2-*c*]quinolin-6,9,10(5*H*)-trione (206f)

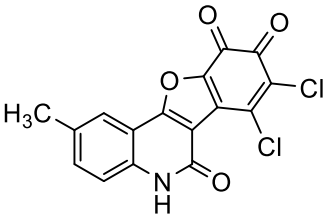

According to **GP9**, 4-hydroxy-6-methylquinolin-2(1*H*)-one (**82f**, 0.175 g, 1.00 mmol, 1.00 equiv.) was refluxed with *o*-CHL (**205**, 0.245 g, 1.00 mmol, 1.00 equiv.) in THF for 12 h. A precipitate of the title compound was obtained as a pale brown solid (0.315 g, 76%, 763 µmol).

R_f = 0.14 (cyclohexane/ethyl acetate; 1:1). – **Mp**: > 350 °C. – **^{1}H NMR** (400 MHz, DMSO-d_6) δ = 11.98 (s, 1H, N*H*), 7.69 (d, *J* = 0.8 Hz, 1H, H^{Ar}), 7.64 (dd, *J* = 1.2, 0.7 Hz, 1H, H^{Ar}), 7.34 (d, *J* = 1.2 Hz, 1H, H^{Ar}), 2.41 (s, 3H, CH_3) ppm. – **^{13}C NMR** (101 MHz, DMSO-d_6) δ = 177.5 (C_q, *C*O), 174.6 (C_q, *C*O), 166.5 (C_q, C^{Ar}), 156.4 (C_q, *C*O), 146.9 (C_q, C^{Ar}), 141.0 (C_q, C^{Ar}), 140.9 (C_q, C^{Ar}), 137.6 (C_q, C^{Ar}), 136.9 (C_q, C^{Ar}), 133.3 (C_q, C^{Ar}), 132.4 (+, *C*H^{Ar}), 128.0 (+, *C*H^{Ar}), 121.4 (+, *C*H^{Ar}), 108.7 (C_q, C^{Ar}), 107.5 (C_q, C^{Ar}), 20.3 (+, *C*H_3) ppm. – **IR** (ATR) $\tilde{\nu}$ = 3330 (vw), 3190 (vw), 2921 (m), 2852 (w), 1722 (s), 1668 (s), 1600 (vs), 1585 (s), 1441 (m), 1392 (vs), 1323 (vs), 1253 (vs), 1202 (vs), 1180 (vs), 842 (m), 758 (m), 723 (s), 629 (m) cm^{-1}. – **MS** (FAB, 3-NBA): *m/z* (%) = 349 (50) $[M+H]^+$, 348 (52) $[M]^+$. – **EA** ($C_{16}H_7Cl_2NO_4$) calc.: C, 55.20; H, 2.03; N, 4.02. found: C, 55.30; H, 2.15; N, 3.93.

General Procedures (GP10)

A suspension of 1,6-disubstituted quinoline-2,4-(1*H*,3*H*)-diones (**82a–f**, 2.00 mmol, 2.00 equiv.) in DMF (10 mL) was added to a solution of 2,3-dichloropyrazine (DCP) (**212**, 0.149 g, 1.00 mmol, 1.00 equiv.) in DMF (15 mL) and Et_3N (0.5 mL). The reaction mixture was gently refluxed for 20–25 h until the starting material had disappeared (monitored by TLC). The resulting precipitates which were obtained after cooling the reaction mixture to room temperature were filtered off and washed with EtOH several times (3 x 20 mL) to afford compounds **213a-f**.

5,12-Dihydropyrazino[2,3-*c*:5,6-*c′*]difuro[2,3-*c*:4,5-*c′*]diquinoline-6,14-(5*H*,12*H*)-dione (213a)

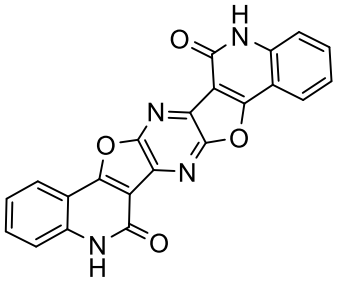

According to **GP10**, 4-hydroxyquinolin-2(1*H*)-one (**82a**, 0.322 g, 2.00 mmol, 2.00 equiv.) was refluxed with DCP (**212**, 0.149 g, 1.00 mmol, 1.00 equiv.) in DMF/Et_3N for 20 h. A precipitate of the title compound was obtained as a buff solid (0.255 g, 65%, 647 μmol).

R_f = 0.18 (cyclohexane/ethyl acetate; 1:1). – **Mp**: 278–280 °C. – **^{1}H NMR** (400 MHz, DMSO-d_6) δ = 12.11 (s, 2H, N*H*), 7.89–7.85 (m, 2H, H^{Ar}), 7.52–7.48 (m, 2H, H^{Ar}), 7.35–7.32 (m, 2H, H^{Ar}), 7.23–7.19 (m, 2H, H^{Ar}) ppm. – **^{13}C NMR** (100 MHz, DMSO-d_6) δ = 165.2 (C_q, *C*O), 160.2 (C_q, C^{Ar}), 153.4 (C_q, C^{Ar}), 139.4 (C_q, C^{Ar}), 138.4 (C_q, C^{Ar}), 130.7 (C_q, C^{Ar}), 125.9 (+, *C*H^{Ar}), 128.4 (+, *C*H^{Ar}), 122.8 (+, *C*H^{Ar}), 115.7 (+, *C*H^{Ar}), 109.5 (C_q, C^{Ar}) ppm. – **IR** (ATR) $\tilde{\nu}$ = 3160 (w), 3080 (w), 2996 (w), 2932 (w), 2863 (w), 1785 (s), 1721 (s), 1650 (vs), 1557 (vs), 1480 (s), 1419 (s), 1333 (m), 1235 (m), 1196 (m), 1140 (vs), 1105 (vs), 967 (vs), 853 (vs), 772 (vs), 704 (vs), 650 (s), 595 (vs), 533 (vs), 453 (vs) cm^{-1}. – **MS** (FAB, 3-NBA): *m/z* (%) = 395 (50) $[M+H]^+$, 394 (27) $[M]^+$. – **EA** ($C_{22}H_{10}N_4O_4$) calc.: C, 67.01; H, 2.56; N, 14.21. found: C, 66.90; H, 2.70; N, 14.30.

2,10-Dichloro-5,12-dihydropyrazino[2,3-*c*:5,6-*c′*]difuro[2,3-*c*:4,5-*c′*]diquinoline-6,14-(5*H*,12*H*)-dione (213b)

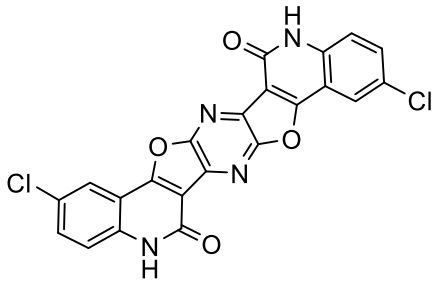

According to **GP10**, 6-chloro-4-hydroxyquinolin-2(1*H*)-one (**82b**, 0.391 g, 2.00 mmol, 2.00 equiv.) was refluxed with DCP (**212**, 0.149 g, 1.00 mmol, 1.00 equiv.) in DMF/Et_3N for 22 h. A precipitate of the title compound was obtained as a buff solid (0.310 g, 67%, 669 µmol).

R_f = 0.20 (cyclohexane/ethyl acetate; 1:1). – **Mp**: 320–322 °C. – **^{1}H NMR** (400 MHz, DMSO-d_6) δ = 12.07 (s, 2H, N*H*), 7.98 (d, *J* = 0.7 Hz, 2H, H^{Ar}), 7.38–7.20 (m, 4H, H^{Ar}) ppm. – **^{13}C NMR** (100 MHz, DMSO-d_6) δ = 167.2 (C_q, *C*O), 160.2 (C_q, C^{Ar}), 154.4 (C_q, C^{Ar}), 139.0 (C_q, C^{Ar}), 138.2 (C_q, C^{Ar}), 128.1 (C_q, C^{Ar}), 126.9 (+, CH^{Ar}), 125.4 (+, CH^{Ar}), 120.0 (+, CH^{Ar}), 118.0 (C_q, C^{Ar}), 109.4 (C_q, C^{Ar}) ppm. – **IR** (ATR) $\tilde{\nu}$ = 3301 (vw), 3053 (w), 2929 (m), 2836 (m), 2621 (w), 1656 (vs), 1601 (vs), 1466 (s), 1384 (vs), 1330 (vs), 1166 (s), 1085 (m), 860 (s), 789 (vs), 769 (vs), 732 (s), 663 (m), 438 (vs) cm^{-1}. – **MS** (FAB, 3-NBA): *m/z* (%) = 464 (60) $[M+H]^+$, 463 (30) $[M]^+$. – **EA** ($C_{22}H_8Cl_2N_4O_4$) calc.: C, 57.04; H, 1.74; N, 12.10. found: C, 57.20; H, 1.70; N, 12.20.

3,11-Dichloro-5,12-dihydropyrazino[2,3-*c*:5,6-*c′*]difuro[2,3-*c*:4,5-*c′*]diquinoline-6,14-(5*H*,12*H*)-dione (213c)

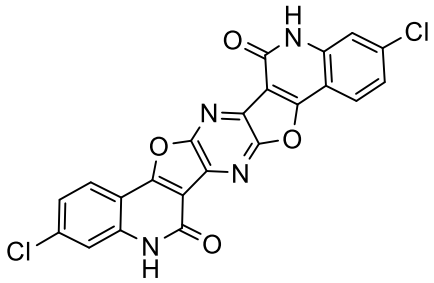

According to **GP10**, 7-chloro-4-hydroxyquinolin-2(1*H*)-one (**82c**, 0.391 g, 2.00 mmol, 2.00 equiv.) was refluxed with DCP (**212**, 0.149 g, 1.00 mmol, 1.00 equiv.) in DMF/Et_3N for 22 h. A precipitate of the title compound was obtained as a buff solid (0.295 g, 64%, 637 µmol).

R_f = 0.20 (cyclohexane/ethyl acetate; 1:1). – **Mp**: 350–352 °C. – **^{1}H NMR** (400 MHz, DMSO-d_6) δ = 12.11 (s, 2H, N*H*), 7.95 (d, *J* = 1.2 Hz, 2H, H^{Ar}), 7.45–7.41 (m, 4H, H^{Ar}) ppm. – **^{13}C NMR** (101 MHz, DMSO-d_6) δ = 167.0 (C_q, *C*O), 160.4 (C_q, C^{Ar}), 152.0 (C_q, C^{Ar}), 138.7 (C_q, C^{Ar}), 138.0 (C_q, C^{Ar}), 130.6 (C_q, C^{Ar}), 127.0 (+, *C*H^{Ar}), 124.9 (+, *C*H^{Ar}), 122.2 (+, *C*H^{Ar}), 120.0 (C_q, C^{Ar}), 108.2 (C_q, C^{Ar}) ppm. – **IR** (ATR) $\tilde{\nu}$ = 3288 (w), 3150 (w), 3067 (m), 3013 (m), 2925 (m), 2836 (m), 1795 (m), 1724 (vs), 1659 (vs), 1611 (vs), 1582 (vs), 1555 (vs), 1492 (vs), 1424 (vs), 1222 (vs), 1143 (vs), 1108 (vs), 1085 (vs), 982 (s), 935 (s), 871 (vs), 792 (vs), 751 (vs), 592 (vs), 465 (vs) cm^{-1}. – **MS** (FAB, 3-NBA): *m/z* (%) = 464 (64) $[M+H]^+$, 463 (36) $[M]^+$. – **EA** ($C_{22}H_8Cl_2N_4O_4$) calc.: C, 57.04; H, 1.74; N, 12.10. found: C, 57.00; H, 1.80; N, 12.15.

2,10-Dibromo-5,12-dihydropyrazino[2,3-*c*:5,6-*c′*]difuro[2,3-*c*:4,5-*c′*]-diquinoline-6,14-(5*H*,12*H*)-dione (213d)

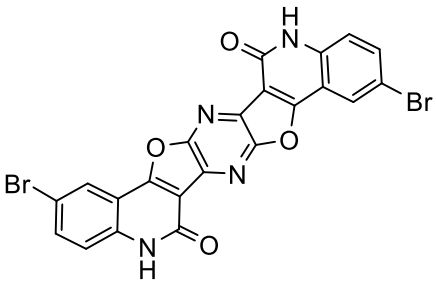

According to **GP10**, 7-bromo-4-hydroxyquinolin-2(1*H*)-one (**82d**, 0.480 g, 2.00 mmol, 2.00 equiv.) was refluxed with DCP (**212**, 0.149 g, 1.00 mmol, 1.00 equiv.) in DMF/Et_3N for 25 h. A precipitate of the title compound was obtained as a pale yellow solid (0.370 g, 67%, 670 μmol).

R_f = 0.19 (cyclohexane/ethyl acetate; 1:1). – **Mp**: 310–312 °C. – **^{1}H NMR** (400 MHz, DMSO-d_6) δ = 12.43 (s, 2H, N*H*), 8.01–7.96 (m, 2H, H^{Ar}), 7.75–7.72 (m, 2H, H^{Ar}), 7.38–7.36 (m, 2H, H^{Ar}) ppm. – **^{13}C NMR** (101 MHz, DMSO-d_6) δ = 166.8 (C_q, *C*O), 160.4 (C_q, C^{Ar}), 150.8 (C_q, C^{Ar}), 141.0 (C_q, C^{Ar}), 135.5 (C_q, C^{Ar}), 131.4 (C_q, C^{Ar}), 128.6 (+, *C*H^{Ar}), 127.8 (+, *C*H^{Ar}), 124.2 (+, *C*H^{Ar}), 118.2 (C_q, C^{Ar}), 103.0 (C_q, C^{Ar}) ppm. – **IR** (ATR) $\tilde{\nu}$ = 3424 (w), 3153 (m), 3080 (m), 2832 (m), 1790 (m), 1715 (vs), 1652 (vs), 1555 (vs), 1496 (vs), 1429 (vs), 1375 (s), 1222 (vs), 1142 (vs), 1109 (vs), 965 (vs), 827 (vs), 795 (vs), 584 (vs), 534 (vs), 506 (vs), 466 (vs) cm^{-1}. – **MS** (FAB, 3-NBA): *m/z* (%) = 553 (58) $[M+H]^+$, 552 (100) $[M]^+$. – **EA** ($C_{22}H_8Br_2N_4O_4$) calc.: C, 47.86; H, 1.46; N, 10.15. found: C, 47.90; H, 1.56; N, 10.25.

5,12-Dihydro-3,11-dimethylpyrazino[2,3-*c*:5,6-*c′*]difuro[2,3-*c*:4,5-*c′*]diquinoline-6,14-(5*H*,12*H*)-dione (213e)

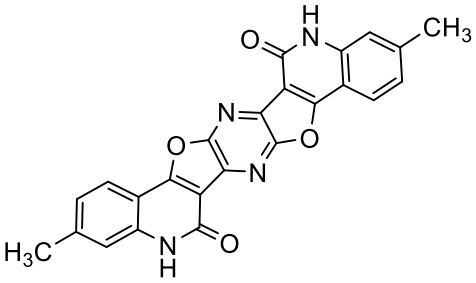

According to **GP10**, 4-hydroxy-7-methylquinolin-2(1*H*)-one (**82e**, 0.350 g, 2.00 mmol, 2.00 equiv.) was refluxed with DCP (**212**, 0.149 g, 1.00 mmol, 1.00 equiv.) in DMF/Et_3N for 23 h. A precipitate of the title compound was obtained as a brown solid (0.280 g, 66%, 663 μmol).

R_f = 0.21 (cyclohexane/ethyl acetate; 1:1). – **Mp**: 276–278 °C. – **^{1}H NMR** (400 MHz, DMSO-d_6) δ = 12.15 (s, 2H, 2 × N*H*), 7.92 (d, *J* = 0.8 Hz, 2H, H^{Ar}), 7.45–7.30 (m, 4H, H^{Ar}), 2.16 (s, 6H, 2 × CH_3) ppm. – **^{13}C NMR** (101 MHz, DMSO-d_6) δ = 166.8 (C_q, *C*O), 159.8 (C_q, C^{Ar}), 150.0 (C_q, C^{Ar}), 138.0 (C_q, C^{Ar}), 137.4 (C_q, C^{Ar}), 130.0 (C_q, C^{Ar}), 128.2 (+, CH^{Ar}), 127.8 (+, CH^{Ar}), 127.2 (+, CH^{Ar}), 125.5 (C_q, C^{Ar}), 110.4 (C_q, C^{Ar}), 20.4 (+, CH_3) ppm. – **IR** (ATR) $\tilde{\nu}$ = 3177 (w), 3126 (w), 3070 (w), 2996 (w), 2925 (w), 2863 (w), 1790 (s), 1714 (vs), 1655 (vs), 1596 (vs), 1554 (vs), 1483 (vs), 1390 (s), 1239 (s), 1203 (s), 1149 (vs), 1108 (vs), 1098 (vs), 965 (vs), 928 (s), 874 (vs), 853 (vs), 796 (vs), 752 (vs), 596 (vs), 465 (vs) cm^{-1}. – **MS** (FAB, 3-NBA): *m/z* (%) = 423 (58) $[M+H]^+$, 422 (28) $[M]^+$. – **EA** ($C_{24}H_{14}N_4O_4$) calc.: C, 68.24; H, 3.34; N, 13.26. found: C, 68.30; H, 3.45; N, 13.35.

5,12-Dihydro-2,10-dimethylpyrazino[2,3-*c*:5,6-*c′*]difuro[2,3-*c*:4,5-*c′*]diquinoline-6,14-(5*H*,12*H*)-dione (213f)

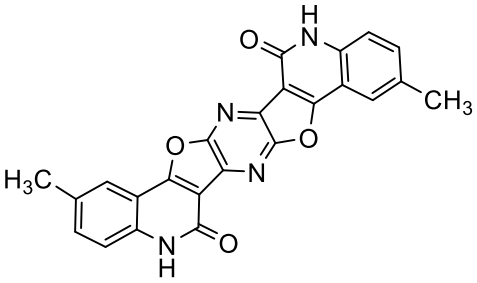

According to **GP10**, 4-hydroxy-6-methylquinolin-2(1*H*)-one (**82f**, 0.350 g, 2.00 mmol, 2.00 equiv.) was refluxed with DCP (**212**, 0.149 g, 1.00 mmol, 1.00 equiv.) in DMF/Et_3N for 23 h. A precipitate of the title compound was obtained as a brown solid (0.287 g, 68%, 679 µmol).

R_f = 0.21 (cyclohexane/ethyl acetate; 1:1). – **Mp**: 300–302 °C. – **^{1}H NMR** (400 MHz, DMSO-d_6) δ = 12.20 (s, 2H, 2 × N*H*), 7.84 (d, *J* = 1.2 Hz, 2H, H^{Ar}), 7.42–7.35 (m, 4H, H^{Ar}), 2.18 (s, 6H, CH_3) ppm. – **^{13}C NMR** (101 MHz, DMSO-d_6) δ = 166.2 (C_q, *C*O), 160.0 (C_q, C^{Ar}), 152.7 (C_q, C^{Ar}), 139.6 (C_q, C^{Ar}), 135.4 (C_q, C^{Ar}), 130.4 (C_q, C^{Ar}), 128.6 (C_q, C^{Ar}), 128.0 (+, *C*H^{Ar}), 127.0 (+, *C*H^{Ar}), 126.2 (+, *C*H^{Ar}), 110.4 (C_q, C^{Ar}), 20.2 (+, *C*H_3) ppm. – **IR** (ATR) $\tilde{\nu}$ = 3318 (w), 3207 (m), 3030 (w), 2912 (w), 2851 (w), 1790 (s), 1711 (vs), 1657 (vs), 1574 (vs), 1503 (vs), 1456 (vs), 1235 (vs), 1106 (vs), 975 (vs), 867 (vs), 829 (vs), 799 (vs), 751 (vs), 697 (vs), 586 (vs), 547 (vs) cm^{-1}. – **MS** (FAB, 3-NBA): *m/z* (%) = 423 (60) $[M+H]^+$, 422 (28) $[M]^+$. – **EA** ($C_{24}H_{14}N_4O_4$) calc.: C, 68.24; H, 3.34; N, 13.26. found: C, 68.20; H, 3.50; N, 13.32.

General Procedures (GP11)

A mixture of 1,6-disubstituted quinoline-2,4-(1*H*,3*H*)-diones (**82a–f**, 1.00 mmol, 1.00 equiv.) and (*E*)-1,2-dibenzoylethene (DBE) (**219**, 0.236 g, 1.00 mmol, 1.00 equiv.) in pyridine (50 mL) and 0.5 ml of Et_3N, was gently refluxed for 10–15 h until the starting material had disappeared (monitored by TLC). The resulting precipitates which were Formed after cooling to room temperature were filtered off and washed with EtOH several times (3 x 20 mL) to afford compounds **220a–f**.

2-(4-Hydroxy-2-oxo-1,2-dihydroquinolin-3-yl)-1,4-diphenylbutane-1,4-dione (220a)

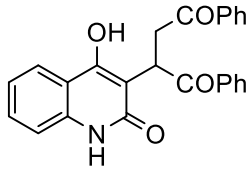

According to **GP11**, 4-hydroxyquinolin-2(1*H*)-one (**82a**, 0.161 g, 1.00 mmol, 1.00 equiv.) was refluxed with DBE (**219**, 0.236 g, 1.00 mmol, 1.00 equiv.) in pyridine/Et_3N for 10 h. A precipitate of the title compound was obtained as a yellow solid (0.295 g, 75%, 746 μmol).

R_f = 0.32 (cyclohexane/ethyl acetate; 1:1). – **Mp**: 325–327 °C. – **^{1}H NMR** (400 MHz, DMSO-d_6) δ = 12.20 (s, 1H, O*H*), 11.55 (s, 1H, N*H*), 8.01 (d, *J* = 7.5 Hz, 2H, H^{Ar}), 7.92 (d, *J* = 8.0 Hz, 1H, H^{Ar}), 7.83 (d, *J* = 7.5 Hz, 2H, H^{Ar}), 7.55 (t, *J* = 7.6 Hz, 2H, H^{Ar}), 7.48 (t, *J* = 7.5 Hz, 1H, H^{Ar}), 7.46 (t, *J* = 7.8 Hz, 1H, H^{Ar}), 7.38 (t, *J* = 7.5 Hz, 2H, H^{Ar}), 7.23 (d, *J* = 8.1 Hz, 1H, H^{Ar}), 7.14 (t, *J* = 7.6 Hz, 2H, H^{Ar}), 5.47 (dd, *J* = 9.6, 2.4 Hz, 1H, C*H*), 4.21 (dd, *J* = 17.3, 9.8 Hz, 1H, CH_2), 2.82 (dd, *J* = 17.2, 2.5 Hz, 1H, CH_2) ppm. – **^{13}C NMR** (101 MHz, DMSO-d_6) δ = 198.5 (C_q, *C*O), 198.3 (C_q, *C*O), 162.4 (C_q, *C*O), 158.9 (C_q, C^{Ar}), 137.8 (C_q, C^{Ar}), 137.0 (C_q, C^{Ar}), 136.7 (C_q, C^{Ar}), 132.9 (C_q, C^{Ar}), 132.3 (+, CH^{Ar}), 130.4 (+, CH^{Ar}), 128.6 (+, 2 × CH^{Ar}), 128.2 (+, 2 × CH^{Ar}), 127.8 (+, 2 × CH^{Ar}), 127.4 (+, 2 × CH^{Ar}), 122.7 (+, 2 × CH^{Ar}), 121.1 (+, CH^{Ar}), 115.2 (+, CH^{Ar}), 115.1 (C_q, C^{Ar}), 111.5 (C_q, C^{Ar}), 40.4 (–, CH_2), 37.4 (+, *C*H) ppm. – **IR** (ATR) $\tilde{\nu}$ = 3271 (w), 3207 (w), 3060 (w), 3023 (w), 2910 (w), 1697 (vs), 1673 (vs), 1632 (vs), 1589 (vs), 1497 (w), 1446 (m), 1271 (vs), 1203 (vs), 1150 (vs), 1105 (vs), 949 (vs), 796 (vs), 739 (vs), 687 (vs), 652 (vs), 547 (vs), 477 (vs), 456 (vs) cm^{-1}. – **MS** (FAB, 3-NBA): *m/z* (%) = 398 (100) $[M+H]^+$, 397 (60) $[M]^+$. – **EA** ($C_{25}H_{19}NO_4$) calc.: C, 75.55; H, 4.82; N, 3.52. found: C, 75.70; H, 4.90; N, 3.62.

2-(6-Chloro-4-hydroxy-2-oxo-1,2-dihydroquinolin-3-yl)-1,4-diphenylbutane-1,4-dione (220b)

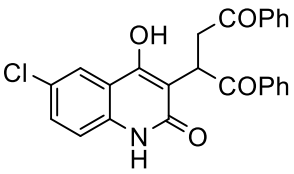

According to **GP11**, 6-chloro-4-hydroxyquinolin-2(1*H*)-one (**82b**, 0.195 g, 1.00 mmol, 1.00 equiv.) was refluxed with DBE (**219**, 0.236 g, 1.00 mmol, 1.00 equiv.) in pyridine/Et_3N for 12 h. A precipitate of the title compound was obtained as a pale yellow solid (0.310 g, 72%, 721 µmol).

R_f = 0.31 (cyclohexane/ethyl acetate; 1:1). – **Mp**: 315–317 °C. – **^{1}H NMR** (400 MHz, DMSO-d_6) δ = 12.30 (s, 1H, O*H*), 11.50 (s, 1H, N*H*), 8.00 (d, *J* = 7.6 Hz, 1H, H^{Ar}), 7.90 (d, *J* = 7.8 Hz, 1H, H^{Ar}), 7.82 (d, *J* = 8.0 Hz, 1H, H^{Ar}), 7.54–7.50 (m, 5H, H^{Ar}), 7.30 (t, *J* = 7.8 Hz, 2H, H^{Ar}), 7.24–7.10 (m, 3H, H^{Ar}), 5.50 (dd, *J* = 10.9, 2.3 Hz, 1H, C*H*), 4.18 (dd, *J* = 17.0, 9.9 Hz, 1H, CH_2), 2.80 (dd, *J* = 17.0, 2.6 Hz, 1H, CH_2) ppm. – **^{13}C NMR** (100 MHz, DMSO-d_6) δ = 198.5 (C_q, *C*O), 198.3 (C_q, *C*O), 164.0 (C_q, *C*O), 158.0 (C_q, C^{Ar}), 136.8 (C_q, 3 × C^{Ar}), 132.6 (+, *C*H^{Ar}), 132.1 (+, *C*H^{Ar}), 130.3 (+, 2 × *C*H^{Ar}), 128.5 (+, 2 × *C*H^{Ar}), 128.0 (+, 2 × *C*H^{Ar}), 127.8 (+, 2 × *C*H^{Ar}), 127.6 (+, 2 × *C*H^{Ar}), 123.0 (+, *C*H^{Ar}), 120.0 (C_q, C^{Ar}), 115.2 (C_q, C^{Ar}), 110.0 (C_q, C^{Ar}), 40.5 (–, *C*H_2), 37.2 (+, *C*H) ppm. – **IR** (ATR) $\tilde{\nu}$ = 3060 (w), 3006 (w), 2932 (w), 2812 (w), 1664 (vs), 1588 (s), 1486 (w), 1428 (m), 1334 (m), 1214 (s), 997 (m), 909 (m), 793 (m), 752 (vs), 686 (vs), 460 (m) cm^{-1}. – **MS** (FAB, 3-NBA): *m/z* (%) = 432 (60) $[M+H]^+$, 431 (23) $[M]^+$. – **EA** ($C_{25}H_{18}ClNO_4$) calc.: C, 69.53; H, 4.20; N, 3.24. found: C, 69.62; H, 4.30; N, 3.32.

2-(7-Chloro-4-hydroxy-2-oxo-1,2-dihydroquinolin-3-yl)-1,4-diphenylbutane-1,4-dione (220c)

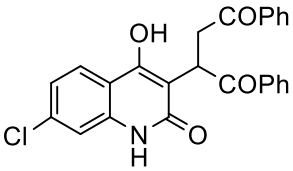

According to **GP11**, 7-chloro-4-hydroxyquinolin-2(1*H*)-one (**82c**, 0.195 g, 1.00 mmol, 1.00 equiv.) was refluxed with DBE (**219**, 0.236 g, 1.00 mmol, 1.00 equiv.) in pyridine/Et_3N for 12 h. A precipitate of the title compound was obtained as a white solid (0.300 g, 70%, 698 µmol).

R_f = 0.30 (cyclohexane/ethyl acetate; 1:1). – **Mp**: 340–342 °C. – **^{1}H NMR** (400 MHz, DMSO-d_6) δ = 12.10 (s, 1H, O*H*), 11.40 (s, 1H, N*H*), 7.98 (d, *J* = 7.8 Hz, 1H, H^{Ar}), 7.80 (d, *J* = 8.0 Hz, 1H, H^{Ar}), 7.60–7.50 (m, 6H, H^{Ar}), 7.20 (t, *J* = 7.8 Hz, 2H, H^{Ar}), 7.18–7.12 (m, 3H, H^{Ar}), 5.45 (dd, *J* = 10.9, 2.3 Hz, 1H, C*H*), 4.20 (dd, *J* = 17.0, 9.9 Hz, 1H, CH_2), 2.85 (dd, *J* = 17.0, 2.6 Hz, 1H, CH_2) ppm. – **^{13}C NMR** (101 MHz, DMSO-d_6) δ = 198.4 (C_q, *C*O), 198.1 (C_q, *C*O), 162.4 (C_q, *C*O), 157.8 (C_q, C^{Ar}), 138.7 (C_q, C^{Ar}), 137.0 (C_q, C^{Ar}), 136.6 (C_q, C^{Ar}), 134.9 (+, *C*H^{Ar}), 132.9 (+, *C*H^{Ar}), 132.4 (+, 2 × *C*H^{Ar}), 129.8 (+, 2 × *C*H^{Ar}), 128.9 (+, 2 × *C*H^{Ar}), 128.6 (+, 2 × *C*H^{Ar}), 128.5 (+, 2 × *C*H^{Ar}), 122.6 (+, *C*H^{Ar}), 119.5 (C_q, C^{Ar}), 121.3 (C_q, C^{Ar}), 114.3 (C_q, C^{Ar}), 40.6 (–, *C*H_2), 39.0 (+, *C*H) ppm. – **IR** (ATR) $\tilde{\nu}$ = 3167 (vw), 3060 (w), 3006 (w), 2932 (w), 2812 (w), 2728 (w), 1664 (vs), 1588 (s), 1486 (w), 1428 (m), 1334 (m), 1214 (s), 997 (m), 909 (m), 793 (m), 752 (vs), 686 (vs), 636 (s), 460 (m) cm^{-1}. – **MS** (FAB, 3-NBA): *m/z* (%) = 432 (60) $[M+H]^+$, 431 (63) $[M]^+$. – **EA** ($C_{25}H_{18}ClNO_4$) calc.: C, 69.53; H, 4.20; N, 3.24. found: C, 69.70; H, 4.15; N, 3.28.

2-(6-Bromo-4-hydroxy-2-oxo-1,2-dihydroquinolin-3-yl)-1,4-diphenylbutane-1,4-dione (220d)

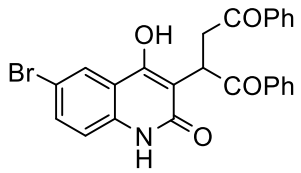

According to **GP11**, 7-bromo-4-hydroxyquinolin-2(1*H*)-one (**82d**, 0.240 g, 1.00 mmol, 1.00 equiv.) was refluxed with DBE (**219**, 0.236 g, 1.00 mmol, 1.00 equiv.) in pyridine/Et_3N for 12 h. A precipitate of the title compound was obtained as a pale yellow solid (0.360 g, 76%, 759 μmol).

R_f = 0.29 (cyclohexane/ethyl acetate; 1:1). – **Mp**: 348–350 °C. – **^{1}H NMR** (400 MHz, DMSO-d_6) δ = 12.30 (s, 1H, O*H*), 11.50 (s, 1H, N*H*), 8.00 (d, *J* = 7.6 Hz, 1H, H^{Ar}), 7.90 (d, *J* = 7.8 Hz, 1H, H^{Ar}), 7.82 (d, *J* = 8.0 Hz, 1H, H^{Ar}), 7.54–7.50 (m, 5H, H^{Ar}), 7.30 (t, *J* = 7.8 Hz, 2H, H^{Ar}), 7.24–7.10 (m, 3H, H^{Ar}), 5.50 (dd, *J* = 10.9, 2.3 Hz, 1H, C*H*), 4.18 (dd, *J* = 17.0, 9.9 Hz, 1H, CH_2), 2.80 (dd, *J* = 17.0, 2.6 Hz, 1H, CH_2) ppm. – **^{13}C NMR** (100 MHz, DMSO-d_6) δ = 198.2 (C_q, *C*O), 197.6 (C_q, *C*O), 165.0 (C_q, *C*O), 158.2 (C_q, C^{Ar}), 138.0 (C_q, C^{Ar}), 137.4 (C_q, C^{Ar}), 133.0 (C_q, C^{Ar}), 132.4 (+, *C*H^{Ar}), 132.0 (+, *C*H^{Ar}), 130.0 (+, 2 × *C*H^{Ar}), 128.8 (+, 2 × *C*H^{Ar}), 127.8 (+, 2 × *C*H^{Ar}), 127.5 (+, 2 × *C*H^{Ar}), 127.0 (+, 2 × *C*H^{Ar}), 122.6 (+, *C*H^{Ar}), 124.0 (C_q, C^{Ar}), 115.0 (C_q, C^{Ar}), 110.0 (C_q, C^{Ar}), 40.6 (–, *C*H_2), 37.0 (+, *C*H) ppm. – **IR** (ATR) $\tilde{\nu}$ = 3169 (vw), 3062 (w), 3006 (w), 2932 (w), 2815 (w), 2728 (w), 1664 (vs), 1580 (s), 1486 (w), 1420 (m), 1334 (m), 1214 (s), 997 (m), 909 (m), 790 (m), 752 (vs), 686 (vs), 630 (s), 465 (m) cm^{-1}. – **MS** (FAB, 3-NBA): *m/z* (%) = 476 (58) $[M+H]^+$, 475 (32) $[M]^+$. – **EA** ($C_{25}H_{18}BrNO_4$) calc.: C, 63.04; H, 3.81; N, 2.94. found: C, 62.96; H, 3.70; N, 3.08.

2-(4-Hydroxy-7-methyl-2-oxo-1,2-dihydroquinolin-3-yl)-1,4-diphenylbutane-1,4-dione (220e)

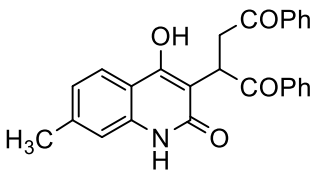

According to **GP11**, 7-methyl-4-hydroxyquinolin-2(1*H*)-one (**82e**, 0.175 g, 1.00 mmol, 1.00 equiv.) was refluxed with DBE (**219**, 0.236 g, 1.00 mmol, 1.00 equiv.) in pyridine/Et_3N for 12 h. A precipitate of the title compound was obtained as a pale yellow solid (0.315 g, 77 %, 769 µmol).

R_f = 0.33 (cyclohexane/ethyl acetate; 1:1). – **Mp**: 352–354 °C. – **^{1}H NMR** (400 MHz, DMSO-d_6) δ = 11.35 (s, 1H, N*H*), 10.77 (b, 1H, O*H*), 8.01 (dd, *J* = 8.5, 1.3 Hz, 2H, H^{Ar}), 7.81 (d, *J* = 7.3 Hz, 2H, H^{Ar}), 7.73 (s, 1H, H^{Ar}), 7.65 (t, *J* = 7.4 Hz, 1H, H^{Ar}), 7.55 (t, *J* = 7.6 Hz, 2H, H^{Ar}), 7.47 (t, *J* = 7.3 Hz, 1H, H^{Ar}), 7.38 (t, *J* = 7.6 Hz, 2H, H^{Ar}), 7.29 (dd, *J* = 8.4, 1.3 Hz, 1H, H^{Ar}), 7.14 (d, *J* = 8.3 Hz, 1H, H^{Ar}), 5.46 (dd, *J* = 9.7, 3.1 Hz, 1H, C*H*), 4.19 (dd, *J* = 17.3, 9.8 Hz, 1H, CH_2), 2.82 (dd, *J* = 17.3, 3.1 Hz, 1H, CH_2), 2.31 (s, 3H, CH_3) ppm. – **^{13}C NMR** (101 MHz, DMSO-d_6) δ = 198.5 (C_q, *C*O), 198.3 (C_q, *C*O), 162.2 (C_q, *C*O), 158.3 (C_q, C^{Ar}), 137.8 (C_q, C^{Ar}), 137.0 (C_q, C^{Ar}), 136.7 (C_q, C^{Ar}), 132.9 (+, *C*H^{Ar}), 132.3 (+, *C*H^{Ar}), 131.7 (+, *C*H^{Ar}), 130.1 (+, 2 × *C*H^{Ar}), 128.6 (+, *C*H^{Ar}), 128.2 (+, 2 × *C*H^{Ar}), 127.8 (+, 2 × *C*H^{Ar}), 127.3 (+, *C*H^{Ar}), 122.1 (+, *C*H^{Ar}), 115.1 (+, *C*H^{Ar}), 114.8 (C_q, C^{Ar}), 111.7 (C_q, C^{Ar}), 40.5 (–, *C*H_2), 37.5 (+, *C*H), 20.6 (+, *C*H_3) ppm. – **IR** (ATR) $\tilde{\nu}$ = 3177 (vw), 3053 (vw), 2915 (vw), 2812 (w), 2735 (vw), 1660 (s), 1594 (w), 1497 (w), 1439 (w), 1336 (w), 1169 (s), 997 (s), 891 (vs), 790 (s), 761 (s), 714 (vs), 686 (vs), 636 (m), 543 (vs), 458 (vs) cm^{-1}. – **MS** (FAB, 3-NBA): *m/z* (%) = 412 (60) $[M+H]^+$, 411 (40) $[M]^+$. – **EA** ($C_{26}H_{21}NO_4$) calc.: C, 75.90; H, 5.14; N, 3.40. found: C, 76.10; H, 5.24; N, 3.50.

2-(4-Hydroxy-6-methyl-2-oxo-1,2-dihydroquinolin-3-yl)-1,4-diphenylbutane-1,4-dione (**220f**)

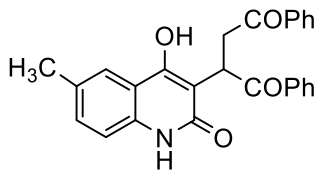

According to **GP11**, 6-methyl-4-hydroxyquinolin-2(1*H*)-one (**82f**, 0.175 g, 1.00 mmol, 1.00 equiv.) was refluxed with DBE (**219**, 0.236 g, 1.00 mmol, 1.00 equiv.) in pyridine/Et_3N for 12 h. A precipitate of the title compound was obtained as a yellow solid (0.315 g, 77 %, 769 µmol).

R_f = 0.33 (cyclohexane/ethyl acetate; 1:1). – **Mp**: 282–284 °C. – **^{1}H NMR** (400 MHz, DMSO-d_6) δ = 12.10 (s, 1H, O*H*), 11.70 (s, 1H, N*H*), 7.98 (d, *J* = 7.7 Hz, 1H, H^{Ar}), 7.86 (d, *J* = 8.0 Hz, 1H, H^{Ar}), 7.80 (d, *J* = 7.8 Hz, 1H, H^{Ar}), 7.62–7.55 (m, 5H, H^{Ar}), 7.28 (t, *J* = 8.0 Hz, 2H, H^{Ar}), 7.30–7.24 (m, 3H, H^{Ar}), 5.48 (dd, *J* = 10.0, 2.4 Hz, 1H, C*H*), 4.22 (dd, *J* = 17.0, 9.9 Hz, 1H, CH_2), 2.82 (dd, *J* = 17.0, 2.6 Hz, 1H, CH_2), 2.20 (s, 3H, CH_3) ppm. – **^{13}C NMR** (101 MHz, DMSO-d_6) δ = 198.0 (C_q, *C*O), 197.6 (C_q, *C*O), 163.0 (C_q, *C*O), 158.2 (C_q, C^{Ar}), 136.8 (C_q, C^{Ar}), 135.4 (C_q, C^{Ar}), 135.0 (C_q, C^{Ar}), 132.4 (+, *C*H^{Ar}), 132.0 (+, *C*H^{Ar}), 131.5 (+, 2 × *C*H^{Ar}), 130.0 (+, 2 × *C*H^{Ar}), 128.9 (+, 2 × *C*H^{Ar}), 127.8 (+, 2 × *C*H^{Ar}), 127.6 (+, 2 × *C*H^{Ar}), 123.0 (+, *C*H^{Ar}), 120.0 (C_q, C^{Ar}), 115.2 (C_q, C^{Ar}), 110.0 (C_q, C^{Ar}), 40.5 (–, *C*H_2), 37.2 (+, *C*H), 21.2 (+, *C*H_3) ppm. – **IR** (ATR) $\tilde{\nu}$ = 3150 (w), 3063 (w), 2912 (w), 2836 (w), 2728 (w), 1693 (vs), 1657 (vs), 1645 (vs), 1605 (vs), 1596 (s), 1476 (w), 1443 (m), 1313 (m), 1282 (vs), 1251 (m), 1203 (s), 1179 (m), 955 (m), 822 (m), 786 (m), 734 (vs), 687 (vs), 649 (s), 611 (s), 582 (s), 564 (s), 534 (s), 450 (vs) cm^{-1}. – **MS** (FAB, 3-NBA): *m/z* (%) = 412 (60) [M+H]$^+$, 411 (42) [M]$^+$. – **EA** ($C_{26}H_{21}NO_4$) calc.: C, 75.90; H, 5.14; N, 3.40. found: C, 76.00; H, 5.22; N, 3.30.

4-(Benzo[*d*]oxazol-2-yl)-3-hydroxy-1*H*-benzo[4,5]oxazolo[3,2-a]pyridine-1-one (224)

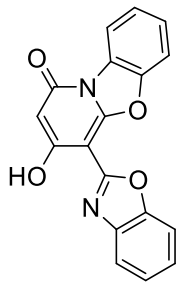

A mixture of 2-hydroxyaniline (**223**, 0.109 g, 1.00 mmol, 1.00 equiv.)) and diethyl malonate (**98**, 20 mL) in polyphosphoric acid (PPA) (20 mL) was heated to 170 °C for 30 min, the temperature was then raised to 200 °C for further 30 min. The hot oily paste was poured into an aqueous saturated sodium acetate solution (250 mL), the formed solid was then collected, washed with water (3 × 20 mL), and recrystallized from a mixture of DMF/CH_3CN (10:50 mL) to afford the title compound as a buff solid (0.255 g, 80%, 799 μmol).

R_f = 0.23 (cyclohexane/ethyl acetate; 1:1). – **Mp**: 270–272 °C. – **^{1}H NMR** (400 MHz, DMSO-d_6) δ = 12.90 (s, 1H, O*H*), 8.40 (dd, *J* = 7.0 Hz, 1H, H^{Ar}), 8.00 (d, *J* = 7.3 Hz, 2H, H^{Ar}), 7.96 (d, *J* = 7.6 Hz, 2H, H^{Ar}), 7.92–7.80 (m, 3H, H^{Ar}), 5.55 (dd, *J* 7.5, 1.2 Hz, 1H, H^{Ar}) ppm. – **^{13}C NMR** (101 MHz, DMSO-d_6) δ = 165.4 (C_q, *C*O), 160.0 (+, *C*H^{Ar}), 153.0 (C_q, C^{Ar}), 149.8 (C_q, C^{Ar}), 148.3 (C_q, C^{Ar}), 147.0 (C_q, C^{Ar}), 138.3 (C_q, C^{Ar}), 126.6 (+, *C*H^{Ar}), 126.3 (+, *C*H^{Ar}), 124.41 (+, *C*H^{Ar}), 125.31 (+, *C*H^{Ar}), 124.24 (+, *C*H^{Ar}), 123.7 (+, *C*H^{Ar}), 118.5 (C_q, C^{Ar}), 116.2 (C_q, C^{Ar}), 111.4 (C_q, C^{Ar}), 110.2 (+, *C*H^{Ar}), 104.2 (+, *C*H^{Ar}) ppm. – **IR** (ATR) $\tilde{\nu}$ = 3143 (w), 3070 (w), 2912 (w), 1677 (vs), 1577 (s), 1451 (s), 1434 (vs), 1323 (w), 1249 (s), 1218 (s), 1140 (s), 999 (m), 908 (m), 769 (s), 762 (s), 745 (vs), 696 (vs), 688 (vs), 679 (s), 543 (s), 514 (s) cm^{-1}. – **MS** (FAB, 3-NBA): *m/z* (%) = 319 (60) $[M+H]^+$, 318 (100) $[M]^+$. – **EA** ($C_{18}H_{10}N_2O_4$) calc.: C, 67.93; H, 3.17; N, 8.80. found: C, 68.10; H, 3.25; N, 8.90.

2-(4-(Benzo[*d*]oxazol-2-yl)-3-hydroxy-1-oxo-1*H*-benzo[4,5]oxazolo[3,2-*a*]pyridin-2-yl)-1,4-diphenylbutane-1,4-dione (225)

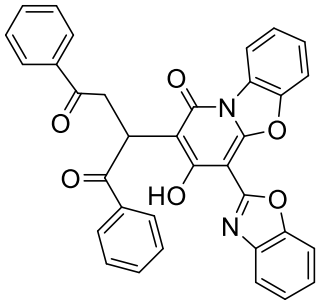

According to **GP11**, 4-(Benzo[*d*]oxazol-2-yl)-3-hydroxy-1*H*-benzo[4,5]oxazolo[3,2-*a*]pyridine-1-one (**224**, 0.318 g, 1.00 mmol, 1.00 equiv.) was refluxed with DBE (**219**, 0.236 g, 1.00 mmol, 1.00 equiv.) in pyridine/Et_3N for 12 h. A precipitate of the title compound was obtained as a white solid (0.472 g, 85%, 853 μmol).

R_f = 0.20 (cyclohexane/ethyl acetate; 1:1). – **Mp**: 278–280 °C. – **^{1}H NMR** (400 MHz, DMSO-d_6) δ = 13.16 (b, 1H, O*H*), 8.45 (dd, *J* = 7.0, 2.0 Hz, 1H, H^{Ar}), 8.03 (d, *J* = 7.3 Hz, 2H, H^{Ar}), 7.95 (d, *J* = 7.6 Hz, 2H, H^{Ar}), 7.90 (d, *J* = 8.2 Hz, 1H, H^{Ar}), 7.86–7.80 (m, 2H, H^{Ar}), 7.66 (t, *J* = 7.3 Hz, 1H, H^{Ar}), 7.56 (t, *J* = 7.6 Hz, 2H, H^{Ar}), 7.54–7.52 (m, 2H, H^{Ar}), 7.50 (t, *J* = 7.3 Hz, 1H, H^{Ar}), 7.48–7.43 (m, 2H, H^{Ar}), 7.41 (t, *J* = 7.3 Hz, 2H, H^{Ar}), 5.55 (dd, *J* = 10.1, 2.9 Hz, 1H, C*H*), 4.36 (dd, *J* = 17.4, 10.2 Hz, 1H, CH_2), 2.85 (dd, *J* = 17.2, 2.6 Hz, 1H, CH_2) ppm. – **^{13}C NMR** (101 MHz, DMSO-d_6) δ = 198.6 (C_q, *C*O), 197.9 (C_q, *C*O), 159.7 (C_q, C^{Ar}), 156.9 (C_q, *C*O), 152.9 (C_q, C^{Ar}), 149.6 (C_q, C^{Ar}), 148.6 (C_q, C^{Ar}), 147.0 (C_q, C^{Ar}), 138.4 (C_q, C^{Ar}), 137.0 (C_q, C^{Ar}), 136.4 (+, *C*H^{Ar}), 132.9 (+, *C*H^{Ar}), 132.5 (+, 2 × *C*H^{Ar}), 128.7 (+, 2 × *C*H^{Ar}), 128.4 (+, 2 × *C*H^{Ar}), 127.9 (+, 2 × *C*H^{Ar}), 127.6 (+, *C*H^{Ar}), 126.9 (+, *C*H^{Ar}), 126.5 (C_q, C^{Ar}), 125.4 (+, *C*H^{Ar}), 125.3 (+, *C*H^{Ar}), 125.2 (+, *C*H^{Ar}), 123.9 (C_q, C^{Ar}), 118.4 (C_q, C^{Ar}), 115.9 (+, *C*H^{Ar}), 111.2 (+, *C*H^{Ar}), 110.8 (+, *C*H^{Ar}), 103.2 (C_q, C^{Ar}), 39.5 (–, *C*H_2), 37.4 (+, *C*H) ppm. – **IR** (ATR) $\tilde{\nu}$ = 3143 (w), 3070 (w), 2912 (w), 1677 (vs), 1650 (vs), 1577 (s), 1526 (vs), 1451 (s), 1434 (vs), 1323 (w), 1249 (s), 1218 (s), 1140 (s), 1120 (vs), 999 (m), 908 (m), 769 (s), 762 (s), 745 (vs), 696 (vs), 688 (vs), 679 (s), 543 (s), 514 (s) cm^{-1}. – **MS** (FAB, 3-NBA): *m/z* (%) = 555 (60) $[M+H]^+$, 554 (100) $[M]^+$. – **EA** ($C_{34}H_{22}N_2O_6$) calc.: C, 73.64; H, 4.00; N, 5.05. found: C, 73.69; H, 4.05; N, 5.11.

5.3. Crystal Structures

Crystal structures in this section were measured and solved by Dr. Martin Nieger at the University of Helsinki.

Table 29: Overview of the numbering and sample coding of crystals from Dr. Nieger.

Numbering in this thesis	Sample Code used by Dr. Nieger
146d	SB1131_HY
159	SB1201_HY
135b	SB1195_HY
135c	SB1199_HY
135f	SB1200_HY
136b	SB1296_HY
136c	SB1297_HY
137b	SB1206_hy_le99
137d	SB1242_HY
138a	SB1232_HY
175	SB1245_HY
139f	SB1228_HY
190	SB1206_SQ
140e	SB1235_HY
141c	SB1314_HY
196	SB1315_HY
220f	SB993_HY
225	SB1057_HY

Crystal Structure Determination

The single-crystal X-ray diffraction studies were carried out on a Bruker D8 Venture diffractometer with the PhotonII detector at 123(2) K using Cu-Kα radiation (λ = 1.54178 Å). Dual space methods (SHELXT)[317] were used for the structure solution and refinement was carried out using SHELXL-2014 (full-matrix least-squares on F^2).[318] Hydrogen atoms were localized by the difference electron density determination and refined using a riding model (H(N) free, except **137b**). Semi-empirical absorption corrections were applied. Due to the bad quality of the data of **137b** the data were not deposited with The Cambridge Crystallographic Data Centre. For **140e** an extinction correction was applied. The absolute structure of **141c** was determined by the refinement of Parsons' x-parameter.[319]

Compound 146d: yellow blocks, $C_{12}H_{11}N_5O_2S$, M_r = 289.32 g mol^{-1}, size 0.14 × 0.08 × 0.04 mm, triclinic, *P-1* (no. 2), a = 4.5032 (1) Å, b = 11.4730 (4) Å, c = 13.0278 (4) Å, α = 80.483 (1)°, β = 84.692 (1)°, γ = 89.314 (1)°, V = 666.97 (3) Å^3, Z = 2, D_{calcd} = 1.454 Mg m^{-3}, F (000) = 300, μ = 2.28 mm^{-1}, T = 123 K 10950 measured reflections ($2\theta_{max}$ = 144.4 °), 2601 independent reflections [R_{int} = 0.025], 190 parameters, 3 restraints, R_1 [for 2515 I > 2σ(I)] = 0.027, wR^2 (for all data) = 0.070, S = 1.07, largest diff. peak and hole = 0.25 e Å^{-3}/- 0.21 e Å^{-3}.

Compound 159: Colorless crystals, $C_{17}H_{18}N_2O$, M_r = 266.33, crystal size 0.16 × 0.06 × 0.02 mm, monoclinic, space group *C*2/c (No. 15), a = 11.8196(4) Å, b = 7.9087(3) Å, c = 28.2370(10) Å, β = 92.708(2)°, V = 2636.58(16) Å^3, Z = 8, ρ = 1.342 Mg/m^{-3}, μ(Cu-K$_\alpha$) = 0.67 mm^{-1}, F(000) = 1136, $2\theta_{max}$ = 144.6°, 10645 measured reflections (2589 independent reflection in the HKLF 5 file, R_{int} = 0.000), 191 parameters, three restraints, R_1 = 0.071 (for 2452 I > 2σ(I)), wR_2 = 0.174 (all data), S = 1.16, largest diff. peak/hole = 0.33/−0.37 e Å^{-3}. Refined as a two-component twin (BASF 0.139(4)). The option TwinRotMat of the program package PLATON[320] was used to create a HKLF 5 file, which was used for the refinement. Therefore, only unique reflections were used for the refinement (Rint = 0.00).

Compound 135b: Colorless crystals, $C_{24}H_{23}N_3OS$, M_r = 401.51, crystal size 0.16 × 0.12 × 0.04 mm, monoclinic, space group $P2_1/c$ (No. 14), a = 12.2835(4) Å, b = 10.5257(3) Å, c = 15.5777(5) Å, β = 104.805(2)°, V = 1947.21(11) Å^3, Z = 4, ρ = 1.0 Mg/m^{-3}, μ(Cu-K$_\alpha$) = 1.64 mm^{-1}, F(000) = 848, $2\theta_{max}$ = 144.8°, 17,562 reflections, of which 3830 were independent (R_{int} = 0.032), 271 parameters, 3 restraints, R_1 = 0.039 (for 3480 I > 2σ(I)), wR_2 = 0.107 (all data), S = 1.04, largest diff. peak/hole = 0.34/-0.20 e Å^{-3}.

Compound 135c: Colorless crystals, $C_{21}H_{23}N_3OS$, M_r = 365.48, crystal size 0.18 × 0.04 × 0.02 mm, orthorhombic, space group *P*bca (No. 61), *a* = 19.5761(14) Å, *b* = 8.2709(7) Å, *c* = 24.0176(17) Å, *V* = 3888.7(5) Å^3, *Z* = 8, ρ = 1.249 Mg/m^{-3}, μ(Cu-K$_\alpha$) = 1.58 mm^{-1}, *F*(000) = 1552, $2\theta_{max}$ = 144.4°, 24,493 reflections, of which 3815 were independent (R_{int} = 0.087), 244 parameters, 198 restraints (a general RIGU restraint was applied), R_1 = 0.059 (for 2913 I > 2σ(I)), wR_2 = 0.141 (all data), *S* = 1.043, largest diff. peak/hole = 0.35/-0.27 e Å^{-3}.

Compound 135f: Colorless crystals, $C_{25}H_{25}N_3OS$, M_r = 415.54, crystal size 0.28 × 0.06 × 0.03 mm, orthorhombic, space group *P*ccn (No. 56), *a* = 19.4444(6) Å, *b* = 25.2548(7) Å, *c* = 8.7599(2) Å, *V* = 4301.7(2) Å^3, *Z* = 8, ρ = 1.283 Mg/m^{-3}, μ(Cu-K$_\alpha$) = 1.50 mm^{-1}, *F*(000) = 1760, $2\theta_{max}$ = 144.4°, 48,155 reflections, of which 4241 were independent (R_{int} = 0.049), 283 parameters, 3 restraints, R_1 = 0.038 (for 3846 I > 2σ(I)), wR_2 = 0.096 (all data), *S* = 1.05, largest diff. peak/hole = 0.27/-0.19 e Å^{-3}.

Compound 136b: Colorless crystals, $C_{24}H_{21}N_3S$, M_r = 383.50, crystal size 0.24 × 0.04 × 0.02 mm, orthorhombic, space group *P*ccn (No. 56), *a* = 19.8459(4) Å, *b* = 25.4981(5) Å, *c* = 7.5772(2) Å, *V* = 3834.31(15)) Å^3, *Z* = 8, ρ = 1.329 Mg/m^{-3}, μ(Cu-K$_\alpha$) = 1.60 mm^{-1}, *F*(000) = 1616, $2\theta_{max}$ = 144.2°, 28166 reflections, of which 3777 were independent (R_{int} = 0.039), 256 parameters, one restraint, R_1 = 0.040 (for 3376 I > 2σ(I)), wR_2 = 0.106 (all data), *S* = 1.04, largest diff. peak/hole = 0.46/−0.36 e Å^{-3}.

Compound 136c: Colorless crystals, $C_{21}H_{21}N_3S \cdot C_2H_6OS$, M_r = 425.59, crystal size 0.24 × 0.06 × 0.02 mm, monoclinic, space group $P2_1/c$ (No. 14), *a* = 24.8195(8) Å, *b* = 7.6344(2) Å, *c* = 11.6051 (4) Å, β = 101.468(1)°, *V* = 2155.06(12) Å^3, *Z* = 4, ρ = 1.312 Mg/m^{-3}, μ(Cu-K$_\alpha$) = 2.38 mm^{-1}, *F*(000) = 904, $2\theta_{max}$ = 144.6°, 28028 reflections, of which 4256 were independent (R_{int} = 0.030), 267 parameters, one restraint, R_1 = 0.050 (for 4009 I > 2σ(I)), wR_2 = 0.134(all data), *S* = 1.07, largest diff. peak/hole = 0.89/−0.63 e Å^{-3}.

Compound 137b: Yellow crystals, $C_{24}H_{21}N_3O$, M_r = 367.44, crystal size 0.20 × 0.12 × 0.03 mm, monoclinic, space group $P2_1/c$ (No. 14), *a* = 13.0346(7) Å, *b* = 14.2304(8) Å, *c* = 10.0713(6) Å, β = 94.353(3)°, *V* = 1862.71(18) Å^3, *Z* = 4, ρ = 1.310 Mg/m^{-3}, μ(Cu-K$_\alpha$) = 0.64 mm^{-1}, *F*(000) = 776, $2\theta_{max}$ = 144.4°, 16984 reflections, of which 3674 were independent (R_{int} = 0.032).

Compound 137d: Violet crystals, $C_{20}H_{21}N_3O$, M_r = 319.40, crystal size 0.16 × 0.08 × 0.02 mm, monoclinic, space group $P2_1/c$ (No. 14), *a* = 17.2016(7) Å, *b* = 8.9605(4) Å, *c* = 10.6470(4) Å, β = 104.112(2)°, *V* = 1591.55 (11)Å^3, *Z* = 4, ρ = 1.333 Mg/m^{-3}, μ(Cu-K$_\alpha$) =

0.66 mm^{-1}, $F(000)$ = 680, $2\theta_{max}$ = 145.4°, 26077 measured reflections (3119 independent reflection in the HKLF 5 file, R_{int} = 0.000), 221 parameters, one restraint R_1 = 0.066 (for 2906 I > 2σ(I)), wR_2 = 0.167 (all data), S = 1.17, largest diff. peak/hole = 0.29/−0.32 e $Å^{-3}$. Refined as a two-component twin (BASF 0.194(5)). The option TwinRotMat of the program package PLATON[320] was used to create a HKLF 5 file, which was used for the refinement. Therefore, only unique reflections were used for the refinement (Rint = 0.00).

Compound 139f: Yellow crystals, $C_{30}H_{27}N_3O_4S$, M_r = 525.60, crystal size 0.14 × 0.12 × 0.04 mm, monoclinic, space group $P2_1/c$ (No. 14), a = 13.0205(4) Å, b = 12.40(4) Å, c = 15.9584(5) Å, β = 92.8(1)°, V = 2574.16(14) $Å^3$, Z = 4, ρ = 1.356 Mg/m^{-3}, μ(Cu-K_α) = 1.46 mm^{-1}, $F(000)$ = 1104, $2\theta_{max}$ = 144.6°, 41,983 reflections, of which 5074 were independent (R_{int} = 0.038), 347 parameters, 1 restraint, R_1 = 0.070 (for 4800 I > 2σ(I)), wR_2 = 0.187 (all data), S = 1.06, largest diff. peak/hole = 1.13 (due to possible disorder in the [2.2]paracyclophane moiety)/-0.35 e $Å^{-3}$.

Compound 190: Colorless crystals, $C_{28}H_{24}N_4O_4S \cdot 0.5\ CH_3OH \cdot 0.5\ H_2O$, M_r = 5.60, crystal size 0.15 × 0.09 × 0.03 mm, monoclinic, space group $C2/c$ (No. 15), a = 19.3130(6) Å, b = 12.4233(6) Å, c = 21.8993(8) Å, β = 90.008(2)°, V = 5254.3(4) $Å^3$, Z = 8, ρ = 1.359 Mg/m^{-3}, μ(Cu-K_α) = 1.49 mm^{-1}, $F(000)$ = 2256, $2\theta_{max}$ = 144.4°, 28,186 reflections, of which 5170 were independent (R_{int} = 0.041), 338 parameters, 1 restraint, R_1 = 0.043 (for 4649 I > 2σ(I)), wR_2 = 0.110 (all data), S = 1.04, largest diff. peak/hole = 0.42/-0.21 e $Å^{-3}$. Refinement with the listed atoms show residual electron density due to a heavily disordered methanol and water in 4 voids around a center of symmetry, which could not be refined with split atoms. Therefore the option "SQUEEZE" of the program package PLATON [51] was used to create a hkl file taking into account the residual electron density in the void areas. Therefore the atoms list and unit card do not agree.

Compound 140e: Red crystals, $C_{31}H_{25}N_3O_3S \cdot 0.625(CH_4O) \cdot 0.375(C_2H_6O)$, M_r = 556.90, crystal size 0.16 × 0.06 × 0.03 mm, monoclinic, space group $P2_1/c$ (No. 14), a = 7.2104(3) Å, b = 14.3984(6) Å, c = 26.4331(12) Å, β = 97.291(2)°, V = 2722.0(2) $Å^3$, Z = 4, ρ = 1.359 Mg/m^{-3}, μ(Cu-K_α) = 1.428 mm^{-1}, $F(000)$ = 1172, $2\theta_{max}$ = 140-2°, 51610 reflections, of which 5279 were independent (R_{int} = 0.039), 367 parameters, 43 restraints, R_1 = 0.058 (for 5006 I > 2σ(I)), wR_2 = 0.175(all data), S = 1.10, largest diff. peak / hole = 0.40 / -0.44 e $Å^{-3}$. The structure was refined as a 2-component twin. There is a solvent disorder (MeOH vs. EtOH). In addition the methylene moieties in C_2H_4-bridges are disordered.

Compound 141c: Colorless crystals, $C_{33}H_{30}N_3OS{\cdot}Br$, M_r = 596.57, crystal size 0.20 × 0.06 × 0.02 mm, orthorhombic, space group *P*na2$_1$ (No. 33), *a* = 17.5892(5) Å, *b* = 25.1597(7) Å, *c* = 12.9433(4) Å, *V* = 5727.9(3) Å^3, *Z* = 8, ρ = 1.384 Mg/m^{-3}, μ(Cu-K$_\alpha$) = 2.87 mm^{-1}, *F*(000) = 2464, $2\theta_{max}$ = 144.4°, 43557 reflections, of which 10648 were independent (R_{int} = 0.028), 698 parameters, 94 restraints, R_1 = 0.033 (for 10402 I > 2σ(I)), wR_2 = 0.083 (all data), *S* = 1.07, largest diff. peak / hole = 0.64 / -0.53 e Å^{-3}, x = -0.017(6). One naphthalene moiety is disordered.

Compound 196: colorless crystals, $C_{33}H_{30}N_3OS{\cdot}Br$, M_r = 596.57, crystal size 0.08 × 0.04 × 0.01 mm, monoclinic, space group *P*2$_1$/c (No. 14), *a* = 16.9166(12) Å, *b* = 9.1979(6) Å, *c* = 18.6636(12) Å, β = 102.929(4)°, *V* = 2830.4(3) Å^3, *Z* = 4, ρ = 1.400 Mg/m^{-3}, μ(Cu-K$_\alpha$) = 2.92 mm^{-1}, *F*(000) = 1232, $2\theta_{max}$ = 144.4°, 22667 reflections, of which 5534 were independent (R_{int} = 0.152), 359 parameters, 2 restraints, R_1 = 0.078 (for 2904 I > 2σ(I)), wR_2 = 0.271 (all data), *S* = 1.01, largest diff. peak / hole = 0.59 / -0.51 e Å^3.

Compound 220f: colorless crystals, $C_{26}H_{21}NO_4$, M_r = 411.44, crystal size 0.16 × 0.08 × 0.06 mm, triclinic, space group *P-1* (No. 2), *a* = 11.1823(3) Å, *b* = 14.3827(4) Å, *c* = 15.3460(4) Å, α = 67.695(1)°, β = 70.666(1)°, γ = 68.389(1)°, *V* = 2069.77(10) Å^3, *Z* = 4, ρ = 1.320 Mg/m^{-3}, μ(Cu-K$_\alpha$) = 0.72 mm^{-1}, *F*(000) = 864, $2\theta_{max}$ = 144.2°, 28,579 reflections, of which 8117 were independent (R_{int} = 0.035), 577 parameters, 5 restraints, R_1 = 0.043 (for 6749 I > 2σ(I)), wR_2 = 0.112 (all data), *S* = 1.01, largest diff. peak/hole = 0.37/−0.50 e Å^{-3}.

Compound 225: colorless crystals, $C_{34}H_2N_2O_6$, M_r = 554.53, crystal size 0.22 × 0.09 × 0.03 mm, triclinic, space group *P-1* (No. 2), *a* = 8.2672(2) Å, *b* = 11.3140(3) Å, *c* = 13.7326(3) Å, α = 91.721(1)°, β = 96.833(1)°, γ = 92.198(1)°, *V* = 1273.64(5) Å^3, *Z* = 2, ρ = 1.446 Mg/m^{-3}, μ(Cu-K$_\alpha$) = 0.82 mm^{-1}, *F*(000) = 576, $2\theta_{max}$ = 144.4°, 18,981 reflections, of which 4987 were independent (R_{int} = 0.037), 382 parameters, 1 restraint, R_1 = 0.048 (for 4212 I > 2σ(I)), wR_2 = 0.127 (all data), *S* = 1.03, largest diff. peak/hole = 0.35/−0.25 e Å^{-3}.

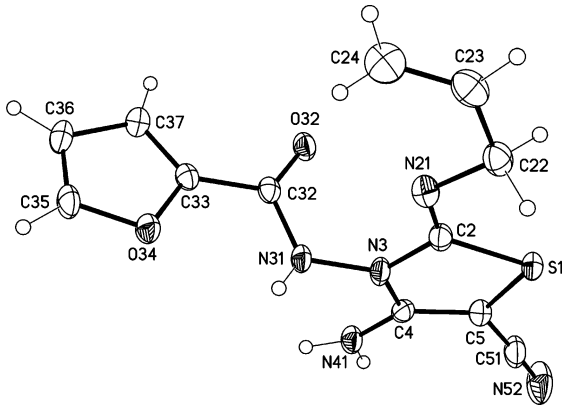

N-(2-(allylimino)-4-amino-5-cyanothiazol-3(2H)-yl)furan-2-carboxamide–SB1131_HY

Crystal data

$C_{12}H_{11}N_5O_2S$	Z = 2
M_r = 289.32	F(000) = 300
Triclinic, P-1 (no.2)	D_x = 1.454 Mg m^{-3}
a = 4.5032 (1) Å	Cu $K\alpha$ radiation, λ = 1.54178 Å
b = 11.4730 (4) Å	Cell parameters from 9058 reflections
c = 13.0278 (4) Å	θ = 3.4–72.1°
α = 80.483 (1)°	μ = 2.28 mm^{-1}
β = 84.692 (1)°	T = 123 K
γ = 89.314 (1)°	Blocks, yellow
V = 660.97 (3) Å^3	0.14 × 0.08 × 0.04 mm

Data collection

Bruker D8 VENTURE diffractometer with PhotonII CPAD detector	2515 reflections with $I > 2\sigma(I)$
Radiation source: INCOATEC microfocus sealed tube	R_{int} = 0.025
rotation in ϕ and ω, 1°, shutterless scans	θ_{max} = 72.2°, θ_{min} = 3.5°
Absorption correction: multi-scan *SADABS* (Sheldrick, 2014)	h = -5→5
T_{min} = 0.730, T_{max} = 0.902	k = -14→13
10950 measured reflections	l = -13→15
2601 independent reflections	

Refinement

Refinement on F^2	Primary atom site location: dual
Least-squares matrix: full	Secondary atom site location: difference Fourier map
$R[F^2 > 2\sigma(F^2)]$ = 0.027	Hydrogen site location: difference Fourier map
$wR(F^2)$ = 0.070	H atoms treated by a mixture of independent and constrained refinement
S = 1.07	$w = 1/[\sigma^2(F_o^2) + (0.0295P)^2 + 0.2705P]$ where $P = (F_o^2 + 2F_c^2)/3$
2601 reflections	$(\Delta/\sigma)_{max} < 0.001$
190 parameters	$\Delta\rangle_{max}$ = 0.25 e Å^{-3}
3 restraints	$\Delta\rangle_{min}$ = -0.21 e Å^{-3}

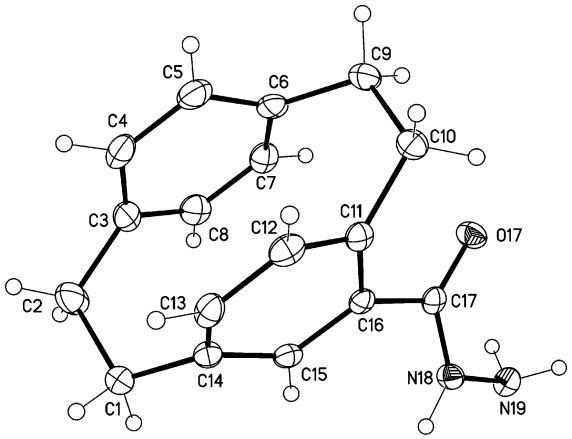

1,4(1,4)-dibenzenacyclohexaphane-1^2-carbohydrazide – SB1201_HY

Crystal data

$C_{17}H_{18}N_2O$	$F(000)$ = 1136
M_r = 266.33	D_x = 1.342 Mg m^{-3}
Monoclinic, *C*2/*c* *(no.15)*	Cu *K*α radiation, λ = 1.54178 Å
a = 11.8196 (4) Å	Cell parameters from 7876 reflections
b = 7.9087 (3) Å	θ = 6.2–72.2°
c = 28.237 (1) Å	μ = 0.67 mm^{-1}
β = 92.708 (2)°	*T* = 123 K
V = 2636.58 (16) Å^3	Plates, colorless
Z = 8	0.16 × 0.06 × 0.02 mm

Data collection

Bruker D8 VENTURE diffractometer with PhotonII CPAD detector	2589 independent reflections
Radiation source: INCOATEC microfocus sealed tube	2452 reflections with $I > 2\sigma(I)$
rotation in ϕ and ω, 1°, shutterless scans	θ_{max} = 72.3°, θ_{min} = 3.1°
Absorption correction: multi-scan *SADABS* V2014/5 (Bruker AXS Inc.)	*h* = -14→14
T_{min} = 0.842, T_{max} = 0.971	*k* = -8→9
(10645) 2589 measured reflections	*l* = -2→34

Refinement

Refinement on F^2	Primary atom site location: dual
Least-squares matrix: full	Secondary atom site location: difference Fourier map
$R[F^2 > 2\sigma(F^2)]$ = 0.071	Hydrogen site location: difference Fourier map
$wR(F^2)$ = 0.174	H atoms treated by a mixture of independent and constrained refinement
S = 1.16	$w = 1/[\sigma^2(F_o^2) + (0.0276P)^2 + 15.106P]$ where $P = (F_o^2 + 2F_c^2)/3$
2589 reflections	$(\Delta/\sigma)_{max} < 0.001$
191 parameters	$\Delta\rangle_{max}$ = 0.33 e Å^{-3}
3 restraints	$\Delta\rangle_{min}$ = -0.37 e Å^{-3}

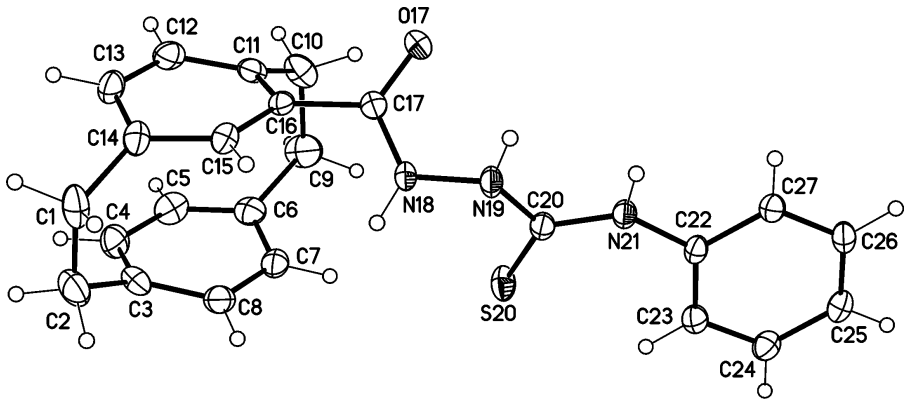

2-(1,4(1,4)-dibenzenacyclohexaphane-1^2-carbonyl)-N-phenylhydrazine-1-carbothioamide SB1195_HY

Crystal data

$C_{24}H_{23}N_3OS$	$F(000)$ = 848
M_r = 401.51	D_x = 1.370 Mg m^{-3}
Monoclinic, $P2_1/c$ (no.14)	Cu $K\alpha$ radiation, λ = 1.54178 Å
a = 12.2835 (4) Å	Cell parameters from 9982 reflections
b = 10.5257 (3) Å	θ = 3.7–72.4°
c = 15.5777 (5) Å	μ = 1.64 mm^{-1}
β = 104.805 (2)°	T = 123 K
V = 1947.21 (11) Å^3	Plates, colorless
Z = 4	0.16 × 0.12 × 0.04 mm

Data collection

Bruker D8 VENTURE diffractometer with PhotonII CPAD detector	3480 reflections with $I > 2\sigma(I)$
Radiation source: INCOATEC microfocus sealed tube	R_{int} = 0.032
rotation in ϕ and ω, 1°, shutterless scans	θ_{max} = 72.4°, θ_{min} = 3.7°
Absorption correction: multi-scan *SADABS* (Sheldrick, 2014)	h = -14→15
T_{min} = 0.812, T_{max} = 0.929	k = -12→13
17562 measured reflections	l = -19→19
3830 independent reflections	

Refinement

Refinement on F^2	Primary atom site location: dual
Least-squares matrix: full	Secondary atom site location: difference Fourier map
$R[F^2 > 2\sigma(F^2)]$ = 0.039	Hydrogen site location: difference Fourier map
$wR(F^2)$ = 0.107	H atoms treated by a mixture of independent and constrained refinement
S = 1.04	$w = 1/[\sigma^2(F_o^2) + (0.0614P)^2 + 0.8925P]$ where $P = (F_o^2 + 2F_c^2)/3$
3830 reflections	$(\Delta/\sigma)_{max} < 0.001$
271 parameters	$\Delta\rangle_{max}$ = 0.34 e Å^{-3}
3 restraints	$\Delta\rangle_{min}$ = -0.20 e Å^{-3}

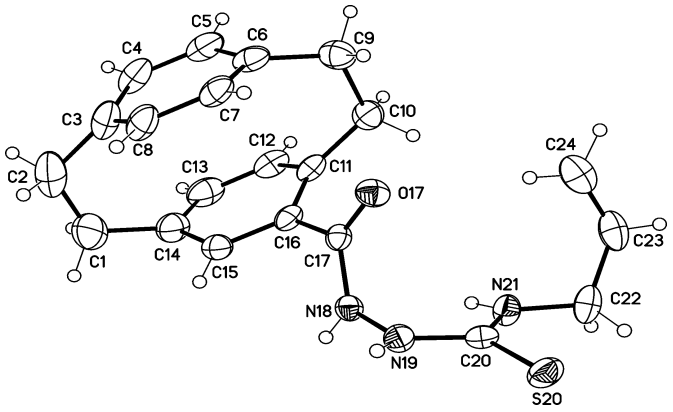

2-(1,4(1,4)-dibenzenacyclohexaphane-1^2-carbonyl)-N-vinylhydrazine-1-carbothioamide – SB1199_HY

Crystal data

$C_{21}H_{23}N_3OS$	D_x = 1.249 Mg m^{-3}
M_r = 365.48	Cu $K\alpha$ radiation, λ = 1.54178 Å
Orthorhombic, *Pbca (no.61)*	Cell parameters from 6225 reflections
a = 19.5761 (14) Å	θ = 3.6–72.0°
b = 8.2709 (7) Å	μ = 1.58 mm^{-1}
c = 24.0176 (17) Å	T = 123 K
V = 3888.7 (5) Å^3	Rods, colorless
Z = 8	0.18 × 0.04 × 0.02 mm
F(000) = 1552	

Data collection

Bruker D8 VENTURE diffractometer with PhotonII CPAD detector	2913 reflections with $I > 2\sigma(I)$
Radiation source: INCOATEC microfocus sealed tube	R_{int} = 0.087
rotation in ϕ, 1°, shutterless scans	θ_{max} = 72.2°, θ_{min} = 3.7°
Absorption correction: multi-scan *SADABS* V2014/5 (Bruker AXS Inc.)	h = -24→23
T_{min} = 0.777, T_{max} = 0.971	k = -10→6
24493 measured reflections	l = -29→29
3815 independent reflections	

Refinement

Refinement on F^2	Primary atom site location: dual
Least-squares matrix: full	Secondary atom site location: difference Fourier map
$R[F^2 > 2\sigma(F^2)]$ = 0.059	Hydrogen site location: difference Fourier map
$wR(F^2)$ = 0.141	H atoms treated by a mixture of independent and constrained refinement
S = 1.03	$w = 1/[\sigma^2(F_o^2) + (0.0467P)^2 + 4.3662P]$ where $P = (F_o^2 + 2F_c^2)/3$
3815 reflections	$(\Delta/\sigma)_{max} < 0.001$
244 parameters	$\Delta\rangle_{max}$ = 0.35 e Å^{-3}
198 restraints	$\Delta\rangle_{min}$ = -0.27 e Å^{-3}

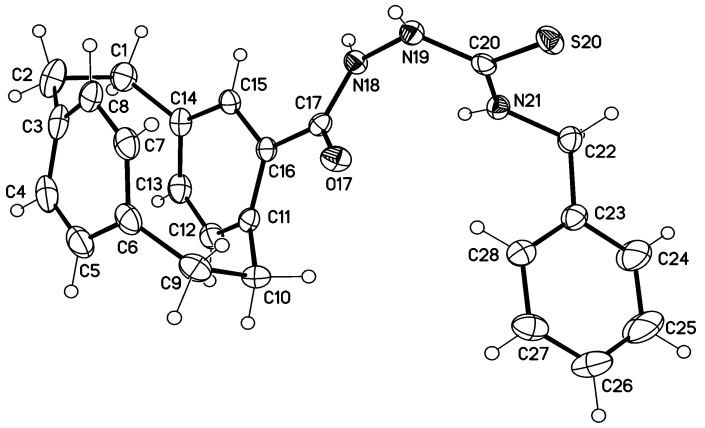

2-(1,4(1,4)-dibenzenacyclohexaphane-1^2-carbonyl)-N-benzylhydrazine-1-carbothioamide – SB1200_HY

Crystal data

$C_{25}H_{25}N_3OS$	D_x = 1.283 Mg m^{-3}
M_r = 415.54	Cu $K\alpha$ radiation, λ = 1.54178 Å
Orthorhombic, *Pccn (no.56)*	Cell parameters from 9977 reflections
a = 19.4444 (6) Å	θ = 2.8–72.2°
b = 25.2548 (7) Å	μ = 1.50 mm^{-1}
c = 8.7599 (2) Å	T = 123 K
V = 4301.7 (2) Å^3	Plates, colorless
Z = 8	0.28 × 0.06 × 0.03 mm
F(000) = 1760	

Data collection

Bruker D8 VENTURE diffractometer with PhotonII CPAD detector	3846 reflections with $I > 2\sigma(I)$
Radiation source: INCOATEC microfocus sealed tube	R_{int} = 0.049
rotation in ϕ and ω, 1°, shutterless scans	θ_{max} = 72.2°, θ_{min} = 2.9°
Absorption correction: multi-scan *SADABS* V2014/5 (Bruker AXS Inc.)	h = -24→23
T_{min} = 0.814, T_{max} = 0.958	k = -31→27
48155 measured reflections	l = -10→9
4241 independent reflections	

Refinement

Refinement on F^2	Primary atom site location: dual
Least-squares matrix: full	Secondary atom site location: difference Fourier map
$R[F^2 > 2\sigma(F^2)]$ = 0.038	Hydrogen site location: difference Fourier map
$wR(F^2)$ = 0.096	H atoms treated by a mixture of independent and constrained refinement
S = 1.05	$w = 1/[\sigma^2(F_o^2) + (0.0437P)^2 + 2.4888P]$ where $P = (F_o^2 + 2F_c^2)/3$
4241 reflections	$(\Delta/\sigma)_{max}$ = 0.001
283 parameters	$\Delta\rangle_{max}$ = 0.27 e Å^{-3}
3 restraints	$\Delta\rangle_{min}$ = -0.19 e Å^{-3}

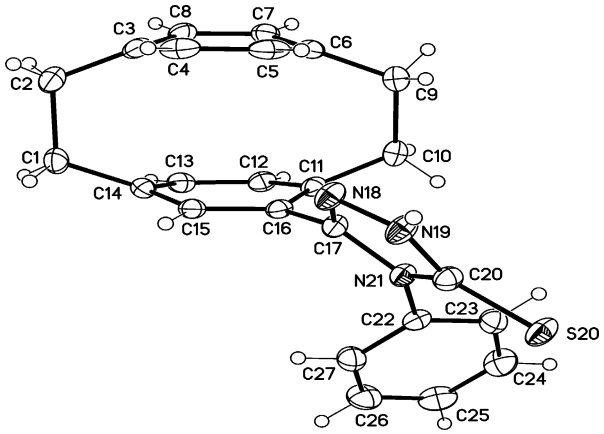

5-(1,4(1,4)-dibenzenacyclohexaphane-1^2-yl)-4-phenyl-2,4-dihydro-3H-1,2,4-triazole-3-thione – SB1296_HY

Crystal data

$C_{24}H_{21}N_3S$	D_x = 1.329 Mg m^{-3}
M_r = 383.50	Cu $K\alpha$ radiation, λ = 1.54178 Å
Orthorhombic, *Pccn (no.56)*	Cell parameters from 9931 reflections
a = 19.8459 (4) Å	θ = 2.8–71.9°
b = 25.4981 (5) Å	μ = 1.60 mm^{-1}
c = 7.5772 (2) Å	T = 123 K
V = 3834.31 (15) Å^3	Rods, colorless
Z = 8	0.24 × 0.04 × 0.02 mm
F(000) = 1616	

Data collection

Bruker D8 VENTURE diffractometer with PhotonII CPAD detector	3376 reflections with $I > 2\sigma(I)$
Radiation source: INCOATEC microfocus sealed tube	R_{int} = 0.039
rotation in ϕ and ω, 1°, shutterless scans	θ_{max} = 72.1°, θ_{min} = 2.8°
Absorption correction: multi-scan *SADABS* (Sheldrick, 2014)	h = -23→24
T_{min} = 0.805, T_{max} = 0.971	k = -31→30
28166 measured reflections	l = -9→8
3777 independent reflections	

Refinement

Refinement on F^2	Primary atom site location: dual
Least-squares matrix: full	Secondary atom site location: difference Fourier map
$R[F^2 > 2\sigma(F^2)]$ = 0.040	Hydrogen site location: difference Fourier map
$wR(F^2)$ = 0.106	H atoms treated by a mixture of independent and constrained refinement
S = 1.04	$w = 1/[\sigma^2(F_o^2) + (0.0539P)^2 + 2.5776P]$ where $P = (F_o^2 + 2F_c^2)/3$
3777 reflections	$(\Delta/\sigma)_{max} < 0.001$
256 parameters	$\Delta\rangle_{max}$ = 0.46 e Å^{-3}
1 restraint	$\Delta\rangle_{min}$ = -0.36 e Å^{-3}

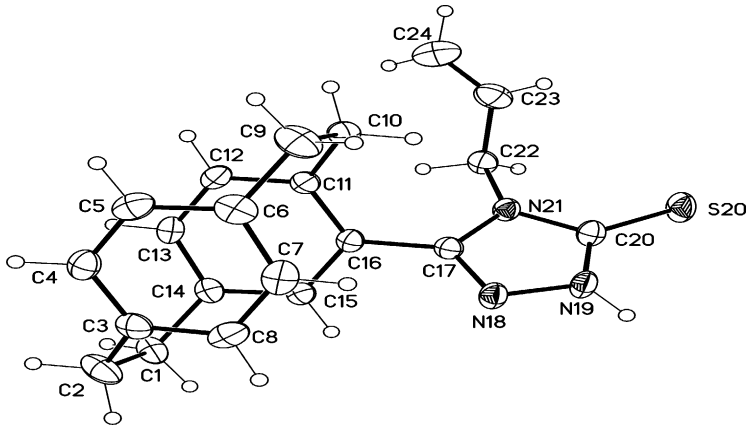

5-(1,4(1,4)-dibenzenacyclohexaphane-1^2-yl)-4-allyl-2,4-dihydro-3H-1,2,4-triazole-3-thione (methylsulfinyl)methane – SB1297_HY

Crystal data

$C_{21}H_{21}N_3S \cdot C_2H_6OS$	$F(000)$ = 904
M_r = 425.59	D_x = 1.312 Mg m^{-3}
Monoclinic, $P2_1/c$ *(no.14)*	Cu $K\alpha$ radiation, λ = 1.54178 Å
a = 24.8195 (8) Å	Cell parameters from 9110 reflections
b = 7.6344 (2) Å	θ = 5.4–72.2°
c = 11.6051 (4) Å	μ = 2.38 mm^{-1}
β = 101.468 (1)°	T = 123 K
V = 2155.06 (12) Å^3	Plates, colorless
Z = 4	0.24 × 0.06 × 0.02 mm

Data collection

Bruker D8 VENTURE diffractometer with PhotonII CPAD detector	4009 reflections with $I > 2\sigma(I)$
Radiation source: INCOATEC microfocus sealed tube	R_{int} = 0.030
rotation in ϕ and ω, 1°, shutterless scans	θ_{max} = 72.3°, θ_{min} = 3.6°
Absorption correction: multi-scan *SADABS* (Sheldrick, 2014)	h = -30→30
T_{min} = 0.766, T_{max} = 0.942	k = -9→9
28028 measured reflections	l = -14→14
4256 independent reflections	

Refinement

Refinement on F^2	Primary atom site location: dual
Least-squares matrix: full	Secondary atom site location: difference Fourier map
$R[F^2 > 2\sigma(F^2)]$ = 0.050	Hydrogen site location: difference Fourier map
$wR(F^2)$ = 0.134	H atoms treated by a mixture of independent and constrained refinement
S = 1.07	$w = 1/[\sigma^2(F_o^2) + (0.0622P)^2 + 2.683P]$ where $P = (F_o^2 + 2F_c^2)/3$
4256 reflections	$(\Delta/\sigma)_{max}$ = 0.001
267 parameters	$\Delta\rangle_{max}$ = 0.89 e Å^{-3}
1 restraint	$\Delta\rangle_{min}$ = -0.63 e Å^{-3}

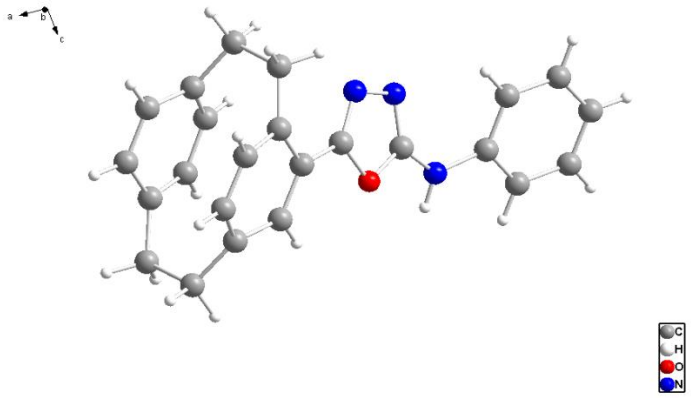

5-(1,4(1,4)-dibenzenacyclohexaphane-1^2-yl)-N-phenyl-1,3,4-oxadiazol-2-amine

SB1206_hy_le99

Due to the bad quality of the data (a probable disorder of the oxadiazol moiety) only the constitution and conformation could be determined.

Crystal data

$C_{24}H_{21}N_3O$	**Z = 4**
M_r = 367.44	**F(000) = 776**
Monoclinic, $P2_1/c$	**D_x = 1.310 Mg m^{-3}**
a = 13.0346 (7) Å	**Cu $K\alpha$ radiation, λ = 1.54178 Å**
b = 14.2304 (8) Å	**μ = 0.64 mm^{-1}**
c = 10.0713 (6) Å	**T = 123 K**
β = 94.353 (3)°	**0.20 × 0.12 × 0.03 mm**
V = 1862.71 (18) Å^3	

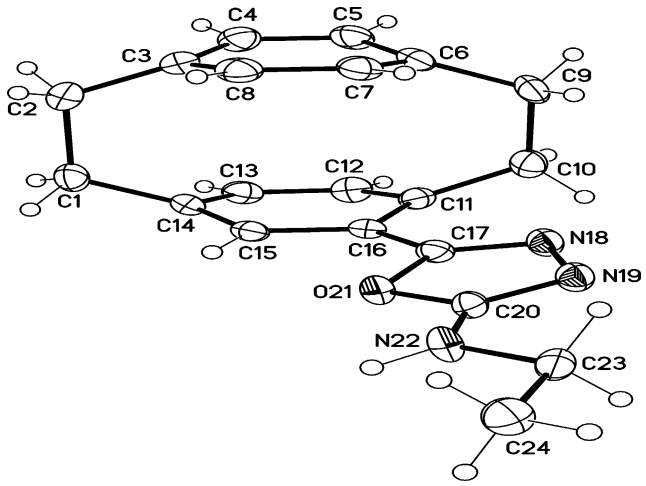

5-(1,4(1,4)-dibenzenacyclohexaphane-1^2-yl)-N-ethyl-1,3,4-oxadiazol-2-amine– SB1242_HY

Crystal data

$C_{20}H_{21}N_3O$	$F(000)$ = 680
M_r = 319.40	D_x = 1.333 Mg m^{-3}
Monoclinic, $P2_1/c$ *(no.14)*	Cu $K\alpha$ radiation, λ = 1.54178 Å
a = 17.2016 (7) Å	Cell parameters from 9853 reflections
b = 8.9605 (4) Å	θ = 2.6–72.2°
c = 10.6470 (4) Å	μ = 0.66 mm^{-1}
β = 104.112 (2)°	T = 123 K
V = 1591.55 (11) Å^3	Plates, violet
Z = 4	0.16 × 0.08 × 0.02 mm

Data collection

Bruker D8 VENTURE diffractometer with PhotonII CPAD detector	3119 independent reflections
Radiation source: INCOATEC microfocus sealed tube	2906 reflections with $I > 2\sigma(I)$
rotation in ϕ and ω, 1°, shutterless scans	θ_{max} = 72.7°, θ_{min} = 2.7°
Absorption correction: multi-scan *SADABS* (Sheldrick, 2014)	h = -21→20
T_{min} = 0.843, T_{max} = 0.981	k = -11→11
3119 measured reflections	l = -9→13

Refinement

Refinement on F^2	Primary atom site location: dual
Least-squares matrix: full	Secondary atom site location: difference Fourier map
$R[F^2 > 2\sigma(F^2)]$ = 0.066	Hydrogen site location: difference Fourier map
$wR(F^2)$ = 0.167	H atoms treated by a mixture of independent and constrained refinement
S = 1.17	$w = 1/[\sigma^2(F_o^2) + (0.021P)^2 + 3.860P]$ where $P = (F_o^2 + 2F_c^2)/3$
3119 reflections	$(\Delta/\sigma)_{max} < 0.001$
221 parameters	$\Delta\rangle_{max}$ = 0.29 e Å^{-3}
1 restraint	$\Delta\rangle_{min}$ = -0.32 e Å^{-3}

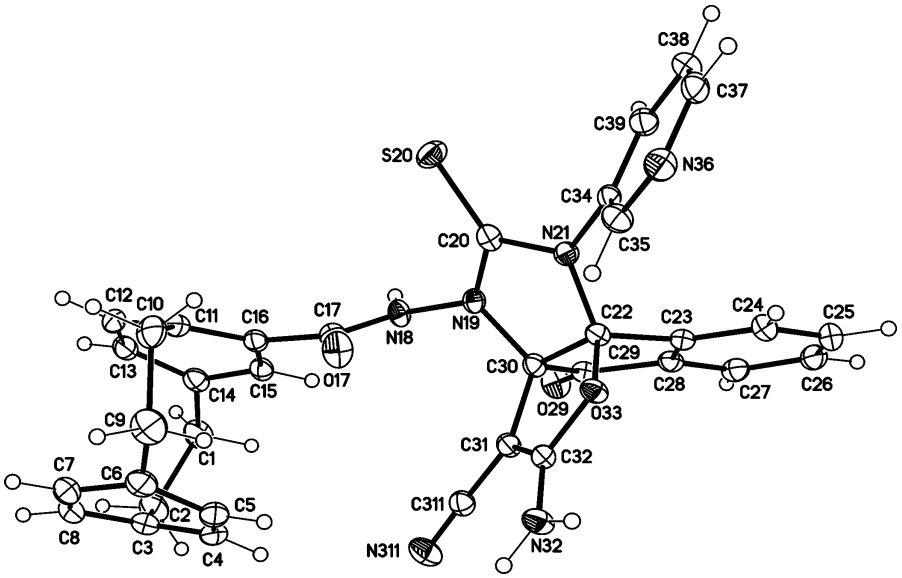

N-(2-amino-3-cyano-4-oxo-9-(pyridin-3-yl)-10-thioxo-4H-3a,8b-(epiminomethano-imino)indeno[1,2-b]furan-11-yl)-1,4(1,4)-dibenzenacyclohexaphane-1^2-carbox-amide methanol solvate – SB1232_HY

Crystal data

$C_{35}H_{26}N_6O_3S \cdot CH_4O$	$F(000)$ = 1344
M_r = 642.72	D_x = 1.383 Mg m^{-3}
Monoclinic, $P2_1/n$ *(no.14)*	Cu $K\alpha$ radiation, λ = 1.54178 Å
a = 9.1660 (2) Å	Cell parameters from 9816 reflections
b = 22.1290 (4) Å	θ = 3.5–72.2°
c = 15.2400 (3) Å	μ = 1.36 mm^{-1}
β = 93.129 (1)°	T = 123 K
V = 3086.59 (11) Å^3	Blocks, colorless
Z = 4	0.18 × 0.12 × 0.06 mm

Data collection

Bruker D8 VENTURE diffractometer with PhotonII CPAD detector	5856 reflections with $I > 2\sigma(I)$
Radiation source: INCOATEC microfocus sealed tube	R_{int} = 0.026
rotation in ϕ and ω, 1°, shutterless scans	θ_{max} = 72.3°, θ_{min} = 3.5°
Absorption correction: multi-scan *SADABS* (Sheldrick, 2014)	h = -11→9
T_{min} = 0.841, T_{max} = 0.915	k = -27→27
31118 measured reflections	l = -18→17
6082 independent reflections	

Refinement

Refinement on F^2	Secondary atom site location: difference Fourier map
Least-squares matrix: full	Hydrogen site location: difference Fourier map
$R[F^2 > 2\sigma(F^2)]$ = 0.035	H atoms treated by a mixture of independent and constrained refinement
$wR(F^2)$ = 0.088	$w = 1/[\sigma^2(F_o^2) + (0.0384P)^2 + 1.8537P]$ where $P = (F_o^2 + 2F_c^2)/3$
S = 1.03	$(\Delta/\sigma)_{max}$ = 0.002
6082 reflections	$\Delta\rangle_{max}$ = 0.33 e Å^{-3}

438 parameters	**$\Delta\rangle_{min}$ = -0.25 e Å^{-3}**
4 restraints	**Extinction correction: *SHELXL2014/7* (Sheldrick 2014, $Fc^{*}=kFc[1+0.001xFc^{2}\lambda^{3}/\sin(2\theta)]^{-1/4}$**
Primary atom site location: dual	**Extinction coefficient: 0.00070 (9)**

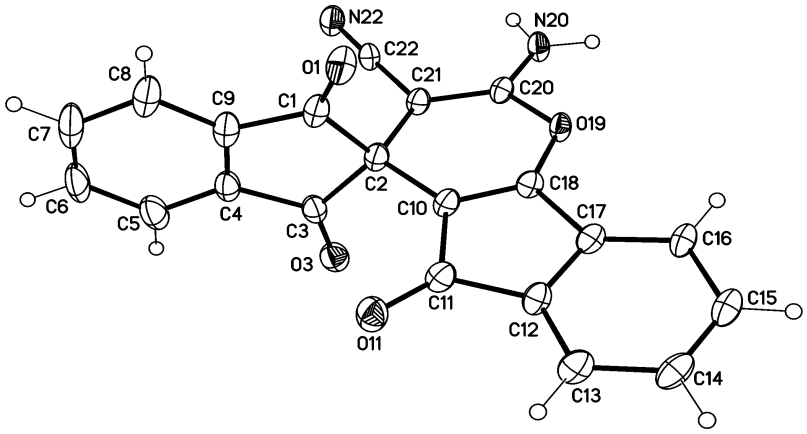

2'-Amino-1,3,5'-trioxo-1,3-dihydro-5'H-spiro[indene- 2,4'-indeno[1,2-b]pyran]-3'-carbonitrile – SB1245_HY

Crystal data

$C_{21}H_{10}N_2O_4$·[+solvent]	Z = 4
M_r = 354.31	F(000) = 728
Triclinic, *P*-1 (no.2)	D_x = 1.310 Mg m^{-3}
a = 8.6840 (3) Å	Cu $K\alpha$ radiation, λ = 1.54178 Å
b = 11.4787 (4) Å	Cell parameters from 7756 reflections
c = 18.2314 (6) Å	θ = 3.8–72.2°
α = 98.215 (2)°	μ = 0.77 mm^{-1}
β = 90.730 (2)°	T = 123 K
γ = 92.430 (2)°	Platers, yellow
V = 1796.73 (11) Å^3	0.08 × 0.04 × 0.01 mm

Data collection

Bruker D8 VENTURE diffractometer with PhotonII CPAD detector	5172 reflections with $I > 2\sigma(I)$
Radiation source: INCOATEC microfocus sealed tube	R_{int} = 0.056
rotation in ϕ and ω, 1°, shutterless scans	θ_{max} = 72.4°, θ_{min} = 2.5°
Absorption correction: multi-scan *SADABS* (Sheldrick, 2014)	h = -10→10
T_{min} = 0.845, T_{max} = 0.996	k = -14→13
24909 measured reflections	l = -22→22
7048 independent reflections	

Refinement

Refinement on F^2	Primary atom site location: dual
Least-squares matrix: full	Secondary atom site location: difference Fourier map
$R[F^2 > 2\sigma(F^2)]$ = 0.055	Hydrogen site location: mixed
$wR(F^2)$ = 0.153	H atoms treated by a mixture of independent and constrained refinement
S = 1.05	$w = 1/[\sigma^2(F_o^2) + (0.0803P)^2 + 0.3748P]$ where $P = (F_o^2 + 2F_c^2)/3$
7048 reflections	$(\Delta/\sigma)_{max} < 0.001$
499 parameters	$\Delta\rangle_{max}$ = 0.47 e Å^{-3}
4 restraints	$\Delta\rangle_{min}$ = -0.28 e Å^{-3}

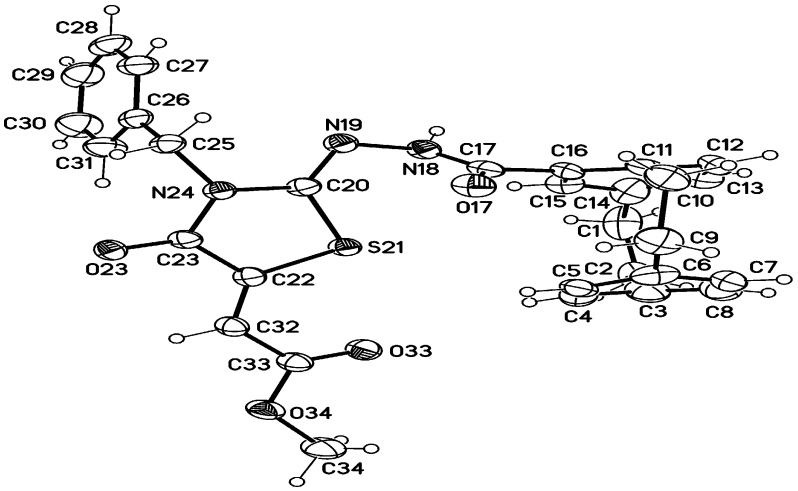

Methyl (Z)-2-((Z)-2-(2-(1,4(1,4)-dibenzenacyclohexaphane-1^2-carbonyl)-hydrazineyl-idene)-3-benzyl-4-oxothiazolidin-5-ylidene)acetate – SB1228_HY

Crystal data

$C_{30}H_{27}N_3O_4S$	$F(000)$ = 1104
M_r = 525.60	D_x = 1.356 Mg m^{-3}
Monoclinic, $P2_1/c$ *(no.14)*	Cu $K\alpha$ radiation, λ = 1.54178 Å
a = 13.0205 (4) Å	Cell parameters from 9767 reflections
b = 12.4037 (4) Å	θ = 3.3–72.3°
c = 15.9584 (5) Å	μ = 1.46 mm^{-1}
β = 92.837 (1)°	T = 123 K
V = 2574.16 (14) Å^3	Plates, yellow
Z = 4	0.14 × 0.12 × 0.04 mm

Data collection

Bruker D8 VENTURE diffractometer with PhotonII CPAD detector	4800 reflections with $I > 2\sigma(I)$
Radiation source: INCOATEC microfocus sealed tube	R_{int} = 0.038
rotation in ϕ and ω, 1°, shutterless scans	θ_{max} = 72.3°, θ_{min} = 3.4°
Absorption correction: multi-scan *SADABS* (Sheldrick, 2014)	h = -16→16
T_{min} = 0.805, T_{max} = 0.942	k = -15→15
41983 measured reflections	l = -19→19
5074 independent reflections	

Refinement

Refinement on F^2	Primary atom site location: dual
Least-squares matrix: full	Secondary atom site location: difference Fourier map
$R[F^2 > 2\sigma(F^2)]$ = 0.070	Hydrogen site location: mixed
$wR(F^2)$ = 0.187	H atoms treated by a mixture of independent and constrained refinement
S = 1.06	$w = 1/[\sigma^2(F_o^2) + (0.0884P)^2 + 4.8752P]$ where $P = (F_o^2 + 2F_c^2)/3$
5074 reflections	$(\Delta/\sigma)_{max} < 0.001$
347 parameters	$\Delta\rangle_{max}$ = 1.13 e Å^{-3}
1 restraint	$\Delta\rangle_{min}$ = -0.35 e Å^{-3}

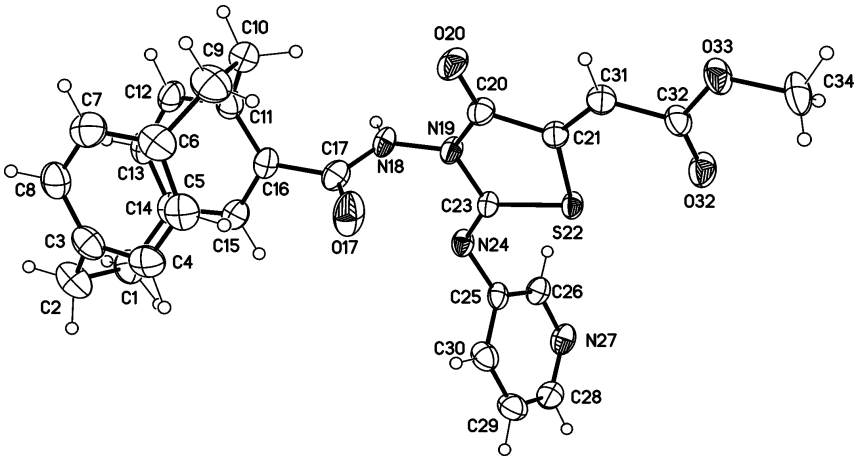

methyl (E)-2-((E)-3-(1,4(1,4)-dibenzenacyclohexaphane-1^2-carboxamido)-4-oxo-2-(pyridin-3-ylimino)thiazolidin-5-ylidene)acetate – SB1206_HY

Crystal data

$C_{28}H_{24}N_4O_4S·0.5(CH_4O)·0.5(H_2O)$	$F(000)$ = 2256
M_r = 537.60	D_x = 1.359 Mg m^{-3}
Monoclinic, *C*2/*c* *(no.15)*	Cu *K*α radiation, λ = 1.54178 Å
a = 19.3130 (6) Å	Cell parameters from 9990 reflections
b = 12.4233 (6) Å	θ = 4.0–72.1°
c = 21.8993 (8) Å	μ = 1.49 mm^{-1}
β = 90.008 (2)°	*T* = 123 K
V = 5254.3 (4) Å^3	Plates, colorless
Z = 8	0.15 × 0.09 × 0.03 mm

Data collection

Bruker D8 VENTURE diffractometer with PhotonII CPAD detector	4649 reflections with $I > 2\sigma(I)$
Radiation source: INCOATEC microfocus sealed tube	R_{int} = 0.041
rotation in ϕ and ω, 1°, shutterless scans	θ_{max} = 72.2°, θ_{min} = 4.0°
Absorption correction: multi-scan *SADABS* V2014/5 (Bruker AXS Inc.)	*h* = -23→23
T_{min} = 0.826, T_{max} = 0.942	*k* = -15→12
28186 measured reflections	*l* = -27→26
5170 independent reflections	

Refinement

Refinement on F^2	Primary atom site location: dual
Least-squares matrix: full	Secondary atom site location: difference Fourier map
$R[F^2 > 2\sigma(F^2)]$ = 0.043	Hydrogen site location: difference Fourier map
$wR(F^2)$ = 0.110	H atoms treated by a mixture of independent and constrained refinement
S = 1.04	$w = 1/[\sigma^2(F_o^2) + (0.0494P)^2 + 6.5503P]$ where $P = (F_o^2 + 2F_c^2)/3$
5170 reflections	$(\Delta/\sigma)_{max} < 0.001$
338 parameters	$\Delta\rangle_{max}$ = 0.42 e Å^{-3}
1 restraint	$\Delta\rangle_{min}$ = -0.21 e Å^{-3}

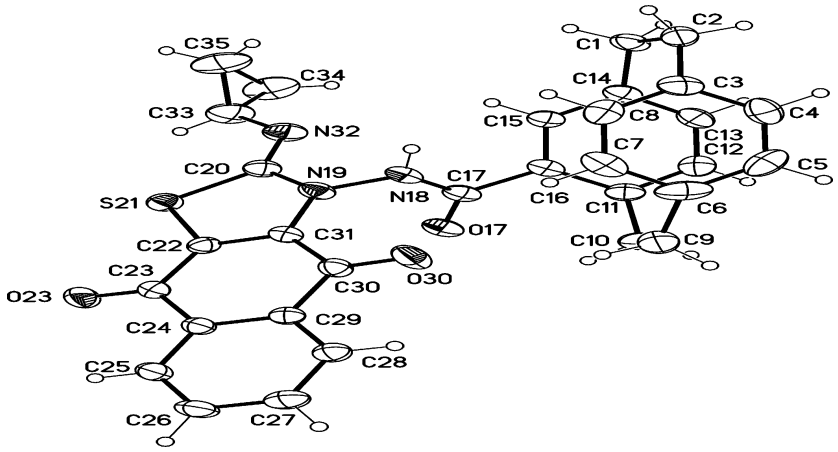

N-(2-(cyclopropylimino)-4,9-dioxo-4,9-dihydronaphtho[2,3-d]thia-zol-3(2H)-yl)-1,4(1,4)-dibenzenacyclohexaphane-1^2-carboxamide – SB1235_HY

Crystal data

$C_{31}H_{25}N_3O_3S·0.625(CH_4O)·0.375(C2H6O)$	$F(000)$ = 1172
M_r = 556.90	D_x = 1.359 Mg m^{-3}
Monoclinic, $P2_1/c$ *(no.14)*	Cu $K\alpha$ radiation, λ = 1.54178 Å
a = 7.2104 (3) Å	Cell parameters from 9937 reflections
b = 14.3984 (6) Å	θ = 3.3–72.2°
c = 26.4331 (12) Å	μ = 1.42 mm^{-1}
β = 97.291 (2)°	T = 123 K
V = 2722.0 (2) Å^3	Plates, red
Z = 4	0.16 × 0.06 × 0.03 mm

Data collection

Bruker D8 VENTURE diffractometer with PhotonII CPAD detector	5006 reflections with $I > 2\sigma(I)$
Radiation source: INCOATEC microfocus sealed tube	R_{int} = 0.039
rotation in ϕ and ω, 1°, shutterless scans	θ_{max} = 70.1°, θ_{min} = 3.1°
Absorption correction: multi-scan *SADABS* (Sheldrick, 2014)	h = -8→8
T_{min} = 0.823, T_{max} = 0.952	k = -17→17
51610 measured reflections	l = -32→32
5279 independent reflections	

Refinement

Refinement on F^2	Primary atom site location: dual
Least-squares matrix: full	Secondary atom site location: difference Fourier map
$R[F^2 > 2\sigma(F^2)]$ = 0.058	Hydrogen site location: mixed
$wR(F^2)$ = 0.175	H atoms treated by a mixture of independent and constrained refinement
S = 1.10	$w = 1/[\sigma^2(F_o^2) + (0.0803P)^2 + 4.1514P]$ where $P = (F_o^2 + 2F_c^2)/3$
5279 reflections	$(\Delta/\sigma)_{max} < 0.001$
367 parameters	$\Delta\rangle_{max}$ = 0.40 e Å^{-3}
43 restraints	$\Delta\rangle_{min}$ = -0.44 e Å^{-3}

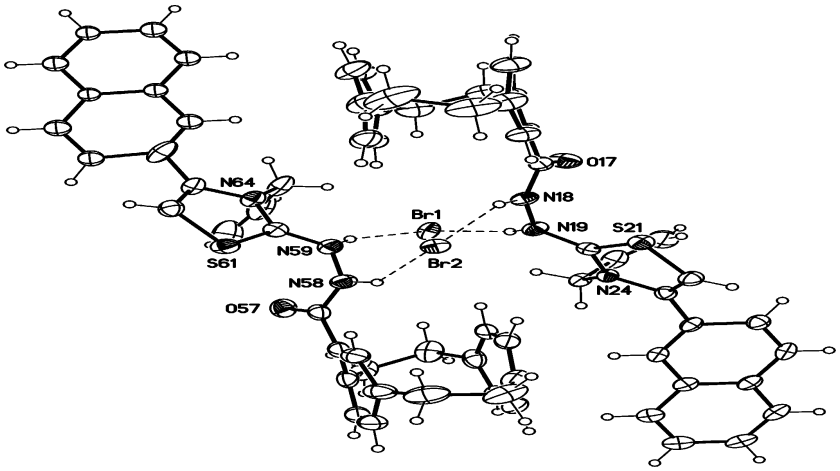

2-(2-(1,4(1,4)-dibenzenacyclohexaphane-1^2-carbonyl)hydrazineyl)-3-allyl-4-(naphthalen-2-yl)thiazol-3-ium bromide – SB1314_HY

Crystal data

$C_{33}H_{30}N_3OS{\cdot}Br$	D_x = 1.384 Mg m^{-3}
M_r = 596.57	Cu $K\alpha$ radiation, λ = 1.54178 Å
Orthorhombic, *Pna*2$_1$ (no.33)	Cell parameters from 9781 reflections
a = 17.5892 (5) Å	θ = 3.0–72.1°
b = 25.1597 (7) Å	μ = 2.87 mm^{-1}
c = 12.9433 (4) Å	T = 123 K
V = 5727.9 (3) Å^3	Rods, colorless
Z = 8	0.20 × 0.06 × 0.02 mm
F(000) = 2464	

Data collection

Bruker D8 VENTURE diffractometer with PhotonII CPAD detector	10402 reflections with $I > 2\sigma(I)$
Radiation source: INCOATEC microfocus sealed tube	R_{int} = 0.028
rotation in ϕ and ω, 1°, shutterless scans	θ_{max} = 72.2°, θ_{min} = 3.1°
Absorption correction: multi-scan *SADABS* (Sheldrick, 2014)	h = -21→20
T_{min} = 0.780, T_{max} = 0.915	k = -31→29
43575 measured reflections	l = -15→14
10648 independent reflections	

Refinement

Refinement on F^2	Secondary atom site location: difference Fourier map
Least-squares matrix: full	Hydrogen site location: mixed
$R[F^2 > 2\sigma(F^2)]$ = 0.033	H atoms treated by a mixture of independent and constrained refinement
$wR(F^2)$ = 0.083	$w = 1/[\sigma^2(F_o^2) + (0.0487P)^2 + 2.6111P]$ where $P = (F_o^2 + 2F_c^2)/3$
S = 1.07	$(\Delta/\sigma)_{max}$ = 0.002
10648 reflections	$\Delta\rangle_{max}$ = 0.64 e Å^{-3}
698 parameters	$\Delta\rangle_{min}$ = -0.53 e Å^{-3}
94 restraints	Absolute structure: Flack x determined using 4467 quotients [(I+)-(I-)]/[(I+)+(I-)] (Parsons, Flack and Wagner, Acta Cryst. B69 (2013) 249-259).
Primary atom site location: dual	Absolute structure parameter: -0.017 (6)

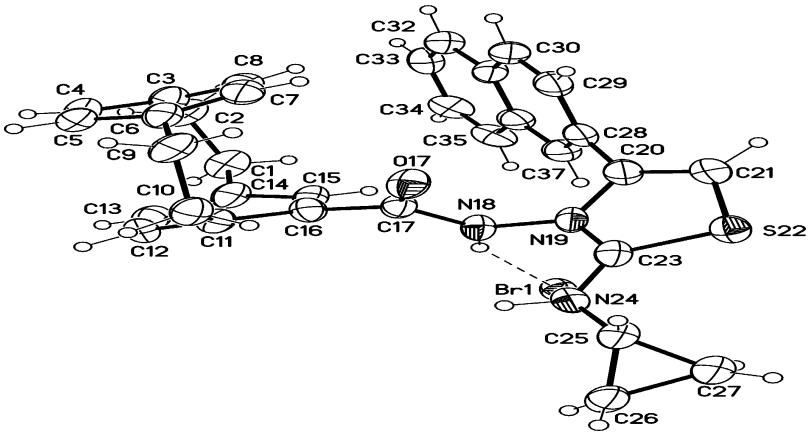

3-(1,4(1,4)-dibenzenacyclohexaphane-1^2-carboxamido)-2-(cyclo-propylamino)-4-(naphthalen-2-yl)thiazol-3-ium bromide – SB1315_HY

Crystal data

$C_{33}H_{30}N_3OS\cdot Br$	$F(000)$ = 1232
M_r = 596.57	D_x = 1.400 Mg m^{-3}
Monoclinic, $P2_1/c$ *(no.14)*	Cu $K\alpha$ radiation, λ = 1.54178 Å
a = 16.9166 (12) Å	Cell parameters from 1949 reflections
b = 9.1979 (6) Å	θ = 2.6–71.3°
c = 18.6636 (12) Å	μ = 2.91 mm^{-1}
β = 102.929 (4)°	T = 123 K
V = 2830.4 (3) Å^3	Plates, colorless
Z = 4	0.08 × 0.04 × 0.01 mm

Data collection

Bruker D8 VENTURE diffractometer with PhotonII CPAD detector	2904 reflections with $I > 2\sigma(I)$
Radiation source: INCOATEC microfocus sealed tube	R_{int} = 0.152
rotation in ϕ and ω, 1°, shutterless scans	θ_{max} = 72.2°, θ_{min} = 2.7°
Absorption correction: multi-scan *SADABS* (Sheldrick, 2014)	h = -18→20
T_{min} = 0.669, T_{max} = 0.971	k = -10→11
22667 measured reflections	l = -22→20
5534 independent reflections	

Refinement

Refinement on F^2	Secondary atom site location: difference Fourier map
Least-squares matrix: full	Hydrogen site location: mixed
$R[F^2 > 2\sigma(F^2)]$ = 0.078	H atoms treated by a mixture of independent and constrained refinement
$wR(F^2)$ = 0.217	$w = 1/[\sigma^2(F_o^2) + (0.0915P)^2]$ where $P = (F_o^2 + 2F_c^2)/3$
S = 1.01	$(\Delta/\sigma)_{max} < 0.001$
5534 reflections	$\Delta\rangle_{max}$ = 0.59 e Å^{-3}
359 parameters	$\Delta\rangle_{min}$ = -0.51 e Å^{-3}
2 restraints	Extinction correction: *SHELXL2014*/7 (Sheldrick 2014), $Fc^*=kFc[1+0.001xFc^2\lambda^3/\sin(2\theta)]^{-1/4}$
Primary atom site location: dual	Extinction coefficient: 0.0020 (2)

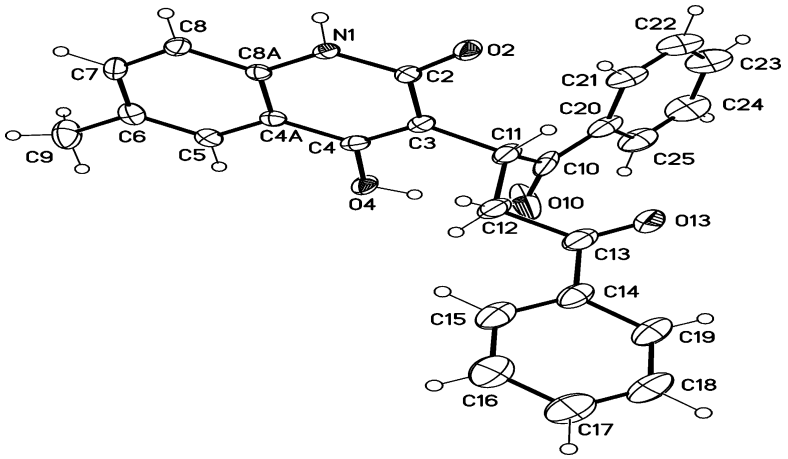

2-(4-hydroxy-6-methyl-2-oxo-1,2-dihydroquinolin-3-yl)-1,4-diphenylbutane-1,4-dione – SB993_HY

Crystal data

$C_{26}H_{21}NO_4$	Z = 4
M_r = 411.44	F(000) = 864
Triclinic, P-1 (no.2)	D_x = 1.320 Mg m^{-3}
a = 11.1823 (3) Å	Cu $K\alpha$ radiation, λ = 1.54178 Å
b = 14.3827 (4) Å	Cell parameters from 9863 reflections
c = 15.3460 (4) Å	θ = 3.1–72.1°
α = 67.695 (1)°	μ = 0.72 mm^{-1}
β = 70.666 (1)°	T = 123 K
γ = 68.389 (1)°	Blocks, colorless
V = 2069.77 (10) Å^3	0.16 × 0.08 × 0.06 mm

Data collection

Bruker D8 VENTURE diffractometer with Photon100 detector	8117 independent reflections
Radiation source: INCOATEC microfocus sealed tube	6749 reflections with $I > 2\sigma(I)$
Detector resolution: 10.4167 pixels mm^{-1}	R_{int} = 0.035
rotation in ϕ and ω, 1°, shutterless scans	θ_{max} = 72.1°, θ_{min} = 3.2°
Absorption correction: multi-scan *SADABS* (Sheldrick, 2014)	h = -13→13
T_{min} = 0.896, T_{max} = 0.958	k = -17→17
28579 measured reflections	l = -18→18

Refinement

Refinement on F^2	Primary atom site location: structure-invariant direct methods
Least-squares matrix: full	Secondary atom site location: difference Fourier map
$R[F^2 > 2\sigma(F^2)]$ = 0.043	Hydrogen site location: difference Fourier map
$wR(F^2)$ = 0.112	H atoms treated by a mixture of independent and constrained refinement
S = 1.01	$w = 1/[\sigma^2(F_o^2) + (0.0508P)^2 + 1.0588P]$ where $P = (F_o^2 + 2F_c^2)/3$
8117 reflections	$(\Delta/\sigma)_{max} < 0.001$
577 parameters	$\Delta\rangle_{max}$ = 0.37 e Å^{-3}
5 restraints	$\Delta\rangle_{min}$ = -0.50 e Å^{-3}

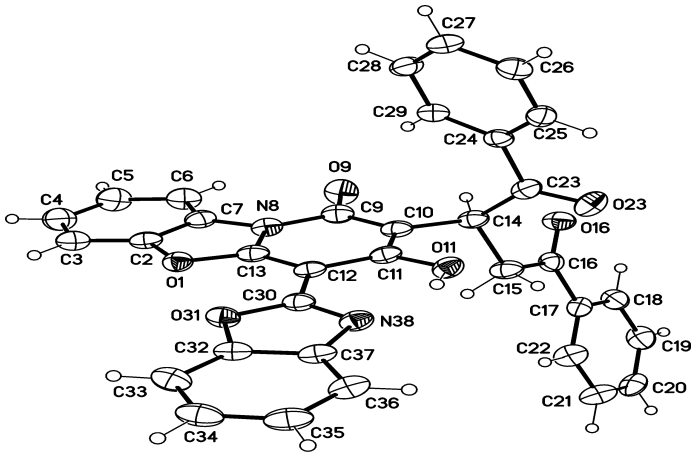

2-(4-(benzo[d]oxazol-2-yl)-3-hydroxy-1-oxo-1H-benzo[4,5]oxazolo[3,2-a]pyridin-2-yl)-1,4-diphenylbutane-1,4-dione – SB1057_HY

Crystal data

$C_{34}H_{22}N_2O_6$	Z = 2
M_r = 554.53	F(000) = 576
Triclinic, P-1 (no.2)	D_x = 1.446 Mg m^{-3}
a = 8.2672 (2) Å	Cu $K\alpha$ radiation, λ = 1.54178 Å
b = 11.3140 (3) Å	Cell parameters from 9918 reflections
c = 13.7326 (3) Å	θ = 3.2–71.1°
α = 91.721 (1)°	μ = 0.82 mm^{-1}
β = 96.833 (1)°	T = 123 K
γ = 92.198 (1)°	Plates, colorless
V = 1273.64 (5) Å^3	0.22 × 0.09 × 0.03 mm

Data collection

Bruker D8 VENTURE diffractometer with Photon100 detector	4987 independent reflections
Radiation source: INCOATEC microfocus sealed tube	4212 reflections with $I > 2\sigma(I)$
Detector resolution: 10.4167 pixels mm^{-1}	R_{int} = 0.037
rotation in ϕ and ω, 1°, shutterless scans	θ_{max} = 72.2°, θ_{min} = 3.2°
Absorption correction: multi-scan *SADABS* (Sheldrick, 2014)	h = -10→10
T_{min} = 0.835, T_{max} = 0.971	k = -13→13
18981 measured reflections	l = -16→16

Refinement

Refinement on F^2	Primary atom site location: dual
Least-squares matrix: full	Secondary atom site location: difference Fourier map
$R[F^2 > 2\sigma(F^2)]$ = 0.048	Hydrogen site location: difference Fourier map
$wR(F^2)$ = 0.127	H atoms treated by a mixture of independent and constrained refinement
S = 1.03	$w = 1/[\sigma^2(F_o^2) + (0.0569P)^2 + 0.8606P]$ where $P = (F_o^2 + 2F_c^2)/3$
4987 reflections	$(\Delta/\sigma)_{max} < 0.001$
382 parameters	$\Delta\rangle_{max}$ = 0.35 e Å^{-3}

6. List of Abbreviations

-	no product
%	percent
(v/v)	volume/volume ratio
°C	degree Celsius
δ	chemical shift
Δ	reflux
$\Delta\psi$mt	mitochondrial transmembrane potential
ΔG	binding free energy
µg	microgram
µL	microliter
µM	micromole
3-NBA	3-nitrobenzyl alcohol
Å	Ångström
abs.	absolute
Ar	aromat(ic)
ACE	angiotensin-converting-enzyme inhibitors
ANRORC	addition nucleophile, ring opening, and ring closure
aq.	aqueous
AQs	alkyl quinolones
ATCAA	2-aryl-thiazolidine-4-carboxylic acid amides
Boc_2O	di-*tert*-butyl dicarbonate
BNE	2-bromo-1-(naphthalene-1-yl)ethanone
br	broad

brs	broad singlet
c	concentration
calc.	calculated
CCDC	Cambridge Crystallographic Data Centre
CDKs	cyclin-dependent kinases
CH_3CN	acetonitrile
o-CHL	3,4,5,6-tetrachloro-1,2-benzoquinone
CNIND	dicyanomethylene-1,3-indanedione
CNS	central nervous system
COSY	correlation spectroscopy
CT	charge transfer
C_q	quaternary carbon
DBE	*E*-dibenzoylethene
DCE	dichloroethane
DCM	dichloromethane
DCNQ	2,3-dichloro-1,4-napthoquinone
DCP	2,3-dichloropyrazine
DEPT	distortionless enhancement by polarization transfer
DMAD	dimethyl acetylenedicarboxylate
DMAP	(4-dimethylaminopyridine)
DMF	*N*,*N*-dimethylformamide
DMSO	dimethylsulfoxide
DNA	deoxyribonucleic acid

Dppm	[μ-bis(diphenylphosphino)methane]dichlorodigold(I)
e.g.	exempli gratia (for example)
EA	elemental analysis
ee	enantiomeric excess
EGFR	epidermal growth factor receptor
ELISA	enzyme-linked immunosorbent assay
equiv.	equivalents
ERK	externally regulated kinases
Et_3N	triethyl amine
EtOAc	ethyl acetate
et al.	*et alii* (and others)
etc.	*et cetera* (and so on)
eV	electron volt
f	oscillator strength
FAB	fast atom bombardement
g	gram
gem	geminal
GI_{50}	growth inhibitory activity
GP	general procedure
h	hour
HSQC	Heteronuclear Single Quantum Coherence
HMBC	Heteronuclear Multiple Quantum Correlation
HOAc	acetic acid

HPLC	high performance liquid chromatography
HRMS	high resolution mass spectrometry
Hz	hertz
i.e.	id est (that is)
IBD	iodobenzene diacetate
in situ	latin for “on site”, without isolation
IR	infrared
*i*PrOH	isopropyl alcohol
IUPAC	International Union of Pure and Applied Chemistry
J	coupling constant
l	liter
LC_{50}	50% loss of initial cells
log	Logarithm
m	meta
m	multiplet
m/z	mass-to-charge ratio
M.p.	melting point
MDR	multidrug resistant
Me	methyl
mg	milligram
MHz	mega Hertz
min	minute
mL	milliliter

mM	milli molar
mmol	millimole
MMFF94X	Merck molecular force field 94x
MOE®	molecular operating environment
MS	mass spectroscopy
MTT	3-(4,5-dimethylthiazol-2-yl)-2,5-diphenyltetrazolium bromide
MW	microwave
N	normality/ equivalent concentration
NBS	*N*-bromosuccinimide
NCI	National Cancer Institute
ng	nanograme
NMR	nuclear magnetic resonance
Nu	Nucleophile
o	ortho
$OPPh_3$	triphenylphosphine oxide
p	para
PC	[2.2]paracyclophane
Ph	phenyl
pH	potential hydrogen, logarithm of the activity of hydrogen ions
PPA	polyphosphoric acid
PPh_3	triphenyl phosphine
ppm	parts per million
PDB: 3HKC	protein data bank

Py	pyridyl
q	quartet
R/*R*$_P$	right-handed (clockwise) stereodescriptor
r.t.	room temperature
rac	racemic
ROS	reactive oxygen species
RMSD	root mean square deviations
s	singlet
s	strong
S/*S*$_P$	left-handed (counter-clockwise) stereodescriptor
SAR	structure activity relationship
SMART	substituted methoxylbenzoylaryl- thiazole
S$_N$Ar	aromatic nucleophile substitution
SRB	suiforhodamine B
t	triplet
TCNE	tetracyanoethylene
TGI	total growth inhibition
THF	tetrahydrofuran
TK	thymidine kinase
TLC	thin layer chromatography
p-TSA	*p*-toluenesulfonic acid
UV	ultraviolet
vs	very strong

vw	very weak
w	weak
wt%	weight percent

7. References

[1] M. Asif, *Mor. J. Chem.* **2014**, *2*, 70-84.
[2] E. Campaigne, *J. Chem. Educ.* **1986**, *63*, 860.
[3] A. R. Katritzky, P. J. Wheatley, *Vol. 1*, Elsevier, **1963**.
[4] I. J. Turchi, M. J. Dewar, *Chem. Rev.* **1975**, *75*, 389-437.
[5] D. V. Patel, N. R. Patel, in *Book*, Elsevier, **2018**, pp. 245-276.
[6] R. Pawlowski, F. Stanek, M. Stodulski, *Molecules* **2019**, *24*, 1533.
[7] A. F. Pozharskii, A. T. Soldatenkov, A. R. Katritzky, *Vol.*, John Wiley & Sons, **2011**.
[8] T. Eicher, S. Hauptmann, A. Speicher, *Vol.*, John Wiley & Sons, **2013**.
[9] T. Creagh, J. L. Ruckle, D. T. Tolbert, J. Giltner, D. A. Eiznhamer, B. Dutta, M. T. Flavin, Z.-Q. Xu, *Antimicrob. Agents Chemother.* **2001**, *45*, 1379-1386.
[10] M. S. Alam, J. U. Ahmed, D.-U. Lee, *Appl. Biol. Chem* **2016**, *59*, 181-192.
[11] J.-Y. Lee, K.-W. Jeong, S. Shin, J.-U. Lee, Y. Kim, *Eur. J. Med. Chem.* **2012**, *47*, 261-269.
[12] Y.-S. Yang, F. Zhang, C. Gao, Y.-B. Zhang, X.-L. Wang, J.-F. Tang, J. Sun, H.-B. Gong, H.-L. Zhu, *Bioorg. Med. Chem. Lett.* **2012**, *22*, 4619-4624.
[13] J.-R. Li, D.-D. Li, R.-R. Wang, J. Sun, J.-J. Dong, Q.-R. Du, F. Fang, W.-M. Zhang, H.-L. Zhu, *Eur. J. Med. Chem.* **2014**, *75*, 438-447.
[14] P. R. Murumkar, R. B. Ghuge, in *Book* (Eds.: M. R. Yadav, P. R. Murumkar, R. B. Ghuge), Elsevier, **2018**, pp. 277-303.
[15] P. K. Gupta, M. K. Hussain, M. Asad, R. Kant, R. Mahar, S. K. Shukla, K. Hajela, *New J. Chem.* **2014**, *38*, 3062-3070.
[16] C. T. Supuran, A. Scozzafava, *Curr. Med. Chem.* **2001**, *1*, 61-97.
[17] Y. Iizawa, K. Okonogi, R. Hayashi, T. Iwahi, T. Yamazaki, A. Imada, *Antimicrob. Agents Chemother.* **1993**, *37*, 100-105.
[18] T. Önkol, D. S. Doğruer, L. Uzun, S. Adak, S. Özkan, M. Fethi Şahin, *J. Enzyme Inhib. Med. Chem.* **2008**, *23*, 277-284.
[19] J. Matysiak, Z. Malinski, *uss. J. Bioorg. Chem.* **2007**, *33*, 594.
[20] D. Kumar, N. M. Kumar, K.-H. Chang, K. Shah, *Eur. J. Med. Chem.* **2010**, *45*, 4664-4668.
[21] A. A. Kadi, E. S. Al-Abdullah, I. A. Shehata, E. E. Habib, T. M. Ibrahim, A. A. El-Emam, *Eur. J. Med. Chem.* **2010**, *45*, 5006-5011.
[22] M. L. Barreca, A. Chimirri, L. De Luca, A.-M. Monforte, P. Monforte, A. Rao, M. Zappalà, J. Balzarini, E. De Clercq, C. Pannecouque, *Bioorg. Med. Chem. Lett.* **2001**, *11*, 1793-1796.
[23] A. K. Jain, S. Sharma, A. Vaidya, V. Ravichandran, R. K. Agrawal, *Chem. Biol. Drug Des.* **2013**, *81*, 557-576.
[24] T. L. Gilchrist, *Heterocyclic Chemistry; Longman; London* **1992**.
[25] K. Tewari, N. Vishnoi, *Vol.*, Vikas Publishing House, **1976**.
[26] D. J. Gorin, N. R. Davis, F. D. Toste, *J. Am. Chem. Soc.* **2005**, *127*, 11260-11261.
[27] J. R. Davies, P. D. Kane, C. J. Moody, *Tetrahedron* **2004**, *60*, 3967-3977.
[28] M. A. Martins, R. Freitag, A. F. Flores, N. Zanatta, *Synthesis* **1995**, *1995*, 1491-1492.
[29] K. Sakai, N. Hida, K. Kondo, *Bull. Chem. Soc. Jpn.* **1986**, *59*, 179-183.
[30] B. Meldrum, R. Horton, M. Sawaya, *J. Neurochem.* **1975**, *24*, 1003-1009.
[31] V. B. Arion, M. A. Jakupec, M. Galanski, P. Unfried, B. K. Keppler, *J. Inorg. Biochem.* **2002**, *91*, 298-305.
[32] C. C. García, B. N. Brousse, M. J. Carlucci, A. G. Moglioni, M. M. Alho, G. Y. Moltrasio, N. B. D'Accorso, E. B. Damonte, *Antiviral Chem. Chemother.* **2003**, *14*, 99-105.
[33] W.-x. Hu, W. Zhou, C.-n. Xia, X. Wen, *Bioorg. Med. Chem. Lett.* **2006**, *16*, 2213-2218.
[34] S. Bondock, W. Khalifa, A. A. Fadda, *Eur. J. Med. Chem.* **2007**, *42*, 948-954.
[35] Y. Zhang, X. Meng, H. Tang, M. Cheng, F. Yang, W. Xu, *J. Enzyme Inhib. Med. Chem.* **2020**, *35*, 344-353.
[36] G. P. Coşkun, T. Djikic, T. B. Hayal, N. Türkel, K. Yelekçi, F. Şahin, Ş. G. Küçükgüzel, *Molecules* **2018**, *23*, 1969.
[37] S. M. Abou-Seri, N. A. Farag, G. S. Hassan, *Chem. Pharm. Bull.* **2011**, *59*, 1124-1132.

[38] H. M. Abumelha, *J. Heterocycl. Chem.* **2020**, *57*, 1011-1022.
[39] U. Salar, M. Taha, K. M. Khan, N. H. Ismail, S. Imran, S. Perveen, S. Gul, A. Wadood, *Eur. J. Med. Chem.* **2016**, *122*, 196-204.
[40] F. Mihalcea, S.-F. Barbuceanu, C. Cristea, C. Draghici, C. ENACHEPREOTEASA, G. L. Almajan, G. Saramet, *Rev. Chim.* **2012**, *63*, 475-480.
[41] G. G. Ladani, M. P. Patel, *New J. Chem.* **2015**, *39*, 9848-9857.
[42] W. A. El-Enany, S. M. Gomha, A. K. El-Ziaty, W. Hussein, M. M. Abdulla, S. A. Hassan, H. A. Sallam, R. S. Ali, *Synth. Commun.* **2020**, *50*, 85-96.
[43] B. Balandis, G. Ivanauskaitė, J. Smirnovienė, K. Kantminienė, D. Matulis, V. Mickevičius, A. Zubrienė, *Bioorg. Chem.* **2020**, *97*, 103658.
[44] Ş. G. Küçükgüzel, I. Küçükgüzel, E. Tatar, S. Rollas, F. Şahin, M. Güllüce, E. De Clercq, L. Kabasakal, *Eur. J. Med. Chem.* **2007**, *42*, 893-901.
[45] I. A. Bessonova, D. Kurbanov, S. Y. Yunusov, *Chem. Nat. Compd.* **1989**, *25*, 39-40.
[46] A. Detsi, V. Bardakos, J. Markopoulos, O. Igglessi-Markopoulou, *J. Chem. Soc., Perkin Trans. 1* **1996**, 2909-2913.
[47] I. Ukrainets, N. Bereznyakova, E. Mospanova, *Chem. Heterocycl. Compd.* **2007**, *43*, 856-862.
[48] D. L. Boger, *J. Pharm. Sci.* **1985**, *74*, 233-233.
[49] S. Heeb, M. P. Fletcher, S. R. Chhabra, S. P. Diggle, P. Williams, M. Cámara, *FEMS Microbiol. Rev.* **2011**, *35*, 247-274.
[50] V. K. Vishwanath K, Latha C, Thangaraj S. , *WO2011161691A1*. **2011**, *P T/IN2011/000404*.
[51] G. S. Bisacchi, *J. Med. Chem.* **2015**, *58*, 4874-4882.
[52] J. P. Michael, *Nat. Prod. Rep.* **2000**, *17*, 603-620.
[53] A. T. Society, I. D. S. o. America, *Am. J. Respir. Crit. Care Med.* **2005**, *171*, 388.
[54] Y. Zuo, J. Pu, G. Chen, W. Shen, B. Wang, *Nat. Prod. Res.* **2019**, *33*, 759-762.
[55] M. Mizuta, H. Kanamori, *Mutat. Res.* **1985**, *144*, 221-225.
[56] A. Debbab, A. H. Aly, W. H. Lin, P. Proksch, *Microb. Biotechnol.* **2010**, *3*, 544-563.
[57] J. J. Li, *Vol.*, Springer Science & Business Media, **2013**.
[58] H. Wang, *Vol. 2*, Wiley, **2010**.
[59] P. Cheng, Q. Gu, W. Liu, J.-F. Zou, Y.-Y. Ou, Z.-Y. Luo, J.-G. Zeng, *Molecules* **2011**, *16*, 7649-7661.
[60] R. A. Bunce, B. Nammalwar, *Org. Prep. Proced. Int.* **2010**, *42*, 557-563.
[61] S. Kafka, A. Klásek, J. Polis, V. Rosenbreierová, C. Palík, V. Mrkvička, J. Košmrlj, *Tetrahedron* **2008**, *64*, 4387-4402.
[62] P. Pitchai, C. Uvarani, T. R. Makhanya, R. M. Gengan, P. S. Mohan, *J. Chem.-NY* **2014**, *3*, 60-71.
[63] W. Steinschifter, W. Fiala, W. Stadlbauer, *J. Heterocycl. Chem.* **1994**, *31*, 1647-1652.
[64] M. S. Katagi, J. Fernandes, S. Mamledesai, D. Satyanarayana, P. Dabadi, G. Bolakatti, *J. Pharm. Res.* **2015**, *14*, 51-56.
[65] I. Ukrainets, E. Mospanova, N. Jaradat, O. Bevz, A. Turov, *Chem. Heterocycl. Compd.* **2012**, *48*, 1347-1356.
[66] A. Klásek, V. Mrkvicka, A. Pevec, J. Košmrlj, *J. Org. Chem.* **2004**, *69*, 5646-5651.
[67] W. Stadlbauers, G. Hojas, *J. Heterocycl. Chem.* **2004**, *41*, 681-690.
[68] E. M. El-Sheref, A. A. Aly, M. A. Ameen, A. B. Brown, *Monatsh. Chem.* **2019**, *150*, 747-756.
[69] C. Brown, A. Farthing, *Nature* **1949**, *164*, 915-916.
[70] C.-F. Shieh, D. McNally, R. Boyd, *Tetrahedron* **1969**, *25*, 3653-3665.
[71] A. Solladié-Cavallo, M. Hibert, *Org. Magn. Reson.* **1981**, *16*, 44-46.
[72] A. Marrocchi, I. Tomasi, L. Vaccaro, *Isr. J. Chem.* **2012**, *52*, 41-52.
[73] P. J. Dyson, B. F. Johnson, C. M. Martin, *Coord. Chem. Rev.* **1998**, *175*, 59-89.
[74] K. A. Lyssenko, M. Y. Antipin, D. Y. Antonov, *Chemphyschem* **2003**, *4*, 817-823.
[75] S. Grimme, *Chem. Eur. J.* **2004**, *10*, 3423-3429.
[76] F. Vögtle, P. Neumann, *Tetrahedron Lett.* **1969**, *10*, 5329-5334.
[77] D. J. Cram, H. Steinberg, *J. Am. Chem. Soc.* **1951**, *73*, 5691-5704.
[78] V. Rozenberg, E. Sergeeva, H. Hopf, in *Secondary*, Wiley Online Library, **2004**, pp. 435-462.
[79] A. A. Aly, A. B. Brown, *Tetrahedron (Oxford. Print)* **2009**, *65*.

[80] S. Banfi, A. Manfredi, F. Montanari, G. Pozzi, S. Quici, *J. Mol. Catal. A: Chem.* **1996**, *113*, 77-86.
[81] D. Y. Antonov, Y. N. Belokon, *J. Chem. Soc., Perkin Trans* **1995**, *1*, 1873-1879.
[82] C. J. Friedmann, S. Ay, S. Bräse, *J. Org. Chem.* **2010**, *75*, 4612-4614.
[83] F. VOeGTLE, P. NEUMANN, *Synthesis* **1973**, *1973*, 85-103.
[84] H. A. Staab, G. H. Knaus, H. E. Henke, C. Krieger, *Chem. Ber.* **1983**, *116*, 2785-2807.
[85] V. Boekelheide, in *Book*, Springer, **1983**, pp. 87-143.
[86] R. A. Meyers, J. W. Hamersma, H. E. Green, *J. Polym. Sci., Part B* **1972**, *10*, 685-689.
[87] A. Marchand, A. Maxwell, B. Mootoo, A. Pelter, A. Reid, *Tetrahedron* **2000**, *56*, 7331-7338.
[88] A. Pelter, B. Mootoo, A. Maxwell, A. Reid, *Tetrahedron Lett.* **2001**, *42*, 8391-8394.
[89] X. W. Wu, X. L. Hou, L. X. Dai, J. Tao, B. X. Cao, J. Sun, *Tetrahedron: Asymmetry* **2001**, *12*, 529-532.
[90] C. Bolm, K. Wenz, G. Raabe, *J. Organomet. Chem.* **2002**, *662*, 23-33.
[91] C. Bolm, T. Focken, G. Raabe, *Tetrahedron: Asymmetry* **2003**, *14*, 1733-1746.
[92] X.-W. Wu, K. Yuan, W. Sun, M.-J. Zhang, X.-L. Hou, *Tetrahedron: Asymmetry* **2003**, *14*, 107-112.
[93] D. K. Whelligan, C. Bolm, *J. Org. Chem.* **2006**, *71*, 4609-4618.
[94] S. M. Ahmad, D. C. Braddock, G. Cansell, S. A. Hermitage, J. M. Redmond, A. J. P. White, *Tetrahedron Lett.* **2007**, *48*, 5948-5952.
[95] V. A. Stepanova, V. V. Dunina, I. P. Smoliakova, *Organometallics* **2009**, *28*, 6546-6558.
[96] K. Mutoh, S. Hatano, J. Abe, *J. Photopolym. Sci. Technol.* **2010**, *23*, 301-306.
[97] A. A. Aly, A. A. Hassan, A. B. Brown, K. M. El-Shaieb, T. M. I. Bedair, *J. Heterocycl. Chem.* **2011**, *48*, 787-791.
[98] B. Hong, Y. Ma, L. Zhao, W. Duan, F. He, C. Song, *Tetrahedron: Asymmetry* **2011**, *22*, 1055-1062.
[99] H. Yamashita, J. Abe, *J. Phys. Chem. A* **2011**, *115*, 13332-13337.
[100] S. Kawai, T. Yamaguchi, T. Kato, S. Hatano, J. Abe, *Dyes Pigm.* **2012**, *92*, 872-876.
[101] M. Busch, M. Cayir, M. Nieger, W. R. Thiel, S. Bräse, *Eur. J. Org. Chem.* **2013**, *2013*, 6108-6123.
[102] K. Mutoh, J. Abe, *Phys. Chem. Chem. Phys.* **2014**, *16*, 17537-17540.
[103] E. Nakano, K. Mutoh, Y. Kobayashi, J. Abe, *J. Phys. Chem. A* **2014**, *118*, 2288-2297.
[104] K. Shima, K. Mutoh, Y. Kobayashi, J. Abe, *J. Am. Chem. Soc.* **2014**, *136*, 3796-3799.
[105] W. Duan, Y. Ma, Y. Huo, Q. Yao, *Aust. J. Chem.* **2015**, *68*, 1472-1478.
[106] S. Kitagaki, K. Sugisaka, C. Mukai, *Org. Biomol. Chem.* **2015**, *13*, 4833-4836.
[107] K. Mutoh, Y. Nakagawa, A. Sakamoto, Y. Kobayashi, J. Abe, *J. Am. Chem. Soc.* **2015**, *137*, 5674-5677.
[108] Z. Niu, J. Chen, Z. Chen, M. Ma, C. Song, Y. Ma, *J. Org. Chem.* **2015**, *80*, 602-608.
[109] K. Shima, K. Mutoh, Y. Kobayashi, J. Abe, *J. Phys. Chem. A* **2015**, *119*, 1087-1093.
[110] Y. Kobayashi, T. Katayama, T. Yamane, K. Setoura, S. Ito, H. Miyasaka, J. Abe, *J. Am. Chem. Soc.* **2016**, *138*, 5930-5938.
[111] A. Perrier, D. Jacquemin, *Tetrahedron* **2017**, *73*, 4936-4949.
[112] D. M. Knoll, Y. Hu, Z. Hassan, M. Nieger, S. Bräse, *Molecules* **2019**, *24*, 4122pp.
[113] V. Aanandhi, S. George, V. Vaidhyalingam, *ARKIVOC* **2008**, *2008*, 187-194.
[114] M. Suni, V. A. Nair, C. Joshua, *Tetrahedron* **2001**, *57*, 2003-2009.
[115] A. A. Hassan, A. M. Shawky, H. S. Shehatta, *J. Heterocycl. Chem.* **2012**, *49*, 21-37.
[116] A. R. Katritzky, N. M. Khashab, A. V. Gromova, *ARKIVOC* **2006**, *3*, 226-236.
[117] A. A. Hassan, S. K. Mohamed, F. F. Abdel-Latif, S. M. Mostafa, J. T. Mague, M. Akkurt, M. Abdel-Aziz, *Tetrahedron Lett.* **2016**, *57*, 345-347.
[118] A. A. Hassan, K. M. El-Shaieb, N. K. Mohamed, H. N. Tawfeek, S. Bräse, M. Nieger, *Tetrahedron Lett.* **2014**, *55*, 2385-2388.
[119] V. M. Patel, K. R. Desai, *ARKIVOC* **2004**, *2004*, 123-129.
[120] J. Matysiak, A. Niewiadomy, *Synth. Commun.* **2006**, *36*, 1621-1630.
[121] A. Aly, A. Brown, T. El-Emary, A. Ewas, M. Ramadan, *ARKIVOC* **2009** *i*, 150-197.
[122] A. Eremkin, O. Ershov, Y. S. Kayukov, V. Sheverdov, O. Nasakin, V. Tafeenko, E. Nurieva, *Tetrahedron Lett.* **2006**, *47*, 1445-1447.

[123] A. A. Hassan, K. M. El-Shaieb, R. M. Shaker, D. Doepp, *Heteroat. Chem* **2005**, *16*, 12-19.
[124] A. A. Hassan, A. F. E. Mourad, A. H. Abou-Zeid, *J. Heterocycl. Chem.* **2008**, *45*, 323-328.
[125] W. A. Arafa, R. A. Faty, A. K. Mourad, *J. Heterocycl. Chem.* **2018**, *55*, 1886-1894.
[126] S. M. Hecht, D. Werner, D. D. Traficante, M. Sundaralingam, P. Prusiner, T. Ito, T. Sakurai, *J. Org. Chem.* **1975**, *40*, 1815-1822.
[127] K. Okuma, Y. Tsujimoto, *Heteroat. Chem* **2001**, *12*, 259-262.
[128] A. A. Hassan, A. A. Aly, S. M. Mostafa, D. Döppb, *Org. Chem. Int.* **2018**, 200-211.
[129] A. A. Hassan, N. K. Mohamed, K. El-Shaieb, H. N. Tawfeek, S. Bräse, M. Nieger, *ARKIVOC* **2016**.
[130] A. H. Alaa, K. M. Nasr, E. A. E.-H. Lamiaa, B. Stefan, N. Martin, *Curr. Org. Synth.* **2016**, *13*, 426-431.
[131] A. A. Hassan, N. K. Mohamed, L. E. Abd El-Haleem, S. Bräse, M. Nieger, *J. Heterocycl. Chem.* **2015**, *52*, 1368-1372.
[132] A. A. Hassan, N. K. Mohamed, L. E. A. El-Haleem, S. Bräse, M. Nieger, *Chin. J. Chem* . **2016**, *34*, 814-822.
[133] H. Hopf, R. Gleiter, in *Secondary*, Wiley-VCH, Weinheim, **2004**.
[134] V. Fritz, N. Peter, *Synthesis* **1973**, 85-103.
[135] H. Hopf, C. Marquard, in *Book*, Springer, **1989**, pp. 297-332.
[136] F. Vögtle, *Vol.*, John Wiley & Sons Inc, **1993**.
[137] C. Braun, S. Bräse, L. L. Schafer, *Eur. J. Org. Chem.* **2017**, *2017*, 1760-1764.
[138] A. A. Aly, N. K. Mohamed, A. A. Hassan, K. M. El-Shaieb, M. M. Makhlouf, S. Bräse, M. Nieger, A. B. Brown, *Molecules* **2019**, *24*, 3069.
[139] A. A. Aly, A. B. Brown, *Tetrahedron* **2009**, *39*, 8055-8089.
[140] A. A. Aly, H. Hopf, P. G. Jones, I. Dix, *Tetrahedron* **2006**, *62*, 4498-4505.
[141] H. Hopf, A. A. Aly, V. N. Swaminathan, L. Ernst, I. Dix, P. G. Jones, *Eur. J. Org. Chem.* **2005**, *2005*, 68-71.
[142] A. A. Aly, *Tetrahedron Lett.* **2005**, *46*, 443-446.
[143] M. Mielczarek, R. V. Thomas, C. Ma, H. Kandemir, X. Yang, M. Bhadbhade, D. S. Black, R. Griffith, P. J. Lewis, N. Kumar, *Biorg. Med. Chem.* **2015**, *23*, 1763-1775.
[144] H. Kandemir, C. Ma, S. K. Kutty, D. S. Black, R. Griffith, P. J. Lewis, N. Kumar, *Biorg. Med. Chem.* **2014**, *22*, 1672-1679.
[145] M. Dutta, B. Goswami, J. Kataky, *J. Heterocycl. Chem.* **1986**, *23*, 793-795.
[146] A. M. Bernardino, A. O. Gomes, K. S. Charret, A. C. Freitas, G. M. Machado, M. M. Canto-Cavalheiro, L. L. Leon, V. F. Amaral, *Eur. J. Med. Chem.* **2006**, *41*, 80-87.
[147] N. Terzioglu, A. Gürsoy, *Eur. J. Med. Chem.* **2003**, *38*, 781-786.
[148] Y. Xia, C.-D. Fan, B.-X. Zhao, J. Zhao, D.-S. Shin, J.-Y. Miao, *Eur. J. Med. Chem.* **2008**, *43*, 2347-2353.
[149] L.-W. Zheng, L.-L. Wu, B.-X. Zhao, W.-L. Dong, J.-Y. Miao, *Biorg. Med. Chem.* **2009**, *17*, 1957-1962.
[150] E. S. Wu, A. Kover, J. T. Loch III, L. P. Rosenberg, S. F. Semus, P. R. Verhoest, J. C. Gordon, A. C. Machulskis, S. A. McCreedy, J. Zongrone, *Bioorg. Med. Chem. Lett.* **1996**, *6*, 2525-2530.
[151] P. Markham, E. Klyachko, D. Crich, M. Jaber, M. Johnson, D. Mulhearn, A. Neyfakh, *PCT Int. Appl. WO 01 70* **2001**, *213*.
[152] H. Zitt, I. Dix, H. Hopf, P. G. Jones, *Eur. J. Org. Chem.* **2002**, *2002*, 2298-2307.
[153] H. Hopf, S. V. Narayanan, P. G. Jones, *Beilstein J. Org. Chem.* **2015**, *11*, 437-445.
[154] D. J. Cram, N. L. Allinger, *J. Am. Chem. Soc.* **1955**, *77*, 6289-6294.
[155] F. N. Diederich, *Vol.*, Royal Society of Chemistry, **1991**.
[156] C. Bolm, T. Kuehn, *Synlett* **2000**, *2000*, 0899-0901.
[157] D. M. Knoll, Y. Hu, Z. Hassan, M. Nieger, S. Bräse, *Molecules* **2019**, *24*, 4122.
[158] D. M. Knoll, H. Šimek, Z. Hassan, S. Bräse, *Eur. J. Org. Chem.* **2019**, *2019*, 6198-6202.
[159] D. M. Knoll, T. B. Wiesner, S. M. Marschner, Z. Hassan, P. Weis, M. Kappes, M. Nieger, S. Bräse, *RSC Advances* **2019**, *9*, 30541-30544.
[160] D. M. Knoll, C. Zippel, Z. Hassan, M. Nieger, P. Weis, M. M. Kappes, S. Bräse, *Dalton Trans.* **2019**, *48*, 17704-17708.
[161] S. E. Gibson, J. D. Knight, *Org. Biomol. Chem.* **2003**, *1*, 1256-1269.

[162] V. Rozenberg, N. Dubrovina, E. Sergeeva, D. Antonov, *Tetrahedron: Asymmetry* **1998**, *9*, 653-656.
[163] N. Eweiss, A. Bahajaj, E. Elsherbini, *J. Heterocycl. Chem.* **1986**, *23*, 1451-1458.
[164] B. Tozkoparan, N. Gökhan, G. Aktay, E. Yeşilada, M. Ertan, *Eur. J. Med. Chem.* **2000**, *35*, 743-750.
[165] M. Ashok, B. S. Holla, B. Poojary, *Eur. J. Med. Chem.* **2007**, *42*, 1095-1101.
[166] A. T. Mavrova, D. Wesselinova, Y. A. Tsenov, P. Denkova, *Eur. J. Med. Chem.* **2009**, *44*, 63-69.
[167] Z. Li, Z. Gu, K. Yin, R. Zhang, Q. Deng, J. Xiang, *Eur. J. Med. Chem.* **2009**, *44*, 4716-4720.
[168] L. I. Kruse, C. Kaiser, W. E. DeWolf, J. A. Finkelstein, J. S. Frazee, E. L. Hilbert, S. T. Ross, K. E. Flaim, J. L. Sawyer, *J. Med. Chem.* **1990**, *33*, 781-789.
[169] J. L. Gilmore, B. W. King, N. Asakawa, K. Harrison, A. Tebben, J. E. Sheppeck II, R.-Q. Liu, M. Covington, J. J.-W. Duan, *Bioorg. Med. Chem. Lett.* **2007**, *17*, 4678-4682.
[170] L. Maingot, F. Leroux, V. Landry, J. Dumont, H. Nagase, B. Villoutreix, O. Sperandio, R. Deprez-Poulain, B. Deprez, *Bioorg. Med. Chem. Lett.* **2010**, *20*, 6213-6216.
[171] Z. Amtul, M. Rasheed, M. I. Choudhary, S. Rosanna, K. M. Khan, *Biochem. Biophys. Res. Commun.* **2004**, *319*, 1053-1063.
[172] P. Vella, W. M. Hussein, E. W. Leung, D. Clayton, D. L. Ollis, N. Mitić, G. Schenk, R. P. McGeary, *Bioorg. Med. Chem. Lett.* **2011**, *21*, 3282-3285.
[173] M. Idrees, R. D. Nasare, N. J. Siddiqui, *Der Chemica Sinica* **2016**, *7*, 28-35.
[174] K. P. Barot, K. S. Manna, M. D. Ghate, *J. Saudi Chem. Soc.* **2017**, *21*, S35-S43.
[175] P. B. Patil, J. D. Patil, S. N. Korade, S. D. Kshirsagar, S. P. Govindwar, D. M. Pore, *Res. Chem. Intermed.* **2016**, *42*, 4171-4180.
[176] C. Adachi, T. Tsutsui, S. Saito, *Appl. Phys. Lett.* **1990**, *56*, 799-801.
[177] M. Idrees, R. D. Nasare, N. J. Siddiqui, *Der Chemica Sinica* **2016,** , *7*, 28-35.
[178] M. Hanif, M. Saleem, M. T. Hussain, N. H. Rama, S. Zaib, M. A. M. Aslam, P. G. Jones, J. Iqbal, *J. Braz. Chem. Soc.* **2012**, *23*, 854-860.
[179] J. Lee, K. Shizu, H. Tanaka, H. Nomura, T. Yasuda, C. Adachi, *J. Mater. Chem.* **2013**, *1*, 4599-4604.
[180] S. G. Deeks, S. Kar, S. I. Gubernick, P. Kirkpatrick, *Nat. Rev. Drug Discov.* **2008**, *7*, 117-118.
[181] Y. Ducharme, M. Blouin, C. Brideau, A. Châteauneuf, Y. Gareau, E. L. Grimm, H. Juteau, S. Laliberté, B. MacKay, F. Massé, *ACS Med. Chem. Lett.* **2010**, *1*, 170-174.
[182] N. D. James, J. W. Growcott, *DRUG FUTURE* **2009**, *34*, 624-633.
[183] J. Boström, A. Hogner, A. Llinàs, E. Wellner, A. T. Plowright, *J. Med. Chem.* **2012**, *55*, 1817-1830.
[184] J. R. Frost, C. C. Scully, A. K. Yudin, *Nat. Chem.* **2016**, *8*, 1105-1111.
[185] A. A. Kadi, N. R. El-Brollosy, O. A. Al-Deeb, E. E. Habib, T. M. Ibrahim, A. A. El-Emam, *Eur. J. Med. Chem.* **2007**, *42*, 235-242.
[186] F. Bentiss, M. Lagrenee, *J. Heterocycl. Chem.* **1999**, *36*, 1029-1032.
[187] V. Mickevičius, R. Vaickelionienė, B. Sapijanskaitė, *Chem. Heterocycl. Compd.* **2009**, *45*, 215-218.
[188] S. Liras, M. P. Allen, B. E. Segelstein, *Synth. Commun.* **2000**, *30*, 437-443.
[189] A. Ramazani, B. Abdian, F. Z. Nasrabadi, M. Rouhani, *Phosphorus Sulfur Silicon Relat. Elem.* **2013**, *188*, 642-648.
[190] A. Ramazani, F. Zeinali Nasrabadi, Y. Ahmadi, *Helv. Chim. Acta* **2011**, *94*, 1024-1029.
[191] A. Ramazani, A. Souldozi, *ARKIVOC* **2008**, *16*, 235-242.
[192] J. Altman, E. Babad, J. Itzchaki, D. Ginsburg, *Tetrahedron* **1966**, *22*, 279-304.
[193] L. Zalkow, R. Harris, D. Van Derveer, *J. Chem. Soc., Chem. Commun.* **1978**, 420-421.
[194] A. S. Feliciano, M. Medarde, M. Gordaliza, E. Del Olmo, J. M. Del Corral, *J. Nat. Prod.* **1988**, *51*, 1153-1160.
[195] A. Alizadeh, A. Rezvanian, L.-G. Zhu, *J. Org. Chem.* **2012**, *77*, 4385-4390.
[196] O. Diels, K. Alder, *Justus Liebigs Ann. Chem.* **1931**, *486*, 191-202.
[197] O. Diels, J. Reese, *Justus Liebigs Ann. Chem.* **1934**, *511*, 168-182.
[198] K. Alder, K. H. Backendorf, *Chem. Ber. (A and B Series)* **1938**, *71*, 2199-2209.
[199] P. Brigl, R. Herrmann, *Chem. Ber. (A and B Series)* **1938**, *71*, 2280-2282.

[200] G. Snatzke, G. Zanati, *Justus Liebigs Ann. Chem.* **1965**, *684*, 62-78.
[201] F. Nerdel, K. Janowsky, D. Frank, *Tetrahedron Lett.* **1965**, *6*, 2979-2981.
[202] J. Qian-Cutrone, Q. Gao, S. Huang, S. E. Klohr, J. A. Veitch, Y.-Z. Shu, *J. Nat. Prod.* **1994**, *57*, 1656-1660.
[203] P. Kaszynski, J. Michl, *J. Am. Chem. Soc.* **1988**, *110*, 5225-5226.
[204] J.-m. Huang, R. Yokoyama, C.-s. Yang, Y. Fukuyama, *Tetrahedron Lett.* **2000**, *41*, 6111-6114.
[205] M. Konishi, H. Ohkuma, T. Tsuno, T. Oki, G. D. VanDuyne, J. Clardy, *J. Am. Chem. Soc.* **1990**, *112*, 3715-3716.
[206] G. A. Ellestad, M. P. Kunstmann, H. A. Whaley, E. L. Patterson, *J. Am. Chem. Soc.* **1968**, *90*, 1325-1332.
[207] J. Dugan, P. De Mayo, M. Nisbet, J. Robinson, M. Anchel, *J. Am. Chem. Soc.* **1966**, *88*, 2838-2844.
[208] K. Okabe, K. Yamada, S. Yamamura, S. Takad, *J. Chem. Soc.* **1967**, 2201-2206.
[209] K. Nakanishi, *Pure Appl. Chem.* **2013**, *14*, 89.
[210] Y. Sugimoto, H. A. Babiker, T. Saisho, T. Furumoto, S. Inanaga, M. Kato, *J. Org. Chem.* **2001**, *66*, 3299-3302.
[211] B.-W. Yu, J.-Y. Chen, Y.-P. Wang, K.-F. Cheng, X.-Y. Li, G.-W. Qin, *Phytochemistry* **2002**, *61*, 439-442.
[212] A. J. Pihko, A. M. Koskinen, *Tetrahedron* **2005**, *37*, 8769-8807.
[213] K. C. Nicolaou, S. A. Snyder, T. Montagnon, G. Vassilikogiannakis, *Angew. Chem. Int. Ed.* **2002**, *41*, 1668-1698.
[214] K. Asahi, H. Nishino, *Tetrahedron* **2008**, *64*, 1620-1634.
[215] B. M. Trost, Y. Shi, *J. Am. Chem. Soc.* **1991**, *113*, 701-703.
[216] J. Jamrozik, M. Jamrozik, P. Ściborowicz, W. Żesławski, *Monatsh. Chem.* **1995**, *126*, 587-591.
[217] D. Ginsburg, in *Book*, Springer, **1987**, pp. 1-17.
[218] I. Yavari, A. Khajeh-Khezri, S. Bahemmat, M. R. Halvagar, *Synlett* **2017**, *28*, 1785-1788.
[219] I. Yavari, A. Khajeh-Khezri, *Mol. Divers.* **2017**, *21*, 849-854.
[220] A. A. Hassan, N. K. Mohamed, A. A. Aly, H. N. Tawfeek, S. Bräse, M. Nieger, *Mol. Divers.* **2020**, 1-10.
[221] A. A. Hassan, S. K. Mohamed, F. F. Abdel-Latif, S. M. Mostafa, M. Abdel-Aziz, J. T. Mague, M. Akkurt, *Synlett* **2016**, *27*, 412-416.
[222] A. A. Hassan, A. A. Aly, N. K. Mohamed, K. M. El Shaieb, M. M. Makhlouf, E.-S. M. Abdelhafez, S. Bräse, M. Nieger, K. N. Dalby, T. S. Kaoud, *Bioorg. Chem.* **2019**, *85*, 585-599.
[223] M. Skultety, H. Hübner, S. Löber, P. Gmeiner, *J. Med. Chem.* **2010**, *53*, 7219-7228.
[224] B. Ortner, R. Waibel, P. Gmeiner, *Angew. Chem. Int. Ed.* **2001**, *40*, 1283-1285.
[225] S. Löber, B. Ortner, L. Bettinetti, H. Hübner, P. Gmeiner, *Tetrahedron: Asymmetry* **2002**, *13*, 2303-2310.
[226] K. Gewald, R. Schindler, *J. Prakt. Chem.* **1990**, *332*, 223-228.
[227] R. Radeglia, *J. Prakt. Chem.* **1985**, *327*, 878-879.
[228] A. Kundu, A. Pramanik, *Mol. Divers.* **2015**, *19*, 459-471.
[229] S. Bommarito, N. Peyret, J. S. Jr, *Nucleic Acids Res.* **2000**, *28*, 1929-1934.
[230] J. Chen, Z. Wang, C.-M. Li, Y. Lu, P. K. Vaddady, B. Meibohm, J. T. Dalton, D. D. Miller, W. Li, *J. Med. Chem.* **2010**, *53*, 7414-7427.
[231] C.-M. Li, Z. Wang, Y. Lu, S. Ahn, R. Narayanan, J. D. Kearbey, D. N. Parke, W. Li, D. D. Miller, J. T. Dalton, *Cancer Res.* **2011**, *71*, 216-224.
[232] R. Romagnoli, P. G. Baraldi, M. K. Salvador, D. Preti, M. Aghazadeh Tabrizi, A. Brancale, X.-H. Fu, J. Li, S.-Z. Zhang, E. Hamel, *J. Med. Chem.* **2012**, *55*, 5433-5445.
[233] Y. Lu, C.-M. Li, Z. Wang, C. R. Ross, J. Chen, J. T. Dalton, W. Li, D. D. Miller, *J. Med. Chem.* **2009**, *52*, 1701-1711.
[234] S. Bestgen, C. Seidl, T. Wiesner, A. Zimmer, M. Falk, B. Köberle, M. Austeri, J. Paradies, S. Bräse, U. Schepers, *Chem. Eur. J.* **2017**, *23*, 6315-6322.
[235] T. Onozawa, M. Kitajima, N. Kogure, H. Takayama, *J. Org. Chem.* **2018**, *83*, 15312-15322.
[236] S. L. Holbeck, R. Camalier, J. A. Crowell, J. P. Govindharajulu, M. Hollingshead, L. W. Anderson, E. Polley, L. Rubinstein, A. Srivastava, D. Wilsker, *Cancer Res.* **2017**, *77*, 3564-3576.

[237] S. A. Rostom, *Biorg. Med. Chem.* **2006**, *14*, 6475-6485.
[238] D. R. Green, G. Kroemer, *Science* **2004**, *305*, 626-629.
[239] H. Nohl, L. Gille, K. Staniek, *Biochem. Pharmacol.* **2005**, *69*, 719-723.
[240] J. M. Rae, C. J. Creighton, J. M. Meck, B. R. Haddad, M. D. Johnson, *Breast Cancer Res. Treat.* **2007**, *104*, 13-19.
[241] O. Polgar, S. Bates, *Biochem. Soc. Trans.* **2005**, *33*, 241-245.
[242] S. Kumar, *Cell Death Differ.* **2007**, *14*, 32-43.
[243] D. R. Matson, P. T. Stukenberg, *Mol. Interventions* **2011**, *11*, 141.
[244] P. R. Clarke, L. A. Allan, *Trends Cell Biol.* **2009**, *19*, 89-98.
[245] M. Higa, N. Noha, H. Yokaryo, K. Ogihara, S. Yogi, *Chem. Pharm. Bull.* **2002**, *50*, 590-593.
[246] A. Schüffler, J. C. Liermann, H. Kolshorn, T. Opatz, H. Anke, *Z. Naturforsch. C,* **2009**, *64*, 25-31.
[247] J. Yue, Z. Lin, D. Wang, Y. Feng, H. Sun, *Phytochemistry* **1994**, *35*, 1023-1025.
[248] M. C. Elliott, M. S. Long, *Org. Biomol. Chem.* **2004**, *2*, 2003-2011.
[249] D. Lednicer, *Vol.*, John Wiley & Sons, **2009**.
[250] B. A. Neto, A. A. Lapis, A. B. Bernd, D. Russowsky, *Tetrahedron* **2009**, *65*, 2484-2496.
[251] G. Meazza, F. E. Dayan, D. E. Wedge, *J. Agric. Food. Chem.* **2003**, *51*, 3824-3828.
[252] C. Zhang, J. G. Ondeyka, D. L. Zink, A. Basilio, F. Vicente, J. Collado, G. Platas, G. Bills, J. Huber, K. Dorso, *J. Nat. Prod.* **2008**, *71*, 1304-1307.
[253] E. Fan, W. Shi, T. L. Lowary, *J. Org. Chem.* **2007**, *72*, 2917-2928.
[254] S. Spyroudis, *Molecules* **2000**, *5*, 1291-1330.
[255] R. P. Verma, *Anticancer Agents Med. Chem.* **2006**, *6*, 489-499.
[256] H. B. Liu, B. Cai, C. B. Cui, Q. Q. Gu, Q. C. Zhao, H. S. Guan, *Chin. J. Chem* . **2006**, *24*, 1683-1686.
[257] C. Gu, J. Zhai, J. Jiang, H. Liu, L. Wang, D. Zhu, Y. Ji, *Chin. J. Chem* . **2014**, *32*, 179-190.
[258] M. Payton, G. Chung, P. Yakowec, A. Wong, D. Powers, L. Xiong, N. Zhang, J. Leal, T. L. Bush, V. Santora, *Cancer Res.* **2006**, *66*, 4299-4308.
[259] A. A. Aly, E. M. El-Sheref, A. B. Brown, S. Bräse, M. Nieger, E.-S. M. Abdelhafez, *J. Sulfur Chem.* **2019**, *40*, 641-647.
[260] B. Parrino, A. Attanzio, V. Spano, S. Cascioferro, A. Montalbano, P. Barraja, L. Tesoriere, P. Diana, G. Cirrincione, A. Carbone, *Eur. J. Med. Chem.* **2017**, *138*, 371-383.
[261] C. H. Spruck, K.-A. Won, S. I. Reed, *Nature* **1999**, *401*, 297-300.
[262] B. Wang, J. Wu, Y. Wu, C. Chen, F. Zou, A. Wang, H. Wu, Z. Hu, Z. Jiang, Q. Liu, *Eur. J. Med. Chem.* **2018**, *158*, 896-916.
[263] H. Matsushime, D. Quelle, S. Shurtleff, M. Shibuya, C. Sherr, J. Kato, *Mol. Cell. Biol.* **1994**, *14*, 2066-2076.
[264] O. M. Abdel-Hamid, A. A. Nafee, E. MA, E. MA, *Benha Veterinary Med. J.* **2018**, *34*, 329-343.
[265] A. Hammam, B. Bayoumy, *Collect. Czechoslov. Chem. Commun.* **1985**, *50*, 71-79.
[266] A. A. Aly, E. K. Ahmed, K. M. El-Mokadem, *J. Sulfur Chem.* **2006**, *27*, 419-426.
[267] Z. Li, Q. Yang, X. Qian, *Biorg. Med. Chem.* **2005**, *13*, 3149-3155.
[268] L. S. Konstantinova, K. A. Lysov, L. I. Souvorova, O. A. Rakitin, *Beilstein J. Org. Chem.* **2013**, *9*, 577-584.
[269] A. Ding, H. Guo, in *Secondary*, Elsevier, Oxford, **2014**.
[270] S. R. Hussaini, R. R. Chamala, Z. Wang, *Tetrahedron* **2015**, *36*, 6017-6086.
[271] E. Olson, *J. Adv. Pract. Oncol.* **2018**, *9*, 43.
[272] N. R. Brown, S. Korolchuk, M. P. Martin, W. A. Stanley, R. Moukhametzianov, M. E. Noble, J. A. Endicott, *Nat. Commun.* **2015**, *6*, 1-12.
[273] E. C. Pesci, J. B. Milbank, J. P. Pearson, S. McKnight, A. S. Kende, E. P. Greenberg, B. H. Iglewski,

Proc. Natl. Acad. Sci. U.S.A. **1999**, *96*, 11229-11234.
[274] S. McGrath, D. S. Wade, E. C. Pesci, *FEMS Microbiol. Lett.* **2004**, *230*, 27-34.
[275] S. P. Diggle, A. Gardner, S. A. West, A. S. Griffin, *Philos. Trans. R. Soc. Lond., B, Biol. Sci.* **2007**, *362*, 1241-1249.

[276] C. E. Dulcey, V. Dekimpe, D.-A. Fauvelle, S. Milot, M.-C. Groleau, N. Doucet, L. G. Rahme, F. Lépine, E. Déziel, *Chem. Biol.* **2013**, *20*, 1481-1491.
[277] Y. Wu, M. R. Seyedsayamdost, *Cell Chem. Biol.* **2017**, *24*, 1437-1444. e1433.
[278] D. A. Burden, N. Osheroff, *Biochim. Biophys. Acta* **1998**, *1400*, 139-154.
[279] Z. Dang, Y. Yang, R. Ji, S. Zhang, *Bioorg. Med. Chem. Lett.* **2007**, *17*, 4523-4526.
[280] A. V. Shindikar, C. Viswanathan, *Bioorg. Med. Chem. Lett.* **2005**, *15*, 1803-1806.
[281] V. T. Andriole, *Clin. Infect. Dis.* **2005**, *41*, S113-S119.
[282] A. A. Aly, E. M. El-Sheref, A.-F. E. Mourad, M. E. Bakheet, S. Bräse, M. Nieger, *Chem. Pap.* **2019**, *73*, 27-37.
[283] A. A. Aly, M. Ramadan, A. A. El-Reedy, *J. Heterocycl. Chem.* **2019**, *56*, 642-645.
[284] A. A. Aly, E. M. El-Sheref, A.-F. E. Mourad, A. B. Brown, S. Bräse, M. E. Bakheet, M. Nieger, *Monatsh. Chem.* **2018**, *149*, 635-644.
[285] E. M. El-Sheref, A. A. Aly, A.-F. E. Mourad, A. B. Brown, S. Bräse, M. E. Bakheet, *Chem. Pap. - Chem. Zvesti* **2018**, *72*, 181-190.
[286] A. A. Aly, E. M. El-Sheref, M. E. Bakheet, M. A. Mourad, S. Bräse, M. A. Ibrahim, M. Nieger, B. K. Garvalov, K. N. Dalby, T. S. Kaoud, *Bioorg. Chem.* **2019**, *82*, 290-305.
[287] A. A. Aly, E. M. El-Sheref, M. E. Bakheet, M. A. Mourad, A. B. Brown, S. Bräse, M. Nieger, M. A. Ibrahim, *Bioorg. Chem.* **2018**, *81*, 700-712.
[288] S. Claerhout, S. Sharma, C. Sköld, C. Cavaluzzo, A. Sandström, M. Larhed, M. Thirumal, V. S. Parmar, E. V. Van der Eycken, *Tetrahedron* **2012**, *68*, 3019-3029.
[289] I. Spartan, *Wavefunction Inc., Irvine, CA, USA* **1997**, *18*.
[290] A. H. Endres, M. Schaffroth, F. Paulus, H. Reiss, H. Wadepohl, F. Rominger, R. Krämer, U. H. Bunz, *J. Am. Chem. Soc.* **2016**, *138*, 1792-1795.
[291] N. Bisballe, M. Hedidi, C. S. Demmer, F. Chevallier, T. Roisnel, V. Dorcet, Y. S. Halauko, O. A. Ivashkevich, V. E. Matulis, G. Bentabed-Ababsa, *Eur. J. Org. Chem.* **2018**, *2018*, 3904-3913.
[292] P. Lont, H. Van der Plas, A. Verbeek, *Recueil des Travaux Chimiques des Pays-Bas* **1972**, *91*, 949-957.
[293] H. C. Van der Plas, *Acc. Chem. Res.* **1978**, *11*, 462-468.
[294] H. C. Van der Plas, *ChemInform* **1999**, *30*, no-no.
[295] G. L. Rusinov, P. A. Slepukhin, V. N. Charushin, O. N. Chupakhin, *Mendeleev Commun.* **2001**, *11*, 78-80.
[296] V. S. Rao, M. Darbarwar, *Synth. Commun.* **1988**, *18*, 2267-2272.
[297] C. Marino, K. Mariño, L. Miletti, M. J. Manso Alves, W. Colli, R. M. de Lederkremer, *Glycobiology* **1998**, *8*, 901-904.
[298] O. M. El din Awad, W. E. Attia, H. El Sayed, *Carbohydr. Res.* **2004**, *339*, 469-476.
[299] E. El Ashry, L. Awad, A. Atta, *Tetrahedron* **2006**, *13*, 2943-2998.
[300] C. Apparu, H. Driguez, G. Williamson, B. Svensson, *Carbohydr. Res.* **1995**, *277*, 313-320.
[301] E. Spuling, *Dissertation, KIT,* **2019.**
[302] R. S. Cahn, C. Ingold, V. Prelog, *Angew. Chem. Int. Ed.* **1966**, *5*, 385–415.
[303] M. Di Grandi, M. Olson, A. S. Prashad, G. Bebernitz, A. Luckay, S. Mullen, Y. Hu, G. Krishnamurthy, K. Pitts, J. O'Connell, *Bioorg. Med. Chem. Lett.* **2010**, *20*, 398-402.
[304] S. J. Dolman, F. Gosselin, P. D. O'Shea, I. W. Davies, *The Journal of organic chemistry* **2006**, *71*, 9548-9551.
[305] L. Tolosa, M. T. Donato, M. J. Gómez-Lechón, in *Book*, Springer, **2015**, pp. 333-348.
[306] P. Pozarowski, Z. Darzynkiewicz, in *Book*, Springer, **2004**, pp. 301-311.
[307] D. Wu, P. Yotnda, *JoVE (Journal of Visualized Experiments)* **2011**, e3357.
[308] A. L. Niles, R. A. Moravec, T. L. Riss, in *Book*, Springer, **2008**, pp. 137-150.
[309] L. X. Peng, M. Wallace, B. Andaloro, D. Fallon, L. Fleck, D. Delduco, G. Tice, *J. AOAC Int.* **2011**, *94*, 172-178.
[310] M. Redmann, G. A. Benavides, W. Y. Wani, T. F. Berryhill, X. Ouyang, M. S. Johnson, S. Ravi, K. Mitra, S. Barnes, V. M. Darley-Usmar, *Redox biology* **2018**, *17*, 59-69.
[311] Y. Lu, J. Chen, M. Xiao, W. Li, D. D. Miller, *Pharm. Res.* **2012**, *29*, 2943-2971.
[312] C. Gilpin, A. Korobitsyn, K. Weyer, *Ther. Adv. Infect. Dis.* **2016**, *3*, 145-151.
[313] J. P. Chow, R. Y. Poon, H. T. Ma, *Mol. Cell. Biol.* **2011**, *31*, 1478-1491.

[314] O. S. S. F. R. E. D. F. Receptor, *version 2.2.5* http://www.eyesopen.com.
[315] M. A. Abdullah, R. El-Baky, H. A. Hassan, E. Abdelhafez, G. E.-D. A. Abuo-Rahma, *Am J Microbiol Res* **2016**, *4*, 81-84.
[316] D. R. Buckle, B. C. Cantello, H. Smith, B. A. Spicer, *J. Med. Chem.* **1975**, *18*, 726-732.
[317] G. Sheldrick, *Acta Crystallogr. A* **2015**, *71*, 3-8.
[318] G. Sheldrick, *Acta Crystallogr. C* **2015**, *71*, 3-8.
[319] S. Parsons, H. D. Flack, T. Wagner, *Acta Crystallogr. B* **2013**, *69*, 249-259.
[320] A. Spek, *Acta Crystallogr. D* **2009**, *65*, 148-155.

8. Appendix

8.1. List of Publications

Publications

1) A. A. Hassan, S. Bräse, A. A. Aly, N. K. Mohamed, **L. E. A. El-Haleem**, M. Nieger, *Monatshefte fuer Chemie, in press*.
   DOI: 10.1007/s00706-021-02853-0
   Stereoselective Synthesis of Homochiral Paracyclophanylindenofuranylimidazo[3.3.3]-propellanes.
2) A. A. Aly, S. Bräse, A. A. Hassan, N. K. Mohamed, **L. E. A. El-Haleem**, M. Nieger, E. M. N. Abdelhafez, *Molecules 2020, 25(23), 5569.*
   https://doi.org/10.3390/molecules25235569
   Design, Synthesis, and Molecular Docking of Paracyclophanyl-Thiazole Hybrids as Novel CDK1 Inhibitors and Apoptosis Inducing Anti-Melanoma Agents.
3) A. A. Hassan, A. A. Aly, N. K. Mohamed, **L. E. A. El-Haleem**, S. Bräse, M. Nieger, *Monatsh. Chem.* **2020**, *151*, 1425–1431.
   Tetracyanoethylene as a building block in the facile synthesis of heteroyl-tetrasubstituted thiazoles.
   DOI: .org/10.1007/s00706-020-02669-4
4) A. A. Aly, A. A. Hassan, N. K. Mohamed, **L. E. A. El-Haleem**, S. Bräse, *J. Chem. Res.*, ***2020****, 44(7-8),* 388-392.
   Regioselective synthesis of new 7,8-dichloro-benzofuro[3,2-c]quinoline-6,9,10(5H)-triones from reactions of 4-hydroxy-2-quinolones with 3,4,5,6-tetrachloro-1,2-benzoquinone.
   DOI:org/10.1177/1747519820902669
5) A. A. Aly, S. Bräse, A. A. Hassan, N. K. Mohamed, **L. E. A. El-Haleem**, M. Nieger, *Molecules* **2020**, *25(15)*, 3315.
   Synthesis of New Planar-Chiral Linked [2.2]Paracyclophanes-N-([2.2]Paracyclophanyl-carbamoyl)-4-([2.2]Paracyclophanylcarboxamide, [2.2]Paracyclophanyl-Substituted Triazolthiones and -Substituted Oxadiazoles.
   DOI:org/10.3390/molecules25153315
6) A. A. Aly, S. Bräse, A. A. Hassan, N. K. Mohamed, **L. E. A. El-Haleem**, M. Nieger, N. M. Morsy, E. M. N. Abdelhafez, *Molecules* **2020**, *25*(13), 3089.

New Paracyclophanylthiazoles with Anti-Leukemia Activity: Design, Synthesis, Molecular Docking, and Mechanistic Studies.
DOI:org/10.3390/molecules25133089

7) A. A. Aly, A. A. Hassan, N. K. Mohamed, **L. E. A. El-Haleem**, S. Bräse, M. Polamo, M. Nieger, A. B. Brown, *Molecules* **2019**, *24*, 3782.
Synthesis of New Fused Heterocyclic 2-Quinolones and 3-Alkanonyl-4-Hydroxy-2-Quinolones.
DOI:org/10.3390/molecules24203782

8) A. A. Hassan, N. K. Mohamed, **L. E. A. El-Haleem**, S. Bräse, M. Nieger, *Curr. Org. Synth.* **2016**, *13 (3),* 426-431.
Synthesis of New Furo-imidazo[3.3.3]propellanes.
DOI:10.2174/1570179412666150513003813

9) A. A. Hassan, N. K. Mohamed, **L. E. A. El-Haleem**, S. Bräse, M. Nieger, *Chin. J. Chem*. **2016**, *34*, 814-822.
Facile Synthesis of Naphtho[2,3-d]thiazoles, Naphtho[2,3-e][1,3,4]thiadiazines and Bis(naphtho[2,3-d]thiazole)copper(II) Derivatives from Heteroylthiosemicarbazides.
DOI:org/10.1002/cjoc.201600195

10) A. A. Hassan, N. K. Mohamed, **L. E. A. El-Haleem**, S. Bräse, M. Nieger, *J. Heterocyclic Chem.* **2015**, *52*, 1368-1372.
Synthesis of Some New Heteroylhydrazono-1,3-thiazolidin-4-ones.
DOI:org/10.1002/jhet.2240

8.2. Acknowledgments

First of all, I would like to express my deepest thanks to my advisor Prof. Dr. STEFAN BRÄSE for being my supervisor and giving me the opportunity to obtain my Ph.D. in such a great environment. I want to thank him for his patience, motivation, immense knowledge, giving me the freedom I needed with a special caring about me and my family. His guidance helped me in all the time of research and writing of this thesis.

I am very grateful to Prof. Dr. ASHRAF A. ALY at the Faculty of Science, Minia University for his supervision in his lab in Egypt, his advice and ideas in chemistry which help me a lot to build this thesis. I appreciate his help in exponential publication growth.

Furthermore, I want to thank Prof. Dr. ALAA A. HASSAN at the Faculty of Science, Minia University for his support and help in my scientific life, I'm really proud that I had my master thesis with him and still complete publishing nice papers together.

For biology collaboration, I would like to thank the National Cancer Institute (NCI, USA) for the anticancer screening for my compounds, also thanks to Dr. EL SHIMAA M. N. ABDELHAFEZ for making all the biological experiments and writing all the results, many thanks for your efforts in producing these great results and also publications.

I want to acknowledge the work of Dr. MARTIN NIEGER for crystal structure analyses at the University of Helsinki, Dr. ANDREAS RAPP, TANJA OHMER-SCHERRER, and DESPINA SAVVIDOU for NMR spectroscopy, ANGELIKA MÖSLE and LARA HIRSCH for mass spectrometry and IR, KAROLIN KOHNLE for elemental analysis. All of them helping me very kindly by analyzing all compounds and without them, this thesis would not have been possible. Thank you ComPlat-Team for taking care of many, many samples, and providing data whenever needed.

I kindly acknowledge Prof. Dr. JOACHIM PODLECH for the acceptance of the co-reference of this thesis.

A great and special thanks to CHRISTOPH ZIPPEL for helping me in my starting in the German lab and learning me all of the new techniques and making it so easy for me, always listing to my chemistry problems and try to solve all of them, giving idea for modifying my results, never annoyed from wasting his time when I need his help, really thanks for your kind efforts

Another special thanks go to SUSANNE KIRCHNER for being a close friend, giving me and my kids a family feeling in Karlsruhe, her great support even if in social or scientific life. I will never forget the happy memories which we spent together.

A particular thank you to CHRISTOPH ZIPPEL, SARAH AL MUTHAFER, GLORIA HONG, ANNA-LENA LEISTNER and SUSANNE KIRCHNER for taking the time to proofread and give me very helpful remarks and suggestions. I am deeply thankful that you have taken the time to correct my thesis thoroughly.

And now time to thank the entire AK Bräse team for this nice and joyful time. It is my pleasure to be part of the team. In particular, many thanks go to Dr. CLAUDIA BIZZARRI, Dr. ROBIN BÄR, Dr. ZAHID HASSAN, Dr. STEFAN MARSCHNER, Dr. JASMIN BUSCH, XUEMIN GAN, SARAH AL MUTHAFER, ROBERTA TABONE, GLORIA HONG, ANNA-LENA LEISTNER, HANNES KÜHNER, CECILIA BRUSCHI, LISA-LOU GRACIA, QAIS PARSA, PETER GÖDTEL, CLAUDINE HERLAN, LISA SCHMIDT and NASRIN SALAEH-AREA, thank you guys for making work time more pleasant.

A huge thanks to CHRISTIANE LAMPERT, JANINE BOLZ, Dr. WELL ILONA, and Dr. CHRISTIN BEDNAREK, whose help cannot be overestimated in keeping the group running.

Also, I want to deeply thanks my Egyptian friends MARWA EISSA, SHAYMAA SHAWKY, and ALAA DOGHDA for supporting me and spending the most beautiful family moments together in Karlsruhe, Dr. AHMED IBRAHIM for advice, support and kind guidance, and for my best friend MAYSA MAKLOUF for being in my life.

The biggest and lovely thanks belong to my parents, my family, my husband ABDELBAKY ABDELALL, and my kids ADAM and DAREEN. Your support and understanding this hard period give me the motivation and courage to study hard and go further, I derive my strength by having you by my side. Your guidance and encouragements give me the determination to success.